Program l·yŘ !ōăúŃJl·Ŏúă

LUNAR AND PLANETARY INSTITUTE

USRA

3rd International Workshop on Instrumentation for Planetary Missions

October 24–27, 2016 • Pasadena, California

Sponsor

Universities Space Research Association (USRA)
Lunar and Planetary Institute (LPI)
Jet Propulsion Laboratory (JPL)

Conveners

Sabrina Feldman, *Jet Propulsion Laboratory*
David Beaty, *Jet Propulsion Laboratory*

Local Organizing Committee

James Ashley, *Jet Propulsion Laboratory*
Lindsay Hays, *Jet Propulsion Laboratory*
Laura Kerber, *Jet Propulsion Laboratory*
Glenn Sellar, *Jet Propulsion Laboratory*

Science Organizing Committee

Carlton Allen, *Johnson Space Center (retired)*
Julie Castillo-Rogez, *Jet Propulsion Laboratory*
Barbara Cohen, *Marshall Space Flight Center*
Anthony Colaprete, *Ames Research Center*
Athena Coustenis, *Observatoire de Meudon/LESIA/CNRS*
Masaki Fujimoto, *Institute of Space and Astronautical Science, Japan Aerospace Exploration Agency (JAXA)*
Daniel Glavin, *Goddard Space Flight Center*
Manuel Grande, *Aberystwyth University, U.K.*
Brook Lakew, *Goddard Space Flight Center*
Scott Murchie, *Applied Physics Laboratory*
Alfred Nash, *Jet Propulsion Laboratory*
Kurt Retherford, *Southwest Research Institute*
Aileen Yingst, *Planetary Science Institute*

Lunar and Planetary Institute 3600 Bay Area Boulevard Houston TX 77058-1113

Loading Your Presentation

In order to facilitate a smooth transition between speakers, all presentations MUST be preloaded in advance. To aid the preloading process, create a folder on your flash drive/CD called "IPM 2016" and place your presentation file in that folder. Please include your last name in the naming of your presentation file. IT assistance will be available in the individual meeting rooms before each session to assist with loading and testing your presentation.

Monday

Morning Sessions	7:30–8:30 a.m.
Afternoon Sessions	12:30–1:15 p.m.

Tuesday-Wednesday

Morning Sessions	7:15–8:15 a.m.
Afternoon Sessions	12:30–1:15 p.m.

Thursday

Morning Sessions	7:15–8:15 a.m.

Abstracts for this workshop are available via the workshop website at

www.hou.usra.edu/meetings/ipm2016/

Abstracts can be cited as

Author A. B. and Author C. D. (2016) Title of abstract. In *3rd International Workshop on Instrumentation for Planetary Missions,* Abstract #XXXX. LPI Contribution No. 1980, Lunar and Planetary Institute, Houston.

Guide to Sessions

Monday, October 24, 2016

8:00 a.m.	Foyer	Registration
8:45 a.m.	San Gabriel Ballroom	Plenary I: Workshop Opening; Future Instrument Needs
10:25 a.m.	San Gabriel Ballroom	Panel I: Perspectives on the Future of Planetary Exploration
1:30 p.m.	San Gabriel Ballroom	Mars 2020 Rover Instruments
	Pasadena	Instruments for Orbiter and Flyby Missions
3:50 p.m.	San Gabriel Ballroom	Jupiter and Its Ocean Worlds: JUICE and Europa Clipper-Lander Missions
	Pasadena	Instruments: Mass Spectrometry and Geochronology

Tuesday, October 25, 2016

8:30 a.m.	International Ballroom	Plenary IIA: Funding and Maturing New Planetary Instruments and Sampling Systems
9:30 a.m.	International Ballroom	Panel II: Bridging the Gap Between Planetary Scientists and Instrument Developers
11:00 a.m.	International Ballroom	Plenary IIB: Surface and Atmospheric Sampling Approaches
11:30 a.m.	International Ballroom	Poster Previews: I
1:30 p.m.	International East	Raman and Vis-NIR Instruments for *In Situ* Mineralogy and Resource Prospecting
1:30 p.m.	International West	Life Detection Instrumentation and Related Technologies for Mars and Ocean Worlds: I
3:05 p.m.	International East	Sub-mm and Radar Instruments for Orbiter and Flyby Missions
3:05 p.m.	International West	Life Detection Instrumentation and Related Technologies for Mars and Ocean Worlds: II
4:10–6:00 p.m.	California Ballroom	Poster Session: I

Wednesday, October 26, 2016

8:30 a.m.	International Ballroom	Plenary III: Winning and Implementing New Planetary Instruments
10:00 a.m.	International Ballroom	Panel III: Lessons Learned for Instrument Development from TRL 1 to 9
11:30 a.m.	International Ballroom	Poster Previews: II
1:30 p.m.	International East	New Technologies for Instruments
1:30 p.m.	International West	Geophysical Instruments and Techniques
3:05 p.m.	International East	Elemental Spectroscopy for Future Missions
3:05 p.m.	International West	SmallSat and CubeSat Instruments
4:10–6:00 p.m.	California Ballroom	Poster Session: II

Thursday, October 27, 2016

8:30 a.m.	International Ballroom	Plenary IV: Emerging Instrument Capabilities and Challenges for Planetary Exploration
10:50 a.m.	International Ballroom	Concluding Discussion

Pasadena Hilton

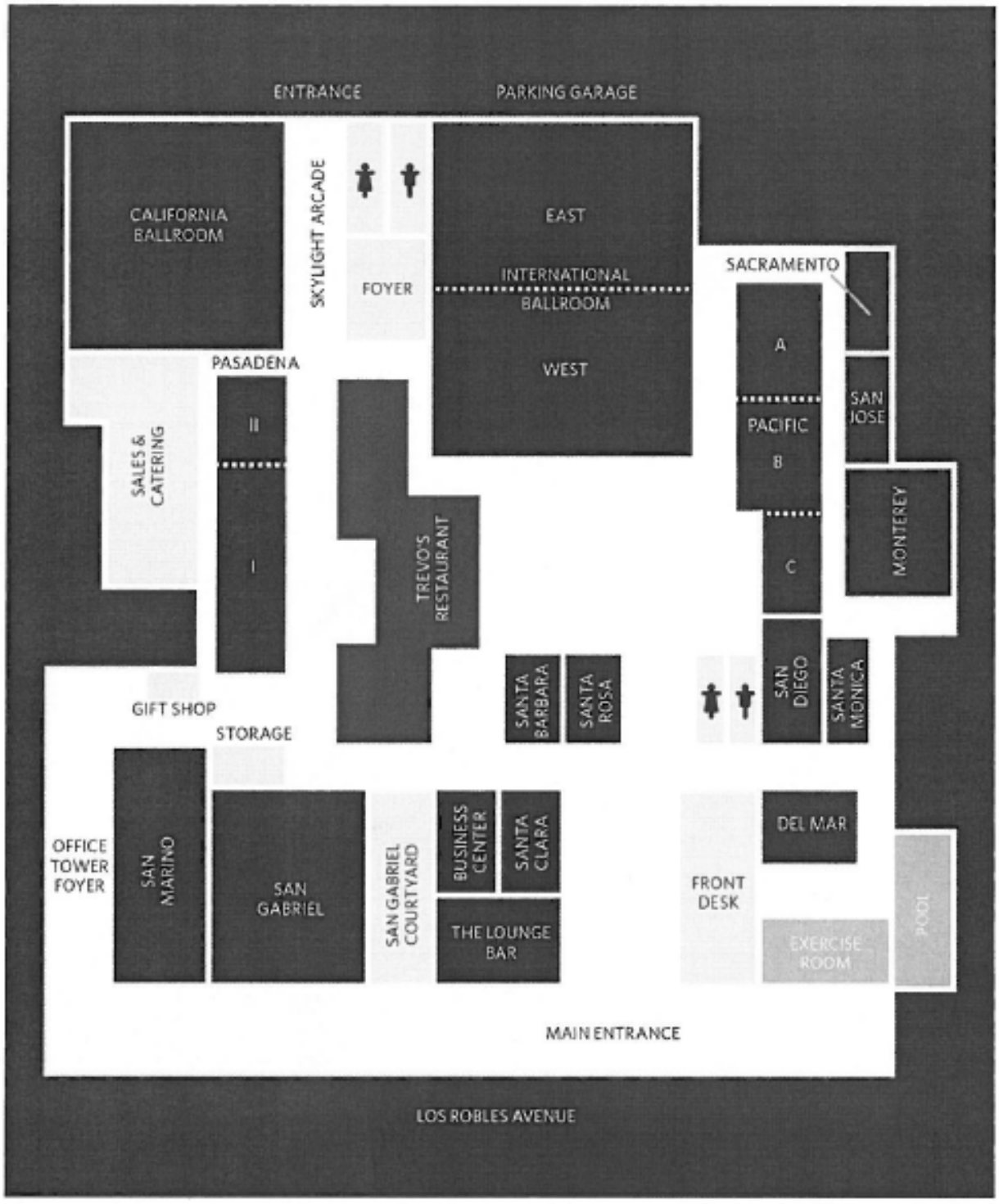

Program

Monday, October 24, 2016
PLENARY I: WORKSHOP OPENING; FUTURE INSTRUMENT NEEDS
8:45 a.m. San Gabriel Ballroom

Chair: **Brook Lakew**

8:45 a.m. Feldman S. Beaty D. *
Opening Remarks

8:55 a.m. Kerber L. *
Introduction to the IWIPM Planetary Instrument Database

9:05 a.m. Voytek M. *
NASA Perspectives on Developing Capabilities to Detect Extant and Extinct Life Beyond Earth

9:25 a.m. Bussey B. *
Current Perspectives on Opportunities for Science Instruments Enabled by Human Exploration

9:45 a.m. Smith D. *
Preliminary Planning for the Next Planetary Science Decadal Survey

10:05 a.m. *Coffee Break*

Monday, October 24, 2016
PANEL I: PERSPECTIVES ON THE FUTURE OF PLANETARY EXPLORATION
10:25 a.m. San Gabriel Ballroom

The purpose of this panel is to present to the workshop a vision of the future of scientific exploration of the solar system over approximately the next 1–2 decades, including science goals and objectives that may require new planetary instruments and measurement techniques.

Moderator: **Louise Prockter**

Panel Members: **Jim Cutts**
Jeff Johnson
Clive Neal
Amy Simon
Tim Swindle

10:25 a.m. Prockter L. *
Introduction

10:30 a.m. Neal C. *
The LEAG Perspective

10:40 a.m. Johnson J. *
The MEPAG Perspective

10:50 a.m. Swindle T. *
The SBAG Perspective

11:00 a.m. Cutts J. A. * Grimm R. Steffes P. I. Izenberg N.
Science Instruments for Venus Exploration **[#4137]**
Venus presents unique challenges and opportunities for scientific exploration. VEXAG is now working on defining needs for laboratory measurements to support the exploration of Venus.

11:10 a.m. Simon A. *
The OPAG Perspective

11:20 a.m. OPEN DISCUSSION

12:00 p.m. *Lunch*

Monday, October 24, 2016
MARS 2020 ROVER INSTRUMENTS
1:30 p.m. San Gabriel Ballroom

Chair: Ken Farley

1:30 p.m. Hamran S.-E. * Amundsen H. E. F. Asak L. Berger T. Brovoll S. Buskenes J. I. Carter L. Damsgård L. Diaz C. Ghent R. Helleren Ø. Kohler J. Mellon M. Nunez D. Paige D. Plettemeier D. Rowe K. Russell P. Sagsveen B. Ødegaard N. Øyan M. J.
The RIMFAX GPR Instrument Development for the Mars 2020 Rover Mission **[#4031]**
The Radar Imager for Mars' subsurface eXperiment (RIMFAX) ground penetrating radar (GPR) experiment for the Mars 2020 Rover will add a new dimension to the rover's toolset by providing the capability to image the shallow subsurface beneath the rover.

1:45 p.m. Beegle L. B. * Bhartia R. DeFlores L. Miller E. Pollack R. Abbey W. Carrier B.
SHERLOC: On the Road to Mars **[#4117]**
SHERLOC is a Deep UV (DUV) native fluorescence and resonance Raman spectrometer that was selected as part of the Mars 2020 payload. It is a robotic arm mounted instrument that generates Raman and fluorescence photons from a targeted 100 μm spot.

2:00 p.m. Rodriguez-Manfredi J. A. de la Torre Juárez M. * Boland J. S. Bridges N. T. Conrad P. Ferri F. Genzer M. Gómez-Gómez F. Gómez-Elvira J. Harri A.-M. Kemppinnen O. Lemmon M. T. Martínez G. Navarro S. Newman C. E. Pérez-Hoyos S. Prieto O. Ramos M. Saiz-López A. Sánchez-Lavega A. Schofield J. T. Sebastián E. Smith M. D. Tamppari L. K. MEDA Team
MEDA: The Mars Environmental Dynamics Analyzer for Mars 2020 **[#4114]**
We describe the status of the Mars Environmental Dynamics Analyzer (MEDA), a suite of environmental sensors that compose one of seven instruments being developed for the science investigations from the Mars 2020 rover.

2:15 p.m. Allwood A. * Wade L. A. Hurowitz J. A.
PIXL Investigation on the Mars 2020 Rover **[4138]**
PIXL data, together with other instruments on the 2020 Mars rover, will make it possible to carry out astrobiological field investigations with sufficient detail and quality to credibly address the search for signs of ancient life on Mars.

2:30 p.m. Bell J. F. III * Maki J. N. Mehall G. L. Ravine M. A. Caplinger M. A. Mastcam-Z Team
Mastcam-Z: Designing a Geologic, Stereoscopic, and Multispectral Pair of Zoom Cameras for the NASA Mars 2020 Rover **[#4126]**
Mastcam-Z is a stereoscopic, multispectral imaging investigation selected for flight on the Mars 2020 rover mission. In this presentation we review our science goals and requirements and describe our CDR-level design and operational plans.

2:45 p.m. Hecht M. H. * Hoffman J. A. The MOXIE team
The Mars Oxygen ISRU Experiment (MOXIE) on the Mars 2020 Rover **[#4130]**
The Mars Oxygen ISRU Experiment (MOXIE) is a technology experiment on the Mars 2020 Rover mission that will demonstrate the production of oxygen from atmospheric carbon dioxide as a precursor to a future human mission.

3:00 p.m. Maki J. N. * McKinney C. M. Sellar R. G. Copley-Woods D. S. Gruel D. C. Nuding D. L. Valvo M. Goodsall T. McGuire J. Litwin T. E.
Enhanced Engineering Cameras (EECAMs) for the Mars 2020 Rover **[#4132]**
The Mars 2020 Rover will be equipped with a next-generation engineering camera imaging system that represents an upgrade over the previous Mars rover engineering cameras flown on the Mars Exploration Rover (MER) mission and the Mars Science Laboratory (MSL) rover mission.

3:15 p.m. Wiens R. C. * Maurice S. Rull F. SuperCam Team
SuperCam Remote Sensing on the Mars 2020 Rover: Science Goals and Overview **[#4136]**
The Mars 2020 Science Definition Team (SDT) report emphasized the importance of fine-scale measurements, suggesting that the numerous pin-point observations made at remote distances by ChemCam was a very desirable capability.

3:30 p.m. *Coffee Break*

Monday, October 24, 2016
INSTRUMENTS FOR ORBITER AND FLYBY MISSIONS
1:30 p.m. Pasadena

Chair: Leslie Tamppari

1:30 p.m. Brageot E. * Lindeman M. Orton G.
Instrument Trade Study and Design for Mid to Far-IR Atmospheric Remote Sensing of an Outer Solar System Planet Based on High Temperature Bolometers **[#4115]**
I will present the design trade study that led us to the concept of an on-orbit or fly-by mid- to far-Infra-Red Fourier Trans-form Imaging spectrometer design for outer planets of the solar system.

1:45 p.m. Kleinboehl A. * Schofield J. T. Kass D. M. McCleese D. J.
The Advanced Mars Climate Sounder (AMCS) — A Proven Atmospheric Profiler for Future Mars Orbiters **[#4066]**
We describe a mature, low-cost, and low-risk infrared atmospheric profiler based on MRO/MCS heritage for measuring atmospheric temperature, dust, water ice, carbon dioxide ice, and water vapor on a future Mars orbiter mission.

2:00 p.m. Burks M. T. * Heffern L. E. Lawrence D. J. Goldsten J. O. Peplowski P. N.
GeMini Plus: A Versatile Gamma-Ray Spectrometer for Planetary Composition Measurements **[#4087]**
GeMini Plus is a high-resolution, low-resource, gamma-ray spectrometer for planetary composition measurements. The core of the instrument has a mass of ~3 kg and requires ~10 watts power, making it well suited for both landed and orbital missions.

2:15 p.m. Clark G. * Westlake J. H. Mitchell D. G. Hoffer E. Brandt P. C.
The Low Energy Neutral Imager (LENI) **[#4042]**
New neutral atom imager that utilizes a novel electro-optical approach to measure low-energy ENAs with high-sensitivity and angular resolution.

2:30 p.m. Panini S. Narendranath S. * Sreekumar P. Athiray P. S. Nayak M.
Soft X-Ray Imager Using Multilayer Mirror Optics for Martian Exospheric Studies **[#4054]**
We will present the conceptual design and developmental status of a X-ray imager for measuring solar wind charge exchange X-ray emission from the martian exosphere from an orbiter around the planet.

2:45 p.m. Davis M. W. * Gladstone G. R. Retherford K. D.
Improving Performance in Planetary Ultraviolet Spectrographs **[#4077]**
Four planetary ultraviolet spectrographs by SwRI have successfully operated on different planetary missions. Two more will operate aboard the JUICE and Europa missions with advancements to allow operations in the Jovian environment.

3:00 p.m. Blaney D. L. * Green R. O. Mouroulis P. Ehlmann B. L. Van Gorp B. McKinnley I. Rodriguez J. M. Lamborn A. Haag J. Cable M.
Ultra Compact Imaging Spectrometer **[#4067]**
The Ultra Compact Imaging Spectrometer (UCIS) is a visible to short wavelength infrared imaging spectrometer with a modular architecture. It is possible to adapt to the instrument details to a variety of mission concepts requiring low mass and low power.

3:15 p.m. Abshire J. B. * Guzewich S. D. Smith M. D. Riris H. Sun X. Gentry B. M. Yu A. Allan G. R.
MARLI: MARs LIdar for Global Wind Profiles and Aerosol Profiles from Orbit **[#4034]**
Winds are the key variable to understand atmospheric transport and to answer fundamental questions about the three primary cycles of the Mars climate. We are developing a new orbital lidar to directly measure both wind profiles and aerosol profiles.

3:30 p.m. *Coffee Break*

Monday, October 24, 2016
JUPITER AND ITS OCEAN WORLDS: JUICE AND EUROPA CLIPPER-LANDER MISSIONS
3:50 p.m. San Gabriel Ballroom

Chair: Scott Murchie

3:50 p.m. Althaus C. * Hussmann H. Lingenauber K. Michaelis H. Kallenbach R. Oberst J.
The Ganymede Laser Altimeter — Instrument Design Overview with Radiation Hard Transmitter **[#4015]**
The Ganymede Laser Altimeter (GALA) onboard of JUICE mission shall investigate Ganymede. A laser provides the measuring signal and has therefore to be robust and reliable in the environment of Jupiter, in particular with regard to radiation.

4:05 p.m. Barabash S. * Brandt P. Wurz P. PEP Team
Particle Environment Package (PEP) for the ESA JUICE Mission **[#4079]**
Description of the particle package for the ESA Jupiter mission JUICE.

4:20 p.m. Turtle E. P. McEwen A. S. Osterman S. N. * Boldt J. D. Strohbehn K. EIS Science Team
The Europa Imaging System (EIS), a Camera Suite to investigate Europa's Geology, Ice Shell, and Potential for Current Activity **[#4091]**
EIS NAC and WAC use identical rad-hard rapid-readout 4 k × 2 k CMOS detectors for imaging during close (≤25 km) fast (~4.5 km/s) Europa flybys. NAC achieves 0.5 m/pixel over a 2-km swath from 50 km, and WAC provides context pushbroom stereo imaging.

4:35 p.m. Westlake J. H. * McNutt R. L. Kasper J. C. Case A. W. Rymer A. M. Stevens M. L. Jia X. Paty C. Khurana K. K. Kivelson M. G. Slavin J. A. Smith H. T. Korth H. Krupp N. Roussous E. Saur J.
The Plasma Instrument for Magnetic Sounding (PIMS) for the Europa Mission **[#4037]**
We present the Plasma Instrument for Magnetic Sounding (PIMS) selected for the Europa Mission. We specifically address how PIMS plasma measurements will improve the accuracy of magnetic sounding of Europa's subsurface ocean.

4:50 p.m. Retherford K. D. * Davis M. W. Greathouse T. K. Monreal R. M. Blase R. C. Raut U. Steffl A. J. Cooke C. M. Siegmun O. Gladstone G. R.
Tests of Microchannel Plate (MCP) Detector Response to MeV Electrons in Support of Juno, JUICE, and Europa Mission UVS Instrument Investigations **[#4102]**
We report our efforts to optimize our UV Spectrograph (UVS) instruments for operating in the intense radiation environment of Jupiter for studying the ocean worlds of Europa and Ganymede in order to share our lessons learned.

5:05 p.m. Grimm R. E. * Delory G. T. Espley J. R. Stillman D. E.
Magnetotelluric Sounding of Europa's Ice Shell **[#4032]**
A magnetometer alone in insufficient to determine thicknesses of water layers in the ice shell because electromagnetic souce geometry is indeterminate at the "high" frequencies (~1 Hz) needed for adequate resolution.

5:20 p.m. Pike W. T. * Standley I. M. Calcutt S. B. Kedar S. Vance S. D. Bills B. G.
The Europa Seismic Package (ESP): 1. Selecting a Broadband Microseismometer for Ocean Worlds. **[#4133]**
We summarize the requirements that would enable a seismic system to provide a probe of the habitability of Europa and introduce a candidate microseismometer for a Europa Seismic Package, comparing to potential competitor technologies.

Monday, October 24, 2016
INSTRUMENTS: MASS SPECTROMETRY AND GEOCHRONOLOGY
3:50 p.m. Pasadena

Chair: Laura Kerber

3:50 p.m. Darrach M. R. Madzunkov S. Neidholdt E. Simcic J. *
Atmospheric Constituent Explorer System (ACES) **[#4065]**
We report on the Atmospheric Constituent Explorer System (ACES), a mass spectrometer based instrument for atmospheric probe missions (e.g. Venus and ice giant) that can determine abundances and isotopic ratios of the noble-gases and trace species.

4:05 p.m. Renard J. B. Verdier N. *
LOAC-S: A Small Aerosol Optical Counter/Sizer for Planetary Measurements of the Size Distribution and Nature of Atmospheric Particles **[#4045]**
The Light Optical Aerosols Counter (LOAC) has been used for years at the surface and under all kinds of balloons in the Earth atmosphere. The reliability of this instrument is now demonstrated and it is light and compact enough for planetary missions.

4:20 p.m. Coleman M. * Christensen L. E. Kriesel J. M. Kelly J. F. Moran J. J. Vance S.
A Very Much Faster and More Sensitive In Situ Stable Isotope Analysis Instrument **[#4052]**
We are developing, Capillary Absorption Spectrometry (CAS) for H and O stable isotope analyses, giving > 4 orders of magnitude improved sensitivity, allowing analysis of 5 nano-moles of water and coupled to laser sampling to free water from hydrated minerals and ice.

4:35 p.m. Cho Y. * Sugita S. Miura Y. N. Okazaki R. Iwata N. Kameda S.
End-to-End Validation of an In-Situ K-Ar Isochron Dating Method for Planetary Landers: Isochron Analysis of Natural Rocks **[#4038]**
End-to-end experiments show the capability of K-Ar isochron dating with a LIBS-QMS combination. Isochron analyses of two natural rocks exhibit the K-Ar ages consistent with their known ages.

4:50 p.m. Anderson F. S. * Whitaker T. J. Levine J. Beck S.
Lead-Lead and Rubidium-Strontium In Situ Dating Using the Chemistry, Organics, and Dating EXperiment (CODEX) **[#4111]**
We describe new results for Pb-Pb dating, and progress on laser development, for the Pb-Pb and Rb-Sr measuring, organics detecting, and elemental abundance mapping Chemistry, Organics, and Dating EXperiment (CODEX) instrument.

5:05 p.m. Cohen B. A. *
The Potassium-Argon Laser Experiment (KArLE): In Situ Geochronology for Planetary Missions **[#4051]**
KArLE is intended to yield in situ geochronology data and enhance functionality of existing flight instruments using flight hardware that would be reliable, reconfigurable and adaptable to multiple partner instruments and mission architectures.

5:20 p.m. Glavin D. P. * Malespin C. A. ten Kate I. L. McAdam A. Getty S. A. Mumm E. Franz H. B. Southard A. E. Bleacher J. E. Mahaffy P. R.
Volatile Analysis by Pyrolysis of Regolith (VAPoR) for Planetary Resource Prospecting **[#4002]**
The Volatile Analysis by Pyrolysis of Regolith (VAPoR) instrument is a pyrolysis mass spectrometer designed to measure the abundance of water and other volatiles released from solids that are heated to temperatures up to 1400C.

Tuesday, October 25, 2016
PLENARY IIA: FUNDING AND MATURING
NEW PLANETARY INSTRUMENTS AND SAMPLING SYSTEMS
8:30 a.m. International Ballroom

Chair: Pat Beauchamp

8:30 a.m. Gaier J. R. *
NASA Planetary Science Division's Instrument Development Programs, PICASSO and MatISSE **[#4003]**
The NASA Planetary Science Division's instrument development programs, Planetary Instrument Concept Advancing Solar System Observations (PICASSO), and Maturation of Instruments for Solar System Exploration Program (MatISSE), are described.

8:50 a.m. Fujimoto M. *
Promoting Planetary Missions at ISAS/JAXA **[#4124]**
How to promote international aspect of ISAS/JAXA planetary missions will be discussed.

9:10 a.m. Grande M. * The Europlanet Community
The Europlanet Research Infrastructure and Technology Foresight **[#4128]**
The Europlanet 2020 Research Infrastructure is a project to integrate and support planetary science activities across Europe. The project is funded under the European Commission's Horizon 2020 programme. Technology Foresight is a key activity.

Tuesday, October 25, 2016
PANEL II: BRIDGING THE GAP BETWEEN
PLANETARY SCIENTISTS AND INSTRUMENT DEVELOPERS
9:30 a.m. International Ballroom

This panel will address challenges and effective approaches to connecting science needs with new instrument technologies and vice-versa.

Moderator: **Alfred Nash**

Panel Members: **Jordana Blacksberg**
Barbara Cohen
Darby Dyar
Glenn Sellar

9:30 a.m. PANEL DISCUSSION

10:45 a.m. *Coffee Break*

Tuesday, October 25, 2016
PLENARY IIB: SURFACE AND ATMOSPHERIC SAMPLING APPROACHES
11:00 a.m. International Ballroom

Chair: Pat Beauchamp

11:00 a.m. Zacny K. * Paulsen G.
1 Meter Class Drill for Acquisition and Transfer of Volatile Rich Samples on the Moon, Mars, and Ocean Worlds **[#4118]**
We present development and testing of the 1 m class drilling system. The system will reach TRL6 by October of 2016 and will be ready for infusion into future planetary surface missions to the Moon, Mars, and Ocean Worlds.

11:15 a.m. Meshik A. * Pravdivtseva O.
New Concept of Sampling Thin Atmospheres of Planetary Bodies for Return Missions **[#4050]**
A new concept of sampling planetary volatiles based on experience from Genesis mission.

Tuesday, October 25, 2016
POSTER PREVIEWS: I
11:30 a.m. International Ballroom

The purpose of this mini-session of lightning talks (1 minute each) is to give the Tuesday poster presenters a chance to introduce themselves and their work.

Chairs: **Lindsay Hays**
David Beaty

11:30 a.m. POSTER PREVIEWS

12:00 p.m. *Lunch*

Tuesday, October 25, 2016
RAMAN AND VIS-NIR INSTRUMENTS
FOR *IN SITU* MINERALOGY AND RESOURCE PROSPECTING
1:30 p.m. International East

Chair: Carlton Allen

1:30 p.m. Moral A. G. * Rull F. Maurice S. Hutchinson I. B. Canora C. P. López G. Canchal R. Gallego P. Seoane L. Prieto J. A. R. Santiago A. Santamaría P. Colombo M. Belenguer T. Ramos G. Parot Y. Ingley R. Woodward S. Shulte W.
Raman Laser Spectrometer for 2020 ExoMars Mission **[#4025]**
The Raman Laser Spectrometer (RLS) is one of the scientific payloads on the ExoMars 2020 mission, within ESA's Aurora Exploration Program. It will perform Raman spectroscopy on crushed powdered samples, obtained from two meters depth under Mars surface.

1:45 p.m. Wang A. * Lambert J. L. Hutchinson I. Monacos S. McHugh M. Wei J. Yan Y. C.
Two High Performance In Situ Raman Spectrometers for Landed Planetary Missions **[#4086]**
We report the results from a CIRS performance test that was accomplished in August 2016. Now both in situ Raman systems, MMRS and CIRS, are ready for missions. We will compare them with other Raman architectures.

2:00 p.m. McHugh M. * Hutchinson I. B. Ingley R. Nelms N.
Optimising the Operation and Performance of a Stand-Off Raman Instrument Developed for Planetary and Lunar Exploration **[#4076]**
We describe the development of a radiometric model for stand-off Raman Spectrometer and discuss the initial results.

2:15 p.m. Ehlmann B. L. * Blaney D. L. Green R. O. Mouroulis P.
VSWIR Microimaging Spectroscopy for Geologic History and Identifying and Quantifying Mineral, Ice, and Organic Abundances on Planetary Surfaces **[#4097]**
VSWIR microimaging spectroscopy is a key tool for landed planetary missions, acquiring simultaneous composition and texture. It has been matured to TRL 6 as UCIS and is presently being used for meteorite and terrestrial earth science studies.

2:30 p.m. Cook A. M. * Colaprete A. Roush T. L. Benton J. E. Forgione J. B. White B. Bielawski R. Fritzler E.
NIR Spectroscopy and Multi-Wavelength Imaging for Volatile Prospecting **[#4023]**
We present a demonstration of an instrument system built at NASA Ames Research Center, for in situ near-infrared spectral observations and visible imagery of planetary surfaces.

2:45 p.m. *Coffee Break*

Tuesday, October 25, 2016
LIFE DETECTION INSTRUMENTATION AND
RELATED TECHNOLOGIES FOR MARS AND OCEAN WORLDS: I
1:30 p.m. International West

Chair: Kurt Retherford

1:30 p.m. Kehl F. * Wu D. Mora M. F. Creamer J. S. Willis P. A.
In-Situ Liquid Extraction and Analysis Platform for Mars and Ocean Worlds **[#4070]**
We present a compact sample extractor and analysis unit, based on subcritical water extraction and flow injection analysis, that could be used to support robotic missions seeking chemical signatures of life on Mars, Europa, Enceladus or Titan.

1:45 p.m. Mojarro A. * Hachey J. Tani J. Smith A. Bhattaru S. A. Pontefract A. Doebler R. Brown M. Ruvkun G. Zuber M. T. Carr C. E.
SETG: Nucleic Acid Extraction and Sequencing for In Situ Life Detection on Mars **[#4095]**
We are developing an integrated nucleic acid extraction and sequencing instrument: the Search for Extra-Terrestrial Genomes (SETG) for in situ life detection on Mars. Our goals are to identify related or unrelated nucleic acid-based life on Mars.

2:00 p.m. Butterworth A. L. * Kim J. Stockton A. M. Turin P. Ludlam M. Mathies R. A.
Instrument for Capturing and Analyzing Trace Organic Molecules from Plumes for Ocean Worlds Missions **[#4100]**
Enceladus Organic Analyzer (EOA) is an innovative miniaturized microfluidic organic chemical and biochemical analysis instrument that will capture plume ice and determine trace organic content.

2:15 p.m. Babu Mannam N. P. * Krishnankutty P.
Biomimetic Planetary Rovers for Ocean Exploration in Space **[#4056]**
Conventional planetary rover designs are wheel operated on firm ground surfaces and proved successful in the exploration of Mars environment. In order to explore liquid medium on Jupiter's Europa, biomimetic planetary rovers are discussed in the current research.

2:30 p.m. Stockton A. M. * Duca Z. Cato M. Cantrell T. Foreman S. Kim J. Putman P. Schmidt B.
An Organic Analyzer Instrument for Highly Sensitive In Situ Organic Detection on an Ice Shell Impact Penetrator Descent Probe **[#4093]**
This work shows the development of LIF and microfluidic subsystems for planetary impact penetrator missions. With structural optimization, EOA can survive a 50,000 g impact, making it the only current optical instrument with this capability.

2:45 p.m. *Coffee Break*

Tuesday, October 25, 2016
SUB-MM AND RADAR INSTRUMENTS FOR ORBITER AND FLYBY MISSIONS
3:05 p.m. International East

Chair: Manuel Grande

3:05 p.m. Tamppari L. K. * Livesey N. J. Read W. G.
A Submillimeter Sounder for Measuring Martian Winds and Water **[#4048]**
We review the scientific need for global vertically resolved observations of martian atmospheric winds, and show that a submillimeter limb sounder can provide such measurements, along with measurements of water vapor and other trace gases.

3:20 p.m. Huang M. * Gautam N. Sherwin M. S. Kawamura J. Stone K. Focardi P. Chahat N. Gulkis S. Karasik B. S. Pfeiffer L.
A Heterodyne Detector for Terahertz Spectroscopy of Planets and Comets **[#4021]**
We are developing a new class of heterodyne detector called a Tunable Antenna-Coupled Intersubband Terahertz (TACIT) detector. TACIT detector promises nearly quantum-limited noise performance and tunable detection frequency in the THz range.

3:35 p.m. Chattopadhyay G. * Reck T. Jung-Kubiak C. Gonzalez-Ovejero D. Lee C. Alonso-Del Pino M.
A Low-Power Low-Mass Dual-Polarization Sensitive Submillimeter-Wave Radiometer/Spectrometer **[#4016]**
Applying CMOS components and silicon micromachining technology that enable low-mass and highly integrated receivers, we are developing a state-of-the-art submillimeter wavelength radiometer/spectrometer instrument for planetary orbiter missions.

3:50 p.m. Carter L. M. * Rincon R. F. Novak M.
A Reduced Power Digital Electronics System for a Digital Beamforming Space Exploration Synthetic Aperture Radar **[#4068]**
We will discuss design of an orbital P-band (70 cm wavelength) digital beamforming radar system that is modular and can be used for imaging polarimetry of Earth and rocky planets and moons, as well as asteroids and comets.

Tuesday, October 25, 2016
LIFE DETECTION INSTRUMENTATION AND
RELATED TECHNOLOGIES FOR MARS AND OCEAN WORLDS: II
3:05 p.m. International West

Chair: Danny Glavin

3:05 p.m. Mora M. F. * Willis P. A.
Microchip Electrophoresis Instrumentation for Determination of Chemical Distributions on Future Spaceflight Missions **[#4083]**
Here we will describe the status of microchip electrophoresis instruments at JPL and the steps we are taking to someday enable the implementation of this technology on other worlds.

3:20 p.m. Arevalo R. Jr. * Danell R. M. Gundersen C. Hovmand L. Southard A. Tan F. Grubisic A. Brinckerhoff W. B. Getty S. A. Mahaffy P. Cottin H. Briois C. Colin F. Szopa C. Vuitton V. Makarov A. Reinhardt-Szyba M.
Advanced Resolution Organic Molecule Analyzer (AROMA): Simulations, Development and Initial Testing of a Linear Ion Trap-Orbitrap Instrument for Space **[#4072]**
AROMA combines a linear ion trap and Orbitrap mass analyzer to enable: quantitative measurements of organic and inorganic compounds; selective isolation of targeted mass ranges; tandem mass spectrometry; and, ultrahigh mass resolution and accuracy.

3:35 p.m. Dasgupta P. K. * Huang W. Stamos B. N. Zhang M. Noell A. C. Davila A.
An Ion Chromatograph for Extraterrestrial Explorations **[#4012]**
Describes a low power low footprint open tubular capillary liquid/ion chromatograph.

3:50 p.m. Serabyn E. * Liewer K. Wallace J. K. Rider S. Lindensmith C. Nadeau J.
Lensless Digital Holographic Microscopy for Life Detection **[#4027]**
Microscopy capable of volume imaging can be used to search for microbial life on ocean worlds. Here we discuss our recent digital holographic microscope (DHM) systems, which provide micron-scale resolution in a very compact package.

Tuesday, October 25, 2016
POSTER SESSION: I
4:10 – 6:00 p.m. California Ballroom

Fletcher Z. J. Cheng A. F. Barnouin O. S. Chabot N. L. Reed C. L.
DRACO: Didymos Reconnaissance and Asteroid Camera for Op-Nav **[#4043]**
The proposed DART mission is the first demonstration of kinetic impact for deflection of an asteroid. We describe DART's instrument DRACO's (Didymos Reconaissance and Asteroid Camera for Op-nav) requirements, resulting design, and planned operations.

Lucey P. G. Sun X. Li S. X. Numata K. Neumann G. A. Abshire J. B. Smith D. E.
An Infrared Multiwavelength Lidar for Compositional Mapping **[#4069]**
A laser altimeter that measures surface reflectance in up to seven bands in the infrared is being developed. Narrow band infrared lasers and infrared avalanche photodiode arrays have been demonstrated. The instrument can detect ppm levels of water.

Osburn S. M. Turner B. Sevy E. T. Austin D. E.
Reducing Impact Fragmentation with a Novel Inlet on a Closed Source Neutral Mass Spectrometer **[#4020]**
High velocity molecular impacts that occur during upper atmosphere flyby missions cause fragmentation of molecules collected from the atmosphere. We are developing a new design for an inlet that will reduce fragmentation of incoming molecules.

Getty S. A. Li X. Brinckerhoff W. B. Elsila J. E. Grubisic A. Cornish T. Balvin M.
Southard A. Ferrance J.
MACROS: Molecular Analyzer for Complex Refractory Organic-Rich Surfaces **[#4071]**
The novel MACROS instrument package will enable the in situ characterization of the inorganic and organic composition of surface samples by coupling liquid extraction with laser desorption/ionization mass spectrometry.

Southard A. E. Getty S. A. Ferrance J. P. Balvin M. A. Elsila J. E. Stewart D. Stamos B.
Kotecki C. Glavin D. P.
Design of an Integrated LC-MS Prototype for an In Situ Mission to an Icy Body in the Solar System **[#4080]**
The OASIS instrument is being developed to perform in situ liquid chromatography-mass spectrometry on icy bodies in the solar system. A chief goal for OASIS is to detect enantiomeric excess in amino acids, a compelling biosignature.

Schröder C. Klingelhöfer G. Morris R. V. Yen A. S. Renz F. Graff T. G.
The Miniaturized Mössbauer Spectrometer MIMOS II for the Asteroid Redirect Mission (ARM): Quantitative Iron Mineralogy and Oxidation States **[#4057]**
We propose a fully-qualified flight-spare Mössbauer spectrometer for the asteroid redirect mission to identify Fe-bearing mineral phases and Fe oxidation states, and for quantitative distribution of Fe between mineral phasesand oxidation states.

Park R. S. Bills B. G. Jorgensen J. Jun I. Maki J. N. McEwen A. S. Riedel E.
Walch M. Watkins M. M.
Advanced Pointing Imaging Camera (APIC) Concept **[#4018]**
The Advanced Pointing Imaging Camera (APIC) concept is envisioned as an integrated system, with optical bench and flight-proven components, designed for deep-space planetary missions with 2-DOF control capability.

Creamer J. S. Mora M. F. Kehl F. Willis P. A.
Enhanced Resolution of Chiral Amino Acids with Capillary Electrophoresis for Biosignature Detection in Extraterrestrial Samples **[#4061]**
This work describes two capillary electrophoresis methods capable of resolving 17 amino acids that are found in high abundance in both biotic and abiotic samples.

Karras J. Carpenter K. Fuller C. Parcheta C.
PUFFER (Pop-Up Flat Folding Explorer Robots) **[#4125]**
PUFFER (Pop-Up Flat Folding Explorer Robots) are origami-inspired folding robots with extreme terrain mobility. PUFFERs are low-volume, low-mass, and low-cost robots for high-reward extreme terrain science.

Arenberg J. W. Harpole G. Zamel J. Sen B. Lee G. Ross F. Retherford K.
Technology for a Thermo-chemical Ice Penetrator for Icy Moons **[#4131]**
This poster introduces a thermo-chemical ice penetrator for Ocean Worlds. It employs a eutectic mix of alkali metals that produce an exothermic with an icy surface. This technology builds on successful classified 1980's era program for the US Navy.

Deleuze M. D. Bernardi P. B. Caïs Ph. C. Perez R. P. Rees J. M. R. Pares L. P. Dubois B. D. Parot Y. P. Quertier B. Q. Maurice S. M. Maccabe K. M. Wiens R. W. Rull F. R.
SuperCam_MastUnit **[#4009]**
This paper will describe and give a development status of SuperCam's mast unit. SuperCam will be carried on the Mars 2020 rover, and consists in an enhanced version of the ChemCam LIBS which is still performing at the surface of Mars, on Curiosity.

Leask E. K. Ehlmann B. L.
Identifying and Quantifying Mineral Abundance Through VSWIR Microimaging Spectroscopy: A Comparison to XRD and SEM **[#4022]**
VSWIR microimaging reflectance spectroscopy is used to identify minerals, quantify abundances, and assess textural relationships at sub-mm scale without destroying the sample. Results are compared to traditional methods such as XRD and SEM-EDS.

Wong M. H.
From Mars to Jupiter and Beyond: In Situ Atmospheric Studies with Synergistic Instrument Payloads **[#4119]**
Two case studies (Curiosity and the Galileo Probe) show how synergistic instrument payloads can overcome some of the challenges of variability over temporal and spatial dimensions, with implications for Saturn/ice giant probe missions.

Wagstaff K. L. Altinok A. Bue B. Chien S. A. Mandrake L.
Instrument Science Autonomy for Orbital and Flyby Planetary Missions **[#4063]**
Autonomous analysis of data as it is collected enables response to dynamic or short-lived events, environmental monitoring, and increased science return. Missions operating at far distances (e.g., ocean worlds) can benefit greatly.

Parker C. W.
PEP-Hi: Energetic Electron, Ion, and Neutral Particle Instrumentation for the JUICE Mission **[#4110]**
The PEP-Hi instruments JENI and JoEE for the ESA JUICE mission will measure middle to high energy electrons, ions, and neutral particles in the jovian particle environment.

Blanc M. Jones G. Prieto-Ballesteros O. Mimoun D. Masters A. Kempf S. Iess L. Martins Z. Lorenz R. Lasue J. Andre N. Bills B. G. Choblet G. Collins G. Cremonese G. Garnier P. Hand K. Hartogh P. Khurana K. K. Stephan K. Tosi F. Vance S. D. van Hoolst T. Westall F. Wolwerk M. Cooper J. F. Sittler E. C. Brinckerhoff W. Hurford T. Europa Initiative
Europa Habitability and Extant Life Exploration with Combined Flyby-Lander-Orbiter Mission **[#4026]**
The optimal configuration for investigation of habitability and any extant life at Europa would be a combined constellation of flyby, lander, and orbiter spacecraft. The Europa Initiative is designing a small orbiter as part of this constellation.

Hong J. Romaine S. Ramsey B. Nittler L. Grindlay J.
Developing Miniature Wolter-I X-Ray Optics for Planetary Science **[#4040]**
We report the development progress and plan of miniature Wolter-I X-ray optics to make powerful, yet compact lightweight X-ray telescopes affordable for many future planetary missions.

Ravine M. A. Schaffner J. A. Caplinger M. A.
ECAM, a Modular Spaceflight Imaging System — First Flight Deliveries **[#4106]**
MSSS has delivered four ECAM systems to four different customers and for widely varying missions and is under contract for two additional systems. The variety of real-world applications has proven the flexibility of the architecture.

Dyar M. D. Breitenfeld L. B. Bartholomew P. Carey C.
Technique Development Needed to Interpret Raman Spectra of Minerals and Mixtures **[#4085]**
Three areas of Raman research are discussed: integration and review of new and existing Raman databases for minerals, assessment of the relationship between peak intensity and mineral abundance, and development of mineral identification software.

Blacksberg J. Alerstam E. Maruyama Y. Cochrane C. Rossman G. R.
High-Speed Pulsed Raman for Mapping of Minerals and Organics on a Microscopic Scale **[#4017]**
We present a miniaturized high-speed pulsed Raman (HiPuR) spectrometer, a planetary surface instrument for in situ identification and quantification of minerals and organics, with surface mapping capabilities on a microscopic scale.

Greenberger R. N. Ehlmann B. L. Green R. O. Blaney D. L.
Scientific Applications of Imaging Spectrometers for Landed Missions: Examples from Terrestrial Field Deployments **[#4028]**
In situ imaging spectroscopy for geology has been field trialed at outcrop scale and lab trialed at hand sample scale. We present key lessons.

Noell A. C. Fisher A. M. Takano N. Fors-Francis K. Sherrit S. Grunthaner F.
Astrobionibbler: In Situ Microfluidic Subcritical Water Extraction of Amino Acids **[#4059]**
A fluidic-chip based instrument for subcritical water extraction (SCWE) of amino acids and other organics from powder samples has been developed. A variety of soil analog extractions have been performed to better understand SCWE capabilities.

Chanover N. J. Aslam S. DiSanti M. A. Hibbitts C. A. Honniball C. I. Paganini L. Parker A. Skrutskie M. F. Young E. F.
Results from the Science Instrument Definition Team for the Gondola for High Altitude Planetary Science Project **[#4078]**
The GHAPS Science Instrument Definition Team presents its report .

Drouin B. J. Tang A. Schlecht E. Raymond A. W. Chang M.-C. F. Kim Y.
A Millimeter Wave Spectrometer on a Chip for In-Situ Molecular Spectroscopy **[#4005]**
We describe the initial gas measurements of a novel cavity resonator spectrometer utilizing low-mass/low power CMOS electronics.

Steininger H. Goesmann F. Raulin F. Brinckerhoff W. B. Mahaffy P. R. Szopa C.
Mars Organic Molecule Analyzer (MOMA) as an Example for Contamination Control for Life Detection Instrumentation **[#4082]**
The contamination control approach for life detection instrument is presented on the example of the Mars Organic Molecule Analyzer. A combined pyrolysis gas chromatograph mass spectrometer and laser desorption mass spectrometer.

Simcic J. Madzunkov S. M. Bae B. Nikolic D. Darrach M.
A Miniature Gas Chromatograph Mass Spectrometer (GCMS) for Planetary Atmospheres Studies **[#4019]**
Presented herein are the latest achievements in developing an instrument with the same analytical performance of commercial Gas Chromatograph Mass Spectrometer systems but approximately an order of magnitude smaller and optimized for space missions.

Willis P. A. Mora M. F. Creamer J. S. Kehl F.
Maximizing Science Return on Astrobiology and Planetary Missions Using Integrated Liquid-Handling Chemical Analysis Systems — A Status Report **[#4089]**
Our team has been developing all components required for liquid-based analysis on planetary missions. Here we summarize our progress in this area, and highlight enhancements to science return on NASA missions that these technologies could provide.

Wednesday, October 26, 2016
PLENARY III: WINNING AND IMPLEMENTING NEW PLANETARY INSTRUMENTS
8:30 a.m. International Ballroom

Chair: Sabrina Feldman

8:30 a.m. Lee G. *
How to Become a Science Instrument Provider

9:00 a.m. Chmielewski A. B. *
Lessons Learned on NASA and European Cooperation Based on the Rosetta Experience **[#4109]**
Lessons learned from the international Rosetta mission.

9:15 a.m. Dyar M. D. * Breves E. A. Lepore K. H. Boucher T. F. Giguere S.
Lessons Learned from LIBS Calibration Development **[#4075]**
More than two decades of work have been dedicated to development of robust standards, data processing, and calibration tools for LIBS. Here we summarize major considerations for improving accuracy of LIBS chemical analyses.

9:30 a.m. Webster C. R. * Flesch G. J. Forouhar S. Christensen L. E. Briggs R. Keymeulen D. Blacksberg J. Alerstam E. Mahaffy P. R.
Tunable Laser Spectrometers for Planetary Science **[#4013]**
Tunable laser spectrometers enjoy a wide range of applications in scientific research, medicine, industry, Earth and planetary space missions. We will describe instruments for planetary probes, aircraft, balloon, landers and CubeSats.

9:45 a.m. *Coffee Break*

Wednesday, October 26, 2016
PANEL III: LESSONS LEARNED FOR INSTRUMENT DEVELOPMENT FROM TRL 1 TO 9
10:00 a.m. International Ballroom

This panel will discuss experiences, pitfalls, keys to success, and lessons learned in the life cycle of instruments: from initial concept to selection, flight operations, and publications.

Moderator: **Chris Webster**

Panel Members: **Jim Bell**
Jason Feldman
Caroline Freissinet
Sam Gulkis
David Paige
Cheryl Reed
David Smith

10:00 a.m. PANEL DISCUSSION

Wednesday, October 26, 2016
POSTER PREVIEWS: II
11:30 a.m. International Ballroom

The purpose of this mini-session of lightning talks (1 minute each) is to give the Wednesday poster presenters a chance to introduce themselves and their work.

Chairs: **Lindsay Hays**
David Beaty

11:30 a.m. POSTER PREVIEWS

12:00 p.m. *Lunch*

Wednesday, October 26, 2016
NEW TECHNOLOGIES FOR INSTRUMENTS
1:30 p.m. International East

Chair: Glenn Sellar

1:30 p.m. Cochrane C. J. * Blacksberg J.
Self-Calibrating Solid-State SiC Magnetometer for Planetary Field Mapping **[#4039]**
We report on the initial stages of development of a new solid-state SiC magnetometer (SiCMag) intended for planetary field mapping. SiCMag measures magnetic field induced changes in spin dependent recombination current within a SiC pn junction.

1:45 p.m. Korth H. * Strohbehn K. Kitching J.
Miniature Dual-Mode Absolute Scalar Magnetometer Based on the Rubidium Isotope ^{87}Rb **[#4073]**
Miniaturized absolute scalar magnetometer based on the rubidium isotope ^{87}Rb takes advantage of recent breakthroughs in micro-fabricated atomic devices, has a total mass of 210 g and uses <1 W of power, and maintains a sensitivity of 0.1 nT rms.

2:00 p.m. Ogasawara K. * Allegrini F. Desai M. I. Livi S. A.
Novel Solid-State Devices as Timing Detectors for Ion Time-of-Flight Measurements **[#4049]**
This study reports on the performance of Avalanche Photodiode (APD) and Multi-Pixel Photon Counter (MPPC) as timing detectors for ion time-of-flight mass spectroscopy. APDs detect >10 keV ions directly, while MPPCs detect sub-keV secondary electrons.

2:15 p.m. Lucey P. G. * Wright R. Honnibal C. Crites S. T. Cahill J. Greenhagen B. T. Glotch T.
Spatial Interferometers for Remote Sensing and In Situ Analysis **[#4024]**
Spatial interferometers allow low power hyperspectral imaging for remote sensing and in situ analysis. Over 20 years of experience with this technology will be summarized in under 20 minutes.

2:30 p.m. Moore T. Z. * Retherford K. D. Davis M. W. Raut U. Mandt K. E.
Mason J. D. Yakovlev V. V.
High Sensitivity Planetary Composition Measurements Using Integrating Cavity Enhanced Spectroscopy **[#4108]**
The desire to understand planetary atmospheres, terrestrial chemistry, or search for potential biological markers often involves optical spectroscopy. We present a new approach to planetary instrumentation based on a novel integrating cavity.

2:45 p.m. *Coffee Break*

Wednesday, October 26, 2016
GEOPHYSICAL INSTRUMENTS AND TECHNIQUES
1:30 p.m. International West

Chair: Diana Blaney

1:30 p.m. Verdier N. * Lognonné P. Banerdt W. B. De Raucourt S. IJpelaan F. Jerjean L. Pont G. Sylvestre-Baron A. Laudet P. Bousquet P. Hohhman T. Umland J. Bone B. Hurst K. Giardini D. Zweifel P. Bramanti C. Pike W. T. Calcutt S. Mimoun D. Bierwirth M. Christensen U.
SEIS Experiment for the INSIGHT Mission: Towards 2018 Launch **[#4046]**
After giving an outline of the InSight mission, with a focus on SEIS activities on Mars, we will describe the SEIS instrument and its performances, and provide a status of its development at the time of the workshop.

1:45 p.m. Palomba E. * Dirri F. Longobardo A. Galiano A. Biondi D. Boccaccini A. Zampetti E. Saggin B. Scaccabarozzi D.
VISTA: A Miniaturized Thermogravimeter to Detect Planetary Dust and Volatiles **[#4010]**
The work here presented is focused on VISTA instrument: a μ-thermogravimeter device, which has been studied and proposed for different planetary in-situ missions. The main scientific goals of VISTA and laboratory tests are described.

2:00 p.m. Stillman D. E. * Oden C. Grimm R. E. Pyke B.
Broadband Ground Penetrating Radar with Conformal Antennas for Subsurface Image from a Rover **[#4011]**
Thin conformal broadband antennas allow a GPR instrument (200–1000 MHz) to be mounted to the underside of a rover. Providing 10's of meters of subsurface imaging through regolith and rock.

2:15 p.m. Cutts J. * Pauken M. Jackson J. Mimoun D. Bowman D.
Venus Exploration with Infrasound Techniques **[#4107]**
We are developing a technique for detecting seismic events and other naturally occurring phenomena on Venus using infrasound from a balloon platform that floats in the upper atmosphere.

2:30 p.m. Pauken M. * Smith K. Sujittosakul S. Li B. Firdosy S. Smrekar S. Morgan P.
Venus Heat Flow Instrument Development **[#4101]**
A heat flux measurement instrument is being developed to determine the heat flow through the Venus surface. Heat flow measurement provides data for distinguishing between various hypotheses of planetary evolution.

2:45 p.m. *Coffee Break*

Wednesday, October 26, 2016
ELEMENTAL SPECTROSCOPY FOR FUTURE MISSIONS
3:05 p.m. International East

Chair: James Ashley

3:05 p.m. Parsons A. M. * Grau J. Lawrence D. J. Miles J. Peplowski P. N. Perkins L. Schweitzer J. S. Starr R. D.
Measuring Venus' Bulk Elemental Composition with BECA **[#4060]**
The Bulk Elemental Composition Analyzer (BECA) instrument uses high energy neutrons and gamma rays to measure the bulk elemental composition of Venus beneath a landed probe. We will present the results of a BECA prototype tested at NASA/GSFC.

3:20 p.m. Hardgrove C. * Prettyman T. Johnson E. Parsons A. Barnaby H. Christian J. Gupta K.
SINGR: A Single Scintillator Neutron and Gamma-Ray Spectrometer for Acquiring Rapid, Remote Geochemical Data on Future Planetary Science Missions **[#4113]**
SINGR is a single scintillator detector coupled with a pulsed neutron generator that is currently being prototyped, modeled, developed and tested in order to acquire rapid geochemical data, hydrogen abundance and depth profiles on planetary missions.

3:35 p.m. Blake D. F. * Sarrazin P. Bristow T. Downs R. Gailhanou M. Marchis F. Ming D. Morris R. Solé V. A. Thompson K. Walter P. Wilson M. Yen A. Webb S.
The Mapping X-Ray Fluorescence Spectrometer (MapX) **[#4006]**
MapX is a full-frame X-ray imager that collects 2.5 × 2.5 cm elemental maps with ≤100 µm spatial resolution. Quantitative XRF spectra from ground- or instrument-selected Regions of Interest (ROI) can be used to identify rock types and mineralogies.

3:50 p.m. Kameda S. * Horiuchi M. Cho Y. Ishibashi K. Wada K. Mikouchi T. Nakamura T. Sugita S.
LIBS for Martian Moons eXploration (MMX) **[#4036]**
JAXA's Martian Moons Exploration (MMX) is planned to be a sample return mission from Phobos, one of the satellites of Mars. We propose adding a laser-induced breakdown spectrometer (LIBS), which enables to determine the origin of the moons.

Wednesday, October 26, 2016
SMALLSAT AND CUBESAT INSTRUMENTS
3:05 p.m. International West

Chair: Barbara Cohen

3:05 p.m. Hosseini S. *
High Spectral Resolution Spectrometry in Compact Sizes in Future Interplanetary Missions Using Spatial Heterodyne Spectrometer **[#4116]**
Spatial Heterodyne Spectrometers (SHS) is a compact reflective two-beam cyclical interferometer that can obtain high spectral resolution spectra (R~100000) at wide FOV (~0.5 degree) using no or small aperture telescopes in very compact sizes.

3:20 p.m. Clark P. E. * Malphrus B. Reuter D. MacDowall R. Hurford T. Brambora C. Folta D. Farrell W.
BIRCHES: Compact Broadband IR Spectrometer and the Search for Lunar Volatiles **[#4007]**
BIRCHES (Broadband InfraRed Compact, High-resolution Exploration Spectrometer) is the payload instrument on Lunar Ice Cube, a science requirements-driven lunar orbiting CubeSat designed to determine volatile distribution as a function of time of day.

3:35 p.m. Atchison J. * Mitch R. Apland C. Kee L.
Small Body In-Situ Multi-Probe Mass Estimation Experiment (SIMMEE) **[#4058]**
A concept and instrument for improving our ability to resolve the mass of asteroids and comets during flybys or orbital phases. A host spacecraft ejects a set of small spheres and optically tracks them pre-and-post flyby to estimate asteroid mass.

3:50 p.m. Riris H. * Abshire J. B. Mumma M. Villanueva G. Hanisco T.
Laser Limb Sounding Approach for Planetary Atmospheres Using CubeSats or SmallSats **[#4035]**
We describe an efficient and sensitive way to map trace gas abundances in planetary atmospheres using small satellites flying in formation and tunable single frequency diode lasers and a sensitive optical detector.

Wednesday, October 26, 2016
POSTER SESSION: II
4:10 –6:00 p.m. California Ballroom

Fillingim M. O. Wishnow E. H. Miller T. Edelstein J. Lillis R. J. Korpela E. England S. Shourt W. V. Siegmund O. McPhate J. Courtade S. Curtis D. W. Deighan J. Chaffin M. Harmoul A. S. Almatroushi H. R.
Wide-Field Ultraviolet Spectrometer for Planetary Exospheres and Thermospheres **[#4008]**
We will present the design for a wide field ultraviolet imaging spectrometer for remote sensing of planetary atmospheres. The imaging spectrometer achieves an extremely large instantaneous 110 degree field of view with no moving scanning mirror.

Kerber L. Nesnas I. A.
The Axel Rover: A Novel Platform for Instruments Making Measurements in Extreme Terrains **[#4122]**
Axel Rover is an extreme terrain rover that can carry a sizeable payload of capable instruments to difficult-to-reach locations in a variety of planetary environments.

Kenyon M. Mariani G. Johnson B. Brageot E. Hayne P.
Next-Generation Thermal Infrared Multi-Body Radiometer Experiment (TIMBRE) **[#4094]**
We have developed an instrument concept called TIMBRE which belongs to the important class of instruments called thermal imaging radiometers (TIRs). TIMBRE is the next-generation TIR with unparalleled performance compared to the state-of-the-art.

Ishimaru R. Sakamoto Y. Kobayashi M. Fujita S. Gonai T. Matsui T.
UV-Visible Observation of Meteors by CubeSat: S-CUBE Project **[#4030]**
We have launched a CubeSat project to observe meteors from space. A space-based observation enables a continuous global observation of meteors. Furthermore, it can access ultra-violet light from meteors which remain largely unknown.

Prettyman T. H. Yamashita N. Burger A. Rowe E. Butler J. Groza M. Stassun K. Lambert J. L. Castillo-Rogez J. C. Raymond C. A. Feldman S. M. Beck P. R. Cherepy N. J. Payne S. A.
Planetary Gamma Ray Spectroscopy with Strontium Iodide **[#4105]**
Strontium iodide, a new scintillator for gamma ray spectroscopy, offers improved performance for orbital and in situ measurements of planetary elemental composition.

Ho G. C. Andrews G. B.
Plasma Composition Instrument for Planetary and Cometary Missions **[#4084]**
We present a new plasma composition instrument design that would extend the energy range of the current plasma instrument and provide higher time cadence and mass measurement that are required for planetary and/or cometry flyover missions.

Kidd R. D. Bae B. Willis P. A. Noell A. C. Scianmarello N. Tai Y.-C.
MEMS Liquid and Gas Chromatography for Miniaturized Planetary In Situ Instruments **[#4062]**
Micro-Electro-Mechanical Systems (MEMS) technology to reduce the size, mass and power of the three classical chromatographic technologies: gas chromatography (GC), capillary electrophoresis (CE) and high performance liquid chromatography (HPLC).

Uckert K. Getty S. Grubisic A. Li X. Yu A. W. Fahey M. E. Brinckerhoff W. B. Li S. X. Cornish T. Farcy B. Elsila J. E.
Organic Detection in Ocean World Analogs with a Two-Step Laser Desorption/Ionization Time-of-Flight Mass Spectrometer **[#4098]**
We explore the analytical advantages offered by a prototype two-step laser desorption/ionization time-of-flight mass spectrometer, and demonstrate the detection of hydrocarbons in organically-doped cryogenic ocean world-relevant ices and mixtures.

Honniball C. I. Wright R. Lucey P. G.
The MIDAS Instrument Design and Characterization **[#4055]**
The Miniaturized Infrared detector of Atmospheric Species (MIDAS) utilizes an uncooled microbolometer coupled with a Sagnac interferometer. MIDAS will be used to detect and quantify atmospheric constituents for a variety of science applications.

Nikolic D. Darrach M.
LADEEView: Elemental Composition Analysis of Lunar Surface **[#4014]**
LadeeView is a comprehensive lunar data analyzer with modular architecture. Mass spectrometry module is designed to map elemental abundances along the LADEE spacecraft trajectories. These maps are useful input for future models of lunar exosphere.

John K. K. Abell P. Brisset J. Britt D. Colwell J. Durda D. Dove A. Fries M. Graham L. Hartzell C. Leonard M. Love S. Sanchez D. P. Scheeres D. J.
Strata-1: A Planetary Science Experiment on the Behavior of Asteroid Regolith in Microgravity **[#4092]**
Strata-1 is an experiment studying asteroid regolith in the microgravity environment of ISS. The prolonged microgravity and vibrational conditions of ISS are analogous to those on small Solar System bodies.

Patel A. Shanmugam M. Ladiya T.
Signal Processing Techniques for Silicon Drift Detector Based X-Ray Spectrometer for Planatary Instruments **[#4033]**
We are developing SDD based x-ray spectrometer using various pulse height analysis techniques. This study will help to identify the proper processing technique based on instrument specifications which can be used for future scientific missions.

Kobayashi M. Okudaira O. Kurosawa K. Okamoto T. Matsui T.
Dust Sensor with Large Detection Area Using Polyimide Film and Piezoelectric Elements **[#4047]**
We describe the development of dust particles sensor in space with large area (1m × 1m scale). The sensor has just a thin film of polyimide attached with small tips of piezoelectric elements. We performed experiments to characterize the sensor.

Lightholder J. Thompson D. R. Huffman W. Boland J. Chien S. Castillo-Rogez J.
Onboard Science Techniques to Optimize Science Data Retrieval from Small Spacecraft **[#4096]**
Software strategies for new onboard science techniques which optimize science return under the constrains of interplanetary small spacecraft. These include size, power, attitude control and communications bandwidth.

Adams E. Y. Murchie S. L. Hohlfeld E. M. Peplowski P. N.
Planetary Object Geophysical Observer (POGO): A New Approach to Small Body Landed Science **[#4053]**
The Planetary Object Geophysical Observer, or POGO, is a geochemical landed package designed for ballistic deployment to its target body, to survive landing at 5 m/s, and to achieve its core objectives from any landed orientation.

Sittler E. C. Jr. Cooper J. F. Paschalidis N. Jones S. L. Brinckerhoff W. L. Paterson W. R. Ali A. Coplan M. A. Chornay D. Sturner S. J. Benna M. Bateman F. B. Fontaine D. Verdeil C. Andre N. Blanc M. Wurz P.
Advanced Ion Mass spectrometer for Giant Planet Ionospheres, Magnetospheres and Moons **[#4088]**
Advanced Ion Mass Spectrometer is being developed to measure both major and minor ion species from 1 V to 25 kV with wide field-of-view in the 1–60 amu mass range at $M/\Delta M \leq 60$ over a wide range of ion intensities within high radiation environments.

Knapp M. Robey F. C. Lind F. D. Hecht M.
Flexible low-band Instrument for RF Measurement and Imaging (FIRMI) **[#4129]**
We propose to apply vector antenna technology, antennas that measures full electric and magnetic field vectors, to RF source characterization, ionospheric sounding, and to surface penetrating radar in the 250 kHz – 30 MHz range.

Wu K. Doran G. B. Thompson D. R. Allwood A. C. Flannery D. T. Sharrow R. F.
Pedersen D. A. K. Liebe C. C.
Performance of Image Registration-Based Instrument Placement for PIXL **[#4081]**
We analyze performance of an algorithm for precise closed-loop instrument placement that uses context camera images to recognize landmark features on a rock surface.

Kedar S. Pike W. T. Standley I M. Calcutt S. B. Bowles N. Blaes B. Irom F. Mojarradi M. Vance S. D. Bills B. G.
The Europa Seismic Package (ESP): 2. Meeting the Environmental Challenge **[#4134]**
We outline a pathway for adapting the SP microseismometer delivered to InSight to provide a Europa Seismic Package that overcomes the three significant challenges in the environmental conditions, specifically gravity, temperature and radiation.

Griggs C. E. Paik H. J. Moody M. V. Rowlands D. D. Lemoine F. G. Li X. Han S.-C.
Superconducting Gravity Gradiometer for Planetary Missions **[#4041]**
A new and innovative design for a compact tensor gravity gradiometer gives a potential sensitivity better than .1 mE $Hz^{-1/2}$ in the measurement band of 1 mHz to 0.1 Hz for a device with a baseline just over 10 cm.

Bar-Cohen Y. Zacny K. Badescu M. Lee H. J. Sherrit S. Bao X. Paulsen G. L. Beegle L.
The Auto-Gopher — A Wireline Rotary-Percussive Sampler for Deep Subsurface Planetary Exploration **[#4001]**
To enable the required capability for subsurface sampling in such bodies as Europa a wireline deep rotary-percussive corer, called Auto-Gopher, was developed and will be described.

Hernandez Schwartz Asphaug Thangavelautham
Micro-Penetrometer Instrument for Small Bodies **[#4135]**
We present a micro-penetrometer instrument for determining hardness, granularity, porosity and composition of asteroid surfaces for use on SmallSat and CubeSat missions. The presentation includes mission concepts and laboratory experiments.

Lerman H. N. Hutchinson I. B. Bannister N. P. McHugh M. Ingley R. Lester M. Wright D. Milan S. Brunskill C. Garton D.
The Development of a Highly Integrated Imaging Payload for Space Weather and Maritime Monitoring **[#4064]**
The results of testing a UV enhanced CCD for a CubeSat-compatible, multi-purpose imaging payload, targeted at space weather monitoring and maritime domain awareness.

Francis R. Estlin T. A. Wagstaff K. Doran G. Mandrake L.
Instrument Autonomy Techniques Enhance Science Return and Efficiency of Surface Missions **[#4121]**
Onboard autonomy at the instrument level can speed mission progress and enable new investigations. We describe the range of roles autonomy can play in surface missions, and survey existing and flight-proven techniques available for new instruments.

Seo M. G. Cho M. H. Tahk M. J.
Common Region Detection Algorithm for Adjacent Lunar Surface Images Using Crater Matching **[#4029]**
The algorithm to figure out the common area of two partially overlapping lunar surface images is proposed in this paper. The performance of this algorithm is demonstrated by the image merging test.

Sellamuthu H. Sharma R. K.
On-Board Orbit Propagator Using Kustaanheimo-Stiefel Elements for Mars Micro Orbiters **[#4004]**
An analytical orbit propagator for small spacecraft missions about Mars is developed using Kustaanheimo-Stiefel regularization method. The perturbation models include the solar gravity and the second zonal harmonic of Mars.

Dell'Agnello S. SCF_Lab Team Currie D. Richards R. Chandler J.
Next-Generation Laser Retroreflectors for the Science and Exploration of the Moon, Mars and Beyond **[#4074]**
We describe next-generation laser retroreflectors for solar system science/exploration, developed at INFN-LNF, Frascati, Italy in collaboration with ASI and NASA-SSERVI, for lunar missions, ExoMars, Mars2020, Phobos, Jupiter icy/rocky moons, asteroids.

Thursday, October 27, 2016
PLENARY IV: EMERGING INSTRUMENT CAPABILITIES AND CHALLENGES FOR PLANETARY EXPLORATION
8:30 a.m. International Ballroom

Chair: Morgan Cable

8:30 a.m. Souders A. K. * Sylvester P. J.
Summary of 2016 GSA Annual Meeting Session T39: 'Go Small or Go Home: Microbeam Techniques Applied to Igneous, Metamorphic, and Sedimentary Petrology of Earth and Planetary Materials' **[#4120]**
Report on 2016 GSA Annual Meeting topical session 'Go Small or Go Home: Microbeam Techniques Applied to Igneous, Metamorphic, and Sedimentary Petrology of Earth and Planetary Materials'.

8:45 a.m. Allen C. C. * Beaty D. W.
Potential Mars Sample Return: The Next Really Big Challenge in Planetary Instrumentation **[#4099]**
We look ahead to the possible return to Earth of samples collected by the Mars 2020 mission, and address the measurements and types of instruments that could provide initial characterization and sample preparation required for planetary protection.

9:00 a.m. Meyer M. A. * Rummel J. D.
Planetary Protection Technology Definition Team: Tasks, Status, and Feedback **[#4090]**
A Planetary Protection and Technology Definition Team will assess challenges to meeting planetary protection requirements to instruments and will suggest technological solutions. Status and initial findings will be reported.

9:15 a.m. Brinckerhoff W. * Grubisic A. Danell R. van Amerom F. Pinnick V. Li X. Arevalo R. Getty S. Trainer M. Mahaffy P. Chu P. Zacny K. Rogacki S.
The Past, Present and Future for the Linear Ion Trap Mass Spectrometer (LITMS) and Related Ion Trap Instrumentation **[#4112]**
Summary of the current status, results and plans for the Linear Ion Trap Mass Spectrometer instrument development project including its contrast to past instrumentation and the outlook for the future.

9:30 a.m. Willis P. *
Overview and Prospects for Microscale Liquid Chemical Analysis on Planetary Missions

9:45 a.m. John K. K. * Botkin D. J. Burton A. S. Castro-Wallace S. L. Chaput J. D. Dworkin J. P. Lupisella M. L. Mason C. E. Rubins K. H. Smith D. J. Stahl S. Switzer C.
Biomolecule Sequencer: Nanopore Sequencing Technology for In-Situ Environmental Monitoring and Astrobiology **[#4103]**
Biomolecule Sequencer will demonstrate, for the first time, that DNA sequencing is feasible as a tool for in-situ environmental monitoring and astrobiology. A space-based sequencer could identify microbes, diseases, and help detect DNA-based life.

10:00 a.m. Castillo-Rogez J. C. Feldman S. * Baker J. D. Vane G.
State of Small Instruments for Nano-Spacecraft Applications **[#4123]**
This presentation reviews the current state of the art in small instruments as well as emerging capabilities.

10:15 a.m. Ravine M. A. * Caplinger M. A. Hansen C. J. Ingersoll A. P. Bolton S. J.
JunoCam: Approach and Orbit 1 Imaging **[#4104]**
Juno went into orbit around Jupiter on 4 July 2016. Junocam took images of Jupiter and its satellites in the weeks before Jupiter Orbit Insertion (JOI) and the weeks after. Much higher resolution data will be acquired in late August 2016.

10:30 a.m. *Coffee Break*

Thursday, October 27, 2016
CONCLUDING DISCUSSION
10:50 a.m. International Ballroom

Chairs: **David Beaty**
Sabrina Feldman

10:50 a.m. Kerber L. *
Report on the IWIPM Planetary Instrument Database

11:05 a.m. GENERAL DISCUSSION

Notes

Notes

MARLI: MARs LIdar for global wind profiles and aerosol profiles from orbit

J. B. Abshire[1], S.D. Guzewich[1,2], M.D. Smith[1], H. Riris[1], X. Sun[1], B.M. Gentry[1], A. Yu[1], and G. R. Allan[3]

[1]NASA Goddard Space Flight Center, Greenbelt MD USA (james.b.abshire@nasa.gov), [2]CRESST/Universities Space Research Association, Columbia MD, USA [3]Sigma Space Corporation, Greenbelt, MD USA.

Introduction: The Mars Exploration Analysis Group's Next Orbiter Science Analysis Group (NEXSAG) has recently identified atmospheric wind measurements as one of 5 top compelling science objectives for a future Mars orbiter [1]. To date, only isolated lander observations of martian winds exist.

Winds are the key variable to understand atmospheric transport and answer fundamental questions about the three primary cycles of the martian climate: CO_2, H_2O, and dust. However, the direct lack of observations and imprecise and indirect inferences from temperature observations leave many basic questions about the atmospheric circulation unanswered. In addition to addressing high priority science questions, direct wind observations from orbit would help validate 3D general circulation models (GCMs) while also providing key input to atmospheric reanalyses.

The dust and CO_2 cycles on Mars are partially coupled and their influences on the atmospheric circulation modify the global wind field. Dust absorbs solar infrared radiation and its variable spatial distribution forces changes in the atmospheric temperature and wind fields. Thus it is important to simultaneously measure the height-resolved wind and dust profiles. MARLI provides a unique capability to observe these variables continuously, day and night, from orbit.

Lidar Measurement Approach: The MARLI lidar [2-3] is being designed to observe the atmosphere from a nominally circular polar orbit around Mars. The lidar measurement concept is shown in Figure 1. The instrument would be pointed ~30° off-nadir in a cross-track viewing direction. The lidar will continuously measure dust aerosol backscatter profiles, cross polarized backscatter profiles (for water ice aerosols), the component of the Doppler shift from wind profiles along the instrument's line-of-sight, and the range to the planet's surface. The MARLI approach uses a pulsed single-frequency Nd:YAG laser, makes measurements at 1064 nm and its measurement types are shown in Figure 2. The MARLI definition work is being supported by the NASA Picasso Program.

LIDAR Description: The laser backscatter from the Mars atmosphere is weak and is distributed in range and thus a highly sensitive lidar approach is necessary. The present MARLI approach measures the height resolved atmospheric characteristics along a single line-of-sight. The lidar uses an efficient pulsed ND:YAG laser with flight heritage, a low-mass receiver telescope and photon-sensitive detectors.

The baseline design of MARLI, shown in Figure 3, utilizes a pulsed single-frequency diode-pumped Nd:YAG laser. Its output pulses are wavelength stabilized near 1064 nm. The laser emits ~50 nsec wide pulses at a 1 kHz pulse rate. Nominally, the receiver uses a ~70 cm diameter telescope and splits the returned signal into 3 paths. One path is a cross-polarized channel to allow dust/ice discrimination. The other two paths are used to illuminate an etalon then are refocused onto detectors This part of the receiver is configured as a double-edge Doppler (optical frequency-shift) discriminator. It is also feasible to measure vector-resolved wind profiles using a dual-telescope-receiver that shares the energy from a single laser.

Our approach leverages new lidar components developed for NASA, including a single frequency laser from Fibertek and photon-sensitive HgCdTe detectors from DRS Technologies. Our targeted instsrument size is a ~80 cm cube, comparable to a medium-sized instrument such as the Mars Orbiter Laser Altimeter (MOLA). Nominal payload parameters are <40 kg, < 90W, and ~50 Kbits/sec. This approach leverages our work on measuring terrestrial winds and lidar technology supported by the NASA ESTO IIP program.

Performance Estimates: Using measurement models developed as part of this project, we have calculated the expected performance of MARLI. The performance estimates are contigent on vertical bin depth and averaging time. The instrument will report measurements at a rate of ≥ 10 Hz. Assuming 2 km vertical bins and 40 second along-track averaging (~2° latt.), the performance estimates are shown in Table 1.

References:

[1] MEPAG: Chaired by B. Campbell and R. Zurek (2015), *Report from the Next Orbiter Science Analysis Group,* http://mepag.nasa.gov/reports.cfm

[2] J.B. Abshire et al., MARLI, 2015 European Planetary Science Congress (EPSC), http://meetingorganizer.copernicus.org/EPSC2015/EPSC2015-258.pdf

[3] S. D. Guzewich et al., MARLI, 2016 Lunar and Planetary Science Confernece (LPSC), http://www.hou.usra.edu/meetings/lpsc2016/pdf/1497.pdf

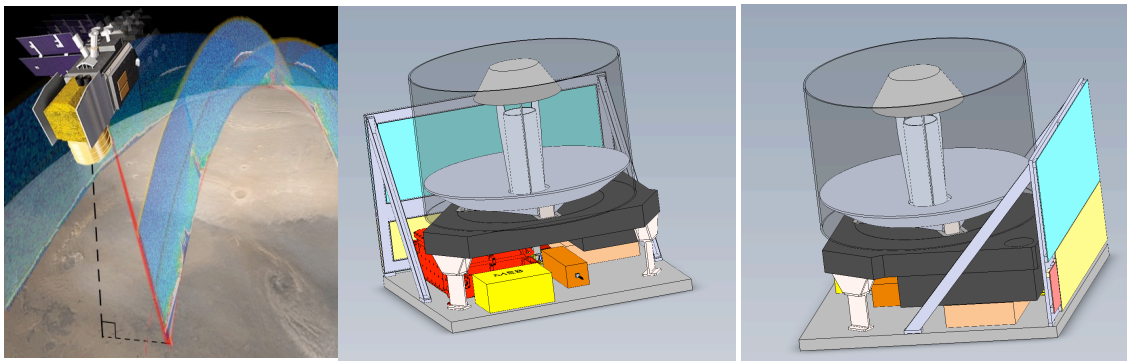

Figure 1. *(Left)* Mars lidar measurement approach, which continuously measures the aerosol backscatter profiles, the cross polarized (ice) backscatter profiles, the Doppler (wind profiles), and the range to the scattering surface from orbit.*)* Nominally the lidar is pointed cross-track at ~ 30 deg off nadir, to measure the Doppler shift of the wind in the cross-track direction. This sketch is for the single beam (cross track direction) approach. *(Middle and Right)* Drawings of the single beam (scalar measurement) version of MARLI from a recent instrument engineering study at NASA Goddard. In this concept the receiver telescope diameter is 80 cm, the laser box is in red, and the radiator panel is in blue and yellow.

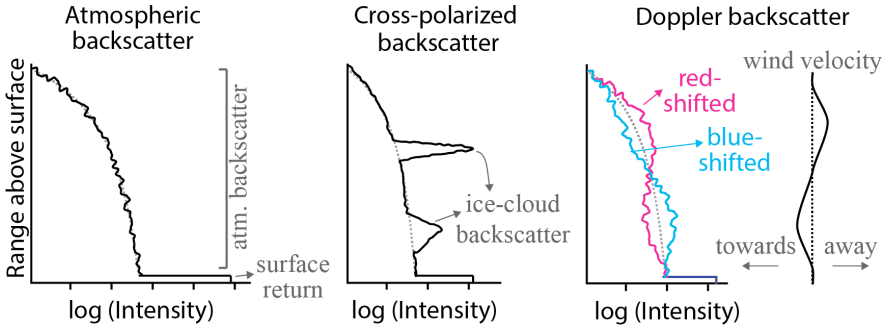

Figure 2. llustrations of the MARLI measurements. *(Left)* Range (height) resolved aerosol backscatter profiles.. *(Middle)* Profiles of cross-polarized backscatter, caused by clouds with ice-crystals. *(Right)* Height resolved Doppler (wind) backscatter profiles as seen by the two detectors after passing through the two etalons comprising the double-edge filter. The horizontal wind profile *(Far Right)* is computed from the ratio (difference/sum) from the detectors after the double-edge filter.

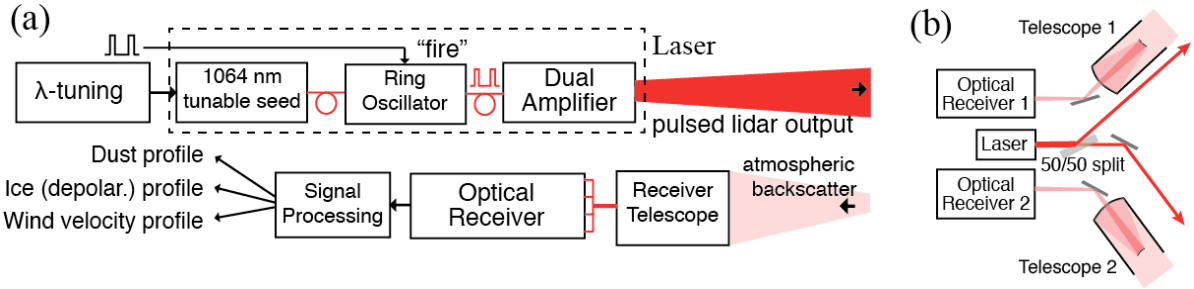

Figure 3 – *(Left -a)* Simplified block diagram of MARLI lidar for single beam (scalar) instrument configuration. *(Right –b)* Approach using a single laser and two identical receivers allow a vector measurement configuration.

Table -1 Summary of MARLI performance for Mars for the single beam configuration

Parameter	*Surface*	*5 km*	*10 km*	*20 km*	*30 km*
Backscatter SNR	400	350	300	170	80
Wind horiz. velocity (m/sec)	0.5	0.7	0.9	1.5	2.5
Range to surface (m)	<1	<1	<1	<1	<1

PLANETARY OBJECT GEOPHYSICAL OBSERVER (POGO): A NEW APPROACH TO SMALL BODY LANDED SCIENCE. E.Y. Adams[1], S.L. Murchie[1], E.M. Hohlfeld[1], and P.N. Peplowski[1]. [1]Johns Hopkins University Applied Physics Laboratory, 11101 Johns Hopkins Road, MS 200-E530, Laurel, MD 20723; elena.adams@jhuapl.edu.

Introduction: The exploration of small bodies, including asteroids, comets, and small planetary satellites, has progressed beyond the stages of purely flyby and orbital studies (e.g., by *Galileo*, *Deep Space 1*, *Cassini*, *NEAR*) to include acquisition of contact science measurements and of samples for return to Earth. Detailed measurements of elemental and mineralogic abundances, isotopic abundances, and the abundances and forms of carbon and volatiles are required to address fundamental questions about the origins and geologic evolutions of small bodies [e.g., 1,2,3]. Thus, collecting a comprehensive set of composional measurements is a high priority for future exploration of small bodies. *Rosetta* included several types of *in situ* compositional measurement, whereas *Stardust*, *Hayabusa*, *Hayabusa 2*, and *OSIRIS-REx* each have the objective of returning some amount of sample to Earth.

A landed package provides a means of obtaining a comprehensive suite of compositional measurements for a mission where cost or mission design precludes return of sample to Earth. A first-order technical challenge is deployment and stability of this package on a body with mill-g or smaller graviational acceleration. We address this technical challenge with a lander concept that fits within the cost envelope of NASA *Discovery* or *New Frontiers* missions, the Planetary Object Geophysical Observer, or POGO (Fig. 1). This development was begun under IR&D funding at APL, and was selected for a 2-year development under NASA's Homesteader program. POGO is targeted for maturation to TRL 6 by Sep. 2017.

POGO Overview: POGO is designed for ballistic emplacement on a target body from 3 km or more in altitude, to survive landing at 5 m/s terminal velocity, and to achieve its core objectives from any landed orientation. No tethering system is required to hold POGO to its target body. The package is tablet-shaped with rounded edges, designed to come to rest on either of two flat faces after bouncing to rest (Fig. 1).

The science instrumentation is chosen to provide a comprehensive investigation of abundances of 20 key major and minor elements that are diagnostic of the origin, provenance, and evolution of primitive, carbonaceous compositions, using a gamma-ray spectrometer (GRS) and an alpha particle X-ray spectrometer (APXS). The GRS uses a low-mass scintillator design developed and matured to TRL 6 under APL IR&D funding [4]. Deploying GRS to the surface, for several days of operation, yields several times larger signal than the threshold for meaningful compositional measurements from orbital altitude (≥10 days inside 1 body radius altitude from the surface [5]). APXS uses the design of the *Rosetta* APXS [6] except with an alternate door mechanism that is operated electrically. Its stimulation of X-ray emissions by a ^{244}Cm source avoids the dependence on solar flares for measurements of many elements by passive X-ray spectroscopy, and enables X-ray spectroscopy to be employed beyond the asteroid belt using only hours-long measurement baselines. GRS is omnidirectional and a single sensor is located inside the lander. One APXS is included on each of the two flat faces of POGO.

POGO's structure is build around a Ti cage that withstands landing shock. The cage houses avionics boards, and encloses upward- and downward-pointed APXS sensors and a voice coil that provides mobility. Power comes from primary batteries outside the cage that support 5 days of landed operation. Communication with the carrier spacecraft is by a UHF antenna.

Concept of Operations: The carrier spacecraft deploys POGO at altitude, and POGO free falls to the asteroid surface. Bouncing is expected, and after several bounces POGO comes to rest on a flat face. A preprogrammed measurement sequence is initiated once motion stops. GRS data collection is initiated, and a 24-hr APXS integration is begun. As data are collected and stored, they are transmitted on a repeating loop to the carrier spacecraft which remains in orbit. After 24 hrs of operation the voice coil is energized, the reaction causes POGO to "hop" a distance of meters or more depending on the target body's gravity and regolith properties, and the measurement sequence is repeated. Hops are initiated every 24 hrs to ascertain composition heterogeneity of the target body.

Tolerance of Landed Orientations: The tolerance of POGO to operation on a realistic asteroidal surface was evaluated using the techniques of Ernst et al. [7]. In a Monte Carlo simulation, an asteroidal surface was simulated by extrapolating Eros' block size-frequency distribution to smaller sizes, using hemispherical caps as proxies for boulders. Starting with POGO in an random orientation, a model of the spacecraft is lowered onto the surface in a random location until it comes to rest on 3 points (Fig. 3). Over 100,000 simulated landings, 99% have the downward-pointed APXS coming to rest with its aperture within the required 10-cm line-of-sight distance to rock or soil for high signal-to-noise ratio measurements.

Technology Development Strategy: POGO has been funded through the NASA New Frontiers Homesteader grant to perform various risk reduction tasks. We are performing relevant environment testing of a fully integrated system, and updates to the mobility mechanism, radio frequency communications (RF) subsystem, and structural design to increase hop distances and communications range to the carrier spacecraft and reduce landing loads on the structure. The new RF design was completed, with the antenna moving from the rim to the top and bottom plates of POGO to ensure communication through dust and better attachment to POGO. The structural analysis has been completed, and the mechanical design was updated to reflect higher loads during landing. The top and bottom plate material is in the process of being selected, with Nomex, aluminum honeycomb, and foam being strong candidates. We perfomed drop tests to 6 m/s that are informing the selection. We are setting up life tests for a variety of battery chemistries, and preparing for Zero-G weightless flight testing in November 2016.

References: [1] Glassmeier, K., et al. (2007) Space Sci. Rev., 128, 1. doi:10.1007/s11214-006-9140-8. [2] Nakamura, T. (2011) Science, 333, 1113-1116. doi:10.1126/science.1207758. [3] Murchie, S. (2014) Acta Astronautica, 93, 475-482, doi:10.1016/j.actaastro.2012.10.014. [4] Peplowski, P.N. et al. (2014) Second International Workshop on Instrumentation for Planetary Missions, abstract #1061. [5] Peplowski, P.N. (2016) The global composition of 433 Eros: First results from the NEAR Gamma-Ray Spectrometer orbital dataset, Planet. Space. Sci., in review. [6] Klingelhöfer, G., et al. (2007) Space Sci Rev, 128, 383-396. doi:10.1007/s11214-006-9137-3. [7] Ernst, C. et al. (2015) Lunar Planet. Sci. 46, abstract #2095.

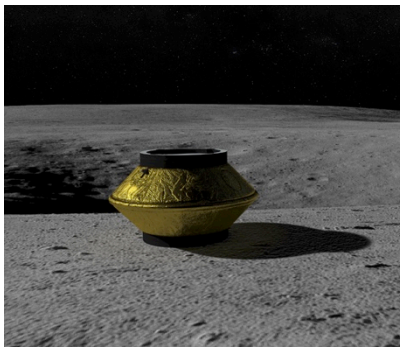

Figure 1. Artist's conception of POGO at rest on the surface of a target asteroidal body.

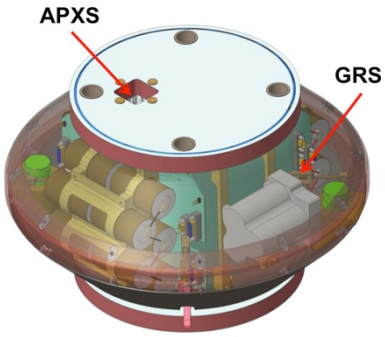

Figure 2. CAD rendering of POGO design with the outer shell and thermal blanket transparent, showing the locations of the GRS and APXS.

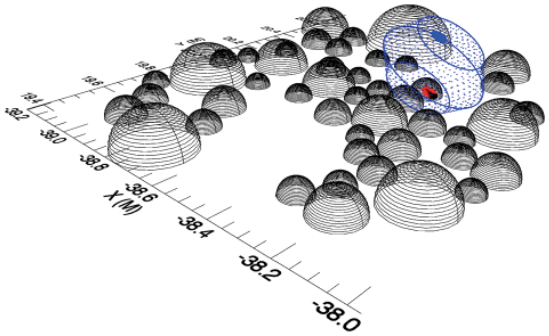

Figure 3. CAD rendering of POGO (in blue) at rest in a block field on its target body, showing the location of the APXS aperture (in red).

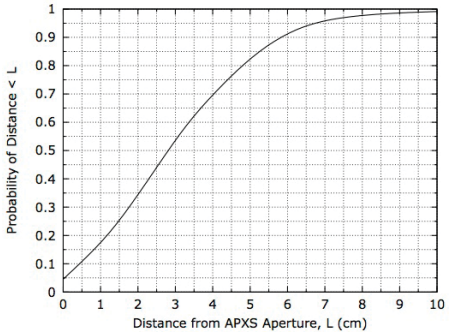

Figure 4. Cumulative probability of the APXS aperture being within a given working distance, over 100,000 trials of a Monte Carlo simulation.

POTENTIAL MARS SAMPLE RETURN: THE NEXT REALLY BIG CHALLENGE IN PLANETARY INSTRUMENTATION.

Carlton C. Allen[1] and David W. Beaty[2], [1]NASA Johnson Space Center (Emeritus), Houston, TX 77058 carlton.c.allen@nasa.gov, [2]JPL/Caltech, Pasadena, CA 91109 david.w.beaty@nasa.gov.

Introduction: This presentation looks ahead to the possible return to Earth of samples collected by the Mars 2020 mission. We specifically address the measurements and types of instruments that could provide the initial characterization and sample preparation required for planetary protection.

The Mission: The Mars 2020 rover mission has four science objectives that support the goals of NASA's Mars Exploration Program:

Looking for Habitability:	Identify past environments capable of supporting microbial life
Seeking Biosignatures:	Seek signs of possible past microbial life in those habitable environments, particularly in special rocks known to preserve signs of life over time
Caching Samples:	Collect core rock and soil samples and store them on the Martian surface
Preparing for Humans:	Test oxygen production from the Martian atmosphere

The mission design envisions preparing as many as 40 rock, soil, and blank samples, measuring approximately 1 cm in diameter and 8 cm in length, and caching them on the Martian surface. These samples could be retrieved by potential future missions, and could ultimately be transported to Earth for detailed analysis. The samples in the Mars 2020 cache could thus become the first Martian samples to be selected for Earth return based on specific scientific criteria and measurements, and with carefully documented field context.

Between extensive analyses of Martian meteorites and the *in-situ* studies carried out by the Viking, Pathfinder, Spirit, Opportunity and Curiosity landers and rovers we understand a great deal about the materials to be expected in the Mars 2020 landing zone. The Mars 2020 rover will carry a suite of instruments to measure mineralogical and elemental composition as well as surface organics. These measurements will feed into the selection of samples for coring and caching. We anticipate that the materials in the Mars 2020 cache will be the best-characterized planetary samples ever selected.

Planetary Protection: The requirements imposed by international planetary protection policies for any future sample return mission from Mars will be specific to that mission. However, current policies suggest that Mars samples would be carried to Earth in containers designed to prevent any accidental release of samples to Earth's environment. Those containers would only be opened in a sample receiving facility (SRF) with protection equivalent to that of a high-level biosafety laboratory. Initial studies of a representative subset of the samples would be required to determine if they contained extant Martian life, and/or if they represented a hazard to the terrestrial biosphere.

The Challenge: There are two primary candidate strategies for operating the SRF: 1). The human operators are inside biosafety suits, and the instruments are out on benches (or for larger instruments, in the middle of the rooms) and the samples are dealt with in the open; 2). The samples are dealt with inside isolator cabinets, with humans on the outside manipulating them with gloves or robots. Although #2 above is far preferable from the point of view of protecting the unique value of the samples (for example, minimizing contamination), substantial technical questions remain about how to integrate modern high-vacuum, high-voltage instrumentation with a biosafety cabinet. These anticipated requirements present a challenge to laboratory, sample preparation system and instrument designers that is unique in the history of planetary science. We need a technology development program in this area.

The Beginnings of an Approach: The instruments for initial rock and soil characterization in the sample receiving laboratory could be complementary to sample measurements on Mars. These include elemental composition, mineralogy and the presence of organics, all measured at the cm- to mm-scale to support detailed subsampling. In addition, knowledge of the internal physical structures of the rock cores would be an invaluable guide for subsampling. To minimize alteration and contamination, the instruments should require little or no physical contact with the samples. The instruments should be capable of remote operation in a controlled environment which preserves sample pristinity while providing a high degree of biosafety protection.

Mineralogical composition: The major minerals in a rock can generally be determined optically, with the

required resolution being determined by the rock's grain size. Visible, UV and near-IR spectrometers, operated thru optical windows, can preserve the samples from alteration and contamination while not interfering with biosafety barriers. Optical spectrometers and spectrophotometers have been flown on numerous planetary missions. The Mastcam-Z instrument on Mars 2020 will help to determine the overall mineralogy of Martian rocks and soils to support rover operations and sample selection.

Such instruments can only sense the samples' surfaces, however, and can be frustrated by optically thick layers of dust or drilling fines. X-ray instruments such as a micro-CT scanner can image mm-scale crystals and show their locations throughout the volume of a rock core. Minerals can be differentiated based on their densities, and the instrument can be calibrated to provide mineral identification. Micro-CT instruments can analyze samples placed in X-ray transparent containers, which can be made compatible with high-level cleanliness and biosafety. A micro-CT system has recently been installed in the curation suite at JSC to characterize the internal mineralogy of lunar and meteorite samples.

Elemental Composition: Identification and characterization of a mineral is considerably enhanced by knowledge of its elemental composition. Non-contact alpha-proton x-ray spectrometers have been flown on all of the Mars rovers to date. The PIXL instrument on Mars 2020 will be an X-ray fluorescence spectrometer that will also contain an imager with high resolution to determine the fine scale elemental composition of Martian surface materials. A modification of this design, operated thru an X-ray transparent window, could provide detailed information on Martian rock and soil cores within the containment of a sample receiving laboratory.

The micro-CT system described above also incorporates detectors which provide X-ray fluorescence analysis. This micro-XRF technology allows the determination of elemental compositions and locations of sub-mm crystals. As noted, this instrument can successfully analyze samples within X-ray transparent containers which could be designed to minimize contamination and provide biosafety protection.

An alternative technique for determining elemental composition remotely is laser-induced breakdown spectroscopy (LIBS). A high-power laser beam interacting with a rock surface produces a plasma with a spectral signature characteristic of the target's composition. The CHEMCAM instrument on Curiosity uses LIBS to analyze rocks at cm to mm resolutions, and could be modified for laboratory use thru an optical window.

Organic analysis: Sample selection for planetary protection would be greatly enhanced by the detection of organic material concentrations. Optical techniques using the natural fluorescence of organics illuminated by specific wavelengths of light have been developed in several laboratories. The SHERLOC instrument on Mars 2020 is a spectrometer that will provide fine-scale imaging and uses an ultraviolet laser to determine fine-scale mineralogy and detect organic compounds. SHERLOC will be the first UV Raman spectrometer to fly to the surface of Mars.

Internal physical structure: The Mars 2020 instruments analyze surfaces, but the core drill will provide samples from as deep as 8 cm into the rock. Knowledge of the internal structure of each core will be critical to the selection of material for subsampling. Cracks and vesicles, perhaps not visible from the sample surface, could provide the most promising sites for the preservation of organics or past life. A micro-CT scanning instrument, discussed above, could provide three-dimensional maps of the internal structure of rocks at the sub-mm scale.

Subsampling: Subsampling soil and rock are two very different challenges. Asteroid dust particles collected by the Hayabusa mission, many smaller than 100 μm, are selected and mounted for analysis in JAXA and NASA curation laboratories. The work is done using micromanipulators inside nitrogen gloveboxes.

Removing selected portions of rock from a core held in biological isolation has yet to be demonstrated. However, computer-controlled microsurgery is an advancing field with technologies clearly applicable to geological investigations.

Looking Ahead: The possibility that samples selected and cached by the Mars 2020 mission could one day be brought to Earth brings issues of sample integrity, contamination and planetary protection into sharp focus. In the case of Mars 2020, the technologies for analyzing, collecting and caching the samples on Mars are essentially locked in. The technologies for dealing with the samples if they are one day brought to Earth, however, require considerable advance planning, laboratory and instrument development, and verification.

We have outlined one approach to one part of the problem – providing data sufficient for planetary protection subsampling. We strongly recommend that a program of laboratory and instrument development be initiated, in order to be ready if the people of Earth are ready to receive samples from the planet Mars.

PIXL Investigation on the Mars 2020 Rover. A. C. Allwood[1], L.A. Wade[1], J.A. Hurowitz[2]. [1]Jet Propulsion Laboratory, California Institute of Technology, 4800 Oak Grove Dr, Pasadena, CA, USA. Stony Brook University, Stony Brook, NY, USA.

Introduction: PIXL (Planetary Instrument for X-ray Lithochemistry) is a micro-focus X-ray fluorescence instrument that is part of the selected science payload for the 2020 rover. From its position on the end of the rover's robotic arm, PIXL will be able to scan a tiny 0.12mm-diameter x-ray beam across a 25x25mm target area on rock or soil, measuring the abundance and distribution of a wide range of elements with high spatial resolution, sensitivity and accuracy. The elemental measurements will be correlated to visible textures and microstructures through an optical fiducial system, consisting of a micro-context camera and a structured light array.

With these capabilities, PIXL will be able correlate chemical measurements with individual grains, crystals, veins, cements, concretions and laminae. These measurements will provide detailed information about past conditions affecting habitability, biosignature formation and biosignature preservation – information that is needed to guide the search for biosignatures. PIXL can also directly detect potential chemical biosignatures such as reduction spots [1] (Fig. 1), and provide critical geochemical characterization of other kinds of potential biosignatures (e.g. stromatolites, organic deposits: Fig. 2) if any are found.

To maximize access to science targets, PIXL will use a hexapod motion system, novel optical fiducial system and a range of algorithms for autonomous positioning and position documentation. Together, these capabilities will allow scientists to investigate targets with uneven surfaces, target specific areas of interest at millimeter scales and to acquire high resolution maps overnight.

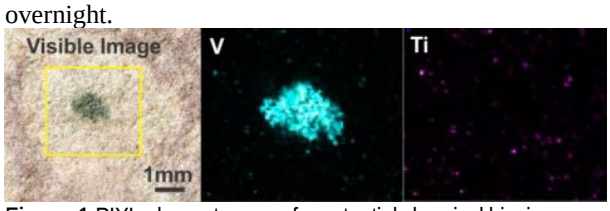

Figure 1 PIXL element maps of a potential chemical biosignature: a vanadium-enriched microbial reduction spot in sandstone. Sample courtesy S. Spinks.

PIXL will have flexible operations enabling the science team to adjust experiment parameters to suit a specific target or operational constraints such as time, power and data volume.

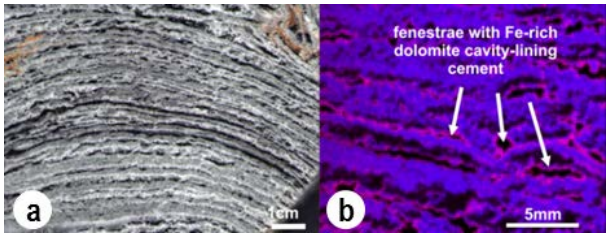

Figure 2: Element map of Early Archean stromatolite: (a) visible image. (b) PIXL element map (Blue = Ca, Pink = Fe) of stromatolite texture shows Fe-rich dolomite cements in fenestrae (voids - black areas, now chert-filled), indicating sedimentary origin of carbonate and microbial influence on texture [2].

In situ science with PIXL: With data produced by PIXL, the science team will be able to:

1. Determine the elemental composition of individual rock components. This includes relative and absolute abundances (point, bulk rock, and bulk of rock sub-components such as cement vs. grains),
2. Measure spatial variations in element abundance and correlate chemistry with visible features at sub-mm resolution
3. Constrain mineralogy from element abundances and correlations
4. Determine the relative timing of formation of chemically distinct components from small scale cross-cutting relationships

PIXL data will be correlated with organic and mineral mapping by the SHERLOC instrument on the rover arm. Together with other instruments on the 2020 rover—including powerful new remote imaging (Mastcam-Z) and spectroscopy (Supercam) instruments—it will be possible to carry out astrobiological field investigations with sufficient detail and quality to credibly address the search for signs of ancient life on Mars.

References:

[1] Spinks, S.C. et al. (2010), *International Journal of Astrobiology*, doi:10.1017/S1473550410000273.

[2] Allwood, A.C. et al. 2009. *Proceedings of the National Academy of Sciences, 106,* 9548-9555

The Ganymede Laser Altimeter – Instrument design overview with radiation hard transmitter.

C. Althaus, H. Hussmann, K. Lingenauber, H. Michaelis, R. Kallenbach, J. Oberst and the GALA team,
German Aerospace Center DLR e.V. (christian.althaus@dlr.de)

Introduction: The JUICE (Jupiter Icy Moons Explorer) mission is part of ESA's Cosmic Vision Programme and its objective is to study Jupiter's plasma environment and the three icy moons Ganymede, Europa and Callisto. The JUICE spacecraft will be launched in 2022 on an Ariane 5 rocket. After its 8 year cruise it will enter an orbit around Jupiter. During the following three years the orbit will be gradually adjusted and after several fly-bys at Callisto, Europa and Ganymede the space-craft will reach its final circular orbit around Gany-mede. One of the ten scientific instruments is the Ganymede Laser Altimeter – GALA (Fig. 1). It will determine the topography and time dependent shape of the moon by direct laser altimetry approach.

Instrument Design: The instrument is composed of three units: Transceiver Unit (TRU), Laser Electronics Unit (LEU) and Electronics Unit (ELU). The TRU contains the transmitter laser

Therefore the instrument is equipped with a Nd:YAG laser system with a nominal pulse repetition frequency of 30 Hz and a pulse energy of 17 mJ. The laser is a side-pumped by laser diodes unstable resonator which is encapsulated in a pressurized compartment. Heritage of this configuration is from BELA which is designed and verified for ESA's BepiColombo mission. For GALA the laser must fulfil strong requirements especially on radiation hardness, power efficiency and lifetime. Furthermore a reflective 25 cm RC telescope is included to receive the transmitted light pulses [1].

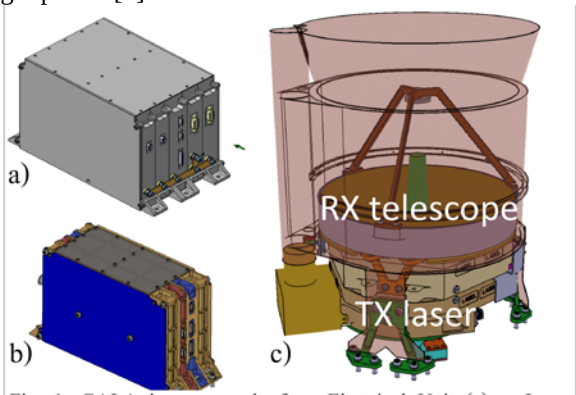

Fig. 1: GALA is composed of an Electrical Unit (a), a Laser Electronics Unit (b) and a Transceiver Unit (c). The latter one is in contrast to the other two accommodated on an space exposed optical bench on the S/C.

Mission constraints: The environment of Jupiter is challenging for a S/C and a laser instrument because besides the common space related factors, e.g. vacuum, thermal loads, limited mass and power, micrometeoroids, plasmas etc., it is strongly dominated by high energetic particles and in particular electrons. These are caught by the strong Jovian magnetic field which with 428 µT at the equator is about one order of magnitude stronger than Earth's [2].

Degradation Mechanisms: The physics of degradation mechanisms by radiation are complex and numerous. A major effect is that protons and electrons cause ionization and displacement damage (DD). These result in darkening of optical glasses, damage of optical coatings as well as loss of adhesion of coatings, increase of laser threshold and loss of optical output power of laser diodes. Furthermore electrons lead, especially in strong dielectrics, to charging which can result in damage or failure of components by discharge arcs.

Methods: In order to realize the goal of achieving the optimal overall configuration of the laser for a Jupiter mission, trade-offs must be made carefully. This is because advantages on one parameter can have contrary impact on others, e.g. increasing the efficiency of the resonator by making the cross-section of the pumped volume smaller leads to increased risk of laser incuced damage (LID) at optical surfaces, e.g. the polarizing beamsplitter (PBS).

Therefore it is investigated which effect or parameter influences the system in which manner, i.e.

for radiation hardness:
- ionizing radiation and non-ionizing radiation
- dielectric charging

for power efficiency:
- laser diodes threshold, slope, pump duration
- laser rod geometry, absorption loss
- Pockels cell rise time

for lifetime:
- redundancy
- laser diodes degradation
- pressurization of resonator

The tools used for assessment of the radiation doses (TID and DD) and fluxes are GRAS, Fastrad and SPENVIS [3]. From those results conditions for representative radiation tests are derived. Particular attention amongst others is paid on charging effects caused by energetic electrons, but also displacement damage.

A tool to quantitatively assess the impact of different factors on the system shall help to design the transmitter of this and other missions. Description of approach and some results are part of this work.

References: [1] K. Lingenauber, H. Hussmann et al. The Ganymede Laser Altimeter (GALA) on ESA's JUICE mission: Overview of the instrument design. (2014) Conference Paper.; [2] Jovian Factsheet: http://nssdc.gsfc.nasa.gov/planetary/factsheet/joviansatfact.html; [3] Space Environment Information System https://www.spenvis.oma.be/

LEAD-LEAD AND RUBIDIUM-STRONTIUM IN SITU DATING USING THE CHEMISTRY, ORGANICS, AND DATING EXPERIMENT (CODEX) F. S. Anderson[1], T. J. Whitaker[1], J. Levine[2], and S. Beck[3], [1]Southwest Research Institute, 1050 Walnut St, Boulder CO; anderson@boulder.swri.edu, [2]Colgate University, Hamilton, NY 13346, 3Aerospace Corporation, Los Angeles, CA 90009.

Introduction: We have continued to develop the Chemistry, Organics, and Dating EXperiment (CODEX) instrument, improving the TRL of the instrument subsystems, and extended previously published Rb-Sr dating [1, 2] to Pb-Pb dating. Our instrument uses laser-ablation (LA) to remove atoms at each of hundreds of analytical spots on a ~1 cm^2 sample, and resonance ionization (RI) to selectively ionize atoms of Pb, Rb, and Sr, thereby mitigating isobaric interferences, followed by mass spectrometry (MS) to determine the abundance of individual isotopes [1]. From our measured isotopic abundances, we are able to construct Pb-Pb and ^{87}Rb-^{87}Sr isochron for the specimen. In addition, we have previously demonstrated that we can measure elemental and organic abundance, using simpler CODEX modes of laser ablation and two-step laser mass spectrometry, respectively [e.g., 3].

Importance: Understanding the relative timing of geologic events using crater counting is the keystone to unraveling the history recorded on the surfaces of rocky bodies. Crater counts, in conjunction with radiometrically-dated Apollo and Luna samples, have been used to estimate the absolute ages of events on the Moon [4]. The resulting cratering flux has been extrapolated to Mars [5], Mercury [6, 7], Venus [8], Vesta [9-11], and used in models of early solar system dynamics [12].

However, recent analysis [13] indicates three major complications to the crater chronology picture: a) crater-counted terrains may not be the sources of dated samples, b) there is a need to extrapolate crater count relationships to very young and old terrains, and c) there is a two-billion year gap of samples with well-known provenance suitable for crater counting from 1 to 3 Ga (**Fig. 1**).

These problems result in billion-year uncertainties for the history of the Moon [13] and solar system. For example, the era of bombardment of the inner solar system, as recorded by lunar impacts, may have effectively ended ~3.7 Ga ago or at some younger time. Because life on Earth is thought to have arisen between ~3.7 and ~3.0 Ga ago, the model improvement could reveal new insights about the habitability of the early Earth. Similarly, the era of liquid water on the Martian

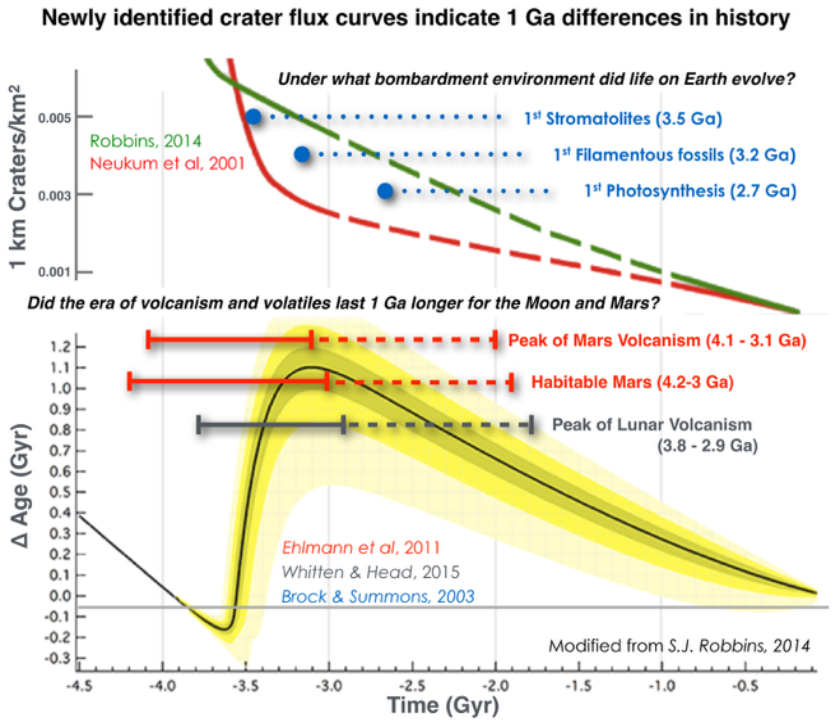

Fig. 1: Illustration of how poorly constrained lunar chronology functions, with up to 1 Ga of uncertainty, influence interpretation of key geologic events for the Moon, Mars, and even Earth.

surface, which is intimately related to possible life on Mars, as well as the eras of voluminous volcanism on the Moon and Mars, might have ended ~3 Ga ago or extended to as recently as ~1.7 Ga ago.

Thus, obtaining new dates from the surfaces of Mars or the Moon are crucial to revealing which of these models of solar system history is correct. To understand the range of terranes and history on another planet will require obtaining samples with a wide geographic distribution. This likely means multiple missions, which due to cost constraints, will need to be comprised of both sample return and in-situ measurements. Fortunately, CODEX provides two chronometry systems, and maps of elemental abundance, enabling us to place measurements in mineralogical and petrological context. Previously published results show that we can readily obtain precision and accuracy better than 200 Ma for the Martian meteorite Zagami [2], and the lunar analog Duluth Gabbro [1]. Our new measurements described below illustrate how CODEX can measure a second independent geochronometer.

New Pb measurements: By adding two lasers to the CODEX system, we can use the LARIMS approach to obtain ~10 ppb sensitivity in isobar-free measurements of ^{204}Pb, ^{206}Pb, ^{207}Pb, and ^{208}Pb. We used wavelengths of 283.3 nm and 600.2 nm for resonance excitation, followed by IR photoionization. These in turn can be used to assess the isochron age of samples. We tested our approach on the Kuehl Lake 91500 Zircon and MIL 05035. The results were in excellent agreement with the known ages, being within 80 Ma of previous measurements **(Fig. 2-3)**.

Progress on instrument development: Under MatISSE 2014 funding, we are currently miniaturizing the Sr and ablation laser subsystem using an all-fiber approach, and are actively working to reduce the overall instrument. In addition, we are in preliminary design and development for the mass spectrometer and sample handling.

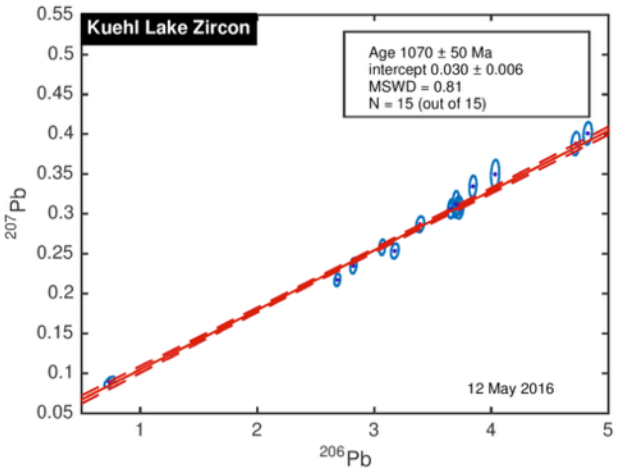

Fig. 2: LARIMS isochron of Zircon Sample. Actual age is 1.067 Ga.

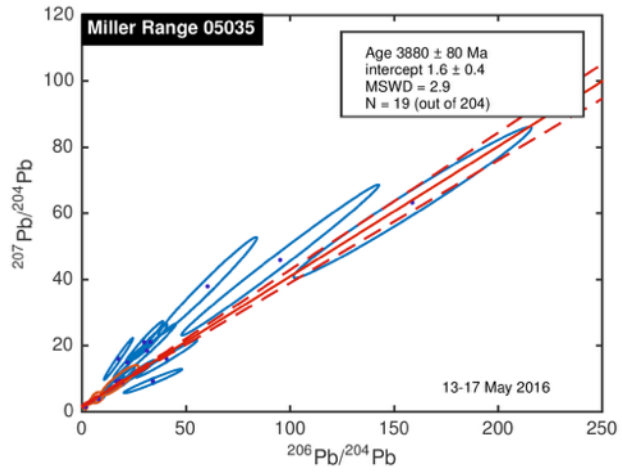

Fig. 3: LARIMS isochron for MIL-05035. Because of the low concentration of Pb in this sample (0.405 ppm) only 19 points out of 204 that we analyzed had adequate signal-to-noise to be used in the isochron. The actual age is between 3.8 and 3.9 billion years.

References:

1. Anderson et al, Rb-Sr resonance ionization geochronology of the Duluth Gabbro: A proof of concept for in situ dating on the Moon. *RCMS*, 2015. 29: p. 1-8. 2. Anderson et al, Dating the Martian meteorite Zagami by the ^{87}Rb-^{87}Sr isochron method with a prototype in situ resonance ionization mass spectrometer. *RCMS*, 2015. 29(2): p. 191-204. 3. Anderson et al, The Case For In-situ Dating In Geologic Context For The Moon And Mars Using The Chemistry, Organics, And Dating Experiment (CODEX), in *IPM-2014,* GSFC: Greenbelt, MD. p. 2. 4. Neukum et al, Cratering records in the inner solar system in relation to the lunar reference system. *SSR*, 2001. 96(1): p. 55-86. 5. Hartmann et al, Cratering Chronology and the Evolution of Mars. *SSR*, 2001. 96: p. 165-194. 6. Fassett, et al., The global population of large craters on Mercury and comparison with the Moon. *GRL*, 2011. 38(10). 7. Marchi., et al., Global resurfacing of Mercury 4.0-4.1 billion years ago by heavy bombardment and volcanism. *Nature*, 2013. 499(7456): p. 59-61. 8. Bougher et al, Venus II, 1997 9. Marchi et al., The violent collisional history of asteroid 4 Vesta. *Science*, 2012. 336(6082): p. 690-694. 10. Scherk et al., The geologically recent giant impact basins at Vesta's south pole. *Science*, 2012. 336(6082): p. 694-697. 11. Schmedemann et al. Crater retention ages from (4) Vesta matching independent Ar-Ar ages of HED meteorites. *EGU* 2013. 12. Michel, P. and A. Morbidelli, Review of the population of impactors and the impact cratering rate in the inner solar system. *MAPS*, 2007. 42: p. 1861-1869. 13. Robbins, New crater calibrations for the lunar crater-age chronology. *EPSL*, 2014. 403: p. 188-198.

Technology for a Thermo-chemical Ice Penetrator for Icy Moons Jonathan Arenberg[1], George Harpole[1], James Zamel[1], Bashwar Sen[1], Greg Lee[1], Floyd Ross[1] and Kurt Retherford[2]
[1]Northrop Grumman Aerospace Systems, One Space Park Drive, Redondo Beach California 90278, email: jon.arenberg@ngc.com, [2]Southwest Research Institute, 6220 Culebra Rd. San Antonio, Texas 78238).

Introduction: The ability to place sensors or to take samples below the ice surface enables a wide variety of potential scientific investigations. Penetrating an ice cap can be accomplished via a mechanical drill, laser drill, kinetic impactor, or heated penetrator. This poster reports on the development of technology for the latter most option, namely a self-heated probe driven by an exo-thermic chemical reaction: a Thermo-chemical ice penetrator (T-ChIP). Our penetrator design employs a eutectic mix of alkali metals that produce an exothermic reaction upon contact with an icy surface. This reaction increases once the ice starts melting, so no external power is required. This technology is inspired by a classified Cold-War era program developed at Northrop Grumman for the US Navy.

Terrestrial demonstration of this technology took place in the Arctic during the 1980's; however, this device cannot be considered high TRL for application at the icy moons of the solar system due to the environmental differences between Earth's Arctic and the icy moons. These differences demand a T-ChIP design specific to these cold, low mass, airless worlds. It is expected that this model of T-ChIP performance will be a complex model incorporating the forces on the penetrator, the thermo-chemistry at the interface between penetrator and ice, and multi-phase heat and mass transport, and hydrodynamics. Our initial efforts are aimed at the development of a validated set of tools to predict the performance of the penetrator for both the environment found on these icy moons and for a terrestrial environment. The inclusion of the terrestrial environment is expected to aid in model validation. Once developed and validated, our model tools will allow us to design penetrators for a specific scientific application on a specific body.

This poster discusses the range of scientific investigations that can be enabled by T-ChIP. We also introduce the development plan to advance T-ChIP to the point where it can be considered for infusion into a program.

Advanced Resolution Organic Molecule Analyzer (AROMA): Simulations, Development and Initial Testing of a Linear Ion Trap-Orbitrap Instrument for Space. R. Arevalo Jr.[1], R. M. Danell[2], C. Gundersen[3], L. Hovmand[4], A. Southard[5], F. Tan[1], A. Grubisic[6], W. B. Brinckerhoff[1], S. A. Getty[1], P. Mahaffy[1], H. Cottin[7], C. Briois[8], F. Colin[8], C. Szopa[9], V. Vuitton[10], A. Makarov[11], and M. Reinhardt-Szyba[11]; [1]NASA GSFC (USA), (ricardo.d.arevalo@nasa.gov), [2]Danell Consulting, Inc. (USA), [3]AMU Engineering (USA), [4]Linear Labs, LLC (USA), [5]USRA (USA), [6]UMBC (USA), [7]LISA (FR), [8]LCP2E (FR), [9]LATMOS (FR), [10]IPAG (FR), [11]Thermo (DE)

Introduction: In collaboration with Thermo Bremen and the French CosmOrbitrap Consortium, NASA GSFC is developing a highly capable mass spectrometer instrument suite that will transform our understanding of cryogenic, potentially organic-rich planetary targets, such as comets, Jupiter's Europa, and Saturn's moons, Enceladus and Titan. This comprehensive, in situ investigation, funded through the ROSES PICASSO Program, promises versatile and high-performance instrumentation capable of:

1. Quantitative measurements of trace levels (e.g., ≤ ppmw) of organic and inorganic compounds over a wide range of volatility, ionization potential and molecular weight;
2. Selective isolation of targeted mass ranges for enhanced signal-to-noise (and by extension limits-of-detection) and controlled ion manipulation and ejection;
3. Induced fragmentation of parent molecules and structural analysis of daughter ions via tandem mass spectrometry (i.e., MS^n operations) for the differentiation of isomers; and,
4. Mass discrimination and disambiguation of isotopologues and organic and inorganic isobaric interferences with high-resolution ($m/\Delta m$ ≥ 50,000) and mass accuracy.

In order to achieve these analytical capabilities, the AROMA instrument combines a mature linear ion trap (LIT) developed at NASA GSFC for the MOMA flight instrument and further augmented through MatISSE efforts (P-I: Brinckerhoff), and an Orbitrap™ mass analyzer adapted for spaceflight by a consortium of French laboratories which is capable of separating isobaric interferences with a resolving power as high as $m/\Delta m$ ≥ 100,000 (FWHM at m/z 100, 1 Hz scan rate; [1]). Together, this powerful combination (**Fig. 1**) will redefine our capabilities to identify complicated organic signatures unambiguously, and assign molecular structures with functional specificity. The primary analytical challenges that will be addressed in this effort are: i) ejection of tight ion packets (≤ µs pulse widths) from a spaceflight LIT; ii) ion collimation and beam steering via simple ion optics; and, iii) analysis of injected ions at suitably high mass resolution (goal: $m/\Delta m$ ≥ 50,000, FWHM at m/z 100 Da) in an Orbitrap™ with limited resources and/or in challenging environments.

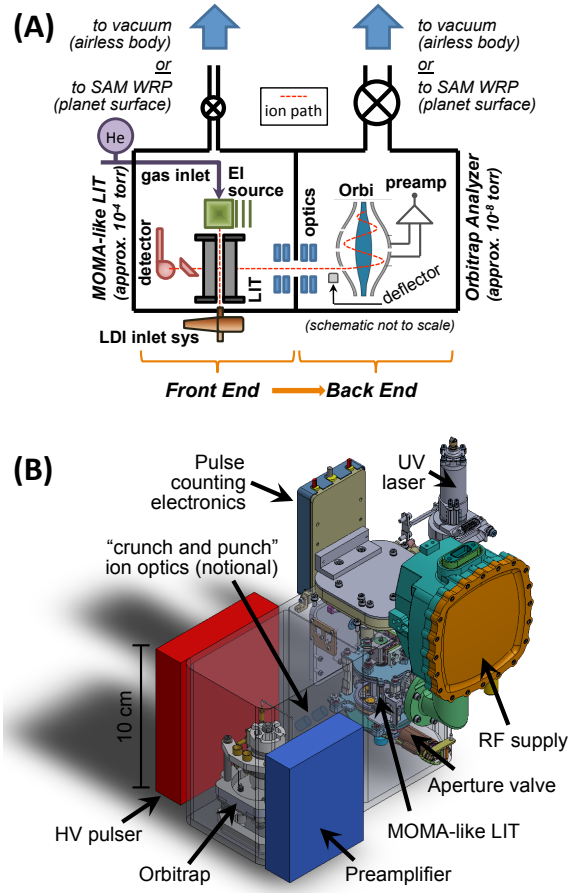

Fig. 1. (A) Schematic representation and (B) 3D model of one possible AROMA flight configuration, including heritage electron ionization (EI) and laser desorption/ionization (LDI) sources, thereby supporting the analysis of gas and solid phases, respectively. A particular flight implementation will require a trade of required mass resolution versus analyzer base pressure and other factors. Greater mass, volume and energy can lead to higher mass resolving powers. As shown, the AROMA concept is estimated at <10 kg and requires <40 W average power (the addition of one or more pumps would increase both mass and power requirements).

Program Schedule: In Phase I of this investigation, the team at NASA GSFC will build a dedicated Orbitrap™ testbed to allow for continuous experi-

mental characterization/tuning of this high-resolution mass analyzer to understand the effect of a number of external variables, including the following:

- Pressures of 10^{-7} – 10^{-9} Torr

(impact: pumping requirements);

- Ion pulse widths from 100 ns up to 2 µs

(impact: ion source requirements);

- Ion residence times up to 1 s

(impact: mass resolution, duty cycle and energy);

- < 3 kV voltage on the central electrode

(impact: instrument power); and,

- Incident energy of the ions from 500 – 1500 eV

(impact: ion optical interface design).

In Phase II NASA GSFC will define the LIT mechanical and electrical interfaces with the CosmOrbitrap subsystem, and build up the LIT assembly and vacuum housing analogous to previous efforts with MOMA prototype instruments. However, rather than employing redundant detector assemblies in a stand alone LIT, one of the ion ejection pathways will direct ions into an array of collimating optics and low-conductance apertures that will interface to the CosmOrbitrap chamber. Once the build is complete, we will verify the analytical capabilities of the LIT subsystem, including sensitivity (limit-of-detection), SWIFT mass excitation (isolation of targeted mass ranges), tandem mass spectrometry (MS^n) operations., and functionality as an ion injection trap (comparable to the C-Trap found in commercial instruments [2]).

In Phase III we will conduct multiple test campaigns with the French CosmOrbitrap Consortium to define system-level analytical capabilities and verify AROMA functional requirements of the fully coupled instrument.

Results: The design of the Phase I Orbitrap™ testbed chamber for use at GSFC has recently been completed and the build of this system is currently underway. As stated above, the purpose of this configuration is to test the effect of various operating parameters on the performance of the Orbitrap™ mass analyzer.

Complete ion optical simulations have been completed of the Phase 1 configuration and the relevant parameters required for successful ion injection have been investigated (**Fig 2**). These models have served to inform the design of this configuration and will also be integrated with a similar model of ion ejection from the LIT to aid in the Phase II system design.

Of particular interest is the effect of operating pressure on the resulting Orbitrap™ mass spectrum, as this will impact the pumping requirements (and therefore mass, volume and power) for a flight system. The CosmOrbitrap portion of our team has recently demonstrated that full performance ($m/\Delta m \geq 100{,}000$) can be maintained at pressures up to 10^{-8} Torr, indicating that ultra high vacuum is not required for many potential applications [1].

A second very important parameter for this coupled LIT/Orbitrap™ instrument is the ion packet pulse width, and its impact on the achievable performance of the instrument (particularly mass range and resolution). In contrast to the CosmOrbitrap system in France, the GSFC testbed employs an ion gun for generating pulsed beams of ions for injection into the Orbitrap™. This allows direct testing of the ion pulse width and its interaction with the other Orbitrap™ operational parameters, and informs the requirements for ion ejection from the LIT. Initial data from these key tests are expected to be available for presentation at the meeting.

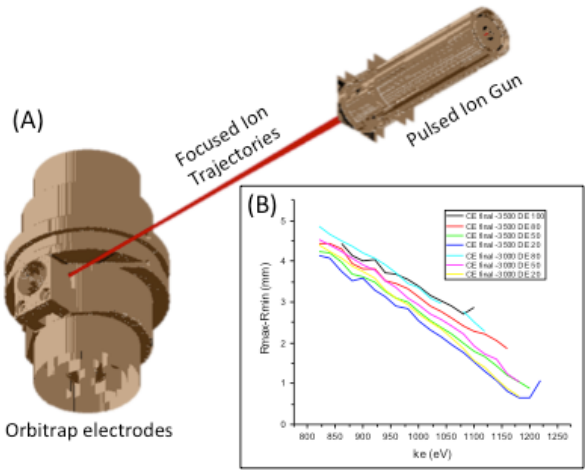

Fig. 2. (A) SIMION model of Phase I testbed configuration. (B) Simulation results showing range of acceptable ion kinetic energies at various Orbitrap electrode operating voltages.

Future Directions: Through the strategic partnership established between NASA GSFC, the French CosmOrbitrap Consrtium and Thermo Bremen, other instrument configurations relying on the CosmOrbitrap analyzer have been submitted for potential funding to complement the AROMA investigation described here. One such concept, the Femtosecond Laser Analysis of Viable Organic Reservoirs (FLAVOR) instrument, promises to characterize the organic and inorganic inventory of planetary materials via in situ stoichiometric laser sampling without contacting or thermally degrading the sample.

References: [1] Briois, C., et al. (2016) *PSS, in press.* [2] Zubarev, R. A. and Makarov, A. (2013) *Anal Chem.*

SMALL BODY IN-SITU MULTI-PROBE MASS ESTIMATION EXPERIMENT (SIMMEE). J. Atchison[1], R. Mitch[1], C. Apland[1], L. Kee[1], [1]Johns Hopkins University Applied Physics Laboratory (11100 Johns Hopkins Road, Laurel, MD, 20723-6099, Justin.Atchison@jhuapl).

Introduction: We explore a concept and instrument for improving our ability to resolve the mass of asteroids and comets during flybys or orbital phases. In this concept, called OpGrav, a host spacecraft releases a group of small white spheres, which it then tracks using an on-board telescope. The spheres, called probes, are deployed such that they pass very near to the small body, and their trajectories are measurably perturbed by the body's gravity. The spacecraft-mounted camera determines the relative measurements of the probes, including right ascension and declination angles with respect to the host spacecraft using background stars. These measurements are then processed on the ground and used to estimate the body's mass. These measurements have the advantages of a high signal-to-noise ratio and a high resolution, owing to the short distance between the host spacecraft to the spheres and the spheres to the body. They are also diverse and numerous, since multiple probes can be deployed to different relative geometries. These benefits enable the accurate determination of mass for bodies that are too small to study using typical ground-based radiometric tracking.

Applicability: The concept is evaluated in a modeling and simulation environment, which includes high-fidelity acceleration models for the small body's gravity, planetary gravity, and solar radiation pressure. The simulation results show meaningful performance during typical flyby scenarios (many kilometers per second) for asteroids as small as 1 kilometer in diameter. Current radiometric techniques require much more massive asteroids, even for missions that are willing to have their spacecraft come very close to the small bodies of interest. The population distribution of asteroid sizes follows a power-law (a larger number of asteroids at smaller sizes). Therefore, this technique greatly increases the number of asteroids that we can collect meaningful scientific gravity information on.

Operations: This approach also enables a greater degree of operational flexibility. Accurate estimation of the small body's mass requires that the host spacecraft pass close enough to the body that the gravitational tug (scaling to first order as the inverse of the distance squared) causes a measureable change in the host's trajectory. In OpGrav, the close approach requirement is instead fulfilled by the probes, and the mass is estimated by tracking their motion in time. There is an additional mission constraint of probe tracking, but this is a benign constraint because there is no requirement of probe tracking during the close approach phase of the small body flyby. Tracking is required for a short period of time following probe deployment (several hours) to fit out initial probe positions and velocities, and an amount of time post-flyby (up to several days) to fit out their perturbed states.

Hardware Design Drivers: The simulations indicate that the measurement success is highly dependent on the deployment accuracy of the hardware (how well one can aim the probe's deployment) and post-deployment knowledge (how well can one determine what the probe's deployment velocity and timing was). The deployment accuracy is important because it determines how close the probe can pass by the body in addition to the observational geometry. Post-deployment knowledge is important because it bounds the estimation problem's *a-priori* uncertainty.

These effects drive the hardware design, requiring an accurate dispenser with a means of measuring the deployment velocity. The hardware implementation of this concept is called the Small Body In-Situ Multi-Probe Mass Estimation Experiment (SIMMEE), and it is being developed on a NASA Innovative Advanced Concepts (NIAC) grant.

Hardware Design: The instrument consists of a dispenser, a probe, and a sabot (Figures 1 and 2). The sabot houses the probe inside the dispenser. The probe is designed to fold compactly into a thick disc. Doing so allows more probes to be stored in a given volume. The probes and sabots are loaded into independent dispenser bays. The bays contain a precompressed spring, which when released via a pin-puller, dispenses the sabot/probe assembly at a predetermined rate of up to 5 m/s. The spring system is designed to accommodate long mission lifetimes (5+ years) while under compression.

The probe deployment state is measured using an LED emitter and detector pair, which is positioned to protrude outside the dispenser. The detector's output is measured to record when the sabot breaks the optical path, and the duration of the blockage. Given a known sabot diameter, this gives an estimate of the deployment speed to within 1 mm/s (1 sigma).

Focus: This research focuses on the key implementation challenges, including a practical concept-of-operations that is consistent with deep space missions. It also evaluates the instrument hardware implementation for the probes and their dispenser, including a test campaign to increase its technology readiness.

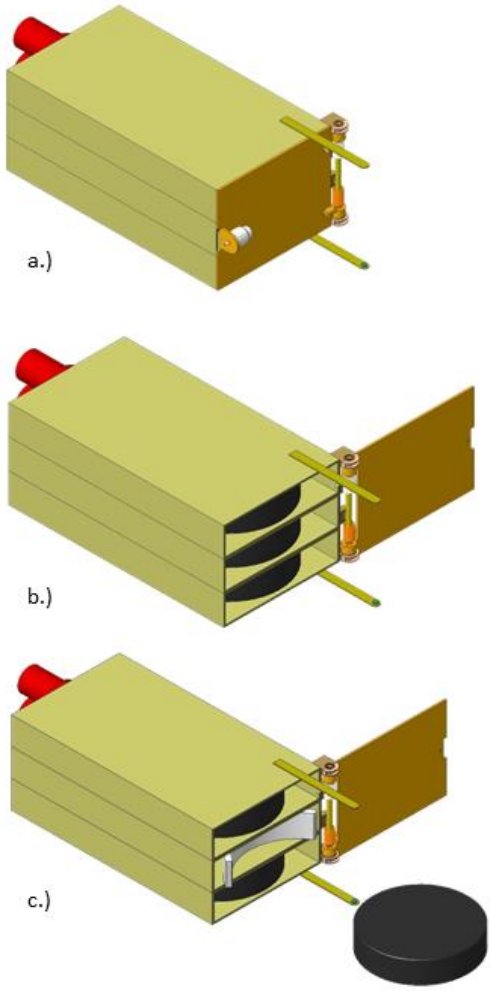

Figure 1: a.) The dispenser assembly is housed inside a single door. b.) The door opens with a pin-puller. c.) The probes are dispensed from independent slots, each of which contains a spring. The two protruding arms contain a LED emitter/detector pair used for velocity and timing measurement.

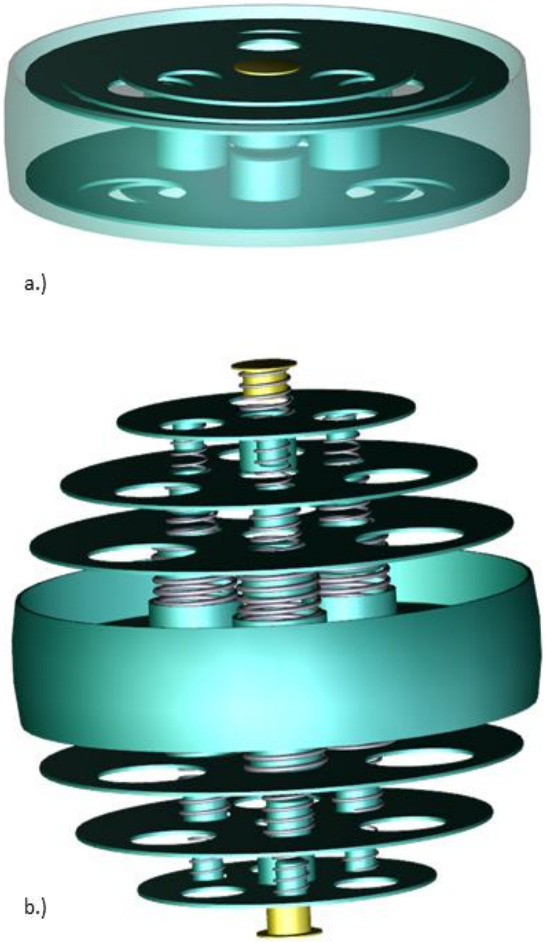

Figure 2: a.) The probe folds compactly into a thick disk. b.) The probe unfolds into a spherical shape using a set of springs. Dissimilar metals prevent stiction during the long mission life. The structure (as shown) is covered with white Beta-cloth for long-range detection in visible bands.

BIOMIMETIC PLANETARY ROBOTS FOR OCEAN EXPLORATION IN SPACE. Mannam Naga Praveen Babu[1] and Krishnankutty. P[2], [1]Department of Ocean Engineering, Indian Institute of Technology Madras, Chennai - 600036, India. [1]E-mail: oe13d006@smail.iitm.ac.in, [2]Department of Ocean Engineering, Indian Institute of Technology Madras, Chennai - 600036, India. [2]E-mail: pkrishnankutty@iitm.ac.in

Introduction: Space exploration is the ongoing discovery and exploration of celestial bodies, planets and moons. The physical exploration of space is carried out by both human spaceflight and unmanned robotic probes (rovers). A rover is a planetary exploration vehicle designed to move acroos the celestial bodies or on surface of the planets. These rovers can be semi-autonomous or fully autonomous bodies. The main function of these rovers is to collect rock samplings, dust and images of the surface. The advantages of planetary rovers compared to stationary landers are they can make obeservations at a microscopic level and can conduct physical experimentations and they can examine more territory. However, the conventional rovers are subjected to limited powering aspects, obstacle avoidance, difficults to maneuver in highly rough terrains and unable to withstand in harsh environments. Naturally the diverse range of environmental conditions that could be encountered during exploration may not be suitable for existing rover systems. The plants and animal species evolved in nature, gives inspiration for designing and buildingof novel and high performance biomiemtic planetary rovers for land and liquid atmospheres on planets. Recently, scientific discoveries creates interest in exploring other planets' moons such as Saturn's Titan and Jupiter's Europa.

Conventional planetary rover designs are wheel operated on firm ground surfaces and proved successful in the exploration of Martian environment (eg: Mars). Hence, the conventional wheel type rovers are not suitable for liquid environments where operation would be in liquid atmospheres on jupiter's europa or within dense gaseous mediums. In order to explore liquid atmospheres in Jupiter's europa (the fourth largest moon on jupiter), the rover should have the ability to propel and manoeuvre effectively within liquid media and its design must reflect these operational requirements.

The current research is to design the planetary rover based on biological species that live in liquid environments on Earth e.g. aquatic mammals and fish. This would involve the development of a robotic system that was able to replicate the swimming aspects of fishes for liquid environments on plantes. This proposed research project will address the design and analysis of a biologically inspired or biomimetic rover concept, for example based on fish swimming, particularly carangiform modes (salmonid). Such robotic systems are highly robust and capable of generating thrust with caudal fin and auxilary (pectroral) fins. These fins increases the powering aspects of the vehicle in liquid environments and the elimiates the needs of rudder devices for maneuvering. Proposed case-studies will involve the exploration of the atmosphere of Europa and Titan.

Biomimetic Planetary Robot: The design considerations will include propulsion mechanisms, efficiencies and power requirements. These will be evaluated through numerical simulations that have been validated against previous studies involving biomimetic autonomous underwater vehicles. The bio-inspired planetary rover is shown in fig. 1. The forward (pectoral) fins have the freedom to oscillate in vertical and/or horizontal plane about the transverse axis and the aft (tail) fin has freedom to oscillate in the horizontal plane about the longitudinal axis. The pectoral fins provides instantaneous stopping ability to rover and helps in reducing the turning circle maneuvering parametes. The modes of operation of pectoral fins is shown in fig.2. The pectoral fins are operated by two servos for flapping motion and two rotational motors for rotation of fins shown in fig. 3. The caudal fin acts as main propulsor for the rover shown in fig. 4. The rover also consits of main controller box, wireless remote.

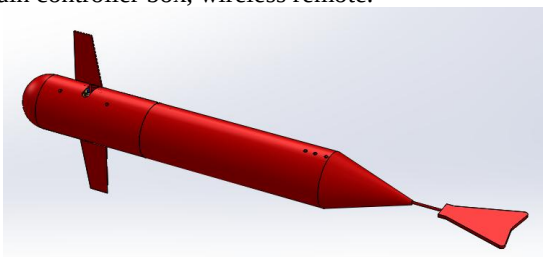

Fig. 1. Bio-inspired Planetary rover

Fig. 2. Pectoral fins in flapping and rotational mode.

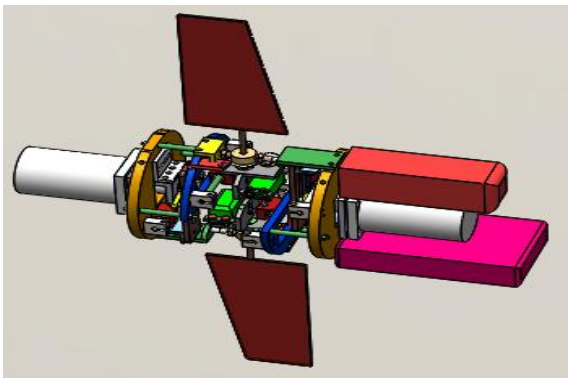

Fig. 3. Pectoral Fins with servo motors and batteries

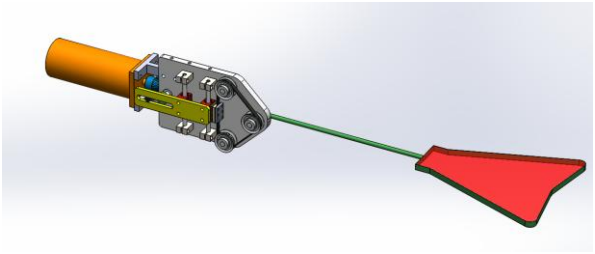

Fig. 4. Caudal fin propulsor for bio-inspired robot

Hydrodynamics of planetary robot: A lift-based propulsion theory is used to estimate the thrust generated by pectoral fins (used as auxiliary thrust device) and an empirical method is used to estimate the torque at the caudal fin. The fish body shape and fin geometrical parameters are also important with regard to the resistance and powering aspects. Numerical studies are conducted with the robotic fish to determine its resistance in bare hull and also for the case fitted with fins. This paper investigates the oscillating motion of caudal fin in yaw mode at different amplitude ratios. The caudal fin generates a reverse von karman vortex street (thrust producing wake) at strouhal number, 0.22. These mechanisms are presented and discussed in the proposed paper. The thrust force on pectoral fins and caudal fin was estimated using strain guage type force sensors in self propulsion mode with the help of towing carriage. These results are discussed in the present paper.

Fig. 5. Bio-inspired robot in testing stage.

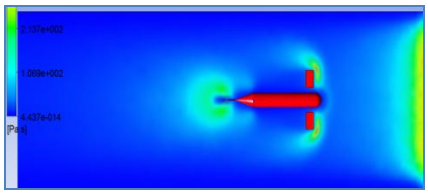

Fig. 6. Flow around the pectoral and caudal fins

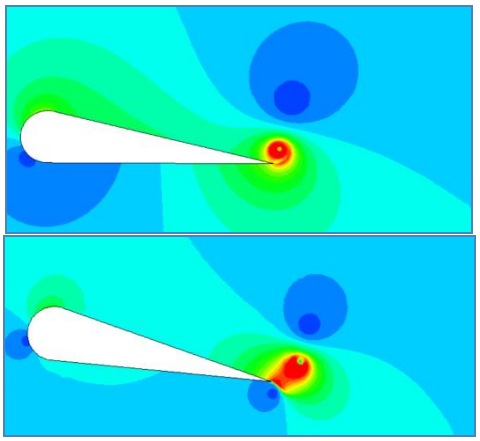

Fig. 7. Reverse von karman vortices around flapping caudal fin

Acknowlodgement: The authors would like to thank Dept. of Ocean Enginnering, Inidan Institute od technology Madras, Chennai, India for suporting this project.

Bibilography:

[1] Anderson J, Streitlien K, Barrett D, Triantafyllou M. Oscillating foils of high propulsive efficiency. Fluid Mechanics 1998;360:41–72.

[2] Taylor GK, Nudds RL, Thomas ALR. Flying and swimming animals cruise at a Strouhal number tuned for high power efficiency. Nature 2003;425:707.

[3] Read DA, Hover F, Triantafyllou M. Forces on oscillating foils for propulsion and maneuvering. Journal of Fluids and Structures 2003;17:163–83.

PARTICLE ENVIRONMENT PACKAGE (PEP) FOR THE ESA JUICE MISSION. S. Barabash[1], C. Brandt[2], P. Wurz[3] and the PEP Team [1]Swedish Institute of Space Physics, Box 812, 98128, Kiruna, Sweden (stas@irf.se), [2]The Johns Hopkins University Applied Physics Laboratory, Laurel, MD, 20723-6099, USA (pontus.brandt@jhuapl.edu), [3]University of Bern, CH-3012, Bern, Switzerland (peter.wurz@space.unibe.ch).

PEP overview: PEP is a suite of six (6) sensors arranged in 4 units to measure charged and neutral particles in the Jupiter magnetospheres and at the moons to answer four overarching science questions:

1. How does the corotating magnetosphere of Jupiter interact with the complex and diverse environment of Ganymede?

2. How does the rapidly rotating magnetosphere of Jupiter interact with the seemingly inert Callisto?

3. What are the governing mechanisms and their global impacts of release of material into the Jovian magnetosphere from seemingly inert Europa and active Io?

4. How do internal and solar wind drivers cause such energetic, time variable and multi-scale phenomena in the steadily rotating giant magnetosphere of Jupiter?

PEP measures positive and negative ions, electrons, exospheric neutral gas, thermal plasma and energetic neutral atoms present in all domains of the Jupiter system over nine decades of energy from < 0.001 eV to > 1 MeV with full angular coverage.

PEP provides instantaneous measurements of 3D flow of the ion plasma and composition to understand the magnetosphere and magnetosphere-moon interactions. It also measures instantaneously 3D electron plasma to investigate auroral processes at the moon and Jupiter. Measurements of the angular distributions of energetic electrons at sub-second resolution probe the acceleration mechanisms and magnetic field topology and boundaries.

PEP combines remote sensing using energetic neutral atoms (ENA) with in-situ measurements and performs global imaging of Europa/Io tori and magnetosphere combined with energetic ion measurements. Using low energy ENAs originating from the particle – surface interaction PEP investigate space weathering of the icy moons by precipitation particles. PEP will first-ever directly sample the exospheres of Europa, Ganymede, and Callisto with extremely high mass resolution (M/ΔM > 1100).

PEP sensors overview: The PEP sensors are (1) an ion mass analyzer, (2) an electron spectrometer, (3) a low energy ENA imager, (4) a high energy ENA and energetic ions imager, (5) an energetic electron sensor, and (6) a neutral gas and ions mass spectrometer. The six (6) sensors are grouped into two (2) groups PEP-Hi for energetic particle measurements and PEP-Lo for low energy particle measurements. PEP-Hi includes two sensors and PEP-Lo 4 sensors and respective electronics. The PEP sensors and their performance are described in Table 1. The overall PEP configuration is shown in Fig. 1.

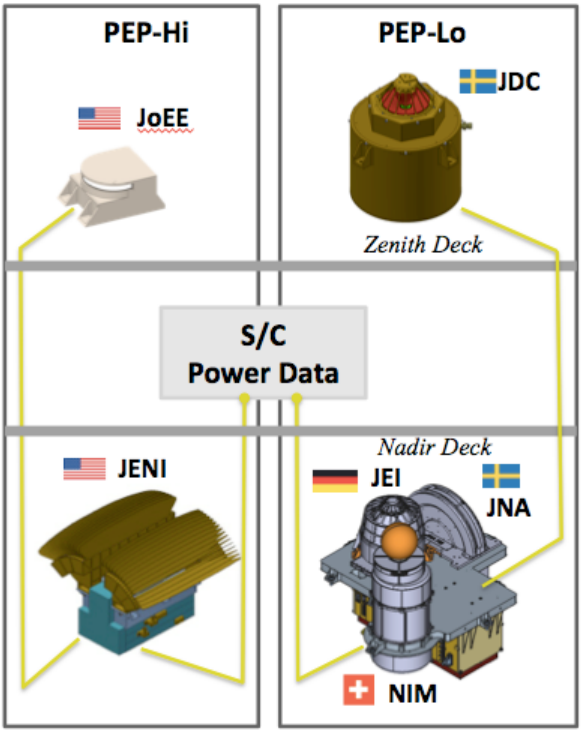

Fig.1 PEP configuration

Table 1. PEP sensors overview

PEP sensor	Key Performance
JDC - Jovian plasma Dynamics and Composition: Design using reflectron and reflecting surface. Instantaneous 3D distributions of positive and negative ions, constraining charge-states, electron measurement capability	Plasma ions and electrons 1 eV – 41 keV, ΔE/E=12% M/ΔM=30 Hemispheric FoV with 5.5˚x19.5˚ ang. resolution
JEI - Jovian Electrons and Ions: Instantaneous 3D distributions of plasma electrons, ion measurement capabilities	Plasma electrons and ions ~1 eV – 50 keV, ΔE/E=4.9% Hemispheric FoV with 20˚x10˚ resolution

JoEE - Jovian Energetic Electrons: Ultra-lightweight energetic electron sensor built on the Galileo energetic particle detector technique. Instantaneous pitch-angle distributions and spectra.	Energetic electrons 25 keV – 1 MeV, $\Delta E/E \leq 20\%$ FoV:12˚x180˚, 12˚x22˚ resolution
NIM - Neutral gas and Ion Mass spectrometer: Compact design based on TOF and reflectron. First-ever exospheric neutral gas and thermal plasma mass spectroscopy at Jupiter's moons.	Thermal neutrals and ions (<5 eV) Mass range: 1-1000 amu $M/\Delta M$=1100 Sensitivity: 2 cm^{-3} ($\sim 10^{-16}$ mbar)
JNA - Jovian Neutrals Analyzer: ENA camera based on successful instrument on the Lunar Chandrayaan-1 mission. Imaging of Io plasma torus, backscattered and sputtered surface products.	Low-energy ENA 10 eV – 3 keV (H) 7˚x10˚ ang. resolution
JENI - Jovian Energetic Neutrals and Ions: Combined energetic ion and ENA camera based on Cassini, IMAGE and Juno. Global imaging of magnetosphere and neutral gas tori.	ENA and ions ~0.5 – 300 keV (ENA), 5 MeV (ions) $\Delta E/E$=14% 90˚x120˚, 2˚ ang. resolution (>10 keV H)

PEP Team: PEP sensors and subsystems have a high technology readiness level and are built on direct flight and team heritage from Galileo, Cassini, Juno, Mars Express (ASPERA-3), Venus Express (ASPERA-4), Rosetta, SOHO, New Horizons, Chandrayaan-1, IMAGE, & RBSP. The PEP team and team member's responsibilities are listed in Table 2.

Table 2. PEP Team

S. Barabash (PI), M. Wieser (SL: JDC, JNA), M. Holmström, Y. Futaana, G. Stenberg, H. Nilsson A. Eriksson (Science with RPWI)	Swedish Institute of Space Physics, Kiruna and Uppsala, Sweden
P. Wurz (Co-PI,SL: NIM), M. Tulej, A. Vorburger, N. Thomas	University of Bern, Physikalisches Institut, Bern, Switzerland
P. Brandt (US Lead), C. Paranicas (SL: JoEE), D. G. Mitchell (SL: JENI), G. Ho, B. H. Mauk, D. Haggerty, J. H. Westlake	Johns Hopkins Univ./Applied Physics Laboratory, Laurel, MD, , USA
Krishan Khurana (Science)	UCLA, Los Angeles, CA, USA
Xianzhe Jia (Science)	University of Michigan, Ann Arbor, MI, USA
C. Paty (Science)	Georgia Institute of Technology, Atlanta, GA USA
M. Fränz (SL: JEI), N. Krupp**,** E. Roussos R. F. Wimmer-Schweingruber B. Heber	Max Planck Institute for Solar System Research, Göttingen, Germany Christian-Albrechts-Universität Kiel, Kiel, Germany)
Asamura Kazushi (JNA electronics)	Institute of Space and Astronautical Science, Kanagawa, Japan
E. Kallio, W. Schmidt (DPU)	Finnish Meteorological Institute, Helsinki, Finland
K. Szego, S. Szalai (Power system, EGSE)	Institute for Particle and Nuclear Physics, Wigner Research Centre for Physics, Budapest, Hungary
M. Grande (Radiation analysis) A. Coates, G. Jones (h/w)	University of Wales Aberystwyth, Wales, UK Mullard Space Science Laboratory, University College London, UK
H. Lammer T. Zhang (Science)	Space Research Institute, Graz, Austria
S. McKenna-Lawlor (h/w)	Space Technology Ireland, Kildare, Ireland
S. M. Krimigis (Science) Th. Sarris (Science, h/w)	Academy of Athens, Athens, Greece Democritus University of Thrace, Xanthi, Greece
D. Grodent (Science)	Université de Liège, Liège, Belgium
N. André, A. Fedorov (h/w)	Institut de Recherche en Astrophysique et Planétologie, Toulouse, France

PI – Principal Investigator
SL – Sensor Lead

The Auto-Gopher – A Wireline Rotary-Percussive Sampler for deep subsurface planetary exploration

Yoseph Bar-Cohen[1], Kris Zacny[2], Mircea Badescu[1], Hyeong Jae Lee[1], Stewart Sherrit[1], Xiaoqi Bao[1], Gale L Paulsen[2], and Luther Beegle[1]

[1] Jet Propulsion Laboratory, California Institute of Technology, Pasadena, CA
[2] Honeybee Robotics Spacecraft Mechanisms Corporation, Pasadena, CA

ABSTRACT

For the "Search for Life" part of the NASA's solar system exploration objectives, it is vital to be able to acquire samples from subsurface regions on planetary bodies that potentially contain extinct or extant biosignatures. To enable the required capability, a wireline deep rotary-percussive corer called Auto-Gopher was developed. The Auto-Gopher can operate as an effective sampling tool reaching great depths (many tens of meters) and is significant to future NASA in-situ exploration mission concepts that would address the important questions of whether life once existed or exists elsewhere in the solar system. The main target for this development effort is Mars although the drill would also be suitable to potential subsurface exploration of Europa and Titan. On Europa, much like Mars, the surface is bombarded with radiation that will destroy fragile biomarkers that may be indicative of life in the Europa Ocean, potentially the largest liquid water repository in the solar system.

The percussive action provides effective material fracturing and the rotation provides efficient cuttings removal. To increase the drill's penetration rate, the percussive and rotary motions are operated simultaneously. To maximize the penetration rate, the lessons learned suggested the need to use a combination of rotation and hammering. This capability was implemented and tested as the Auto-Gopher-1 deep drill which was demonstrated to reach 3-meter deep in gypsum. Currently, the second generation wireline system is being developed, called Auto-Gopher-2, and it is integrated in a single drilling unit to execute all the necessary functions and to include the drive electronics. To maximize the probability of success, the coring mechanism is being replaced with a full face drill head and an auger. The integrated wireline drill functions include cutting removal, retention and delivery in addition to drilling. In this paper, the Auto-Gopher-2, its predecessors and their capability will be described and discussed.

SHERLOC: ON THE ROAD TO MARS. L. W. Beegle[1], R. Bhartia[1], L. DeFlores[1], E. Miller[1], R. Pollack[1], W. Abbey[1], B. Carrier[1], S. Asher[2], A. Burton, M. Fries[3], P. Conrad[4], S. Clegg[5], K. S. Edgett[6], B. Ehlmann[7], W. Hug[8], R. Reid[8], L. Kah[9], K. Nealson[10], T. Nelson[5], M. Minitti[11], J. Popp[12], F. Langenhorst[12], P. Sobron[13], A. Steele[14], N. Tarcea[12], R. Wiens[5], K. Williford [1], R. A. Yingst[11]. [1]Jet Propulsion Laboratory, California Institute of Technology, Pasadena Ca, 91109 (Brandi.L.Carrier@jpl.nasa.gov, Rohit.Bhartia@jpl.nasa.gov, Luther.Beegle@jpl.nasa.gov),[2]University of Pittsburgh, [3]Johnson Space Center, [4]Goddard Space Flight Center, [5]Los Alamos National Laboratory, [6]Malin Space Sciences, [7]California Institute of Technology, [8]Photon Systems Inc., [9]University of Tennessee, [10]University of Southern California, [11]Planetary Science Institute, [12]University Of Jena, [13]SETI Institute, [14]Carnegie Institute Washington

Introduction: SHERLOC is a Deep UV (DUV) native fluorescence and resonance Raman spectrometer that was selected as part of the Mars 2020 payload. It is a robotic arm mounted instrument that utilizes a DUV laser to generate characteristic Raman and fluorescence photons from a targeted spot. The DUV laser is co-boresighted to a context imager and integrated into an autofocusing/scanning optical system that allows us to correlate spectral signatures to surface textures, morphology and visible features. Additionally, it has recently been augmented with an imaging system that is a built-to-print version of the MArs Hand Lens Imager (MAHLI) instrument on the Mars Science Laboratory (MSL).

The SHERLOC investigation combines two spectral phenomena, fluorescence and pre-resonance/resonance DUV Raman scattering. Raman scattering enables classification of bonds such as C-H, CN, C=O, C=C, NHx, NOx, SOx, POx, ClOx, and OH. These spectral features are resolvable when a high-radiance, narrow linewidth, laser source illuminates a sample. In fluorescence, the incident photons are absorbed and re-emitted at a longer wavelength. The difference between the excitation and emission wavelength is the difference between the excitation frequency and the lowest electronic state frequency that increases with increasing aromatic structure (i.e., number of aromatic rings). Typical fluorescence cross-sections are 10^4 greater than traditional Raman, enabling the detection of sub-picograms levels of aromatic organic compounds. Through the use of an internal scanning mirror, autofocusing lens, and a depth of focus of ±500 µm, the 100 µm laser spot can be systematically scanned over a 7x7 mm area with a fine-scale spatial resolution on natural or abraded surfaces and boreholes to a depth of at least 13 mm, without further arm movement. Through the use of the context imager, SHERLOC's data products can be combined with observations made by other instruments on the Mars 2020 payload. By bringing to bear multiple scientific instruments on a single sample, our ability to assess the habitability of ancient environments and search for potential biosignatures preserved within the geologic record will be greatly enhanced, making possible the selection of high-priority samples for caching.

Fluorescence emission of organics extends from ~270 nm into visible wavelengths. On the other hand, mineral fluorescence emission stemming from crystalline defects and impurities is weak in the deep UV, and typically begins longward of 360 nm continuing through the visible and into the NIR. Mineral fluorescence is very unlikely to be seen in samples found on Mars. The DUV fluorescence technique employed by SHERLOC is well-suited to the detection of organics on mineral surfaces.

The road from concept to eventual flight for SHERLOC first started in 1998. An internal program at JPL called the "Grand Challenge" awarded grants to multiple instrument teams to designed and develop instrumentation to detect evidence of extant and extinct life. In the time between that first endeavor and the submission of Mars 2020 proposal, multiple different funding from sources including DARPA, ASTID, NAI and PIDDP were obtained. After selection, the design of the instrument underwent several changes including the including of WATSON, the modification of the optical path and packing all the hardware on the resource constrained arm.

Acknowledgement: This work was carried out at the Jet Propulsion Laboratory, The California Institute of Technology under a contract from NASA.

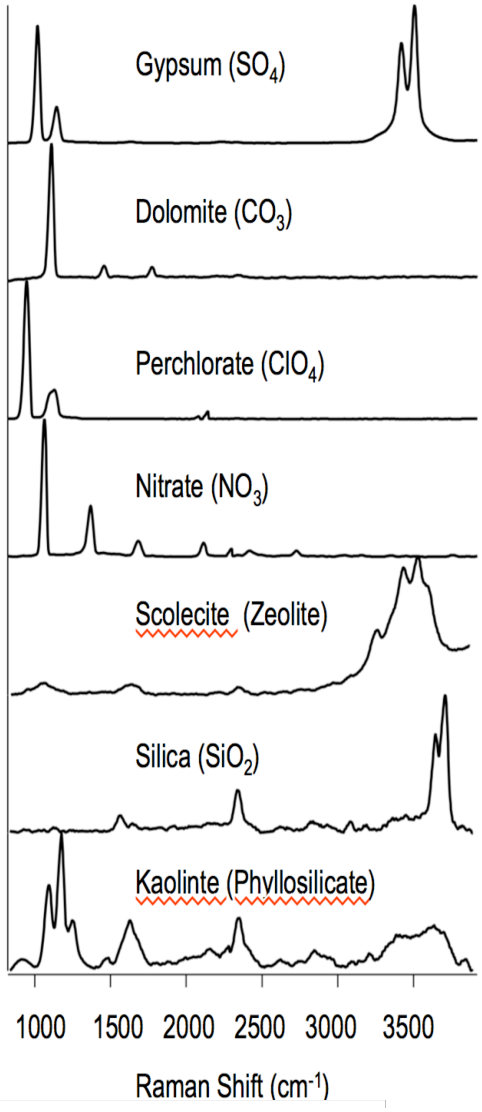

Figure 1 (above): Figure 1 (above) Raman Spectra of minerals of astrobiological importance and indicators of water activity that are targeted by the SHERLOC Raman Spectrometer.

Figure 2 (Right) Raman and fluorescence spectra demonstrating organic molecule detectability. These spectra including organics ranging from PAHs (polyaromatic hydrocarbons), condensed carbon, and proposed mars carboxylic acids. In the SHERLOC investigation, these Spectra are obtained on the same CCD at the same 100 micron condensed spot that is then related to images obtained by the SHERLOC imaging system.

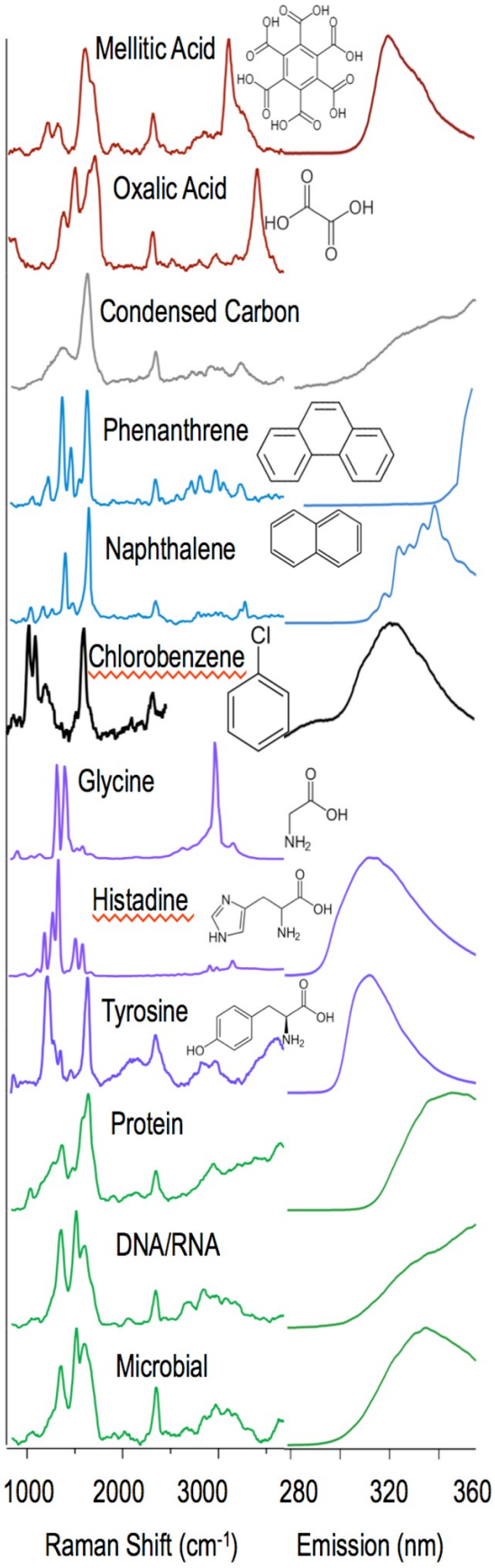

MASTCAM-Z: DESIGNING A GEOLOGIC, STEREOSCOPIC, AND MULTISPECTRAL PAIR OF ZOOM CAMERAS FOR THE NASA MARS 2020 ROVER. J. F. Bell III[1], J. N. Maki[2], G.L. Mehall[1] , M.A. Ravine[3], M.A. Caplinger[3], and the Mastcam-Z Team. [1]Arizona State Univ., Tempe, AZ (Jim.Bell@asu.edu); [2]JPL/Caltech, Pasadena, CA; [3]Malin Space Science Systems, Inc., San Diego, CA.

Introduction: The Mast Camera Zoom (Mastcam-Z; [1,2]) is a stereoscopic, multispectral imaging investigation selected for flight on the Mars 2020 rover mission. The cameras and their associated electronics and software are being designed and developed primarily at Malin Space Science Systems, Inc. (MSSS) and associated subcontractors, under the academic leadership of Arizona State University and in cooperation with the Mars 2020 Payload Office at JPL.

The Mastcam-Z instrument hardware and software have very high heritage from the Mastcam instruments on the MSL *Curiosity* rover, and the operations strategy will leverage heavily the experience and lessons learned from both MSL/Mastcam and MER/Pancam. We passed our PDR in late 2015 and are preparing for CDR in late 2016 and delivery in mid-late 2018. In this presentation we review our science goals and requirements and describe our CDR-level design and operational plans. Additional high-level details about the development of Mastcam-Z can be found in [1-3].

Science Goals: The Mastcam-Z investigation goals and objectives respond directly to Objectives A-D of the Mars 2020 mission [4,5]. Specifically, the primary goals of Mastcam-Z are:

Goal 1: *Characterize the overall landscape geomorphology, processes, and the nature of the geologic record (mineralogy, texture, structure, and stratigraphy) at the rover field site.* Mastcam-Z observations will provide a full description of the topography, geomorphology, geologic setting, and the nature of past and present geologic processes of the Mars 2020 field site, especially as they pertain to habitability and other astrobiology topics [6]. This includes observations of rocks and outcrops to help determine morphology, texture, structure, mineralogy, stratigraphy, rock type, history/sequence, and associated depositional, diagenetic, and weathering characteristics. Meeting this goal also requires observations of regolith to help evaluate physical and chemical alteration, along with stratigraphy, texture, mineralogy, and depositional/erosional processes.

Goal 2: *Assess current atmospheric and astronomical conditions, events, and surface- atmosphere interactions and processes.* This will be achieved by Mastcam-Z observations of clouds, dust-raising events, properties of suspended aerosols (dust, ice crystals), astronomical phenomena, and aeolian transport of fines. This goal also encompasses characterization of potential ice- or frost-related (periglacial) geomorphic features, and even the characterization of frost or ice, if present, and its influence on rocks and fines.

Goal 3: *Provide operational support and scientific context for rover navigation, contact science, sample selection, extraction, and caching, and the other selected Mars 2020 investigations.* Mastcam-Z images will assist rover navigation by determining the location of the Sun and of horizon features, and by providing information pertinent to rover traversability (*e.g.*, distant hazards, terrain meshes, etc.). This goal also includes observations enabling other Mars 2020 science instruments to identify and characterize materials to be collected for in situ analyses, coring, and caching, or other purposes (*e.g.*, hardware monitoring).

Instrument Description: Mastcam-Z consists of an identical pair of zoom-lens cameras that provide images in broad-band Bayer red/green/blue (RGB), 11 unique narrow-band visible/near-infrared colors, and 4-color direct solar imaging, with fields of view (FOV) from ~5° to ~15°. The cameras will have the ability to resolve (across 4-5 pixels) features ~1 mm in size in the near field and ~3-4 cm in size at 100 m distance.

Each Mastcam-Z camera consists of newly-designed (compared to MSL) optics and associated focus, ~3:1 zoom, and 8-position filter wheel mechanisms, a CCD detector assembly that is identical to that used on MSL/Mastcam, and digital electronics cards (one per camera) and firmware that are nearly identical to those used on MSL. A newly-designed external passive color/grayscale calibration target, based on the MSL/Mastcam cal target design but enhanced based on lessons learned, will be mounted on the rover deck at a similar place as the MSL target. The two Mastcam-Z cameras will be separated by ~24.5 cm and mounted on the Mars 2020 rover's Remote Sensing Mast (RSM), which sits approximately 2 meters above the local surface.

References: [1] Bell *et al., Internat. Workshop on Instrum. for Plan. Missions,* Abstract #1151, 2014. [2] mars.nasa.gov/mars2020/mission/instruments/mastcam-z/ [3] www.planetary.org/explore/projects/mars-2020/ [4] mars.nasa.gov/mars2020/mission/overview/ [5] Mustard, J.F. *et al.* (2013) Report of the Mars 2020 Science Definition Team, http://mepag.jpl.nasa.gov/reports/MEP/Mars_2020_SDT_Report_Final.pdf. [6] Williford, K. and K. Farley, *Biosig. Pres. & Detec. in Mars Analog Env. Workshop,* Abstract #2070, 2016.

High-speed Pulsed Raman for Mapping of Minerals and Organics on a Microscopic Scale

Jordana Blacksberg[1], Erik Alerstam[1], Yuki Maruyama[1], Corey Cochrane[1], George R.Rossman[2]. [1]Jet Propulsion Laboratory, California Institute of Technology, 4800 Oak Grove Dr., Pasadena, CA 91109, [2]California Institute of Technology, Division of Geological and Planetary Sciences, Pasadena, California 91125, *Jordana.blacksberg@jpl.nasa.gov

Overview: We present a miniaturized planetary surface instrument for *in situ* identification and quantification of minerals and organics, with surface mapping capabilities on a microscopic scale. We have previously demonstrated the benefits of time-resolved Raman spectroscopy using spectra obtained on planetary analogs [1]. Recent technological advances in the high-speed pulsed Raman (HiPuR) spectrometer presented here have enabled further expansion in capabilities, encompassing a much wider range of samples. For example, with HiPuR it is possible to obtain diagnostic Raman spectra from samples exhibiting a large interfering background from short-lifetime fluorescence as well as from samples traditionally sensitive to damage.

Introduction: The High-speed Pulsed Raman (HiPuR) instrument builds on the widely used 532 nm (green) laser Raman technique, but uses *time gating* to separate out pervasive background interference caused by fluorescence (from minerals and organics) resulting in unambiguous Raman spectra as illustrated in Fig. 1. This fluorescence rejection capability ensures that every point measurement making up a Raman map yields a diagnostic spectrum, unlike conventional methods where many spectra are unusable because of fluorescence [*e.g.* see ref. 2]. In addition to fluorescence rejection, time-gating also enables operation in daylight conditions without the need for light shielding, an important factor, especially for power-constrained missions where measurements are only feasible during the warmer daylight hours.

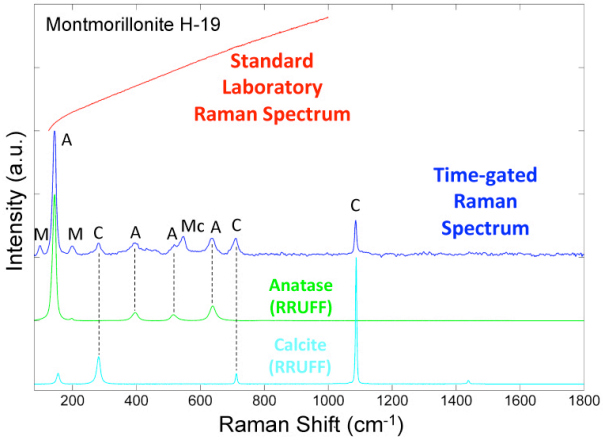

Figure 1. Time-gated Raman spectrum (dark blue) of a highly fluorescent phyllosilicate sample measured by our 1024 x 8 time-gated SPAD detector. Minerals identified are (M) montmorillonite, (A) anatase, (Mc) mica clay, and (C) calcite. This spectrum could not be obtained without time-gating as evidenced by the overwhelming fluorescence background visible in the standard laboratory Raman spectrum (shown in red with a different intensity scale for clarity).

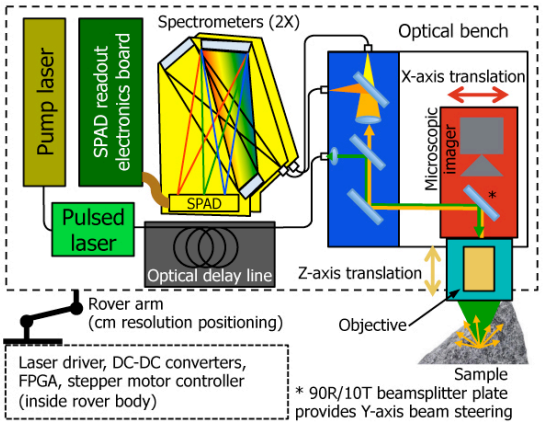

Figure 2. Block diagram of the prototype High-Speed Pulsed Raman Spectrometer.

Fig. 2 shows the overall instrument architecture as it would be mounted on a rover or lander arm. Modular design allows for straightforward adaptation to a broad range of missions with different accommodation requirements. The ability to perform high-speed pulsed Raman spectroscopy in a miniaturized arm-mounted package can be attributed to two key enabling technologies: a sub-ns time-gated single photon avalance diode (SPAD) detector synchronized with a High-speed Microchip (HMC) laser capable of emitting ~100 ps pulses at repetition rates as high as several MHz. We focus in particular on the design of the HMC lasers currently under development, and their optimization with SPAD detectors.

Custom time-gated detectors: The high-speed pulsed Raman spectrometer relies on two custom time-gated 1024 x 8 pixel arrays of Single Photon Avalanche Diode (SPAD) arrays operated in single photon counting mode and capable of sub-ns time gating down to 700 ps [3], each paired with a spectrometer to cover the complete spectral range in Raman shift from ~100 cm^{-1} to 4000 cm^{-1}. Because the SPAD is a solid state detector, it offers a significant reduction in size, weight, power, and complexity when compared to traditional photocathode-based detectors such as streak cameras that have until now been the only technology available for achieving sub-ns time resolution. This

means that fast time-gating has now become feasible for planetary surface missions, offering the enhanced science return associated with fluorescence rejection and daylight rejection, with minimal added complexity.

The time-gating process is illustrated in Fig. 3. The detector collects returned light only during the time gate. In order to get the maximum benefit from fluorescence rejection, the detector and laser can be synchronized to line up the laser pulse near the falling edge of the detector gate. In that way, the time resolution of the instrument can be approximated as the laser pulse width.

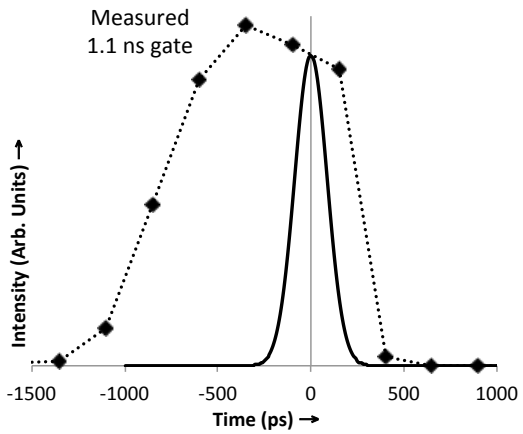

Figure 3. Illustration of the time-gating process shown for a 1.1 ns SPAD time gate and a 200 ps laser pulse. In the early gating scheme, the gate begins before the laser pulse in order to maximize fluorescence rejection. Note that the SPAD cannot produce an ideal rectangular gate, but rather has a 250 ps fall time which reduces the ultimate time resolution slightly.

High-speed microchip lasers: At the heart of our most recent advancement is the high-speed microchip (HMC) laser, a passively Q-switched diode-pumped solid state (DPSS) laser built in-house and based on a laser microchip from BATOP Gmbh with a novel semiconductor saturable absorber [4-6]. This laser offers significant advantages over conventional passively Q-switched DPSS lasers, in particular shorter pulses, higher repetition rates, and electrically tunable output power. In this way we can improve the instrument sensitivity by increasing the repetition rate, which allows for lower peak power on the sample for any given average power. This means that the laser power on the sample can be increased without inducing sample damage. We can use the electrical tunability to adjust the power on the sample for optimal return. The narrower pulse width provides improved time resolution, beneficial for samples with short lifetime fluorescence.

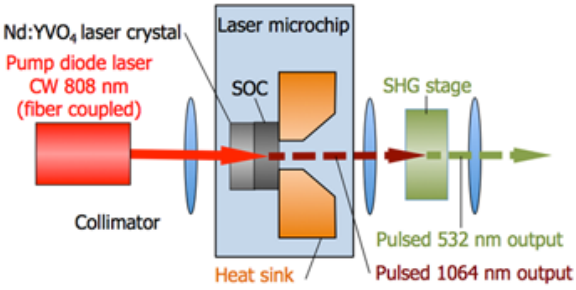

Figure 4. Laser architecture for the high-speed microchip laser.

Applications for future NASA missions: By combining capabilities for the identification of minerals present in geological materials, with capabilities to detect organic matter, laser Raman spectroscopy is a compelling technique for landed missions targeting rocky and icy bodies. Raman is non-destructive, requires no sample preparation, and is well suited for deployment on a lander or rover arm. In combination with micro-scale imaging, Raman can directly interrogate rocks and regolith materials, while placing compositional analyses within a microtextural context. The combination of these advantages of Raman spectroscopy combined with the fluorescence and daylight rejection capabilities of HiPuR makes this an ideal instrument for future robotic exploration of planetary surfaces at a wide range of Discovery, New Frontiers, and Flagship class mission destinations, including asteroids, comets, the Moon, Mars, Venus, Europa, and Titan.

References: [1] J. Blacksberg *et al.* (2016) *Applied Optics*, 55(4), 739-748. [2] Frosch et al. (2007), *Anal. Chem.* 79, p.1101 [3] Y. Maruyama *et al.* (2014) *IEEE JSSC*, 49 (1) [4] B. Bernard *et al.(2014), Proc. of SPIE* Vol. 8960 [5] E. Mehner *et al.* (2013) *Appl. Phys. B*, 112, 231-239 [6] A. Steinmetz *et al.* (2009), *Appl. Phys. B*, 97, 317-320

Acknowledgement: The research described here was carried out at the Jet Propulsion Laboratory, California Institute of Technology, under a contract with the National Aeronautics and Space Administration (NASA). Funding for this work is provided by the NASA Planetary Instrument Concepts for the Advancement of Solar System Observations (PICASSO) Program. Continuous-wave Raman measurements were per-formed at the Mineral Spectroscopy Laboratory at the California Institute of Technology. SPAD development was performed at Delft University of Technology by the group of Professor Edoardo Charbon.

THE MAPPING X-RAY FLUORESCENCE SPECTROMETER (MAPX). David Blake[1], Philippe Sarrazin[2], Thomas Bristow[1], Robert Downs[3], Marc Gailhanou[4], Franck Marchis[2], Douglas Ming[5], Richard Morris[5], Vicente Armando Solé[6], Kathleen Thompson[2], Philippe Walter[7], Michael Wilson[1], Albert Yen[8] and Samuel Webb[9], [1]NASA Ames Research Center, Moffett Field, CA - david.blake@nasa.gov, [2]SETI Institute, Mountain View, CA, [3]Univ. of Arizona, Tucson AZ, [4]IM2NP, Université Paul Cézanne, Marseille, France, [5]NASA Johnson Space Center, Houston, TX, [6]ESRF, Grenoble, Fr, [7]Université Pierre et Marie Curie, Paris, Fr., [8]JPL, Pasadena, CA, 9SLAC, Stanford, CA.

Introduction: Many planetary surface processes leave traces of their actions as features in the size range 10s to 100s of μm. The Mapping X-ray Fluorescence Spectrometer (MapX) will provide elemental imaging at ≤100μm spatial resolution, yielding elemental chemistry at a scale where many relict physical, chemical, or biological features can be imaged and interpreted in ancient rocks on Mars or on the surfaces of other planetary bodies/planetesimals.

MapX: MapX is an arm-based instrument positioned on soil or regolith with touch sensors. During an analysis, an X-ray source (tube or radioisotope) bombards the sample with X-rays or α-particles / γ-rays, resulting in sample X-ray Fluorescence (XRF). X-rays emitted in the direction of an X-ray sensitive CCD imager pass through a 1:1 focusing lens (X-ray μ-pore Optic (MPO)) that projects a spatially resolved image of the X-rays onto the CCD. The CCD is operated in single photon counting mode so that the energies and positions of individual X-ray photons are recorded. In a single analysis, several thousand frames are both stored and processed in real-time. The MapX concept is illustrated in Fig. 1.

Higher level data products include single-element maps with a lateral spatial resolution of ≤ 100 μm and quantitative XRF spectra from ground- or instrument-selected Regions of Interest (ROI). XRF spectra from ROI are compared with known rock and mineral compostions to extrapolate the data to rock types and putative mineralogies.

Proof of concept prototypes: Earlier prototypes [1-3] demonstrated proof-of-concept using COTS components. MapX-II (Fig. 2) utilizes an Andor iKon M camera with 1024x1024 back illuminated deep depletion CCD. Two 40kV-4W Au target transmission window X-ray tubes (Moxtek) illuminate the sample. An MPO X-ray focusing lens (PHOTONIS) is placed equidistant between the sample location and the CCD. The lens derives from "lobster-eye" multichannel optics used for X-ray astronomy [4]. It is implemented here in a flat geometry for 1:1 focusing. This lens provides a much improved aperture when compared to pin-hole camera optics having similar spatial resolution, and true focusing when compared to polycapillary collimating optics also used for X-ray mapping. The camera is driven at up to 3 frames per second, and the X-ray sources are shuttered during read cycles.

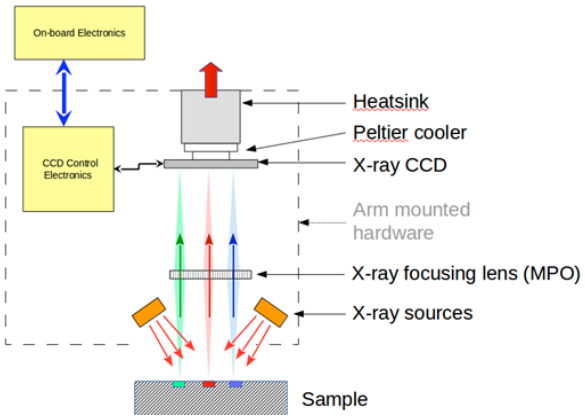

Fig. 1: Schematic drawing of the MapX concept.

Other work in progress:

Development of data processing software. The instrument collects a large number of short acquisitions that are combined into X-Y-time data cubes. Python code was developed for processing raw CCD data from the prototypes. This code includes background correction, split charge removal and optional binning features. The resulting X-Y-energy data cubes are stored in HDF5 format and quantified with PyMca [5] using fundamental parameters methods.

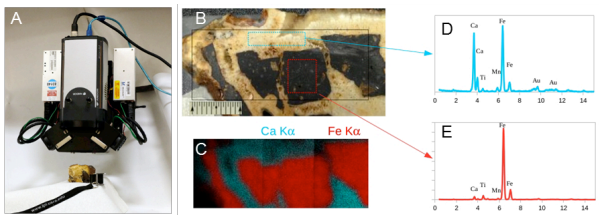

Fig. 2. MapX-II Prototype. A) MapX-II in position to analyze a rock sample. B) Optical image of sample composed of basalt fragments and light-toned cement (scale in mm). C) FeKα/CaKα map obtained by tiling 3 analyses of 1000s integration. D-E) XRF spectra of ROI chosen from the MapX-II image shown in "C."

Characterization and correction of the MPO Point Spread Function (PSF). The MPO lens causes a signal spread on the detector that must be corrected for optimum spatial resolution. The PSF varies with photon energy and with X-Y position due to morphological or stacking defects of the micro-channels. Experiments are being performed at the Stanford SSRL to character-

ize the PSF, and ray-tracing models of the MPO have been developed in parallel to evaluate the effects of various types of defects on the PSF and to assist in the development of PSF deconvolution algorithms [6] (e.g., Fig. 3). Figure 4 shows results in which a deconvolution algorithm based on an observed PSF was applied to data from an imaging standard.

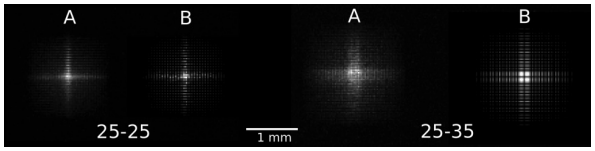

Fig. 3. Comparison of MPO PSF data (A) collected at SSRL BL2-3 and (B) obtained by ray tracing simulations at a nominal CCD-MPO distance of 25mm. Left: sample in focus (25-25); Right: sample out of focus by 10mm (25-35). A 10 mm defocus condition results in a point resolution decrease of ~100 μm.

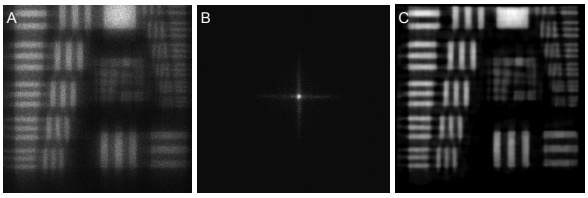

Fig. 4. MapX PSF Deconvolution Example (1951 USAF resolution standard, Cr on glass). A) Original image. CrKα, taken with MapX-II (MPO-CCD, MPO-Target = 50 mm). The resolution of this image is estimated to be 200μm. B) Measured PSF from the SLAC experiment (FWHM ~165μm). C) AIDA [6] deconvolution with automatized cost function parameters (resolution ~160 μm).

X-ray and γ-ray/α-particle radioisotope source requirements. Source requirements for MapX are determined through Monte Carlo modeling and experiment. XMIMSIM [7], GEANT4 [8] and PyMca [5] are being used along with a dedicated XRF test fixture to determine detection limits and accuracy/precision for elements of interest. Preliminary results indicate that either a 3W X-ray tube source, or a 30mCi ^{244}Cm radioisotope source (as carried on the APXS instruments) will be sufficient to meet MapX science objectives.

Development of high-TRL MapX components. In parallel with method development and laboratory and field prototype refinement, engineering efforts are being pursued to increase the TRL of the instrument. MapX-III (Fig. 5) is being built with a CCD224 imager (MSL CheMin heritage) driven by dedicated CCD electronics using flight design standards. The new camera prototype will demonstrate the basic architecture of a flight camera for an arm mounted instrument and will serve a base for an in-vacuum MapX prototype to characterize the system capabilities at the low X-ray energies (e.g., Kα lines for Na) that are absorbed in the in-air current prototypes.

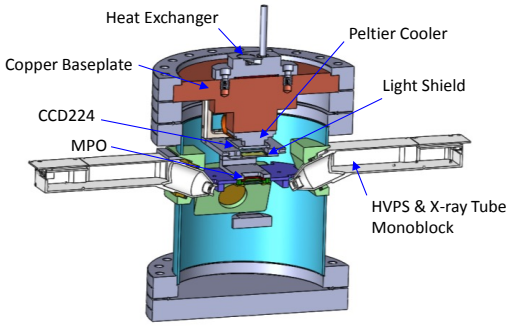

Fig. 5. TRL-4 MapX-III prototype with X-ray tube sources, MSL CheMin heritage CCD224 CCD package, exchangeable MPO and modifiable geometry.

Flight instrument concept: Fig. 6 shows a conceptual illustration of an arm-deployed MapX instrument (with X-ray tube sources). Replacing X-ray sources with radioisotope sources would reduce the mass by 1 kg. and the power by 10W. Not shown is a Rover Avionics Mounting Platform (RAMP) unit that houses the Control and Processing Electronics (CPE).

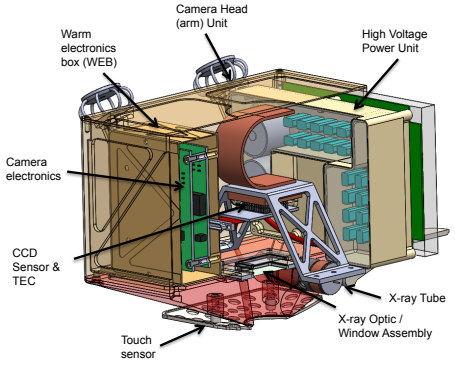

Fig. 6. Notional Flight configuration of MapX Arm Unit (X-ray Tube version) enclosing the Camera Head Electronics (CPE).

References: [1] D.F. Blake et al. (2014) IPM-2014, #1080. [2] D.F. Blake et al. (2015) LPSC XLVI #2274. [3] P. Sarrazin et al. (2016) LPSC XLVII #2883. [4] G. W. Fraser et al. (2010) Planet. Space Sci. 58 (1-2), 79–95. [5] V.A. Solé, et al. (2007) Spectrochim. Acta B 62 63-68. [6] Hom, E.F.Y. et al. (2007) *J. Opt. Soc. of America. A,* 24(6), pp. 580–600. [7] Schoonjans T. et al. (2012) *Spectrachim. Acta Part B, 70*, 10-23. [8] Agostinelli, S. et al. (2003) *Nucl. Instr. and Methods in Phys. Res. A*, **506**, 250-303.

Acknowledgements: DB is grateful for support from NASA/ARC's Center Innovation Fund and NASA's PICASSO program (grant # NNX14AI28A).

EUROPA HABITABILITY AND EXTANT LIFE EXPLORATION WITH COMBINED FLYBY-LANDER-ORBITER MISSION. M. Blanc[1], G. Jones[2], O. Prieto-Ballesteros[3], D. Mimoun[4], A. Masters[2], S. Kempf[5], L. Iess[6], Z. Martins[7], R. Lorenz[8], J. Lasue[9], N. Andre[1], B. G. Bills[10], G. Choblet[11], G. Collins[12], G. Cremonese[13], P. Garnier[14], K. Hand[10], P. Hartogh[15], K. K. Khurana[16], K. Stephan[17], F. Tosi[18], S. D. Vance[10], T. van Hoolst[19], F. Westall[20], M. Wolwerk[21], J. F. Cooper[22], E. C. Sittler[22], W. Brinckerhoff[22], T. Hurford[22] and *the Europa Initiative*, [1]L'Institut de Recherche en Astrophysique et Planétologie (IRAP), CNRS/Université Paul Sabatier, 9 avenue du colonel Roche, 31028 Toulouse, France (e-mail: michel.blanc@irap.omp.eu), [2]Mullard Space Sciences Laboratory, University College London, United Kingdom, [3]Center for Astrobiology, INTA-CSIC, Spain, [4]Airbus, Toulouse, France, [5]LASP, University of Colorado at Boulder, Boulder, Colorado, [6]Università di Roma Sapienza, Rome, Italy, [7]Imperial College London, London, United Kingdom, [8]Applied Physics Laboratory Johns Hopkins University, Laurel, Maryland, [9]Observatoire Midi-Pyrenees IRAP, Toulouse, France, [10]Jet Propulsion Laboratory, Pasadena, California, [11]Laboratoire de Planétologie et de Géodynamique, Université de Nantes, France, [12]Wheaton College, Norton, Massachusetts, [13]INAF, Osservatorio Astronomico di Padova, Padova, Italy, [14]Université de Toulouse, Toulouse, France, [15]P. Hartogh, Max Planck Institüt für Solar System Research, Katlenburg-Lindau, Germany, [16]Krishan K. Khurana, University of California at Los Angeles, Los Angeles, California, [17]DLR, Institute of Planetary Research, Berlin, Germany, [18]INAF-IAPS, Rome, Italy, [19]Royal Observatory of Belgium, Brussels, Belgium, [20]CNRS-Centre de Biophysique Moléculaire, Orleans, France, [21]Space Research Institute, Austrian Academy of Sciences, Graz, Austria, [22]NASA Goddard Space Flight Center, Greenbelt, Maryland (e-mail: John.F.Cooper@nasa.gov).

1. Introduction. Complementary to the on-going intensive effort by NASA to design an ambitious Europa Lander mission which will focus on the search for life, we describe the important potential benefits of adding scientific investigations performed in Europan orbit as well as by the NASA flyby mission. This can be done by operating scientific instruments either directly on the carrier/relay platform of the lander mission, or on an additional small orbiter platform which will fly to Jupiter and Europa together with the main spacecraft.

2. Measurements. A combination of gravity, magnetic field and plasma instruments, possibly augmented by an altimeter and/or a neutral and ion mass spectrometer, operating in conjunction with magnetic field and gravity/geodesy experiments on the lander platform, will open the way to an in-depth characterization of Europa as a geophysical object made of a set of coupled layers. These layers include the core, mantle, ocean, ice crust, neutral atmosphere, ionosphere, and local magnetospheric environments. Orbital measurements would be optimized to investigate responses to periodic forcing of the Europa multi-layer system at key time scales, 85 hours for the moon's orbital motion around Jupiter and 11 hours for magnetospheric corotation relative to the moon. The deepest probes of the ocean and the lower layers would require several months of continuous observations in low-altitude orbit. This mission duration is possible due to more favorable radiation environment in moon orbit as compared to elsewhere in Europa's orbit around Jupiter.

3. Flyby-Orbiter-Lander Combined Campaign. Best results for exploration of the habitability of this ocean moon, as combined with the lander's search for life, would come from orbital measurements contemporaneous with the 45 flybys of the Europa Multiple Flyby Mission that would likely launch earlier but on a slower trajectory to Jupiter and Europa. Synchronicity of orbiter and flyby measurements can provide a powerful combination, e.g. changes of state in external magnetospheric environment for each flyby can be correlated to orbiter measurements to extract information on intrinsic response of the moon layers as compared to external forcing. Maximum sensivity to ocean depth and thickness, and to magnetic properties of the core, would come from joint flyby, lander, and orbiter measurements. The intrinsic chemical composition of Europa can be better separated from that due solely from the external interactions, i.e. the thin patina of materials passed to the moon surface through the jovian magnetosphere from Io volcanic emissions. Environmental conditions at the landing site would be best characterized by the combined campaign.

The tantalizing prospect of water plume emissions would also be best addressed by the orbiter-flyby combined observational campaign. *There would be no need to wait two weeks for the next flyby to follow up on a plume emission detection.* Smaller plumes would likely be more frequent and easier to detect with the orbiter, while remote imaging during flybys would provide the more global perspective for large plumes.

4. Conclusions. Europa with its putative modern ocean is potentially promising as a habitat for extant and future life, as Mars may have been for past life. Europa's multi-layered responses to external gravitational, magnetic, and plasma forcing can best be investigated with a combined mission campaign, as the lander searches for signs of life in-situ, and with excellent prospects for international collaboration.

ULTRA COMPACT IMAGING SPECTROMETER. D. L. Blaney[1], R.O. Green[1], P. Mouroulis[1], B.L. Ehlmann[1,2], B. Van Gorp[1], I. McKinley[1], Jose Rodriguez[1], A. Lamborn[1], J. M. Haag[1], M. Cable[1]. [1]Jet Propulsion Laboratory, 4800 Oak Grove Drive, Pasadena, California, 91109 (Diana.L.Blaney@jpl.nasa.gov) [2]Division of Geological & Planetary Sciences, California Institute of Technology, 1200 E. California Blvd., Pasadena, California, 91125.

Summary: The Ultra Compact Imaging Spectrometer (UCIS) [e.g. 1,2] is a visible to short wavelength infrared (VSWIR) imaging spectrometer with a modular architecture (Figure1). It is possible to adapt the instrument details to a variety of mission concepts requiring low mass and low power. Imaging spectroscopy is an established technique to address complex questions of geologic processes by mapping diagnostic absorption features due to minerals, organics, and volatiles throughout our solar system. At the core of UCIS is an Offner imaging spectrometer using M^3 heritage spectrometer and a miniature pulse tube cryo-cooler developed under the NASA Maturation of Instruments for Solar System Exploration (MatISSE) program to cool the focal plane array. The TRL 6 integrated spectrometer and cryo-cooler provide a basic imaging spectrometer capability that is used with a variety of fore optics to address surface mission science goals (e.g. lunar, Mars, small bodies). Potential configurations include: remote sensing from small orbiters and flyby spacecraft; in situ panoramic imaging spectroscopy; and in situ micro-spectroscopy. An integrated spectrometer / micro-cooler / micro-spectroscopy front end is being developed using MatISSE funding.

Reflectance Imaging Spectroscopy: Reflectance imaging spectroscopy is a non-destructive technique for remote mineral identification and mapping of distribution by measuring the reflected light from a surface. Compositional mapping enables the linkage of mineral assemblages to specific locations where geological processes are occurring. Reflectance spectroscopy is an established technique with well-developed spectral libraries and theoretical basis. A wide range of material can be identified and mapped including igneous and sedimentary minerals, ices, volatiles, and organics. It has been successfully used on a wide range of objects ranging from Mercury, the Moon, Mars, asteroids, comets and the outer solar system planets and moons. The technique works at all spatial scales ranging from 100's of kilometers to 10's of microns [5].

UCIS Modular Architecture: The utility of imaging spectroscopy given the range of materials it can measure, the range of spatial scales, and the types of bodies it can be use on makes development of a single instrument challenging. Science requirements, wavelength ranges, platform and the object itself provide distinct instrument requirements. The need for small instruments for in situ and small spacecraft also drive optimization. To develop a technology that works for a such a wide range of applications, for UCIS we adopted modular architecture approach. The desired science, target, and platform then feed into choices for the thermal design, spectrometer design, and optical design. Several variations have been recently proposed for flight. Including:

- Min Map: Panoramic, Mars (Blaney, PI): Mars 2020, CAT 1 (Cryo-cooler, Spectrometer, Panoramic)
- CIMMBA: Micro, Mars (Ehlmann, PI): Mars 2020, CAT 1 (Cryo-cooler, Spectrometer, Microscopic)
- M6 on Merlin Phobos Discovery Proposal (Murchie, PI) (not selected) (Cryo-cooler, Spectrometer, Microscopic)
- Korean Pathfinder Lunar Orbiter (KPLO) mission RFI (Morgan Cable, JPL Lead) (Cryro-cooler, spectrometer, telescope)

References: [1] Van Gorp et al. (2011) Proc. SPIE. 8158, Imaging Spectrometry XVI [2] Van Gorp et al. (2014) J. Appl. Remote Sens. 8(1), 084988 doi:10.1117/1.JRS.8.084988 [3] Ehlmann et al. (2016) This meeting.

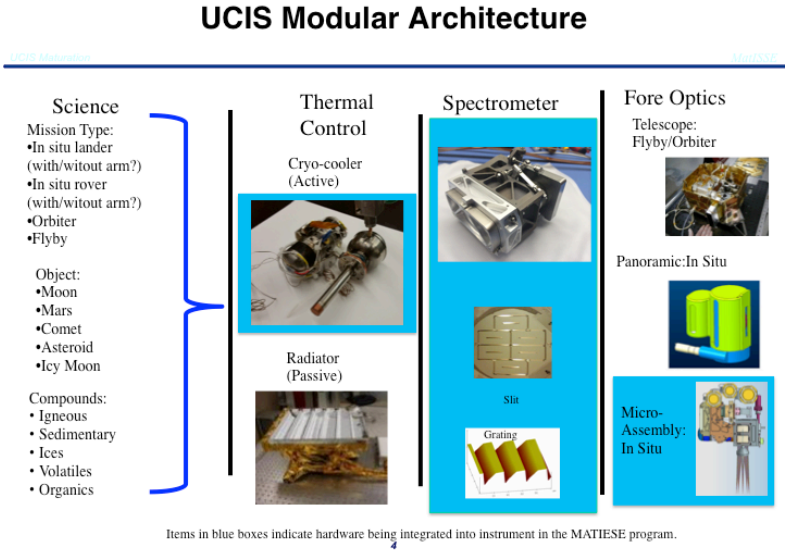

INSTRUMENT TRADE STUDY AND DESIGN FOR MID TO FAR-IR ATMOSPHERIC REMOTE SENSING OF AN OUTER SOLAR SYSTEM PLANET BASED ON HIGH TEMPERATURE BOLOMETERS. E. C. Brageot[1], M. A. Lindeman[1] and G. Orton[1]. [1]NASA-Jet Propulsion Laboratory, California Institute of Technology, 4800 Oak grove Drive, Pasadena CA 91109, Emily.C.Brageot@jpl.nasa.gov, Mark.A.Lindeman@jpl.nasa.gov.

1. Introduction: The study of the atmospheres of giant planets their satellites such as Saturn, Titan, Uranus or Neptune requires a wide range of wavelengths to probe different depths into the atmosphere, with longer wavelengths generally able to peer to greatest depths. The atmospheres of these bodies are opaque at shorter wavelengths due to the broad pressure-broadened absorption of H_2 and He and, in some cases (e.g. Neptune and Titan), CH_4 and N_2. For this reason, the composition of the atmosphere of the gas and ice giants and their satellites has been studied by remote sensing using far-IR thermal radiance spectroscopy. In addition, new science would be unlocked by imaging fast dynamic processes, such as moving clouds or storms, while resolving narrow and weak spectral features to detect their composition as they are moving in the atmosphere.

Performing these studies requires a high sensitivity, high-spectral and -spatial resolution instrument capable of acquiring spectra in a short time window. Such an instrument would be ideally installed on-board an orbiting or fly-by spacecraft in the outer solar system and provide the next generation of Cassini CIRS-like measurements.

Recent advances in the yttrium barium copper oxide (YBCO) high temperature superconducting kinetic inductance bolometers (KIBs) and their development into pixel arrays have enabled the design study of such an instrument. These detectors have multiple advantages for the considered science applications including a high sensitivity over a wavelength range potentially spanning from the visible to the far Infra-Red (500microns) and a fairly high operation temperature of 50K which opens up the possibility of a passively cooled instrument considering its use in the outer solar system. Furthermore, these capabilities would allow us to merge the three separate channels of the CIRS instrument to obtain a smaller instrument with a 2-dimension array of pixels instead of line arrays, and with a two orders of magnitude higher predicted sensitivity.

In this paper, I will first present the design trade study based on both science goals and the projected performance of the YBCO KIBs array through radiometric modelling and how that led us to the concept of an on-orbit or fly-by mid- to far-Infra-Red Fourier Transform Imaging spectrometer design for outer planets of the Solar System. I will then present its current optical design and main instrument parameters as well as the remaining challenges of its design.

2. Science goals and trade-off study: The ideal instrument we are envisioning would be able to characterize the methane cycle, D/H and He/H_2 ratios and atmospheric dynamics of these outer solar system bodies. The equivalent black-body temperatures of these planets range between 50 and 100K, which corresponds to peak wavelengths between 30 and 60µm. The He/H_2 ratio measurement corresponds to tracking the shape of a spectral continuum and therefore does not require high spectral resolution [1]. On the other hand, trace constituents such as CH_4, NH_3 and PH_3 display sharp spectral features that require a spectral resolution of at least $0.5cm^{-1}$ to resolve different emission bands and retrieve mixing ratios accurately [2]. A higher spectral resolution of $0.1cm^{-1}$ adds further insight to the H/D ratio measurements in methane by singling out isolated lines of CH_3D and CH_4 whose ratio can be used to eliminate uncertainty on the abundance of CH_4 [3,4].

An on-orbit instrument wavelength range of 20 to 100µm (100 to $500cm^{-1}$) with a spectral resolution better than $0.1cm^{-1}$ would therefore enable these measurement with a high spatial resolution. A radiometric model of the Signal-to-Noise Ratio (SNR) in the case of Titan showed this design is possible with an all reflective Fourier Transform Imaging Spectrometer using YBCO KIBs arrays, and would yield a predicted spectra SNR value of 2960 for an equivalent scene black body temperature of 90K while keeping the instrument volume as small as possible.

3. Current instrument parameters and optical design: The instrument parameters were set by both the detector performance, the desired IFOV and spectral resolution, and the need for a compact design. All of these were input and balanced out using the afore mentioned radiometric model and yielded the results listed in table 1.

Instrument parameter	*Value*
IFOV	1 mrad
FOV	2.86x2.29 deg

F-number	11.2
Focal length	1000 mm
Spectral resolution	0.1 cm^{-1}
Complete spectra acquisition time	200s
Modelled Spectra SNR for 90K scene	2960

Tab 1- Main instrument parameters.

Due to the large wavelength range to cover, the optical design is all-reflective and therefore both achromatic and isothermal save for the synthetic diamond beam splitter [5]. Both the telescope design and the focusing optics are off-axis to avoid having a central obscuration that would lower the SNR of the instrument.

The optical design illustrated in Figure 1 is kept as compact as possible by using a corner cube mirror as the moving mirror. This effectively shortens the needed travel of the mirro by a factor 2.

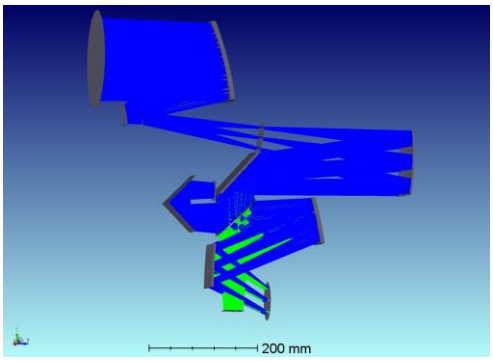

Fig 1- 3D rendering of the interferometer optical design. The 2-mirror telescope can be seen on top the image while the detector is at the bottom right. The corner cube moving mirror can be seen in the middle left of the image. The two paths of the light in the interferometer part of the instrument are represented in blue and green.

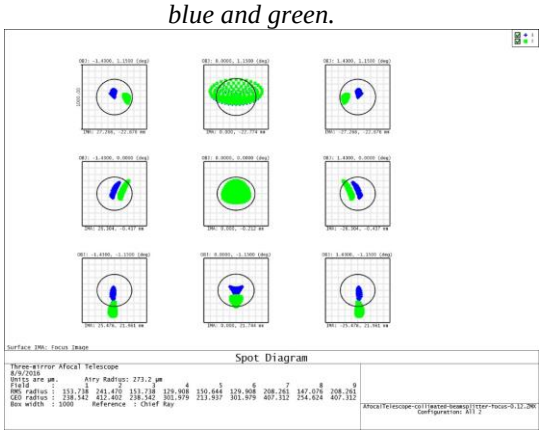

Fig 2- Spot diagram of the interferometer optical design. The blue and green color correspond to the image spots at extreme positions of the moving mirror while the box size corresponds to the pixel size.

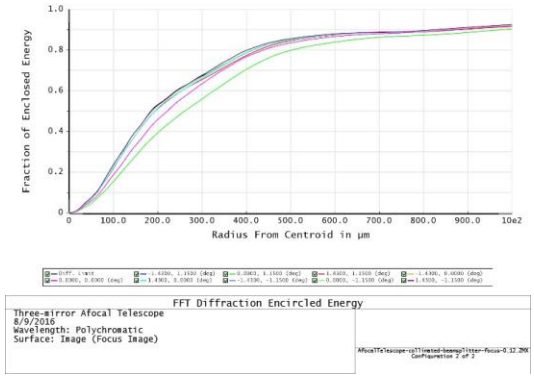

Fig 3- Diffraction encircled energy of the interferometer optical design across the Field Of View.

3. Remaining challenges: Several challenges remain for the complete design of this instrument concept. Firstly, the optical aberrations over the FOV vary a lot due to the off-axis design, a study of the variation of the spectral resolution across the FOV will be done to quantify them and attempt to calibrate them out. Second, the large FOV will make the baffling design a challenge even though the telescope image plane is accessible for a stop to be installed. Thirdly, the YBCO KIBs currently have a fill ratio of 50%. We are thus pursuing options to focus the light with an addtionnal array on top of the detector plane to be able to use all the incoming light beam. Finally, we are investigating the passive thermal designs available to this instrument.

References:

[1] P. G. J. Irwin. (2009) Giant Planets of Our Solar System : Atmospheres, Composition and Structure. Springer-Praxis, 427 pp.

[2] S. Vinatier et al. (2010), *Icarus*, Volume 205, Issue 2, 559-570.

[3] G. Orton (1992), *Symposium on Titan, ESA SP-338, pp. 81–85.*

[4] O. Mousis (2002), *Icarus*, 159, 156-165.

[5] J. Brasunas et al. (1998), *Applied Optics, Vol. 37, no19, 4226-4229.*

The Past, Present and Future for the Linear Ion Trap Mass Spectrometer (LITMS) and Related Ion Trap Instrumentation. W. Brinckerhoff[1], A. Grubisic[2], R. Danell[3], F. van Amerom[4], V. Pinnick[5], X. Li[5], R. Arevalo[1], S. Getty[1], M. Trainer[1], P. Mahaffy[1], P. Chu[6], K. Zacny[6], S. Rogacki[7], [1]NASA Goddard Space Flight Center (8800 Greenbelt Road, Mailstop 699, Greenbelt, MD 20771) william.b.brinckerhoff@nasa.gov; [2]CRESST, University of Maryland at College Park, College Park, MD ; [3]Danell Consulting, Inc., Winterville, NC; [4]Mini-Mass Consulting, Hyattsville, MD; [5]Center for Research and Exploration in Space Science and Technology (CRESST), University of Maryland, Balti- more County, Baltimore, MD; [6]Honeybee Robotics Spacecraft Mechanisms Corp., New York, NY; [7]Space Physics Research Laboratory (SPRL), University of Michigan, Ann Arbor, MI.

Introduction: Over the next decade, the in situ investigation and chemical characterization of high-priority planetary bodies will require progressively more compact and analytically capable payloads. From the Pioneer Venus Program in the 1970's up through the ongoing MSL and MAVEN missions, quadrupole mass spectrometer (QMS) systems have served as low-risk, cost-efficient means to explore the inner and outer reaches of the solar system. However, spaceflight QMS instruments are inherently limited, as they are designed for the analysis of volatile phases only, require high vacuum, and offer only a limited mass range (≤ 550 Da). Moreover, QMS sensors do not provide any detailed information regarding molecular structure. In contrast, ion traps enable the measurement of both volatile (via electron ionization, EI) and non-volatile (via laser desorption/ionization, LDI) compounds, operate under relaxed vacuum conditions (reducing pumping requirements) and can disambiguate molecular structures via tandem mass spectrometry and/or high mass resolving power.

Although traditional 3D ion traps have been operated on the International Space Station [1] and Rosetta's Philae Lander [2], the Mars Organic Molecule Analyzer (MOMA) on the ExoMars rover represents the first planetary application of a 2D (or linear-type) ion trap. The workhorse MOMA breadboard instruments have demonstrated the detection of ppmw-levels of nonvolatile organics embedded in geological materials, even in the presence of perchlorate salts, via LDI techniques [3]. The MOMA Engineering Test Unit (ETU), which simulates the form, fit and function of the flight model, has been shown to detect < pmol/mm^2 levels of analyte [4]. In order to further advance these capabilities of MOMA and its fundamental 2D ion trap architecture, a next-generation Linear Ion Trap Mass Spectrometer (LITMS) has been under development at NASA GSFC with support from the ROSES MatISSE Program.

The LITMS investigation is focused on the ability to conduct fine-scale organic and inorganic analyses of short (5 – 10 cm) rock cores, such as those that could be acquired by a drill-enabled robotic arm on a planetary lander or rover. Like MOMA, the LITMS investigation supports both pyrolysis/gas chromatograph mass spectrometry (GCMS) and laser desorption/ionization mass spectrometry (LDI-MS). However, unlike MOMA the LITMS instrument enables the compositional analysis of subsampled core fines. Further, LITMS offers an extended mass range (up to 2000 Da), high-temperature (up to 1300°C) evolved gas analysis and dual-polarity ion detection.

Current Status: The complete LITMS brassboard, including the sensor and mechanical housing (**Fig. 1**), pulsed laser system and RF power supply, is scheduled for integration in the late summer of 2016. Following the functional checkout of the system, the brassboard will be interfaced to the Precision Core Sampler (PCS) at Honeybee Robotics in Pasadena, CA, and the performance of the combined instrument will be verified under Mars relevant atmospheric conditions over the course of several dedicated integration and test campaigns. Following these campaigns, the brassboard will be returned to NASA GSFC and undergo vibration qualification (GEVS-levels) to reach TRL 6 maturity.

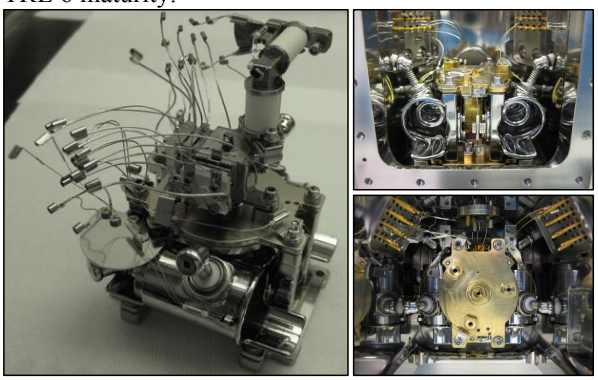

Fig. 1. (Left) LITMS ion trap subassembly, including electron ionization (EI) source with flying leads, shielded conversion dynodes, hyperbolic rods, and gas inlet. (Top right) Front view and (bottom right) overhead view of the ion trap subassembly (EI source removed for easier visual access) integrated into the LITMS mechanical housing.

Results: Initial testing of a LITMS prototype instrument was completed with both 700 kHz and 1.6 MHz RF supplies. Using these two frequencies, an *m/z*

range down to 18 Da in EI mode and up to >2000 Da in LDI mode as well as sub-unit mass resolution up to at least 500 Da has been demonstated (**Fig. 2**). Recently the flight-like dual frequency RF supply that will be used for final brassboard instrument testing has become available, and initial performance testing has been completed.

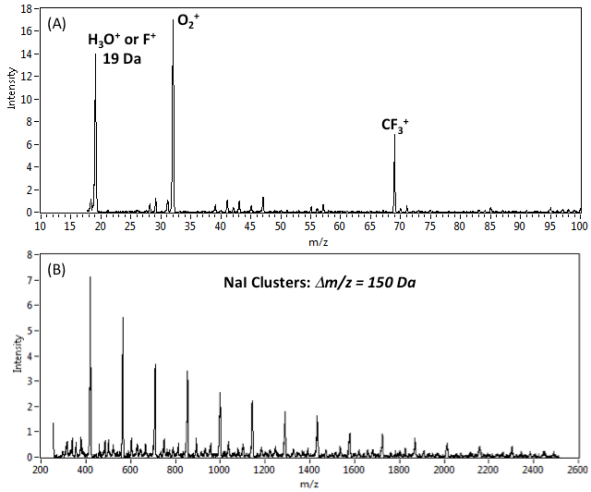

Fig. 2. (A) Low mass range GCMS spectrum of PFTBA with 1.6 MHz RF supply. (B) High mass range LDMS spectrum of NaI clusters with 700 kHz RF supply.

The detection of negative ions, particularly in LDMS mode, can provide complementary information and improve identification of electronegative species, containing elements such as S and Cl, as well as classes of organics (including several carboxylic and amino acids) that favor anion formation. This results in one ion polarity providing a significantly clearer mass spectrum than the other polarity, depending on the physicochemical properties of the compound under study (**Fig. 3**). Negative ion mode also allows the detection of the strong oxidant perchlorate (ClO_4^-), which has been measured at high levels (up to 0.7 wt.%) in the Martian soil by the Phoenix Mars Lander [5,6] and could have presented analytical challenges to the pyrolysis experiments on Viking and Phoenix [7], and may also do so on MSL.

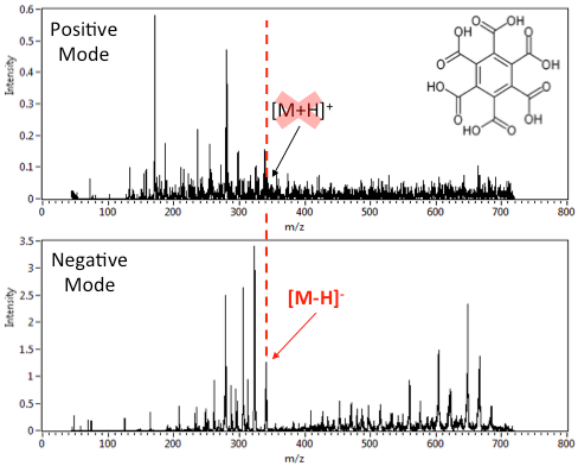

Fig. 3. Positive and negative mode spectra of mellitic acid demonstrating the clear detection and higher signal-to-noise in negative mode vs. positive mode.

Future Plans: Because mobile exploration of the surface and subsurface of the red planet is critical to address current and future astrobiology goals, the LITMS instrument will join the rest of the payload instruments on the Atacama Rover Astrobiology Drilling Studies (ARADS; PI: Brian Glass) project and be tested in the field in early 2017. This analog Mars mission, which is supported by the ROSES PSTAR Program, seeks to integrate and test progressively an innovative rover-drill system with a small collection of highly capable and technically mature scientific instruments. The scientific objective of the project is to understand the mobility and distribution of soluble salts, organic compounds, organic biomarkers, and life in extremely arid environments.

However, the application of the LITMS is not limited to Mars or remote terrestrial destinations. Rather, simple modifications to the gas processing subsystem and laser desorption ion inlet interface can adapt the LITMS instrument to the exploration of higher or lower pressure environments, including ultrahigh vacuum conditions found at Europa and Enceladus.

References: [1] Chutjian, A. et al. (2007) *SAE Tech Paper Series, 37th ICES*; [2] March, R. E. and Todd, J. F. J. (2005) *John Wiley & Sons, Inc.*; [3] Li, X. et al. (2015) *Astrobiology*; [4] Arevalo Jr., R. et al. (2015) *IEEE Aerospace*; [5] Hecht M. et al. (2009) Science 325: 64-67. [6] Kounaves S. et al. (2009) J. Geophys. Res. 115: E00E10 doi: 10.1029/2009JE003424. [7] Navarro- González R. et al. (2010) J. Geophys. Res., 115: E12010, doi:10.1029/2010JE003599.

GeMini Plus: A Versatile Gamma-Ray Spectrometer for Planetary Composition Measurements. Morgan T. Burks[1], Lena E. Heffern[1], David J. Lawrence[2], John O. Goldsten[2], Patrick N. Peplowski[2], [1]Lawrence Livermore National Laboratory, Livermore, CA (burks5@llnl.gov), [2]Johns Hopkins University Applied Physics Laboratory (JHU/APL), Laurel, MD.

Introduction: We are developing a next-generation, high-purity Ge (HPGe) gamma-ray spectrometer (GRS) for planetary composition measurements. This instrument, called GeMini Plus, is unique in that it offers the best available gamma-ray energy resolution in a low-resource package (small size, low mass, low power). GeMini Plus (Figure 1) is thus well suited for resource-constrained missions, including landed and orbital missions, to planets, moons and asteroids.

Fig. 1. GeMini Plus sensor housing including cryostat and miniature cryocooler. Not shown are power supplies and readout electronics.

Gamma-ray spectroscopy is a valuable tool in measuring and quantifying planetary surface composition. This knowledge in turn helps address many science questions including constraining the formation history of the planetary body [1]. GeMini Plus is sensitive to a range of elements commonly found at a planetary surface. These elements include: H, C, O, Na, Mg, Al, Si, S, Cl, K, Ca, Ti, Fe, Th and U. Furthermore, due to the long penetration length of gamma-rays, this technique is sensitive to elements down to several tens of cm below the surface.

GRS instruments have previously flown on planetary missions to the Moon, Mercury, Mars and asteroids, and have made significant contributions to our understanding of these bodies [2-4]. However, most of these instruments had large mass, high power consumption and/or were low energy-resolution scintillator-based systems. The first high-resolution gamma-ray spectrometer that was also small size and low power was the GRS that flew on the MESSENGER mission to Mercury [5]. GeMini Plus is the next generation of the MESSENGER GRS, incorporating lessons learned and updated design to reduce the mass and power, while maintaining the ruggedness and performance.

Figure 2 shows the value of high-energy-resolution for elemental analysis. GeMini Plus was used to measure a Mars soil simulant and compared to a CsI-based scintillator. The soil was bombarded by neutrons to give a gamma-ray signature similar to that expected at Mars. Scintillator detectors are generally less complex and less expensive to deploy than germanium detectors, which have to be cryogenically cooled. However, GeMini Plus provides higher signal to background, better discrimination between gamma-ray lines, and resolves lines that are not resolvable by the scintillator. The result is a higher sensitivity to a wide range of elements.

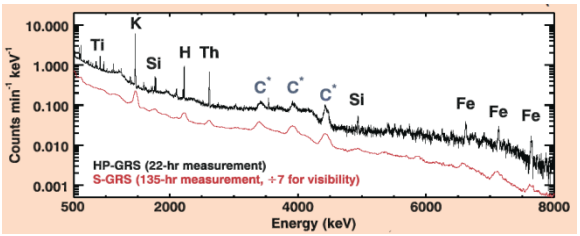

Fig. 2. Measured gamma-ray spectra for the GeMini Plus HPGe spectrometer and a CsI-based gamma-ray spectrometer of Mars soil simulant at the JHU/APL Planetary Gamma-Ray and Neutron Simulation Facility.

GeMini Plus Development: The goal of the GeMini Plus development is to build on the success of the MESSENGER GRS to make the next generation HPGe spectrometer. GeMini Plus incorporates improved infrared shielding, a robust suspension to reduce conductive heat load, and is compatible with the various low-power cryocoolers. The result is a low-resource instrument at Technical Readiness Level 6 or 7 that is suitable for a wide range of planetary missions. Specific development tasks include:

Cryocooler trade study. When the MESSENGER GRS was being designed and built (early 2000's) it was difficult to select a cryocooler that met all the desired specifications of low-mass, low-power, high heat lift, and longevity. However, in the past decade, significant progress in cryocooler technology has been made. GeMini Plus has been designed to work

with many different cryocoolers and can be optimized for the needs of a specific mission.

One cryocooler currently being tested is from Lockheed Martin (Figure 3) with a mass of 450 grams, 750 mW heat lift at 77K, and an expected lifetime of ~10 years of continuous operation.

Fig. 3. Lockheed Martin cryocooler. This cryocooler is low mass (450 grams), has a long life expectancy (10 years) and has sufficient heat lift (500 mW heat lift at 77 K). It is well suited for integration with GeMini Plus

Radiation damage and annealing. Although germanium-based spectrometers give the highest resolution of any competing technology, the resolution degrades over time due to radiation damage from cosmic ray bombardment. These effects are seen at a fluence around $10^8/cm^2$, which is about a year in space (depending on Solar cycle and proximity to planetary bodies). Fortunately this damage can be repaired *in situ* by annealing the detector to 100 ^oC for several days.

GeMini Plus will be irradiated at the NASA Space Radiation Laboratory with GeV protons to reproduce the damage expected in space. The instrument will then be annealed under various conditions in order to optimize annealing time and temperature. This will allow us to verify the performance of GeMini Plus for long duration missions in harsh radiation environments.

Vibration and shock tests. The GeMini Plus sensor housing has been mounted on a shake table and subjected to vibration loads mimicking rocket launch. Testing includes

- Sinusoidal strength test: 35 G at 42 Hz
- Random vibe: 14 G rms from 20 to 2000 Hz
- Shock: up to 2500 G at 2000 Hz.

These tests were performed an all three axes and showed that any resonances are well outside the measurement bandwidth. Thus the design is well-suited for rocket launch.

Design flight electronics. A flight-heritage data processing unit (DPU) has been developed for GeMini Plus (Figure 4). The DPU minimizes mass and allows quick reuse of standard flight-proven designs. Four modular "slices" are coupled together to form a compact electronics stack without the need or added mass of a backplane. These slices include a Low Voltage Power Supply, a High Voltage Power Supply, a Processor board containing the central FPGA, and a Cryocooler Controller capable of driving several types of cryocoolers. All-digital filtering algorithms have been implemented within the FPGA and shown to achieve similar performance to a commercial laboratory analyzer (Figure 5).

Fig 4. Digital Processing Unit (DPU) showing two "slices".

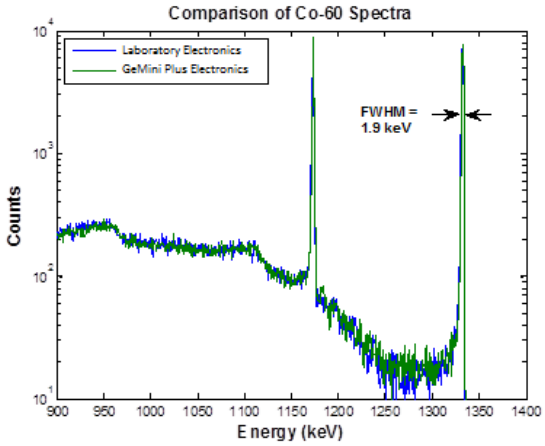

Fig 5. Energy resolution performance of the DPU compared to standard laboratory electronics for a germanium detector and a ^{60}Co point source.

References: [1] Evans, L. G. et al. *Remote Geochemical Analysis: Elemental and Mineralogical Composition* 167198 (1993); [2] Peplowski et al. (2011) *Science*, *333*(6051), 1850-1852; [3] Boynton et al., *Space Science Reviews*, *110*(1-2), 37-83 (2004); [4] Goldsten et al. In *The Near Earth Asteroid Rendezvous Mission*, pp. 169-216. Springer Netherlands, 1997; [5] Goldsten et al. *Space Science Reviews* 131, no. 1-4 (2007), 339-391; [6] Burks, M. (2008), *IEEE Nuc. Sci. Symp*., 1375.

INSTRUMENT FOR CAPTURING AND ANALYZING TRACE ORGANIC MOLECULES FROM PLUMES FOR OCEAN WORLDS MISSIONS. Anna Butterworth[1], Jungkyu Kim[2], Amanda Stockton[3], Paul Turin[1], Michael Ludlam[1] and Richard A. Mathies[4] [1]Space Sciences Laboratory, University of California, Berkeley, CA. [2]Texas Tech University, Lubbock, TX, [3]Georgia Institute of Technology, Atlanta, GA. [4]College of Chemistry, University of California, Berkeley, CA (ramathies@berkeley.edu).

Introduction: Enceladus Organic Analyzer (EOA) is an innovative miniaturized microfluidic organic chemical and biochemical analysis instrument that will sample and determine trace organic content from plumes or comas. *In situ* organic analysis is a powerful and cost effective approach for detecting molecules of relevance for chemical evolution in our solar system. Furthermore, biologically important classes of compounds, such as amino acids, show a strong chiral bias on Earth, and are ideal for probing the presence of extraterrestrial life. The goal of the EOA is to sample the Enceladus south pole plumes and perform sensitive organic measurements and probe for indications of life.

Heritage: A miniature lab-on-a-chip approach for detection and chirality determination of trace organic compounds has been developed extensively over 15 years at UC Berkeley College of Chemistry and the Berkeley Space Sciences Lab [1-3]. Portable prototypes have been field tested in the Panoche Valley, CA and in the Atacama Desert in Chile, where amino acid biomarkers of ancient life were detected and dated based on their chiral ratios [1].

The technique employs an integrated microfluidic device (typically 10-cm diameter) to analyze microliter aqueous volume samples for a wide variety of molecular species with part-per-million sensitivity. The projection of a typical microfluidic chip is shown in Fig. 1. First, organic compounds are automatically labeled according to their chemical functional groups with specific fluorescent reagents in a Programmable Microfluidic Analyzer (PMA). Next, the labeled organic species are separated by high-resolution electrophoretic separation in a microfabricated capillary electrophoresis (μCE) device. Finally, high sensitivity laser-induced fluorescence detection results in molecular identification and chirality (by separation time) and quantitation (by peak intensity). This miniaturized instrument is ideal for deployment for *in situ* organic analysis of multiple and varied planetary science targets. We describe here the use of this technology to solve the challenging problem of acquiring samples from the Enceladus plumes by an orbiter or fly-by and analyzing for organic components.

Enceladus Organic Analyzer (EOA) Instrumentation: The icy plumes arising from Enceladus provide an outstanding opportunity to look for organic rich life or potential for life [4]. This sampling opportunity suggested a novel design for a flight-ready Lab-on-a-Chip organic analyzer instrument, where we capture elusive volatile samples such as comet comae or Enceladus plumes and analyze them operating an integrated microfluidic device in a low gravity environment.

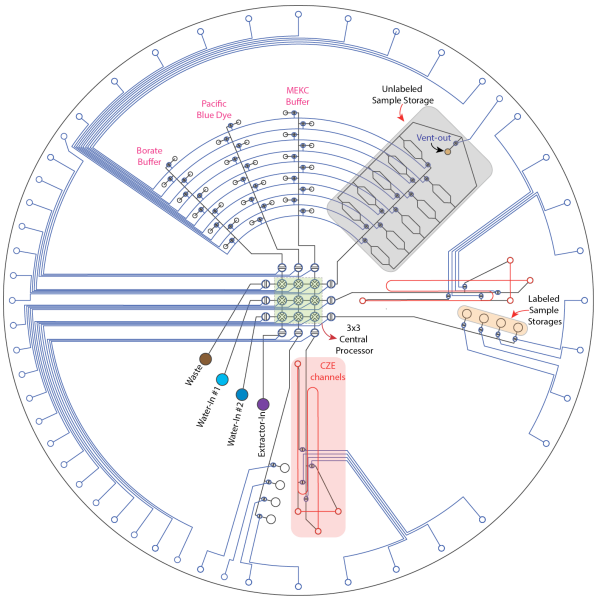

Figure 1: Microdevice at the heart of the Enceladus Organic Analyzer instrument. The processing core is a rectilinear array of valves at the center of the microdevice highlighted green. Reagent storage for multiple samples radiate from the center along spokes towards the top, and sample storage has been highlighted grey. The capillary electrophoresis channel is highlighted red.

EOA analysis schematic is shown in Fig 2 and the instrument design is shown in Fig. 3. The instrument is flown through the Enceladus plume where a capture plate is used for ice-particle collection; adsorbed organics are dissolved and transported to the PMA-μCE microfluidic device for analysis. The key question is the design and function of the capture plate that picks up the sample in a 1-5 km/s fly-by through the plume. It is important to dissipate the kinetic energy of impact in such a way that the organic molecules in the ice particles are not isomerized or significantly altered by the impact. We have performed detailed mechanical modeling calculations to determine the partitioning of

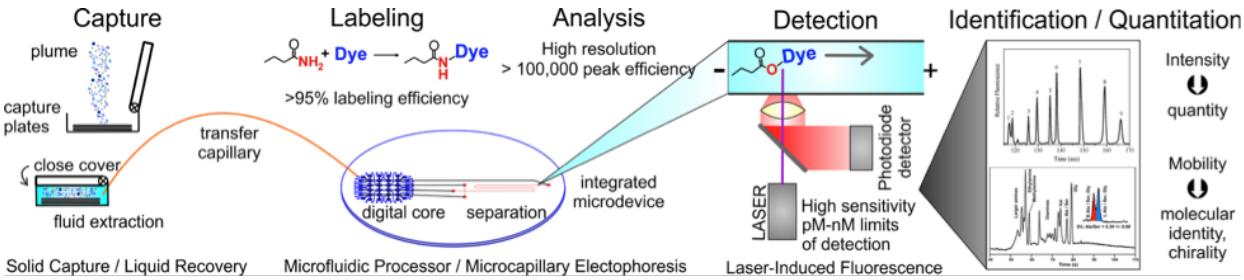

Figure 2. Schematic of functional elements and analysis process of Enceladus Organic Analyzer (EOA). The ice plume impacts the capture plate when the lid is open depositing organic molecules. After the lid is closed, the molecules are dissolved and, after passage to the microfluidic processor, the amine-containing molecules in the extract including amino acids are labeled with a fluorescent dye, separated by high resolution capillary electrophoresis, and detected with ppm sensitivity. Biologically significant molecules which may indicate life such as amino acids are identified by their unique mobility and their chirality is determined.

the input kinetic energy into the work of deformation of the target material, thermal transfer from the ice particle into the target material during the impact and heating of the projectile material. These calculations demonstrate that with the correct impact material, organic molecules in the incoming ice are not heated sufficiently to cause isomerization or thermal decomposition. A design that enables over 25% capture of the input material has also been developed providing micrograms of captured material for analysis by EOA.

EOA is a ~2.5 kg mass instrument, with a 16 cm by 16 cm footprint, and low power operation requirement. It is capable of ppm-organic species detection and chiral measurement of organic molecules such as amines and amino acids in 5 µg ice. Fluidic management is achieved by using pressured nitrogen. A microfluidic valve array, the Programmable Microfluidic Analyzer, is used to perform labeling of the sample with fluorescent dyes and to process the sample for high resolution electrophoretic analysis and sensitive fluorescence detection. In particular the measurement of amino concentration composition and chirality is especially important for probing for the potential for life or perhaps its actual existence on Enceladus.

Many missions, especially to outer Solar System targets like the icy moons of Saturn and Jupiter, or comets, are best approached with *in situ* instruments because of the formidable risks and costs of sample return. The identity and concentration of a wide range of organic molecules including amines, amino acids, aldehydes, ketones, organic acids, thiols and to polycyclic aromatic hydrocarbons (PAHs) in extraterrestrial samples can be determined with sub-part-per-billion sensitivity using the EOA concept. The demonstration and deployment of such technology should dramatically advance our knowledge of molecular planetary science.

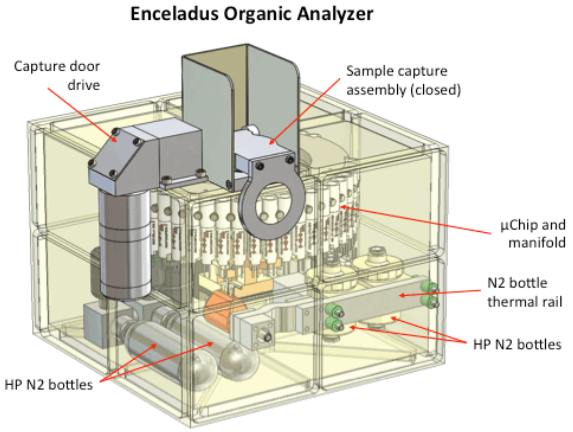

Figure 3: Schematic CAD of the EOA Instrument. The EOA is a 16x16x12 cm instrument with a mass of 2.5 kg that can be used for sensitivity part-per-million chemical analysis of organic molecules from plumes or comet tails that impact the capture plate assembly.

References: [1] Skelley A.M. et al. (2005) *PNAS USA, 102*, 1041-1046. [2] Kim J. et al. (2013) *Anal. Chem.*, *85*, 7682−7688. [3] Stockton A.M. et al. (2014) *Second International Workshop on Instrumentation for Planetary Missions*. [4] Porco C.C. (2006) *Science 311*, 1393-1401.

A REDUCED POWER DIGITAL ELECTRONICS SYSTEM FOR A DIGITAL BEAMFORMING SPACE EXPLORATION SYNTHETIC APERTURE RADAR. Lynn M. Carter[1], Rafael F. Rincon[1], and Markus Novak[2], [1]NASA Goddard Space Flight Center (lynn.m.carter@nasa.gov), [2]Ohio State University.

Introduction: We are designing a P-band (70 cm wavelength) digital beamforming radar system that is modular and can be used for imaging polarimetry of Earth and rocky planets and moons, as well as asteroids and comets. This radar (Space Exploration SAR, SESAR) is based off the successful P-band EcoSAR airplane radar that was developed at NASA Goddard for biomass measurements [1]. A major design problem with orbital beamforming radars is the power required to drive and steer the multiple beams. To adapt the airplane radar to an orbital format, it is particularly important to reduce the power of the digital electronics and RF elements.

Science Goals: Synthetic aperture radar (SAR) is the only remote sensing technique capable of penetrating through meters of material and imaging buried surfaces at high (meter-scale) spatial resolution. Multiple decadal survey science goals require a high-resolution view of subsurface stratigraphy, and in dust-covered environments it is critical to be able to expose bedrock and search for buried features that hold clues about the geologic history.

SESAR is particularly well-suited to studies of Mars and the Moon. Locating habitable regions, finding water, and determining the evolution of Martian hydrology and cryosphere is a primary goal of Mars exploration. Because ice and water outside the polar regions will be buried, radar is a key technology for cryosphere studies. Ice has a distinct radar polarization signature (high backscatter and Circular Polarization Ratio values) that can be used to locate buried ice deposits. A P-band radar instrument could map subsurface ice deposits [2]. P-band polarimetric radar would also reveal the internal structure in the upper tens of meters of the polar deposits, which is needed to detect seasonal changes and decipher how recent changes in climate have affected the cryosphere. High-resolution radar mapping has the potential to reveal buried fluvial systems on Mars (Fig. 1).

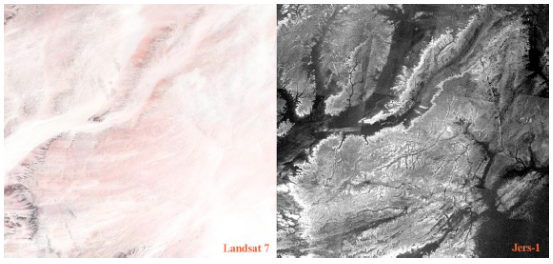

Fig. 1: Radar (right) reveals buried fluvial networks in southern Sudan that are not visible in Landsat imagery (left). SESAR would provide meter-scale imaging of buried channels on Mars. Image from [3].

The lunar surface is covered in a ~2-10 m of regolith that often hides geology that is crucial to our understanding of lunar processes. Radar can image through the regolith to characterize the near-surface stratigraphy of the Moon. High-resolution (<5 m) morphologic mapping and polarimetry would provide details about the volcanic processes that built the mare (e.g. size of flows, emplacement scenarios) and would enable comparisons to terrestrial analogs. The radar images could be used to locate and track lava tubes [4], which is important for both science and future exploration purposes. P-band will provide a new depth of penetration and rock population measurement that can be used to determine how the regolith varies across the Moon. Mapping the column structure of the regolith will provide new data on how airless surfaces age [5] as well as provide critical information for future landed missions that involve digging and/or sampling.

P-band (70 cm) is an ideal wavelength because 1.) it is capable of seeing beneath 2-15 m of material, 2.) it penetrates to a depth that is reachable by human and robotic explorers, 3.) it provides high-resolution, few meter-scale imaging, and 4.) it will not scatter off cm-sized rocks that are prevalent in near-surface regolith. Although P-band requires a larger antenna than prior shorter wavelength radar systems (Mini-RF on Lunar Reconnaissance Orbiter, the Magellan radar), P-band provides the penetration depth needed for science goals like mapping buried ice on Mars and looking for lava tubes and mapping buried lava flows on the Moon.

Digital beamforming allows for "smart" data collection [6], where one radar system can provide different data types (e.g. high- or low-res polarimetry, stereo imaging, altimetry, scatterometry, nadir sounding) depending on the science requirements defined for each surface target. Digital beamforming is also highly beneficial for spacecraft operations because it allows multiple look angles to be acquired without rolling the spacecraft. Nadir operations like scatterometry and sounding can also be performed with no rolls. The multi-mode and beamforming operation of SESAR SESAR's onboard processing capabilities are a significant advancement over prior radars and can return quick-look processed products that can be used to assess which data to send back.

The SESAR Instrument Concept: SESAR is an advanced digital beamforming radar instrument concept that will enable a new class of observations suitable to meet Decadal Survey science goals for planetary exploration. The instrument design will employ a modular approach that allows for the customization of the instrument architecture to meet scientific mission requirements for a specific planetary body. The modular approach distributes the radar systems into instrument panels composed of active subarrays, as illustrated in Fig 2.

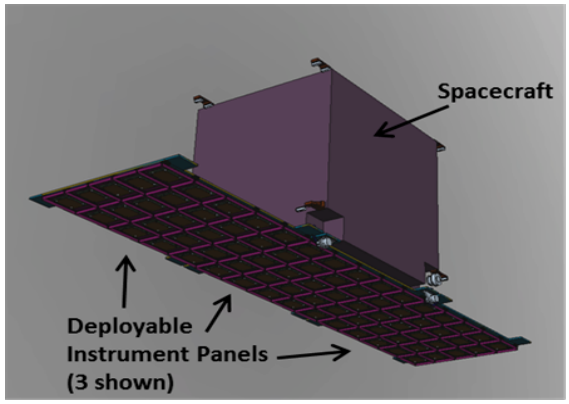

Fig. 2: SESAR employs a modular approach that permits customizing the architectures for a given planetary mission. SESAR's distributed architecture enables advanced operational modes.

SESAR's architecture will be fully programmable and capable of multi-mode radar operation including polarimetric SAR imaging, nadir SAR altimetry, and scatterometry. Some of its advanced programmable features include single, dual, or full polarimetry; multi-look angle data collection; simultaneous left and right of the track imaging; selectable resolution and swath width; digital beam steering (no moving parts); and beam pattern control; among others.

Under the technology-development program awarded by NASA's Planetary Instrument Concepts for the Advancement of Solar System Observations program (PICASSO), the SESAR team is developing innovative techniques to reduce the mass and power consumption of the radar.

The SESAR instrument will use a distributed digital electronics architecture that implements frequency domain multiplexing (FDM) techniques to provide the full beam steering agility while providing significant reductions in power consumption. The FDM approach reduces the number of digital-to-analogue converters (DACs) and analogue-to-digital converters (ADCs) and enables centralized waveform generation and data acquisition with reduced power and mass.

In addition, the SESAR team will use an ultra-wideband (UWB) tightly-coupled dipole array (TCDA) that will permit the reduction of the size and weight of the SESAR antenna. This is achieved by designing the element such that the sensing band lies at the lower range of the antenna's total operational bandwidth (approximately 2 GHz bandwidth).

Using these innovations, SESAR will be able to synthesize multiple antenna beams, simultaneously or interleaved, permitting the implementation of non-conventional imaging that can overcome fundamental limitations of conventional radar systems [6,7,8]. Some of its benefits include an increase in the measurement swath without reducing the received antenna gain, and the suppression of ambiguities or localized interference in the receiver signal by appropriate null-steering of the antenna pattern. The antenna gain, beam pointing angle, and sidelobe structure can be programmed in real-time for specific tasks. Furthermore, multiple beams can be synthesized on both sides of the flight-track, as well as nadir, using a single nadir-looking antenna, thus increasing the coverage area.

Summary: The SESAR instrument approach would be a first in planetary exploration. SESAR's agile radar operation, modularity, and multimode operation, while using technology that can be optimized to produce the best possible data set for the individual science goals, will help pave the way for the next generation planetary radar systems. SESAR's innovative approach to lower mass and power consumption will make these future missions feasible.

References: [1] Rincon, R.F. et al. (2015), IEEE Radar Conference (RadarCon), pp. 0699-0703. [2] MEPAG NEX-SAG Report (2015), Report from the Next Orbiter Science Analysis Group (NEX-SAG), Chaired by B. Campbell and R. Zurek, posted Dec. 2015 by MEPAG at http://mepag.nasa.gov/reports.cfm. [3] Paillou, P. et al. (2006), J. Geophys. Res., 111, E06S11, doi:10.1029/2005JE002528. [4] Campbell, B. A. et al. (2009), Geophys. Res. Lett., 36, L22201, doi:10.1029/ 2009GL041087. [5] Ghent, R. R. et al. (2016), Icarus, 273, 182-195. [6] Rincon, R. F. et al (2011), IEEE Trans. Geosci. Rem. Sens., vol.49, no.10, pp.3622-3628, doi:10.1109/TGRS.2011.2157971. [7] Krieger, G. et al (2008), IEEE Trans. Geosci. Rem. Sens., vol. 46, No. 1, pp. 31 – 46. [8] Younis, M. et al (2003), IEEE Trans. Geosci. Rem. Sens., vol. 41, No. 71, pp. 1735 – 1739, Jul. 2003.

Acknowledgement: Part of this work is funded by a NASA ROSES PICASSO grant.

STATE OF SMALL INSTRUMENTS FOR NANO-SPACECRAFT APPLICATIONS – A REVIEW. J. C. Castillo-Rogez, S. M. Feldman, J. D. Baker, G. Vane, Jet Propulsion Laboratory, California Institute of Technology, 4800 Oak Grove Drive, Pasadena, CA 91109.

Introduction: Nano-platforms, in the 1-10 kg range, are gaining maturity for deep space exploration thanks to increased investments from various space agencies into miniaturized subsystems and instruments. The last decade has seen the introduction of small platforms such as JAXA's Minerva hopper and the MASCOT (Mobile Asteroid Surface Scout) [1] developed by the German Space Agency (DLR), both of which are flying on the Hayabusa 2. Rover missions to Mars developed by NASA (e.g., Pathfinder, Mars Exploration Rovers, Mars Science Laboratory) and ESA (Beagle 2, Huygens, Rosetta's Philae, ExoMars) have fostered the development of small instruments some of which can be leveraged on future nano-spacecraft. NASA's recent focus on Cubesat have led to the development of a reference 3U bus (INSPIRE, Interplanetary Nanospacecraft Pathfinder in Relevant Environment, [2]) and a 6U bus (NEAScout and Lunar Flashlight missions, MSFC/JPL [3]) developed under the sponsorship of the Advanced Exploration Systems (HEOMD). The growing interest across the community for Cubesats and other nanosatellites for deep space exploration requires the availability of small instruments that can be easily implemented on these platforms and yet remain performant.

We review the current state of the art in small instruments that may be applicable to future missions involving independent or deployable platforms in the 1-10 kg range. We first highlight instruments inherited from past missions and then address requirements and way forward for the development of future small instrument.

Framework: Nano-spacecrafts open a new dimension in planetary exploration with the introduction of new architectures that carry the potential to increase science return at low cost: distributed network, complementary vantage point between mothership and daughterships, expandable assets for the exploration of high-risk areas (e.g., cometary plumes) [4]. An obvious trade to the low scale and cost of these platforms is a degradation in science data quality and quantity in comparison to the science return of larger missions, which the planetary science community is used to.

Mass and power are obvious limitations intrinsic to nano-spacecraft. Smaller detectors and apertures generally imply degraded spectral resolution and spatial resolution; the latter may be compensated for by flying the spacecraft closer to the target.

Short lifetime and limited data rates require science to be returned shortly following acquisition. Operational complexity, associated for example with material sampling and processing, or calibration, may simply preclude the implementation of certain measurement techniques into small spacecraft. As the field of miniaturized instruments progresses, it will be important to consider new ways of implementing old techniques. This is expecially true for optical instruments which could benefit greatly from the most recent technological advances enabling miniaturization, for example computational methods, on-chip spectrometers, and new semiconductor-based devices.

State of the Art in Small Instruments: A review of instruments that have flown on past and current missions shows the availability of a spectrum of geophysical and fields and particles instruments (seismometers, penetrometers, thermal probes, particle detectors, etc.); only a few optical and spectrometer instruments are available in a small form factor, including visible cameras (e.g., NEAScout imaging system [3]), ultraviolet sensors [5], new generation of small IR-spectrometer such as the Lunar Flashlight point spectrometer [6], the LunarCubes' BIRCHES [7], as well as micro-bolometers; a few analytical chemistry instruments have already been demonstrated on small landers, such as alpha-particle X-ray spectrometer [8] and gas chromatograph-mass spectrometer [9]. More advanced spectrometers for chemical measurements, especially isotopes, typically require larger platforms, especially when solid material sampling and processing is required. However a new class of miniaturized mass spectrometers (e.g., JPL's quadrupole ion trap mass spectrometers [10]) will open up possibilities in atmospheric sampling with small probes [11]. Tunable laser spectrometers have seen a huge success in recent years, with the tunable laser spectrometer (TLS) on Curiosity, capable of measuring gas abundances and isotope ratios to extremely high precision [12]. Pathways exist for further miniaturization, and instruments targetting specific gases and isoptope ratios (e.g., D/H in H_2O) could be designed to fit on small platforms. These instruments could, for example, sample cometary plumes, or deploy mechanisms for surface heating and gas capture on icy bodies. Key technological gaps have been identified in the area of radar instruments, although novel approaches such as passive radio exper-

iments should enable probing deep interiors with small spacecraft from orbit or even during flybys [13].

Many instruments required for addressing strategic knowledge gaps at Near Earth Asteroids and Mars' moons are already small enough to be deployed on small spacecraft as is illustrated by recent Cubesat concepts: NEAScout [3] and the Hedgehog platform currently developed under NASA's Space Technology Mission Directorate [14].

Emerging Technologies for the Next Generation of Small Instruments:

- Advanced detector technologies, for example the HOTBIRD (High Operating Temperature Barrier Infrared Detector [15]), enables instrument miniaturization without loss of performance.
- Increased aperture, for example in the context of Cubesat-based exoplanet search and characterization; origami-inspired deployable optics have been recently introduced as a promising approach [16].
- Increased on-board intelligence can help optimize science return when lifetime and downlink resources are tight and/or when observing opportunities are time constrained, e.g., in the case of a flyby or impacting experiment. Agile Science algorithms [17] can help optimize science return via on-board data processing, compression, and triage.
- Deployment mechanisms: low-cost nano-spacecraft should ideally avoid the number and complexity of internal mechanisms. However deployable booms have been recently introduced, for example for the INSPIRE magnetometer and RainCube Ka-band radar mission [18].
- Smart configuration of the lander may help optimize the shielding of electronics [19], as well as relax operational requirements, e.g., thermal control
- Low-temperature electronics would be suitable in order to relax requirements on thermal control.
- Smart packaging, for example foldable electronics, can help to significantly decrease instrument volume.
- The development of standard instrument interfaces will also be instrumental to the introduction of reference nano-spacecraft flight systems that may be considered for a variety of missions.

Environment Specific Requirements: The availability of small instruments for future small-class deployable platforms at Europa is limited to fields and particles. High-g investigations (penetrators) set requirements on instrument survivability that may be out of reach from the current generation of instruments, except for seismometers [20]. Significant tailoring to high-radiation, atmospheric, or in situ environments may conflict with the perception that nano-spacecraft, and especially Cubesats, may offer reference platforms for plug and play experiments.

Acknowledgements: This study is being developed at the Jet Propulsion Laboratory, California Institute of Technology, under contract to NASA.

References: [1] Jaumann, R. (2013) LPS 44, 1500. [2] Klesh, A., et al. (2013) *Proc. 27th Annual AIAA/USU Conference on Small Satellites*. [3] Castillo-Rogez, J. C., et al. (2016) NASA Exploration Science Forum, https://ac.arc.nasa.gov/p82b7is9fqr/. [4] Klesh, A., Castillo-Rogez, J. (2012) *Proc. Space 2012 Conference*. [5] Ishimaru, R., et al. (2016) This Conference. [6] Cohen, B., et al. (2014) NASA Exploration Science Forum. [7] Clark, P. E., et al. (2016) This conference. [8] Foley, C., et al. (2003) *J. Geophys. Res.* 108, E12. [9] Raulin, F., et al. (1989) *Origins of Life and Evolution of the Biosphere* 19, 497-498. [10] Madzunkov, S. M., Nikolic, D. (2014) J. Am. Soc. Mass. Spectrom. 25, 1841-1852. [11] Darrach, M., et al. (2015) Workshop on Harsh-Environment Mass Spectrometry, http://www.hems-workshop.org/10thWS/Talks/Durrach.pdf; [12] Webster, C.R. et al. (2014) "Tunable Laser Spectrometers For Space Science", *Instrumentation for Planetary Mission Workshop* 2014. [13] Romero-Wolf, A., et al. (2014) eprint arXiv:1404.1876. [14] Pavone, M., et al. (2013) *Proc. IEEE Aerospace Conference* 2013. [15] Ting, D. Z.−Y., et al. (2011) In: *Semiconductors and Semimetals* 84, 1–57, Eds. S.D. Gunapala, D.R. Rhiger, and C. Jagadish, Elsevier, Amsterdam. [16] Marchis, F., (2014) SPIE Astronomical Telescopes+Instrumentation Conference, #9143-128. [17] Thompson, D. R. (2012) SpaceOps http://ml.jpl.nasa.gov/papers/thompson/Thompson_2012_SpaceOps.pdf. [18] Sauder, J., et al. (2015) 29th Annual AIAA/USU Conference on Small Satellites, SSC15-VI-7. [19] Castillo-Rogez, J. C. (2013) *Low-Cost Planetary Mission Workshop*, http://lcpm10.caltech.edu/pdf/session-6/3_LCPM10-Castillo_Final.pdf. [20] Gowen, R. A., et al. (2011) *Adv. Space Res.* 48, 725-742.

RESULTS FROM THE SCIENCE INSTRUMENT DEFINITION TEAM FOR THE GONDOLA FOR HIGH ALTITUDE PLANETARY SCIENCE PROJECT. N. Chanover[1], S. Aslam[2], M. A. DiSanti[2]. C. A. Hibbitts[3], C. I. Honniball[4] L. Paganini[2], A. Parker[5], M. F. Skrutskie[6]. E. F. Young[5]
[1]Astronomy Department, New Mexico State University, Las Cruces, NM 88003, nchanove@nmsu.edu, [2]NASA Goddard Space Flight Center, Greenbelt, MD, [3]Johns Hopkins University Applied Physics Laboratory, Laurel, MD, [4]University of Hawaii at Manoa, Manoa, HI, [5]Southwest Research Institute, Boulder, CO, [6]Univerisity of Virginia, Charlottesville, VA.

The Gondola for High Altitude Planetary Science (GHAPS) is an observing asset under development by NASA's Planetary Science Division that will be hosted on stratospheric balloon missions intended for use by the broad planetary science community. GHAPS is being designed in a modular fashion to interface to a suite of instruments as called for by science needs. It will operate at an altitude of 30+ km and will include an optical telescope assembly with a 1-meter aperture and a pointing stability of approximately 1 arcsecond with a flight duration of ~100 days. The spectral grasp of the system is envisaged to include wavelengths spanning the near-ultraviolet to near/mid-infrared (~0.3-5 μm) and possibly to longer wavelengths.

The GHAPS Science Instrument Definition Team (SIDT) was convened in May 2016 to define the scope of science investigations, derive the science requirements and instrument concepts for GHAPS, prioritize the instruments according to science priorities that address Planetary Science Decadal Survey questions, and generate a report that is broadly disseminated to the planetary science community. The SIDT examined a wide range of solar system targets and science questions, focusing on unique measurements that could be made from a balloon-borne platform to address high-priority planetary science questions for a fraction of the cost of space missions. The resulting instrument concepts reflect unique capabilities offered by a balloon-borne platform (e.g., observations at spectral regions inaccessible from the ground due to telluric absorption, diffraction-limited imaging, and long duration uninterrupted observations of a target). We discuss example science cases that can be addressed with GHAPS and describe a notional instrument suite that can be used by guest observers to pursue decadal-level science questions.

A Low-Power Low-Mass Dual-Polarization Sensitive Submillimeter-Wave Radiometer/Spectrometer.

Goutam Chattopadhyay[1], Theodore Reck[1], Cecile Jung-Kubiak[1], David Gonzalez-Ovejero[1], Adrian Tang[1], Choon-sup Lee[1], and Maria Alonso-DelPino[1]

[1]Jet Propulsion Laboratory, California Institute of Technology, Pasadena, CA, 91109 USA

Introduction: Using newly developed CMOS components and silicon micromachining technology that enable low-mass and highly integrated receivers, we are developing a state-of-the-art submillimeter-wavelength radiometer/spectrometer instrument for planetary orbiter missions to Mars, Venus, Titan, and the Galilean moons. Our flexible receiver architecture provides a powerful instrument capability in a light-weight, low-power consuming compact package, which offer unprecedented sensitivity performance, spectral coverage, and scalability to meet the scientific requirements of multiple missions. The instrument will allow a large number of chemical species, such as water, NO_2, N_2O, NH_3, SO_2, H_2S, CH_4, and HCN, among others. It will also be able to pinpoint their location in latitude, longitude, and in altitude.

Space-based terahertz heterodyne radiometry-spectrometry at these frequencies has proven useful for measuring trace constituent abundances and physical properties under all climate conditions, including high dust loading [1]. The terahertz transitions of polar molecules permit detection of numerous trace species at parts per trillion to parts per billion sensitivity. As an emission measurement, observations are carried out continuously in a passive mode without the need for any time-restricted event such as a solar occultation. At these wavelengths, a moderate-sized antenna (30-cm effective) can yield high-spatial resolution measurements ($\lambda/D \approx 1.8 \times 10^{-3}$ at 550 GHz), while ultrahigh spectral resolution ($\lambda/\Delta\lambda > 10^6$) provides clear line separation and well-defined line profiles. Submillimeter-wave measurements are an ideal complement to infrared measurements of thermal inertia. Moreover, they offer several advantages over the infrared (IR) measurements: (i) much higher spectral resolution ($>10^6$) is possible because of the smaller absolute Doppler line broadening at lower frequencies, (ii) terahertz measurements are not blinded by aerosols or dust because the wavelengths are much longer than dust grain/aerosol size, eliminating scattering, (iii) some constituents (such as nitriles) have much stronger line intensities at submillimeter wavelengths, thus making possible detection at much lower concentrations, and (iv) radiometry allows characterization of surface properties by measuring thermal emission from dielectric surfaces.

Instrument Design: Fig. 1 shows the block diagram of the instrument under development. The instrument features a dual-polarized, sideband separating receiver sensitive to 520-600GHz, backed by a high-speed digital spectrum analyzers. The two-polarizations are received by a dual-polarization horn followed by a orthomode-transducer (OMT), which separates the two polarizations into two separate channels. Each channel is down-converted to 3GHz by a sideband separating Schottky-diode mixers pumped by a diode-based multiplier chain. A CMOS synthesizer is used to generate the fundamental LO signal that is multiplied up to 520-600GHz. The four IF channels (upper and lower sidebands for both polarizations) are amplified using low-power Silicon-Germanium amplifiers. Finally, the signal is digitized and a spectrum is generated by a CMOS spectrometer [2].

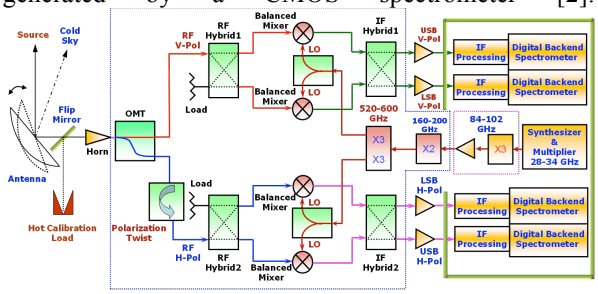

Figure 1: Schematic block diagram of a 520-600 GHz dual-polarized sideband separating receiver with two sideband outputs in each polarization for radiometry and spectroscopy applications.

Several innovations have enabled the radical increase in capabilities of submillimeter-wave instruments while reducing the total power consumption of the instrument. Most significantly, the CMOS components have reduced the power of the spectrometer and synthesizer, which previously have consumed tens of watts on previous submillimeter-wave instruments. Compared to a FPGA-based spectrometer, the power has been reduced from 12W to less than 1W per channel. Similarly, the CMOS synthesizer consumes less than 0.5W, saving over 5W compared to a DRO-based synthesizer. Higher submillimeter-wave circuit complexity is enabled by a novel silicon-micromachining process that utilizes microfabrication processes to produce precision waveguide structures. Finally, advances in commerical Gallium Nitride power ampliers reduce the LO power consumption from 20W to 6W.

Technological Advances: Discussion of each of the technological advances that enable this instrument follow.

CMOS Spectrometer: Previously, wide-bandwidth digital spectrometer processors were implemented as auto-correlators architectures or chirp-transform spec-

trometers (CTSs). These components have been massive and power hungry. Due to the much higher circuit speeds available from modern sub-micron CMOS technology, it is now possible to construct a much lighter and lower-power consuming system-on-chip (SoC) replacing even FPGA based spectrometers. The chip has integrated 7-bit digitizers, channel offset self-calibration, interleaving functions, clock management system, and vector accumulation. Currently it has a 512 channel quadrature output with integrated USB 2.0 controller. The entire back end including support PCB is 5cm x 8cm x 1cm and consumes only 200mW of total power. A higher speed 10 GS/s SoC chip with 8K channels is also under development [3].

CMOS Synthesizer: The CMOS synthesizer uses a conventional (charge-pump / phase detector / freq divider / VCO) phase-locked-loop (PLL) which provides coverage across 43-53 GHz followed by an on-chip frequency doubler to provide the higher 83-100 GHz output. Decreased frequency steps are achieved by clocking the synthesizer with a direct-digital frequency synthesizer (DDFS), enabling frequency steps less than 500MHz at the detection frequency. Also integrated within the same device is an integrated W-band power amplifier, allowing the module to output at least 1 mW of output power across the band. The entire synthesizer module consumes 220 mW with a phase noise of -90 dBc [4].

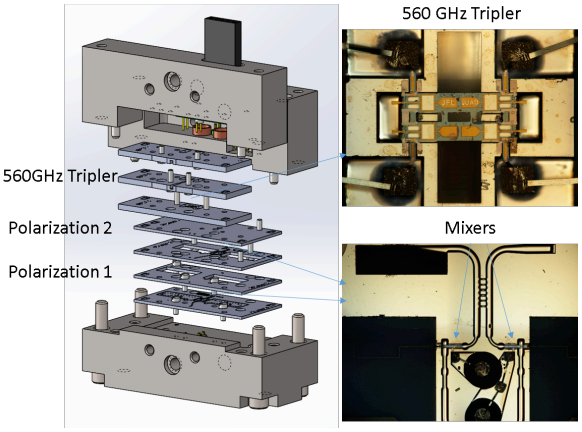

Figure 2: An exploded view of the silicon micromachined assembly. (Left) Seven layers are used to house the tripler and two sideband separating receivers, one for each polarization. (Top Right) The quad-chip 560GHz tripler used to pump the Schottky mixers. (Bottom Right) A sideband-separating receiver that supports two fundamental-balanced Schottky mixers.

Silicon Micromachining: Increased submillimeter-wave circuit complexity is achieved by manufacturing the 520-600 GHz, dual-polarization receiver with silicon micromachining. This process uses a combination of photolithographic techniques and Deep Reactive Ion Etching (DRIE) of silicon to form the waveguide-based circuit. This process provides high precision structures (+/-1um), allowing for higher-density waveguide circuit integration. Fig. 2 shows an exploded view of the front-end assembly, showing the seven silicon layers that support the two receivers and the 560GHz tripler [5].

Conclusion: A compact, low-power and mass, dual-polarization submillimeter-wave radiometer/spectrometer instrument is being developed for future planetary missions to Mars, Venus, Titan, the Galilean moons and other sites around the solar system. In additional to performing remote limb sounding of planetary atmospheres, the dual-polarizition capability allows for remote measurement of a surface's dielectric properties. Several technological innovations have enabled this advance in capabilities while reducing the power budget of the system; namely development of custom CMOS SoCs and silicon micromachining.

References:

[1] M. A. Janssen, Atmospheric Remote Sensing by Microwave Radiometry, Wiley, New York, 1993.

[2] G. Chattopadhyay, T. Reck, A. Tang, C. Jung-Kubiak, C. Lee, J. Siles, R. Schlecht, Y. M. Kim, M-C F. Chang, and I. Mehdi, "Compact Terahertz Instruments for Planetary Missions", *IEEE European Antennas and Propagation*, 2015.

[3] F. Hsiao, A. Tang, Y. Kim, B. Drouin, G. Chattopadhyay, M-C Frank Chang, "A 2.2 GS/s 188mW Spectrometer Processor in 65nm CMOS for supporting Low-Power THz Planetary Instruments", *IEEE Custom Integrated Circuit Conference* 2015.

[4] A. Tang, T. Reck, Y. Kim, G. Virbila, G. Chattopadhyay, M-C. Frank Chang, "A 65nm CMOS 88-105 GHz DDFS-Based Fractional Synthesizer For High Resolution Planetary Exploration Spectroscopy", *International Microwave Symposium* 2016.

[5] C. Jung-Kubiak, T. J. Reck, J. V. Siles, R. Lin, C. Lee, J. Gill, K. Cooper, I. Mehdi, and G. Chattopadhyay, "A Multistep DRIE Process for Complex Terahertz Waveguide Components," *IEEE Transactions on Terahertz Science and Technology*, vol.6, no.5, 2016.

Acknowledgements: The research described herein was carried out at the Jet Propulsion Laboratory, California Institute of Technology, Pasadena,California, USA, under contract with National Aeronautics and Space Administration.

NASA and European Cooperation Lessons Learned Based on the Rosetta Experience. Arthur B. Chmielewski[1]
Jet Propulsion Laboratory (4800 Oak Grove Drive, Pasadena, CA 91109, abc@jpl.nasa.gov)

Introduction: Rosetta is an international mission to the comet Churyumov-Gerasimenko 67P. The mission is led by ESA with participation from NASA and 12 countries. Approximately 300 scientists who represent an international plethora of universities, institutes, government agencies and private entities and hundreds of engineers, business managers, technicians and media personnel have taken part in Rosetta. Rosetta is truly a cornerstone or, as we call it in the US, a flagship mission.

The author of the paper has been the Project Manager of the NASA portion of the mission for the last six years. In that time, science mission operations have been developed, the spacecraft went in and out of hibernation, encountered an asteroid, orbited the comet and landed both the lander and the orbiter on its surface. There were numerous technical and progtammatic issues on both sides, changes in personnel and adjustments to the budget.

The mission taught us a lot about comets and the early solar system but it also gave NASA great lessons on how to conduct international cooperation.

The paper will discuss the following topics based on the Rosetta experience:

- How the Project tailored the management structure of instrument teams depending if the PI is from NASA or Europe.
- What are the major differences between ESA and NASA management structure and how Rosetta made them work for the benefit of the mission.
- NASA and ESA reviews are very, very different. How to conduct joint reviews without creating chaos.
- ESA missions are funded in a completely different way, on a different cycle, governed by different political forces than those present in the US.
- ESA and NASA have different approach to risk management, operations and mission assurance. It is important to understand these differences and use them to strengthen the mission and not to defeat it.
- ITAR is an unavoidable component.
- Coordination of media and public outreach requires careful planning to assure that the credit is given to the proper research institution or sponsor.
- International cooperation among the instrument teams is a daily staple of the mission. This can be a source of frustration or, if well designed, can strengthen the teams.

The paper will conclude with a Rosetta cookbook of recommendations for the future managers and PI's of international missions.

END-TO-END VALIDATION OF AN IN-SITU K−AR ISOCHRON DATING METHOD FOR PLANETARY LANDERS: ISOCHRON ANALYSIS OF NATURAL ROCKS. Y. Cho[1, 2], S. Sugita[3], Y. N. Miura[4], R. Okazaki[5], N. Iwata[6], T. Morota[7], and S. Kameda[8], [1]NASA Marshall Space Flight Center (320 Sparkman Dr. Huntsville, AL 35805, yuichiro.cho@nasa.gov), [2]University of Alabama in Huntsville, Huntsville, AL 35805. [3]The University of Tokyo, Tokyo 1130033, Japan. [4]Earthquake Research Institute, University of Tokyo, Tokyo 1130032, Japan. [5]Kyushu University, Fukuoka, 8190395, Japan. [6]Yamagata University, Yamagata 9908560, Japan. [7]Nagoya University, Aichi 4648601, Japan. [8]Rikkyo University, Tokyo 1718501, Japan.

Introduction: The absolute age of a rock is an important observable for interpreting the geologic record of planetary surfaces. In the Curiosity mission, Farley et al. [1] performed a milestone in situ geochronology experiment on Mars, demonstrating the feasibility of K−Ar dating on another planet. While the interpretation of the obtained age (4.21 ± 0.35 Ga) is still difficult due to the complexity of the nature of the measured mudstone, this measurement underscored the value of geochronology during rover explorations.

Several groups or researchers including ours have been developing an isochron-based in situ K−Ar dating method [2−14] to improve the capability of K−Ar dating on Mars and to solve problems concerning whole-rock analyses, including excess ^{40}Ar and insufficient Ar degassing with an onboard furnace [15]. This approach uses the combination of flight-proven techniques: laser-induced breakdown spectroscopy (LIBS) [16] and a quadrupole mass spectrometer (QMS) [17] for K and Ar measurement, respectively. For example, Cohen et al. [10] developed a K−Ar dating method called KArLE (K−Ar Laser Experiment) and reported isochron ages for a 28 Ma tuff and a 1714 Ma granite using their breadboard instrument. Devismes et al. [13] reported the measurement of a 160 Ma basalt using a UV laser. Our group has developed a possible design of the actual geochronology instrument suite for a rover [4, 7]. We also conducted end-to-end experiments using our breadboard instrument to examine the performance of the K−Ar isochron method. In this abstract, we summarize the results obtained in our recent paper where we measured two gneiss slabs to validate the isochron analysis [6].

K−Ar dating experiment: We placed two gneiss samples in a vacuum chamber. The different portions of the samples, preferably various minerals containing different K concentrations, were measured by laser pulses. The laser spot was approximately 500 μm in diameter. A series of laser pulses excavate the samples and liberate K and Ar simultaneously. The emission line of K at 769 nm was measured to obtain the concentration of K in each ablation pit [5]. The QMS measured the abundance and the isotopic composition of Ar after the purification by a getter. Here, the mass of the sample needs be determined to relate the concentration of K (wt%) with the absolute amount of Ar (cm^3 STP, or mol). We estimate the ablated volume and multiply it by the density of the sample to estimate the sample mass that released K and Ar. In this study, however, we used an external microscope to measure the volume of the pits. In actual missions, the pit volume would be measured either with an imager [18] or with the feature of LIBS spectra [12]. We also used the bulk density of the rock slabs here for age calculations. The elemental and mineral compositions obtained by LIBS may be used for the density estimation in a flight instrument [10].

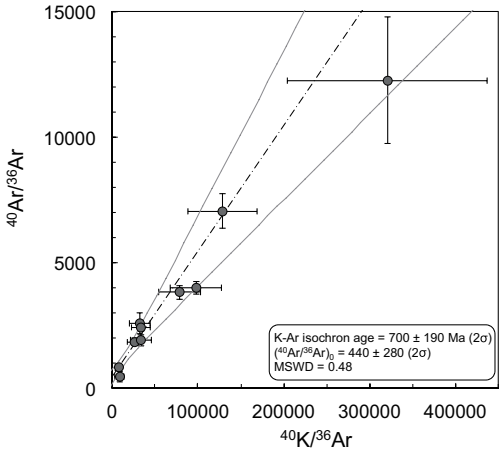

Fig. 1 K−Ar isochron for the hornblende-biotite bearing gneiss [6].

Isochron results and discussion: We obtained a K−Ar isochron (^{40}Ar/^{36}Ar vs. ^{40}K/^{36}Ar) for a gneiss containing hornblende and biotite phenocrysts. The data points distribute along a straight line, strongly suggesting the feasibility of isochron measurements with our LIBS−MS approach (Fig. 1). The isochron slope yielded the age of 700 ± 190 Ma (2σ), which is consistent with the K−Ar age obtained with conventional method with biotites. The isochron intercept exhibited a trapped Ar isotopic ratio of ^{40}Ar/^{36}Ar = 440 ± 280, which is consistent with that of atmospheric contamination (^{40}Ar/^{36}Ar = 296). This non-zero intercept suggests that the isotopic composition of trapped Ar is measurable with our approach. Such a measure-

ment is useful for understanding the evolution of parent magmas or planetary atmosphere trapped as the magma solidified.

In contrast, we could not derive the K−Ar isochron for the other sample (a gneiss containing pyroxene crystals) because it had very low ^{36}Ar contents from the terrestrial atmosphere. Thus, we also constructed ^{40}Ar−K plots based on the concentrations of K and ^{40}Ar. The "isochron" slopes yielded 420 ± 210 Ma of age for the 492 ± 30 Ma hornblende-biotite gneiss and 1050 ± 190 Ma for the 1052 ± 58 Ma pyroxene gneiss, demonstrating the validity of this approach. The intercept of the ^{40}Ar−K plot of the pyroxene gneiss yielded a best-fit trapped ^{40}Ar concentration on the order of 10^{-6} cm^3 STP/g, comparable with the amount of excess ^{40}Ar contained in the shergottites [15]. These results strongly suggest that the LIBS−MS method is capable of deriving both isochron age and the contribution of initially trapped ^{40}Ar with local analyses of different minerals in a single rock.

The spot-by-spot analysis has several advantages over whole-rock analysis techniques proposed in previous studies. For example, a wide range (e.g., a factor of ~50 in this study) of K contents obtained from different minerals in a single rock is favorable for obtaining accurate isochron. In addition, the degree of the departure of data points from a single straight line would enable us to assess whether or not the sample consists of minerals of different origins. Furthermore, if minerals with different closure temperatures coexist in a rock, these spots will follow different isochrons and thus we cannot obtain a single age. Nevertheless, such a result could provide information on the cooling rate of the parent magma.

Error assessment indicates that the in situ K−Ar dating with our LIBS−MS approach would determine the absolute ages of a variety of key geologic events for Mars evolution, such as Noachian/Hesperian and Hesperian/Amazonian transitions with 10−15% and 10−20% errors, respectively. Because no radiometric age data have been directly linked to a geologic unit on Mars yet, such a measurement will greatly improve our understanding of Martian history. Since the LIBS−MS system used in this study can be constructed with flight-equivalent components, landing geochronology using our method could be achieved with existing technologies.

Acknowledgments: Y. Cho was supported by Japan Society for the Promotion of Science (JSPS) Postdoctoral Fellowship of Research Abroad Program. This study was supported by funds from the Institute of Space and Aeronautical Science (ISAS)/Japan Aerospace Exploration Agency (JAXA) and by JSPS Grant-in-Aid in Scientific Research Grant Number 26247092.

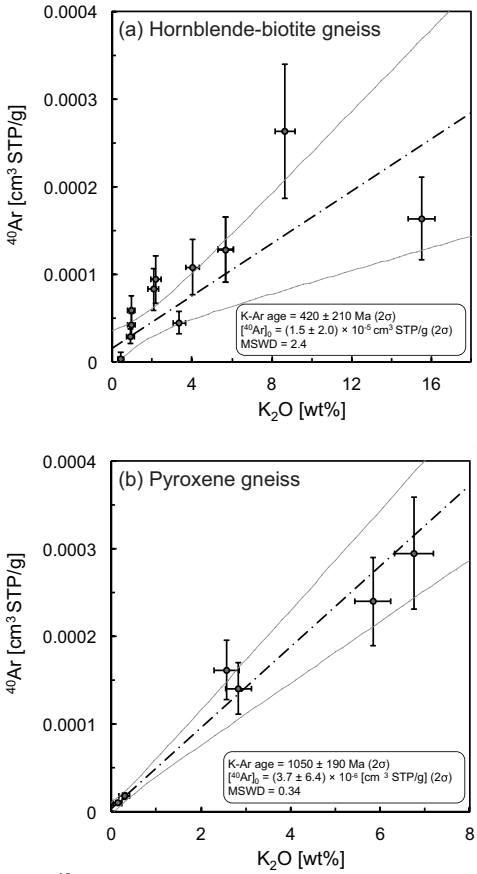

Fig. 2: ^{40}Ar−K plots for two gneiss samples [6].

References: [1] Farley, K. A. et al. (2014) *Science*, *343*, 1247166. [2] Cho, Y. et al. (2011) *PERC Planet. Geo. Field Symp.*, 30 [3] Cho, Y. et al. (2014a) *LPSC 45*, 1205. [4] Cho, Y. et al. (2014b) *IPM-2014*, 1157 [5] Cho, Y. et al. (2015) *Spectrochim. Acta B*, *106*, 28-35. [6] Cho, Y. et al. (2016a) *Planet. Space Sci.*, *128*, 14-29. [7] Cho, Y. et al. (2016b) *Trans. JSASS*, in-press. [8] Swindle, T. D. et al. (2003) *LPSC 34*, 1488. [9] Cohen B. A. (2012) *LPSC 43*, 1267. [10] Cohen, B. A. et al. (2014) *Geostand. Geoanal. Res. 38*, 421-439. [11] Stipe, C. B., et al. (2012) *Spectrochim. Acta B*, *70*, 45-50. [12] Devismes, D. et al. (2016a) *LPSC 47*, 2046. [13] Devismes, D. et al. (2016b) *Geostand. Geoanal. Res.,* doi: 10.1111/ggr.12118. [14] Solé, J. (2014) *Chem. Geol. 388*, 9-22. [15] Bogard, D. D. (2009) *MAPS*, *44*, 3-14. [16] Maurice, S. et al. (2012) *SSR*, *170*, 95-166. [17] Mahaffy, P. R. et al. (2012) *SSR*, *170*, 401-478. [18] French, R. A. et al. (2014) *LPSC 45*, 1936.

The Low Energy Neutral Imager (LENI) G. Clark[1], J. H. Westlake[1], D. G. Mitchell[1], E. Hoffer[1], and P. C. Brandt[1], [1]Johns Hopkins University Applied Physics Laboratory (george.clark@jhuapl.edu)

Introduction: To achieve breakthroughs in the areas of heliospheric and magnetospheric energetic neutral atom (ENA) imaging a new class of instruments is required. We present a high angular resolution ENA imager concept aimed at the suprathermal plasma populations with energies between 0.5 and 20 keV. This instrument is intended for understanding the spatial and temporal structure of the heliospheric boundary recently revealed by Interstellar Boundary Explorer (IBEX) instrumentation and the Cassini Ion and Neutral Camera (INCA). The instrument is also well suited to characterize magnetospheric ENA emissions from low-altitude ENA emissions produced by precipitation of magnetospheric ions into the terrestrial upper atmosphere, or from the magnetosheath where solar wind protons are neutralized by charge exchange, or from the ring-current region. We present a new technique utilizing ultra-thin carbon foils, 2D collimation, and a novel electron optical design to produce high-angular resolution (≤2°) and high-sensitivity (≥ 10^{-3} cm^2 sr/pixel) ENA imaging in the 0.5-20 keV energy range [1].

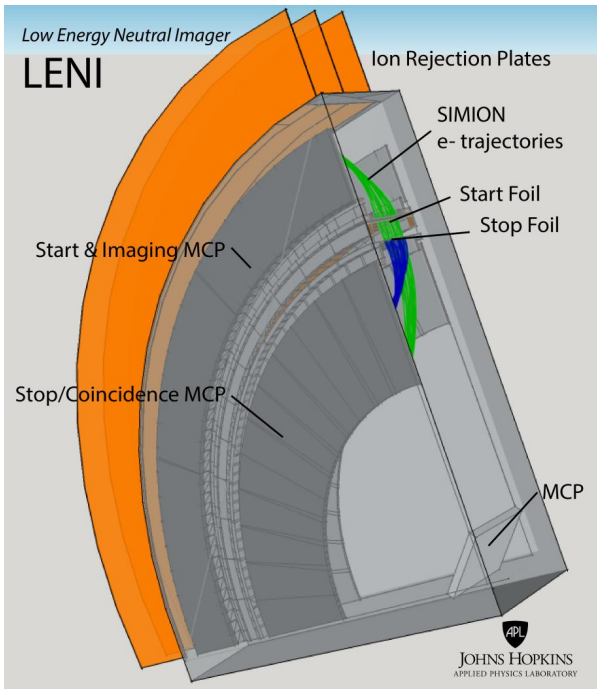

Figure 1: Conceptual drawning of LENI.

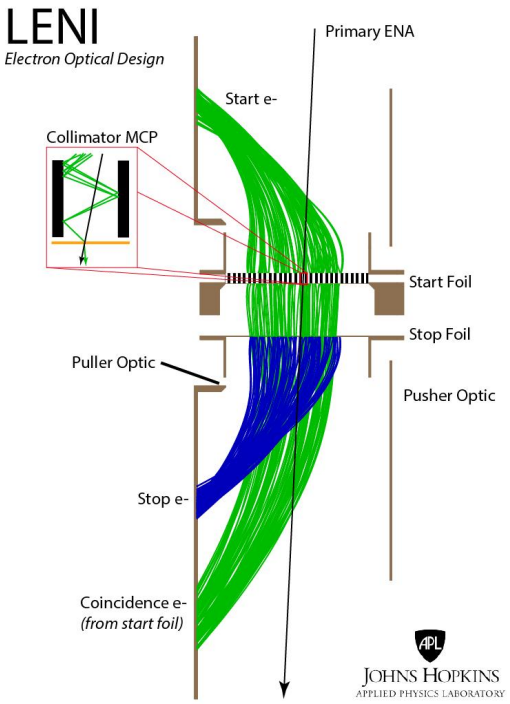

Figure 2: Schematic illustrating the electro-optics design using a particle simulation software package (SIMION).

References:

[1] Westlake, J. H., D. G. Mitchell, P. C. Brandt, B. G. Andrews, and G. Clark (2016), The Low Energy Neutral Imager (LENI), J. Geophys. Res. Space Physics, 121, doi:10.1002/2016JA022547.

BIRCHES: Compact Broadband IR Spectrometer and the Search for Lunar Volatiles . P. E. Clark[1], Ben Malphrus[2], Dennis Reuter[3], Robert MacDowall[3], David Folta[3], Terry Hurford[3], Cliff Brambora[3], William Farrell[3], [1]Jet Propulsion Laboratory, California Institute of Technology (pamela.e.clark@jpl.nasa.gov), [2]Morehead State University, [3]NASA/GSFC.

BIRCHES (Broadband InfraRed Compact, High-resolution Exploration Spectrometer) is the payload instrument on Lunar Ice Cube, a science requirements-driven lunar orbiting 6U cubesat designed to determine volatile distribution as a function of time of day. Led by Morehead State University, the Lunar Ice Cube mission was selected for a NASA HEOMD NextSTEP slot on the EM1 launch. The versatile instrument is being developed for a high priority science application: understanding volatile origin, distribution, and ongoing processes in the inner solar system. BIRCHES, a miniaturized version of OVIRS on OSIRIS-Rex, is a compact (1.5U, 2.5 kg, 10W including cryocooler and electronics) point spectrometer with a compact cryo-cooled HgCdTe focal plane array for broadband (1 to 4 micron) measurements, achieving sufficient SNR (>400) and spectral resolution (10 nm) through the use of a Linear Variable Filter to characterize and distinguish important volatiles (water, H2S, NH3, CO2, CH4, OH, organics) and mineral bands. We are also developing compact instrument electronics which can be easily reconfigured to support the instrument in 'imager' mode on future missions, once the communication downlink band-width becomes available, and the H1RG family of focal plane arrays. Thermal design is critical for the instrument. The newly-available compact and efficient AIM cryocooler (with iris controller) is designed to maintain the detector temperature below 115K. In order to maintain the optical system below 230K, a special radiator is dedicated to optics alone, in addition to a smaller radiator to maintain a nominal environ-ment for spacecraft electronics.

Self-calibrating solid-state SiC magnetometer for planetary field mapping C.J. Cochrane*, J. Blacksberg, [1]Jet Propulsion Laboratory, California Institute of Technology, 4800 Oak Grove Dr., Pasadena, CA 91109, *Corey.J.Cochrane@jpl.nasa.gov

Overview: We report on the initial stages of development of a new solid-state SiC magnetometer (SiCMag) intended for planetary field mapping. SiCMag measures magnetic field induced changes in spin dependent recombination (SDR) current within a SiC pn junction [1]. This change in SDR current arises from the interaction of external magnetic fields with the atomic scale defects intrinsic to the SiC semiconductor [2]. Although SiCMag, in its present form, is characterized as having a sensitivity of 440 nT/Hz$^{1/2}$, a custom sensor will be designed in the near future which will achieve a sensitivity below the 1 nT/Hz$^{1/2}$ limit.

Introduction: It's commonly known that fluxgate and optically pumped atomic gas based magnetometers are the instruments of choice because of their proven performance, reliability, and ability to adhere to the strict requirements associated with space missions. However, their complexity, size, and cost prevent their applicability in smaller missions involving cubesats. Conventional solid-state based magnetometers pose a viable solution, though many are prone to radiation damage and plagued with temperature instabilities. In this work, we report on the development of a new self-calibrating, solid-state based magnetometer based on a SiC pn junction. Unlike heritage designs, the magnetometer does not require inductive sensing elements, high frequency radio, and/or optical circuitry and can be made significantly more compact and lightweight. Additionally, the robustness of the SiC semiconductor allows for operation in extreme conditions such as the hot Venusian surface and the high radiation environment of the Jovian system. These features enable a variety of magnetic field sensing applications, including planetary entry probes, landers, and swarms of small picosats capable of science returns not possible with a single large-scale satellite. Our large scale prototype and planned coil system are illustrated in fig. 1.

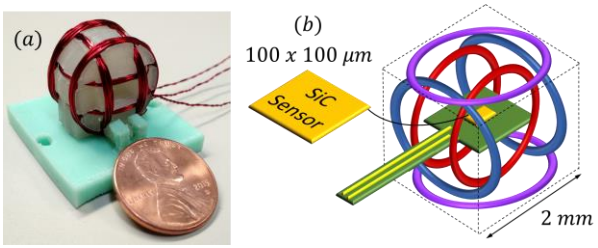

Figure 1: (a) Current "large scale" prototype and (b) planned coil system which will house the SiC sensor.

Operation: SiCMag is based on a magnetic field cancellation scheme that maximizes the SDR current in a SiC pn junction by maintaining a local region of zero-magnetic field across the volume of the device. The device is housed within three sets of Helmholtz coils (one for each dimension) that are driven independently to provide a low-frequency (<10Hz) cancellation field and a modulation field at audio frequencies. As the low-frequency driving current in these Helmholtz coils is directly proportional to the magnetic field it generates, its measure will serve as an indirect measure of the field being cancelled in each dimension.

Self-calibration: By measuring the electron nuclear hyperfine interactions that are observed in the higher

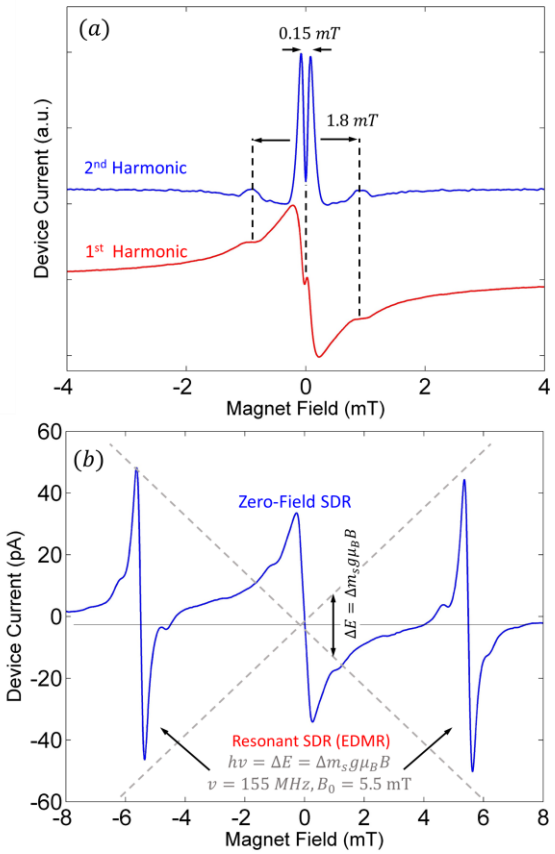

Figure 2: Self-calibration modes of SiCMag. (a) Well defined and stable electron nuclear hyperfine interactions observed in the higher order harmonic SDR responses can be used to self-calibrate the magnetometer. (b) EDMR measurement provides an absolute and redundant field measurement.

order harmonic SDR responses as illustrated in fig. 2a, SiCMag can leverage their stable magnetic field spacing to self-calibrate the magnetometer. Additionally, at the cost of adding a low radio frequency source and coil for offset field, one can leverage the electrically detected magnetic resonance (EDMR) response of the SiC defect electrons to provide an absolute and redundant magnetic field measurement as illustrated in fig 2b.

Sensitivity: Because the magnetometer relies on a magnetic field modulation scheme, the sensitivity of the instrument can be defined by the zero crossing slope of the response and the noise retained in the bandwidth of interest of the modulation frequency used. Figure 3a illustrates the measured sensitivity of the magnetometer at different biases applied to the SiC pn junction. As illustrated, the optimal sensitivity for this device is 440 nT/sqrt(Hz) when forward biased with 2.35 V. Figure 3b illustrates the magnetometer's response for three different axes (each offset by 1.5 pA for clarity) in the presence of an external, alternating axis, square wave magnetic field with amplitude of +/- 1500 nT. As illustrated in the figure, a frequency division multiplexing technique allows for simultaneous measurement of the x, y, and z magnetic field components. The signal-to-noise ratio of the data is consistent with the sensitivity metric depicted in fig. 3a

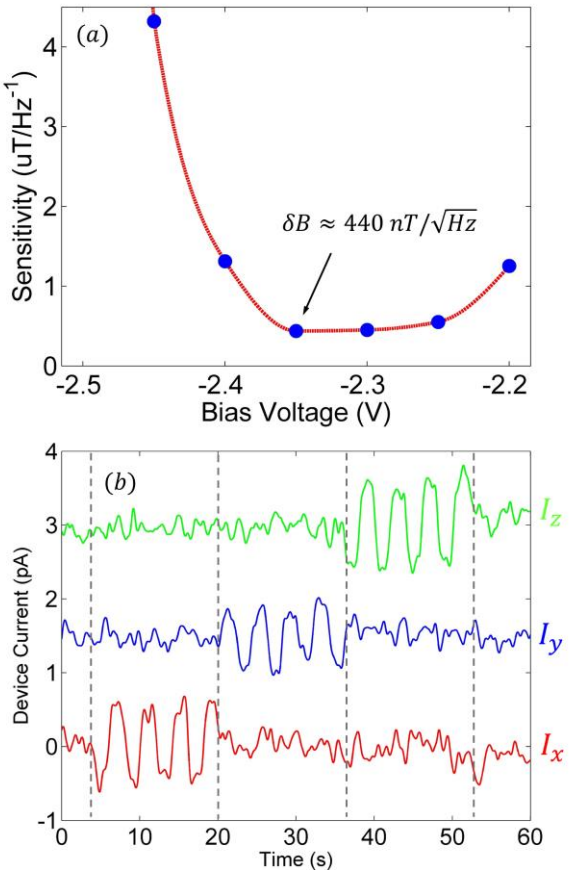

Figure 3: (a) Measured sensitivity of the magnetometer for a range of applied junction biases using a non-optimal SiC device. (b) Measurement of three current components versus time, each offset by 1.5 pA for clarity, in the presence of an alternating axis, ±1500 nT square wave magnetic field.

Applications for future NASA missions:

There are numerous relevant mission opportunities applicable for SiCMag, ranging from the large flagship missions to the smaller New Frontiers and Discovery missions. Because of the extremely small scale of the technology, it has significant potential for use on small spacecraft such as nanosats and picosats, where fluxgate and optically pumped sensors are too large for implementation. These small satellites can be used in swarms, thereby allowing for synchronous mapping of a planet's geomagnetic field without the need to make multiple orbits as required for large spacecraft. Additionally, if used on larger spacecraft, SiCMag's size and simplicity allows for multiple sensors to be placed around the spacecraft which would provide redundancy and inter-sensor calibration, allow for cancelation of stray fields from the satellite payload, make differential measurements for gradiometric science needs, and also allow for simultaneous measurements of magnetic fields at different frequencies. The collection of this information would make it significantly easier to distinguish between magnetic fields generated by internal dynamos, crustal magnetic fields, induced magnetic fields, and the interplanetary magnetic fields carried by the solar wind.

References: [1] C.J. Cochrane *et. al.* (2015) *Mat. Sci. Forum., Proc. 16th ICSCRM*, 858, 265-268. [2] C.J. Cochrane *et. al.* (2012) *J. Appl. Phys*., 112, 123714. [3] H. Kraus *et. al.* (2014) Nature Sci. Reps, 4, 5303. [4] D. Simin *et. al.* (2015) *Phys. Rev. Appl*., 4, 014009. [5] S.-Y. Lee *et. al.* (2015) Phys. Rev. B, 92, 115201.

Acknowledgement: The research described here was carried out at the Jet Propulsion Laboratory, California Institute of Technology, under a contract with NASA under Center Innovation Funding (CIF). Further development will be carried out with the Planetary Instrument Concepts for the Advancement of Solar System Observations (PICASSO) Program. We would like to thank Gerardo Hernandez from University of California Riverside for the design and construction of the 3D printed magnet, Neil Murphy of JPL for his help and assistance with JPL magnetometer facilities, and Aivars Lelis of the Army research lab for contributing the SiC device for study.

THE POTASSIUM-ARGON LASER EXPERIMENT (KArLE): IN SITU GEOCHRONOLOGY FOR PLANETARY MISSIONS. B. A. Cohen, NASA Marshall Space Flight Center, Huntsville AL 35812 (Barbara.A.Cohen@nasa.gov).

Introduction: Isotopic dating is an essential tool to establish an absolute chronology for geological events. It enables a planet's crystallization history, magmatic evolution, and alteration to be placed into the framework of solar system history. The capability for in situ geochronology will open up the ability for this crucial measurement to be accomplished as part of lander or rover complement. An in situ geochronology package can also complement sample return missions by identifying the most interesting rocks to cache or return to Earth. Appropriate application of in situ dating will enable geochronology on more terrains than can be reached with sample-return missions to the Moon, Mars, asteroids, outer planetary satellites, and other bodies that contain rocky components.

The capability of flight instruments to conduct in situ geochronology is called out in the NASA Planetary Science Decadal Survey and the NASA Technology Roadmap as needing development to serve the community's needs. Beagle 2 is the only mission launched to date with the explicit aim to perform in situ K-Ar isotopic dating [1], but it failed to communicate and was lost. The first in situ K-Ar date on Mars, using SAM and APXS measurements on the Cumberland mudstone [2], yielded an age of 4.21 ± 0.35 Ga and validated the idea of K-Ar dating on other planets, though the Curiosity method is not purpose-built for dating and requires many assumptions that degrade its precision. To get more precise and meaningful ages, multiple groups are developing dedicated in situ dating instruments [3-8].

KArLE methodology: KArLE uses currently available, flight-proven instruments to measure the age of a planetary sample, in addition to providing the original analyses of the instrument. KArLE is a science experiment whose implementation yields geochronology data and improvement in mission data quality and functionality enhancement to existing on-board instruments. KArLE measures K using laser-induced breakdown spectroscopy (LIBS), measures the Ar liberated by the laser ablation using mass spectrometry (MS) and relates K and Ar by measuring the volume of the ablated pit using optical imaging (Fig. 1). We have previously reported experimental results confirming the KArLE methodology [5]. Here, we describe requirements for KArLE flight hardware that would be reliable, reconfigurable and adaptable to multiple instruments and mission architectures.

KArLE Point Design: We used the GSFC Instrument Development Laboratory (IDL) to create a KArLE point design integrated into a notional lunar or martian lander or rover. We adopted a mission configuration from the Curiosity platform, assuming a mast unit, interior volumes, and a sample acquisition system (arm) as mission design elements. We used the more extreme lunar environment to further drive mission design elements such as lifetime, thermal environment, and sample type (regolith rather than hard rock).

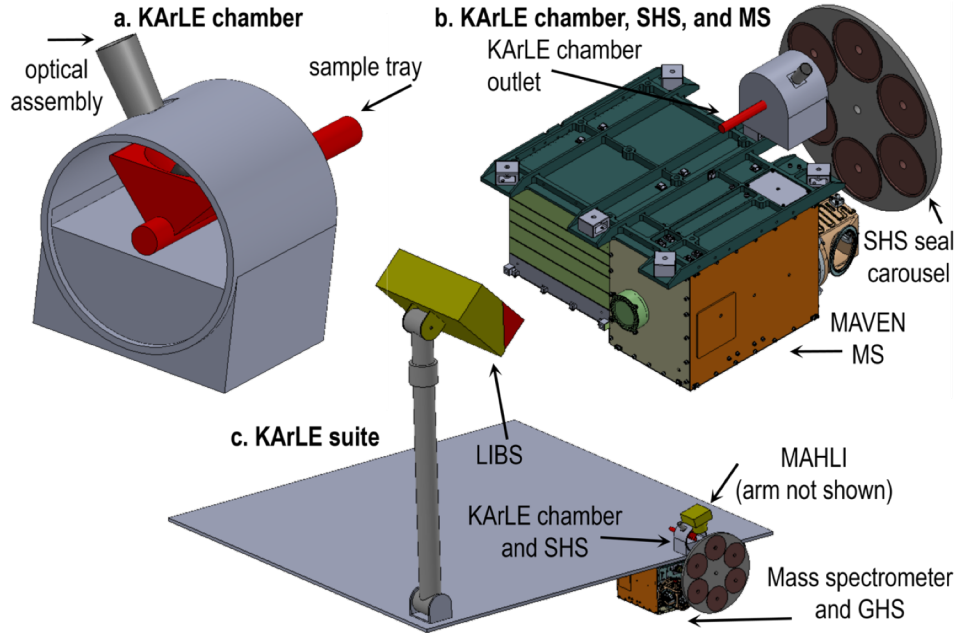

Figure 1. Point design for candidate KArLE flight configuration. Mass and volume etimates were derived for the MS from the MAVEN design, for LIBS from ChemCam, and for imaging from MAHLI, all currently aboard Curiosity.

The KArLE designs for all candidate missions have elements in common (Fig. 1). KArLE relies on measurement of the ^{40}Ar liberated by the LIBS laser ablation;

therefore, the ablation needs to take place within an enclosed chamber that does not allow sample gases to escape (or atmosphere to enter). A sample handling system must be able to introduce a rock sample for multiple KArLE laser spot analyses. The KArLE experiment is flexible to the exact sampling system; some examples might be a rough, natural sample such as a pebble, a prepared sample such as a cut face, or a core sample from a drill. While not a requirement, the ability to examine candidate samples outside the KArLE chamber and choose the appropriate ones for analysis prior to sample introduction is desired.

The KArLE sample handling system (SHS) is the hardware that meets these functional requirements. The KArLE SHS is physically mounted either to the spacecraft deck or internal volume. The sample chamber assembly has a resealable sample inlet port, an optical port to allow the LIBS instrument to operate on the sample, and a gas transfer line to allow the vaporized sample to expand to the MS for ^{40}Ar measurements. A calibration target composed of natural or synthetic rock resides inside the SHS, available to the LIBS and camera. An external housing or cover may be added to protect the optics from dust contamination during landing and/or extended inactivity.

The optical interface to the KArLE chamber permits the laser wavelength to enter and the visible light to be collected by the spectrometer. In addition, the laser must focus at the sample and must be able to impinge on multiple spots on the sample in serial. These two functions may be performed in multiple ways. For example, it is possible to package the LIBS instrument so that it is optimized for analysis in a chamber inside the spacecraft body [9], but the more synergistic situation would be to take advantage of a mast-mounted LIBS and body-mounted mass spectrometer that would be able to independently interrogate the environment.

The Curiosity mast has a pointing accuracy of 0.3 mrad relative to elements on the rover deck, allowing it to accurately point at the ChemCam calibration target set. This pointing accuracy implies that successive spots of 1 mm separation could be achieved on the sample with the mast pointing through a window. However, at 2 m distance, the spot diameter is ~0.035 cm, giving a peak intensity of ~13 GW/cm2, exceeding the sapphire damage threshold. To mitigate window damage, the beam is focused at infinity (collimated) coming from the mast, and focused on the sample using a short focal length optic embedded into the SHS window. This window may be placed at a distance from the sample to minimize deposition onto it from the LIBS ablation process by mounting it in a "snout" protruding from the SHS.

After LIBS ablation, evolved gas is sent to the mass spectrometer via a gas handling system consisting of a getter to remove active gases (and enrich the noble gases), pumps, a calibration gas tank, and microvalves, connected by capillary tubing. There is no requirement on how far the mass spectrometer can be from the KArLE chamber; although, increased distance increases the dilution volume and equilibration time.

The KArLE measurements themselves are made via the KArLE suite instruments: mass spectrometer, LIBS, and camera. These instruments have full and independent functionality outside of the KArLE experiment, and do not need to be re-designed or re-qualified. However, there are several KArLE-specific parts that will need to be monitored and/or controlled, including stage motors, environmental sensors, dust covers, and any decision-making algorithms that trigger the experiment to begin or end. The KArLE-specific electronics are assumed to be able to be kept within a thermal range common to electronics (-10°C to +40°C) via thermally coupling to a spacecraft thermal loop or radiator. Thermal-insulating blankets or a passive housing as a shield may also need to be added to protect the chamber from sunlight, depending on the spacecraft configuration.

A KArLE operations sequence consists of multiple sub-sequences, including sample acquisition, placement in the KArLE SHS, evacuation, blanks, backgrounds and standards, sample interrogation (LIBS, MS, and imaging) and sample removal. Built-in checkpoints may be included throughout the combined sequence; for example, a preload confirmation or a threshold MS background level.

Because several of the KArLE components are already flight-proven under similar conditions, they do not need to be requalified for flight. However, we have proposed to build a test article to qualify elements of the KArLE experiment under relevant environments by subjecting it to thermal vacuum (TVAC), vibration, and field tests. With this activity, we hope to show that the KArLE approach is a low-risk, synergistic way to implement a first attempt at in situ geochronology.

References: [1] Talboys, et al. (2009) Planetary and Space Science 57, 1237-1245, doi:10.1016/j.pss.2009.02.012. [2] Farley, et al. (2014) Science 343, doi:10.1126/science.1247166. [3] Anderson, et al. (2015) Rapid Comm. Mass Spec. 29, 191-204, doi:10.1002/rcm.7095. [4] Solé (2014) Chem. Geo. doi: 10.1016/j.chemgeo.2014.08.027. [5] Cohen, et al. (2014) Geostand. Geoanaly. Res. 38, 421-439, doi:10.1111/j.1751-908X.2014.00319.x. [6] Farley, et al. (2013) Geochim. Cosmochim. Acta 110, 1-12, doi:10.1016/j.gca.2013.02.010. [7] Cho, et al. (2016) Planet. Space Sci. 128, 14-29. [8] Devismes, et al. (2016) Geostand. Geoanaly. Res. doi:10.1111/ggr.12118. [9] Cho et al. (2015) Int. Symp. Space Tech. Sci. 30, #2015-k-2042.

A VERY MUCH FASTER AND MORE SENSITIVE IN SITU STABLE ISOTOPE ANALYSIS INSTRUMENT. M. Coleman[1,2], L. E. Christensen[1], J. M. Kriesel[3], J. F. Kelly[4], J. J. Moran[5], S. Vance[1,2]. [1]NASA Jet Propulsion Laboratory, California Institute of Technology, Pasadena, CA 91109, USA, max.coleman@jpl.nasa.gov. [2]NASA Astrobiology Institute, USA. [3]Opto-Knowledge Systems Inc., Torrance, CA 90502, USA. [4]J. F. Kelly, Pasco, WA, 99301, USA. [5]Pacific Northwest National Laboratory, Richland, WA 99354, USA.

Introduction: We are exploiting an emerging infrared absorption spectrometry technology to develop an in situ measurement system which should offer at least four orders of magnitude improvement in sensitivity relative to currently operating systems. Although the approach eventually will have many applications, we are focusing initially on isotopic analysis of hydrogen and oxygen in water ice and hydrated minerals, sampled at high spatial resolution by laser.

Why start with water analysis: The search for life outside the Earth remains a very high-profile topic. For a planet or moon to be habitable requires availability of volatile materials. Water is a key ingredient for life, and a mediator of geophysical processes on Earth such as mantle convection and atmospheric chemistry. The solar system's store and distribution of water constrains planetary evolution and habitability. Water makes up much of the mass in the outer solar system, including primordial meteorites and comets that might have formed our oceans [1]. Spectroscopic observations and rare sample analyses show considerable heterogeneity of D/H ratios of comets [2] and while it is likely that cometary cores are primordial [3], it is not clear if the surface material observed remotely has been reworked. Processes such as weathering, evaporation, precipitation, freezing, radiolysis, etc., affect the isotopic compositions of ices. Furthermore, comet samples returned by the Stardust mission [4] showed both large and small isotopic variations and also extreme differences between grains. Therefore, there is a need for multiple in situ isotopic analyses of comets and asteroids with high resolution sampling.

Analytical method: IR absorption spectrometry with a tunable diode laser source is well-established for stable isotope analysis for many gaseous compounds, whether directly in a Herriot cell with an extended path length after many bounces between opposing mirrors [5] or by cavity ring down spectroscopy [6]. The spectrum for water offers good expression of all relevant isotopologues (Fig. 1).

While using the same spectral features for analysis, our instrument utilizes a hollow optic fiber instead of a chamber, greatly reducing the sample volume [8] (Fig. 2).

The fiber is a waveguide, enhancing the laser-water-vapor interaction. A longer fiber would give a longer path length, more absorption and thus more sensitivity. However that would also increase sample volume. Initially, we have chosen a 2 meter fiber length, which should give sufficient absorption. With a 2 m long fiber, we estimate that we will be able to analyze a 5 nanomole water sample to precision of 1‰ in 1 seconds and 0.1‰ in 10 seconds. This is a more than four orders of magnitude increase in sensitivity, despite a shorter optical path length.

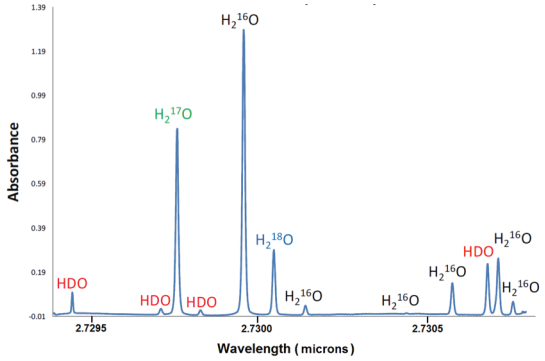

Figure 1. IR absorption spectrum for water isotopes [7].

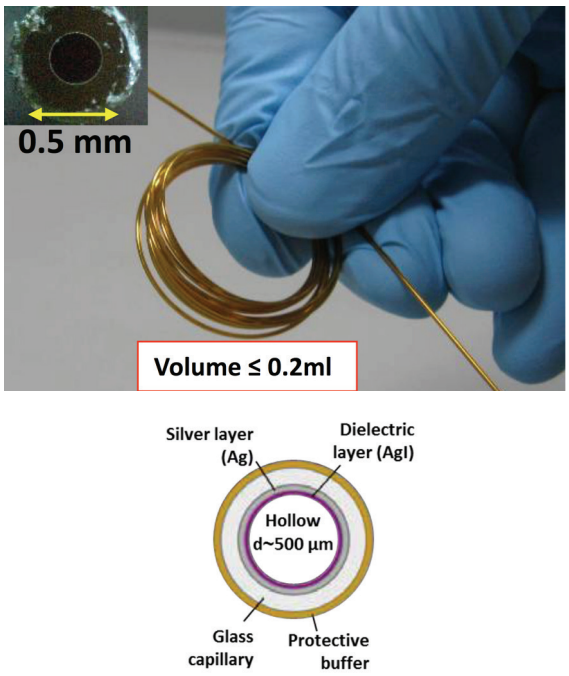

Figure 2. Hollow optic fiber, the absorption chamber.

Laser sampling: The wavelength of IR laser light chosen for spectrometry clearly is strongly absorbed by water vapor. Therefore our plan is to use the same wavelength, and indeed the same laser, for vaporizing water for analysis. This is shown in Fig.3, a schematic view of the three units that comprise the complete instrument. Although not shown in detail here, we have designed the sampling head so that it would make a sufficient seal to the surface being analyzed, being deployed on a simple arm. The sampling beam is intended to have just sufficient power to volatilize ice or release water from hydrated minerals without causing ablation and ejection of particle that might obstruct the camera or enter the hollow fiber. However, to avoid that unlikely possibility, we have designed the head to have an oblique sampling incidence and have included baffles to impede particle movement.

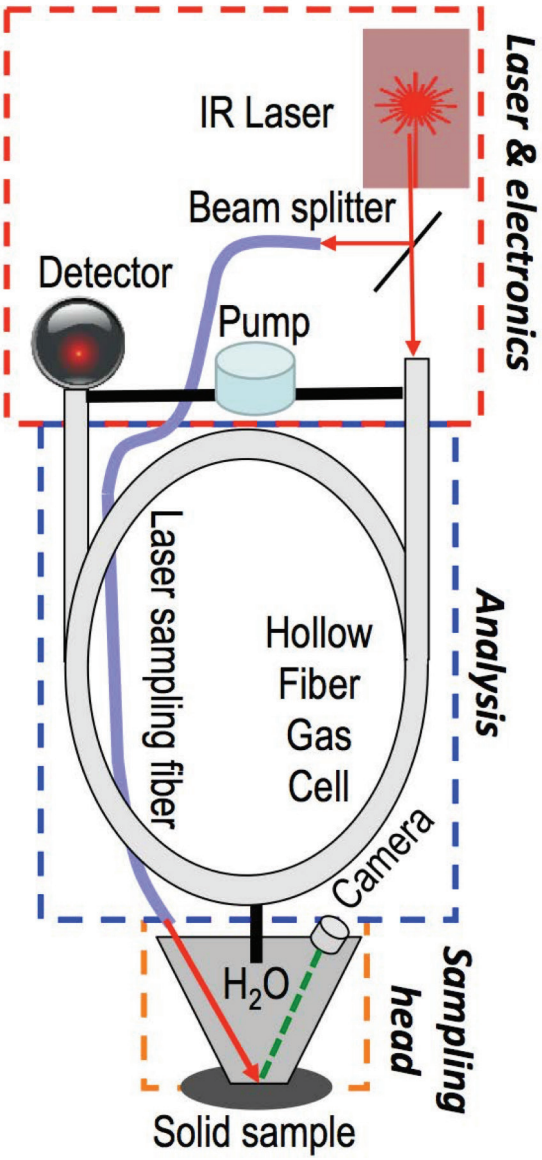

Figure 3. Schematic of the complete instrument.

Conclusion: We have chosen water analysis as the first attempt to use this very sensitive analytical technology for a flight instrument because of the magnitude of the scientific problem. However, having established this way of measuring, we can envision many other applications for astrobiology and planetology. CO_2, SO_2 and CH_4 are routinely analyzed by laser absorption spectrometry and this approach would be amenable to undertaking such analyses in situ, either directly or after a simple sample processing front end.

References: [1] Javoy M. (1998). *Chem. Geol. 147*, 11-25. [2] Bockelée-Morvan D. et al. (2015) *Space Sci Rev 197,* 47–83. [3] Davidsson B. J. R. et al. (2016) *A&A 592,* A63. [4] McKeegan K. D. et al. (2006) *Sci., 314,* 1724-1728. [5] Wahl E. H. et al (2006) *Isotop. Env. Health Stud., 42,* 21–35. [6] McManus J. B. et al (2010) *Isotop. Env. Health Stud.*,46, 49-63. [7] Chen P. et al. (2011) NASA PIDDP Final Report, JPL Project/Task Number: 103957. [8] Kelly J.F.et al. (2012) *Rev. Sci. Inst. 83*, 023101.

NIR SPECTROSCOPY AND MULTI-WAVELENGTH IMAGING FOR VOLATILE PROSPECTING.
A. M. Cook[1,2], A. Colaprete[1], T. L. Roush[1], J. E. Benton[1,3], J. B. Forgione[1], B. White[1], R. Bielawski[1], E. Fritzler[1,2]. [1]NASA Ames Research Center, M/S 245-6, Moffett Field, CA 94035, [2]Millennium Engineering and Integration, M/S 213, Moffett Field, CA 94035, [3]Wyle Engineering, Moffett Field, CA 94035.

Introduction: We present a demonstration of an instrument system built at NASA Ames Research Center, for in situ near-infrared spectral observations and visible imagery of planetary surfaces. The Near-InfraRed Volatile Spectrometer System (NIRVSS)[1] is comprised of two main structural components, pictured in Figure 1: the spectrometer box, which houses two NIR spectrometers, and the "bracket assembly" which includes a camera, 8 LEDs, optical fiber mounts for the spectrometers, a near-infrared source lamp, and 4 radiometers for long-wave infrared characterization. The primary science goal of NIRVSS is to detect and characterize the abundance of H_2O/OH and other volatiles on planetary surfaces.

Resource Prospector Mission: The current instrument design is driven primarily by requirements of the Resource Prospector rover mission to the lunar poles in ~2022. For this mission, NIRVSS serves as a prospecting instrument, mounted to the underside of the rover, viewing the ground as the rover traverses. The two spectrometers span adjacent wavelength ranges (1.59 - 2.39 and 2.31- 3.39 microns) that target the detection of OH bands indicative of water and other volatiles on the lunar surface. The near-IR tungsten filament lamp on the bracket projects a beam onto the ground beneath the rover, which reflects back up in to the viewports for the spectrometer fibers. The four radiometers (8, 10, 12.5, and 25 microns) provide calibration for higher temperature surfaces that can contribute thermal radiance within the range of the spectrometers. They can also characterize surface temepratures between approximately 80 to 400K.. Finally, the newly-updated Drill Observation Camera (DOC) is accompanied by 8 LED illumination sources with the following peak wavelengths: 410, 540, 640, 740, 905, 940, 1050, and a white broadband LED.

All components of NIRVSS are meant for use during both rover prospecting and drilling operations over specific targets of interest. The system could provide the mission's first measurements of increased OH-signatures, as subsurface soils are delivered to the surface by the RP drill.

Other Missions and Field Applications: The NIRVSS instrument provides a capability that is relevant beyond the moon. Remote observations of Mercury [2], Ceres [3], Phobos [4], and other airless bodies indicate the likely presence of water and other volatiles. The NIRVSS instrument is an ideal in situ in-

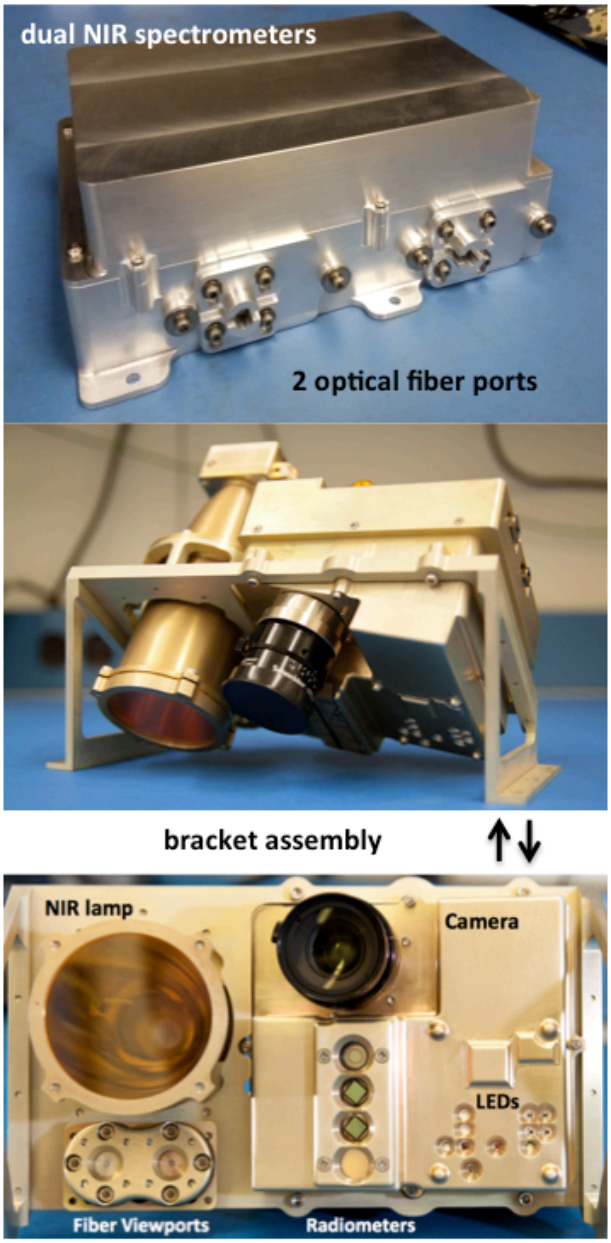

Figure 1. The NIRVSS instrument. Top panel: the dual spectrometer housing, with fiber ports. Middle Panel: a side view of the bracket assembly, pointing diagonally downward as it will from the Resource Prospector rover. Bottom Panel: Front view of the bracket assembly, annotating the location of various components discussed in the text.

strument to characterize the distribution of hydrated and/or hydroxylated deposits on these bodies.

In addition, the InField instrument is a version of NIRVSS that is being modified to study its potential use during human exploration missions. For InField, the same capabilities are being packaged into a < 35-lb backpack, with supporting equipment (batteries, harnessing, laptop, etc.) for field testing in collaboration with the BASALT (Biologic Analog Science Associated with Lava Terrains) team expeditions [5]. This iteration of the instrument provides adjustable fields of view for the spectrometers, by integrating a set of lenses to the bracket assembly in front of the fiber viewports. Smaller fields of view provide an opportunity to examine the spectral signal from much smaller features, some of which may contain biomarkers.

The range of wavelengths included in the camera's accompanying LEDs allow the NIRVSS system to capture images at individual wavelengths. The resulting images at each wavelength allow fluourescing features and OH-bearing mineral inclusions to be highlighted in contrast to surrounding material. The images are a highly informative complement to the spectral data.

Laboratory & Field Demonstrations:

We will present data from engineering tests in Glenn Research Center's VF13 vacuum chamber, where NIRVSS observed the Honeybee Robotics Resource Prospector drill deliver cuttings of a cryogenically cooled, water doped lunar simulant from depth into the NIRVSS field of view. Spectral data and images from this test demonstrate the ability of the NIRVSS system to sense water in real time, as it's being delivered to the surface.

We will also present data from initial testing of InField, which is slated for its first in-simulation field test in Hawaii Volcanoes National Park in November 2016.

References: [1] Roush, T. L. et al. (2016) *AIAA SCiTech Forum 2016*, Doc. ID: 20160000304. [2] Neumann, G. A. et al. (2013) *Science*, 339, 296-300. [3] Küppers, M. et al. (2014) *Nature*, 505, 525-527. [4] Fraeman et al. (2014), *Icarus*, 229, 196-205 [5] Lim, D. S. S. et al. (2015) AGU Fall Meeting 2015, #P31A-2031.

ENHANCED RESOLUTION OF CHIRAL AMINO ACIDS WITH CAPILLARY ELECTROPHORESIS FOR BIOSIGNATURE DETECTION IN EXTRATERRESTRIAL SAMPLES. J. C. Creamer[1], M. F. Mora[1], F. Kehl[1], and P. A. Willis[1], [1]NASA Jet Propulsion Laboratory, California Institute of Technology 4800 Oak Grove Dr. Pasadena, CA 91109

Introduction: Amino acids are the fundamental building blocks of all of the proteins needed for life on Earth. However, they are also a common byproduct of abiotic chemical reactions. The distribution of amino acids can be indicative of extinct or extant life on other worlds, but in order to use amino acids as biomarkers we need to be able to distinguish between those generated from abiotic and biotic reactions. By targeting detection of a small subset of 17 amino acids found in high abundance in terrestrial life (biotic) and meteorites (abiotic) it is possible to look for three distinct patterns, namely: 1) which amino acids are present; 2) the relative abundance of those amino acids to glycine; 3) the presence of an enantiomeric excess.

However, the in situ analysis of amino acids in extraterrestrial environments remains a challenge. Because of the low expected abundances of organics in planetary samples (amino acids in terrestrial soil can be as low as parts-per-billion) in situ sampling techniques are preferable over remote optical ones because they provide increased sensitivity [1].

Capillary electrophoresis (CE) is an extremely promising analytical technique for polar organic molecules in environments where water is present. Since CE is a liquid-based technique, all sample preparation can be done without leaving the aqueous phase. CE can be coupled to a wide variety of detection methods including laser induced fluorescence detection (LIF) to achieve selective and sensitive detection. Moreover, CE-LIF has been used for many decades for chiral amino acid analysis.

Here, we present two CE methods capable of resolving 17 amino acids labeled with 5-carboxyfluorescein succinimidyl ester. These 17 amino acids (seven enantiomer pairs L/D-Ala, -Asp, -Glu, -His, -Leu, -Ser, -Val and plus the achiral Gly, β-Ala, and GABA) represent the amino acids found in the highest abundance in biotic and abiotic samples. Resolution of the neutral amino acids was achieved using cyclodextrin (CD) mediated MEKC, with dual chiral selectors sodium taurocholate and γ-CD (Figure 1A). The acidic amino acids were resolved by CZE, using γ-CD alone (Figure 1B).

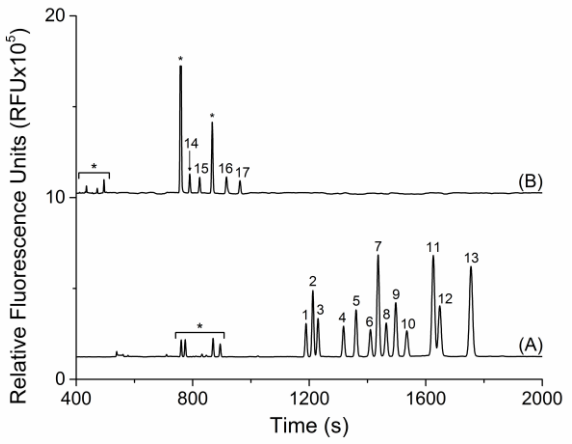

Figure 1: Electropherograms of the two optimized separations for the analysis of 17 amino acids found in high abundance in abiotic and biotic samples. A) The 13 neutral amino acids were resolved with a BGE composed of 80 mM sodium tetraborate, 30 mM γ-CD, 30 mM STC, and 5% v/v CAN. B) The 4 acidic amino acids were resolved with a BGE of 80 mM sodium tetraborate, 30 mM g-CD. Both separations were done on a 40 cm effective length capillary (50 cm total) with a 25 kV separation voltage. Peaks: 1. D-His; 2. D-Leu; 3. D-Val; 4. L-His; 5. L-Leu; 6. D-Ser; 7. GABA; 8. L-Val; 9. D-Ala; 10. L-Ser; 11. β-Ala; 12. L-Ala; 13. Gly; 14. D-Glu; 15. D-Asp; 16. L-Glu; 17. L-Asp; *Dye side products

Acknowledgements: The work done in this article was done at the Jet Propulsion Laboratory, California Institute of Technology, under a contract with the National Aeronautics and Space Administration. Financial support was provided by The Planetary Instrument Concepts for the Advancement of Solar System Observations (PICASSO) Program and the NASA Postdoctoral Program (NPP) at the Jet Propulsion Laboratory, administered by Universities Space Research Association through a contract with NASA.

References:

[1] Willis, P.A., Creamer, J.S., Mora, M.F. (2015) ABC, 23, 6939-6963.

Venus Exploration with Infrasound Techniques

J. A. Cutts , M. Pauken, Jet Propulsion Laboratory, California Institute of Technology, Pasadena, CA U.S.A, J.M. Jackson, Division of Geological and Planetary Sciences, California Institute of Technology, Pasadena, Cal-ifornia, U.S,A., David Mimoun, Institut Supérieur de l'Aéronautique et de l'Espace, Toulouse, France and Daniel Bowman, University of North Carolina at Chapel Hill

Introduction:

The formation, evolution and structure of Venus remains a puzzle more than fifty years after the first visit by a robotic spacecraft. Radar images have re-vealed a surface that is much younger than those of the Moon, Mercury and Mars as well as a variety of enigmatic volcanic and tectonic features quite unlike those generated by plate tectonics on Earth. To un-derstand how Venus works as a planet it is necessary to probe the interior of Venus. This paper describes the application and adaptation of seismic and infra-sonic techniques to exploit and cope with the unique environment of Venus in order to probe its interior and characterize its seismicity.

Background

The Venus environment, with surface temperatures of 460°C, makes conventional seismology using sen-sors in contact with the planetary surface impractical with current technology. However, the dense atmos-phere of Venus, which efficiently couples seismic energy into the atmosphere as infrasonic waves, ena-bles an alternative: detection of infrasonic waves in the upper atmosphere using either high altitude bal-loons or orbiting spacecraft. In June 2014, the Keck Institute for Space Studies (KISS) at the California Institute of Technology sponsored a one week work-shop with 30 specialists in the key techniques and technologies relevant to investigating Venus's inte-rior structure. The report of that study (Cutts, Mimoun, & Stevenson, 2015) identifies the most promising approaches for developing seismic sensors tolerant of the high temperatures as well as means of observing the infrasonic signal.

High Temperature Seismic Sensors

The surface of Venus, with temperatures near 460°C is a very hostile environment for instruments. Con-ventional electronics are out of the question as there are currently, nor are there in prospect, techniques for protecting components from the environment for more than a few hours. Technologies for tolerating the environment involving vacuum electronics and high temperature semiconductors require many years of development (Cutts, Mimoun, & Stevenson, 2015). Work continues on these technologies but alternative techniques are needed for near term mis-sions and that is the focus of this paper.

Infrasonic Techniques

Infrasonic techniques for probing the Venus interior can be implemented without exposing sensors to the severe environment of the Venus surface. This approach takes advantage of the fact that approxi-mately 60X the energy from a seismic event on Ve-nus is coupled into the atmosphere on Venus as would occur for a comparable event on Earth. (Lognonne, Geophysics of the Terrestrial Planets, 2010). The KISS report (Cutts, Mimoun, & Stevenson, 2015) evaluates the possibility of detect-ing seismic events on Venus as infrasonic waves from balloon platforms floating at altitudes where conventional electronics and sensor components can be used and from orbital spacecraft by observing an optical signal produced by the infrasonic wave as il-lustrated in Figure 1. A direct or epicentral wave can be detected where infrasonic energy is generated right above the event by the piston-like motion pro-duced by the quake. An indirect wave produced at distance can be detected where seismic energy propagates through the crust and interior of the planet and vertical motions at the surface atmosphere interface then excite the vertically moving infrasonic wave. Only the indirect wave probes the interior of the planet. However, the epicentral wave can be a sensi-tive detector of seismicity across the planet which is itself a subject of considerable interest.

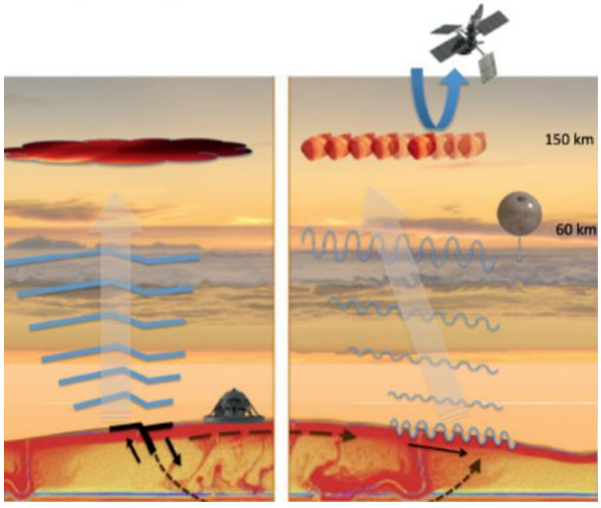

Figure 1 Generation of infrasonic waves by a seismic event on Venus. The direct or epicentral wave (left) propagates vertically above the event. The indirect wave (right) propagates through the planet as a Rayleigh wave and then couples to an infrasonic wave.

Balloon Infrasonic Detection – Sensitivity

Despite the much larger losses at the ground-atmosphere interface on Earth quite small earthquakes can be detected. For example, (Arrowsmith, et al., 2011) report the detection of a magnitude 4.7 quake in Utah across a statewide network of ground based infrasonic stations.

In addition to the fact that more seismic energy will be communicated into the atmosphere on Venus, the balloon station is moving with the medium which will substantially reduce the wind noise which gener-ally determined the threshold of detection for quakes on Earth. This sensitivity advantage of a balloon plat-form was recently established by comparison of infra-sonic measurements from a stratospheric balloon on earth with nearby ground stations as shown in Figure 2 (Bowman & Lees, 2016).

The instrumental limits for detection of seismic events on Venus are likely to be well below the Earth and may be determined by the background for other types of infrasonic source. While no inventions are needed at the component level, developments of ex-perimental techniques are needed and these should in-volve terrestrial flights on both tropospheric and strat-ospheric balloons. During the last two years, one of us (Bowman) conducted two stratospheric flights from New Mexico and demonstrated that the background noise levels were lower than for simultaneous meas-urements made at infrasound networks on the surface of the Earth (Bowman & Lees, 2016). Further meas-urements from balloon platforms are planned to de-velop and refine techniques for identifying quakes on Venus as well as to learn more about the Earth's in-frasound signature including both naturally occurring and anthropogenic events.

Relevance to Future Missions:

The great advantage of the infrasonic approach to studying the Venus interior is that the basic technol-ogy is ready today. While independent balloon and orbital missions could contribute valuable infor-mation, the real strength of this technique will involve the synergies between them as shown in Figure 3. The balloon technique provides a synoptic view but there is less energy particularly at the higher frequencies that propagates to the top of the Venus atmosphere and will be visible from space.

Opportunities for a mission with multiple platforms are currently being considered for Russia's Venera D but the baseline mission does not currently include balloons. The U.S. National Research Coun-cil's Planetary Science Decadal Survey of 2011 advo-cated a Venus Climate Mission which did feature a synoptic orbiter and balloon platforms but focused ex-clusively on atmospheric objects. The same flight el-ements could be employed to extend the capabilities of that mission as a Venus Climate and Interior Mis-sion. As NASA prepares for its next decadal survey this option should be considered.

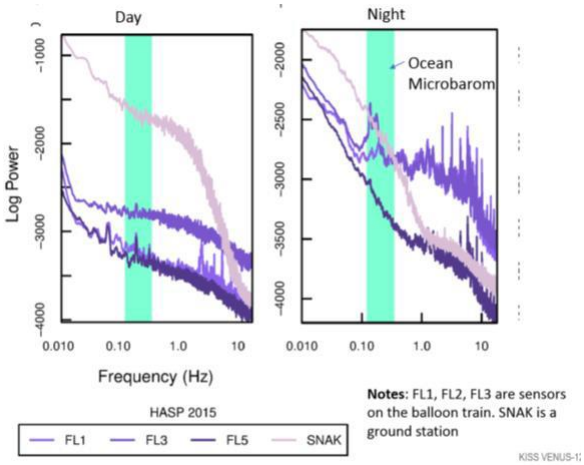

Figure 2. Comparison of acoustic signatures from a strat-ospheric balloon platform with a ground station during day and night time in the same location.

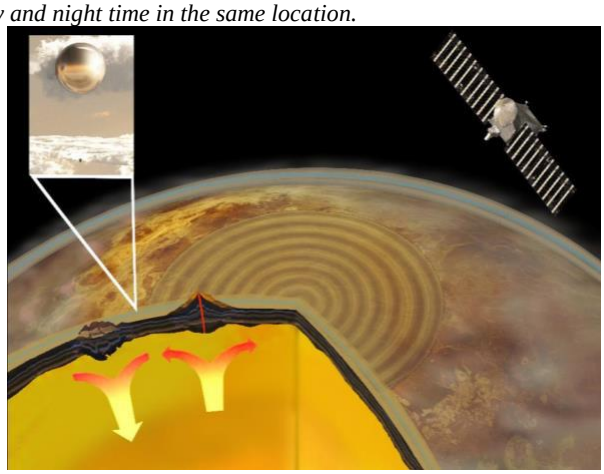

Figure 3. Coordinated observations of the infrasonic sig-natures from an orbital spacecraft and a balloon platform could provide confirmation of seismic event detections and complementary information

SCIENCE INSTRUMENTS FOR VENUS EXPLORATION: J. A. Cutts[1,] R Grimm.[2], Pl. Steffes[3], N. Izenberg[4], [1]Jet Propulsion Laboratory, California Institute of Technology, MS 321-550, 4800 Oak Grove Drive, Pasadena, CA 91109, James.A.Cutts@jpl.nasa.gov [2] South West Research Institute, Boulder, CO 80302, [3] Georgia Tech, Atlanta, GA 30332, [4]Applied Physics Lab, Laurel, MD 20723

Venus presents unique challenges and opportunities for scientific exploration. The dense atmosphere and high surface temperatures at the surface render many techniques irrelevant that are routine for use at the other inner planets. The environmental conditions have the greatest impact on remote sensing measurements from orbit and in situ measurements at the surface. However, the deep atmosphere with regions of benign temperatures permits long duration aerial platforms to operate with conventional sensors and electronics and apply both remote sensing and in situ techniques to observations of the surface, atmosphere and interior.

From orbit, a rich variety of remote atmospheric investigations are practical but the deep atmosphere blocks surface signals for vast region of the electromagnetic spectrum. As a result, UV, visible and infra instrumentation has played a key role in investigating the atmosphere on ESA's Venus Express mission and now on JAXA's Akatsuki mission. However, when it comes to investigating surface features at high resolution radar is the preferred technique. The VERITAS mission, selected as a candidate NASA Discovery mission, uses radar in conjunction with infrared in narrow spectral windows. Advances in both radar and infrared instrument technology will provide a major advances over what was accomplished by Magellan.

For in situ missions, there has been a long hiatus since the lander and balloon missions performed by the Soviet Union in the mid-1980s. Although there is little immediate prospect of extending the lifetime of these missions beyond a few hours, advances in instrumentation will enable remarkable gains in science. For example, the DAVINCI probe mission, also selected as a Discovery candidate mission in 2015, will be able to conduct descent imaging and high precision molecular analysis not possible with the Soviet technology of 30 years ago. Equally, the Venus In Situ Explorer, A New Frontiers class mission that NASA plans to issues a solicitation for this fall, requires the adaptation of the technologies developed for Mars and lunar surface in situ exploration to the high temperature and pressure of the Venus surface environment.

Prospects for long duration surface operation on Venus hinge on the development of sensing and electronics technologies that can function for weeks to months at almost 500C. Although individual components have been developed, we are far from having the range and complexity of components needed for a spacecraft system. Refrigeration systems that could allow the use of conventional components are also decades away from feasibility and would require powerful energy sources that have yet to be defined.

For long term in situ observations on Venus the near future lies with floating or flying platforms that operate in the upper atmosphere where temperatures are clement. From this vantage point it is possible to both conduct long term observations of the atmosphere and also use infrasound and magnetic and electrical signatures to investigate seismicity, explosive volcanic events and interior structure.

A series of documents prepared by VEXAG and published in 2014 (1),(2),(3), lay out the science goals for future Venus exploration, a mission roadmap and the technologies needed to realize these objectives. This information was supplemented in May 2014 with targets and target zones on the surface and in the atmosphere and measurement details by the with the Venus Exploration Targets workshop (4). A month later a Venus Seismology workshop(5) was sponsored by the Keck Institute for Space Studies (KISS) and compared in situ surface, atmospheric platforms and orbital platforms for seismic investigation of the Venus interior

Most recently, a detailed examination of the state of spacecraft and instrument technologies for exploring Venus was provided in a short course held in conjunction with the International Planetary Probe Workshop (IPPW) held in June 2016 and titled Destination Venus: Science, Technology and Mission Architectures (6). VEXAG is now working on defining needs for laboratory measurements to support the exploration of Venus.

References:

(1) Goals, Objectives and Investigations for Venus Exploration, 2014 http://www.lpi.usra.edu/vexag/reports/GOI-140625.pdf

(2) Roadmap for Venus Exploration, 2014 http://www.lpi.usra.edu/vexag/reports/Roadmap-140617.pdf

(3) Venus Technology Plan 2014 http://www.lpi.usra.edu/vexag/reports/Venus-Technology-Plan-140617.pdf

(4) Venus Targets Workshop Final Report 2015 http://www.lpi.usra.edu/vexag/WorkshopTargets20160115.pdf

(5) Probing the interior of Venus http://kiss.caltech.edu/study/venus/2015_KISS_Venus_Final_Report.pdf

(6) IPPW Short Course Destination Venus, Science, Technology and Mission Architecture http://ippw2016.jhuapl.edu/course.php

Atmospheric Constituent Explorer System (ACES)

M. Darrach, S. Madzunkov, E. Neidholdt, and J.Simcic
Planetary Surface Instruments Group, Jet Propulsion Laboratory, Pasadena, CA, 91109

Abstract

We report on the Atmospheric Constituent Explorer System (ACES), a mass spectrometer (MS) based instrument for atmospheric probe missions. In its current embodiment, ACES has been specifically matured to address the top three decadal science measurements of the Venus and Ice Giant atmospheres; to determine abundances and isotopic ratios of the noble-gases, to inventory and quantify the trace species, and to measure key isotopic ratios of the elements. ACES is designed to perform these measurements rapidly and to exceed the required precision and accuracy. The rapid measurement capability is specifically valuable for proposed investigations of Venus, enabling rapid atmospheric profiling of, for example, the unknown UV absorber at high altitudes.

ACES employs the JPL quadrupole ion trap mass spectrometer (QITMS) that has been developed over more than a decade (since 2001). The ACES QITMS is based on the mass spectrometer that flew in the successful Vehicle Cabin Atmosphere Monitor (VCAM), which monitored the atmosphere of the International Space Station (ISS) continuously for two years. The QITMS has been improved and matured for the ACES instrument. The QITMS is engineered in a "wireless" design, where all electrical connections are made through the structure, obviating all wires. The structural posts then plug directly into the vacuum flange electrical connectors. This approach significantly improved the shock and vibration loads the QITMS can survive and operate under, more than sufficient for the entry and descent loads for a Venus mission (300G axial, ±30G random radial). The QITMS employs two *rf* signals, applied to the MS cap electrodes, in addition to the main (high voltage) *rf*. Operating the QITMS in resonant injection modes enables, selective mass trapping (or ejection) and high mass resolution ($m/\Delta m \geq 5000$ @ 28 Da, full width at half maximum) and high mass range (1000 Da) with unprecedented long-term instrument stability. The ACES has been developed to introduce atmospheric gases such that the QITMS operate QITMS in the ultra-high vacuum environment (≤ 5E-10 Torr base pressure with operating pressure of <5E-8 Torr). This is highly advantages as, for example, it minimizes or eliminates ion-molecule reactions that are typically commonplace in ion trap MS. In combination with stability and virtually no background signal, the QITMS has a signal to noise/background ratio greater than 10^8.
The front end gas inlet system, has been matured under a 2014 NASA Homesteader award. It is comprised of as a system of valves (4) and micro leaks (4) which maintain gas flow within to the sensor as probe descends through planetary atmosphere. Our approach is unique in a sense that all valves but one as well as microleaks are based on MEMS technology which makes them light, high G load insensitive, low power consumption (mW) small mass and volume.

As part of the ACES instrument development we are performing a numerous measurements with analog gas mixtures of planetary atmospheres. Shown in Figure 1 is an ACES measurement of the ratio of intensities of 44 Da and 45 Da mass lines from CO2 using a Venus atmosphere analogue. The measurement, requiring only 10 sec of integration time, yields the expected 44/45 intensity ratio to within 5% uncertainty.

Figure 1: Isotopic measurement of CO2 with Venus analogue sample

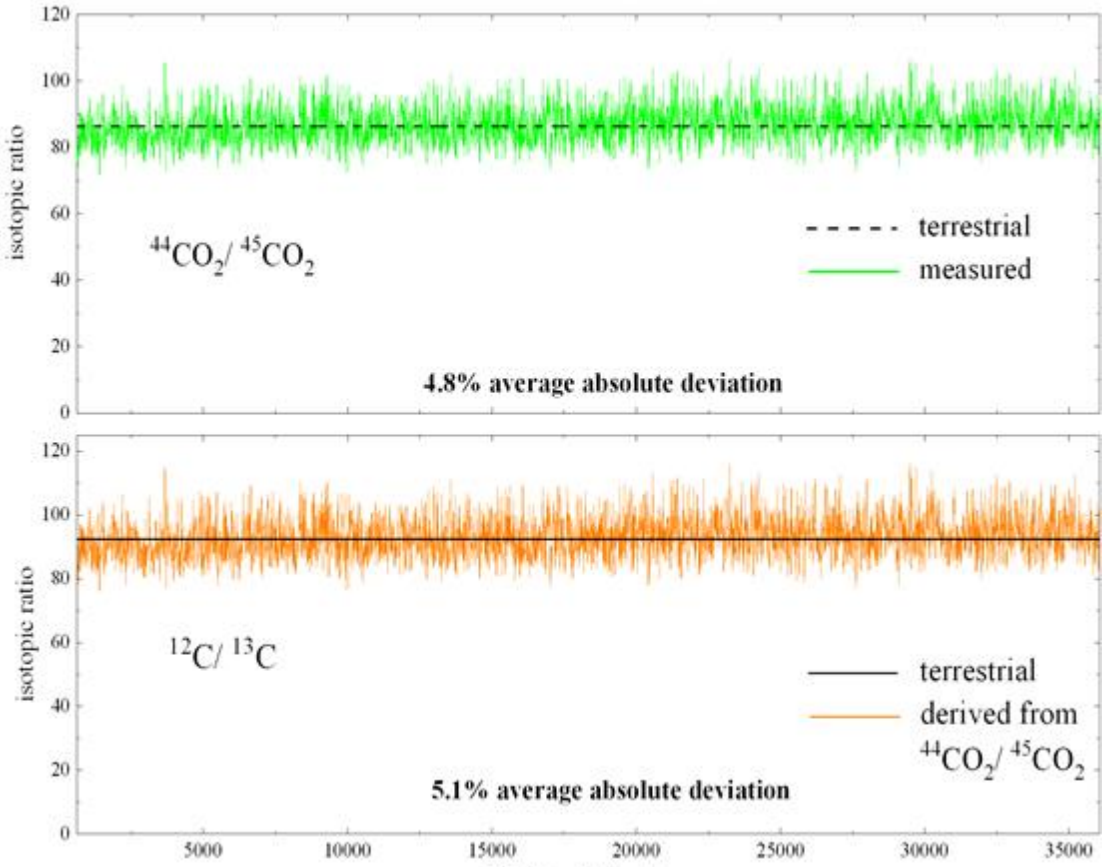

AN ION CHROMATOGRAPH FOR EXTRATERRESTRIAL EXPLORATIONS.

P. K. Dasgupta[1], W. Huang[1], B. N. Stamos[2], M. Zhang,[1] Y. Bedoustani,[1] A. C. Noell,[2] and A. Davila[3]
[1]Department of Chemistry and Biochemistry, University of Texas at Arlington, Arlington Texas 76019-0065 (Dasgupta@uta.edu), [2] Jet Propulsion Laboratory, 4800 Oak Grove Dr. MS 183-401 Pasadena, CA 91109, [3] SETI Institute, NASA Ames Research Center. MS 245-3, Moffett Field, CA 95136

Introduction: Ion chromatography (IC) is the benchmark technique for ion analysis. Recent technological developments allow us to build small and compact IC prototypes that can make key contributions in a variety of areas in planetary exploration, including investigations of inorganic and organic chemistry, habitability, and even the search for evidence of life [1]. For example, the surprising detection of perchlorate in Martian soil demonstrated both the importance of performing soluble ion measurements and the need for improved instrumentation to unambiguously identify all of the species present. Versatile designs and operational simplicity make *in situ* IC suitable for multiple spacecraft configurations and mission classes, including landers, rovers, and orbiters to planets, asteroids or icy moons.

IC vs. CE: Present day commercial ion chromatographs are far too bulky and power consuming to be directly considered. In addition, current technology relies on particle packed columns that must be kept wet and unfrozen even when they are not used to perform reliably. For this reason, many researchers have advocated electrophoresis, both in the microchip and the traditional capillary format. Capillary/ μchip electrophoresis (CE) can provide extraordinarily efficient high speed separations under ideal circumstances but its Achilles heel is lack of robustness. Any adsorption of injected material on the wall changes flow and makes future separations unpredictable and analyte identification tenuous, if not impossible. In the 90's, after Waters introduced a "Capillary Ion Analyzer" system demonstrating excellent separation performance, several other manufacturers introduced similar instrumentation. Suffice it to say that the entire breed has now become extinct.

Open Tubular Ion Chromatography (OTIC): Much of the benefits of CE can be realized in ion chromatography in an open tubular format. The columns can be dried and frozen and wetted and reused. However, whereas CE is typically carried out in 50-75 μm bore columns, open tubular liquid chromatography at these radial dimensions is inefficient. The mass transfer efficiency to the wall depends on the inverse square of the inner diameter, as such, even small changes in diameter can have a large effect.

As Jorgenson, the father of capillary zone electrophoresis, famously quipped, *CE is a wonderful technique, except it has three small problems: Injection, Separation and Detection,* this triad of Jorgenson problems exponentially increase with decreasing column bore. In addition, in OTIC, unlike CE, it not sufficient to have a narrow bore tube, the walls of that tube must be appropriately functionalized. Carrying out chemistry within sub-50 μm bore tubes without blocking them is not a high yield process.

Current Progress: In last several years, aided by generous sponsorship from NASA first through an ASTID and now through a PICASSO grant, we have made significant progress towards a miniature IC in the OT format that can be powered by a pneumatic pump (under 100 psi, 7 bars, often as low as 2 bars), that uses flow rates in the 10's to a few hundred nL/min with injected volumes in the pL-nL range and can separate and detect many analyte ions, both organic and inorganic, in the sub- to single-digit μM levels. Our experience indicates that the conflicting demands of functionalizing walls and sensitive detection vs. separation efficiency reaches an optimum compromise in the 10-30 μm column diameter range. The system operates off a pressure source like a keyboard duster via a miniature digital pressure controller. It uses a set of miniature solenoid valves governed by a Cypress Semiconductor System on a Chip (SoIC, PSoC5) to perform variable volume injections (as small as 40 pL for a 19 μm bore column up to the entire column volume) with a reproducibility of ±2% and with very little dependence on the sample viscosity. While we started with silica columns, the eventual goal being suppressed anion chromatography which uses alkaline eluents, we needed to use polymeric columns that are stable in strong base. We have had thence fabricated capillaries from polymethylmethacrylate, and cyclic olefin polymers (COP) and copolymers. We chemically treated the interior surface of these capillaries to endow them with carboxylic acid or sulfonic acid groups and then coated them with a suspension of anion exchanger latex nanoparticles, the same types as commercial packed columns so that extant separation protocols can be readily transferred. Special procedures had to be

developed to quantitatively measure the capacity of these columns (low nanoequivalents) [2]. Detection in such small capillaries proved to be the biggest challenge as none of the extant commercial contactless conductivity detectors produced consistent or meaningful responses. An extensive effort towards theatrically understanding the behavior of such detectors through modeling and simulation led us to the conclusion that one must operate at an altogether much lower excitation frequency domain to be successful [3]. These findings and appropriate electronic design led to the development of a simple, compact detector that could even be used in capillaries as small as 2 µm in bore [4]. The pneumatic eluent delivery and injection systems, coupled to latex coated polymeric capillary columns led then to complete ion chromatograph [5]. A sub-3 kg, sub-watt portable OTIC, field tested once in the Atacama Desert, is presently being refined for a second, more rigorous testing. Meanwhile the cyclic olefin polymer (COP) OTIC columns (these can be coiled into small diameter coils, increasing column efficiency, already reaching 150,000 plates/m in favorable cases) and their sulfonation conditions have been thoroughly characterized. Finally we have been able to fabricate electrodialytic suppressors small enough to be coupled to 28 µm bore columns without measurable loss of efficiency (suppressor size must be further reduced to work properly with 19 µm bore columns) that now permit hydroxide eluent gradient IC with performance unequaled by any commercial IC available today.

Presently we are attempting to develop a small enough pulsed amperometric detector and carry out amino acid separations in this format.

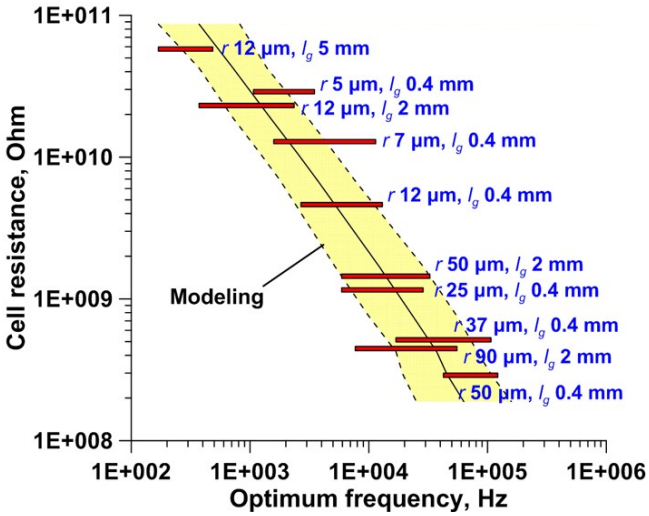

Figure 1. The river of optimum frequency. l_g is the gap between the probe electrodes, $2r$ is the capillary bore.

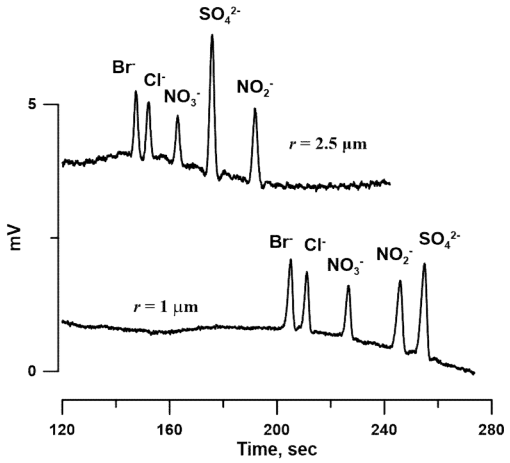

Figure 2. Capillary Electrophoresis in very small capillaries with new admittance detector.

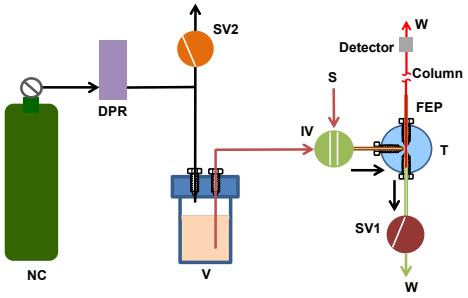

Figure 3. Operational Schematic of OTIC.

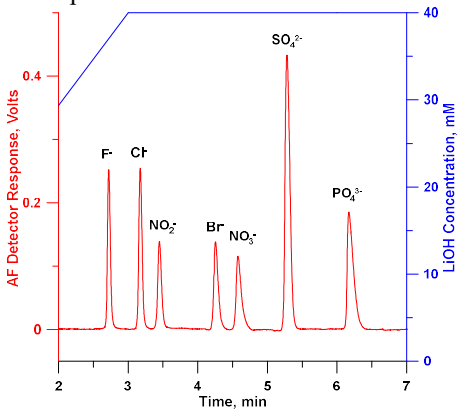

Figure 4. Gradient suppressed OTIC on a 75 cm 28 µm column, 100 µM each analyte, phosphate 200 µM, 6.7 nL.

References:[1] Shelor, C. P. et al. (2014) *Astrobiology, 14,* 577-588. [2] Zhang, M. et al. (2013) *Anal. Chem. 85,* 7,994-8,000. [3] Zhang, M. et al. (2014) *Anal. Chem. 86,* 11,538-11,546. [4] Zhang, M. et al. (2014) *Anal. Chem. 86,* 11,554-11,553. [5] Yang, B. C. et al. (2014) *Anal. Chem. 86,* 11,554-11,561

Acknowledgment: Supported by NASA through NNX11AO66G, NNX15AM76G, NSF through CHE-1506572 and the Hamish Small Chair Endowment to PKD at the University of Texas at Arlington.

IMPROVING PERFORMANCE IN PLANETARY ULTRAVIOLET SPECTROGRAPHS. M. W. Davis[1], G. R. Gladstone[1] and K. D. Retherford[1], [1]Space Science and Engineering Division, Southwest Research Institute, 6220 Culebra Road, San Antonio, TX 78238 (mdavis@swri.edu).

Introduction: Four compact planetary ultraviolet spectrographs have been built by Southwest Research Institute and successfully operated on different planetary missions: Rosetta-Alice [1], New Horizons-Alice [2], LRO-LAMP [3], and Juno-UVS [4]. Two more are in the works to observe Jupiter and its moons aboard the JUICE and Europa missions. Both of these spectrographs feature advancements that improve spatial resolution, maximum instantaneous count rates, and radiation background rejection when compared to previous spectrographs. The new designs also allow solar occultations at Jovian distances.

UVS Instrument Summary: Light enters the instrument through the main airglow port (AP; a 40-mm square aperture), the high-resolution port (HP; a 10-mm diameter aperture co-aligned with a door at the AP), or the solar port (SP; a 0.25-mm pinhole that feeds a small, gold-coated pickoff mirror). The light is then focused by the off-axis paraboloid (OAP) mirror onto a slit plane. The slit passes the solid angle of interest (7.5° by 0.1°) to a toroidal grating co-aligned with the location of the pupil image. The grating then focuses the spectral image onto a cylindrical MCP detector over the 55-210 nm range. The detector is read out by cross-delay-line (XDL) electronics. The detector and its accompanying electronics are inside the local tantalum shields, which act to both reduce the total MeV electron dose on the electronics as well as reduce the background noise on the detector (Figure 1). The shielding design is derived from the Juno-UVS instrument that arrived at Jupiter in July 2016.

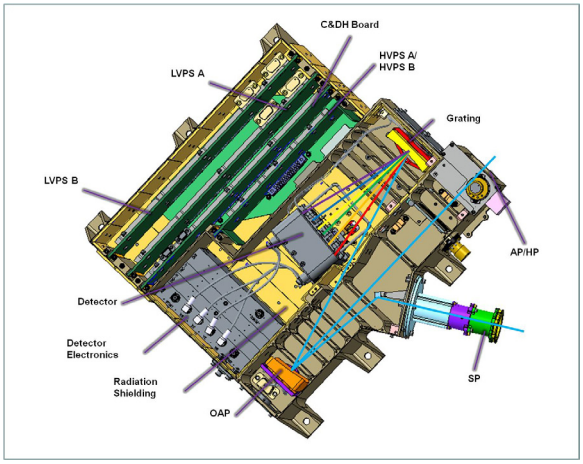

Figure 1. JUICE-UVS instrument design.

JUICE features dual low-voltage and high-voltage power supplies. Both HVPSs fit on one board. The LVPSs, however take up one board each. Europa-UVS features single-string power supplies, so it only has one LVPS board. As such, the Europa-UVS width is slightly smaller than JUICE-UVS by 1.125 inches, with a corresponding mass reduction of approximately 2 kg. Europa-UVS also features the solar port at 40° incidence to the airglow port, instead of 60° for JUICE-UVS. Otherwise, the designs are currently identical.

Design Improvements: The following changes maximize performance in the Jovian environment:

Spatial Resolution. The HP is designed to improve the spatial resolution of the base UVS design by a factor of approximately 4 at a cost of 20 times worse signal-to-noise. In practice, there are variations in optical aberrations that do not always scale with aperture size, so the HP spatial resolution varies as a function of wavelength. Furthermore, the optical resolution must be convolved with the native resolution of the detector to determine the final PSF as a function of wavelength. As shown in Figure 2, the resulting HP resolution is best at 90 nm (0.04°), and varies between 0.05° and 0.11° across the 55-210 nm bandpass.

Solar Port. The Solar Port is derived from the SOCC that flew on P-Alice past Pluto. This heritage assembly has been reworked for use at Jupiter in a few ways. First, the actuator is updated from a one-shot to a reusable actuator, similar to the scan mirror launch lock on Juno-UVS. Second, the pinhole has been resized from 1-mm to 0.25 mm to reduce solar flux. Finally, the pickoff mirror will be coated with gold to further reduce incoming solar flux to a safe level.

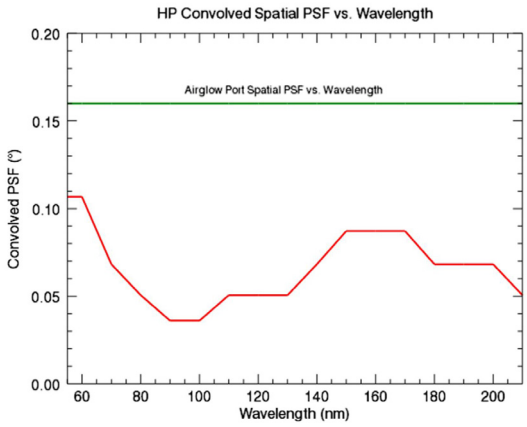

Figure 2. HP resolution as a function of wavelength.

Faster Detector Count Rates. The Juno-UVS cross-delay line (XDL) detector was limited to a maximum count rate of 85 kHz. While this rate exceeds the maximum rate seen by P-Alice by approximately a factor of three, it is still too low to ensure good science during the 300 kHz background rates expected at Europa closest approach. The JUICE and Europa-UVS XDL detectors are specified to have no worse than 30% deadtime loss at 300 kHz rates. The detectors achieve this rate by reducing the native resistance of the microchannel plates as well as optimizing the readout speed of the XDL electronics. Furthermore, the data connection to the spacecraft will be fast enough to handle sustained data rates over 300 kHz.

Improved Radiation Background Rejection. The pulse height distribution of detected UV photons differs from both electrons and gamma rays. The JUICE- and Europa-UVS detector electronics will feature a couple of improvements to the pulse height recording that will enhance rejection of background radiation. First, the number of recorded pulse height bins is increasing from 32 on Juno-UVS to 256. This improved resolution allows finer rejection of background events with large pulse height, potentially reducing background rates by 30%. As shown in Figure 3, potentially half of the detected electrons have pulse heights higher than any of the photons, so they may be rejected outright [5]. Second, an additional analog-to-digital converter has been added to the detector electronics to allow accurate reporting of the pulse heights even at high count rates. Previous electronics would report "sag" in the pulse height as count rate increased, which is inadequate for a high radiation background environment.

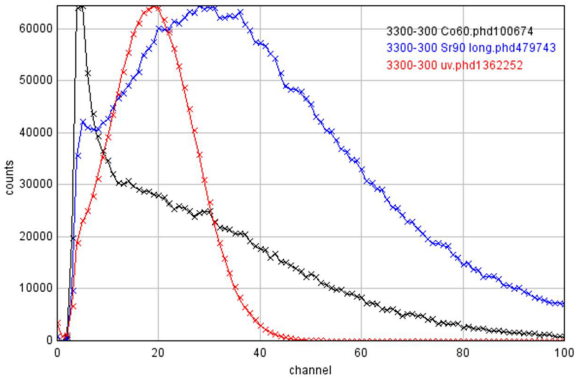

Figure 3. Pulse height distributions for UV photons (red), MeV electrons (blue), and MeV gamma rays (black) [5].

References:

[1] Stern S. A. et al. (2007) *SSR, 128,* 1, 507–527. [2] Stern S. A. et al. (2008) *SSR, 140,* 155-187. [3] Gladstone G. R. et al. (2010) *SSR, 150,* 161-181. [4] Gladstone G. R. (2014) *SSR,* doi:10.1007/s11214-014-0040-z. [5] Siegmund O. H. W. et al. (2015) *Proc of SPIE, 9601*, 96010S

THE SUPERCAM MAST UNIT ON THE NASA MARS2020 MISSION. M. Deleuze[1], P. Bernardi[2], Ph. Caïs[3], R. Perez[1], J.-M. Reess[2], L. Pares[4], B. Dubois[4], Y. Parot[4], B. Quertier[3], S. Maurice[4], K. Maccabe[5], R. Wiens[5] and F. Rull[6], [1]CNES, 18 avenue Edouard Belin, 31401 Toulouse cedex 4, France, [2]LESIA, Observatoire de Paris, 5 place Jules Janssen 92195 Meudon Cedex, France, [3]LAB, Université de Bordeaux, Allée Geoffroy Saint-Hilaire, 33615 Pessac Cedex, France, [4]IRAP, Observatoire Midi-Pyrénées, 14 avenue Edouard Belin, 31400 Toulouse France, [5]LANL, P.O. Box 1663, Los Alamos, NM 87545, USA., [6]Uva, Universidad de Valladolid, Spain

Introduction: The Mars 2020 rover mission is part of NASA's Mars Exploration Program, a long-term effort of robotic exploration of the Red Planet. The Mars 2020 mission addresses high-priority science goals for Mars exploration, including key questions about the potential for life on Mars. The mission takes the next step by searching for signs of past microbial life. The Mars 2020 rover introduces a drill that can collect core samples of the most promising rocks and soils and set them aside in a "cache" on the surface of Mars. The mission also provides opportunities to gather knowledge and demonstrate technologies that address the challenges of future human expeditions to Mars. These include testing a method for producing oxygen from the Martian atmosphere, improving landing techniques, and characterizing weather, dust, and other potential environmental conditions that could affect future astronauts living and working on Mars.

SuperCam Instrument: The SuperCam instrument is an evolution from the successful ChemCam (CCAM) instrument on MSL-Curiosity. SuperCam is an instrument package capable of five different remote-sensing techniques: Laser-Induced Breakdown Spectroscopy (LIBS), Raman and time-resolved fluorescence (TRF), passive visible and infrared (VISIR) reflectance spectroscopy, remote micro-imagery (RMI) and a sound recording device (MIC).

The SuperCam package consists of three separate major components: the SuperCam Body Unit (SCBU), the SuperCam Mast Unit (SCMU) and the SuperCam Calibration Target (SCCT). The SCMU is provided by IRAP (Toulouse, France, funding from CNES), while LANL (Los Alamos, NM) is building the SCBU. The IRAP and LANL subunits are entirely separate mechanically, greatly simplifying development across international boundaries. The University of Valladolid (UVa, Spain) is primarily responsible for the SuperCam on-board calibration target assembly.

SuperCam Mast Unit : The SuperCam Mast Unit (SCMU) combines several functions: it focuses the telescope, generates the laser beam to trigger the LIBS plasma and Raman scattering, it collects LIBS/Raman/VISIR light which is redirected to the spectrometers, reads RMI images and records sound. The SCMU consists of 2 units which are thermally separated: the Electronics Box (EBOX) and the Optical Box (OBOX). Within the SCMU; four modules are identical or minimally adapted from CCAM (LIBS Laser, Red Line optical path, Telescope, Focus), one is improved from CCAM (color imager), and three are completely new (InfraRed Spectrometer, Green line optical path and microphone).

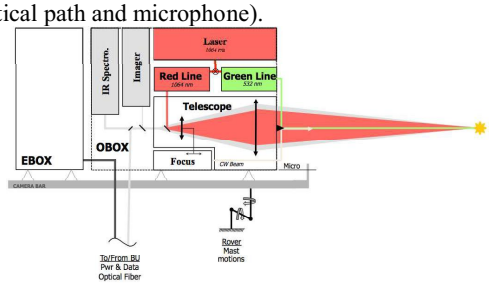

Figure 1: SCMU functional block diagram

Laser. The laser is the heart of the LIBS and Raman experiments. It has CCAM laser heritage but differs in a couple of important ways: a new Nd:YAG crystal to support higher firing rates (10 Hz/1000 shots). Simultaneously, the beam quality is improved for a better focus quality and a doubling crystal (KTP) is added to convert the 1064 nm line in 532 nm on demand.

Red Line. The 1064 nm laser beam is expanded to 1 cm diameter by a compact Galilean telescope and injected into the main Cassegrain telescope, which is unchanged from CCAM.

Green Line. The 532 nm laser beam is also expanded to 1 cm diameter by a compact Galilean telescope, but it remains collimated and is co-aligned along the telescope axis by a 2-mirrors periscopic system.

Telescope. The Cassegrain telescope has high CCAM heritage : it focuses the laser red beam onto the target and collects the photons through the laser dichroic. Then light below 950 nm is fed into a 300 µm-core fiber for LIBS/Raman/Vis reflectance analysis while longer wavelengths are diverted to the IRS. Moreover, light from a 20 mrad cone around the analysis spot goes to the color camera (RMI).

Focus. The focus capability relies on fine displacements of the secondary mirror. With high CCAM heritage, the table focus is used in autofocus mode at distances lower than 12 m and manual focus at greater distances.

Remote Micro-Imager. The RMI is a context imager of the laser pits on targets. It is located at the rear of the telescope. The optical path to the camera is unchanged from CCAM but the panchromatic 1 Mpx CCD is replaced by a color CMOS. The CMV4000 device constituted of 2048 x 2048 5.5µm pitch pixels, with a Bayer filter from CMOSIS was selected. RGB pixels of the Bayer filter are illuminated, providing color images with the same resolution as for CCAM. The RMI will benefit from the High Dynamic Range (HDR) mode.

InfraRed Spectrometer. The IRS is a compact and independent subsystem, linked to the telescope objective with a periscope. The band pass lies between 1.3 µm and 2.6 µm. The IRS concept is based on the scan of an Acousto-Optical Tunable Filter (AOTF). Applying a Radio Frequency (RF) signal on a transducer mounted on the AOTF, the crystal will transmit a zero order and diffract two useful orders (e-ray and o-ray) at the same wavelength depending on the excitation RF frequency. The zero order is trapped in a light trap while the e-ray and o-ray are focused on the two different HgCdTe (MCT) photodiodes. The photodiodes are embedded in a TO66 package including a triple-stage Thermo-Electric Cooler (TEC) to decrease the photodiode temperature up to 70°C below the spectrometer temperature. Only one of the two photodiodes is powered at the same time, the other one is carried as a cold redundancy. Considering the simplicity of the design, the IRS provides extremely valuable science using minimal resources.

Microphone. The MIC primary science objective is to support the LIBS investigations to obtain unique properties of Mars rocks and soils through their coupling with the LIBS laser. In addition, the MIC can monitor various artificial sounds of the rover and contribute to basic atmospheric science. The MIC assembly is composed of two parts: the microphone finger mounted on the RWEB window bracket and the front-end electronics fixed on the OBOX. The microphone is a Commercial Off-The-Shelf (COTS) unit, but has heritage from Mars Polar Lander (MPL) and Phoenix missions. The microphone has been implemented lately in the SCMU and is designed to add no risk on the developments, and to be plug-and-play up to ATLO.

EBOX. The EBOX is mechanically independent of the OBOX, and isolated from the baseplate, using fiberglass mounting feet. Four electronics boards are interconnected with a wiring flex and outer connectors (data, power, safety) to the SCBU.

LVPS board. The Low Voltage Power Supply (LVPS) board is connected to the rover +28V via the SCBU, to allow on/off switching of the SCMU and to distribute digital and analog secondary power lines.

DPU board. The Digital Processor Unit (DPU) board communicates with the SCBU, controls and monitors all the SCMU subsystems and hosts some operational algorithms. The DPU incorporates a re-programmable FPGA.

Laser board. The Laser board drives the Laser with high current (up to 230A) for lasing, and then triggers the Pockels cell with a high voltage signal (1450V) for firing. Another Pockels cell is triggered to switch the laser from red to green color.

IR board. The IR board functions are to power the AOTF with adequate frequency (from 33.8 to 68.7MHz), to control the TEC cooler and to sample the IR photodiodes signal. The RF frequency range covers the 1.3-2.6 µm range at 30 cm^{-1} resolution.

Development and Test Approach of the SCMU: The overall philosophy maximizes heritage and focuses strong attention on the few lower-heritage areas to ensure success. The plan is rich in development models :

EDU Model: The SCMU Engineering and Development Unit (EDU) Model was built to be fully functional, but not fully form and fit. All the functions are present and characterized at ambient. During last spring, the SCMU EDU has been shipped temporarily to LANL for a coupling test with SCBU EDU, for a successful first Raman end-to-end check.

TU Model : The SCMU EDU will be refurbished to be the SCMU Testbed Unit (TU) and delivered to JPL after being integrated with the SCBU for Mars 2020 Vehicle System TestBed purposes.

STM Model: The SCMU STM (Structural and Thermal Model) was built last spring and passed successfully the environemental tests (vibration, shock, thermal vacuum).

EQM Model: A fully representative SCMU Engineering and Qualification Model (EQM) model will be built and tested at Qualification level in 2016/2017. Performance will be verified and characterized. The EQM model will be delivered to LANL, for tests at Instrument level, then, for Calibration. This model will stay at LANL, as a ground model, during the mission.

Flight Model: This model, for flight, will be very similar to the EQM, but with screened EEE parts. The FM model will go through Acceptance tests campaign and will be delivered to LANL and then to JPL in 2018.

References: [1] Wiens et al. (2012) *Space Sci. Rev. 170*. [2] Maurice et al. (2012) *Space Sci. Rev. 170.* [3] Maurice et al. (2015) *LPSC 46*. [4] Clegg et al. (2015) *LPSC 46*. [5] Wiens et al. (2016) *LPSC 47*. [6] Maurice et al. (2016) *LPSC 47*. [7] Fouchet et al. (2015) *LPSC 46*. [8] Gasnault et al. (2016) *LPSC 47*. [9] Virmontois et al. (2016) *LPSC 47*.

Next-Generation Laser Retroreflectors for the Science and Exploration of the Moon, Mars and Beyond.

S. Dell'Agnello[1] for the SCF_Lab Team, D. Currie[2], R. Richards[3], J. Chandler[4]
[1]Istituto Nazionale di Fisica Nucleare – Laboratori Nazionali di Frascati (INFN-LNF), via E. Fermi, Frascati (Rome), Italy, email Simone.DellAgnello@infn.infn.it
[2]University of Maryland (UMD) at College Park, MD, USA
[3]Moon Express Inc (MEI), 19-2060 N Akron Rd, Moffett Field, CA 94035
[4]Harvard-Smithsonian Center for Astrophysics (CfA), MA, USA

Introduction. We developed next-generation laser retroreflectors for solar system science and exploration in the framework of the Affiliation membership of INFN to NASA/SSERVI (Solar System Exploration Virtual Institute), INFN National Science Committees n. 5 (devoted to R&D) and n. 2 (devoted to science) [1] and in collaboration with ASI, the Italian Space Agency. Applications cover landing and roving missions to the Moon, Mars (ExoMars 2016 lander, ExoMars 2020 Rover and Mars 2020 Rover) to future or proposed missions to Phobos/Deimos (sample return), icy/rocky moons of Jupiter/Saturn and asteroids/comets (ESA's AIM). These retroreflectors have been or will be fully characterized at the SCF_Lab (Satellite/lunar/gnss laser ranging/altimetry Cube/microsat Characterization Facilities Laboratory), a unique and dedicated infrastructure of INFN-LNF, in Frascati (Rome), Italy (www.lnf.infn.it/esperimenti/etrusco/) [2] and at vibration qualified at certified facilities.

We will present analysis work and simulations performed with CfA's Planetary Ephemeris Program sw package to test General Relativity (GR) and new gravitational physics with missions to the Moon (under an agreement among INFN, Moon Express Inc and the Univ. of Maryland) and Mars, continuing and extending the work done for the Moon with Apollo and Lunokhod cube corner laser retroreflectors (see [3] [4] [5] and refs. by March et al in [6]).

Next-Generation Lunar Laser Retroreflectors

Concerning the Moon, our main goals are lunar exploration, geodesy and precision tests of General Relativity (GR) and new gravitational physics, continuing and extending up to a factor 100 the reach of Apollo and Lunokhod laser retroreflectors. We developed a large (4" = 100 mm optical diameter), single retroreflector (MoonLIGHT, Moon Laser Instrumentation for General relativity High accuracy Tests). Since it is unaffected by the lunar librations that currently limit the accuracy of Lunar Laser Ranging (LLR) to Apollo/Lunokhod reflectors, MoonLIGHT will support significantly measurements by ground stations of the International Laser Ranging Service (ILRS). MoonLIGHT, also dubbed LLRRA21, Lunar Laser Retroreflector Array for the 21st century, is shown in Fig. 1, next to an Apollo laser retroreflector.

Figure 1: MoonLIGHT (4"), Apollo (1.5") reflectors

INFN, UMD and MEI signed a private-public partnership, multi-mission agreement to deploy MoonLIGHT on the Moon (1st mission: end 2017/early 2018). The results of an optical performace characterization of MoonLIGHT carried out at the SCF_Lab is in Fig. 2.

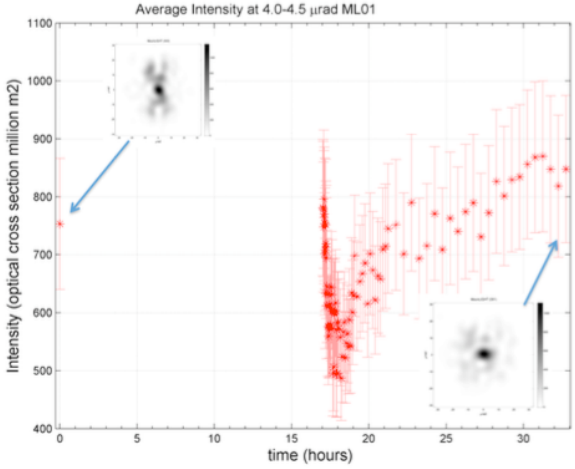

Figure 1: MoonLIGHT laser return (Oprical Cross Section) at 4.0-4.5 μrad velocity aberration.

Current LLR GR tests and improvements expected with MoonLIGHT are shown in Table 1 [7][8].

Gravitational measurement	1st generation LLR accuracy (∼ cm)	next-generation LLR accuracy (1 mm)	next-generation LLR accuracy (0.1 mm)
EP	$< 1.4(10^{-13})$	10^{-14}	10^{-15}
SEP	$< 4.4(10^{-4})$	$3(10^{-5})$	$3(10^{-6})$
β	$< 1.1(10^{-4})$	10^{-5}	10^{-6}
$\dot{G}/G$	$< 9(10^{-13})yr^{-1}$	$5(10^{-14})$	$5(10^{-15})$
Geodetic precession	$6.4(10^{-3})$	$6.4(10^{-4})$	$6.4(10^{-5})$
$1/r^2$ Deviation	$< 3(10^{-11})$	10^{-12}	10^{-13}

Table 1: Current and future LLR test of GR.

First laser retroreflector on the surface of Mars

During Summer 2015 the SCF_Lab Team of INFN-LNF, with support by ASI, carried out an intense activity of final design, manufacturing and testing in order to construct, space qualify and finally integrate INRRI-EDM/2016 on ESA's ExoMars EDM spacecraft (also dubbed 'Schiaparelli'), which was successfully launched on March 14, 2016. INRRI (INstrument for landing-Roving laser Retroreflector Investigation) for the EDM (Entry descent and landing Demonstration Module) 2016 mission is a compact, lightweight, passive, maintenance-free array of eight cube corner laser retroreflectors fixed to an aluminium alloy frame through the use of silicon rubber suitable for space applications. INRRI was installed on the top panel of the EDM Central Bay on October 14, 2015. It will enable the EDM to be laser-located from Mars orbiters, through laser ranging and altimetry, lidar atmospheric observations from orbit, laser flashes emitted by orbiters, and lasercom. One or all of the above means of observation can be supported by INRRI when there is an active, laser-equipped orbiter, especially after EDM end-of-life and for a long time. INRRI goals will cover science (Mars geodesy/geophysics, future Mars test of General Relativity, GR), technology and exploration. Concerning the latter two, INRRI will support *mars-georeferencing* of the EDM landing site, support potential precision lidar-based landing next to the EDM, support test and diagnostics of lasercom for data exchange among Mars orbit, Mars surface and Earth, and it will be a precursor for additional Mars surface retroreflectors on exploration rovers like the ExoMars 2020 of ESA (already foreseen, through ASI) and NASA's Mars 2020 Rover. Infact, recently NASA-HQ formally invited ASI to deliver a flight INRRI unit for Mars 2020. We will describe our innovative payload, hopefully the very first to be deployed safely with the lander Schiaparelli on the Mars surface, its space qualification for the ExoMars EDM 2016 mission and the prospects for its deployment on Mars 2020.

Finally: 1) note that INRRI on the Moon landers, like the one forseen to be deployed on the 1st MEI lander, is to be observed by laser-ranging capable orbiters, like NASA's LRO; 2) we will describe future applications to Phobos sample return, icy/rocky moons of Jupiter/Saturn and to asteroid/comets missions.

References:

[1] Advanced Laser Retroreflectors for Astrophysics and Space Science, Dell'Agnello, S., et al, *Journal of Applied Mathematics and Physics, 3, 218-227 (2015).*

[2] Creation of the new industry-standard space test of laser retroreflectors for the GNSS and LAGEOS, S. Dell'Agnello et al, *Adv. Space Res. 47, 822–842 (2011).*

[3] Probing gravity with next-generation lunar laser ranging, M. Martini and S. Dell'Agnello, *in R. Peron et al. (eds.), Gravity: Where Do We Stand?, DOI 10.1007/978-3-319-20224-2_5, Springer International Publishing, Switzerland (2016).*

[4] Constraining spacetime torsion with Moon and Mercury, R. March, G. Bellettini, R. Taursaso, S. Dell'Agnello, *Phys. Rev D 83, 104008 (2011).*

[5] Constraining nonminimally coupled gravity with laser ranging to the moon, N. Castel-Branco, J. Paramos, R. March and S. Dell'Agnello, *in 3rd European Lunar Symposium, Frascati, Italy (2014).*

[6] The 1/c expansion of nonminimally coupled curvature-matter gravity model and constraints from planetary precession, R. March, J. Paramos, O. Bertolami, S. Dell'Agnello, submitted to Phys. Rev. D (2016), arXiv:1607.03784v1 [gr-qc], 7 Jul 2016.

[7] [3] Williams, J. G., Turyshev, S. G., Boggs, D. H., Ratcliff, J. T., Lunar laser ranging science: Gravitational physics and lunar interior and geodesy, *Adv. Space Res. 37(1), 67-71 (2006).*

[8] INRRI-EDM/2016: the first laser retroreflector on the surface of Mars, Dell'Agnello S., et al, submitted to Adv. Space Res., Manuscript ASR-S-16-00054.

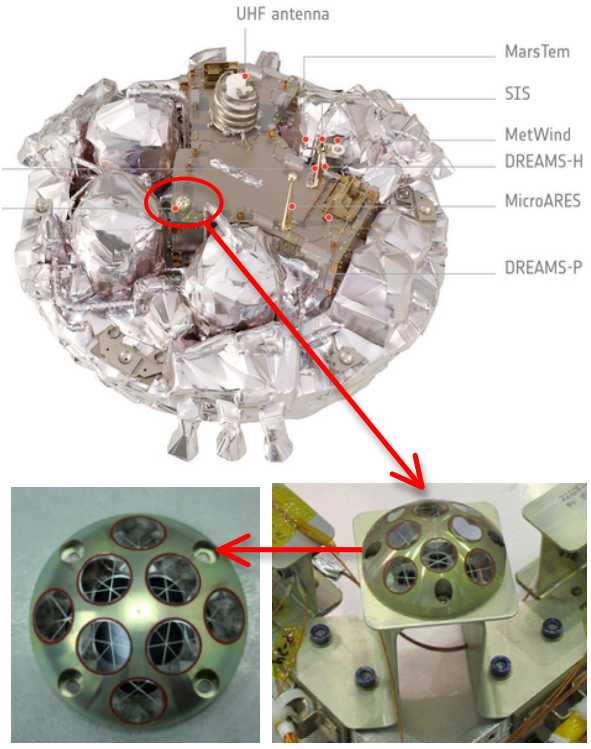

Figure 2. Top picture (courtesy of ESA): Schiaparelli lander with science payloads. Bottom right zoom (courtesy of ESA and Thales Alenia Space Italia): INRRI integrated on the central bay of Schiaparelli. Bottom left: close-up of INRRI.

A millimeter wave spectrometer on a chip for *in-situ* molecular spectroscopy Brian J. Drouin[1] A. Tang[1], E. Schlecht[1], A. W. Raymond[1,3], Mau-chung Frank Chang[2], Y. Kim[2], [1]brian.j.drouin@jpl.nasa.gov, Jet Propulsion Laboratory, California Institute of Technology, Pasadena, CA 91109-8099 [2]University of Calfornia, Los Angeles, Los Angeles, CA, 90095, 3 Harvard University, School of Engineering and Applied Science, Cambridge, MA, 02138.

Introduction: Exploration of extra-terrestrial objects demands small, efficient investigative tools, ideally with highly specific and sensitive detections. Multiple science objectives outlined in the planetary science decadal survey [1] involve the detection of small molecular tracers and determination of their abundance and origin. For detections in the gas phase the rotational spectrum of a polar molecule typically provides a strong interaction with centimeter and shorter wavelength radiation, which has been exploited for remote sensing for half a century with data repositories growing to support these widespread efforts [2,3]. *In-situ* instruments are now being developed [4,5] but have lagged behind remote sensors due to the large equipment traditionally required for generation and detection of this radiation. These first generation instruments are man-portable, but not yet compact enough for space applications. Furthermore, the Fourier Transform microwave technique[6] has been utilized in research laboratories for three decades to determine fundamental physical properties of molecules and molecular complexes and extension of the technique to higher frequencies furthers study of the lightest molecules (*e.g.* hydrides) and complexes (particularly with Helium). Other research laboratories have built cavity resonators for sensitive detections in the millimeter[7] and submillimeter [8], however the injection losses reduce the potential to streamline the technique.

To realize the goal of a compact low-power system, we take advantage of new advances in both the transistor speed and size of commercial CMOS technology [9] that have enabled entire millimeter wave transmitters and receivers to be built on a single chip. This effort leverages these technological advances to enhance microwave techniques for *in-situ* gas detection. We have applied these advances in millimeter wave CMOS technology to standard microwave spectroscopic techniques [6,10] and realized the goal of developing a highly compact *in-situ* gas detection system. Extension of this technique into the millimeter had been slow due to difficulties with coupling radiation efficiently into high finesse cavities. Some exploratory work on wire-polarizer based coupling schemes have recently been described [11,12], but limitations of available hardware have precluded molecular detections. Extension of the traditional technique of incorporating back-fed coupled light directly behind a spherical mirror has reported sensitive detections at 59.1 GHz [13] and measurements up to 88 GHz have recently been demonstrated [14], as well as a demonstration of the potential for cavity ringdown absorption spectroscopy at 94 GHz [7]. Our demonstrated method is similar to that proposed for mm-wave cavities by Braakman and Blake [11] except their wire grid coupler is replaced with a gold-plated coupler and the mm-wave light is created and detected at this coupler. The technique may be generally applicable across the THz spectrum and provides a template design for a multitude of planetary mission profiles. This instrumentation goal leaps forward in two important ways (1) there has not been an efficient means to a build cavity resonator for the millimeter and submillimeter wavelengths, and (2) the volume and mass of the electronics and optics (in comparison to traditional millimeter wave systems) decrease by more than an order of magnitude.

Results: In this first generation system, shown in Figure 1, the CMOS transmit and receive chips are demonstrated at the input/output interface of a planar coupler that injects the light into a semi-confocal Fabry-Perot cavity. The mirror position is adjusted to provide throughput in the range of one or more molecular resonances and light generated at the coupler interface is pulsed into the cavity.

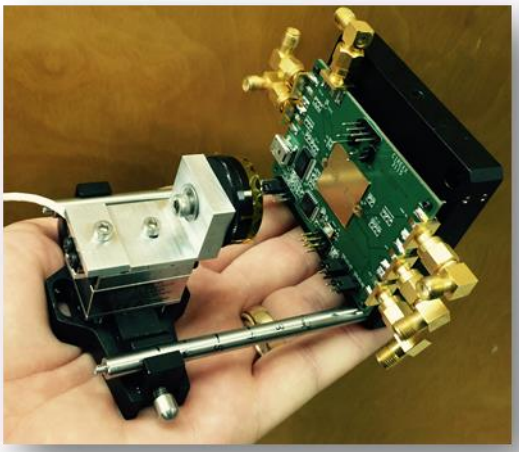

Figure 1. The CMOS devices that generate and receive the mm-wave radiation are each 1 mm^2. These are located on either side of the gold square (the coupler) on the circuit board. A 25 mm diameter, 25 mm focal length spherical mirror is positioned normal to the coupler plane on a precision translation stage that allows mode tuning across the 92-102 GHz bandwidth of the CMOS devices.

The mixer contains an embedded local oscillator tuned several MHz away from the resonance (and transmitted frequency) and the analog output of the mixer is fed to a digitizing oscilloscope for Fourier transform of the post-pulse echo response from molecules that are pumped into an excited state by the transmission pulse. An example of gas detection is shown in Figure 2. The CMOS circuitry draws only 250 mW of power during nominal operations, and total instrument power is dominated by the command/control hardware (USART and Atmega) that draw about 300 mW in the current configuration.

The example spectrum of N_2O allows an initial sensitivity derivation. Using an interaction volume of 0.2 cm^3, the measured pressures and the signal to noise ratios (22 in center channel and integrating out over the width of the feature) of the measurements, we estimate the minimal detection for the system in its current configuration to be $5x10^{11}$ N_2O molecules, or 70 ppm in a 100 mTorr gas mixture for an integration time of 100 ms. Other molecules will have differing (typically lower) detection limits due to variation in dipole moment, which is very weak for N_2O (0.16 Debye).

Numerous volatile species are detectable in the bandwidth of the spectrometer, and efforts are underway to characterize the sensitivity to key molecular tracers that are relevant to planetary science including deuterated water and a variety of organic compounds. A system trade study is also underway that will examine trade-offs in the cavity dimensions. There is also a plan to miniaturize the data processing (CMOS analog to digital conversion as well as Fast Fourier Transform) to dramatically reduce the output bandwidth of the system without significantly increasing the power consumption.

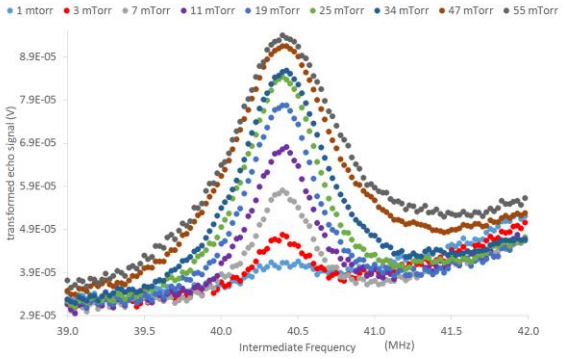

Figure 2. Data recorded with the system shown in Figure 1 embedded in a vacuum chamber with different gas flows of nitrous oxide (N_2O).

References:

[1] Vision and Voyages for Planetary Science in the Decade 2013-2022, Committee on the Planetary Science Decadal Survey, Space Studies Board Division on Engineering and Physical Sciences, The National Academies Press, Washington, D.C. [2] H. M. Pickett, R. L. Poynter, E. A. Cohen, M. L. Delitsky, J. C. Pearson, and H. S. P. Meuller (1998) *J. Quant. Spectrosc. & Rad. Transfer* 60, 883. [3] H. S. P. Mueller, F. Schloeder, J. Stutzki, and G. Winnewisser (2005) J. Mol. Struct. 742, 215227. [4] Brian J. Drouin, Ken Cooper, Robert Dengler, Marcoanto Chavez, William Chun, Tim Crawford (2012) *Aerospace Conference, IEEE*, 3-10, 1 - 4. [5] Christopher F. Neese, Ivan R. Medvedev, Grant M. Plummer, Aaron J. Frank, Christopher D. Ball, and Frank C. De Lucia (2012), *IEEE Sens. J.*, 12. [6] T. J. Balle and W. H. Flygare (1981), *Rev. Sci. Instrum.* 52, 33. [7] N. Gopalsami, A.C. Raptis, J. Meier, Review of Scientific Instruments (2002), 73 (2) 259-262. [8] A.I. Meshkov and F.C. De Lucia, Review of Scientific Instruments (2005), 76 083103. [9] A. Tang, D. Murphy, F. Hsiao, G. Virbila, Y.-H. Wang, H. Wu, Y. Kim and M.-C. Frank Chang (2012) *IEEE Transactions Microwave Theory and Techniques IMS 2012 special issue*, 60 4129-4137. [10] R. N. Clarke and C. B. Rosenberg (1982) J. Phys. E: Sci. Instrum., 15, 9-24. [11] R. Braakman, G.A. Blake (2011) *J. Appl. Phys.* 109, 063102. [12] B. A. DePrince, B. E. Rocher, A. M. Carroll, and S. L. Widicus Weaver (2013) *Review of Scientific Instruments* 84, 075107. [13] D. Halfen, L.M. Ziurys (2016) presentation WH03, International Sysmposium on Molecular Spectroscopy. [14] J. K. Anderson, D.T. Halfen, L.M. Ziurys (2015) *J. Mol. Spec.* 307, 1-5.

Additional Information: This material is based upon work supported by the National Aeronautics and Space Administration under Grant No. NN13D485T issued through the Planetary Science Division PICASSO program. AR is supported by NSTF grant NMX13AM67H. Portions of the research described in this paper were performed at the Jet Propulsion Laboratory, California Institute of Technology, under contract with the National Aeronautics and Space Administration, government sponsorship acknowledged.

TECHNIQUE DEVELOPMENT NEEDED TO INTERPRET RAMAN SPECTRA OF MINERAL MIXTURES. M. D. Dyar[1], L. B. Breitenfeld[1], P. Bartholomew[2], CJ Carey[3]. [1]Mount Holyoke College, Dept. of Astronomy, South Hadley, MA, 01075, mdyar@mtholyoke.edu, Department of Biology and Environmental Science, University of New Haven, West Haven, CT 06516, [3]College of Information and Computer Science, University of Massachusetts, Amherst, MA 01003.

Introduction: Planetary scientists who use reflectance and thermal emission spectroscopy are spoiled by the availability, breadth, and sophistication of unmixing software and spectral libraries available for commonly used techniques. Many techniques for extracting quantitative abundances of minerals from visible through mid-infrared (and thermal emission) spectra of mineral mixtures are available [1-3]. *However, there is no analogous methodology for mineral unmixing for the technique of Raman spectroscopy* because most development work has been focused on micro-Raman techniques [4] that probe pure minerals. Because the beam sizes of the Raman instruments on SuperCam (~1.3 mm) [5] and SHERLOC (50 μm) [6] on *Mars 2020* are larger than most expected grain sizes on Mars, it is likely that their Raman spectra will contain mixtures of mineral signatures. Other impending possible uses of Raman spectroscopy, such as on Europa and Venus landers, may also face this issue. An infusion of work is needed to support these instruments.

Three interrelated areas of research are reported here: 1) integration and review of new and existing mineral databases of well-characterized mineral samples, 2) acquisition of quantitative data to assess the relationship between Raman peak intensity and mineral abundance, and 3) development of mineral identification software with quantified accuracy.

Databases: The importance of robust Raman databases of appropriate well-characterized minerals cannot be overstated. In addition, spectra of single crystals may not be appropriate for identification (or quantification) of fine grained mineral mixtures and/or powders. Raman spectral data for powders and mixtures of minerals are nearly nonexistent and, while work has already begun to remedy this [7], the necessary investment of time and effort needed is significant.

While a number of public/internet Raman spectral databases exist, the largest, by far, is the RRUFF spectral database (http://rruff.info) created by Bob Downs and the University of Arizona mineralogy group through the support of both private donors and federal research grants [8,9]. While every spectrum in these databases has scientific value, not every spectrum meets the criteria to be included in a reference dataset for mineral identification [10]. These criteria include:

1. Use only spectra from verified samples – ideally with both structure and chemistry verified.
2. Strong, clear spectra are preferred, so a minimum S/N ratio must be set.
3. Use spectra that are free of artifacts – for Raman the concern is features due to photo-fluorescence.

Because many of the >4000 known mineral species are truly rare, an effective reference database for petrologic mineral identification also needs to contain flags to distinguish rock-forming minerals from rare ones, while still maintaining thorough coverage of rock-forming minerals. To this end, we are assembling and reviewing publicly-available Raman data from RRUFF and other on-line datasets to filter out weaker (low S/N) spectra, those contaminated by fluorescence, and from unverified samples. We are also evaluating gaps in the resulting dataset that are relevant to rock-forming and planetary minerals. We are obtaining Raman spectra on well-characterized samples in order to fill those gaps. Particularly important are pyroxenes and olivines. We plan to acquire data on samples synthesized by Don Lindsley at Stony Brook University that span the Ca-Fe-Mg pyroxene quadrilateral and the fayalite-forsterite solid solution series.

Finally, because fluorescence peaks are often not inherent characteristics of the individual minerals and have the potential to confuse matching algorithms, we plan to study mineral fluorescence under experimental conditions relevant to Raman spectrometry. Although the use of time-resolved Raman in some planetary missions will exclude fluorescence effects, nearly all existing spectral libraries (to which they will be compared) contain data with this problem.

To address the lack of data on fine-grained minerals, we plan to collect data on a petrologically relevant subset of >10,000 powdered minerals available in our laboratory as funding allows. We are also creating fine-grained mixtures of mineral and glass phases for Raman testing, including 256 binary mineral mixtures described in [11,12] and 140 glass-mineral mixtures designed to test detection limits.

Understanding Raman Peak Intensities: It is well-known that experimental factors affect Raman peak intensities (and thus mineral identification). Spectra of the same mineral species in existing datasets show variations in peak presence/absence and relative intensity. These can result from sample factors (grain size, transparency, crystallographic orientation, grain surface/boundary effects [4]), instrument factors (laser wavelength, power, and spot size, spectrometer apertures, gratings, and detectors), experimental factors

(angle of incidence and takeoff and the use/absence of polarizers) and data gathering factors (integration time, averaging, method/frequency of calibration). Some differences in peak intensities can be mitigated through pre-processing steps such as normalization, smoothing, and squashing [13,14]. We are also working on a calibration transfer methodology that will correct for many of these instrumental and experimental factors [15].

Raman cross-section of minerals is the primary *species-specific* intensity factor; it arises primarily from variations in bond polarizability in mineral structures. Mineral-specific proportionality factors (comparable to optical constants used to relate peak intensities to mineral abundances) of common rock-forming minerals are needed. These can be determined from calculations of remote Raman efficiency based on laboratory measurements [16] or by comparing peak intensities of minerals mixed with known amounts of a standard such as diamond [12]. Of these, the latter is more generally useful and easier to implement in practice. We plan to acquire those data in our laboratory for hundreds of mineral species before the *Mars 2020* landing.

Matching and Unmixing of Raman Data: Traditional Raman matching software packages, including the CrystalSleuth program [17], have been found to have limited accuracy, especially at the species level. However, machine learning techniques using automated whole spectrum matching (AWSM) [14] dramatically improve matching accuracy for Raman spectra of pure minerals. For example, a weighted-neighbor cosine similarity classifier [13] achieved 97.8% group-level and 89.2% species-level accuracy on average for a subset of RRUFF data, far outperforming existing methods for matching.

Moving forward, unmixing approaches that build on techniques currently used for FTIR should provide a starting point for Raman theoretical umixing models. Raman features arise from scattering of energy while FTIR spectra have absorption features. Raman provides information on covalency of molecular bonds, while FTIR indicates ionic character. Raman peaks reflect changes in bond polarization, while FTIR peaks record dipole changes. These commonalities suggest the potential of future unmixing algorithms to assist with interpretation of Raman data, but that promise is years away from becoming a reality.

As an alternative, our AWSM algorithms are now being adapted for the purpose of mineral unmixing. However, determining the components is one problem, but quantifying them is another. Consider the mixtures of minerals in known proportions shown in **Figure 1**. These are Raman data of three mixtures, all with 20 volume% gypsum and 80 volume % of another common phase (forsterite, siderite, or labradorite). In these

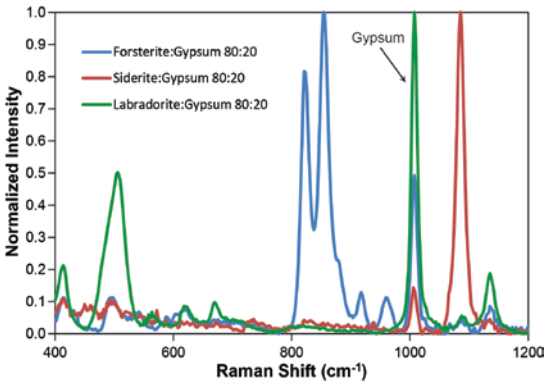

Figure 1. Mixtures of 20% gypsum with 80 volume% of other phases (pyroxene, carbonate, and feldspar). Note the large variations in the intensities of the gypsum peak ca. 1010 cm^{-1} despite its constant modal abundance.

mixtures, the amount of gypsum is identical but the magnitudes of the gypsum peaks are highly variable. This is emblematic of problems to be faced in quantifying mineral abundances using Raman spectra. We expect that Raman proportionality factors measured against our diamond internal standard will provide an empirical solution for this challenge.

Resources: Current models for Raman mineral matching and unmixing of up to three components [18] are available on our web site for beta-testing at http://nemo.cs.umass.edu:54321/. Ongoing development work and new data will be posted there for interested users. Please contact the first author for full site access.

Acknowledgments: This work was supported by NASA SSERVI grant NNA14AB04A (RIS^{4}E) and the Massachusetts Space Grant Consortium.

References: [1] Rull F. et al. (2014) *8th Intl. Mars Conf.*, Abstr. #1277. [2] Beegle L. W. et al. (2014) *11th Intl. GeoRaman Conf.*, Abstr. #5101. [3] Maurice S. et al. (2015) *LPS XLVI*, Abstr. #2818. [4] Haskin L. A. et al. (1997) *JGR*, 102, 19293-19306. [5] Clegg S. M. et al. (2015) *LPS XLVI*, Abstr. #2781. [6] Beegle L. et al (2014) *LPS XLV*, Abstr. #2835. [7] Dyar M.D. et al. (2016) *LPS XLVII*, Abstr. #2240 [8] LaFuente B. et al. (2015) *Highlights Mineral. Crystallography*, pp. 1-29. [9] Stone N. et al. (2015) *AbSciCon*, Chicago, IL. [10] Bartholomew P.R. et al. (2014) *GSA Abstr.* 46, 321. [11] Breitenfeld et al. (2016) *LPSXLVII*, Abstr. #2430. [12] Breitenfeld et al. (2016) *LPS XLVII*, Abstr. #2186. [13] Carey C. et al. (2015) *J. Raman Spectrosc.*, 46, 894-903. [14] Carey C. et al. (2015) *AI in Space, IJCAI 2015*. [15] Boucher, T. et al. (2016) *LPS XLVII*, Abstr. #2784. [16] Stopar J.D. et al. (2005) *Spectrochim. Acta A*, 61, 2315-2323. [17] Laetsch T. and Downs, R.T. (2006) *19th General IMA Meeting*, Kobe, Japan, 23–28. [18] C. Carey et al. (2016) *LPS XLVII*, Abstr. #2626.

LESSONS LEARNED FROM LIBS CALIBRATION DEVELOPMENT. M. D. Dyar[1], E. A. Breves[1], K. H. Lepore[1], T. Boucher[2], S. Giguere[2]. [1]Mount Holyoke College, Department of Astronomy, South Hadley, MA, 01075, mdyar@mtholyoke.edu, [2]College of Information and Computer Science, University of Massachusetts, Amherst, MA 01003.

Introduction: More than ten years of work in our and others' research groups have been dedicated to development of robust standards, data processing, and calibration tools for laser-induced breakdown spectroscopy (LIBS). Here we summarize major considerations relating to LIBS calibrations as we and others have encountered them, with a focus on our group's work.

Calibration suites. As with most analytical techniques, the number of standards and their elemental compositions must represent the magnitude of variation in the unknowns to be analyzed. This is particularly important for LIBS because matrix effects (largely arising from interactions within the plasma) have a first order effect on peak intensities, especially for light elements. Currently the largest set of LIBS calibration data on rocks comes from a suite of 2883 rock and mineral powders acquired in our laboratory [1], each shot 30 times at >5 locations using 3 different laser powers. Included in this suite are 320 samples consisting of 8 rock matrices doped with Ni, Zn, Cr, Mn, Co, Rb, Sr, Y, Zr, Ce, La, Se and Pb in concentrations ranging from 10 ppm to 10 wt%. Preliminary analyses suggest that a significant improvement in prediction accuracy results from such a broad training set.

Laser Power. Work by [2] used the ratio of intensities of the Si II line at 644.7 nm against that of neutral Si at 288.2 nm to demonstrate that the plasma temperature recorded in Mars ChemCam spectra is variable. This effect can be reproduced in the laboratory as well, where even under ideal conditions, the laser power on target has some variability. Because the population of species and their ionization states is temperature-specific, it is critical for LIBS calibration data to be collected over a range of plasma temperatures that spans those used in the instrument of interest.

Normalization. LIBS data require normalization for comparisons among conditions, data sets, and instruments, but the optimal method for this is still being investigated. The ChemCam team [3,4] and most workers normalize to the total intensity on each of the three spectrometers. Some workers [5] have suggested that other types of normalization, such as to the magnitude of the continuum or to specific spectral lines (e.g., C at 247.9 or 658.0 nm or O ca. 777.2 nm) may be required for analysis of trace elements.

Continuum removal. There is as yet no consensus on the best practice for continuum (baseline) removal in LIBS spectra. We have recently [6] examined the causes, effects, and optimization of continuum removal in LIBS from geological samples. Nine previously published methods for baseline subtraction generally produce equivalent prediction accuracies for major elements after optimizing their adjustable parameters. Ideally, these parameters should be determined separately for each variable. We proposed a new technique for custom baseline removal (BLR) [7] that significantly improves prediction accuracy over existing methods across varying geological data sets, instruments, and analytical conditions. The current practice of using generalized, one-method-fits-all-spectra baseline removal results in poorer predictive performance for all methods. The extra steps needed to optimize baseline removal for each predicted variable are shown to be well worth the additional computations required.

Angle of incidence. Spectral variability due to changes in collection geometry is typically ignored, despite work [8,9] showing that differences in orientation of continuum and emission lines could complicate the practice of normalization. So we [10] have tested results of varying ablation and collection angles from 0-60° on LIBS spectra of glasses and rocks with compositions from basalt to rhyolite. We varied ablation and collection angle together as well as separately. Summed spectral intensity increases as ablation or collection angle approaches normal to the standard surface. Spectral intensity of the fitted continuum varies more with ablation or collection angle than spectral intensity of the emission lines. Most importantly, results show that an additional analytical uncertainty of >30% is added to LIBS errors if the ablation angle onto the target surface is unconstrained or unknown.

Univariate vs. multivariate analyses. Analysis techniques for LIBS data fall in two categories. Univariate analyses use the intensity of a single peak (or peaks) to determine concentration using a calibration curve relating those two variables, but they suffer greatly from the matrix effects mentioned above. The alternative is multivariate analysis, generally partial least-squares (PLS), which is currently used in tactical activities for ChemCam [3]. We and others [11-16] have worked to find ways to improve upon PLS, either by applying more modern methods or through novel approaches to data preprocessing; 10-30% improvements in prediction accuracy result depending on the element predicted and the training set used.

We have recently [17] investigated the issue of univariate vs. multivariate prediction accuracy using 1356 spectra from 452 geologically-diverse samples,

the largest suite of LIBS rock spectra ever assembled. Univariate predictions are by far the least accurate, regardless of the region of channels/wavelengths chosen and the prominence of the selected emission lines. The best wavelength region choice for any given univariate analysis is an inherent property of each specific training set that cannot be generalized. In comparison, multivariate analysis using PLS almost universally outperforms univariate analysis, producing results that improve in accuracy by 63% for major elements and 3% for minor elements. This difference is likely a reflection of signal to noise ratios, which are better for major elements than for minor elements, and likely limit their prediction accuracy by any technique. Masking out channels to focus on emission lines from a specific element [17] worsens prediction accuracy for major elements but is useful for minor elements with low signals and proportionally much higher noise; use of PLS rather than univariate analysis is still recommended for the elements tested, which included Si, Al, Ti, Fe, Mg, Ca, Na, K, Ni, Mn, Cr, Co, and Zn [17].

Components in PLS Models. A key parameter of models like PLS is the number of components used. In a manner analogous to choosing the polynomial order in a multiple regression model, the fewest possible number of components should provide the most generalizable prediction model. For this reason, the number of components in LIBS PLS models is usually held to be <12 [e.g., 3,4]. Tests using a dataset with 1356 LIBS spectra [18] showed that after increasing the search range to include up to 50 components, prediction accuracy improved in 30.8% of cases, stayed the same in 57.0% of cases, and became worse in 12.2% of cases. This implies that the complex interactions resulting from variation in elemental composition produce a system with an intrinsic dimensionality larger than 12 components, so use of predictive models with a larger numbers of components is justified. The fact that model performance converges on <50 components indicates the compressibility of LIBS data in general.

Calibration Transfer. We have learned that LIBS data are extremely sensitive to instrumental differences as well as all the factors discussed above. Machine learning provides tested techniques for resolving discrepancies among datasets from different instruments, a task known as calibration transfer (CT). For example, CT can be used to correct for differences found between spectra of deployed extraterrestrial instruments, like ChemCam, and Earth-based laboratory facilities.

Using a latent variable CT method, we showed that the predictive accuracy of major elements like CaO can be improved up to 60% [19]. CT can also be used to align and aggregate suites of spectra with a small number of common samples, allowing better models to be built with combined data sets. With a linking set size >10 samples, models trained on a suite of data sets aligned with piecewise direct-standardization (PDS) were more generalizable with lower prediction error [20] than those of the individual data sets. Unfortunately, PDS requires the differing instruments to share the same sampling wavelength range and frequency and cannot correct for larger differences.

Our group has introduced a novel framework for CT based on recent advances in the field of convex optimization [21]. A customizable CT loss function is constructed using a series of penalty terms that target specific behaviors, spectroscopies, and task types. It is optimized using alternating direction method of multipliers capable of transferring multiple data sets with millions of samples and thousands of channels. We have introduced a framework for CT that does not require any overlapping subset of samples [22]; it aligns disparate data sets by embedding samples in a shared low-dimensional latent-space to preserve their local geometric structures. This is effective when data sets are large but the overlapping subset is small or absent, though overlapping subset CT methods are preferred.

Future Work. Although much has been done to improve accuracy of LIBS as a chemical analysis tool, several issues remain. These include effects of uneven/porous surfaces/grain size, problems relating to prediction of trace and light elements, and experimental factors such as laser stability/power distribution. As these are studied, the usefulness of LIBS in planetary exploration will continue to improve.

Acknowledgments: Work supported by NSF grants CHE-1306133, CHE-1307179 and NASA NNX14AG56G, NNX12AK84G, and NNX15AC82G. We thank the Massachusetts Space Grant Consortium for student support.

References: [1] Dyar M.D. et al. (2016) *LPS XLVII*, Abstract #1510. [2] Tokar R.L. et al. (2015) *LPS XLVI*, Abstract #1369. [3] Wiens R. et al. (2013) *Spectrochim. Acta B*, 82, 1-27. [4] Clegg S.M. et al. (submitted) *Spectrochim. Acta B.* [5] Rapin W. et al. (2016) *LPS XLVII*, Abstract #226. [6] Dyar M.D. et al., *Spectrochim. Acta B*, submitted. [7] Giguere, S. et al. (submitted) *Appl. Spectr.* [8] Piepmeier E.H. and Malmstadt H.V. (1969) *Anal. Chem.*, 50, 1483-1499. [9] Multari R.A. et al. (1996) *Appl. Spectr*., 50, 1483-1499. [10] Breves, E.S. et al. (submitted) *Spectrochim. Acta B.* [11] Boucher T.F. et al. (2015) *Spectrochim. Acta B*, 107, 1-10. [12] Boucher T.F. et al. (2015) J. Chemometrics, 29, 484-491. [13] Boucher T.F. et al. (2015) *5th AI in Space IJCAI Workshop*, Buenos Aires. [14] Anderson, R. et al. (submitted) *Spectrochim. Acta B.* [15] Kochelek, K.A. et al. (2015) *Amer. Mineral.*, 100, 1921-1931. [16] Yang, J.Y. et al. (2015) *J. Anal. Atomic Spectr*., 30, 1541-1551. [17] Lepore, K.. et al. (2016) *Appl. Spectr.*, in press. [18] Dyar M.D. et al. (2016) *Spectrochim. Acta B*, in press. [19] Boucher, T.F. et al. (2015) *LPS XLVI*, Abstract #2773. [20] Boucher, T.F. et al. (2016) *LPS XLVII*, Abstract #2784. [21] Boucher T.F. et al. (submitted) *J. Chemometrics*. [22] Boucher T.F. et al. (2015) *Proc. 29th AAAI Conf.*

VSWIR MICROIMAGING SPECTROSCOPY FOR GEOLOGIC HISTORY AND IDENTIFYING AND QUANTIFYING MINERAL, ICE, AND ORGANIC ABUNDANCES ON PLANETARY SURFACES B.L. Ehlmann[1,2], D.L. Blaney[2], R.O. Green[2], P. Mouroulis[2], [1]Division of Geological & Planetary Sciences, California Institute of Technology, 1200 E. California Blvd., Pasadena, California, 91125 (ehlmann@caltech.edu), [2]Jet Propulsion Laboratory, 4800 Oak Grove Drive, Pasadena, California, 91109.

Introduction: Visibile to shortwave infrared (VSWIR) microimaging spectroscopy provides simultaneous fine-scale composition (mineralogy, ices, and organics) and fine-scale imaging at a grain scale. A major advantage of assessing composition with texture preserved is the ability to infer a time-ordered history of geologic processes. An ultra-compact imaging spectrometer (UCIS) has been built and demonstrated [1], a flight configuration is being matured to TRL 6 under MatISSE [2], and UCIS and commercial instruments (e.g. at Ehlmann's lab at Caltech) are presently being used for science investigations of meteorite [e.g. 3, 4], terrestrial sedimentary, hydrothermal, igneous, impactite, and biological samples [5, 6, 7]. Here, we briefly describe the specifications and choices for flight implementation, characteristics of the instrument approach, and science use scenarios.

Instrument Characteristics Summary: The UCIS flight implementation, SPIM [8], and commercial VSWIR microimaging spectrometers are, like proven orbiting/airborne systems, pushbroom sensors and build up the complete image using a scanning approach to build an image line-by-line (vs. MicrOmega [9] which adopts a framing camera approach and has an order of magnitude longer data acquisition time). Desired target measurement area, desired spatial resolution, and choice of focal plane array size, lead to selection of microscopic foreoptics to set a desired pixel size (typically 20-150 μm). Full spectral information is obtained for each pixel by projecting light from a spatial slit, through a grating onto the focal plane array. Acquisition is typically optimized for a specific wavelength range between 400 nm and 5000 nm, a spectral range which includes most diagnostic spectral information of most minerals, ices, and organics. The target temperature, desired NR, and chosen spectral range and resolution dictate cooling requirements. A simple visible to shortwave infrared light source further shortens measurement time.

Example flight implementations are discussed in [10, 11]. Typically, a 12x12x12 cm arm-based sensor of 2-2.5 kg with a DPU of 1-2 kg acquires several hundred thousand simultaneous independent measurements (pixels) of composition over a few cm^2 area of sample in <10 min. Data can be downlinked as full images (~200-500Mb/each) or processed onboard to downlink compositional summary products and "best" spectra when downlink volume-constrained.

Datasets and Use Cases: We are presently using microscopic imaging spectroscopy to investigate clast heterogeneity in impact melts [5,6], serpentinization and biomatter entombment in travertine springs [7], mafic composition of HED meteorites from Vesta [3], the nature of aqueous alteration in carbonaceous chondrite and martian meteorites (Figs. 1, 2), stromatolite

Figure 1. VSWIR Microimaging spectroscopy of a fragment of Allende demonstrates the ability to map mineralogical variability in fine-grained dark materials characteristic of small bodies. We map the compositional variability of chondrule fragments and the matrix.

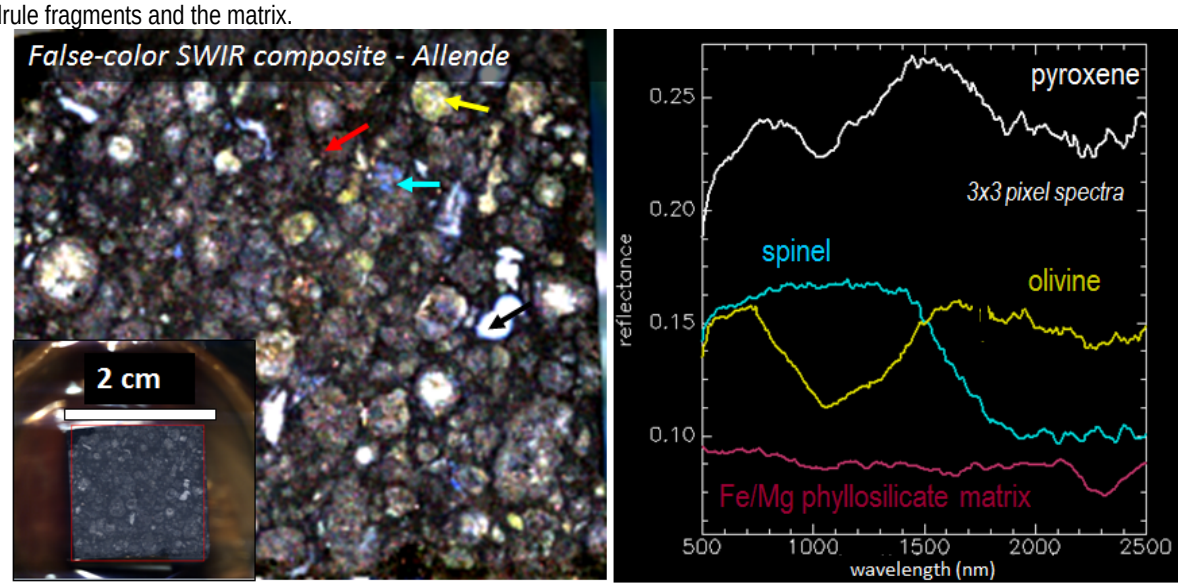

Figure 2. Laboratory microspectrometer test data demonstrate the ability of microVSWIR imaging spectroscopy to directly interrogate primitive materials to determine the products of aqueous alteration in the early solar system. Samples of Tagish Lake matrix minerals compared to single large crystal serpentine and chlorite from the Rossman lab collection show Mg-serpentine, identified by Blinova et al [2014] in their Tagish Lake study (thanks to G. Rossman for spectra).

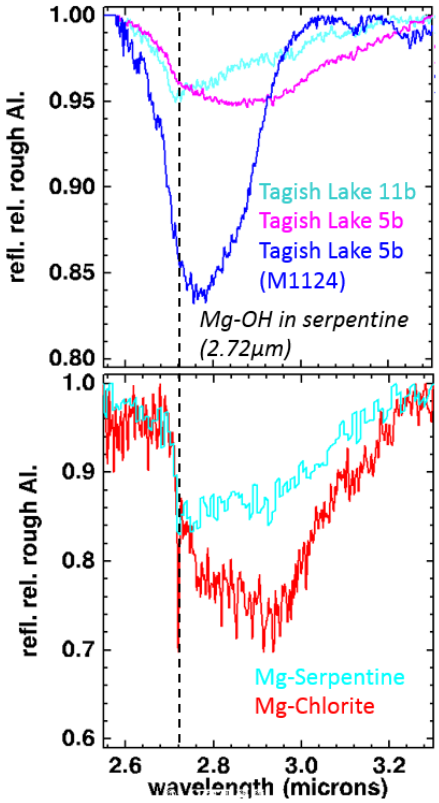

Figure 3. VSIWR microimaging spectroscopy of a stromatolite showing laminae with discrete sediments and zone of later metamorphic overprinting (sample courtesy W. Fischer).

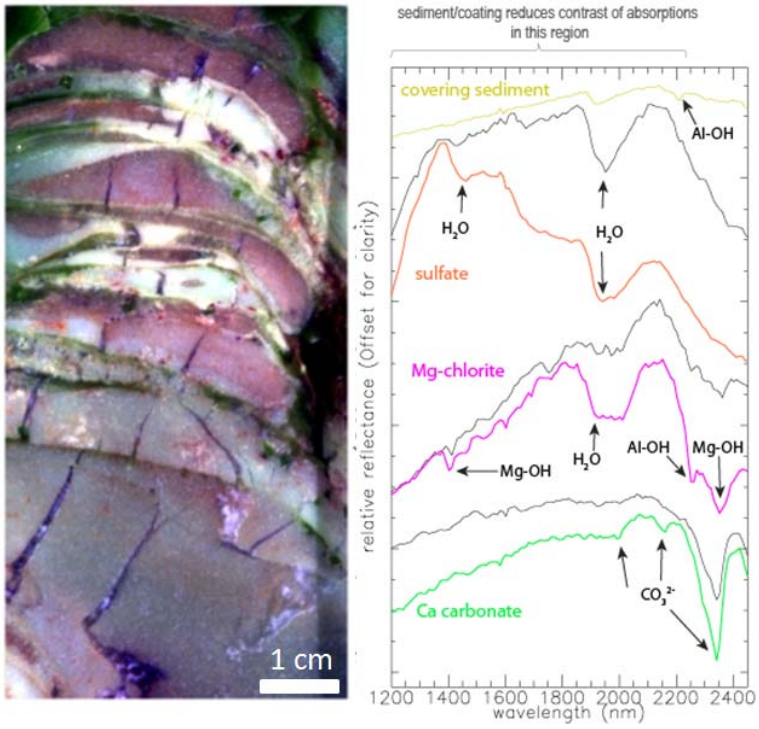

sedimentation, and the structure of microbialites (Fig. 3).

Advantages and Disadvantages for Science: VSWIR microimaging spectroscopy has been developed to maturity for flight [1,2] and demonstrated in the laboratory and in the field to be useful in unraveling geologic histories. Disadvantages are few but include (i) relative insensitivity to anhydrous silicates with no iron (e.g. quartz); (ii) relative insensitivity to some metal oxides and some kerogens; (iii) semi-quantitative information only when the grain size of the sample is significantly below the spatial resolution (e.g. mudstones). These are relatively less important for many planetary targets and can be circumvented by use of VSWIR microimaging spectroscopy in concert with a synergistic payload (e.g. with chemistry, other spectroscopies). There are at least 7 key advantages: (1) demonstrated effectiveness in telescopic, spacecraft, aircraft, field, and lab modes for science objectives [5] with highly mature spectral libraries [12]; (2) provision of simultaneous composition and texture measurements (petrology); (3) non-destructiveness, ideal for reconnaissance for sample collection; (4) little to no sample preparation requirements as the technique works equally well on regolith and natural, rough rock surfaces (the Mars-2020 proposed implementation choice allowed 1cm of roughness over a 9 cm^2 area [10]); (5) rapid data acquisition with >100,000 independent samples of composition per each 5-10 minute measurement; (6) VSWIR spectra acquired provide direct linkages to remotely acquired datasets; and (7) the technique is robust under multiple planetary environments with significant measurement margin and well-understood cooling and radiation shielding requirements [1,2].

References: [1] Van Gorp, B., et al. (2014) *J.App. Rem. Sensing 8(1)*, 084988. [2] Blaney et al., this conf. [3] Fraeman et al., LPSC 2016, #2237 [4] Ehlmann, et al. 2016,. Asteroid Met. Connection, UCLA [5] Greenberger et al., 2015, *GSA Today* [6] Greenberger et al., this conf. [7] Leask & Ehlmann, this conf. [8] Manzari, P., et al., 2016, *Earth and Space Science*, doi:10.1002/2015EA000153. [9] Pilorget & Bibring et al., 2013, *Plan. Space Sci.*, doi:10.1016/j.pss.2012.11.004 [10] Ehlmann et al., Inst. Plan. Missions, 2014 [11] Green et al., LPSC 2015, #2154 [12] Clark et al., 2007, USGS spectral library

WIDE-FIELD ULTRAVIOLET SPECTROMETER FOR PLANETARY EXOSPHERES AND THERMOSPHERES. Matthew O. Fillingim[1], Edward H. Wishnow[1], Tim Miller[1], Jerry Edelstein[1], Robert J. Lillis[1], Eric Korpela[1], Scott England[1], William Van Shourt[1], Oswald Siegmund[1], Jason McPhate[1], Sasha Courtade[1], David W. Curtis[1], Justin Deighan[2], Michael Chaffin[2], Abdalla Harmoul[3] and Hessa Rashid Almatroushi[3], [1]University of California, Berkeley, Space Sciences Laboratory, 7 Gauss Way, Berkeley, CA, USA, 94720 (matt@ssl.berkeley.edu), [2]University of Colorado at Boulder, Laboratory for Atmospheric and Space Physics, 1234 Innovation Drive, Boulder, CO, USA, 80303, [3]Mohammed Bin Rashid Space Center, Al Khawaneej Street, Al Khawaneej, Dubai, United Arab Emirates.

Introduction: Understanding the composition, structure, and variability of a planet's upper atmosphere – the exosphere and thermosphere – is essential for understanding how the upper atmosphere is coupled to the lower atmosphere, magnetosphere and near-space environment, and the Sun. Ultraviolet spectroscopy can directly observe emissions from constituents in the exosphere and thermosphere. From such observations, the structure, composition, and variability can be determined.

We will present the preliminary design for a wide field ultraviolet imaging spectrometer for remote sensing of planetary atmospheres. The imaging spectrometer achieves an extremely large instantaneous 110 degree field of view with no moving scanning mirror. The imaging resolution is very appropriate for extended atmospheric emission studies, with a resolution of better than 0.3 degrees at the center to 0.4 degrees at the edges of the field. The spectral range covers 120 - 170 nm, encompassing emissions from H, O, C, N, CO, and N_2, with an average spectral resolution of 1.5 nm. The instrument is composed of a 2-element wide-field telescope, a 3-element Offner spectrometer, and a sealed MCP detector system contained within a compact volume of about 40 x 25 x 20 cm. We will present the optical and mechanical design as well as the predicted optical performance.

The wide instantaneous FOV simplifies instrument and spacecraft operations by removing the need for multiple scans (either from a scan mirror or spacecraft slews) to cover the regions of interest. This instrumentation can allow for two-dimensional spectral information to be built up with simple spacecraft operation or just using spacecraft motion. Applications to the terrestrial geocorona and thermosphere will be addressed as well as applications to the upper atmospheres of other planetary objects.

DRACO: DIDYMOS RECONNAISSANCE AND ASTEROID CAMERA FOR OP-NAV. Zachary J. Fletcher[1], Andrew F. Cheng[1], Olivier S. Barnouin[1], Nancy L. Chabot[1], and Cheryl L. Reed[1], [1]Johns Hopkins University Applied Physics Laboratory, 11100 Johns Hopkins Rd., Laurel, MD, 20723, USA. Zachary.Fletcher@jhuapl.edu.

Introduction: The Double Asteroid Redirection Test (DART) [1] is a low-cost mission concept developed in response to the threat of an asteroid impact and the need to mitigate such a threat. In particular, the *NRC Defending Planet Earth* report [2] recommended that "the first priority for a space mission in the mitigation area is an experimental test of a kinetic impactor along with a characterization, monitoring, and verification system." DART is designed to be the first planetary defense demonstration of the kinetic impactor concept, the impulsive deflection of an asteroid.

The DART target is the binary asteroid system 65803 Didymos. The primary member of the binary system (Didymos A) has a diameter of 780 m, the secondary member (Didymos B) has a diameter of 160 m, and the two objects are separated by roughly 1.2 km with an orbital period of 11.9 hrs [3]. The Didymos system is the ideal target because: 1) Didymos is highly accessible with a close pass by Earth in 2022. 2) The DART impact produces a change in the Didymos binary orbit period that can be measured from Earth-based observations during its close pass. 3) Didymos B is of a size typical of potentially hazardous asteroids (PHA) and likely an S-type asteroid, suggesting that its composition and physical properties are shared by a large fraction of PHAs. DART is planned to impact Didymos B at ~6 km/s in October 2022.

The sole payload instrument on DART is DRACO, the Didymos Reconnaissance and Asteroid Camera for Op-nav. Here, we describe DRACO's responsibilities on the DART mission, the resulting design, and the planned operations.

DRACO Requirements: DRACO's highest priority is to support onboard navigation and terminal guidance to ensure the DART spacecraft impacts Didymos B. DRACO images will feed directly into onboard software that will autonomously target Didymos B. At 30 days prior to DART impact, DRACO will be able to image the Didymos system with a signal/noise ratio to support this onboard navigation need.

In addition, DRACO images will characterize the Didymos system and provide detailed views of the DART impact site. The final DRACO images returned prior to impact will resolve features within the impact site at a smaller scale than the impacting DART spacecraft, providing important constraints for modeling efforts to interpret the results of the DART hypervelocity impact event.

DRACO Overview: DRACO (Fig. 1) is derived from the Long Range Reconnaissance Imager (LORRI) instrument on New Horizons. DRACO is required both to image the Didymos system 30 days in advance, when the target is faint, and to image the impact site shortly before impact, when the scene is considerably brighter. DRACO uses a complementary metal–oxide–semiconductor (CMOS) detector to support <1 ms exposure times for the final images prior to impact to avoid saturation, a capability not supported by the LORRI charge-coupled device (CCD) detector. The CMOS detector chosen for DART also costs significantly less than the LORRI detector and maintains the low noise and high sensitivity needed for faint imaging. DRACO is mounted inside the spacecraft structure via a support ring and flexures to the spacecraft.

DRACO Optics: DRACO optics are based on the optical design from LORRI, which consists of a f/12.6 Ritchie-Chrétien telescope with an aperture of 208 mm [4]. LORRI operated in a varying thermal environment from 1 AU to over 30 AU while DART remains ~1 AU from the sun for the duration of the mission. This more stable thermal environment allows DRACO optics to be made from Al rather than LORRI's SiC, re-

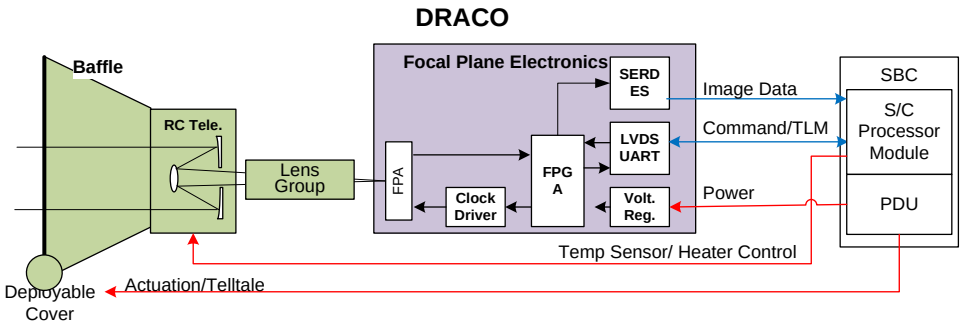

Figure 1. DRACO block diagram

ducing cost and complexity. Other changes include removal of image ghosts via planned changes to the field-flattening lens group [4].

DRACO Electronics: The DRACO detector is the BAE sCMOS CIS2521, which is a 2560x2160 format, has 6.5 um 5T pixels and has low (<5e-) read and dark noise. The CIS2521 has been radiation tested up to 50 krad, the maximum dose possible for DART, and the corresponding dark current increases have been characterized [5]. The detector is digitized on chip with two different gain states, a high-gain and a low-gain mode, each with 11 bits. The detector data are sent to the DRACO Focal Plane Electronics (FPE), which also commands and provides power to the detector. The FPE takes the two 11 bit pixel streams and converts them into a single 16 bit stream.

The FPE passes image data to the Single Board Computer (SBC), which hosts the DART processing. The SBC is built around the UT700 LEON3 processor and an RTG4 FPGA for supporting firmware. It also includes MRAM for hosting the software image, 32 MB of SRAM for processing and 16 GB of flash storage. The SBC also sends commands and receives telemetry from the FPE as it hosts all instrument software.

DRACO Processing: DRACO processing will have many options for reducing data volume due to limited time to return images prior to final impact with Didymos B. These include: 2x2 pixel binning, reduction to 12b data, lossless image compression algorithms, and windowing of the image. In addition to these, DRACO will process images for background removal and bad pixel removal. All of these processing steps occur in the firmware inside the RTG4.

Additionally, the images from DRACO will be used in closed-loop terminal guidance to Didymos B. Flight software handles the guidance and navigation filters, but DRACO is responsible for thresholding, blobbing, and centroiding the images in the RTG4 firmware in a single-pass approach [6]. DRACO creates a bitmask of pixels above a threshold signal, looks for contiguous pixels to group together in blobs, and identifies the centroid of the blob. These centroids are passed to the navigation software.

DRACO Operations: DRACO operations support the characterization of the Didymos system and the impact site and can be considered in two main phases: long-range imaging, conducted when the Didymos system is not resolvable, and proximity imaging, when Didymos A and B can be distinguished

Long-range imaging observations will begin approximately 30 days before impact to provide ground based optical navigation images which include Didymos and at least 3 stars. These data will be downlinked to Earth for navigation's processing and will also be used to refine the rotation rate of Didymos A and the orbit of Didymos B, complementing Earth-based observations. These images will also enable a search for any additional members of the Didymos system.

Beginning at roughly 4 hrs prior to impact, DRACO can separate Didymos A and B, and by about 1 hr prior, Didymos B becomes a resolved object. Starting at 4 hrs before impact, DRACO is targeted on Didymos B, and DRACO processes images to pass centroids to navigation for closed-loop control to the target system. As many images as the available downlink supports will also be sent to Earth, estimated at roughly one image every 5 s. These proximity imaging observations will provide information about the shapes of the two objects and their geologic properties. The hemisphere of Didymos A visible to DRACO will be imaged with meter-sized pixel-scales. Figure 2 provides a modeled DRACO view of the Didymos system two minutes prior to impact. The final set of images obtained by DRACO will be of the DART impact site on Didymos B, and the final image returned to Earth will be acquired at 20 cm/pixel or better.

An operational test of the onboard autonomous targeting software is planned to be conducted prior to DART's impact of Didymos B, during an opportunistic asteroid flyby during DART's cruise to the Didymos system, currently planned for near-Earth asteroid 2001 CB21 in March 2022. DRACO inflight calibrations will utilize the Moon and imaging of star fields. All inflight calibration and Didymos system characterization images will be returned to Earth for analysis

Figure 2. A modeled DRACO view of the Didymos system two minutes prior to DART impact.

References: [1] Cheng A. F. et al. (2016) *Planet. Space Sci., 121,* 27-35. [2] National Research Council (2010) *Defending Planet Earth,* National Academies Press, 152 pp. [3] Michel P. et al. (2016) *Adv. Space Res., 57,* 2529-2547. [4] Cheng A. F. et al. (2008) *Space Sci Rev. 140,* 189-215. [5] Rodricks B. et al. (2010) *Proc. SPIE 7805* [6] Trein J. et al. (2008) *MPC-Workshop, Ravensburg-Weingarten,* 71-77.

INSTRUMENT AUTONOMY TECHNIQUES ENHANCE SCIENCE RETURN AND EFFICIENCY OF SURFACE MISSIONS. R. Francis[1], T. A. Estlin[1], K. Wagstaff[1], G. Doran[1] and L. Mandrake[1] [1]Jet Propulsion Laboratory, California Institute of Technology, Pasadena, California (raymond.francis@jpl.nasa.gov)

Introduction: Robotic exploration missions, operating spacecraft at great distances from Earth, face challenges in data throughput and latency, with consequences for mission scope, productivity, and science return. This abstract describes advances achieved for surface missions; autonomous science for orbital and flyby missions is described in [1].

Surface missions, which often study very localized, fine-scale, and diverse features, face further obstacles due to short mission durations and restricted communications geometry. Many of these can be addressed by including capabilities for instrument autonomy and onboard intelligence with respect to acquiring or prioritizing measurements. A number of such techniques have already aided planetary missions, and new capabilities are under development. Given the significant increase in science return and the new observations that can be enabled, capabilities for instrument autonomy should be an important part of the design and selection of instrument systems for planetary missions.

Autonomy as a scalable class of tools: Instruments equipped with a degree of autonomy can be more powerful tools for the science team on Earth than those without – just as an autofocus capability increases the ease and reliability of operating a camera. The degree of autonomous operation can vary greatly, and should be selected based on the particular science goals, instrument capabilities, and working environment to best enhance the outcome the observations. A number of specific examples are given below.

Data triage: Data budgets for planetary missions are always very constrained. An onboard system capable of recognizing high-value observations and prioritizing them for downlink increases the average value of transmitted data, and the overall value of the mission's data set. The WATCH software system aboard the MER Opportunity rover analyzes images for the presence of clouds and dust devils – both rare features of interest to the science team – and prioritizes images containing them for transmission to Earth [2]. WATCH demonstrated a 70% reduction in data volume for dust devil monitoring campaigns [3].

Novelty detection: Techniques exist to automatically recognize data, which are out of family with past observations. Whether in images, spectra, or other data, onboard recognition of novel features can be used in a number of ways – as part of the data triage process, or to command additional observations with the same or another instrument. The DEMUD algorithm [4] has been applied to LIBS data from the Curiosity rover's ChemCam instrument, for example, to automatically recognize unusual geochemical spectra [5], and autonomous onboard use of such a system would provide many of the benefits discussed above.

Pointing refinement: There are numerous technical and operational challenges to precise pointing of narrow-field instruments. ChemCam is often used to target small-scale features such as veins in rocks, which may be as small as a few millimeters in width. The AEGIS software system aboard the Curiosity rover allows autonomous real-time pointing refinement for observing such features [6]. The science team on the ground selects a desired target (such as bright-toned veins in an outcrop) and commands ChemCam to observe it with the Remote Micro-Imager (RMI) context camera. AEGIS identifies the desired features, in the image, and, retargets ChemCam to correct any offset. In this way, a few minutes of imaging and automated analysis can save a day or more of delay of making a second targeting attempt. The capability has been demonstrated on Mars and is available whenever the science team finds suitable targets.

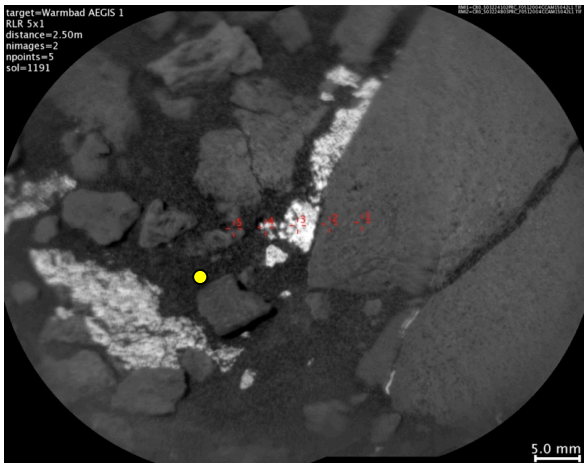

Fig 1, AEGIS pointing refinement: ChemCam RMI mosaic, showing LIBS spots measured on sol 1191. ChemCam initial pointing shown in yellow.

A new capability under development for narrow-field instruments on the Mars 2020 rover allows operators to specify a particular target of interest in an instrument's view on one sol, then return precisely to this location on a subsequent sol using a visual alignment of the instrument's view across the two sols to

account for any drift that might have occurred in the intervening period due to thermal fluctuations or rover settling [7]. This capability will be essential for arm-mounted instruments like PIXL, for which the region targeted for science measurements is on the order of the error in arm placement from sol-to-sol (~1 cm).

Autonomous targeting: AEGIS is also capable of selecting targets on its own, following criteria set by the science team [8]. AEGIS analyzes images from the Curiosity rover's navigation cameras (NavCams) and identifies distinct geological features by a combination of computer vision techniques. It then filters and ranks these objects, choosing one or more which best match the science team's request(s). ChemCam measurements of these targets are then automatically made.

Such a capability is very useful, for example, after driving into new terrain not yet seen by the team on Earth; rather than waiting for post-drive images to be downlinked at the next opportunity, and for the science team to inspect them, select targets, and uplink commands, AEGIS can quickly deliver geochemical spectra from the post-drive location. The science team employs a mix of ground-targeted observations (when possible) and AEGIS automated targeting (when appropriate), with the latter occurring after most drives since the system became available.

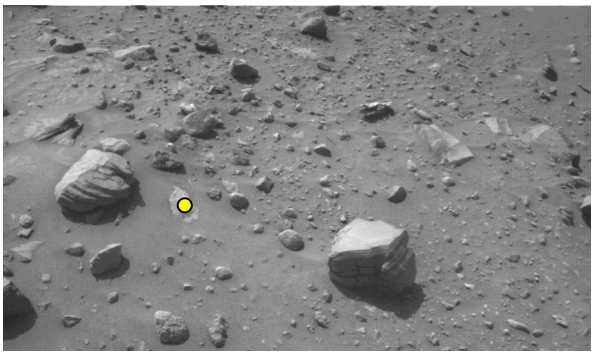

Fig 2, Autonomous targeting: NavCam scene analyzed by AEGIS on MSL sol 1400, set to find bright patches of outcrop. The top-ranked target (yellow marker) was automatically measured with ChemCam.

An upgrade in development would augment AEGIS targeting with automated pixelwise classification of geological materials using the TextureCam system [9], which demonstrated full-image classification onboard its instrument in under 1 second.

Autonomous rescheduling: An instrument that can detect notable events and measurements can also be set to trigger changes in the spacecraft's schedule of activities. This can be used to acquire more data of a recognized novel or high-priority feature or event, or to defer a routine or low-priority activity in response to a high-priority observation opportunity. For example, the Earth-observing EO-1 satellite is able to autonomously recognize active volcanoes in hyperspectral data, acquire opportunistic data on those targets quickly, and reschedule the originally-planned observations for later opportunities [10]. Similar replanning could be used for a rover to recognize particular types of geological material, or an airborne system (on Titan or Venus) to respond to certain types of terrain or other conditions.

Where autonomy contributes: Instrument autonomy, at any level, is most useful when circumstances reduce the ability of the science team to be in the loop for operations. Long periods without communication, or long light-time delays, make it difficult to share information between the Earth and a distant planet. Transient events require either autonomous detection or routine monitoring with autonomous data triage to reduce data volumes. For mobile platforms (roving or airborne), important or novel features may pass entirely by before Earth sees them; autonomous detection, response, and data acquisition can allow discovery and study of things that would have been missed entirely.

Even now, AEGIS on MSL contributes 'opportunistic science', by making valuable measurements on as-yet-unseen-by-Earth materials during post-drive periods which would otherwise be idle or underused time on Mars. Similar underused periods occur on many missions. When data throughput is limited, the mission science return is enhanced by systems, which can intelligently select the most desirable, most representative, or most unusual data to send to Earth.

Conclusion: Existing, flight-proven, and near-future autonomy capabilities can enhance the value of science instruments, and consequently of planetary missions, by increasing the quality and throughput of data, and by making more efficient use of precious planetary surface time. Instrument and mission design benefits from considering and promoting these capabilities – at the concept definition, proposal, development, and operation phases.

This work was carried out at the Jet Propulsion Laboratory, California Institute of Technology, under a contract with NASA.

References: [1] Wagstaff, K. et al. (2016) 3rd Workshop on Inst. for Planetary Missions (this meeting) [2] Castaño A. et al. (2008) *Machine Vision and Apps.* [3] Chien S. et al. (2008) *ISAIRAS*. [4] Wagstaff K.L. et al. (2013) *AAAI Conf. on Art. Intell.* [5] Wagstaff K.L. et al. (2014) *LPS XXXXV*. [6] Francis R. et al. (2015) 44th IEEE AIPR [7] Doran G. et al. (2016) 25th IJCAI, [8] Estlin T. et al. (2012) *ACM TIST.* [9] Bekker D. et al. (2014) Astrobiology 14, 486-501 [10] Davies A. et al. (2006) *Remote Sens. Env.*

PROMOTING PLANETARY MISSIONS AT ISAS/JAXA. M. Fujimoto, Department of Solar System Sciences, ISAS, JAXA (3-1-1 Yoshinodai, Chuo-ku, Sagamihara, 252-5210, Japan).

Introduction: At ISAS, it is fully recognized that international collaborations are necessary to make a space science mission a truly successful one. This recognition has led to the recent reformulation of the space science program at ISAS. Now it is clearly formulated that ISAS has three mission lines, (A) Strategic L-class mission to be launched by H-IIA/III launchers, (B) Competetive M-class mission to be launched by Epsilon launchers, and (C) Small-sized opportunities including those for participation to foreign missions. (A) is expected to be a mission that is so attractive to the international community as to collect substantial fraction of its instruments from abroad. Martian Moons eXplorer (MMX), the Phobos sample return mission that is under study at ISAS, is a typical example. (B) is expected to perform nice focused science theme and it is a good challenge for planetary sciencetists to come up with a compelling mission idea.SLIM, a lunar landing technology demonstrator having a decent science instrument onboard, is an example. (C) is set so that a well defined path for Japanese participation to NASA and ESA missions, whose sizes JAXA cannot afford, exists and be visible from abroad. An onging one is for ESA JUICE.

This is a substantial change from what it used to be: Every science mission was launched by M-V without clearly defined path for international collaboration, and all that proposers had to care was to design a good mission that fits the mostly-single boundary. The change in the landscape is leading to the necessity to reconsider the schemes by which pre-proposal activities, ranging from (A) to (C), are supported by ISAS. Here a better way to promote smoother international collaboration is the key issue. Ideas under discussion will be presented in expectation of fruitful feedback from the international audience.

NASA Planetary Science Division's Instrument Development Programs, PICASSO and MatISSE. J. R. Gaier, NASA Glenn Research Center, 21000 Brookpark Road, Cleveland OH 44135; james.r.gaier@nasa.gov.

Introduction: Historically, the NASA Planetary Science Division (PSD) had three instrument development programs that were solicited through the Research Opportunities in Space and Earth Sciences (ROSES) annual proposal call. These were the Planetary Instrument Definition and Development Program (PIDDP), the Astrobiology Science and Technology for Instrument Development (ASTID) Program, and the Mars Instrument Development Project (MIDP). As of ROSES-2011, the PIDDP and ASTID programs supported technology readiness levels (TRL) 1-6 development maturation. TRLs are summarized in Table 1, and described more fully beow. The MIDP program supported the development of Mars instrument systems that would achieve TRL 6; however the last call for MIDP proposals was solicited in ROSES-2007. In order to have a more integrated instrument development pipeline the PSD combined the PIDDP, ASTID and MIDP programs into two new instrument development programs; the Planetary Instrument Concept Advancing Solar System Observations (PICASSO), a TRL 1-4 program, and the Maturation of Instruments for Solar System Exploration Program (MatISSE), a TRL 3-6 program.

PICASSO: PICASSO is a PSD program specifically designed to support the development of spacecraft-based instrument systems that show promise for use in future planetary missions. The goal of the program is to conduct planetary and astrobiology science instrument feasibility studies, concept formation, proof of concept instruments, and advanced component technology development to the point where they may be proposed in response to the MatISSE Program.

The PICASSO program is competed every year at a nominal level of $3.5M. Efforts typically are funded at the $250k-$300k per year level for two or three years, so about a dozen awards per year are expected.

MatISSE: The MatISSE Program supports the advanced development of spacecraft-based instruments that show promise for use in future planetary missions. The goal of the program is to develop and demonstrate planetary and astrobiology science instruments to the point where they may be proposed in response to future announcements of flight opportunity without additional extensive technology development (approximately technology readiness level TRL6. The proposed instrument must address specific scientific objectives of likely future planetary science missions.

The MatISSE program is competed in even numbered years at a nominal level of $6M. Efforts typically are funded at the $1M per year level for three years, so about a six awards per cycle are expected.

Instrument Development Strategy: The nominal mode for PSD instrument development is to progress through the TRLs. First a new principle or technology is developed that has the potential to be the basis of a new instrument or a significant improvement in a current instrument. (TRL 1). From that, new instrument or instrument component is conceived based on it and an application is formulated (TRL 2). Then experiments are carried out to demonstrate proof-of-concept or critical fundtion – that the idea works. (TRL 3). Instrument concepts at this early stage of development are eligible for support through the PICASSO program. Instruments may enter PICASSO at TRLs 1-3, and must advance at least one TRL during the course of the program which can be for up to three years. Components or instruments that start out at low TRLcould be selected for more than one PICASSO award.

After proving the concept, the next step is to validate the instrument in a laboratory environment, that is, to build hardware that makes the measurement (TRL 4). Then an integrated brassboard instrument is developed and validated in a relevant environment (TRL 5). To achieve TRL 6, the instrument must have the form, fit, and function of a flight-like instrument that is validate in a relevant environment. Instruments may enter the MatISSE program at TRL 3-5 and expected to achieve TRL6 within three years.

After an instrument reaches TRL 6 it can be proposed to individual mission programs for further development and placement on a spaceraft, lander, or rover. So the instrument development flow is:

PICASSO → MatISSE → Mission

Interested parties are referred to the latest ROSES call for current details, proposal due dates, and points of contact of the PICASSO and MatISSE programs.

Table 1. Technology Readiness Levels

TRL 1	Basic principles observed and reported
TRL 2	Technology concept/application formulated
TRL 3	Critical function/proof of concept
TRL 4	Breadboard validation in lab
TRL 5	Brassboard validation in relevant environment
TRL 6	Prototype validation in relevant environment
TRL 7	Demonsration in space environment
TRL 8	Space qualified
TRL 9	Flight proven through sussessful mission ops

MACROS: Molecular Analyzer for Complex Refractory Organic-rich Surfaces S. A. Getty[1], X. Li[2], W. B. Brinckerhoff[1], J. E. Elsila[1], A. Grubisic[3], T. Cornish[4], M. Balvin[1], A. Southard[5], and J. Ferrance[6], [1]NASA Goddard Space Flight Center (8800 Greenbelt Road, Mailstop 699, Greenbelt, MD 20771; Stephanie.A.Getty@nasa.gov), [2]University of Maryland, Baltimore County (1000 Hilltop Cir, Baltimore, MD 21250), [3]University of Maryland, College Park (College Park, MD), [4]C&E Research, Inc. (Columbia, MD), [5]Universities Space Research Association (Greenbelt, MD), [6]J2F Engineering (Charlottesville, VA).

Introduction: The objectives of future landed missions to solar system destinations of high astrochemical and astrobiological interest will require science instrumentation capable of conducting broad, comprehensive, and highly sensitive in situ analyses of surface materials. A primary goal of any such landed mission will be a detailed characterization of the local chemical environment. The Molecular Analyzer for Complex Refractory Organic-Rich Surfaces (MACROS; Figure 1) addresses the limitations of predecessor instrument technologies, namely the propensity of indigenous salts and oxidants to confound the detection and identification of trace organics in an acquired surface sample with state-of-the-art flight instrumentation. MACROS goes several steps beyond current spaceflight analytical capabilities to integrate laser desorption/ionization mass spectrometry (LDMS) [1,2] with *in situ* solvent extraction and liquid-phase analysis using liquid chromatography (LC) [3]. This integration will achieve unprecedented capabilities within a compact instrument footprint, compatible with a Discovery or New Frontiers mission to high-priority targets, including Europa, Enceladus, Titan, Mars, a comet, or a carbonaceous asteroid.

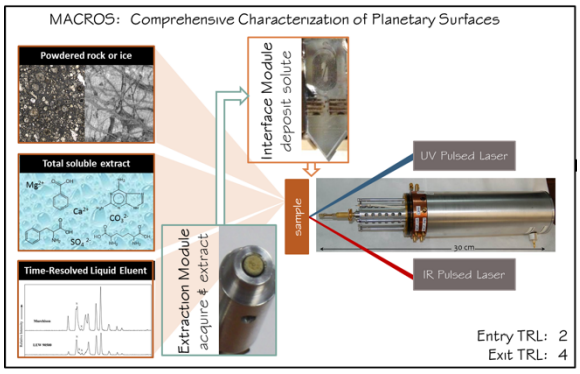

Figure 1. Instrument concept of MACROS, in which analysis of a native unprepared sample is then compared to the solvent-extracted fraction and chromatographically separated eluents.

Instrument Concept: MACROS combines drill and sample acquisition development, solvent-based sample extraction, and liquid deposition interfaced to laser desorption/ionization (LDI).

Drill and Sample Acquisition Development: A 1.5 mm ID diamond coring drill, as shown in Figure 2, can be used as both a means to collect ground powdered specimens from rock surfaces, as well as to provide a sample holder that can be interfaced directly to the ion source of a miniature time-of-flight mass spectrometer (TOF-MS) for LDMS broad survey mode. For an airless body, no vacuum interface between the sample and TOF-MS will be required. The drill further provides an internal volume to capture rock powder for extraction in the MACROS solvent extraction module. To realize this additional capability, current testing is focused on characterizing the powdered mineral sample accumulated in the drill under various conditions, including as a function of sample hardness and drill dimensions.

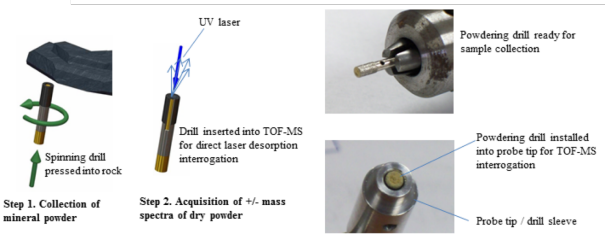

Figure 2: A potential design of drill bit that will have the capabilities to both present drilled fines to the LDMS for survey mode, and also contain extraction solvent and deliver the extracted sample to the fluidic components of MACROS.

Sample Extraction: We tested various solvent extraction procedures using a variety of analog samples, including powdered Allende meteorite, Green River Shale, and samples from the Painted Desert. Two different solvent systems were used: isopropanol:water (50:50, targeting polar compounds) and dichloromethane (DCM, which targets non-polar compounds). DCM also extracts elemental sulfur, which can dominate the LDMS spectrum, so a simple sulfur removal step was added to our procedure using a copper surface.

Extract Interface Module Development: MACROS is designed to analyze the composition of solvent-extracted sample for detailed analysis of the soluble organic fraction of a planetary sample. This component of the instrument is intended to be compatible with

liquid chromatography but does not rely on separation to accomplish the baseline objectives of the MACROS development. The interface module enables an interface between the liquid eluent from the extraction module to a vacuum region necessary for MS analysis. We have demonstrated spray desposiiton from a number of geometries and nozzle dimensions to deposit liquid analyte onto a secondary LDI substrate. This element enables several compelling analytical capabilities: (1) enrichment of total soluble extract through controlled deposition duration, (2) front-end coupling to an ion exchange column or solid phase extraction component for desalting and purification, and (3) time-resolved mass analysis of chromatographically resolved eluent.

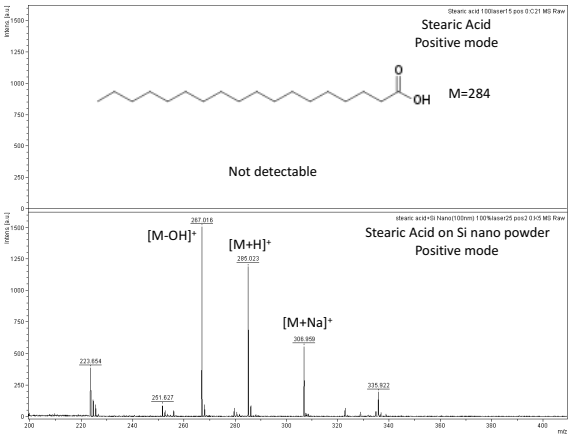

Figure 3. Enhanced detection of stearic acid is seen for a silicon nanoparticle iMALDI underlayer.

To increase the detection sensitivity of organics, particularly those that are difficult to detect by LDI alone, in the deposited liquid extracts, a substrate covered with thin matrix layer is used. In traditional matrix-assisted LDI (MALDI), an organic acid (or "matrix") is used to promote the ionization of intact large organic molecules during the MS analysis. However, organic matrix is not well suited to a robotic flight configuration given the complexity of the required sample preparation and the risk for cross- and forward-contamination with terrestrial organics. As an alternative path, the development of inorganic matrix-assisted laser desorption/ionization (iMALDI) has now been demonstrated allowing the detection of a broader suite of organic composition. A series of inorganic microparticle and nanoparticle chemistries have been investigated for their effectiveness in promoting the desorption and ionization process with a 266 nm ultraviolet (UV) laser. Likewise, the optimal choice for iMALDI matrix will impart minimal background signal to the mass spectra obtained with MACROS. Evaluating the trade between sensitivity and background signal, we have selected the silicon nanoparticles for pursuant sample analyses, and one example enhancement is shown in Figure 3 for stearic acid, a model lipid and key biosignature.

Sample Analysis: MACROS will feature different modes of operation to allow systematic measurements of the broad inorganic and organic composition using LDMS mode (survey mode) [1], the aromatic composition of the sample using L2MS mode (detailed mode) [2] and the soluble inorganic salts at low mass and soluble organics at mid-molecular weights. An comparison between LDMS and L2MS is shown for the Murchison meteorite, using GSFC miniature mass spectrometer prototypes for demonstration of MACROS capabilities (Figure 4). Improved sensitivity and selectivity to key classes of organics, as in L2MS, can be used to differentiate between structural isomers that appear at the same nominal mass in an organically complex sample.

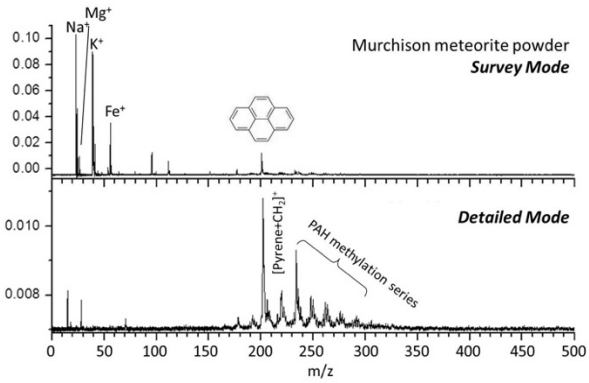

Figure 4: Sample Analysis of Murchison meteorite under LDI survey mode and detailed mode.

Conclusion: MACROS is a hybrid LC/LDMS instrument that will provide sophisticated sample analysis beyond the capabilities of either technique alone. This new instrument package can be used to determine inorganic mineral composition, broadband organic sample content, and detailed structural analysis of high-priority compound classes for a thorough understanding of the chemistry of planetary surface materials.

References: [1] Li X. et al. (2015) *IEEE Aerospace Conference*. [2] Getty S. A. et al. (2012) *Rapid Communications in Mass Spectrometry*, *26,* 1. [3] Getty S. A. et al. (2013) *IEEE Aerospace Conference*.

VOLATILE ANALYSIS BY PYROLYSIS OF REGOLITH (VAPOR) FOR PLANETARY RESOURCE PROSPECTING. D. P. Glavin[1*], C. A. Malespin[1,2], I. L. ten Kate[3], A. McAdam[1], S. A. Getty[1], E. Mumm[4], H. B. Franz[1,5], A. E. Southard[1,2], J. E. Bleacher[1], and P. R. Mahaffy[1]. [1]NASA Goddard Space Flight Center, 8800 Greenbelt Rd, Greenbelt, MD 20771, [*]email: daniel.p.glavin@nasa.gov; [2]Universities Space Research Association, 10211 Wincopin Circle, Columbia, MD 21044; [3]Utrecht University Budapestlaan 4, 3584 CD Utrecht, The Netherlands; [4]Honeybee Robotics, 460 W. 34th Street, New York, NY, 10001, USA; [5]Center for Research and Exploration in Space Science and Technology, 5523 Research Park Drive, University of Maryland Baltimore County, Baltimore MD 21228, USA.

Introduction: Measuring the chemical composition of planetary bodies and their atmospheres is key to understanding the formation of the Solar System and the evolution of the planets and their moons. *In situ* volatile measurements enable a ground-truth assessment of the distribution and abundance of resources such as water-ice and oxygen, important for a sustained human presence on the Moon and beyond. The Volatile Analysis by Pyrolysis of Regolith (VAPoR) instrument is a compact pyrolysis mass spectrometer designed to detect volatiles released from solid samples that are heated to elevated temperatures and is one technique that should be considered for resource prospecting on the Moon, Mars, and asteroids.

There are several key lunar science and exploration measurement objectives that can be achieved by the VAPoR instrument: (1) Measure the abundance of water that can be released from lunar regolith for *in situ* resource utilization (ISRU) technology development, (2) .Measure the isotope ratios of carbon, hydrogen, oxygen, and nitrogen (CHON)-containing volatiles including water in polar regolith to establish their origin, and (3) Understand the processes by which terrestrial organic compounds are dispersed and/or destroyed on the surface of the Moon to prepare for future human exploration and life detection on Mars.

Here we will describe the VAPoR instrument concept that is based on the Sample Analysis at Mars (SAM) instrument on Curiosity currently operating on Mars and discuss the key science and resource prospecting measurement objectives enabled by evolved gas analysis.

Evolved Gas Analysis on Mars: The SAM instrument has been an essential tool in understanding the nature, abundance, and isotopic composition of volatiles and organics in Gale crater sediments [1]. The SAM instrument receives scooped or drilled soils or sediments from the rover sample acquisition system delivered to individual quartz cups. The cup is placed inside a pyrolysis oven under He flow at 25 mbar and heated at a rate of 35ºC/min up to ~860ºC. Evolved gases (e.g., H_2O, CO_2, O_2, SO_2) released from the sample are detected by a quadrupole mass spectrometer and their abundances determined from their characteristic masses and an estimate of the weight of the sample delivered to the oven. The SAM evolved gas analysis of eolian drift material called Rocknest have reported the detection of evolved water, SO_2, CO_2, O_2 and other trace volatiles (Fig. 1). The water abundances measured by SAM in Rocknest fines correspond to ~ 2.0 ± 0.5 wt.% [2]. Under the SAM heating conditions adsorbed water is released below 200ºC while bound water from amorphous phases, phyllosilicates, and hydrated salts and oxides are released at higher temperatures. Carbonate decomposition and oxidation of organics are the most likely sources of CO_2. Iron sulfates and oxidation of iron sulfides are possible sources of SO_2 and the oxygen releases are consistent with the presence of perchlorate and chlorate phases. Although SAM has a gas chromatography (GC) system, the GC was not required to determine the abundances of the major volatiles released from the sample.

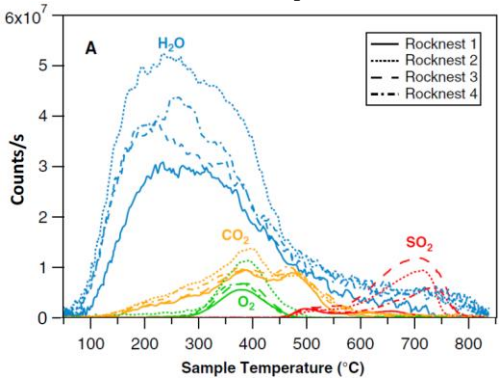

Fig. 1. SAM evolved gas analysis of four individual portions (50 ± 8 mg) of the Rocknest soil showing the major gases released as a function of temperature [2].

VAPoR Instrument: The VAPoR flight instrument concept based on SAM is shown in Fig. 2 and combines a sample carousel of up to six individually heated pyrolysis ovens with a time of flight mass spectrometer. The VAPoR gas processing system includes two gas manifolds, heated transfer lines, and two separate gas reservoirs for calibration of the mass spectrometer and oxygen for combustion experiments. One of the benefits of making evolved gas measurements on an airless body such as the Moon or an asteroid is that a vacuum pump is not required like it is on Earth or on Mars. Powdered rock or soil

samples collected from a rover or lander drill or scoop and delivered through the solid sample tube to one of the VAPoR ovens can then be heated by a controlled ramp from ambient to temperatures up to 1400ºC to release the volatile constituents for direct measurement by the mass spectrometer. Two independent units have been built and tested to understand the performance of the different instrument components.

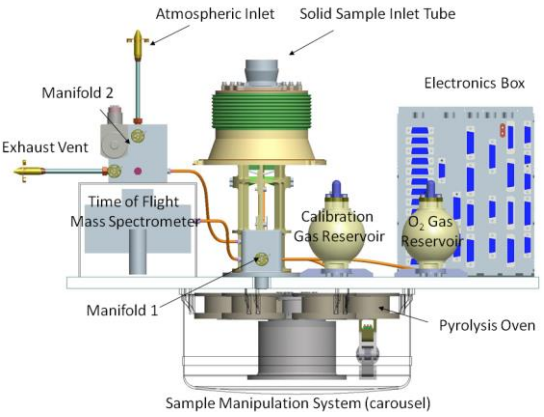

Fig. 2. Cross sectional view of the preliminary VAPoR flight instrument concept which combines a sample carousel containing six separate pyrolysis ovens integrated to a reflectron time of flight mass spectrometer for volatile analyses on the surface of planetary bodies throughout the Solar System.

A laboratory breadboard was developed to test, optimize, and calibrate the reflectron time of flight mass spectrometer (TOF-MS) component of VAPoR inside a separate vacuum chamber and is discussed in more and elsewhere [3]. A separate portable field unit (Fig. 3) consisting of a custom made pyrolysis oven coupled to a commercial RGA quadrupole mass spectrometer, vacuum manifold and turbomolecular pumping station, was built to demonstrate the feasibility of conducting vacuum pyrolysis evolved gas measurements on Apollo samples and meteorites in the laboratory as well as analyses in the field [4,5].

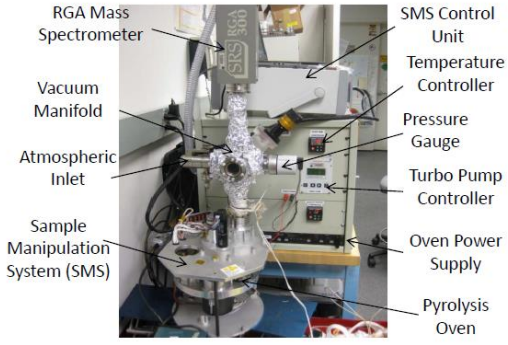

Fig. 3. The VAPoR laboratory and field instrument, which includes a new sample manipulation system and high temperature pyrolysis oven for evolved gas analysis of powdered solid samples.

The instrument is set up to enable direct line of sight from the heated sample in an oven to the ionization region of the RGA mounted at the top of the manifold. The RGA was setup to scan over the mass range 1-100 amu during the pyrolysis heating experiment. The current VAPoR field instrument does not include the TOF-MS, which is being tested and optimized separately in a larger vacuum chamber at NASA GSFC.

The custom VAPoR ovens are designed to bring solid samples up to a maximum temperature of 1400° C in order to release high temperature volatiles such as O_2 from the breakdown of silicates, SO_2 from the decomposition of gypsum, and high temperature noble gas releases of Ar, Kr, and Xe. The oven design was based off of the design of the two flight pyrolysis ovens in the SAM instrument suite, but unlike the SAM oven design where a cup containing solid powder is raised up into the oven, sample can be dropped directly inside the VAPoR alumina crucible which enables direct heating of the sample and lower power to achieve the desired temperature.

Conclusions: *In situ* pyrolysis evolved gas measurements of the lunar regolith and other airless bodies including asteroids are needed to characterize and determine the nature, distribution and abundance of volatiles, particularly, water, an important resource for future human exploration. SAM has demonstrated that *in situ* abundance measurements of water and other major volatiles released from martian surface samples by heating can be made by evolved gas analysis. Using the VAPoR instrument during NASA's 2011 Desert RATS field campaign, we successfully demonstrated that high temperature vacuum pyrolysis of solid samples to temperatures exceeding 1300°C coupled with line of sight detection of volatiles by mass spectrometry can be used for the identification of resources including water and oxygen in powdered rock samples [4]. The inclusion of volatile analysis capability in the field and continued testing of instruments such as VAPoR in future field tests will be critical to the success of future robotic and human planetary resource exploration missions.

References: [1] Mahaffy, P. R. and Conrad, P. G. (2015) *Elements* 11: 51. [2] Leshin, L. A. et al. (2013) *Science* 341: (6153), DOI:10.1126/science.1238937. [3] Getty S. A. et al. (2010) *International Journal of Mass Spectrometry* 295: 124-132. [4] Glavin D. P. et al. 2012 IEEE Aerospace Conference, March 3-10, 2012, pp. 1-11, doi: 10.1109/AERO.2012.6187065. [5] ten Kate I. L. et al. (2010) *Planetary and Space Science* 58: 1007-1017.

Acknowledgements: We appreciate support for the VAPoR instrument development from the NASA ASTID and MMAMA Programs, and Goddard IRAD.

THE EUROPLANET RESEARCH INFRASTRUCTURE AND TECHNOLOGY FORESIGHT.

M. Grande on behalf of the Europlanet Community

Aberystwyth University, Penglais, Aberystwyth, SY233BZ United Kingdom, m.grande@aber.ac.uk

The **Europlanet 2020 Research Infrastructure (RI)** is a project to integrate and support planetary science activities across Europe. The project is funded under the European Commission's Horizon 2020 programme; it was launched on 1st September 2015 and will run until 31 August 2019. has 33 beneficiary institutions from 19 European countries. Europlanet 2020 RI is a European Research Infrastructure that is addressing key scientific and technological challenges facing modern planetary science by providing open access to state-of-the-art research data, models and facilities across the European Research Area.

Europlanet 2020 RI provides:

- Transnational access to world-leading laboratory facilities that simulate conditions found on planetary bodies as well as specific analogue field sites for Mars, Europa and Titan.
- Virtual access to diverse datasets and visualisation tools needed for comparing and understanding planetary environments in the Solar System and beyond.
- Networking activities to enhance cooperation and effective synergies between its different components: space exploration, ground-based observations, laboratory and field experiments, numerical modelling, and technology. EPN2020-RI will disseminate its results to a wide range of stakeholders including industry, policy makers, the media and the public. It will use a combination of traditional media activities and new educational and social media tools to engage the widest possible European audience with the science resulting from EPN2020-RI.
- Europlanet 2020 RI places particular emphasis on widening the participation of previously under-represented research communities and stakeholders.

Europlanet 2020 Innovation and Foresight Working Group

The Innovation and Foresight group brings together science and industrial teams to promote the innovation that is inherent in space activities because of the challenging environments they work in. The very existence of a structured community of European planetary scientists is of considerable added value for the European industry, not only for the large companies of the space sector but even more importantly for SMEs and non-space industry, which must identify

relevant interlocutors. Identifying a market is vital in order to invest in technology. For an SME or for a larger non-space company, assessing opportunities for planetary science applications remains a challenge. The technical foresight group helps to identify specific topics relevant to SMEs. We promote thematic workshops with participants from industry and academia. Outcomes from will be rapidly disseminated to build industry involvement in later years. This will result in:

- ✓ Topical Working Groups with participants from planetary science groups, SMEs and other industrial partners to promote innovation in planetary science (with SMEs);
- ✓ Workshops on innovative instrumentation for planetary missions. The specific new observational challenges suggested by the scientific groups will be assessed in the light of existing technological possibilities, and the need/cost of new instrumentation development will be discussed and analysed;
- ✓ Workshops on cooperation between EUROSPACE and the European planetary science academia. (EUROSPACE - www.eurospace.org- is the trade association of the European Space Industry representing 90% of the total turnover of the European Space Industry.)

We also aim to provide a way of responding to our stakeholders in industry. Will to promote innovative measurement techniques in forthcoming planetary science/missions, with commercial and industrial companies including SMEs;

Key questions to address are:

- What are the major science drivers for the next 15 years? (i.e. from now to 2030)
- How will science instrumentation change over the next 15 years?
- What methods will we need to address these science challenges (Resolution, radiation Hardness, readout speed etc.)?
- What are the priority technologies that we must invest in now to meet these future science challenges?
- What are the priority constituent technologies that we must invest in now to meet these future science challenges? (e.g. materials technology, computing, etc.)
- Are there nearer term technologies that we can significantly improve, and how?
- What will the planetary technology road-map look like from now to 2030?

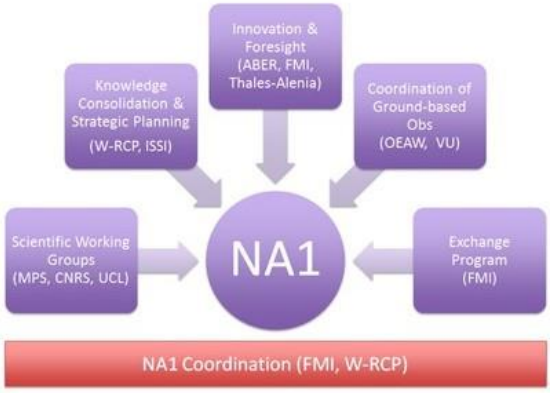

SCIENTIFIC APPLICATIONS OF IMAGING SPECTROMETERS FOR LANDED MISSIONS: EXAMPLES FROM TERRESTRIAL FIELD DEPLOYMENTS. R. N. Greenberger[1], B. L. Ehlmann[1,2], R. O. Green[1], D.L. Blaney[1]. Jet Propulsion Laboratory, California Institute of Technology, 4800 Oak Grove Drive, Pasadena, CA, 91109; Rebecca.N.Greenberger@jpl.nasa.gov. [2]California Institute of Technology, 1200 E. California Blvd., Pasadena, CA 91125.

Introduction: Visible-shortwave infrared (VSWIR) imaging spectroscopy from orbiter missions has revolutionized our understanding of the history of solar system bodies (e.g., most recently, CRISM on MRO, M^3 on Chandrayaan-1, VIR on Dawn). New technological advances in instrument miniaturization now enable imaging spectroscopy at sub-cm spatial resolution in landed packages (<2-3 kg mass), which has exciting geological applications on Earth and other solar system bodies [4]. Here, we show three science applications of imaging spectroscopy in different environments at scales relevant to landed planetary missions (landscape to microscopic) highlighting the utility of this technique, which combines information on morphology and composition in a single dataset. The imaging spectrometers used in the following examples are commercially available but are similar in wavelength coverage, spatial resolution, and data output to those developed to TRL 6 for spaceflight (e.g., the Ultra Compact Imaging Spectrometer, packaged in mast- or microscope mode [1-3]).

Example 1 – Sedimentary unit sequence stratigraphy: Sedimentary processes have been discovered on Mars and Titan. Changing compositions of minerals and ices recorded in layered units provide insight into the type of environments in which the sediments were deposited and record environmental change. For example, [5] used imaging spectroscopy to map lithologies of the Green River Formation, Utah (Fig. 1). The lithologies identified include carbonates (incl. distinctly calcite- and dolomite- rich units), silicates (hydrated), and organic-rich units. A general transition from siliciclastic to carbonate facies indicates deepening of the basin's lake, consistent with previous, traditional field-based geologic mapping [6]. Key new results also include identification of a dolomitized stratum as well as gypsum in enriched lenses and as a weathering product [5]. The ability to remotely map sedimentary lithologies during a planetary mission would provide a significant advance in spatial resolution (and thus paleoenvironment temporal resolution) vs. orbital data and identify the most crucial locations for further in situ investigations.

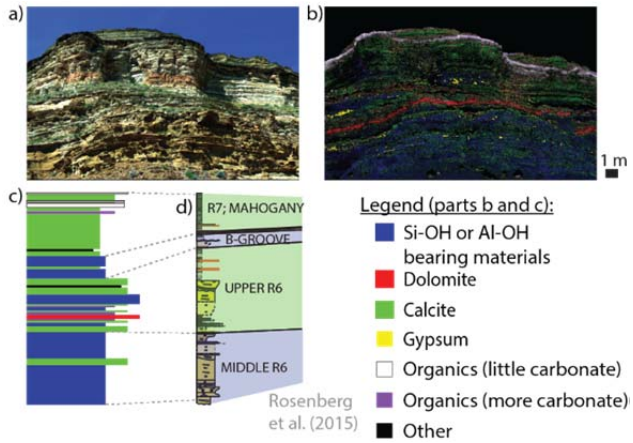

Fig. 1. a) Approximate true color image of outcrop of Green River Formation outcrop. b) Lithologic map from spectral image. c) Lithostratigraphy from (b). d) Stratigraphy made with traditional geologic methods by [6]. Modified from [5].

Example 2 – Interpretation of volcanic and hydrothermal processes: Volcanism occurs on bodies throughout the solar system, and the resulting mineralogies characteristic of different temperatures, pressures, and source compositions have unique spectral signatures at VSWIR wavelengths [e.g. pyroxenes, olivine, ilmenite, spinel, anorthites; 7]. Furthermore, VSWIR imaging spectroscopy is a powerful technique to discern hydrothermal alteration and weathering of volcanic materials. For example, a microimaging spectroscopy study of lacustrine pillow lavas from the Hartford Basin, Connecticut, identified the composition of the lavas and then multiple episodes of fluid interaction that could be time-ordered: (1) initial >400°C temperature formation of calcic clinopyroxenes and aegirine, (2) lower temperature formation of Fe/Mg-smectite and chlorite along with fine-grained hematite, and (3) two episodes of calcite precipitation and albitization [8]. Small areas of datolite ($CaBSiO_4OH$), significant because of its flagging of the existence of past boron-rich fluids, were also identified with imaging spectroscopy that were not apparent through visual inspection of the sample. The results of these detailed micro-scale analyses were then scaled to the larger samples and outcrops using imaging spectroscopy, highlighting alteration trends at a larger scale. Imaging spectroscopy is a key technique for a planetary mission to integrate individual point measurements to the surrounding outcrops.

Example 3 – Impact cratering and investigation of subsurface-derived clasts: Impact cratering is the most ubiquitous geologic process in the solar system, affecting every planetary body. Ground-

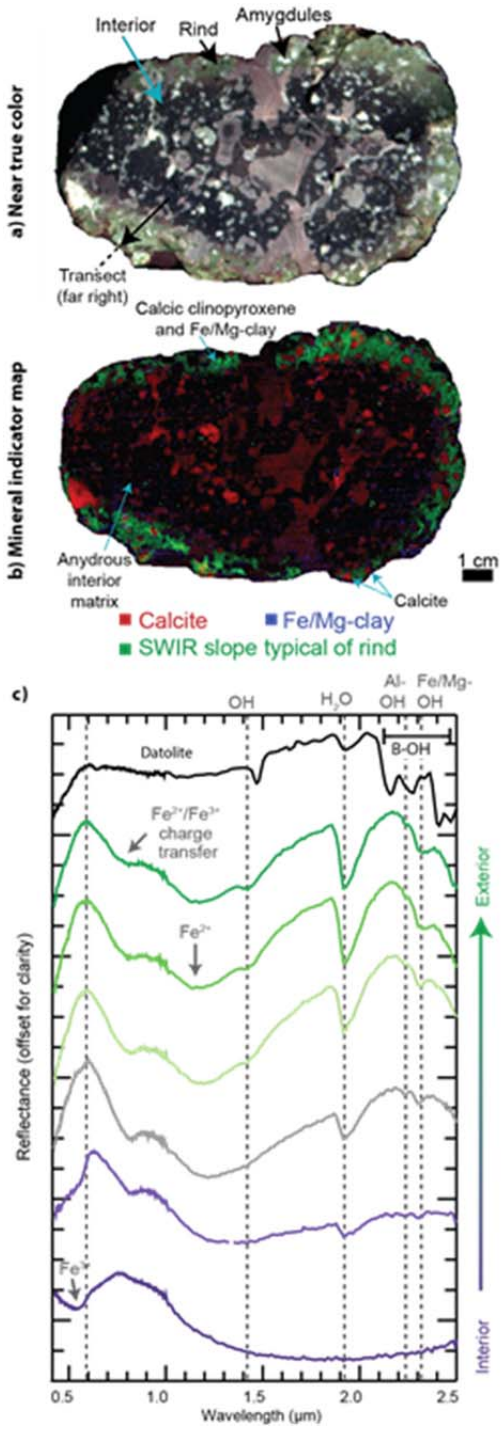

Fig. 2. a) Approximate true color image of lacustrine pillow lava cross-section. b) Spectral parameter map. c) Spectral transect across alteration rind and spectrum of small patch of datolite. Location of transect shown in (a). Figure modified from [Greenberger 4, 8].

based imaging spectroscopy field campaigns have been conducted at the Haughton impact structure, Nunavut, Canada in 2013 [9] and 2016 [10]. Using imaging spectroscopy, lithologies within highly heterogeneous, impact-disrupted materials can be identified and mapped, permitting identification of rare lithologies that might otherwise be missed. On water-bearing bodies such as Mars and Ceres, the heat from meteorite impacts can generate hydrothermal systems [e.g., 11-12]. Those deposits and their weathering products can be mapped, providing insights into the chemistries and temperatures of the fluids and guiding sampling to search for evidence of microbial colonization (Fig. 3).

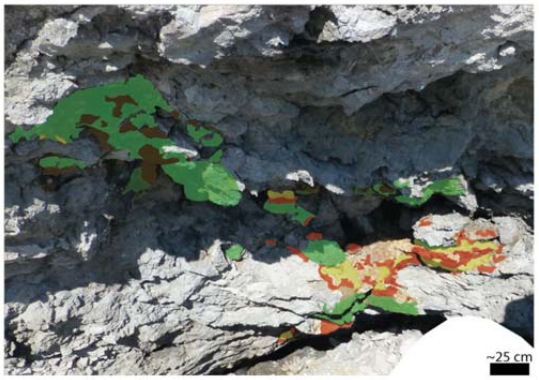

Fig. 3. Mapping of primary and weathering lithologies at a hydrothermal calcite-marcasite vug, Haughton impact structure, Canada. Green=marcasite, brown=thin sulfate and oxide coatings on marcasite, yellow=copiapite+fibroferrite, red=gypsum+Fe^{3+}-oxides and sulfates (fig. modified from [9])

Conclusions: Imaging spectroscopy on a landed planetary mission is uniquely suited to remotely mapping lithologies in a variety of terrains, combining morphology and composition in a single dataset to determine geologic histories. The results guide tactical mission planning, identifying the most promising sites for in situ sampling and finding rare compositional components that may be key to understanding the geologic and/or aqueous history. Finally, field tests on Earth provide opportunities to characterize and test the instrumentation and develop the analytical methods to maximize the science return from future missions.

References: [1] Van Gorp B. et al. (2014), *J. Appl. Rem. Sens., 8*, 084988. [2] Ehlmann B. L. et al. (2014), *Intl. Workshop on Instr. for Plan. Missions*, #1046. [3] Blaney D. L. (2014), *Intl. Workshop on Instr. for Plan. Missions*, #1148. [4] Greenberger R. N. et al. (2015), *GSA Today*, *25*, 4-10. [5] Greenberger R. N. et al. (accepted), *IEEE Proceedings, WHISPERS*. [6] Rosenberg M. J. (2015), *Strat. and Paleolimn. of the Green River Formation, Western USA*, 211-249. [7] Burns R. G. (1993), *Mineralogical Appl. of Crystal Field Theory*, *2*. [8] Greenberger R. N. et al. (2015), *GCA, 171*, 174-200. [9] Greenberger R. N. et al. (accepted), *MAPS*. [10] Greenberger R. N. et al. (2016), *AGU Fall Meeting*. [11] Newsom H. E. (1980), *Icarus, 44*, 207-216. [12] Osinski G. R. et al. (2013), *Icarus, 224*, 347-363.

Acknowledgments: R.N.G. is supported by the NASA Postdoctoral Program with an appointment at the Jet Propulsion Laboratory, California Institute of Technology, administered by Universities Space Research Association under contract with NASA.

SUPERCONDUCTING GRAVITY GRADIOMETER FOR PLANETARY MISSIONS. C. E. Griggs[1], H. J. Paik[1], M. V. Moody[1], D. D. Rowlands[2], F. G. Lemoine[2], X. Li[3], S.-C. Han[4], [1]Department of Physics, University of Maryland, College Park, MD 20742, [2]Planetary Geodynamics Laboratory, NASA Goddard Space Flight Center, Greenbelt, MD 20771, [3]Cryogenics and Fluids Branch, NASA Goddard Space Flight Center, Greenbelt, MD 20771, [4]University of Newcastle, NSW 2308, Australia.

Introduction: We are developing a compact tensor superconducting gravity gradiometer (SGG) for obtaining accurate gravimetric measurements from planetary orbits. A new and innovative design gives a potential sensitivity better than 10^{-4} E $Hz^{-1/2}$ (1 E $\equiv 10^{-9}$ s^{-2}) in the measurement band of 1 mHz to 0.1 Hz for a device with a baseline just over 10 cm.

The SGG requires cooling to ≤ 6 K, and the goal for a space mission is to use a cryocooler to enable mission lifetimes of ≥ 5 years. The most significant issue has been the potential for vibration from the cryocooler to couple into the gradiometer. On this front, there has been a *major breakthrough*. A 10-K turbo-Brayton cryocooler for space application has recently been demonstrated by Creare, LLC [1]. With the only vibration sources being low-mass, precisely balanced, rotors turning at > 1 kHz, and turbulent pressure forces from helium fluid, **the vibrations from the turbo-Brayton cryocooler will *not* affect the SGG performance even without active control or isolation**.

The original SGG, fully developed in the 1990's, had *mechanically suspended* test masses, which limited the sensitivity to ~ 10^{-2} E $Hz^{-1/2}$ with a baseline nearly 20 cm [2]. *Magnetic levitation* gives a number of advantages. The resulting magnetic spring is much more compliant and gives two degrees of freedom to each test mass. Hence a tensor gradiometer can be constructed with only six test masses, and the 10^{-4} E $Hz^{-1/2}$ sensitivity can be achieved with a device miniaturized by an order of magnitude in volume and mass.

With 10^{-4} E $Hz^{-1/2}$ sensitivity, **the expected resolution (*l* ~ 220, where *l* is the maximum degree of harmonic coefficients) of the gravity field for Mars is better than the expected resolution (*l* ~ 180) using satellite-to-satellite tracking (SST) from two co-orbiting spacecraft.** The more sensitive measurements from the SGG should also enable mapping the regional scale of seasonal gravity variations due to mass transport of CO_2 every month or every season.

SGG Instrument: Both a diagonal and an off-diagonal-component SGG have been developed at the University of Maryland (UM) [2,3]. Signal differencing by means of stable persistent currents *before* detection is a unique feature of the SGG. **This assures excellent *null stability* of the device, which in turn improves the overall common-mode (CM) rejection. The mechanical stability of materials at cryogenic temperatures guarantees that misalignments are also stable.** These error coefficients can therefore be measured once for all during the initial setup, multiplied by the proper acceleration components, and subtracted from the gradiometer output. By applying this 'residual CM balance' [4], the error coefficients have been reduced to $\leq 10^{-7}$ and $\leq 10^{-9}$ for the diagnonal and off-diagonal components, respectively.

A simple levitation scheme, which provides stiff suspension for unwanted degrees of freedom while permitting complete compliance along the sensitive axis, has been devised and demonstrated at UM. Figure 1 illustrates the principle of levitation by current induced along a superconducting tube. Inside the levitation tube, each of *N*-turn wires carries current I_L. This induces a screening current on the tube, NI_L, to flow along the inner surface of the tube and return along the outer surface. **The current density on the outer surface is *uniform*, independent of the current distribution inside the tube. This generates a *cylindrically symmetric* magnetic field,** as shown in Fig. 1(a). A tube-shaped superconducting test mass with a bigger diameter surrounds the levitation tube. When the test mass is concentric with the levitation tube, the field is uniform around the levitation tube and does not exert a net force on the test mass. However, if the test mass is displaced radially, as shown in Fig. 1(b), the field becomes stronger at *P* and weaker at *Q*, resulting in a radial restoring force.

The guiding principle in designing the SGG for laboratory test is the capability to levitate the test masses in 1-g. This led to a test mass design using thin "wings" to produce a light mass (m = 0.10 kg). On the ground, a relatively large current (I_L ~ 10 A with N = 120) is required to levitate the test masses against

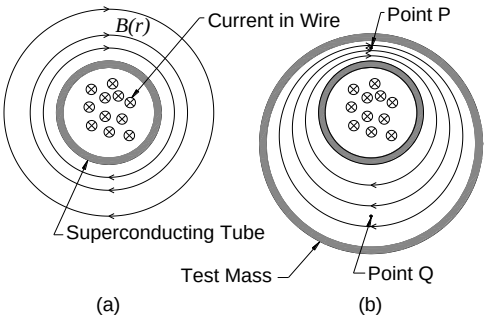

Figure 1. Principle of levitation by current induced on a superconducting tube.

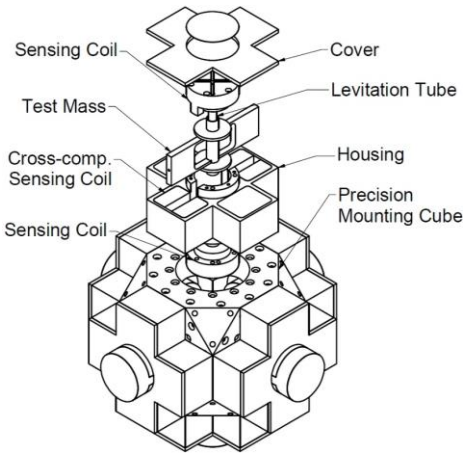

Figure 2. Partially exploded view of the tensor SGG.

Earth's gravity. **In space, the levitation becomes easier and the g-related errors disappear.**

A partially exploded view of the tensor SGG is shown in Fig. 2. The device will measure all six components of the gradient tensor, as well as all six components of the linear and angular accelerations of the platform. The entire SGG assembly weighs 12 kg and fits within a sphere of 22 cm in diameter.

Expected Sensitivity: The intrinsic noise of the diagonal components is better than 2×10^{-4} E $Hz^{-1/2}$ in the 0.001 to 0.1 Hz frequency band. This represents two orders of magnitude improvement over the performance of the GOCE gradiometer over a wider bandwidth. **The intrinsic noise at $f \leq 1$ mHz could be improved by a factor of 30 by lowering the resonance frequency f_D to 0.2 mHz. With such frequency tuning, SGG outperforms SST at low degrees, where time-varying signals are, as well as at high degrees yielding a superior spatial resolution.**

***Test Results*:** The first of the three axes of the tensor SGG has been assembled and is undergoing tests. A test mass has been successfully levitated and its dynamics is being investigated. Figure 3 shows the observed resonance frequency squared versus the sensing current squared for the translational mode. The excellent fit to a straight line shows that the acceleration-to-current transfer function is highly linear. The successful levitation proved that the magnetic field from the levitation tube not only *levitates* the mass but indeed provides *stable suspension* in two linear and two angular degrees of freedom, as predicted.

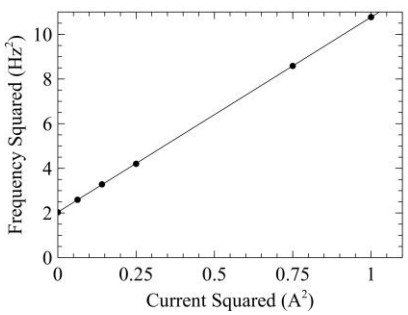

Figure 3. Frequency squared vs. current squared for the translational mode.

SGG Cryogenic System: The turbo-Brayton technology cryocoolers developed by Creare produce lower vibration levels than any of the competing cryocooler technologies. The successful operation of the turbo-Brayton cryocooler on the HST application combined with subsequent component and system developments at Creare to improve system efficiency, reduce weight, and provide cooling to < 10 K make the Creare turbo-Brayton an *ideal enabling technology* for providing the low vibration cooling required for the SGG.

Enabled Planetary Science: The unique high sensitivity of the gravity gradiometer has been demonstrated with the ESA's GOCE mission for the Earth [5]. Those measurements were particularly useful to characterize the lithospheric and (steady-state) oceanic processes at an unprecedented spatial resolution, substantially better than the GRACE mission [6] that exploits SST, while the latter has been addressing large-scale time-variability of the global gravity fields that the former is not capable of observing.

The SGG technology will bring similar advances to the planet's gravity fields. By virtue of inherent sensitivity to high-frequency gravity signals exceeding the spectrum attainable from Doppler tracking and SST, our gradiometer technology will significantly enhance the resolution of the global gravity field. Gradiometer measurements will help the trajectory determination of the spacecraft, and thus will improve the quality of surface height measurements from the laser altimeter.

Acknowledgement: This work was supported by NASA grants NNX12AK18G and NNX14AI43G, as well as by the Science Engineering Cooperative Program (SECP) of NASA GSFC.

References: [1] Breedlove, J. J. *et al*. (2014), 52nd Aerospace Sciences Meeting, AIAA SciTech (AIAA 2014-1075). [2] Moody, M.V., Paik, H.J. and Canavan, E.R. (2002), *Rev. Sci. Instrum.* **73**, 3957. [3] Moody, M.V. (2011), *Rev. Sci. Instrum.* **82**, 094501. [4] Moody, M.V., Chan, H.A. and Paik, H.J. (1986), *J. Appl. Phys*. **60**, 4308. [5] Drinkwater, M.R. *et al*. (2003), *Earth Gravity Field from Space − from Sensors to Earth Sciences* (Kluwer, Dordrecht, Netherlands), Space Sciences Series of ISSI, Vol. 18, p. 419. [6] Tapley, B.D. *et al*. (2004), *Science* **305**, 503.

Magnetotelluric Sounding of Europa's Ice Shell. R.E. Grimm[1], G.T. Delory[2], J.R. Espley[3], and D.E. Stillman[1], [1]Planetary Science Directorate, Southwest Research Institute, 1050 Walnut St. #300, Boulder CO 80302, grimm@boulder.swri.edu; [2]Space Sciences Laboratory, University of California Berkeley, Berkeley CA; [3]Goddard Space Flight Center, Greenbelt, MD.

Introduction. Electromagnetic (EM) sounding has revealed subsurface oceans on the three icy Galilean satellites [1-3] and a magma ocean on Io [4]. An additional objective for a Europa Lander is to detect any water layers within the ice shell [5]. However, a magnetometer alone is insufficient for this task, because the source strength and geometry are indeterminate at the higher frequencies required to resolve intra-shell structure. By measuring the horizontal components of the electric field and comparing them to the magnetic field, electrical conductivity structure can be determined without any additional information This is the magnetotelluric method, which has been used on Earth for more than a half-century [6].

EM Methods. We parameterize the EM response by the apparent conductivity σ_a, which is the conductivity of uniform half-space having the same EM response as the target. Then EM sounding can be considered simply in terms of exploiting the skin-depth effect to invert true conductivity $\sigma(z)$ from $\sigma_a(f)$, where z is depth and f is frequency. Alternatively, the complex impedance Z can used when considering measurement methods: the familiar Ohm's Law Z=V/I calls for two independent quantities to determine the impedance, and the same applies to EM sounding.

There are two approaches to determining Z that are relevant to Europa [7,8]. The Transfer Function (TF) compares the magnetic field at or near a planetary body (the sum of source and induced fields) to a known, distant source field. The Galileo induction studies can be considered a special case of the TF, wherein the source field is modeled a priori [9]. In the Magnetotelluric Method (MT), the horizontal electric field E and the magnetic field B are used to form Z. Because E supplies the required second piece of information, the source field is not needed separately.

EM Sources at Europa. The synodic rotation of Jupiter's magnetic field creates a "kinematic" time-varying signal that is the largest induction source. Additional signals are at the orbital period and the harmonics of the synodic period [10]. We show below that these low frequencies (~10^{-6}Hz), while well-suited to investigating the subsurface ocean, cannot resolve structure within the ice shell. Higher frequencies are required, which can be exploited from magnetospheric waves [e.g. 11-13]. Now the MT method must be applied because the source amplitude amplitude and phase are not independently known from the induction response near the body. Elimination of plasma effects

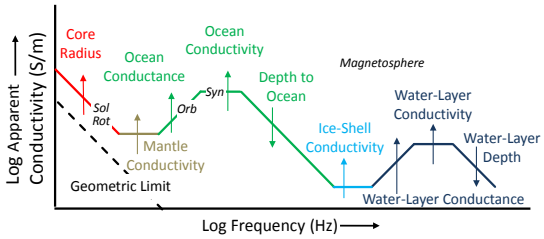

Fig. 1. Schematic broadband EM sounding for Europa. Apparent conductivity is the conductivity of a halfspace having the measured EM response at the specified frequency. All segments can be imagined extending over the whole bandwidth so vertical shifts with varying layer thicknesses and conductivities determine which are visible and which are obscured. Relevant EM sources are indicated but have effects beyond their marked locations.

is actually more straightforward, because the inductive parts of B and E must satisfy certain dispersion relations [14] and responses to strong conductors like briny water layers have distinct forms (Fig. 1).

Europa Response. We calculate a suite of induction models for a radially symmetric Europa [7]. The reference model is water-layer depth, thickness, and conductivity 3 km, 2 km, and 1 S/m, respectively; ice-shell thickness and conductivity 10 km and 10^{-4} S/m, respectively; ocean thickness and conductivity 100 km and 1 S/m, respectively, and mantle conductivity 10^{-3} S/m. We confirm that ocean thickness and conductivity both strongly affect σ_a at the kinematic frequencies (Fig. 2), and that the spread in frequency is useful in separating the "equivalence" in these two quantities. There is no response to these parameters at magnetospheric frequencies, as these signals negligibly penetrate the ocean. Both the kinematic and magnetosphere signals have some sensitivity to ice-shell thickness, with opposite, complementary, dependencies.

In contrast, the kinematic frequencies have no sensitivity to the depth or thickness of a water layer in the ice shell at nominal conductivity and only begin to respond when conductivity is very high. However, clear responses are evident in the magnetospheric band for all of these properties; in fact, diagnostic responses are mostly bounded between 0.01 and 100 Hz. Depth and conductivity are well-determined; resolution o fthickness improves for shallower, thinner, and less conductive water layers, or a thicker ice shell.

In Situ Measurement. A fluxgate magnetometer is already specified for a Europa lander [5], so a complete MT sounder only requires adjustment of sam-

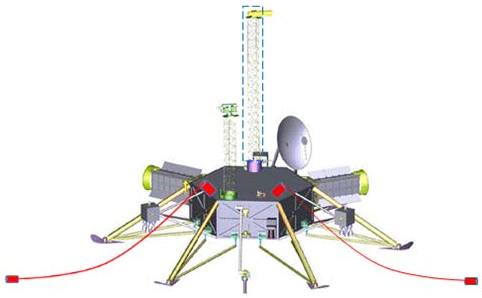

Figure 2. Top: Europa Magnetotelluric Sounder (EMS) sensors comprise magnetometer on vertical boom (dashed blue box; specified by ref. 5) and two remote electrodes (red cylinders on ground) that have been deployed by spring launchers (red cylinders on lander) to ~20 m distance (not to scale). Bottom: Drawing of electrode and spring launcher (connecting cable not shown).

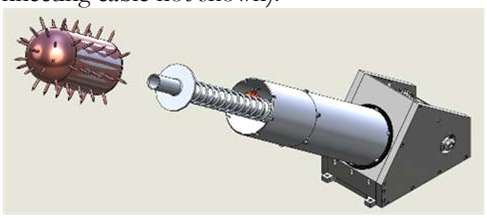

pling rates and addition of an appropriate electric-field measurement (Fig. 3). The fluxgate can be reconfigured to sample up to a few hundred sps in order to measure magnetospheric waves up to 100 Hz. The electrometer needs a long baseline (up to a few tens of meters) between the electrodes or voltage probes in order to achieve the necessary voltage SNR from the ambient electric field ($\Delta V = E\Delta x$). To attain this separation, the electrode can be spring launched and ballistically deployed (Fig. 3); our prototype-deployments to several meters translate to >20 m on Europa. Resources for a Europa Magnetotelluric Sounder (EMS) are modest, ~3 kg ~4 W CBE, and the system is readily adapted to the low temperature (70 K) and high radiation (500 krad) environment of Europa.

References. [1] Khurana, K.K. et al. (1998) *Nature, 395*, 777. [2] Zimmer, C. et al. (2001) *Icarus, 147*, 329. [3] WHERE IS GANYMEDE. [4] Khurana, K.K. et al. (2011) Science, 332, 1186. [5] Europa Study Team, JPL D-71990, 2012. [6] Simpson F., and Barr K. (2005) *Practical Magnetotellurics*, Cambridge, 254 pp. [7] Grimm, R.E., and G.T. Delory (2012), *Adv. Space Res.*, ASR-D-11-00329. [8] Banerdt, W.B. et al. (2014) in Encyclop. Solar Sys. (ed. T. Spohn), Elsevier. [9] Khurana, K.K. (1992), *JGR, 102*, 11295. [10] Seufert, M. et al. (2011), *Icarus, 214*, 477. [11] Khurana, K.K. and M.G. Kivelson (1989) *JGR, 94*, 5241. [12] Kurth, W.S. et al (2001) *PSS, 49*, 345. [13] Volwerk, M. et al. (2001), *JGR, 106*, 26,033. [14] Wiedelt, P. (1972) *Z. Geophys. 38*, 257.

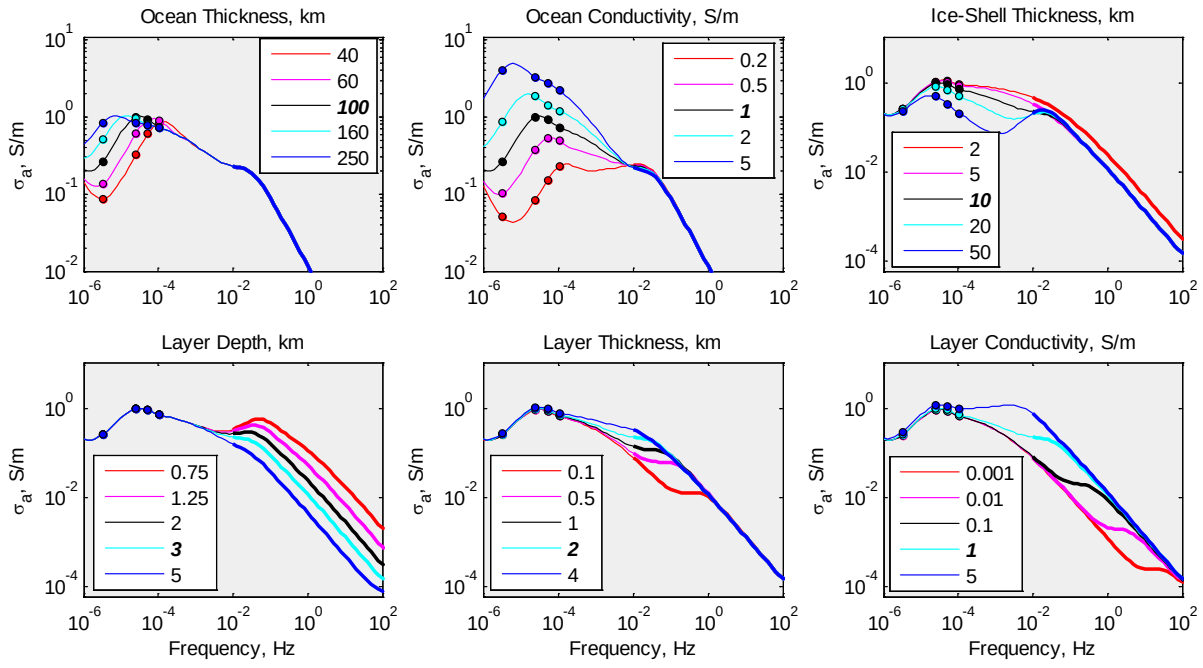

Fig. 2: Broadband EM sounding of Europa expressed as apparent conductivity σ_a. Reference value for each parameter (i.e., that used in other panels) is labeled in bold italic. Symbols are discrete kinematic frequencies; heavy lines specify instrument range to measure broadband magnetospheric phenomena. Kinematic frequencies can determine ocean properties and shell thickness, but magnetospheric frequencies are necessary to resolve water-layer properties

THE RIMFAX GPR INSTRUMENT DEVELOPMENT FOR THE MARS 2020 ROVER MISSION.

Svein-Erik Hamran[1], Hans E.F. Amundsen[2], Linn Asak[1], Tor Berger[1], Sverre Brovoll[1], Jo Inge Buskenes[1], Lynn Carter[3], Leif Damsgård[1], Christina Diaz[7], Rebecca Ghent[4], Øystein Helleren[1], Jack Kohler[5], Michael Mellon[6], Daniel Nunes[7], David Paige[8], Dirk Plettemeier[9], Kathryn Rowe[8], Patrick Russell[8] Bendik Sagsveen[1], Nina Ødegaard[1], and Mats Jørgen Øyan[1], [1]FFI, Kjeller, Norway, Svein-Erik.Hamran@ffi.no, [2]Vestfonna Geophysical, Trondheim, Norway, [3]NASA GSFC, MD, United States, [4]Univ. of Toronto, Canada, [5]Norwegian Polar Institute, Tromsø, Norway, [6]JHU/APL, MD, United States, [7]Jet Propulsion Lab, CA, United States, [8]UCLA, CA, United States, [9]Technical University of Dresden, Germany.

Introduction: The Radar Imager for Mars' subsurface eXperiment (RIMFAX) ground penetrating radar (GPR) experiment for the Mars 2020 Rover will add a new dimension to the rover's toolset by providing the capability to image the shallow subsurface beneath the rover. Radar waves can be transmitted through the air and will penetrate the surface of Mars with minimal interference with rover activities. A GPR instrument can provide subsurface imaging capabilities at sufficient depth, resolution, and timing to be of operational value to the rover mission, while also providing valuable geologic context. A GPR on the Chinese Lunar rover Chang'E-3 successfully penetrated several meters into the lunar subsurface [1]. The WISDOM GPR is planned on the ExoMars mission to be launched in 2020 [2].

2. Scientific Objectives: The principal goals of the RIMFAX investigation are to image subsurface structure and to provide information regarding subsurface composition.

RIMFAX will allow the rover science team to quickly assess the extent and depths of possible buried layers and their stratigraphic relationship to nearby outcrops. RIMFAX will provide a unique view of the stratigraphic section and cross-cutting relations, and thus a window into the geological and environmental history of Mars. Depending on the geologic setting, RIMFAX has the potential to detect a wide range of subsurface geologic features and can provide valuable information regarding the past surface exposure history of sedimentary rock layers.

Depending on materials, RIMFAX will image the subsurface stratigraphy to depths of more than 10 meters with vertical resolutions < 20 cm and a horizontal sampling distance of 10 cm along the rover track. The data provided by RIMFAX will aid the Mars 2020 rover in its mission to explore the ancient habitability of its field area, and in the selection of scientifically compelling samples for caching and eventual sample return.

3. The Radar System: The RIMFAX radar system consist of an electronics box mounted in the rear left tower of the rover. The electronics box is in a thermally controlled area. The RIMFAX antenna is externally mounted underneath the RTG on the back of the rover and has no thermal control. Fig. 1 illustrates where the different radar parts are mounted on the rover body.

The Frequency Modulated Continuous Wave (FMCW) signal is gated so that a single antenna will be used both as a transmitter and receiver antenna. The gating is basically switching the transmitted signal on and off [3]. When the transmitter is off the receiver is switched on and will receive the reflected signal. The radar transmits a frequency sweep starting at 150 MHz up to a maximum of 1200 MHz depending on operation mode. The radar can switch to a calibration cable and measure the reflection from the end of the cable, which is used to monitor the instrument performance and calibrate the radar response.

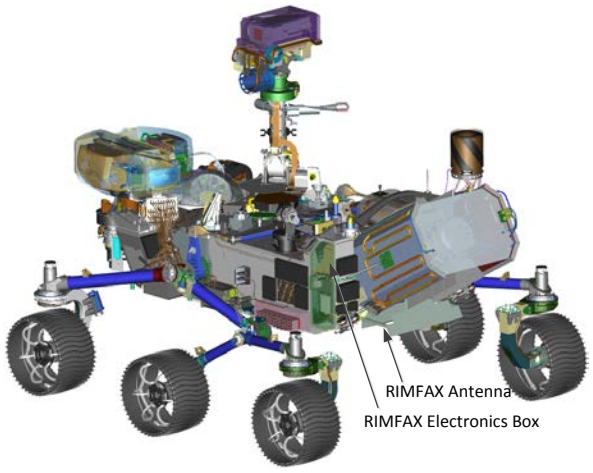

Fig 1. The RIMFAX Electronics box is mounted in the rear left tower and the antenna is externally mounted underneath the RTG on the back of the rover. (Illustration courtesy of NASA/Caltech/JPL).

3. Operation on Mars: The RIMFAX radar will collect data when the rover is either driving or stationary. The radar receiver has a limited instantaneous dynamic range for each sounding. To capture the reflection from the surface and deeper attenuated layers at the same time is not possible. The radar sounding is therefore split into three different modes, which to-

gether can capture the full surface and subsurface dynamic range.

- **Surface Mode** where the reflections from the antenna and surface is within the receiver dynamic range window.

- **Shallow Mode** where the antenna reflection is removed by gating and the surface reflection and shallow reflectors are within the receiver dynamic range window.

- **Deep Mode** where the antenna, surface reflection and shallow reflectors are removed from the receiver dynamic range window by gating.

All three modes will be collected every 10 cm along the rover path. Every sounding from the Surface Mode is expected to be downlinked back to Earth. Both the Shallow Mode and the Deep Mode will be collected with an instrumented depth range that is deeper than the expected penetration depth. Data for the Shallow and Deep modes can be both stacked and clipped in range while onboard as to tactically meet, when strictly necessary, operational constraints imposed on downlink volume.

The radar may also collect data while the rover is stationary at a given time interval between each sounding. A sounding can, for example, be taken every hour over a Sol, thereby measuring the effects of thermal changes in the subsurface over the diurnal cycle.

A longer integration mode will be used while the rover is stationary. In this mode the soundings are integrated in the rover allowing bit growth and thereby higher dynamic range in the receiver. A long integration sounding will be collected every time the rover stops for a time period in the order of a several minutes.

The radar also has two passive modes where the received noise is captured either on the calibration cable to measure the radar internal noise, or on the antenna to measure external noise.

3. Field test: A prototype version of the antenna that is very close to the expected Flight Model was tested on Svalbard in April 2016. The antenna was mounted on a glass fiber pole sticking out on the back of a snow mobile sled, see Fig. 2. The field test was mainly an instrument test to verify the antenna performance. An earlier prototype version of the RIMFAX radar was hooked up to the antenna. The radar was programmed to emulate the different operation modes. Fig. 3 shows a profile using the surface mode where the antenna and surface reflection are captured within the radar receiver. A background removal is used to remove the strong stationary reflections from the antenna. The radar profile shows the surface reflection from the air/ice interface together with a shallow reflection from the ice/ground interface. The radar was tested on several poly-thermal glaciers in the area.

Fig 2. Prototype version of the RIMFAX antenna during field test on Svalbard in 2016.

References:

[1] Xiao et. Al (2015) Science 347 (6227), 1226-1229.
[2] Ciarletti et al., (2011), Proc. IEEE, Vol. 99, No. 5.
[3] Hamran et. al. (1995), J of App. Geophysics, 33, 7-14.

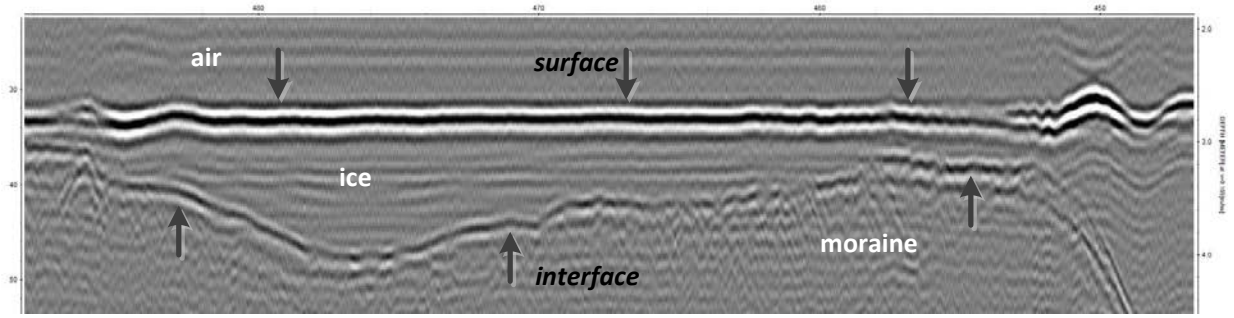

Fig 3. Radar profile using the Surface Mode. The length of the profile is around 40 meters and the depth scale is about 1.5 meters below the surface reflection.

SINGR: A SINGLE SCINTILLATOR NEUTRON AND GAMMA-RAY SPECTROMETER FOR ACQUIRING RAPID, REMOTE GEOCHEMICAL DATA ON FUTURE PLANETARY SCIENCE MISSIONS

C. Hardgrove[1], E. Johnson[2], T. Prettyman[3], A. Parsons[4], H. Barnaby[1], J.Christian[2], K. Gupta[1], [1]Arizona State University (School of Earth and Space Exploration, Tempe, AZ craig.hardgrove@asu.edu), [2]Radiation Monitoring Devices (Watertown, MA), [3]Planetary Science Institute (Tucson, AZ), [4]NASA Goddard Space Flight Center (Greenbelt, MD).

Introduction: Geochemical planetary science data can be acquired at a variety of scales and play an important role constraining the geologic history of a planetary body, as well as in understanding formation and post-depositional processes experienced by local outcrops on a planetary surface. Several future NASA missions identified by the Planetary Decadal Survey would benefit from rapid acquisition of geochemical data, including a Venus lander, Moon or Mars rovers, and missions to comets, Phobos or Deimos. Acquiring lander- or rover-scale geochemical data on planetary surfaces is often achieved through robotic, arm-mounted instrumentation or via scoops/drills that sample a subset of near-surface material that is subsequently portioned to the instrument via a sample delivery system. These types of observations can require significant spacecraft resources (*i.e.* time, power) and often only a subset of bulk material can be characterized due to particle size or sample preparation limitations. Geochemical data can also be acquired through laser ablation spectroscopy, however, individual observations are typically at size scales on the order of ~microns, do not penetrate at significant depth, and are ideally suited for study of small-scale textures, minerals, or individual rocks. Observations at scales of several meters can integrate the geochemical signatures from multiple rock units and are typically sensitive to greater depths (tens of centimeters to meters) than other instruments. These measurements can be used to place other measurements in geologic context, to identify geochemical trends throughout a rover traverse, or for comparison with orbital (regional/planetary-scale) data sets.

The Curiosity Mars rover has successfully demonstrated the ability of an active-source neutron spectrometer (Dynamic Albedo of Neutrons (DAN)) to map multiple geologic units throughout an ~11km traverse in Gale Crater [1] DAN uses a new technique in planetary science called neutron die-away to rapidly assess H content and its distribution with depth. Using ^{3}He detectors and a pulsed neutron generator (PNG), DAN bins neutron counts by their energy and arrival time to acquire a high signal-to-noise measurement of neutron counts in ~20 minutes. The use of a PNG as a neutron source overcomes the limitation imposed by relatively low counting rates for gamma-rays and neutrons due to GCR reactions. For the Moon and Mars, there are about 9 neutrons created per GCR particle

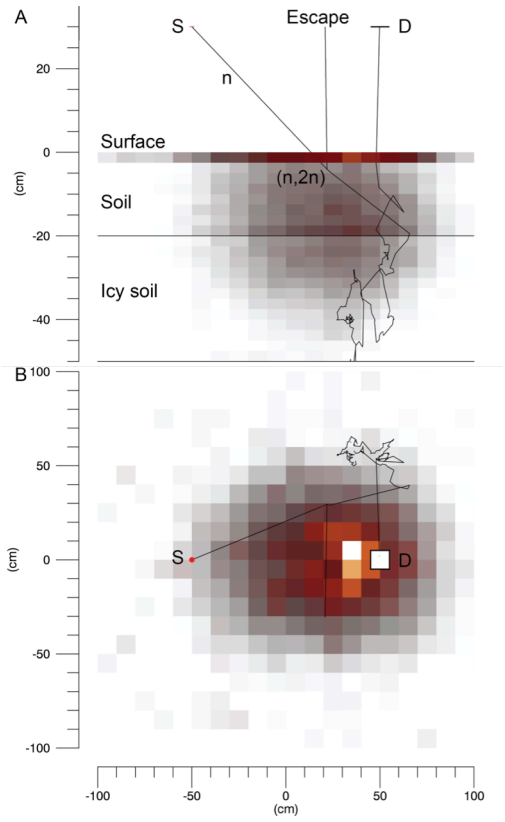

Figure 1. Measurement geometry and sample volume (temperature map) for active interrogation of an asteroid regolith with hydrogen layering, 1 wt.% water-equivalent hydrogen (WEH) covering 20 wt.% WEH. The source (**S**) is 14 MeV neutrons from a D-T pulsed neutron generator. The detector (D) is a 100 cm^2 × 2.5 cm CLYC scintillator. Side (A) and top (B) views of the geometry are shown along with a selected neutron trajectory.

interaction with regolith, and typical gamma-ray fluxes produced by inelastic neutron scattering reactions vary between 0.1 - 2.6 photons/min-cm^2 for GCR-produced gamma rays [2]. A PNG can emit ~10^8 neutrons/s, greatly increasing the number of nuclear reactions in the subsurface, which will result in higher signal- to-noise (statistical uncertainty in count rate ~ $\sqrt{N}$) and significantly shortened measurement times [3]. As an example, DAN has acquired measurements with the PNG at every end-of-drive location utilizing short, 20

minute observations. This has generated a significantly large data set of thermal and epithermal neutron counts over the first four years of surface operations [1, 4, 5]. Although not detected, characteristic prompt and delayed gamma-rays are produced by interactions of atomic nuclei with neutrons from the PNG are not detected by DAN's ^{3}He tubes. While other studies have demonstrated the use of individual neutron and gamma-ray detectors with a PNG [6,7,8], new high-efficiency scintillator materials that are sensitive to both neutrons and gamma-rays allow for one detector element to acquire counting data and spectra for both. One new scintillator material, CLYC, is an ideal candidate for use on future planetary science missions due to its sensitivity to thermal, epithermal and fast neutrons CLYC also provides gamma-ray resolution <4% at 662 keV [9,10].

Modeling: The objectives of our modeling effort are to support characterization of the response of CLYC to gamma-rays, neutrons, and energetic particles and to optimize the design of PNG-CLYC-based systems for in situ measurements of regolith composition and layering. For this purpose, we use a Monte Carlo radiation transport code [11] to sample particle interactions within a vehicle, regolith and detector. The detector response model includes a detailed treatment of light ouput, including quenching effects for swift electrons, protons, and ions produced by nuclear reactions (e.g. ^{6}Li(n,α)t in CLYC). Application of the code to determine the regolith volume sampled by 14 MeV neutrons is illustrated in **Fig. 1**.

Design: SINGR will utilize a 5cm dia. x 5cm long CLYC crystal coupled to a R6233-100 photomultiplier tube (PMT). The PMT is biased using a active voltage divider network to minimize non-linear behavior associated with high event rates. The predicted neutron flux based on the DAN measurements indicate that around 100 to 1000 ns after the neutron pulse will result in a 20-50% probability that more than one neutron will be detected in the crystal. This indicates that there will be some events that are piled up. To account for this, a signal processing algorithm will be implemented on the CLYC signals to identify separate neutron events. This algorthim is based on research [12] showing that CLYC can be used to discriminate neutrons from gamma rays at high gamma ray event rates exceeding 1x10^{6} cps (**Fig. 2**).

The signal processing algorithm uses a simplied readout hardware, consisting of a buffer, differential amplifier, an analog to digital converter, and a field programmable gate array (FPGA). The front-end signal processing is conducted on the FPGA (filtering, trigerring, integration), and post-signal processing (energy conversion, particle type discrimination calculations, histogramming) are conducted on the processor. The system is designed to provide both neutron and gamma spectroscopy. The ability to detect both neutrons and gamma-rays on a single scintillator makes CLYC a compelling option for small spacecraft like CubeSats, such as the Lunar Polar Hydrogen Mapper (LunaH-Map) CubeSat mission, which will utilize a detector array of CLYC within its Miniature Neutron Spectrometer (Mini-NS) [13].

Future Work/Tests: Future tests will allow us to demonstrate the use of CLYC in an active configuration using a PNG. This prototype CLYC instrument will be tested in early 2017 using a commercial Thermo MF Physics Model MP320 D-T PNG at an outdoor test site at NASA/ Goddard Space Flight Center [14]. This test facility consists of two large (1.8 m x 1.8 m x .9 m) Columbia River basalt and Concord Gray granite test monuments located in the middle of an open field surrounded by a 50-meter radius radiation safety zone. The complete bulk elemental composition of both basalt and granite materials has been independently measured to ppm levels so that they will act as measurement standards for our tests. In addition, the test site provides thin plates of basalt, granite and polyethylene that can be layered on top of the monuments to physically simulate buried hydrogen-rich material at a specified depth. These tests will allow the CLYC instrument to measure the depth of this material as well as the bulk elemental composition of the monuments.

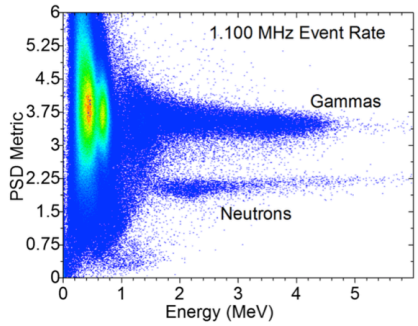

Figure 2: Pulse shape discrimination plot for CLYC with an AmBe and Cs-137 source at an event rate of 1100 kHz

References: [1] Mitrofanov et al., 2014 JGR-P [2] Woolum et al, 1975, Moon 12 [3] Knoll, 2010 Rad Detect Measurement [4] Litvak et al, 2014 JGR-P [5] Hardgrove et al, 2014 AGU 2128 [6] Parsons et al., 2011 Nucl Instr Meth A 652 [7] Bodnarik, J.G et al 2012. Nucl Instr Meth A 707 [8] Litvak et al., 2015 JGR-P [9] D'Olympia et al., 2012 Nucl Instr Meth A 694 [10] Johnson et al., 2015. IEEE HST Symposium [11] Prettyman, T. H. et al. (2011), SSR 163 [12] E. B. Johnson, et al., 2015 IEEE International Symposium, pp. 1-7. [13] Hardgrove et al., 2016 47th LPSC [14] Parsons, A.M., et al, 2016. 47th LPSC 2476.

The Mars Oxygen ISRU Experiment (MOXIE) on the Mars 2020 Rover Michael H. Hecht,[1] and Jeffrey A. Hoffman[2] for the MOXIE Team. [1]MIT Haystack Observatory, Westford, MA. Email: mhecht@haystack.mit.edu. [2]M.I.T. Dept. of Aeronautics and Astronautics, Cambridge, MA. Email: jhoffma1@mit.edu.

Introduction: A substantial reduction in the cost and complexity of a human mission to Mars can be realized by *in situ resource utilization (ISRU),* using resources at our destination to supplement the payload brought from Earth. Low-hanging fruit for such a mission is *in situ* production of oxygen, which is consumed in prodigious quantity by the lift-off of an ascent vehicle from Mars. The most readily accessible source of oxygen is the martian atmosphere itself.

The Mars Oxygen ISRU Experiment (MOXIE), a technology demonstration on NASA's 2020 Mars rover, is a progenitor of the "oxygenator" used by the fictional Mark Watney as portrayed in Andy Weir's *The Martian*. MOXIE ingests the thin CO_2 that comprises 96% of the Martian air, and exhales O_2 – somewhat like a tree, but without benefit of water as a reactant.

Mission models suggest that in excess of 30 metric tons of oxygen will be needed as the oxidant for the ascent of a human crew from Mars, representing ~78% of the propellant mass in a CH_4/O_2 propulsion system. This would translate into 400 metric tons in Earth orbit – requiring 4 to 5 heavy lift launches [1].

Approach: In development at the Jet Propulsion Laboratory, MOXIE is a ~1% scale model of an oxygen processing plant that might support a human expedition sometime in the 2030s. MOXIE is expected to produce ~10g/hr of O_2 on Mars with >99.6% purity. Fig. 1 illustrates the two major steps in O_2 production – CO_2 accumulation and compression, and conversion of CO_2 to O_2. Also of importance is the process monitoring and control system, our primary source of knowledge from experiments on Mars and in the laboratory. MOXIE fills a 24x24x31 cm volume within the rover body, as shown in Fig. 2.

MOXIE's solid oxide electrolysis (SOXE) stack for converting CO_2 to O_2 [2] is designed and built by Ceramatec, Inc.. Its working elements are stacked scandia-stabilized zirconia (ScSZ) electrolyte-supported cells with thin screen-printed electrodes, coated with a catalytic cathode on one side and an anode on the other. These are separated by expansion-matched interconnects that direct the source, exhaust, and product gases to and from their respective manifolds. The stacks nominally operate at 800°C.

When CO_2 flows over the catalyzed cathode surface under an applied electric potential, it is electrolyzed according to the reaction $CO_2 + 2e^- \Rightarrow CO + O^=$. The CO is exhausted, while the oxygen ion is electrochemically driven through the solid oxide electrolyte to the anode, where it is oxidized ($O^= \Rightarrow O + 2e^-$). The O atoms combine to produce the gaseous O_2 that is released from the anode cavity at a rate proportional to current, $\dot{n}_{O_2} = \frac{I}{4F}$, where F is Faraday's constant.

Having designated atmospheric CO_2 as the source of oxygen, the choice of solid oxide electrolysis is largely uncontested, though lower-temperature solutions such as polymer electrolytic membranes may become important in the future. For MOXIE and future systems, the more contentious trade is over the method of collecting and compressing CO_2. In the context of the Mars 2020 mission direct mechanical pumping was chosen as the most practical and resource-efficient solution, as it allows real time operation without intermediate storage despite the limited mass, volume, and power resources of Mars 2020. A scroll pump is under development from Air Squared, Inc. for this purpose. Future implementations, possibly less limited by either space or power, may choose an integrated approach that uses cryogenics for CO_2 collection, gaseous product separation, and liquefied gas storage.

Dust filtering is also a critical technology, not so much because Mars is so dusty, but because small pressure drops that would be of no significance in the Earth environment can severely impact the throughput of a collection system at Mars ambient pressure. For MOXIE, conventional pleated HEPA filters appear to offer sufficient collecting area to treat the air drawn through the filter with tolerable degradation during the limited allocated operating time (nominally 15 two-hour runs during the primary mission). Recent experiments in a Mars wind tunnel addressed this issue, as well as exploring the impact of dust passively accumulated when MOXIE is not in operation. In future implementations, a dust-tolerant first-stage pump, electrostatic dust removal, or cyclonic particle separation may be preferred.

Performance: MOXIE oxygen production rate is limited by several factors:

- SOXE capability
- Pump capability
- Power supply capability
- Safe operating conditions
- Atmospheric pressure
- Impedance from filters and dust accumulation

The production capability of the SOXE itself is uniquely determined from knowledge of the area-

specific resistance (ASR), typically ~2.0 for this system; the open-circuit voltage (OCV), typically 0.8V; the overall cell area (A), 10 cells at 22.7 cm^2 each; and the choice of operating voltage, typically 1.2 V. This voltage is adjusted such that the SOXE doesn't use more than a selected fraction of the available CO_2, the utilization fraction, which is expected to be ~50% to allow for spatial variation that might result in carbon deposition in CO_2-starved areas.

Since MOXIE's scroll pump is volumetric, oxygen production is limited both by its capacity and by the external conditions that determine the density and quantity of air that can be drawn in. The atmospheric pressure of Mars varies by as much as a factor of 2 with elevation, by up to 30% with season, and by up to ~10% with time of day. Weather variations, by comparison, are a few percent or less, except during severe dust storms, which can increase the pressure by up to ~12%. The available CO_2 is largely predictable as a function of time-of-day and season once the landing site is known; but that decision is unlikely to be made until after MOXIE is delivered. MOXIE has therefore been designed to accommodate the full range of sites under consideration, all at relatively high elevation compared to previous landings.

Other production constraints include the SOXE power supply limit of 4A current, corresponding to 12 g/hr O_2 production for the 10-cell stack. Also, since MOXIE is inside a warm rover box, production may be limited at times by its own heat generation. Safe operating conditions are currently being determined for SOXE voltage, temperature, and pump speed.

Fig. 3 factors all these limits together for anticipated operating conditions. It is notable that SOXE performance is not anticipated to be the limiting factor under any conditions.

Acknowledgments: MOXIE development is supported by the NASA HEOMD, STMD, and SMD Directorates. The technical progess reported here is largely due to the tremendous effort of the implementation team at JPL, as well as our partners at Ceramatec and Air Squared.

References: [1] Drake B. ed. (2007) Mars Design Reference Architecture 5.0, NASA/SP–2009–566-ADD. [2] Hartvigsen, J.J. et al. (2015), proc. ECS Conf. on Electrochemical Energy Conversion & Storage with SOFC-XIV, Glasgow, Scotland.

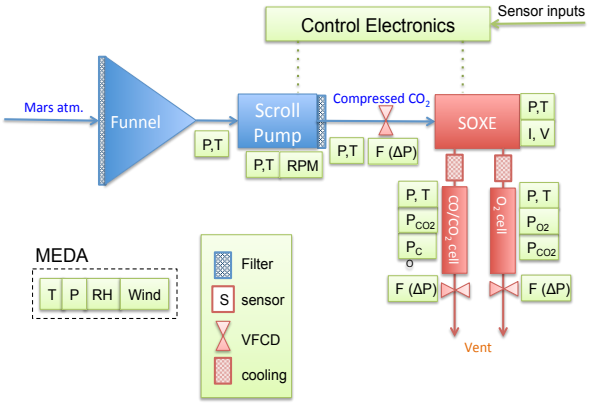

Fig 1. SOXE design components showing collection and compression system, electrolysis, monitor and control. MEDA is a separate meteorological instrument that characterizes environmental conditions of inlet gas.

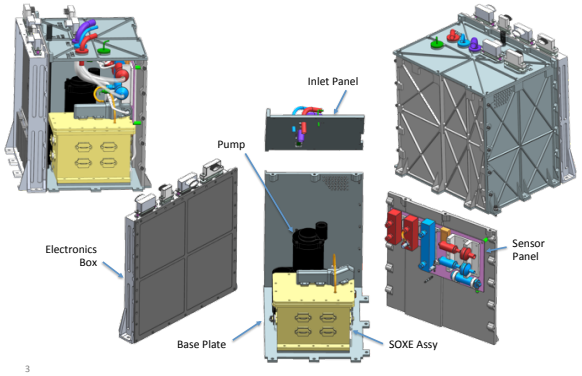

Fig 2. The MOXIE assembly consists of the SOXE and pump, electronics, analytical equipment, plumbing, and structure. All fits in a 24x24x31 cm volume.

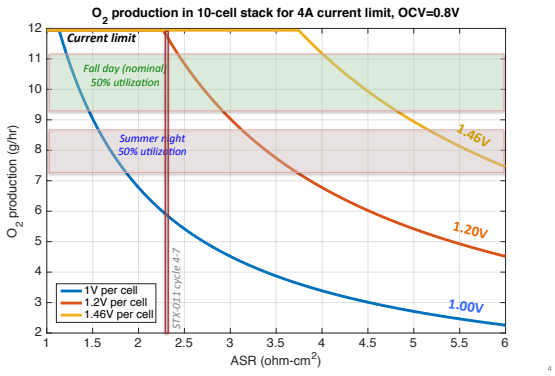

Fig 3. Anticipated O_2 production falls on the intersection of the red vertical line, showing a characteristic SOXE ASR, and a horizontal line representing the external pressure. The voltage is then adjusted accordingly. Once a site is chosen, the pink and green bands will collapse into horizontal lines representing high and low pressure conditions at the site. A 50% CO_2 utilization fraction is assumed for the y-axis.

MICRO-PENETROMETER SCIENCE INSTRUMENT FOR SMALL BODIES. V. Hernandez[1], S. Schwartz[1], E. Asphaug[1], and J. Thangavelautham[1], [1]Space and Terresterial Robotic Exploration (SpaceTREx) Laboratory, School of Earth and Space Exploration, Arizona State University, 781 E. Terrace Mall, Tempe, AZ, 85287, jekan@asu.edu.

Introduction: Asteroids and comets hold tantalizing clues to the formation history of our Solar System as well as to the origins life. They are also potential sources for water and off-world resources. Asteroids and comets range enormously in size and surface properties, and it is important to determine the specific environment in advance to ensure a safe landing and to conduct in-situ exploration, resource exploitation or for near-Earth object (NEO) hazard mitigation. Images of asteroids, even those at very high resolution such as those taken of Itokawa by the Hayabusa spacecraft [1], can give clues to the surface properties and composition, but due to various complex deposition and layering processes, some of this data can be deceiving given our current limited understanding. Use of an instrument to physically interact with an asteroid or cometary surface and obtain its hardness and other physical properties can provide valuable insight for landing, risk assessment, or for in-situ resource extraction.

Penetrometer: A suitable instrument to perform this task is a micro-penetrometer. A penetrometer was flown on the Cassini Huygens probe to estimate the surface hardness of Titan [2]. Percusive penetrometers are in development for lunar surface missions [3]. A micro-penetrometer is an instrument that consists of a rod with a conical tip that is pushed into regolith. The rod is mounted with force sensors. By pushing the rod into the regolith and measuring the reactive forces, it may be possible to determine the granularity, the porosity, the hardness, and the chemical composition of the top layers of the asteroid surface. In our present work, we are developing a penetrometer that would fit into a 1U CubeSat body. The penetrometer could be pushed into place using linear actuators that can be readily space-qualified.

Asteroid Missions: An important advantage of the penetrometer as a science instrument for a small (~0.1–1 km diameter) asteroid mission is that it can be used in touch and go exploration, where a spacecraft has brief encounters with an asteroid surface (Fig. 1), but due to the very low gravity, does not land. Touch and go operations, demonstrated in the Hayabusa mission [1] and to be used by OSIRIS-REx and Hayabusa-2 sample return missions, require low-delta V and limits risk when the surface properties of an asteroid are unknown. Repeated touch and go operations can enable sampling of the asteroid surface to determine relative hardness and distribution of surface material.

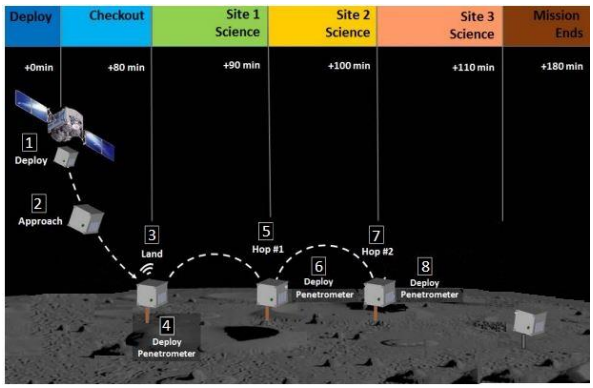

Figure 1: Penetrometers can be used on low-cost NanoSat sized asteroid surface explorers to obtain readings of hardness, porosity and granularity. This data can be used to reduce risk of landing a large spacecraft.

The data obtained from a penetrometer are not readily obtained from imagers, due to surface ambiguity (e.g. porous crusts, aggregate clods, etc.) and will allow for an assessment of surface properties prior to more ambitious engagement with the surface. In this work, we propose use of a penetrometer for a touch and go microsatellite mission to an asteroid and for use on nanosat-sized asteroid surface explorers. Microsat missions offer the possibility of getting to an asteroid, performing touch and go operations and obtaining samples. Nanosat sized surface explorers can be sent by the tens or hundreds to image the surface and characterize surface properties. These surface explorers would hop, roll and fly over the asteroid. In both cases, a penetrometer would be an important instrument that would complement the capabilities of onboard imagers and spectrometers.

Prototype Development: A prototype penetrometer is being built in our laboratory (Fig. 2) and is being used to characterize the properties of fine to coarse grain material and soft rock (Fig. 3). Next steps include testing the penetrometer on asteroid simulant.

Figure 2: Penetrometer Prototype.

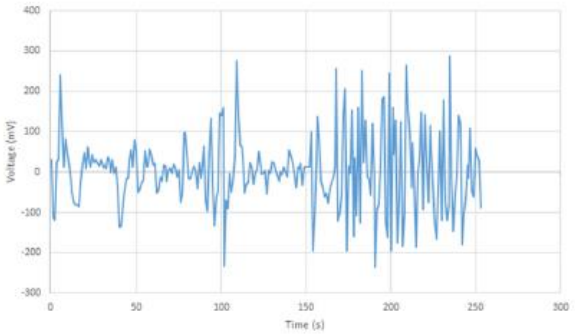

Figure 3: Preliminary readings of a penetrometer tested using sand and gravel mixture.

Deployment shown in Fig. 1 includes repeated touch and go attempts with small delta-V to keep the spacecraft engaged at the point of contact of the penetrometer. These results will be compared against computer simulations and conventional hardness testing of materials. Our laboratory development paves the way for further refinement of the instrument and flight qualification aboard an Asteroid science laboratory such as AOSAT [4], in preparation for an asteroid surface mission.

References: [1] Fujiwara A. et al. (2006) Science 312, 1330–1334. [2] Zarnecki J. et al. (2005) Nature 438, 792–795. [3] Bar-Cohen Y. and Zacny C. (2009) Extraterresterial Drilling and Excavation, 400–410. [4] Asphaug E. and Thangavelautham J. (2014) 45th LPSC, 2306.

PLASMA COMPOSITION INSTRUMENT FOR PLANETARY AND COMETARY MISSIONS. G. C. Ho[1] and G. B. Andrews[1], [1]The Johns Hopkins University Applied Physics Laboratory, Laurel, MD 20723 (George.Ho@jhuapl.edu).

Introduction: Plasma exists in all space environments, whether planetary, cometary, or interplanetary space. There are two types of plasma measurement: 1) Fast plasma; and 2) Plasma composition. Fast plasma instruments measure the core plasma moments (temperature, density, and energy) in very fast time scale (~seconds or faster), while plasma composition instruments measure all of the above (at slower time scale ~minutes) plus the charge state and elemental composition of the plasma by the addition of a time-of-flight section. In almost all space missions a plasma instrument has been part of the core payload, since it measures the basic properties of the environment the spacecraft is exploring. In addition, the plasma composition measurement provides a key diagnostic tool in deciding the origins of the plasma. In interplanetary space, the plasma composition measurement can tell us whether particular plasma comes from the Sun (coronal hole or coronal mass ejection), nearby planet, or nearby comet. In a planetary mission, as demonstrated recently by MESSENGER, plasma composition measurements have not only been key to understanding of the structure of the magnetosphere, but the plasma composition has shown that materials from the planet's surface are being scoured by solar wind, magnetospheric, and physical impact processes. Most of the heavier ions in the plasma originated as neutral atoms on the surface. In a cometary mission, plasma composition measurements can remotely sense the composition of the comet tail as far out as 1.6 AU from the nucleus [1]. (Neugebauer et al., ApJ, 667, 1262-1266, 2007). When closer to the comet, plasma composition measurements provide the basic understanding of the gas jets leaving the comet and their interaction with the solar wind.

Plasms Composition: As demonstrated recently by MESSENGER, the role of low energy thermal plasma is key to many science investigations. In particular, its measurement can infer the surface composition and other key physical processes operating in many celestial bodies without ever touching the surface. A typical plasma composition instrument consists of an electrostatic analyzer (ESA) that selects the energy per charge of an ion. It is followed by post acceleration (<30 kV) into a time-of-flight (TOF) section that measures the ion velocity and energy with solid-state detectors (mass and energy).

New Approach. In this paper, we present a new ESA design that would extend the energy range of the current plasma instrument and provide higher time cadence measurement that are required for planetary and/or cometry flyover missions. The new ESA design covers a large field-of-view on a 3-axis stabilized spacecraft and can make simultaneous energy measurement over a broad range.

A preacceleration system will be used to raise the energy of low-energy particles after exit from the ESA and before entrance into a high TRL compact TOF chamber. Within the TOF chamber, the particles velocity will be measured using electrostatic mirror, thin carbon foils and micro-channel plates. And at the end of the TOF chamber, the preaccelerated ions will overcome the thin window of the solid-state detectors (SSDs) and its total energy will then be measured. The novel use of compact TOF chamber together with thin window SSDs is capable of resolving all the major species (He, C, N, O, etc.).

Challenges: The challenges to be addressed with regards to plasma composition measurements in planetary science require more capable instrument in resoure limited missions. Instruments to date have collected critical data that have helped us understand formation and physics processes in many celestial bodies. Those instruments and their data have opened a field of planetary science that needs to be further explored with more tailored/dedicated instrumentation.

References:

[1] Neugebauer M. *et al.* (2007) *ApJ, 667,* 1262–1266.

Developing Miniature Wolter-I X-ray Optics for Planetary Science. J. Hong[1], S. Romaine[2], B. Ramsey[3], L. Nittler[4] and J. Grindlay[1], [1]Havard University, Cambridge, MA, USA (jhong@cfa.harvard.edu), [2]Smithsonian Astrophysics Observatory, Cambridge, MA, USA, [3]Marshall Space Flight Center, Huntsville, AL, USA, [4]Carnegie Institution Of Washington, Washington, DC, USA

Introduction: Comparative study of surface variation of the elemental abundance of diverse planetary bodies can provide clues to their formation and evolutionary history. X-ray fluorescence (XRF), intrinsic to atomic energy levels, carries a unique signature of the elemental composition of the emitting bodies (e.g., Figure 1 (*a*) [1]). Unlike optical and infrared spectra that can be altered by space weathering, XRF can probe more than 10–20 μm deep below the surface (e.g., see [2, 3]), and thus it is a powerful diagnostic tool to understand the true chemical and mineralogical composition of the planetary bodies.

The optical images of Comet 67P/Churyumov–Gerasimenko taken by the Rosetta mission such as the image shown (e.g, Figure 1 (*b*), see also [4]) have revealed rich surface features and outgassing activities. If the Rosetta mission was equipped with a high resolution X-ray *Imaging* spectrometer, it could have directly identified elemental composition of diverse structures of the comet nuclei surface and coma in the image. For instance, an X-ray telescope with sub-arcminute angular resolution and a square degree field of view (FoV) can measure the surface elemental abundance of ~1000 different segments in the region marked by the orange square in Figure 1 (*b*). Such an X-ray observation can greatly improve our understanding of the geological history of the comet nuclei and the physics behind the volatile activity.

Applications of X-ray imaging spectroscopy reach far beyond the study of elemental composition. Whether it is exospheric escape from Mars, pion reactions on Venus or sprite lighting on Saturn, sensitive X-ray imaging spectroscopy of planetary objects will greatly improve our understanding of the target bodies and the Solar System as a whole. Until now virtually all the X-ray spectrometers employed in planetary missions have been limited to simple collimator-type instruments without imaging capability. To make powerful, yet compact lightweight X-ray optics affordable for many future planetary missions where mass, volume and power for each instrument are limited, we have started a new program to develop miniature X-ray optics (MiXO) using metal-ceramic hybrid shells.

Technical Approach and Status: Nearly all modern X-ray astronomy missions utilize grazing-incidence optics with Wolter-I geometries which combines reflection from a parabolic and a hyperbolic surface in a barrel shape mirror. To increase the collecting area of these telescopes, several mirror shells of varying diameter can be nested one inside the other along the same optical axis. The majority of X-ray missions employ either Al foil, glass or nickel as the telescope substrate material.

Our new approach illustrated in Figure 2 (*a*) combines the plasma thermal spray technology with the electroformed Nickel replication process to largely replace thick high density NiCo shell (8.9 g/cm^3) with thin, light ceramic compound (2.3–2.9 g/cm^3) [5, 6]. In our metal-ceramic hybrid technology, the ceramic (~200 μm thick) provides the necessary stiffness to hold the figure of the mandrel and supply the rigidity needed for handling, while the thin metal (~ 30 μm thick) provides micro-roughness required for X-ray reflection. In parallel, we are also investigating minimum thickness of NiCo layer required for self-supporting NiCo-only shells. Thin (<~120 μm) NiCo-only shells can be potentially used for inner small shells without need for the supporting ceramic layers.

Figure 3 (*a*) shows recently fabricated hybrid shells (62 mm diameter × 18 cm long, designed for small FoV: <~ 0.1 deg^2) composed of 100 μm NiCo + 50 μm Bond layer + 200 μm Al_2O_3. A hybrid shell shows 2.1 arcmin resolutions with X-rays, whereas a 100 μm NiCo-only shell from the same mandrel shows about 1.1 arcmin resolution, which is limited by the polishied figures of the mandrel used for shell fabrication. Currently measures to reduce stress in the bond coat of conical shells are explored to improve the resolution using relatively thick (100 μm) NiCo substrate. Our new program for planetary science will start with flats (e.g., Figure 3 (*b*)) to identify minimal thickness (~ 30–50 μm) of NiCo layers where the newly found spray parameters remain valid without leaving imprints on NiCo layers during thermal spray, and thus eliminating need for an additional barrier layer between the metal and ceramic layers. We also started a new mandrel design to produce wide field (~1 deg^2) miniature X-ray shells suitable for planetary applications.

Telescope Design: Nearly all planetary targets for in-situ observations are diffuse sources, and thus a large FoV coverage with high resolution is essential in achieving sensitive X-ray observations. Modified Wolter-Schwarzschild or polynomial mirror geometries enable high angular resolution (<30 arcsec to 1 arcmin) over a wider FoV (~1 deg) than the standard Wolter geometry consisting of parabolic and hyperbolic sur-

faces [7, 8]. The off-axis resolution improvement with non-Wolter surfaces, however, requires the best focal surface, i.e., non-planar detector, which is not likely feasible for small instruments of planetary application. We, therefore, employ mirror shells of the standard Wolter geometry but with varying lengths, and we defocus each shell slightly to improve off-axis resolution. Defocusing trades off the on-axis resolution against off-axis resolution, leveling out the resolution over the FoV.

A baseline telescope configuration using MiXO (Figure 2 (*b*)) consists of ~50 shells with diameters of 6 cm to 14 cm and matching shell lengths of 7 cm to 10 cm, providing a grasp of ~30 cm^2 deg^2 at 1 keV. The focal length is set at 70 cm, but it offsets about 400 μm – 1.2 mm from the outer most to the inner most shell. This enables ~30 arcsec geometric resolution over 1 deg^2 FoV. Thus, even with additional degradation (<~20 arcsec) from surface roughness and shell alignments, sub arcmin resolution (~40 arcsec) is expected to be maintained over 1 deg^2 FoV.

Plan and Application: We plan to build three working modules of two shells each suitable for use in the baseline telescope configuration to demonstrate the feasibility of the technology for planetary science. Their performance will be fed back to modeling full X-ray telescope designs with high-fidelity.

MiXO enables diverse telescope configurations suited for various mission profiles. For instance, a modular version utilizing seven small optics with one common focal plane can cover about 7 deg^2 with relatively higher sensitivity in the hard (> 2 keV) X-ray band (Figure 2(*c*)). Given the relatively rapid development and deployment, CubeSAT is becoming a popular platform for space application. A free-flying CubeSAT configuration using MiXO can be envisioned in a 1 × 6 U package with 3–9 cm diameter optics with ~50 cm focal length. Another 1 × 6 U would be needed for the spacecraft functions including star cameras, so such a free-flyer MiXO telescope can be complete in a 2 × 6 U form factor.

References: [1] Weider S. Z. et al., (2015) *Earth & Planetary Science Letters*, 416, 109. [2] Tormbka J. L. et al., Science 289, 2101, [3] Binzel R. P. et al., 2010) Nature 463, 331 [4] Capaccioni, F. et al., 2015 Science, 347, a0628. [5] Hong J. et al. (2015) *Earth Planets & Space* 68, 35. [6] Romaine S. et al., (2015) SPIE, 91441H [7] Conconi et al. (2010) *MNRAS*, 405, 877 [8] Saha et al., (2014) *SPIE*, 914418

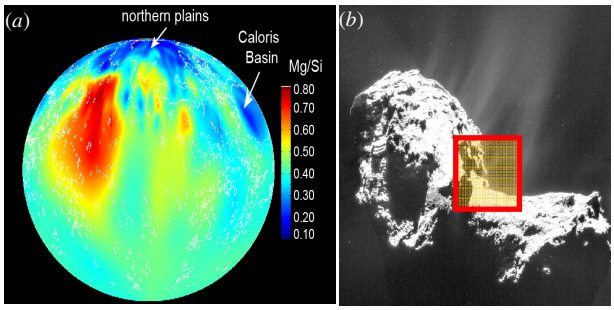

Figure 1 (*a*) Mg/Si abundance distribution of Mercury measured by the X-ray Spectrometer on MESSEGER. [1] (*b*) Comet 67P/Churyumov–Gerasimenko taken by NAVCAM on the Rosetta mission reveals the outgassing jets (Courtesy of European Space Agency-ESA, see also [4]).

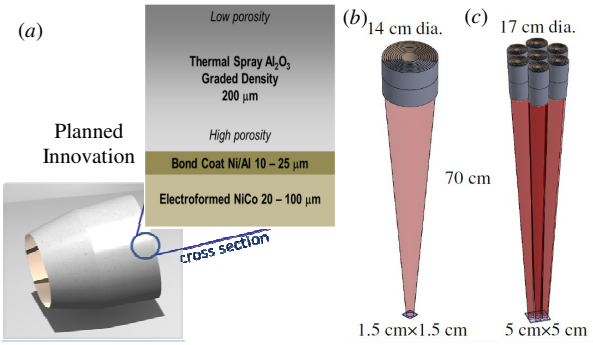

Figure 2 (*a*) Planned layer composition of lightweight metal/ceramic hybrid X-ray mirror shell: 30 μm NiCo + 10 μm Bond coat + 200 μm Al_2O_3. (*b*) A baseline MiXO telescope (optics mass ~1.1 kg, ~1 deg^2 FoV) (*c*) A wide-field version (optics mass ~1.8 kg, ~7 deg^2 FoV) optimized for hard (> 2 keV) X-ray bands. The design is easily scalable for smaller or bigger telescopes.

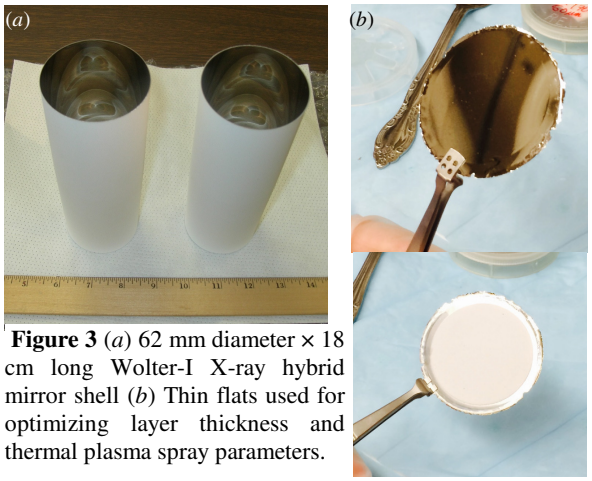

Figure 3 (*a*) 62 mm diameter × 18 cm long Wolter-I X-ray hybrid mirror shell (*b*) Thin flats used for optimizing layer thickness and thermal plasma spray parameters.

The MIDAS instrument design and characterization. C. I. Honniball, R. Wright, and P. G. Lucey, Hawai'i Institute of Geophysics and Planetology, University of Hawai'i at Manoa (1680 East-West Road, POST 517 Honolulu, HI 96822; cih@higp.hawaii.edu)

Introduction: Remote sensing in the mid-wave IR (MWIR) from 3–5 μm can provide essential information for a range of Earth and planetary science applications for both gaseous and solid targets. For example thermal observations of lava lakes on Io, the most volcanically active body in the solar system, will aid in defining their dynamics and origin as well as their compositions [1]. Applications for Earth science include the detection of CH_4 from industrial gas leaks and the remote measurements of the energy at 4 μm emitted by wildfires. The energy emitted is used to quantify fire radiative power, which is a quantitative measure of global biomass burning that can be used to estimate the amount of carbon liberated into the Earth's atmosphere, and is thus an essential climate variable [2]. Many atmospheric species exhibit strong absorption features in the MWIR region. Although there are several good reasons to make scientific measurements at these wavelengths, there are also challenges to working in the MWIR.

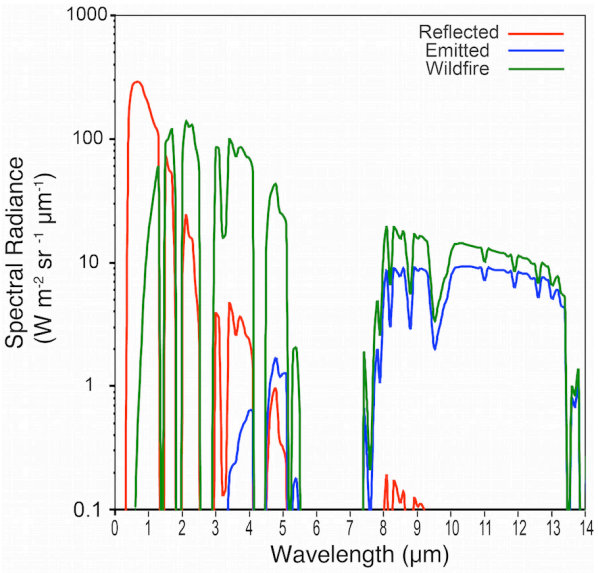

Figure 1. Spectral radiance levels (measured in units of W m^{-2} sr^{-1} μm^{-1}) available for measurement at the top of Earth's atmosphere. The red, blue, and green curves show the at-satellite spectral radiance from the Sun (assuming reflectivity of 1.0), from a 300K surface, and from a wildfire at 1400K [1] (where the flame occupies 1% of the instantaneous field of view and the remainder—99%—is occupied by the ground at 300K). A model atmosphere was assumed for all calculations.

Compared with the long-wave IR (LWIR) spectral region (8–14 μm), there is significantly less light available to measure in the MWIR (for surfaces at, near, or below Earth's ambient temperature). For instance, the availability of light over the IR region for both reflected (red line) and emitted (blue line) light is shown in Figure 1. To overcome this lack of signal, it is typically necessary to cool MWIR instruments. Such cooling, however, causes the instruments to consume substantial amounts of power, which leads to large masses and volumes. However, emerging interferometric techniques allow uncooled microbolometer arrays to be used for hyperspectral imaging. This is primarily a result of the higher signal-to-noise ratio attainable with an interferometer when compared to a dispersive spectrometer, allowing for higher signal-to-noise even when using relatively insensitive microbolometers. Moreover, uncooled microbolometers require much less power than cooled photon-detecting arrays. This makes them attractive candidates for imaging instruments on small satellites.

The Instrument: At the University of Hawai'i we have developed the Miniaturized IR Detector of Atmospheric Species (MIDAS) to demonstrate the utility of microbolometers for the detection of gaseous constituents for Earth and planetary atmospheres. MIDAS is a MWIR hyperspectral imager, which can be seen in Figure 2 outlined in blue. The instrument consists of an uncooled microbolometer that is coupled with a Sagnac interferometer and a set of three lenses – an objective, a collimator, and an imaging lens. MIDAS operates as a conventional remote sensor with a large distance between the sensor and target. However, removing the objective allows MIDAS to be used as a microscope with 1:1 magnification.

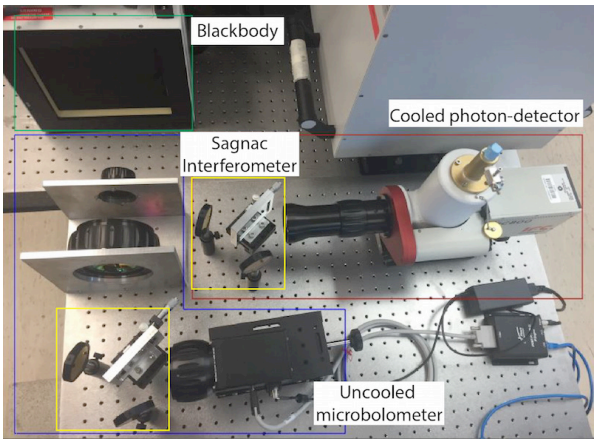

Figure 2. Benchtop setup of the MIDAS instrument

(outlined in blue). In this configuration, MIDAS is positioned to look through the Sagnac interferometer (outlined in yellow) and lenses to a hot blackbody (outlined in green). The cooled photon detector looking through the Sagnac interferometer is outlined in red.

Measured light is decomposed into its component frequencies by the Sagnac interferometer, which comprises a beam splitter and two mirrors. An interference pattern is thus generated, which we then sample and process (using standard Fourier transform techniques) to derive a calibrated radiance spectrum for each scene element. The configuration of the mirrors and beam splitter causes the optical path to vary linearly across the detector array. The interferometer allows us to leverage the well-known multiplex advantage, allowing for higher signal-to-noise when compared to the more common dispersive methods for acquiring spectral data when employing read-noise limited detectors such as microbolometers [3]. Part of our research will be to determine whether the signal-to-noise advantages that accrue from this interferometric approach allow us to make valid science measurements in the MWIR using uncooled microbolometers.

Instrument characterization: To quantify the precision and accuracy with which MIDAS can quantify thermal emission in the MWIR, it will be benchmarked against a cooled photon-detector used in the same Sagnac interferometer configuration. Both systems are subjected to numerous standard characterization procedures—including, but not limited to, the determination of noise equivalent differential temperature, signal-to-noise ratios, and spectral response. For most of the characterization tests, the use of a standard large format blackbody and a high temperature cavity radiator as our target allows for accurate temperature variation; providing information on which temperature ranges MIDAS is best suited for.

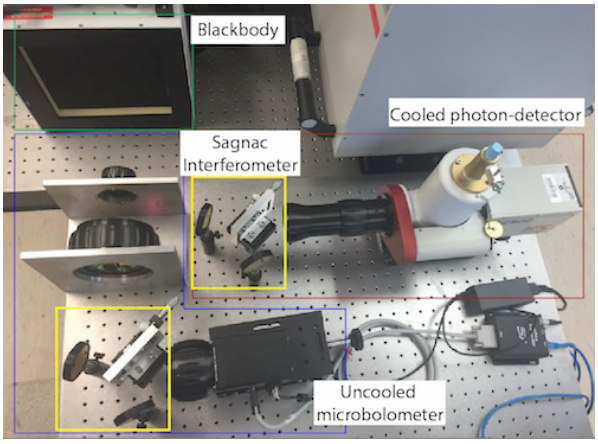

Figure 3. Cooled photon-detector system set up to look through a gas cell at a large format blackbody.

In addition to benchtop characterization we will also quantify the performance of MIDAS by simulating the aforementioned science cases. Both MIDAS and the cooled photon-detector system will look through gas cells filled with known concentrations of gases, such as CO_2 and CH_4, at a large format blackbody, an example setup can be seen in Figure 3. This will allow us to simulate the performance of MIDAS for gas detections (and fire and active lava measurements) under representative field conditions. Detection of CH_4 from industrial gas leaks depends on the contrast between the background and the plume. There are two ways MIDAS may look for CH_4 leaks, the first by looking at the plume in absorption with the ground as the background and the second by looking at the plume in emission with the sky as the background. Detection of CH_4 may prove to be difficult in the MWIR if the temperature of the plume and the background are similar. The remote detection of lava lakes on Io and wildfires on Earth are targets for which MIDAS is not signal limited. Wildfires reach temperatures of 1400 K [2] and emit substantial levels of energy in the MWIR, with a peak emission around 5 μm while measured temperatures for Pele on Io have been up to ~1700K [4].

Summary: Due to the lack of moving parts in the Sagnac interferometer and the minimal power requirements of uncooled microbolometers, MIDAS is well suited for adaption to small satellite platforms such as CubeSat's. For this presentation we will present results from benchtop characterization testing.

References: [1] Lopes, R.M.C. et al. (2004) Icarus, 169, 140-174. [2] Wooster, M., Zhukov, B., and Oertel, D. (2003) Remote Sens. Environ. 86, 83–107. [3] Griffiths, P. and De Haseth, J. (1986) Fourier Transform Infrared Spectroscopy, Wiley. [4] Lopes, R.M.C. et al. (2001) J. Geophys. Res. 106, 33053–33078.

Additional Information: The authors would like to thank Andrea Gabrieli, Harold Garbell, Eric Pilger, Mark Wood, Tim Williams, Lance Yoneshige and the Geology and Geophysics department at UH. Funding is provided by NASA grant NNX14AN15A.

HIGH SPECTRAL RESOLUTION SPECTROMETRY IN COMPACT SIZES IN FUTURE INTERPLANETARY MISSIONS USING SPATIAL HETERODYNE SPECTROMETER

Sona Hosseini, Jet Propulsion Laboratory, California Institute of Technology, Pasadena, California, USA (sona.hosseini@jpl.nasa.gov)

Introduction: We can coarsely sort the performance of narrow bandpass imagers or traditional dispersive grating spectrometers into two classes of instruments with large effective aperture A_{eff} that emphasize spectral resolving power (e.g., HST-STIS or Keck-HIRES) and those with large étendue (e.g., Cassini UVIS). The most common instrument to obtain high spectral resolving power (R) in UV are the classical grating spectrometer, but their high R implementations are physically large and require large aperture telescopes to overcome the small field of view (FOV) of the apertures required. In grating spectrometers, R is derived from both the dispersion relation at the detector and the width of the aperture in the diffraction plane. This convolution drives the R lower if the size of the instrument is reduced and its FOV is increased. Thus, the typical high R (~50,000) spectrometer is quite large, has a very narrow FOV and is attached to a large telescope (2.4 m HST), while the typical low-resolving power spectrograph on a remote probe (e.g., Voyager-UVS or New Horizon-ALICE) is compact, has a wide FOV, and low R (<1000). The FOV in SHS is not convolved with the spectral response and therefore, to a large degree, the R is decoupled from the size of the area that is being sampled. Thus allows SHS to sample closer to the full theoretical R of the grating.

Interferometry is another technique that is used to obtain high étendue measurements at high R. They emphasize sensitivity for long-term temporal studying at high R from wide FOV (e.g., planetary disks, nebula, large galaxy structures, interstellar medium, etc.). Some technologies that demonstrate the utility for these targets include Hydrogen absorption cells (e.g., SOHO-Solar Wind experiment [2]), field-summing instruments such as FPIs (e.g., Wisconsin H-alpha Mapper [3]), and scanning Fourier Transform Spectrometers (FTSs). However, below 300 nm many commercially, available glasses begin to become opaque, and the transmitting optics issue dominates around 100-130 nm. The number of transmitting crystals, especially below 160nm, is sharply reduced, and performances degrade. The last known transmitter, LiF, becomes opaque at ~105 nm and is difficult to make optically flat beam splitter or etalon. Getting spectra below 100 nm requires Boron-Carbide or Silicon-Carbide coatings (≤35% reflectivity) [4] or multi-layer coatings for narrow-band filters. Therefore, these designs are limited at different points in UV by their use of transmitting optics, demanding low optomechanical tolerances, a narrow acceptance bandpass, and physical size [5, 6].

Spatial Heterodyne Spectrometer (SHS): SHS is a compact reflective two-beam cyclical interferometer that produces a 2-D fizeau fringe pattern from which the input spectrum can be obtained via a Fourier transform [5, 7, 8]. SHS-based instruments have been used in a series of ground and space-based project, or observations of atmospheric and interstellar emission line feature [9, 10]. To date, the majority of the SHS projects are in the Michelson SHS format [5] in which the mirror in each interferometer arm was replaced by a grating [5, 11], and a two-dimensional camera CCD detector imaged the fringes [5, 9, 12, 13]. But a major weakness of Michelson SHS instruments is their use of transmitting elements, which limits their usefulness in shorter wavelengths (UV). Reflective SHS [8] combines the high étendue (É= telescope effective area (A_{eff}) × FOV) and high R of FTS with higher optomechanical tolerance and simpler optomechanical design associated with grating spectrometers.

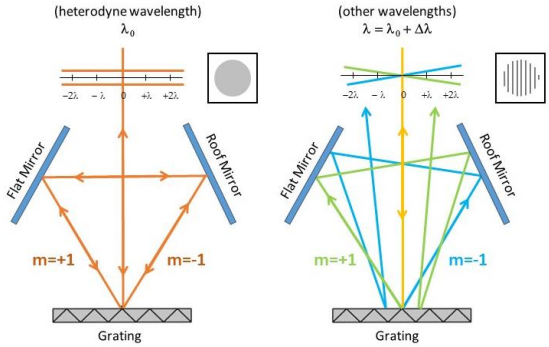

Fig 1. (Left) PHI is based on a remarkably simple cyclical design. The incoming collimated light hits the grating at normal incidence, splits to two orders, travel in opposite directions, and diffract off the grating before exiting. For the tuned wavelength λ_0 everything is symmetric, there is no path or phase differences between the emerging beams. **(Right)** However the exiting wave fronts of other wavelengths ($\lambda=\lambda 0+\Delta\lambda$) are tilted in respect to each other producing a fringe pattern.

The significance of the FOV for SHS is that it increases the étendue of the instrument, the capability of an optical system to accept and gather light, and is the product of the collecting area A_{eff} and FOV (É = FOV×A_{eff}). Provided the source is aperture-filling, the FOV of the SHS can fill the same role that a large telescope does for a grating spectrometer. The quantity of

Étendue is widely used to express the sensitivity of an optical instrument. However, for practical reasons in building new instruments, usually the goal is to optimize grasp per cost. Grasp [8] is defined as G = É×R and it is used to quantify the overall potential of an instrument considering the input aperture, FOV, and resolving power. One of the implementations of low grasp in common high R spectrometers is the steep

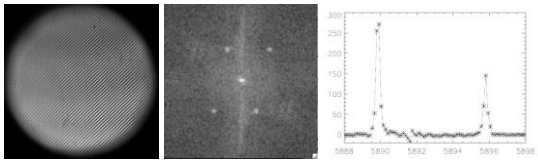

Fig 2. (Left) Fringe pattern from Na Hollow Cathode Lamp when the ground-based tunable reflective SHS built by PI at Mt. Hamilton [1]. The interferometer is tuned to the vicinity of the Na D lines at $\lambda_{\Delta 1}$= 5895.9 Å, $\lambda_{\Delta 2}$= 5889.9 Å . This image contains two set of fringe patterns each for one of the Na D lines. **(Middle)** The reduced power spectra shows both lines indicating both fringe pattern are present in the data. The top half of the 2D FFT is the repetition of the bottom half with an inverse wave-vector sign. **(Right)** The Na D lines' power spectra: the separation of $\Delta\lambda$=5.97 Å, indicates a resolving power of R~48000 which is same with the calculated R [1].

trade-off between R and FOV; by increasing the FOV, the instrument loses the R sensitivity.

Developing the SHS instrument has a wider significance to planetary science. SHS provides integrated spectra at high R, over a wide FOV in compact designs in which it offers the ability to make key science measurements for a variety of planetary targets. SHS could be implemented on a dedicated SmallSat or ISS that can sit and stare at its target for the long duration of time that cannot be done from the ground or on big missions. SmallSats are lower cost, faster to build, relatively easy to correct and upgrade. High R spectrometers are usually limited by the telescope aperture size and complicated optomechanical tolerances, but that's not the case for SHS. Preliminary SNR and flux calculation on extended targets show that the signal flux levels will allow robust measurements by SHS performing sequential high R observation in UV to IR from Earth's orbit. Such temporal studies on any one scientific objective would not be a practical request for any large-scale mission because of the high competitive subscription rates.

References:

1. Hosseini, S., *Tunable Reflective Spatial Heterodyne Spectrometer: A Technique for High Resolving Power, Wide Field of View Observation of Diffuse Emission Line Sources* in *Engineering Applied Science* 2015, University of California Davis. p. 122.
2. Combi, M.R., Reinard, A. A., Bertaux, J. L., Quemerais, E., Mäkinen, T., *SOHO/SWAN Observations of the Structure and Evolution of the Hydrogen Lyman a Coma of Comet Hale–Bopp (1995 O1).* Icarus, 2000. **144**: p. 191-202.
3. Reynolds, T., Haffner, Jaehnig, Percival, *The Wisconsin H-Alpha Mapper (WHAM): A Brief Review of Performance Characteristics and Early Scientific Results.* Publ. Astron. Soc. Aust., 1998. **15**(14).
4. Nikzad, S., Hoenk, Michael E., Greer, Frank, Jacquot, Blake, et al, *Delta-doped electron-multiplied CCD with absolute quantum efficiency over 50% in the near to far ultraviolet range for single photon counting applications.* Optical Society of America, 2012. **51**(3).
5. Harlander, J.M., *Spatial Heterodyne Spectroscopy: Interferometric Performance at any Wavelength Without Scanning.* 1991, University of Wisconsin-Madison.
6. Harlander, J., Reynolds, R.J., Roesler, F. L., *Spatial heterodyne spectroscopy for the exploration of diffuse interstellar emission lines at far-ultraviolet wavelengths.* Astrophysical Journal, 1992(396): p. 730-740.
7. Hosseini, S., Harris, Walter *First calibration and visible wavelength observations of Khayyam, a tunable spatial heterodyne spectroscopy (SHS).* Proc. SPIE 9147, Ground-based and Airborne Instrumentation for Astronomy, 2014. **91478L**: p. 9.
8. Hosseini, S.S., *Tunable Reflective Spatial Heterodyne Spectrometer: A Technique for High Resolving Power, Wide Field Of View Observation Of Diffuse Emission Line Sources,* in *Engineering Applied Science* 2015, University of California Davis.
9. Harris, W., et al., *Applications of spatial heterodyne spectroscopy for remote sensing of diffuse UV-vis emission line sources in the solar system.* Journal of Electron Spectroscopy and Related Phenomena, 2005. **144**: p. 973-977.
10. Chakrabarti, S., Cotton, Daniel M., Vickers, James S., Bush, Brett C., *Self-compensating, all-reflection interferometer.* Applied Optics, 1994. **33**(13).
11. Dohi, T., Suzuki, T., *Attainment of High Resolution Holographic Fourier Transform Spectroscopy.* Applied Optics, 1971. **10**.
12. Englert, C.R., et al., *Spatial Heterodyne Imager for Mesospheric Radicals on STPSat-1.* Journal of Geophysical Research-Atmospheres, 2010. **115**.
13. Florjanczyk, M., et al. *Development of a slab waveguide spatial heterodyne spectrometer for remote sensing*. 2010. SPIE.

A HETERODYNE DETECTOR FOR TERAHERTZ SPECTROSCOPY OF PLANETS AND COMETS

M. Huang,[1] N. Gautam,[1] M. S. Sherwin,[1] J. Kawamura,[2] K. Stone [2], P. Focardi,[2] N. Chahat,[2] S. Gulkis[2], B. S. Karasik,[2] and L. Pfeiffer [3]

[1]Physics Department and Institute for Terahertz Science and Technology, University of California at Santa Barbara, Santa Barbara, CA 93106 (Sherwin@physics.ucsb.edu)

[2]Jet Propulsion Laboratory, California Institute of Technology, Pasadena, CA 91109

[3]Department of Electrical Engineering, Princeton University, Princeton, NJ 08544

Gaseous species on comets and in planetary atmospheres have unique spectral fingerprints between 100 GHz and 5 THz. The Microwave Instrument for the Rosetta Orbiter (MIRO)[1] with heterodyne receivers based on Schottky diodes at 188 GHz and 562 GHz, hasrecently demonstrated the power of high-resolution sub-THz spectroscopy in planetary missions as it records spectra of volatile molecules sublimating from a comet. Both the density and strength of microwave transitions increases with increasing frequency, so high-resolution spectroscopy at frequencies between 1 and 5 THz is even more attractive. High resolution spectroscopy in the 1-5 THz region with a nearly quantum limited heterodyne receiver will greatly improve spectral coverage and sensitivity over existing submillimeter heterodyne receivers designed for planetary space applications. The improved sensitivity will reduce the column abundances needed to detect known spectral lines, and open up the possibility of detecting new molecular species never before detected in space.

We are developing a new class of heterodyne detector called a Tunable Antenna-Coupled Intersubband Terahertz (TACIT) detector.[2] TACIT heterodyne detectors promise nearly quantum-limited noise performance at frequencies above 1 THz using only microwatts of local oscillator (LO) power while operating at temperatures compatible with passive cooling. TACIT detectors are sensitive in a ~100 GHz wide frequency window that can be tuned broadly in the THz frequency range by simply varying gate voltages.[3] Thus the detection frequencies on an instrument flying a TACIT heterodyne receiver could be reconfigured during a mission, adding the flexibility to search for a range of species with spectral signatures in different frequency bands.

A TACIT mixer is a four-terminal transistor-like device, shown schematically in Fig. 1. The heart of a TACIT mixer is a GaAs "quantum well" containing a two-dimensional electron gas (2DEG) whose resistance is a strong function of the electron temperature. The signal and LO are coupled into the 2DEG by an antenna that is terminated by front- and back-gate contacts located above and below an active region in the 2DEG. When the signal and LO are resonant with an "intersubband transition"—a transition between quantum-confined states in the quantum well-- the THz radiation is efficiently absorbed, heating the 2DEG and changing its mobility. The intermediate frequency (IF) of a TACIT mixer is read out through a pair of ohmic contacts (source and drain) to the 2DEG. The frequency of the intersubband resonance can be broadly tuned by changing the voltage difference between the front and back gates. Independently, the impedance presented by the active region to the signal and LO can be matched, *in-situ*, to the antenna impedance by varying the carrier concentration in the active region via the field effect, ensuring high quantum efficiency.[2]

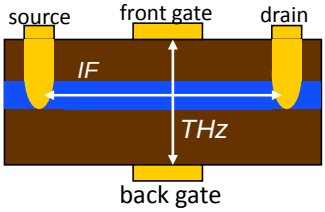

Fig. 1 Schematic of THz detection and intermediate frequency (IF) generation in a TACIT device, where 2DEG channel is shown in blue.

In order to realize TACIT devices, 40 nm GaAs quantum wells with very low impurity concentration containing a 2DEG whose mobility is a strong function of temperature above 10K are grown by molecular beam epitaxy (MBE) at Princeton University. A novel rf embedding circuit is designed at JPL which enables coupling of signal, LO, IF, and DC biases to the four terminals of the device. A fabrication procedure involving multiple photolithography, wet etching and metallization steps is under development at UCSB, aiming to produce low reistance Ohmic contacts as the source and drain leads and metal gates on both surface and backside. In order to have a high responsivity, it is necessary for the resistance of the 2DEG near the TACIT operating temperature to be dominated by thermally-excited phonons rather than impurities or other quenched disorder. This requires the 2DEG have a mobility in excess of 10^6 $cm^2/V*s$ at 10 K after the complete fabrication process. Moreover, the fabrica-

tion process needs guarantee no short between the gates and source/drain leads.

The research plan is to implement a complete cycle of design, fabrication and testing of a new generation of TACIT detectors. This cycle includes materials science (growth and characterization of a specially-designed, very clean quantum well by molecular beam epitaxy), rf engineering (design of novel antenna and rf embedding circuit), the development and implementation of a new microfabrication procedure, and testing of TACIT detector under DC, microwave and terahertz fields. We are aiming to bring TACIT detectors much closer to realizing their enormous potential for studying gases near comets and planets.

Currently, preliminary test devices have been achieved which undergo dc characterization (dc conductivity and magnetoresistance). These measurement yield the electron gas paremeters essential for understanding of the device. More data including current-voltage characteristics, device microwave noise and impedance, as well as the integrated THz circuit (antenna) design are expected soon. These data and their implication regarding the physics of the mixing process in TACIT device will be reported at the meeting.

A part of the research described in this work is carried out at the Jet Propulsion Laboratory, California Institute of Technology, under a contract with the National Aeronautics and Space Administration. Research activities at UC Santa Barbara and Princeton University are carried out under a subcontract from the Jet Propulsion Laboratory.

References Cited

1. Gulkis, S.; Frerking, M.; Crovisier, J.; Beaudin, G.; Hartogh, P.; Encrenaz, P.; Koch, T.; Kahn, C.; Salinas, Y.; Nowicki, R.; Irigoyen, R.; Janssen, M.; Stek, P.; Hofstadter, M.; Allen, M.; Backus, C.; Kamp, L.; Jarchow, C.; Steinmetz, E.; Deschamps, A.; Krieg, J.; Gheudin, M.; Bockelee-Morvan, D.; Biver, N.; Encrenaz, T.; Despois, D.; Ip, W.; Lellouch, E.; Mann, I.; Muhleman, D.; Rauer, H.; Schloerb, R.; Spilkeri, T., MIRO: Microwave instrument for rosetta orbiter. *Space Sci Rev* **2007,** *128*, 561-597.

2. Sherwin, M. S.; Cates, C.; Serapiglia, G. B.; Dora, Y.; Williams, J. B.; Maranowski, K.; Gossard, A. C.; McGrath, W. R. In *Tunable antenna-coupled intersubband terahertz (TACIT) mixers: the quantum limit without the quantum liquid.* Proceedings of Far-IR, Submm and mm Detector Technology Workshop (Monterey, CA, 2002), http://www.sofia.usra.edu/det_workshop/papers/manuscript_session6.html

3. Serapiglia, G. B.; Sherwin, M. S.; Hanson, M.; Doty, M. F.; Focardi, P.; McGrath, W. R.; Gossard, A. C. In *Ultrafast tunable antenna-coupled quantum-well THz detectors operating above 100K*, Infrared and Millimeter Waves and 13th International Conference on Terahertz Electronics, 2005. IRMMW-THz 2005. The Joint 30th International Conference on, 19-23 Sept. 2005, 2005; pp 267-268 vol. 1.

UV-VISIBLE OBSERVATION OF METEORS BY CUBESAT: S-CUBE PROJECT. R Ishimaru[1], Y. Sakamoto[2,1], M. Kobayashi[1], S. Fujita[2], T. Gonai[2], and T. Matsui[1], [1]Planetary Exploration Research Center (PERC), Chiba Institute of Technology (Chitech) (2-17-1 Tsudanuma, Narashino, Chiba 275-0016, Japan; ishimaru@perc.it-chiba.ac.jp), [2]Tohoku University (6-6-11, Aza-Aoba, Aramaki, Aoba-ku, Sendai, Miyagi 980-8579, Japan).

Introduction: Meteors are a luminous phenomenon caused by the entry of meteoroids into the Earth's atmosphere at hypervelocity. Most meteoroids originate from comets and asteroids. So, the meteor gives us valuable opportunities of an indirect exploration of the primordial objects, such as comets and asteroids, in our Solar System. Although meteors have been observed mainly from the ground so far, the ground-based observations have weak points: narrow observational range and weather dependent. In contrast to ground-based observations, a space-based observation by an earth-orbiting satellite enables a continuous global observation of meteors. It has an advantage in estimating the flux of meteoroids colliding with the Earth. Furthermore, a satellite can access ultra-violet light from meteors, because the light is not hindered by the ozone layer. The meteor's UV light contains emission lines, which have not been observed previously by ground-based observations. As a result, it would offer new information about the composition of comets or asteroids. Carbary et al. [1] observed UV spectra from a meteor for the first time by using five spectrographic imagers onboard the Midcourse Space Experiment satellite during the Leonid meteor shower on 18 November 1999. Unfortunately, however, no observation from space has been applied since 1999. Therefore, the intensity and emission mechanism of meteor's UV light remain largely unknown.

Thus, the Planetary Exploration Research Center of the Chiba Institute of Technology (PERC/Chitech) has launched a CubeSat project to observe meteors from space [2]. The standard ~10×10×10 cm cubic satellite is often called a "1U" CubeSat meaning one unit, and has a mass of ~1 kilogram. A CubeSat project can be carried out with a reasonable cost, suitable technology, and effective manpower. Therefore, CubeSat has been a familiar tool for engineers to test new technologies in space and often used for Earth remote-sensing. With its successful missions to date, CubeSat is primed and ready to proceed with science missions, although use of CubeSat for astronomical and planetary sciences has been rare.

Our satellite, a "3U" CubeSat, is called S-CUBE (Fig. 1). S-CUBE stands for Shootingstar Sensing Satellite (S^3). The S-CUBE is being developed by a partnership between PERC/Chitech and Tohoku University. We develop the 3Unit CubeSat S-CUBE based on the

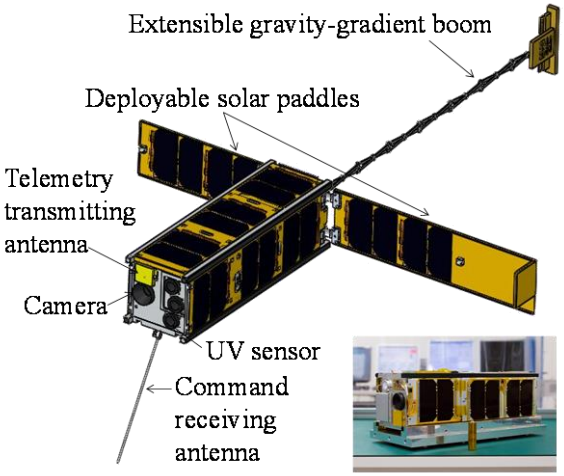

Fig.1. Appearance of S-CUBE

design of 2U CubeSat RAIKO that was developed and launched by the Tohoku University in 2012 [3].

Scientific instruments: The scientific instruments of the S-CUBE consists of one visual camera and 3 UV sensors (Fig. 1). The camera has been proven in the flight of the CubeSat RAIKO [3]. The camera has a field of view of 37.5 × 27.7 degrees. The camera takes visible images to estimate the meteoroid size from the brightness of meteors. According to our sensitivity estimate, the camera can image meteoroids larger than ~1cm. From the camera observation,we aim to estimate the size distribution of meteors.

The UV sensors can observe UV emissions from meteors. The sensors are attached with UV band-pass filters so as to extract emission lines in the meteor's light. The first UV sensor is designed to observe meteors at bloadband wavelength (200-300 nm), which enables photometric measurement of UV emissions from meteors.

The second sensor is designed to detect a singly ionized magnesium (Mg^+) line (~280 nm). Magnesium is one of the most typical metal elements in meteoroids. The line was detected as the strongest line by Carbary et al. (2003) [1]. From this data we aim to estimate not only the magnesium abundance but also the ionization degree.

The third sensor is designed to detect a neutral line of sulfur (~180 nm). Although sulfur in meteors has not been observed yet, an inclusion of the line is suggested because the line has been identified by the laser-

induced breakdown spectroscopy in the ultraviolet region [4]. Because sulfur is a volatile element, the abundance of sulfur in meteors would give a indicator of the thermal alteration of meteoroids and thermal history of their parent body. Sulfur is also one of the most important chemical elements which make up biomolecules and, therefore, the detection of sulfur in meteors would be important in terms of Astrobiology.

Signals of UV sensors is also used as a trigger of the camera. Because the ozone layer blocks UV lights from the Earth, detecting UV lights in the low earth orbit can be regareded as the occurrence of a meteor. The trigger makes it possible to capture only images of meteors, lowering the downlink data amount.

Satellite bus system: The S-CUBE is equipped with two solar paddles which are deployed after release in orbit. Attitude control subsystem of the S-CUBE consists of magnetic torquers, deployable gravity-gradient boom, and 3-axis reaction wheels. The boom can maintain an Earth-facing orientation, which make it possible for sensors (camera and UV sensors) to point nadir direction during the meteor observation. On the other hand, the reaction wheels are not to be used during meteor observation. The wheels are to be tested for future missions, such as space telescope missions. The communication system consists of an UHF receiver for command data uplink and an S-band transmitter for sending observation data.

Ground station: Communication with the S-CUBE can be conducted by a ground station at Chiba Institute of Technology: U-band uplink (400 MHz approx.) and S-band downlink (2 GHz approx.) with 2m diameter antenna.

Orbital requirements: Most of meteors occur on the leading edge of the Earth [5] where the Earth collides with dusts producing meteors at hypervelocity. In addition, to take images of meteors, the observation of the night side of the Earth is required. Therefore, we wish to observe the leading edge of the shadow area. A possible solution to meet our requirements is low inclination orbits such as those of CubeSats deployed from the International Space Station.

System specifications

Size	W100 × D100 × H327 mm (structure) W113 × D113 × H340.5 mm (envelop)
Weight	< 3.99kg
Orbit	Low earth orbit
Attitude control	3-axis magnetic torquers, gravity-gradient boom, 3-axis reaction wheels
Communication	Uplink: UHF-band, 401.25MHz, 50 W, 1200 bps Downlink: S-band, 2.285GHz, 0.1 W 9600 bps to 100 kbps S-band beacon, 2.285GHz, 2 mW 32 bps Ground station: Chitech
Power	Solar cells: ZTJ 2series×18parallels Batteries: 6-cell NiMH (7.2V) Power generation: 5.3 W (avg. in sunshine w/o paddle) 7.4 W (avg. in sunshine with paddle) Power comsuption: 1.0 W (stanby mode) 3.1 W (observation mode)
Instruments	Camera×1, UV sensor×3

References: [1] Carbary J. F. et al. (2003) *Icarus*, 161, 223–234. [2] Ishimaru R. et al. (2013) *LPS XXXXIV*, Abstract #1944. [3] Sakamoto Y. et al. (2013) *ISTS*, f-13, 1-6. [4] Radziemski L. et al. (2005) *Spectrochimica Acta Part B*, 60, 237-248. [5] Campbell-Brown (2008) *Icarus*, 196, 144-163.

STRATA-1: A PLANETARY SCIENCE EXPERIMENT ON THE BEHAVIOR OF ASTEROID REGOLITH IN MICROGRAVITY.

K. K. John[1] (kristen.k.john@nasa.gov), P. Abell[1], J. Brisset[2], D. Britt[2], J. Colwell[2], D. Durda[3], A. Dove[2], M. Fries[1], L. Graham[1], C. Hartzell[4], M. Leonard[5], S. Love[6], D.P. Sánchez[7], D.J. Scheeres[7]., [1]Astromaterials Research and Exploration Science Division, NASA JSC, Houston, TX, [2]University of Central Florida, [3]Southwest Research Institute, [4]University of Maryland, [5]T STAR, Bryan, TX, [6]Astronaut Office, NASA JSC, Houston, TX, [7]University of Colorado Boulder.

Introduction: Strata-1 is an experiment studying asteroid regolith in the microgravity environment of the International Space Station (ISS). Strata-1 is answering questions about how regolith evolves under extended microgravity and ambient vibration, as well as what roles particle density, shape, and composition play in the evolution of regolith dynamics. The prolonged microgravity and vibrational conditions of ISS are analogous to those on small Solar System bodies.

Strata-1 Experiment Description: Strata-1 contains four clear tubes containing different regolith simulant materials, each being autonomously imaged. On the ground, each tube was filled with a different simulant and evacuated to mTorr pressure. Each tube includes an "entrapulator" that was used to compress the simulants during launch. Once on-orbit, the entrapulator was retracted to allow the simulants to move freely. Strata-1 is currently operating. At the conclusion of the experiment, the entrapulator will trap the materials in place and Strata-1 will be returned to Earth for further analysis. Strata-1 is located in an Express Rack locker with the long axes of the tubes aligned with the microgravity acceleration vector of ISS. A sensitive three-axis accelerometer, SAMS, is mounted to the face of Strata-1 for the entire one-year experiment to record the vibration environment (0.01 Hz to 400 Hz). Data is being analyzed now, including vibrational data from the SAMS sensor, as well as imagery from each of the four tubes. The latest results from the first set of images will be presented.

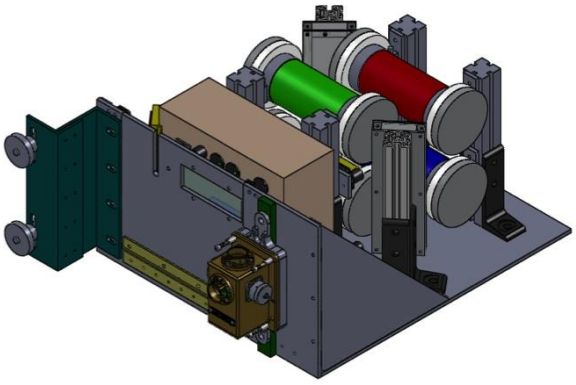

Figure 1: CAD model of Strata-1, including four regolith tubes, four cameras, an electronics box, and two sets of lights. The gold SAMS accelerometer is mounted to the front.

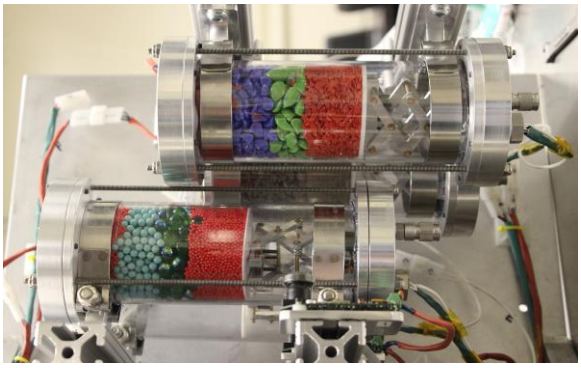

Figure 2: View of the Strata-1 interior, showing the regolith simulant tubes.

A new type of payload: Strata-1 launched to ISS in March 2016. Strata-1 is a Class-1E payload. The new Class-1E payloads are developed with an approach to streamline the payload development, review, approval, and integration processes. Strata-1 went from concept to flight-ready in just 10 months. The payload development team was led at NASA JSC, with hardware built primarily at UCF and JSC. The electronics were provided by T STAR, and the science team members are located at several institutions around the country.

Figure 3: Strata-1 launched to ISS on March 22, 2016 at KSC onboard Orbital ATK's Cygnus spacecraft.

Regolith Simulant Materials & Experiments: The Strata-1 regolith simulants were chosen by the science team to include a range of complexity including a relatively simple system of glass spheres, a tube of glass fragments, a more complex system of crushed/sieved meteorite material, as well as a carbonaceous chondrite simulant. Each tube was sorted into three sizes and maintained in that configuration during launch using the entrapulator.

Experiment 1: The first tube is composed of spherical particles with three discrete grain sizes and colors. This allows for comparison of the size segregation observed on-orbit with Earth-based experiments, which have previously demonstrated that size segregation will occur with spherical glass beads, and computational simulations of the system, as spherical grains are most easily modeled by Discrete-Element-Method (DEM) codes. The grain sizes and quantity of each species were chosen due to numerical constraints and constraints involving interaction with the sample tube walls, porosity of the sample, and the Knudsen number (a measure of the mean free path of the grains). The Knudsen number was chosen to be 0.003 so that particle-particle collisions dominate [1]. The largest grain size was limited to 10 mm in order to keep the grains relatively small compared to the inner diameter of the tube (63 mm).

Experiment 2: The properties of the second tube are identical to Experiment 1, except with angular particles, created by manually fracturing hemispherical particles and then sieving to achieve the desired size distributions. A major limitation of current modeling efforts is the difficulty of including aspherical grains. Thus, by comparing Experiments 1 and 2, we will be able to identify the influence and significance of grain shape on the segregation process.

Experiment 3: The third tube contains a crushed and sieved ordinary chondrite to simulate the behavior of an ordinary chondrite-based regolith. It was sorted to three size distributions similar to Tubes 1 and 2, but contains particles of a wider range of density to include metal- and sulfide-bearing meteorite fragments.

Experiment 4: The fourth tube contains a carbonaceous chondrite simulant, sieved to three size fractions. The simulant was designed to mimic the mineralogy, particle size, and strength properties of CI carbonaceous chondrites. The behavior of materials in this tube will directly inform missions to carbonaceous bodies such as OSIRIS-REx, Hayabusa2, and the ARM mission concept.

Figure 4: One of the first images downlinked from Strata-1. This images shows the angular, silica glass particles representing Experiment 2. Analysis is being performed now and results will be presented.

Simulation Methods: Two simulation methods are proposed for this research, Soft-sphere Discrete Element Method (SSDEM) [2,3] and Contact Dynamics Method (CD) [4,5]. In SSDEM, the particles interact through soft potentials (spring dashpot-type) that model the forces and deformation that occurs during collisions or enduring contacts. In CD, particles are not allowed to interpenetrate and forces are calculated unilaterally so that this premise is upheld.

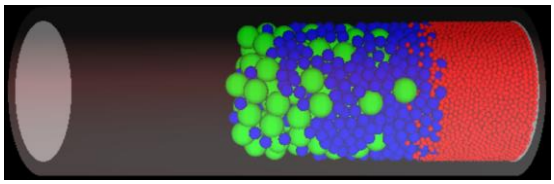

Figure 5: Prototype simulation (SSDEM) of one of the experimental tubes. The cylinder contains 2 mm, 5 mm and 10 mm glass-like spherical beads. Gravity is pushing to the right. All particles are frictional and are contained in a cylindrical container with the same material characteristics. This container can also be made to vibrate so that the experimental conditions in the ISS are matched.

A tool for studying regolith: Strata-1 will help us understand regolith dynamics and will inform design and procedures for landing and setting anchors, safely sampling and moving material on asteroidal surfaces, processing large volumes of material for in situ resource utilization (ISRU) purposes, and, in general, predicting the behavior of large and small particles on disturbed asteroid surfaces. This experiment will provide new insight into small body surface evolution.

Post-Flight Analysis & Strata-2: At the conclusion of the experiment (approximately one year on ISS), all tubes will be returned to Earth. Each tube will be cored and quantitatively analyzed for the particle size and density (where appropriate) distribution to form a data set that is complimentary to the time-lapse imagery. Imagery will be processed into time-lapse video showing the evolution of the simulants. These will be compared to simulation results and will allow for refinement of models.

Strata-1 is the first of several regolith investigations. Strata-2 is currently being developed. Future Strata investigations will involve active components such as probes to study regolith properties, impacts, inter-particle interactions, and anchoring techniques.

References: [1] Harth, K. *et al.* (2015) *Adv. Space Res., 55,* 1901-1912. [2] P. Sanchez, et al. (2011) *Astrophys. J.* **727**(2):120. [3] P. Cundall (1971) in *Proc.Int'l. Sym. on Rock Mechanics V.1* 129–136 -, Nancy. [4] C. M. Hartzell, et al. (2014) in *LPSC 45* 2849. [5] J. J. Moreau (1994) *Eur J Mech A* 13:93.

BIOMOLECULE SEQUENCER: NANOPORE SEQUENCING TECHNOLOGY FOR IN-SITU ENVIRONMENTAL MONITORING AND ASTROBIOLOGY.

K. K. John[1] (kristen.k.john@nasa.gov), D. J. Botkin[2], A. S. Burton[3], S. L. Castro-Wallace[4], J. D. Chaput[5], J. P. Dworkin[6], M. L. Lupisella[7], C. E. Mason[8], K. H. Rubins[9], D. J. Smith[10], S. Stahl[11]. C. Switzer[12]. [1]NASA Postdoctoral Program, NASA Johnson Space Center (JSC), Houston, TX, [2]Formerly JES Tech, Houston, TX, [3]Astromaterials Research and Exploration Science Division, NASA JSC, Houston, TX [4]Biomedical Research and Environmental Sciences Division, NASA JSC, Houston, TX, [5]Department of Pharmaceutical Sciences, University of California-Irvine, Irvine, CA, [6]Solar System Exploration Division, NASA Goddard Space Flight Center (GSFC), Greenbelt, MD, [7]Exploration Systems Projects Office, NASA GSFC, Greenbelt, MD, [8]Department of Physiology and Biophysics, Weill Cornell Medical College, New York, NY, [9]Astronaut Office, NASA JSC, Houston, TX [10]Space Biosciences Division, NASA Ames Research Center, Mountain View, CA, [11]Wyle / NASA JSC, Houston, TX, [12]Department of Chemistry, University of California-Riverside, Riverside, CA.

Introduction: Future missions to planetary bodies such as Mars require the next generation of tools and instrumentation. As we venture further, it will become increasingly challenging to transfer materials back to Earth for analysis, creating a need for in-situ diagnostic capabilities. Human missions will present challenges associated with crew health and safety, as well as contamination. One tool in particular, the Biomolecule Sequencer, has applications for in-situ environmental monitoring, medical diagnostics, and even life detection experiments for astrobiology investigations.

Nucleotide Sequencing: Nucleotide sequencing (the process of determining the order of nucleotides within a molecule such as DNA) can be used to: (1) mitigate microbial risks to crew by allowing identification of microbes in water, in air, and on surfaces; (2) identify optimal treatment strategies for infections that arise in crew members; and (3) track how crew members, microbes, and mission-relevant organisms respond to conditions on Mars through transcriptome- and genome-level changes. On the surface of other bodies, sequencing can be used as a tool for identifying Earth-derived contamination in samples. Additionally, if Mars contains indigenous life that is based on nucleic acids or closely related molecules, sequencing could serve as a tool to characterize those molecules. For these reasons, it is necessary to develop spaceflight-compatible nucleic acid sequencing tools.

Nanopore Sequencing: Until recently, sequencing technology has not been space-compatible due to size, power, and operational constraints. However, the development of nanopore-based sequencing has produced devices that are much smaller, consume less power, and use detection methods more conducive to the challenges of spaceflight. Nanopore sequencers measure changes in current caused by DNA passing through nanopores, as shown in Figure 1.

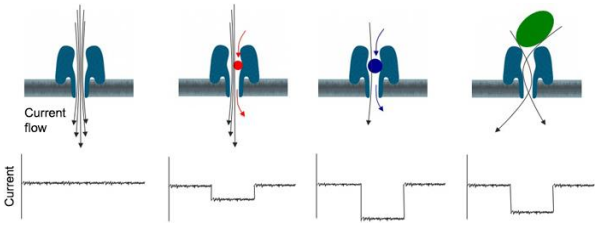

Figure 1. Nanopore-based sequencers measure changes in current caused by molecules (ex. DNA strands) passing through the pore. The changes in current are diagnostic of the sequence of the molecule passing through the pore. This method of measurement means that the sequencing capability is not limited to DNA and RNA with canonical nucleobases (A, G, C, and T/U).

Biomolecule Sequencer Project: In July of 2016, the Biomolecule Sequencer project launched to the International Space Station (ISS), creating history by becoming the first experiment to sequence DNA in space. The Biomolecule Sequencer project is the first step towards evaluating nanopore sequencing as a tool for future exploration [1]. This project involves testing the MinION™ device (see Figure 2), a commercially available product developed by Oxford Nanopore Technologies, to determine how the device performs after flight to the ISS and under continuous microgravity conditions. The MinION™ device is lightweight (< 150 g), small (9.5 x 3.2 x 1.6 cm), and powered by a USB connection. On the ISS, it is powered by a Microsoft Surface Pro3™.

Figure 2: The MinION™ device is a nanopore sequencer that weighs less than 150 g, with a volume of less than 100 cm^3.

Three different types of DNA will be sequenced: lambda bacteriophage, *Escherichia coli* and mouse genomic DNA. The ground-prepared samples are stored frozen until experiment initiation. Identical ground controls will be run in parallel with the flight experiment. Immediately prior to sequencing, the crew member will thaw a frozen sample, inject the thawed sample into a new flow cell, and initiate sequencing. After 6 hours, sequencing will be terminated and the data downlinked to Earth for analysis. The concept of operations, from sample preparation to termination of sequencing, was successfully tested aboard a parabolic flight [2]. The first effort of the Biomolecule Project is a technology demonstration. The next step involves demonstrating end-to-end in-flight sequencing, from sample collection to data analysis. The latest results from the first set of experiments will be presented.

Sequencing as a tool for astrobiology: For the future of astrobiology, nucleic acid sequencing will serve as a critical tool. Sequencing can place extremophiles in evolutionary context [e.g., 3-5], provide insights into the origin and evolution of the ribosome itself [e.g., 6, 7], and give key information regarding organismal metabolism [e.g., 8]. Sequence data have been successfully obtained from samples including: DNA from bones that were hundreds of thousands of years old [9,10]; insects trapped in amber over 100 million years old [11]; and archaea entrained in halite crystals over 400 million years old [12]. The preservation of DNA combined with the amount of possible information obtained from genomic sequences, provide strong support for the inclusion of nucleic acid sequencing as part of a life detection mission.

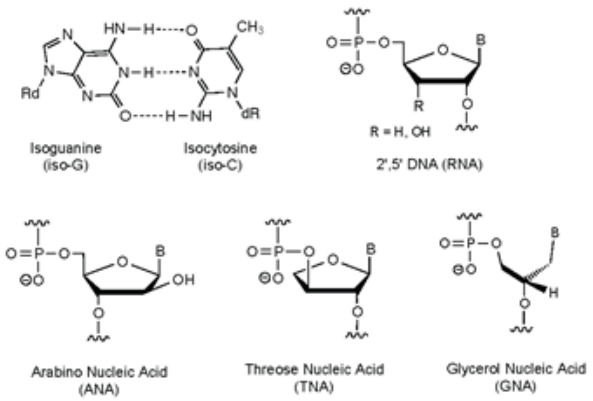

Figure 3. Examples of nucleic acid-like molecules that could support life. Nanopore-based sequencers have the potential to detect these kinds of molecules, whereas sequencers that require synthesis or incorporation of chromophores would not.

Sequencing beyond DNA and RNA: Traditional sequencing methods for life detection can only sequence DNA or RNA. It is possible that life existing elsewhere uses informational molecules other than DNA or RNA. Traditional sequencers would be not able to obtain data, even from closely related nucleic acid analogs such as arabinose or threose nucleic acids shown in Figure 3. However, nanopore-based sequencers measure changes in current based on the polymer passing through them, so they can also read RNA, proteins, and other polymers [13]. Therefore, nanopore-based sequencing is more versatile as a life detection tool than other sequencers that require nucleic acid synthesis or other detection methods.

Figure 4: The Biomolecule Sequencer launched to the ISS on July 18th, 2016 aboard the SpaceX Falcon 9 Dragon capsule. [Photo credit: Ken Kremer, kenkremer.com]

References:

[1] "Sequencing DNA in the palm of your hand"; http://www.nasa.gov/mission_pages/station/research/news/biomolecule_sequencer; September 29, 2015 [2] McIntyre et al., Nanopore Sequencing in Microgravity, (in press) *npj Micrograv.* [3] Ciccarelli F. D. et al. (2006) *Science* 311, 1283-1287. [4] Puigbò P. et al. (2009) *J. Biol.* 8, 59 – 59. [5] Wolf Y. I. et al. (2002) *Trends Gen.* 18, 472-479. [6] Fox G. E. (2010) *Cold Spr. Harb. Persp. Biol.* 2, a003483 [7] Petrov A. S. (2014) *Proc. Natl. Acad. Sci. USA* 111, 10251-10256. [8] Oren A. (2008) *Sal. Syst.* 4, 2-2. [9] Dabney J. et al. (2013) *Proc. Natl. Acad. Sci USA* 110, 15758-15763. [10] Orlando L. et al. (2013) *Nature* 499, 74-78. [11] Cano R. J. et al. (1993) *Nature* 363, 536-538. [12] Park J. S. et al. (2009) *Geobiology* 7, 515-523. [13] Oukhaled A. et al. (2012) *ACS Chem. Biol.* 7, 1935-1949.

LIBS FOR MARTIAN MOONS EXPLORATION (MMX). S. Kameda[1], M. Horiuchi[2], Y. Cho[3], K. Ishibashi[4], K. Wada[4], T. Mikouchi[5], T. Nakamura[6], and S. Sugita[5], , [1]Rikkyo University (3-34-1 Nishi-Ikebukuro, Toshima, Tokyo 171-8501, Japan, kameda@rikkyo.ac.jp). [2]Rikkyo University, Tokyo, Japan. [3]NASA Marchall Space Flight Center, AL. [4]Chiba Institute of Technology, Chiba, Japan. [5]The University of Tokyo, Tokyo, Japan. [6]Tohoku University, Miyagi, Japan.

Introduction: JAXA's Martian Moons Exploration (MMX) is planned to be a sample return mission from Phobos, one of the satellites of Mars. The nominal instruments have been selected: a telescopic camera, wide angle multiband camera, near infrared spectrometer, gamma-ray and neutron spectrometer (GNS), ion mass spectrometer, dust monitor, and LIDAR. Because one or two additional instruments may be acceptable, we propose adding a laser-induced breakdown spectrometer (LIBS).

One of the scientific objectives of MMX is to determine the origin of the two martian moons. Phobos and Deimos seem to be asteroids captured by Mars' gravity according to the result of spectroscopic observation of the surface reflectance. Conversely, they also seem to have been formed by a large impact of a body with Mars and subsequent accretion [1]. Elemental analysis is necessary to clarify the origin of the moons.

The MMX mission will acquire more than 10 g of regolith on the surface of the moon. A coring unit will be installed with a core diameter of 10–20 mm. Assuming that the sample is representative of Phobos, we will be able to clarify the origin of the moons. To test this assumption, we should determine suitable landing sites and identify the uniformity or nonuniformity of the distribution of surface material. Though we can obtain the globally averaged elemental compositon using the GNS, the distribution of the elemental compositon cannot be obtained by the selected instruments with a resolution of ~10 mm.

Laser induced breakdown spectroscopy (LIBS): LIBS is widely used for chemical composition analysis. A high-intensity pulsed laser is focused to ablate the surface of the target material in order to form a light-emitting plasma. The composition of this ablated material can then be analyzed using atomic emission spectroscopy. This technique has already been successfully used in ChemCam onboard Mars Curiosity [2,3]. The result clearly shows the emission lines of the major elements—Mg, Si, Ca, Fe, Ca, Na, K, and Al—and the light elements—H, C, and O. This new technique will be the standard for future planetary exploration. We can also expect an innovative performance of LIBS on the surface of Phobos because in principle, it can be used in vacuum as well.

The rotation period of Phobos is 7.65 hours. In the nominal plan, the spacecraft has to take off from the surface before dusk. Thus, the operation time is limited to be approximately 1 hour. We conducted an experiment to demonstrate that we can determine whether the surface composition resembles that of Martian meteorites or that of a carbonaceous chondrite in a short time with an instrument similar to that designed for MMX. Figure 1 shows the obtained LIBS spectra in vacuum for NWA1068 and Zagami, (Martian meteorites), and Allende (a carbonaceous chondrite). The emission lines of major elements are clearly detected. Figures 2 and 3 show the differences between the Martian meteorites and the carbonaceous chondrites. It is known that Allende is Mg-rich and Martian meteorites are rich in Al and Ca, and our result shows that we may distinguish Martian meteorites from carbonaceous chondrites using LIBS. The required observation time is ~30 minites including the time for focusing and shifting the field of view, which is within MMX operation time on the surface.

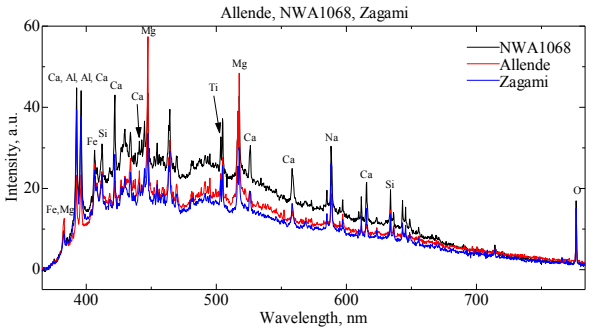

Figure 1: LIBS spectra for NWA1068, Zagami and Allende

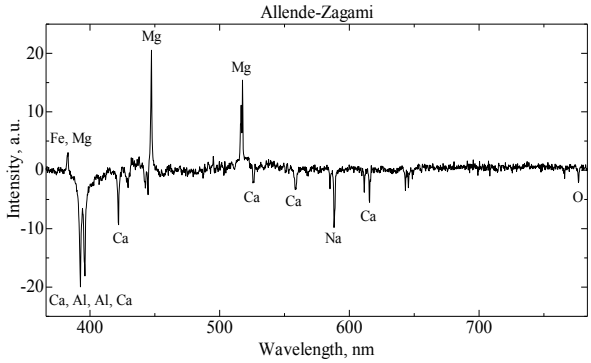

Figure 2: Difference between LIBS spectra of Allende and Zagami.

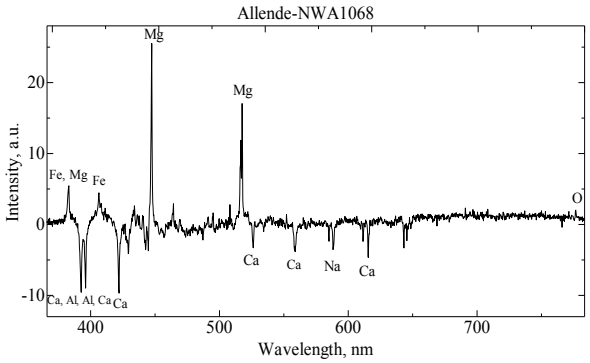

Figure 3: Difference between LIBS spectra of Allende and NWA1068

References: [1] Rosenblatt et al. (2016) Nat. Geosci., 9, 581–583. [2] Maurice, S. et al. (2012) Space Sci. Rev., 170, 95–166. [3] Wiens, R. C. et al. (2012) Space Sci. Rev., 170, 167–227.

PUFFER (Pop-Up Flat Folding Explorer Robots)

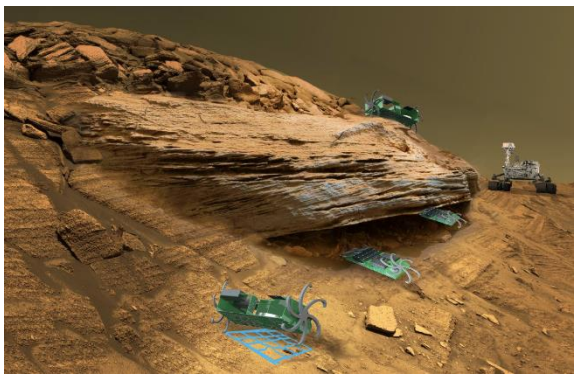

Figure. 1. Illustration of multiple PUFFERs exploring overhung rocks on Mars.

PUFFER (Pop-Up Flat Folding Explorer Robots) is a current Game Changing Development Program effort developing origami-inspired folding robots with extreme terrain mobility. PUFFERs are low-volume, low-mass, and low-cost robots for high-reward extreme terrain science. Multiple folded PUFFERs could be included as a secondary payload on future missions. The parent platform would release one or more PUFFERs near interesting, but otherwise inaccessible terrain. PUFFER then expands and explores. PUFFER could image stratigraphy on steep slopes by using its low center-of-gravity and high, image features of interest with a ground-facing microscope, and transmit the images to the parent platform for relay to Earth. PUFFER could also evaluate microenvironments in confined spaces. For this scenario, PUFFER folds to drive beneath features such as rock overhangs where it can measure temperature and radiation levels using environmental sensors. Beyond this basic instrument suite, PUFFER looks to incorporate instruments of high science return that need to be taken to areas outside of traditional mission scope.

THE EUROPA SEISMIC PACKAGE (ESP): 2. MEETING THE ENVIRONMENTAL CHALLENGE. S. Kedar[1], W. T. Pike[2], I. M. Standley[3], S. B. Calcutt[4], N. Bowles[4], B. Blaes[1], Farokh Irom[1], M. Mojarradi[1], S. D. Vance[1], B. G. Bills[1], [1]Jet Propulsion Laboratory, Caltech, Pasadena, CA 91109, CA [2]Dept. of Electrical and Electronic Engineering, Imperial College, London, UK, [3]Standley Technology Consulting, Claremont, CA, [4]Dept. of Physics, Oxford University, UK. sharon.kedar@jpl.nasa.gov

Introduction: NASA is currently studying a potential Europa lander mission, and instrumentation must be ready within 3-4 years. In a companion paper [1] we summarized the requirements that would enable a seismic system to provide a probe of the habitability of Europa and introduced a candidate broadband instrument capable of delivering those requirements, the SP microseismometer built around a micromachined silicon suspension and delivered for the InSight mission to Mars. Here we outline an approach for adapting this design without any compromise in performance to provide a Europa Seismic Package (ESP) that overcomes the three significant challenges in the environmental conditions, specifically gravity, temperature and radiation.

Gravity for ESP: The change in gravity from 3.7 m/s^2 to 1.3 m/s^2 will result in a different offset of the sensor's suspended proof mass for the vertical axis. This requires minor modification of the sensor-die design with the reduced deflection allowing an increased range of tilt for deployment with no compromise in performance. As tailoring the suspension for the higher offset of Mars has already been achieved in the SP sensor die, we assess this to be a low risk development for ESP.

Temperature for ESP: The seismometer sensor head has to be mechanically coupled to the surface of Europa and so is expected to operate at close to ambient temperatures (fig. 1). Day-night temperatures on Europa's surface span 80-125 K up to 45° latitude [2, 3] and may reach as low as 50 K in shadowed regions. Temperatures on more distant ocean worlds such as Enceladus can dip to around 30 K [4]. Hence to adapt SP to ESP requires a reduction in the minimum operational temperature from 210 K to 80 K. Both this drop and the variation in temperature can affect the performance of the microseismometer.

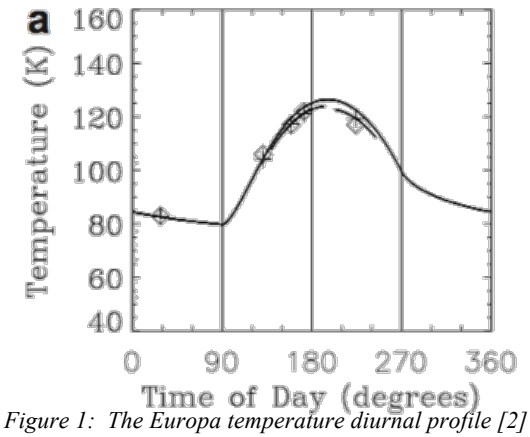

Figure 1: The Europa temperature diurnal profile [2]

The SP sensor's mechanical functionality has already demonstrated in liquid nitrogen at 77K and the lower temperature has the beneficial effect of reducing the suspension's thermodynamic noise floor with the root of absolute temperature, an improvement of up to 30% depending on the thermal coupling to the Europa ambient. Hence we plan to avoid using any sensor-head heating for operation. The variability in temperature is more challenging due to the unwanted thermal contribution of the seismic output through the thermal coefficient of the suspension's Young's modulus. This contribution affects the vertical component of the seismic output for those frequencies unattenuated by the thermal isolation of the sensor die, below ~10 mHz. For Mars we successfully balanced thermal elasticity and expansion coefficients in SP to minimise the overall thermal sensitivity of the vertical axis. This sensitivity is reduced by more than 3 in the lower Europa gravity. Depending on the tilt range required for deployment for ESP we can implement either:

- identical three-axis sensors without thermal compensation deployable over a full 4π solid angle and use die-temperature decorrelation to minimise the thermal contribution, or
- adjusted compensation for the specified tilt range for the vertical-axis sensor, as for the SP.

We achieved a thermal time constant of 2000s for SP to attenuate the unwanted thermal contribution at seismic frequencies above 10 mHz. We will reduce the thermal conductance of the pathways on the sensor die to further increase this attenuation.

Radiation for ESP: Europa sets the most stringent requirements for radiation [5,6]. The total dose depends on the cruise duration, configuration and approach, but is dominated by the lander location, and surface-mission duration. The SP is able to achieve its full performance with the majority of the components located away from the sensor head on the SP's feedback board within the warm electronics box of the InSight lander. This board is connected through a 2 m tether to the proximity electronics on a single hybrid within each sensor head. This distributed electronics scheme allows for optimum protection of the components from the Mars environment, with only the proximity electronics

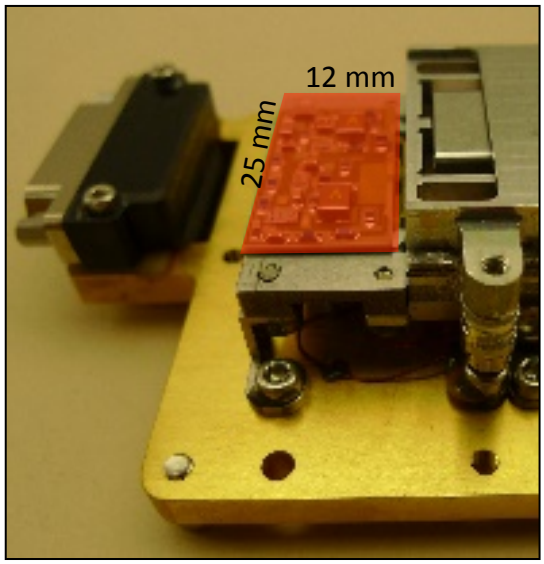

Figure 2: The SP proximity electronics hybrid (shaded red) is likely to see the highest radiation dose, but can be spot shielded with an additional mass of ~40 g.

substantially exposed. We anticipate an analogous approach on the Europa lander, with a shielded, thermally insulated vault available within the lander body as a shared facility for all the payload electronics, reducing the total dose to below 100 krad. For ESP's more exposed sensor-head electronics we have a working assumption of a maximum a total dose of 300 krad. This corresponds to the worst-case scenario of the higher radiation received on the trailing side of Europa, shielded under 8 mm of Al during a 30-day mission, including a margin of 2.

The SP electronics design has to be adapted to this radiation environment through a combination of swap-in of flight-qualified radiation-hard parts and additional localized 8-mm Al shielding for the proximity electronics. A preliminary radiation review of all the microelectronic components used in SP indicates that there are alternatives available for all parts that do not currently meet our assumed Europa radiation requirements already, with no predicted compromise in performance. Spot shielding of the proximity electronic components outside the vault comes with a minimal additional mass due to the small area of the SP's front-end hybrid (fig. 2).

In addition to the high sensitivity and broad frequency response, a seismic system placed on Europa will be required to have the ability to observe a wide range of surface displacements [1]. 24-bit (~140dB) ADCs are the standard in all terrestrial seismic recording systems, and are used on InSight. This high dynamic range is crucial when placing a first seismometer on a planetary body whose range of seismicity and seismic amplitudes are unknown, and even more so for a short-lived mission such as the Europa Lander. This ADC will be located beyond the feedback electronics in the shielded vault and we have identified a candidate design that delivers our performance while meeting our assumed radiation requirements.

Testing ESP: We have already developed cold-test facilities to validate the performance of the SP down to 200K at the sub-1ng/rtHz level, and we are extending the range down to 80K to simulate Europa surface temperatures. As the SPs can operate in tilted configurations to simulate Mars gravity on Earth, we can similarly provide complete performance validation under Europa temperature and gravity simultaneously. We have also developed rapid swap-in procedures to identify any performance degradation from the introduction of radiation-hard components.

Conclusions: Europa confronts any instrument designer with formidable challenges. We have outlined a low risk path to adapt InSight's SP broadband microseismometer for the Europa gravity, temperature and radiation environment, identifying specific solutions that meet these challenges. In particular, the distribution of electronics on SP already minimizes the shielding required for the most exposed components on Europa.

The development of the SP itself has already demonstrated much of the testing required to validate this pathway, including the ability to determine performance at reduced gravity and temperature with radiation-hard space-qualified parts.

Acknowledgments: A portion of this work was performed at the Jet Propulsion Laboratory, California Institute of Technology, under a contract with NASA. U.S. Government sponsorship is acknowledged. A portion of this work was also funded by the UK Space Agency.

References: [1] Pike et al., THE EUROPA SEISMIC PACKAGE (ESP): 1. SELECTING A BROADBAND MICROSEISMOMETER FOR OCEAN WORLDS, *this volume*. [2] Spencer, J. R., L. K. Tamppari, T. Z. Martin, and L. D. Travis (1999). *Science*, **284**(5419):1514–1516. [3] Rathbun, J., N. Rodriguez, and J. Spencer (2010). *Icarus*, **210**(2):763–769. [4] Spencer, J. R., J. C. Pearl, M. Segura, F. M. Flasar, A. Mamoutkine, P. Romani, B. J. Buratti, A. R. Hendrix, L. J. Spilker, and R. M. C. Lopes (2006). *Science*, **311**:1401 – 1405. [5] Paranicas, C., J. Cooper, H. Garrett, R. Johnson, & S. Sturner. in *Europa*. Univ. of Arizona Press, Tucson, pp. 529–544. [6] Patterson, G. W., C. Paranicas, and L. M. Prockter (2012). *Icarus*, **220**(1):286–290.

IN-SITU LIQUID EXTRACTION AND ANALYSIS PLATFORM FOR MARS AND OCEAN WORLDS.
F. Kehl[1], D. Wu[1], M. F. Mora[1], J. S. Creamer[1], and P. A. Willis[1]. [1]Peter.A.Willis@jpl.nasa.gov, Jet Propulsion Laboratory, California Institute of Technology, Pasadena CA 91109.

Introduction: Mars, Europa, Enceladus and Titan are particularly auspicious worlds to search for signatures of past or present alien life in our Solar System. Here we present a compact, integrated sample extractor and analysis unit that could be used to support robotic missions seeking these chemical signatures of life on these destinations. In a first step, inorganic and putative organic compounds are automatically extracted from approximately 1 cm^3 of regolith or ice/soil mixtures by subcritical water extraction (SCWE) at 175 - 250°C and elevated pressures [1]. Following the extraction, miniaturized electrochemical probes quantify the eluate's pH, redox potential and electrical conductivity to better understand the sample (ice or soil) chemistry and mineralogy. Colorimetric measurements by flow injection analysis (FIA) in a fully integrated microfluidic manifold (MicroFIA) furthermore allow additional assessment of the soil's ionic composition [2]. Besides the evaluation of the potential for past or present biology, this system can be employed as a front-end instrument for subsequent, more sophisticated organic analyzers such as capillary electrophoresis (CE) or mass spectrometer (MS) systems, to put these down-stream measurements in context [3].

Approach: The presented sensor platform consists of two sub-systems, comprising a SCWE and a MicroFIA unit. *SCWE* uses liquid water as extraction solvent at temperatures above the atmospheric boiling point of water (273 K, 0.1 MPa), but below the critical point of water (647 K, 22.1 MPa). At elevated temperatures, the permittivity, viscosity, ionization constant and surface tension of water are decreased, whereas its diffusion rate increases, making it a powerful solvent for extraction of both polar and non-polar compounds.

The presented automated and multiplexed SCWE system (Figure 1 and 2) allows for four independent extractions. The crucibles are mounted on a rotary holder and automatically moved by a stepper motor to four positions, where: 1. the sample is ingested and filled into the extraction crucible via the sample funnel, 2. the extraction crucible is capped and hermetically sealed by a linear motor and, 3. engaged with liquid interface to inject the extraction solution. At the 4. position, the crucible is heated up to 250°C by the cell's internal heater to initiate the extraction. After concluding the extraction, the crucible engages again with the liquid interface to release the extract to the MicroFIA system for downstream compositional analysis.

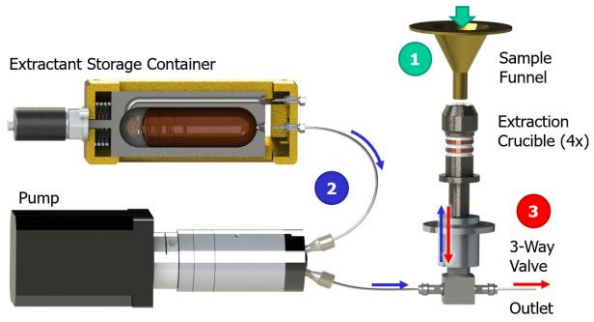

Figure 1: The solids enter one of the four extraction crucibles through the sample funnel (1). Thereafter, the crucible is hermetically sealed by a linear motor and pre-pressurized with the extractant by a high pressure pump (2). Subsequently, the temperature of the crucible is increased up to 250°C by an internal resistive heater, initiating the extraction of the compounds. The extraction is concluded by releasing the eluate via a 3-way valve (3).

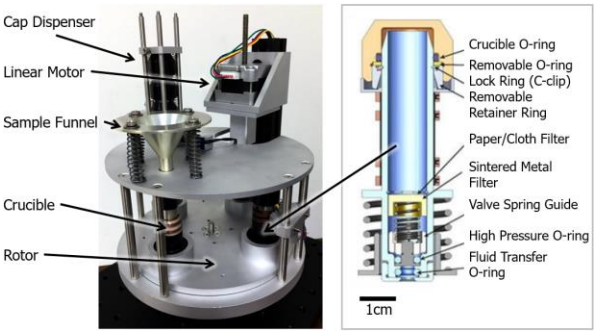

Figure 2: SCWE system (left) and cross-section of a sealed extraction crucible (right) [4].

FIA is a technique where a liquid sample is injected into a moving carrier stream. The two liquids form a reaction plug, which is transported toward a detector that continuously measures changes in e.g. absorbance and electrode potential. FIA is a powerful but simple tool to measure ion concentrations, pH, ORP and electrical conductivity of a liquid sample, such as the extract from the SCWE unit. The general concept of the presented MicroFIA platform is graphically depicted in Figures 3 and 4.

The liquid sample enters the 3D-printed MicroFIA manifold (Figure 5) and is routed via various 3-way valves. A liquid plug of reagent is injected into the carrier stream by switching one of the 3-way valves, accessing the reagent reservoir. The sample and rea-

gent mix and react, leading to an absorbance change depending on the reagent and the concentration of the analyte of interest in the sample. These colorimetric changes and therefore the analyte concentration can be determined by a white-light LED and RGB photodiode. Custom-made, miniaturized electrochemical sensors additionally measure pH, oxidation reduction potential (ORP) and temperature of the liquid sample.

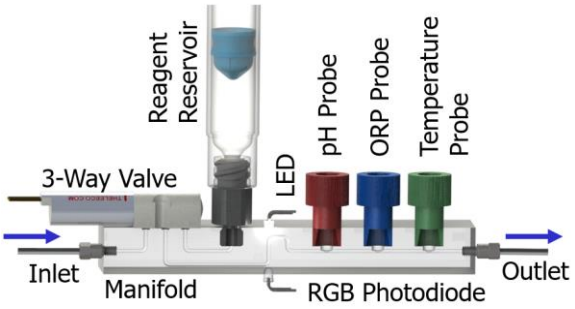

Figure 3: General MicroFIA concept: fluidic manifold, 3-way valve for liquid routing and reagent injection, colorimetric absorption cell and electrochemical sensors for in-line measurement of pH, ORP and temperature.

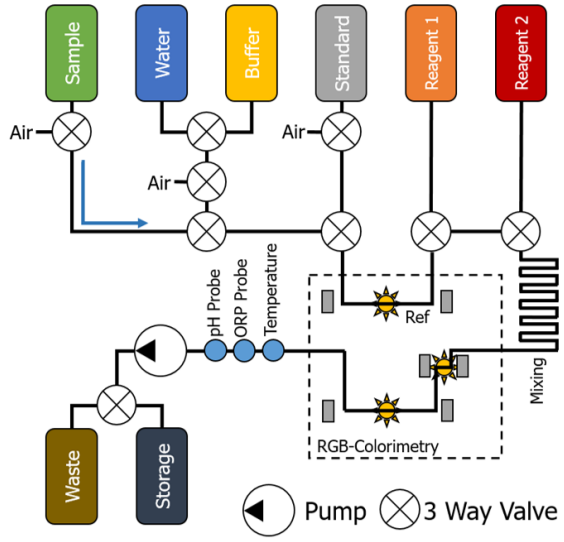

Figure 4: MicroFIA schematics: The liquid sample is pulled through the fluidic manifold by a pump mounted at the system's outlet. Controlled switching of the 3-way valves allows to inject different indicator reagents in the sample solution. Resulting color changes can be quantified in the colorimetric absorption cells.

The presented, fully automated MicroFIA system (Figure 6) allows to quantify up to six different analytes (such as, but not limited to, Mg^{2+}, PO_4^{3-}, Cu^{2+}, NH_3-N, H^+, and formaldehyde) by colorimetry, and pH and ORP by electrochemical sensors.

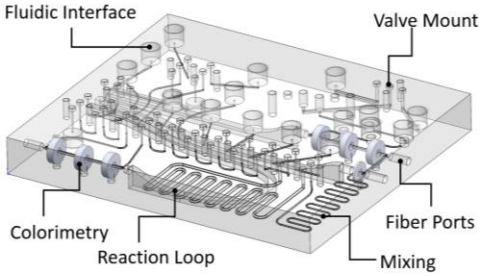

Figure 5: 3D printed MicroFIA manifold.

Outlook: After the prototype development and successful technology demonstration, extended measurement campaigns are planned to evaluate both efficiency of the extractor as well as limit of detection of the FIA system. In the near future, the two systems will be combined for an end-to-end analysis of Mars analogue samples. In 2017, a fully-integrated version will be installed on the K-Rex Rover (NASA Ames) for in-situ measurements in the Atacama Desert (Chile).

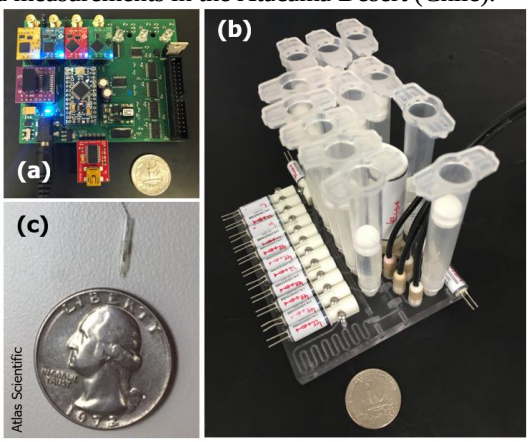

Figure 6: Photographs of (a) MicroFIA electronics, (b) assembled MicroFIA system, (c) miniature pH probe.

Acknowledgements: The presented work was done at the Jet Propulsion Laboratory, California Institute of Technology, under a contract with the National Aeronautics and Space Administration. Financial support was provided by Planetary Science and Technology from Analog Research (PSTAR) Program and the NASA Postdoctoral Program (NPP) at the Jet Propulsion Laboratory, administered by Universities Space Research Association through a contract with NASA.

References:

[1] Amashukeli, X., et al. (2007). *J Geophys Res Biogeosci*, 112(G4), [2] Worsfold, P. J., et al. (2013). *Anal Chim Acta*, 803, 15–40. [3] Willis, P. A., et al. (2015). *Anal Bioanal Chem*, 407(23), 6939–6963. [4] Beegle, L., et al. (2011). *Aerospace Conference* (pp. 1–10). IEEE.

Next-generation thermal infrared multi-body radiometer experiment (TIMBRE). M. Kenyon[1], G. Mariani[1], B. Johnson, E. Brageot[1], and P. Hayne[1] [1]Jet Propulsion Laboratory, 4800 Oak Grove Dr., Pasadena, CA 91109, mkenyon@jplnasa.gov

Introduction: We have developed an instrument concept which is a next-generation Thermal Infrared Multi-Body Radiometer Experiment called TIMBRE. TIMBRE is build around a new focal plane architecture consisting of a 128 x 64 element array of thermopiles and incorporates an optical design with a novel intentional aberration [1] at the intermediate focus which reduces the size of the optical bench by a factor of 2 over a conventional design.

TIMBRE is a versatile instrument that makes spectral maps of terrestrial surfaces and atmospheres with wavelengths ranging between ~1-100 um. It belongs to a class of important instruments called thermal imaging radiometers (TIRs) that provide high priority science as demonstrated by the inclusion of this class of instrument on Pioneer 10 \& 11 (Infrared Radiometer), Voyager (IRIS instrument), Viking Orbiter (IRTM), Cassini (CIRS), Mars Odyssey (THEMIS), Mars Reconnaissance Orbiter (MCS), Lunar Reconnaissance Orbiter (Diviner), and Europa Clipper (E-THEMIS). TIRs are also included on the model payload for New Frontiers 4 & 5 missions [Trojan Tour and Rendevous (TTR), Comet Surface Sample Return (CSSR), Io Volcano Observer (IVO)] and proposed Discovery missions (BASiX) [2].

The power of a TIR is determined by several properties including the capacity to measure faint signals (e.g. sensitivity), the spatial resolution, the number of spectral channels, radiometric accuracy, and the swath width or coverage of the instrument as it passes over a target. In terms of these properties, MCS, Diviner, and THEMIS are the gold standard currently flying and have provided breakthrough science by measuring the infrared/far-infrared (~1-100 um) properties of Mars and the Moon; however, these instruments suffer from limitations in both spatial resolution and sensitivity at low temperatures (i.e. > 200 K) due to limitations in the focal plane.

TIMBRE overcomes these shortcomings by incorporating a diffraction-limited and sensitive modern thermopile array and an optical design with a novel intentional aberration to achieve an instrument with unparalleled performance.

TIMBRE is specifically designed for demanding future missions to small bodies (e.g. NEO, main-belt comets, Trojan asteroids), planets (e.g. Jupiter, Mars, Venus), and satellites (e.g. Io).

References: [1] W. Johnson *et al.* (2015) NASA New Technology Report 49552. [2] R. C. Anderson *et al.* (2014) *45th Lunar and Planetary Science Conference, 1571*, A74.

THE AXEL ROVER: A NOVEL PLATFORM FOR INSTRUMENTS MAKING MEASUREMENTS IN EXTREME TERRAINS. L. Kerber[1] , I.A. Nesnas[1] , [1]Jet Propulsion Laboratory, California Institute of Technology, 4800 Oak Grove Dr., Pasadena, CA 91109 (kerber@jpl.nasa.gov).

Introduction: Many interesting geological exploration targets exist in regions with steep and rough terrain, such as impact crater walls, lava tube skylights, volcanic pit craters, chasms, graben, and fissures. Unfortunately, these places are often out of reach for traditional rover concepts. The Axel rover is a platform that can navigate difficult topography and steep slopes, allowing it to carry a wide variety of instruments to a new array of target sites. The Axel rover consists of two wheels connected by a thick axle containing a winch and a tether [1]. Two Axels can be combined to form a "DuAxel" (**Fig. 1**), or one Axel can replace an axle on a more traditional rover body [1]. Over flat terrains (for example, from the landing site to the investigation area), Axel rover can traverse just like an ordinary rover. Across rough terrain, Axel rover can maneuver across large rocks up to one wheel radius in height. Once it approaches a steep section, the Axel rover can set an anchor and rappel down the steep slope by letting out the tether stored inside the axle [1; **Fig. 1**].

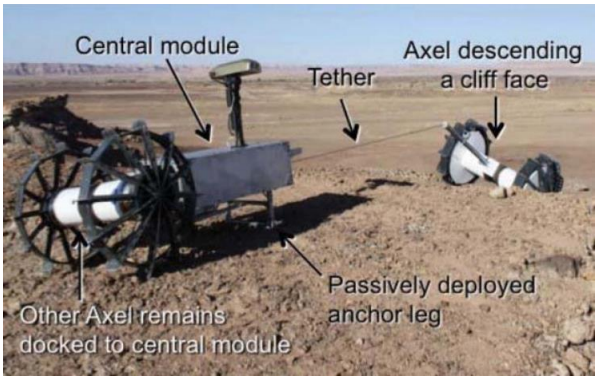

Figure 1. The DuAxel rover configuration at work in the field (figure from [1])

This functionality allows the rover to descend steep to vertical slopes (and ascend them again). The rover can even dangle in free space and continue to let out its tether. The rappelling module is symmetrical top to bottom, allowing it to flip over while navigating steep terrain and remain operational. The rover can communicate through its cable, alleviating common communication problems facing other extreme terrain robots. The rover can also receive power through its tether, meaning that it could leave a solar panel on the surface and still receive power to explore a dark cave or permanently shadowed crater below [1]. At the edge of a steep slope, the Axel rover can anchor itself in the regolith and rappel down the side of the slope using its tether for support, communication, and power. Axel has undergone extensive testing in terrestrial desert environments on steep slopes and various rock types [1].

Figure 2. The Axel rover taking spectroscopic measurements on a slope of 40º (figure from [1]).

Possibility for Carrying Scientific Instructments: Axel can carry scientific instruments in the 8 instrument bays contained within its wheel wells (16 for a DuAxel). When Axel stops, the instrument comes out of the bay and makes a measurement (**Fig. 2**). Before moving again Axel can independently rotate its wheel well to access all of the other instruments in that wheel for collocated measurements of the same target [1]. The Axel wheel can also make a trench in the surface to expose fresh regolith to the instruments. The location of the instruments inside the wheel of the rover protects them from rocks, dust, and falling debris. In addition, whether used as an addition to a traditional rover, or as part of a DuAxel configuration, Axel could scout for interesting targets and collect samples to be carried back to heavier or bulkier instruments located on the main rover body. Commercial off-the-shelf instruments that have been successfully integrated into the rover wheel payload space include a microimager, a miniature spectrometer, and a thermal probe [1].

Moon Diver: A Sample Axel Mission Concept

The lunar mare basalt deposits serve as natural probes into the lunar interior. Recent images returned by the Kaguya and Lunar Reconnaissance Orbiter missions have revealed the presence of deep mare pits containing meter-scale layer stratigraphy exposed in their walls ([2-

4]). Such an exposure would offer a wealth of information about the compositional, petrologic, and emplacement conditions of the mare basalts through time. While normal rovers would not be able to reach these layers, the functionality of Axel rover would allow a mission to examine and characterize the lava layers exposed in the wall of a mare pit crater during abseil descent [**Fig. 3**; 5]. Mineralogy (provided by a VIS/NIR spectrometer), texture (provided by a microimager), elemental chemistry (provided by an X-ray spectrometer), and age (provided by a mass spectrometer situated on the main rover body) would reveal the evolution of the mare lavas through the section. Axel's onboard cameras could record layer thicknesses and document the presence and characteristics of intervening regolith layers. Once on the floor of the pit, the Axel rover could continue to explore. If the pit opened into a lava tube or other subsurface void, the rover could attempt to negotiate the floor up to the length of its tether (currently 250-300 m, potentially up to 1 km; [1]). After exploring the pit, the rover could reel itself back up the wall and either continue roving across the surface or rappel down a different side of the pit.

The Axel rover provides enhanced mobility which would enable it to land, rove to a pit, cave, cliff, or slope, approach the science targets, explore with a suite of high-priority science instruments, and exit, all with existing or highly developed technologies. This approach would revolutionize our capability to carry diverse instruments to many previously inaccessible terrains on a variety of planetary bodies.

References: [1] Nesnas, I. et al. (2012) J. of Field Robotics, 29, 663-685. [2] Haruyama, J., et al. (2009) GRL 36, L21206 [3] Robinson, M.S. et al. (2012) PSS 69, 18- 27. [4] Wagner, R.V. and Robinson, M.S. (2014) Icarus 237, 52-60. [5] Kerber L. et al. (2016) LPSC 47, Abs. 2969.

Figure 3. A mission concept using Axel rover's capabilities to bring instruments into a volcanic pit crater on the Moon [5].

MEMS LIQUID AND GAS CHROMATOGRAPHY FOR MINIATURIZED PLANETARY IN SITU INSTRUMENTS. R. D. Kidd[1], B. Bae[1], P. A. Willis[1], A. C. Noell[1], N. Scianmarello[2] and Y.-C. Tai[2], Jet Propulsion Laboratory, California Institute of Technology, 4800 Oak Grove Dr., Pasadena CA 91109, Richard.D.Kidd@jpl.nasa.gov, [2] California Institute of Technology, Pasadena, CA 91125.

Introduction: Our objective is to design, build and demonstrate a miniaturized instruments for analysis of organic and inorganic compounds in planetary materials with high sensitivity (parts-per-billion/trillion depending on target species) and accuracy, with a particular focus on detecting biomarkers extracted (or direct entry) from rocks, soils and ices. The ultimate goal of this research is to develop a miniaturized instruments for both robotic and human missions.

We have been using Micro-Electro-Mechanical Systems (MEMS) technology to reduce the size, mass and power of the three classical chromatographic technologies (Fig. 1): gas chromatography (GC), capillary electrophoresis (CE) and high performance liquid chromatography (HPLC) [1-4]. Both CE and HPLC are liquid chromatographic (LC) technologies.

SMD (Science Mission Directorate) Goals. Our instruments are meant to address two fundamental questions in astrobiology, namely, "how does life begin and evolve?" and "does life exist elsewhere in the universe?" For these reasons, the science objectives for instruments are to look for: (1) signs of extinct life by detecting carboxylic acids and lipids - the longevity and preservation of carboxylic acids and lipids offer a chemical insight into potential primordial biological activity; (2) extant life by searching for amino acids, peptides and proteins - molecules that strongly indicate a biotic origin; (3) provide organic molecular detection and life detection capabilities for future landed missions to Mars, Europa, Titan, Enceladus, and other planetary bodies; (4) astrobiology field research on Earth.

HEOMD (Human Exploration & Operations Mission Directorate) Goals. Our instrumentation is cross-cutting with the human program and, in fact, we have already flown a GC system to the International Space Station for environmental monitoring [5] and will fly a MEMS-GC in 2018 [1]. HEOMD goals include (1) experiments on ISS (2), astronaut health monitoring, (3) environmental monitoring, (4) field laboratory.

Detectors: There are a variety of compact detectors commonly used for GC: mass spectrometry (MS), flame ionization detection (FID), and thermal conductivity detection (TCD). For a compact system, such as for cubesat-sized instruments, a MEMS-TCD would be preferred. For all else, our preferred detector is an ion trap MS [1,5].

For LC, UV/VIS absorption or fluorescence, refractive index, electrochemical, conductivity, evaporative light scattering are few common detectors in use. However, none of these types of detectors can give a definitive identification of molecules nor can they identify, and in some cases, even detect unknown compounds. The coupling of LC to MS is recognized as the premier technique for any application, which requires high sensitivity, selectivity, and complete unambiguous identification of an unknown collection of chemical species. These are exactly the requirements and conditions found in a planetary robotic exploration. The coupling of LC to MS via electrospray ionization (ESI) is the terrestrial standard and is especially useful in producing ions from macromolecules because it overcomes the propensity of these molecules to

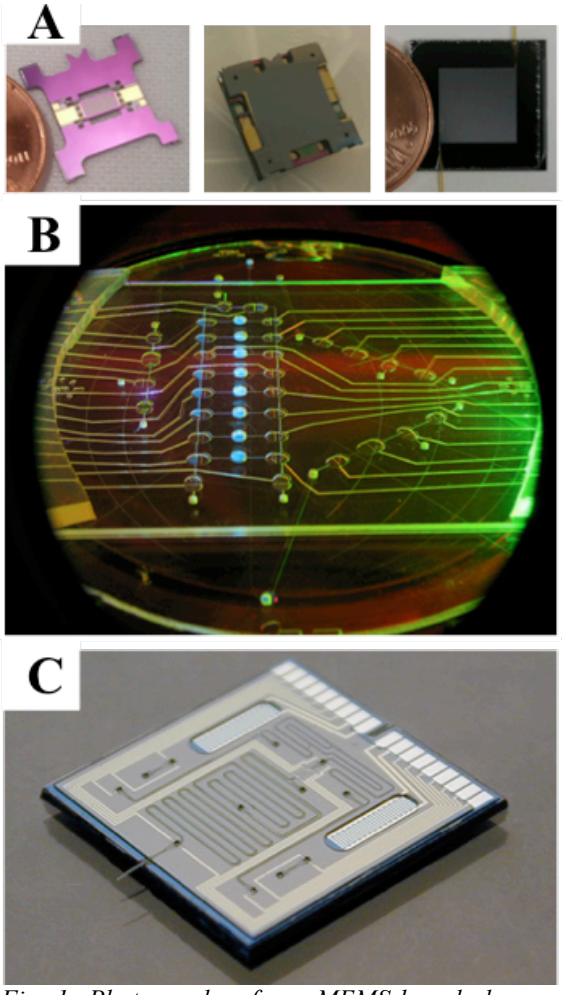

Fig. 1: Photographs of our MEMS-based chromatography chips. (A) left-to-right, MEMS-GC preconcentrator, 4-electrostatic valve array, 1 m column; (B) CE-chip; (C) HPLC-chip.

fragment when ionized through other methods (e.g. electron impact, laser ionization). A further advantage for LC/MS is that the need for chemical labeling (for optical detectors) and/or derivatization (for gas chromatography) are eliminated.

Until recently, HPLC systems have been considered to be unsuitable for *in situ* planetary applications due to their large mass and operational complexity. However, starting in 2004 the Caltech Micromachining Laboratory demonstrated the first complete microfluidic reverse-phase HPLC-chip instrument (pumps, injector, mixer, column), which is capable of separating a wide range of organic compounds based on their varying elution times through the separation column [6]. The HPLC-chip integrates three electrolysis based electrochemical pumps, one for loading the sample and the other two for delivering the solvent gradient; a static mixer; a column packed with silica-based reversed-phase support; and an electrospray nozzle directly on the polymer chip. The technology eliminates many of the traditional fittings and connections associated with traditional HPLC systems, dramatically reducing the possibility of leaks and dead volumes and significantly improving ease of use, sensitivity, and reliability during analysis.

Ion Trap Mass Spectrometer: The Planetary Surface Instruments Group at JPL is drawing upon its experience in successfully developing and constructing MS flight instruments for the MEMS GC, CE, and LC systems. Our group has been responsible for the original research and flight development of several different miniature mass spectrometers including a Paul quadrupole ion trap (QIT) MS that was used in the Vehicle Cabin Atmosphere Monitor [5] and will be used in the Spacecraft Atmosphere Monitor (Fig. 2) [1].

Value-Added Sensors - Ion Selective Electrodes: Although we have been developing ion chromatographs on a chip [4], for inorganic measurements (inorganic ions, conductivity, pH, etc), simpler technology can be added on to LC-based systems.

The identification of perchlorates on Mars, one of the most notable instance of sample matrix effects in planetary science, was made possible by a wet chemistry instrument, JPL's Wet Chemical Laboratory (WCL) [7] onboard the Phoenix Lander. Using ion selective electrodes (ISEs) as part of its suite of soluble ion electrochemical sensors, WCL made the surprising discovery of perchlorate salts in the Martian regolith. This discovery helped explain how reactions between perchlorate and organics in the pyrolysis oven during sample volatilization had prevented every gas chromatograph-mass spectrometer instrument sent to Mars since Viking from conclusively detecting organic molecules.

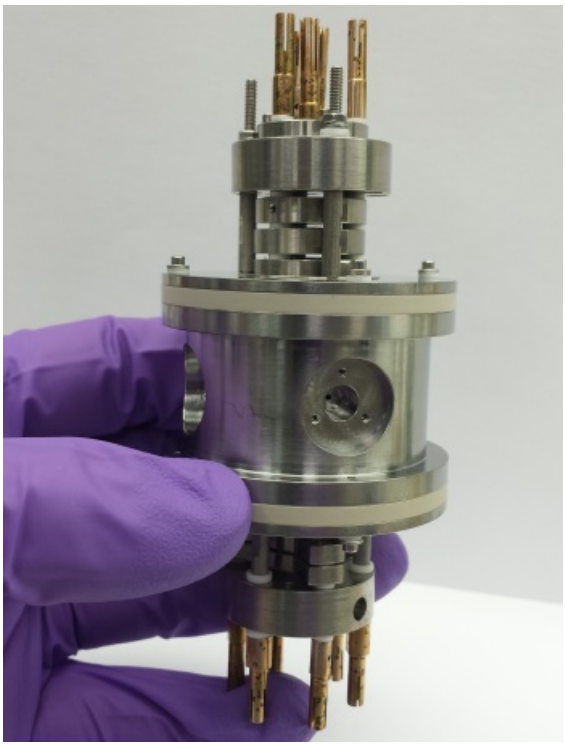

Fig. 2: Photograph of our 10 mm Paul ion trap mass spectrometer. This is the axial ionization version of our MS.

The clear success of the WCL instrument makes it, or a subset of its electrochemical sensors, a natural choice for future missions that will benefit from inorganic ion analysis such as the Europa Lander or a New Frontiers mission to Enceladus. However, the ISEs that were the main class of sensors in WCL are currently not robust enough to avoid drying out during a long duration mission to the outer planets. JPL is working to address that issue by developing solid contact ISEs (SC-ISEs) that no longer rely on a wetted hydrogel material in order to function. Taking advantage of the switch to SC-ISEs and advances in the technology since WCL was built will also allow reductions in sensor size and improvements in the limits-of-detection.

References: [1] Madzunkov S. M. et al. (2016) *ICES*, Abstract #2016-284. [2] Willis P. A. and Stockton A. M. (2013) *CE and Microchip CE*, John Wiley & Sons, Inc. pp 277–291. [3] Xie J. et al. (2005). *Anal. Chem. 77,* 6947–6953. [4] Kidd R. D. et al. (2015) *ICES*, Abstract# 2015-141. [5] Madzunkov S. M. et al. (2013) *J. Am. Inst. Aeronautics & Astronautics*. Abstract# 2012–3453. [6] Xie J. et al. (2005) *Anal. Chem. 77*, 6947–6953. [7] Hecht M. et al. (2009) *Sceince 325*, 64–67.

Acknowledgements: The research described here was carried out at the Jet Propulsion Laboratory, California Institute of Technology.

THE ADVANCED MARS CLIMATE SOUNDER (AMCS) - A PROVEN ATMOSPHERIC PROFILER FOR FUTURE MARS ORBITERS. A. Kleinböhl, J. T. Schofield, D. M. Kass, and D. J. McCleese, Jet Propulsion Laboratory, California Institute of Technology, Pasadena, CA (armin.kleinboehl@jpl.nasa.gov).

Introduction: Remarkable progress has been made in understanding the structure and dynamics of the Martian atmosphere. A decades-long climatology has been acquired, revealing significant interannual variability, dust storms that disrupt the seasonal mean circulation, and complex surface/atmosphere interactions. Many of the underlying dynamical and radiative processes that govern the Martian atmosphere remain poorly quantified. To a large extent the structure and dynamics of the Martian atmosphere are controlled by the atmospheric aerosols of dust, H_2O, and CO_2. Dust storms lift dust into the atmosphere and while some patterns in their occurrence are well characterized [e.g. 1,2], the processes that cause these storms to expand and become global while others dissipate in a matter of days or weeks are still not understood. Water ice clouds are abundant on Mars. Their radiative effects on the atmosphere are profound [3,4] but not well quantified to date. Our understanding of the water cycle is limited by extremely sparse water vapor profile observations [5]. Column water vapor measurements [e.g. 6] have provided insight, but the 3-D water vapor distribution and the processes controlling it are virtually unexplored. Hence there is a continued need for global, vertically resolved measurements of atmospheric temperature, water vapor, and aerosols (dust, water ice, CO_2 ice), and their evolution on diurnal, seasonal, and interannual time scales. Measured climatologies and near real-time atmospheric density profiles support landing, aerocapture and surface operations of future human and robotic missions to Mars.

Here we describe the Advanced Mars Climate Sounder (AMCS), a mature, low-cost, and low-risk infrared atmospheric sounder for a future Mars orbiter mission that is ideally suited to address these outstanding questions and support landed missions. AMCS builds on the instrument and measurement heritage of the Mars Climate Sounder (MCS, Fig. 1) [7], which has been operating on Mars Reconnaissance Orbiter (MRO) for ~10 years. It also incorporates flight development work completed for the ExoMars Climate Sounder (EMCS) instrument [8], which was selected to fly on ESA's ExoMars Trace Gas Orbiter. AMCS would provide daily, global, pole-to-pole profiles of atmospheric temperature, dust, water ice, CO_2 ice, and water vapor. Atmospheric profiles would be assimilated into Mars General Circulation Models to generate global, interpolated fields of measured and derived parameters such as winds.

AMCS would address the highest priority MEPAG Goal II to "understand the process and history of climate" and the high priority decadal survey goal on climate on Mars [9]. It would provide several of the highest priority precursor measurements for manned missions based on MEPAG Goal IV and the Human Mission Strategic Knowledge Gaps.

Figure 1: The MRO/MCS flight instrument during thermal vacuum testing at JPL.

AMCS Instrument: Like MCS and EMCS, AMCS is a passive infrared limb-sounding filter radiometer. It would use 8 spectral channels in the IR from 12-45 µm as well as a visible/near-IR channel to address its measurement objectives. The instrument would consist of two telescopes, with visible and mid-IR channels in one and far-IR channels in the other. Azimuth and elevation actuators, with a range of 270° each, would allow pointing of the telescopes anywhere in the downward hemisphere from a nadir-oriented spacecraft. Each channel would consist of a linear array of uncooled thermopile detectors, which instantaneously measures a radiance profile when vertically pointed at the limb. This results in better sensitivity and geometrical stability than scanning the limb with a single detector. While an MRO/MCS detector array consists of 21 detectors, the AMCS array size could be increased to achieve improved vertical resolution or preserve a target vertical resolution from a higher orbit altitude. Accurate calibration of the IR channels would be achieved with thermally stabilized blackbody targets and frequent spaceviews. A solar target would enable calibration of the visible/near-IR channel.

An overview of the AMCS channels and their measurement functions is given in Tab. 1. Most channels are heritage from MRO/MCS. The combination of channels B2 and B3 would enable water vapor profiling by discriminating between water vapor and aerosols (Fig.

2). This was not achieved with MCS because B3 was sensitive to water vapor. The B3 design was improved during EMCS development to address this issue.

Telescope/ Channel #	Bandpass cm^{-1}	Band Center - µm	Measurement Function
A1	595 - 615	16.5	Temperature 0 - 30 km
A2	615 - 645	15.9	Temperature 30 - 50 km; Pressure
A3	635 - 665	15.4	Temperature 50 - 90 km, Pressure
A4	820 - 870	11.8	Water ice extinction 0 - 90 km
A5	400 - 500	22.2	Dust extinction 0 - 90 km
A6	3300– 33000	1.65	High altitude hazes and particle size discrimination
B1	290 - 340	31.7	Dust and CO_2 ice extinction 0 - 90 km
B2	220 - 260	41.7	Water vapor 0 - 40 km
B3	231 - 243	42.2	Dust and Water ice extinction 0 - 30 km

Table 1: AMCS spectral channels and their measurement functions.

AMCS has heritage in MRO/MCS and the Diviner instrument on the Lunar Reconnaissance Orbiter. It would make use of the EMCS design heritage and utilize mechanical and optical flight hardware already fabricated by the time of EMCS closeout. Based on the maturity of its design, AMCS would be very compact with a mass of only 9 kg, a power consumption of 18 W and a very low data rate of 2000 bps. The instrument would be built at JPL by the hardware and science teams that developed EMCS. The mature design would allow AMCS to be built for the next available opportunity, e.g. a potential Mars orbiter in 2022.

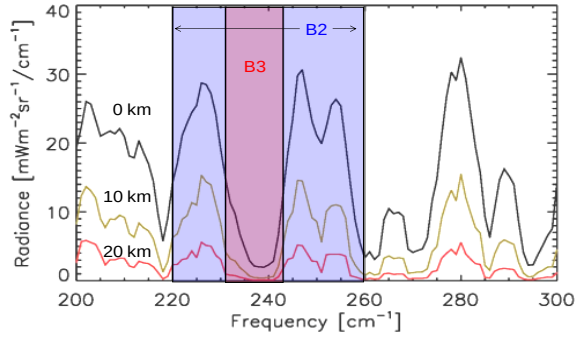

Figure 2: Limb radiance spectrum showing water vapor bands in the far-IR. The positions of channels B2 and B3 are indicated. B2 would be used to measure water vapor while B3 would be designed to be insensitive to water vapor, allowing the discrimination between water vapor and aerosols.

AMCS Observations and Data Products: AMCS can accommodate a large range of orbital geometries. A nadir-oriented spacecraft in near-polar orbit would allow limb observations in all directions and provide daily, global, pole-to-pole coverage, similar to MRO/MCS (Fig. 3). Coverage at multiple local times could be achieved from a precessing orbit and by slewing the instrument in azimuth in order to view perpendicular to the orbit track [3]. From typical orbit altitudes AMCS would achieve 0-90 km vertical coverage with a vertical resolution of 5 km or better. Data products would consist of profiles of temperature, water vapor, and dust, water ice and CO_2 ice extinction. Retrieval algorithms have heritage from MRO/MCS [10,11]. Column quantities of dust, water ice and water vapor would be provided along with atmospherically corrected surface temperature [12] and albedo. Assimilation of the measured atmospheric fields into Mars General Circulation Models would be an integral part of the AMCS investigation and would provide globally interpolated and derived fields, such as winds.

MRO/MCS has demonstrated the ability to rapidly process data into geophysical quantities in order to support the successful landings of Phoenix and MSL as well as MAVEN operations. AMCS would retain this key capability well into the next decade.

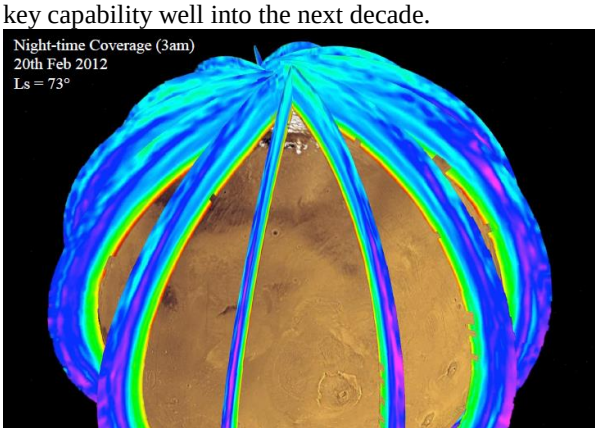

Figure 3: Coverage for one day of nighttime temperature profiles from MRO/MCS. From a near-polar orbit, this kind of coverage would be achieved daily, day and night, for temperature, dust, water ice, water vapor, and CO_2 ice.

Acknowledgments: Work at the Jet Propulsion Laboratory, California Institute of Technology, is performed under contract with the National Aeronautics and Space Administration.

References: [1] Kass, D. et al. (2016) *GRL 43*, 6111-6118. [2] Wang, H. and Richardson, M. (2015) *Icarus 251*, 112-127. [3] Kleinböhl, A. et al. (2013) *GRL 40*, 1952-1959. [4] Madeleine, J. et al. (2012) *GRL 39*, L23202. [5] Maltagliati, L. et al. (2011) *Science 333*, 1868-1871. [6] Smith, M. et al. (2009) *JGR 114*, E00D03. [7] McCleese, D. et al. (2007) *JGR 112*, E05S06. [8] Schofield, J. et al. (2011) *Mars atmosphere workshop*, Paris. [9] Visions and Voyages (2012) *NRC Press*. [10] Kleinböhl, A. et al. (2009) *JGR 114*, E10006. [11] Kleinböhl, A. et al. (2016) *JQSRT*, 10.1016/j.jqsrt.2016.07.009. [12] Piqueux, S. et al. (2016) *JGR 121*, 10.1002/2016JE005034.

Flexible low-band Instrument for RF Measurement and Imaging (FIRMI). M. Knapp[1], F. C. Robey[2], F. D. Lind[3], M. Hecht[3], [1] MIT Dept. of Earth, Atmospheric, and Planetary Science, 77 Massachusetts Ave. Cambridge, MA 02139, [2] MIT Lincoln Laboratory, 244 Wood St., Lexington, MA 02420, [3] MIT Haystack Observatory, 99 Millstone Rd, Westford, MA, 01886.

Introduction: Recent antenna technology has the potential to significantly improve space-based sensing, particularly at the low end of the radio band. The vector antenna, a structure that measures full electric and magnetic field vectors [1], [2], is a novel approach to radio frequency sensing that provides angular resolution, polarization state information, and improves sensitivity in a compact, electrically short structure. As such, vector antennas promise to substantially reduce the mass and volume of spacecraft RF sensor antennas and, in some cases, eliminate the need for spatially distributed arrays of elements. Here we propose to apply this novel technology to RF source characterization, ionospheric sounding, and to surface penetrating radar in support of planetary sciences data collection. **FIRMI will operate from 250 kHz – 30 MHz and will be capable of both active radar sounding and passive imaging.**

Vector Sensor: An electromagnetic vector sensor (EMVS) samples the electric *(E)* and magnetic *(H)* field at a single location in space and with a common phase center. To do this, a vector sensor is composed of three orthogonal dipole elements and three orthogonal loop elements. These six elements allow for a complete measurement of the E-field and H-field amplitude and phase of incoming radiation. The vector sensor is named for its capacity to fully measure the electromagnetic vector field rather than the single scalar measurement associated with a single element antenna. One consequence of sensing the full E and H vectors is that the vector sensor natively measures full polarization information. The advantages of a vector sensor are described as follows.

- Vector sensors are able to determine direction of arrival of sources [1] without resorting to multiple poses as required for a tripole.
- Vector sensors can null or isolate specific sources [2] based on spatial and polarization characteristics of the sources.
- Vector sensors can distinguish between electrostatic and electromagnetic in-situ plasma waves in the sensor frequency range.
- Vector sensors maximize the statistics collected from a single point in space.
- Vector sensor data is invariant to rotation of the spacecraft and omni-directional in coverage.

Instrument Description: FIRMI's compact form factor, low mass, and low power requirements will provide novel capabilities while minimizing resource (mass, power, volume) competition with other mission instruments. The vector sensor antenna provides unique capabilities to achieve angular resolution on a variety of static or transient sources and to perform simultaneous radar measurements when required. The vector sensor is somewhat more complex than a simpler antenna (e.g. dipole) but enables performance which easily justifies the increased complexity. **The proposed instrument is lightweight and compact, fitting in a stowed volume of 1.5 L (10 x 10 x 15 cm), weighing less than 2.5 kg, and consuming less than 10 W.**

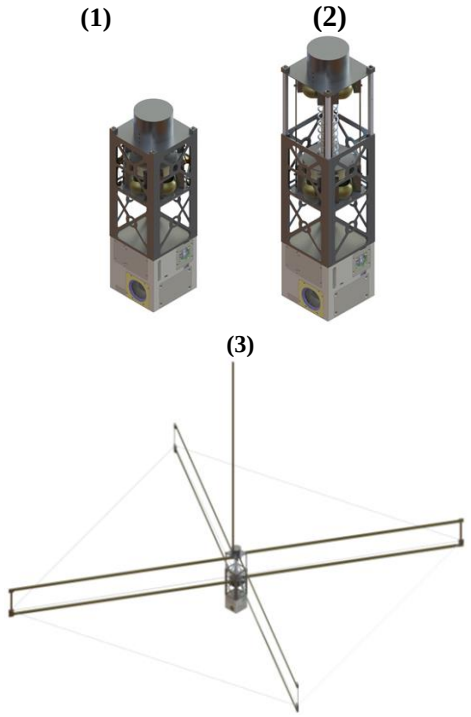

Figure 1. FIRMI antenna fully stowed (1), telescoped but not deployed (2), and fully deployed (3). The vertical monopole is stowed in the cylinder on the top of the 3U CubeSat frame and the remaining five elements (two rectangular loop/dipoles and square perimeter loop) are stowed in the top 1U.

The vector sensor that will be implemented will utilize two crossed elements that serve to simultaneously provide both loop and dipole sensing modes [3,4]. A

perimeter loop provides mechanical stability to the crossed loop/dipole elements, and a final monopole provides the sixth element to create the full complement of sensing modes. The stowed and deployed instrument is shown in Figure 1 on a 3U CubeSat body for reference.

Applications to Planetary Science:

Active sensing (sounder/radar). FIRMI's active sensing capabilities are well suited to a variety of subsurface imaging and ionospheric sounding tasks on various solar system bodies. For example, surface-penetrating radar offers the potential for detection of ice / water interfaces on Europa [5], the study of subsurface geyser structures on Enceladus [6], and searching for lava tubes and basaltic caves which have significant potential as astrobiological habitats [7] among many other potential targets. **FIRMI's small mass, volume, and power requirements compare favorably to previously flown radar payloads that address similar science needs.**

FIRMI's sounding capability also offers significant potential for the study of planetary ionospheres in the solar system using radio sounding and radar techniques. Targets include the Martian ionosphere as well as planets such as Venus, Jupiter, and Saturn that have have significant and complex ionospheres. Several moons in the solar system also have relatively dense atmospheres, ionospheres, and complex interactions with the planets that they orbit (e.g. Io, Titan, Enceladus, etc.). These bodies offer the opportunity to examine atmosphere/solar wind interactions, neutral atmosphere to ionosphere coupling, the transport of plasma in planetary ionospheres, and the occurrence of plasma turbulence and non-linear plasma phenomena which can also exhibit large radar cross-sections.

Passive Imaging. Imaging of transient phenomena with even modest angular resolution has been difficult or impossible with past single-spacecraft instruments that operate in the low frequency regime. FIRMI will allow resolved imaging of planetary electrostatic discharge (ESD) phenomena, such as lighting and impact flashes. Planetary lightning is a probe for atmospheric dynamics, including cloud layering and composition, storm evolution, neutral atmosphere-ionosphere coupling, volcanic plumes, and disequilibrium chemistry.

Passive imaging at low frequencies also offers access to plamsa wave and driven emission from auroras, moon-influenced plasma emission, and solar wind-magnerospheric interactions. FIRMI offers remote sensing capability in the frequency range where cyclotron magnetospheric emission is brightest, enabling monitoring of planetary rotation and magnetosphere/ionosphere/atmosphere coupling via time variability of auroral emission. FIRMI will be able to localize the emission region(s) and measure polarization in a single snapshot observation, enhancing the study of the fundamental plasma processes that give rise to the auroral radio emission and related phenomena.

FIRMI's remote sensing capabilities provide useful overlap with in-situ plasma instruments and complement IR/Vis/UV imagers and spectrometers. FIRMI's small size is well suited to micro/nanosat applications as well.

Applications Beyond Planetary Science:

Spatially and spectrally resolved HF measurements from space have numerous applications in disciplines beyond planetary science.

Heliophysics. Observations of the polarization, refraction field and angular broadening properties of the cosmic radio sky carry information on the plasma within the heliosphere. A small interferometric array of spacecraft equipped with FIRMI would provide images of solar burst radio emission source regions. FIRMI's frequency range would enable spatially resolved tracking of Type II radio bursts farther from the solar corona than is currently possible.

Earth Observation. Of radio emissions from the Earth, auroral kilometric radiation (AKR) is the strongest distributed source. The FIRMI instrument in an appropriate orbit would observe and locate AKR and provide polarimetric measurements. FIRMI will also be capable of top-side sounding the terrestrial ionosphere as well as detection and localization of some terrestrial plasma wave phenomena.

Astrophysics. FIRMI would provide a capability that for the first time could enable cost-effective long baseline astronomical radio interferometry in the < 10 MHz window, which is inaccessible from the ground due to the ionospheric cut-off frequency. These observations can be especially useful for studies of the interstellar medium where propagation effects are large, allowing observations of dispersion measure, interstellar turbulence, and interstellar free-free absorption. A moderate resolution map of the low frequency sky (better than 60° angular resolution achieved by RAE-2) would be a significant step forward.

References:

[1] Wong K T and Zoltowski M D (1997) *IEEE Trans. Antennas Propag.* **45** 1467–74. [2] Robey F C (2012) HFGeo Phase 1B Proposers' Day Briefing: HFGeo Phase 0 and Phase 1B Test and Evaluation. [3] King R (1959) *IRE Trans. Antennas Propag.* **7** 53–61. [4] Meloling J H et. al. [5] Chyba C F et. al. (1998) *Icarus* **134** 292–302. [6] Walker C C et. al. (2010) *2010 IEEE International Geoscience and Remote Sensing Symposium* (IEEE) pp 4522–5. [7] Léveillé R J and Datta S (2010) *Planet. Space Sci.* **58** 592–8.

Dust Sensor with Large Detection Area Using Polyimide Film and Piezoelectric Elements. M. Kobayashi[1], O. Okudaira[1], K. Kurosawa[1], T. Okamoto[1] and T. Matsui[1], [1]Planetary Exploration Research Center, Chiba Institute of Technology (2-17-1, Tsudanuma, Narashino, Chiba, Japan 275-0016; kobayashi.masanori@it-chiba.ac.jp).

Introduction: Dust that escapes from gravitational sphere of the celestial body exists in the interplanetary space and is observed as various events. For instance, there are some dust particles from comets, satellites and so on.

Dust particles from comets are observed as a meteor stream when their orbit intersects with the earth orbit, the night sky will be colored as a meteor stream. However, the dust trail of comet has never directly been observed except for such special case as meteor stream.

On the other hand, for dust particles from satellites, some previous theoretical studies predict dust torus that Phobos and Deimos supply with dust particles over those satellites orbits. However, they have not been discovered yet.

Those are important events for understanding the material transfer of inside the solar system. However, sensor to be onboard on spacecraft is difficult from the viewpoint of the resource requirement to the spacecraft system because large detection area (> $1m^2$) is necessary to observe dust particles (tens of micron to millimeter) which exist in low spatial density. Pegasus mission had such large detection area for observe meteoroids in space as environment assessment before Apollo mission [1], and there have been no similar mission performed after that.

For enlargement of detection area, previous works used a metallic plate at which incident dust particles collides and vibration is induced and the vibration is detected with piezoelectric elements as dust particle hit signals [2]. Assuming aluminum plate, sensor using metallic materials with > $1m^2$ detection area has a mass of greater than 2 kg which is unreasonably heavy just for detecting medium.

Using non-metallic materials, we developed several type of large area dust sensors [3] [4]. ALADDIN uses piezoelectric polyimide PVDF having 30cm x 30 cm detection area and had successful observations in the interplanetary space. The PVDF sensor converts mechanical impact of incident dust particle to electrical signal and the following electronics read out the signals as dust particle impact. However, PVDF has a large permittivity and a thin film sensor has a large capacitance which is like to induce electrical noise. On the other hand, SDM is a penetration type sensor which is a polyimide film having thin strip electrodes on [4]. When the incident dust particle penetrates the sensor film and breaks electrode(s), the broken electrodes can be detection by applying current and then one can estimate the size of the incident dust particles from the number of broken electrodes. SDM has been onboard HTV-5 (5^{th} H-II transfer vehicle) for demonstration flight. SDM worked extremely well. However, the electronics is not simple and needs more resource requirement.

In this paper, we describe a dust particle sensor with a large detection area (1m x 1m scale) using just a film of polyimide (10 – 20 μm in thickness) attached with pieces of piezoelectric elements (~2 cm) as pick-up sensor.

Measurement principle: Figure 1 illustrates measurement principle of a sensor of our current work. We use a polyimide film (no piezoelectricity, no electrodes, and just normal polyimide) and small tips of piezoelectric element adhesively attached on the film. When an incident dust particle hit on the film and penetrate, stress waves occur in the film material and propagate away from the penetration points. When the stress wave reaches a tip of piezoelectric sensor and some of the stress wave energy transfer to the piezoelectric sensor, oscillation is induced in the sensor and is converted to electric signal which is read out by the following electronics. The piezoelectric sensor picks up the stress waves caused by the incident dust particle. Assuming the pick-up sensor has a dimension of 20 mm x 20 mm x 2mm, the electric signal has two components in frequency; 200 kHz and 1.1 MHz for thickness and radial direction oscillation, respectively.

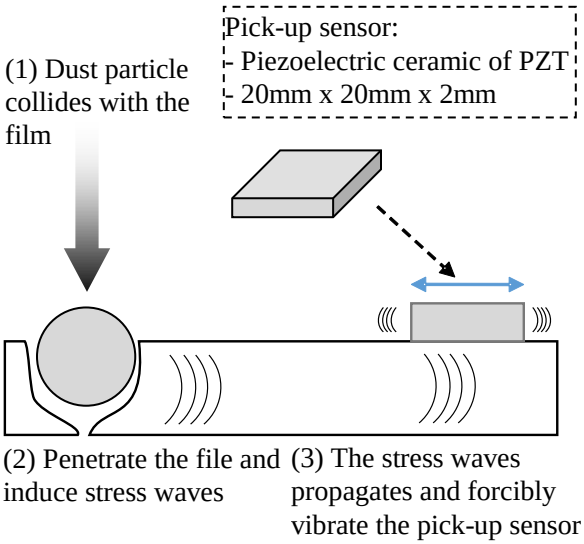

Figure 1 Principle of dust particle detection

Experiments: We performed two experiments that microparticles were accelerated to hypervelocity speed using two-stage light gas gun, one is from ISAS, JAXA and another from PERC, CIT. In the experiments, we had micro particles (150 μm to 3 mm) accelerated up to 4 – 5km/s. The first experiments used a sensor of SDM prototype and four pick-up sensor on the corners, while the second experiment used a multi-layer insulator, typical thermal device for spacecraft, three pick-up sensors were attached at the apex of a triangle on a rectangular MLI. Figure 2 shows an example of results, the measurement of raw signal from a pick-up sensor (top), calculated FFT spectrum (middle) and filtered signal with 200 kHz band pass (bottom). Applying the band pass filter makes clearer signal detection and timing determination.

The propagation speed of stress wave in the film is constant (~2.6 km/s) and the penetration point as "sound source" can be positioned by a typical algorithm of sound source positioning using the arrival times of stress waves at multiple pick-up points. Figure 3 shows four examples of actual penetration points (star) and ones derived from positioning algorithm (red diamond). In that example, there are three pick-up sensors located at "+" positions to detect signals to determine arrival timing of the stress waves. Actual penetration points and calculated ones have a good agreement within 1 cm.

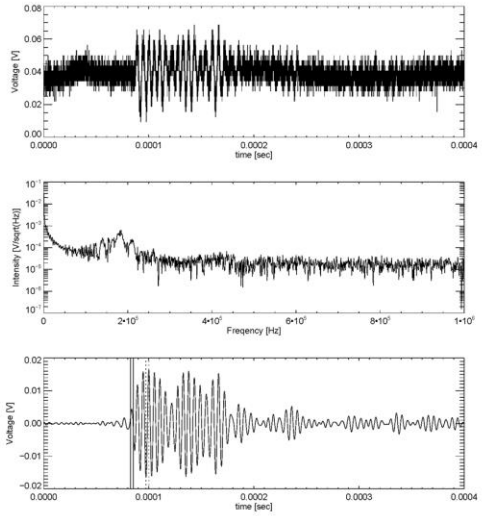

Figure 2 Example of experimental results

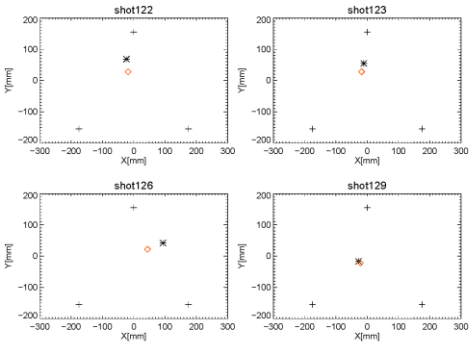

Figure 3 Positioning of penetration point

Future prospective: The polyimide film as detection medium can be easily expanded to observe large-sized micro particles (> 10 μm) of which the statistics is lower than one of smaller particles. The sensor of the current works uses just a typical polyimide film and piezoelectric elements as pick-up sensor. Exploiting those characteristics, MLI which covers a spacecraft can be a large-area dust particle sensor being attached piezo electric elements without significant resource impact on spacecraft system.

References: [1] Naumann, R. J. "Pegasus satellite measurements of meteoroid penetration (February 16 - July 20, 1965)", NASA-TM-X-1192. [2] Auer S. : "Instrumentation in Interplanetary Dust", eds. E. Gruen, B. A. S. Gustafson, S. F. Dermott and H. Fechtig (Springer-Verlag, Berlin, Heidelberg, 2001) p. 385. [3] Takayuki Hirai, Michael J. Cole, Masayuki Fujii, Sunao Hasegawa, Takeo Iwai, Masanori Kobayashi, Ralf Srama, Hajime Yano,"Microparticle impact calibration of the Arrayed Large-Area Dust Detectors in INterplanetary space (ALADDIN) onboard the solar power sail demonstrator IKAROS", Advances in Space Reaech, Vol.100, Pages 87–97, 2014. [4] Maki Nakamura, Yukihito Kitazawa, Haruhisa Matsumoto, Osamu Okudaira, Toshiya Hanada, Akira Sakurai, Kunihiro Funakoshi, Tetsuo Yasaka, Sunao Hasegawa, Masanori Kobayashi: "Development of In-Situ Micro-Debris Measurement System", Advances in Space Research, Volume 56, Issue 3, 1 August 2015, Pages 436 - 448 (2015).

MINIATURE DUAL-MODE ABSOLUTE SCALAR MAGNETOMETER BASED ON THE RUBIDIUM ISOTOPE ^{87}Rb. H. Korth[1], K. Strohbehn[1], J. Kitching[2], [1]The Johns Hopkins University Applied Physics Laboratory, Laurel, Maryland, USA. [2]National Institute of Standards and Technology, Boulder, Colorado, USA.

Introduction: The magnetic field is a fundamental physical quantity, and its precise measurement plays a central role in addressing the scientific objectives of many planetary, solar, and interplanetary science missions. Magnetic fields in space have been measured by fluxgate magnetometers, proton-precession magnetometers, and optically-pumped magnetometers. The measurement technique in the latter two categories is based on absolute frequency standards and does not require calibration. As such, the instruments provide an ideal in-flight calibration source for fluxgate magnetometers on missions that necessitate ultra-precise measurements or which are of extended duration. However, a major disadvantage of atomic magnetometers, i.e., proton-precession and optically-pumped instruments, is their significant mass and high power requirements, which effectively prevent their routine use in space. Hence, to allow for more widespread use of atomic magnetometers in space, mass, size, and power consumption of these instruments must be substantially reduced.

In response to an on-going paradigm shift in space research, we have developed a low-resource, miniaturized, absolute scalar magnetometer based on the rubidium isotope ^{87}Rb. Our instrument takes advantage of recent breakthroughs in micro-fabricated atomic devices, which have demonstrated reductions of power requirements and mass by one to two orders of magnitude over conventional instruments. The resulting instrument has a total mass of 210 g and uses <1 W of power, while maintaining sensitivity, 15 pT/√Hz at 1 Hz, comparable to present state-of-the-art absolute magnetometers.

Hardware Description: Most atomic optically-pumped magnetometers are based on the Larmor precession of electron or nuclear spins in a magnetic field [1]. A cell containing a suitable gas is illuminated with light with a wavelength that correspond to resonance with an optical (electronic) transition in the atoms. Under these conditions, atoms are optically pumped into a non-thermal population distribution and the gas cell becomes largely transparent to the optical beam. If the cell is then subjected to a radio frequency (rf) signal at the Larmor precession frequency, an oscillating population distribution is excited within the atoms, which causes a time-dependent modulation of the optical absorption. By detecting the phase shift (M_x mode) or the amplitude (M_z mode) in the resonance of the atomic response, the Larmor frequency can be

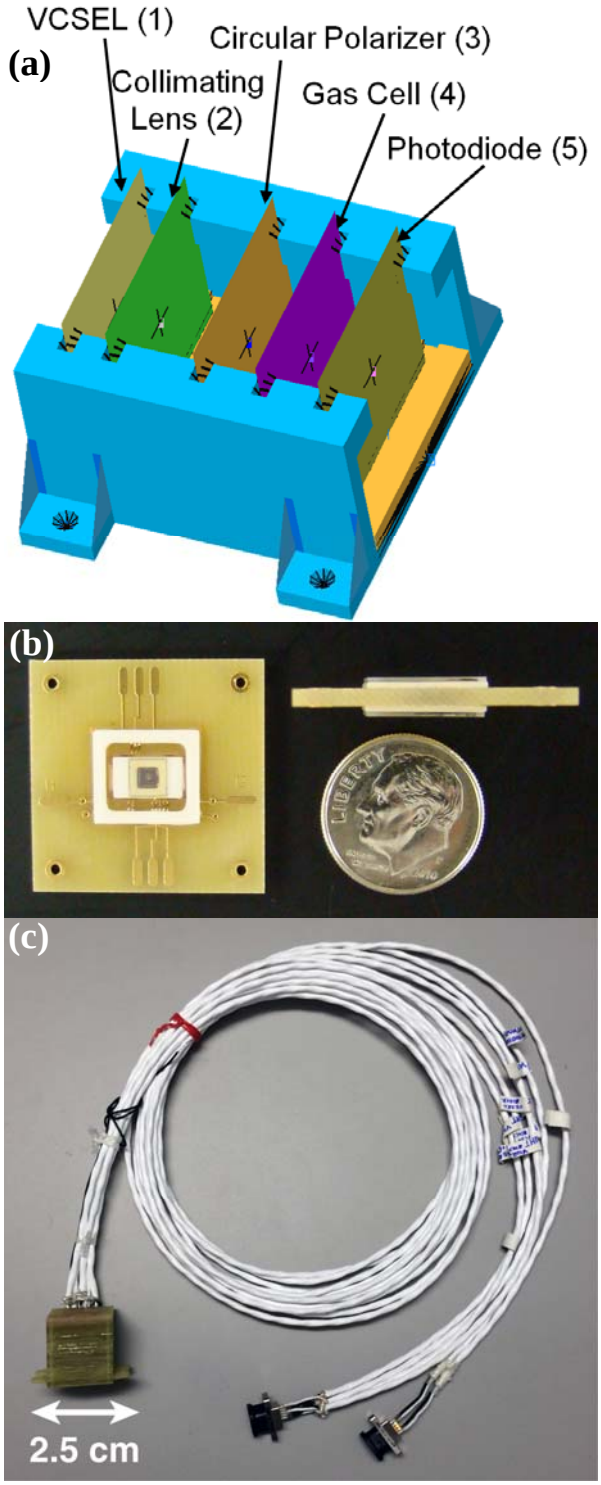

Figure 1: Atomic magnetometer (a) configuration, (b) vapor cell assembly, and (c) sensor.

determined and from that the magnetic field can be deduced. Our sensor technology is based on the isotope ^{87}Rb selectively uses M_x- or M_z-mode magnetic field detection.

Our device [2] employs a low-power semiconductor laser and a miniature rubidium vapor cell of millimeter dimensions produced using modern micro-fabrication processes [3]. In recent years, MEMS vapor cells have been employed in chip-scale sensitive magnetometers [4]. The combination of MEMS vapor cell and a semiconductor diode laser has allowed a substantial reduction in mass, size, and power dissipation of atomic magnetometers with only modest decrease in performance. The MEMS vapor cell has been integrated into a magnetic field sensor configured as shown in Figure 1a. The micro-fabricated rubidium vapor cell (4) is illuminated by light emitted from a vertical-cavity surface-emitting laser (VCSEL) (1). The laser light passes through an optics package, where the laser light is collimated (2) and circularly polarized (3). The resonant response of the atoms is detected using a discrete photodiode (5). The assembled prototype sensor, shown in Figure 1c, measures 35 × 25 × 25 mm^3 and has a mass of 40 g without harness; future reductions in size and mass are anticipated.

An additional key aspect in the miniaturization of the device is the monolithic integration of the vapor cell with heaters and Helmholtz coils using silicon-on-sapphire (SOS-CMOS) technology. The latter are glued to the two faces of the vapor cell perpendicular to the optical axis. The SOS-CMOS technology was chosen because the sapphire substrate is intrinsically transparent to the light emitted at the wavelength of the laser. The SOS-CMOS chips heat the vapor cell to its operating temperature of about 100°C using 0.5 W of power generated by a 10 mA current from a 50 V power supply. Even though the heater current is low, extreme care must be taken in the implementation of the heater because the flow of current generates a contamination magnetic field in close vicinity of the detection volume. To minimize interference with the measurement of the ambient field, the integrated conductor widths and spacing are on micrometer scales, and near-perfect magnetic compensation was achieved using two sets of dual square loops arranged in neighboring conducting layers of the chip. The contamination due to the heater was measured to be less than 10 nT, and comparison with numerical calculations shows that the finite residual field is largely due to limitations in the accuracy of the alignment of the two SOS-CMOS dies. The second function of the SOS-CMOS die is to generate the rf magnetic field necessary to establish the atomic resonance via a single-turn circular coil. To maximize the uniformity of this field across the detection volume, the coils of both SOS-CMOS dies are sized to yield the Helmholtz arrangement, where the coil radius matches their separation prescribed by the thickness of the vapor cell. Finally, the SOS-CMOS die includes circuits to support temperature measurements and signal conditioning. The system reported in this paper does not use the latter electronic circuits to stay compatible with external instrumentation. The assembled vapor cell including transparent SOS-CMOS dies is shown in Figure 1b.

The sensor is controlled by a dedicated electronics and software in an FPGA, which generates the signals to excite the rubidium atoms within the vapor cell and measures and processes the resonant response at a rate of 10 samples per second. The prototype electronics are implemented on two 10×10 cm^2 printed circuit boards and has a mass of 170 g.

Performance: The sensor response to different step-like changes in the magnetic field magnitude between 0.5 nT to 2 nT is illustrated in Figure 2. The sensor has a sensitivity is 15 pT/√Hz at 1 Hz or about 0.1 nT rms. The prototype instrument demonstrates that absolute magnetometers can be miniaturized to serve future planetary missions even under severe resource constraints.

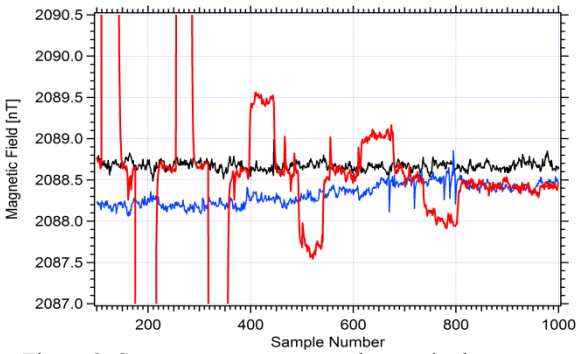

Figure 2: Sensor response to step changes in the magnetic field (red) vs. ambient field (black, blue).

References: [1] Bloom, A. L. (1962), Principles of Operation of the Rubidium Vapor Magnetometer, *Appl. Optics*, *1*, 61-68. [2] Korth, H., et al. (2016), Miniature atomic scalar magnetometer for space based on the rubidium isotope ^{87}Rb, *J. Geophys. Res. Space Physics*, doi: 10.1002/2016JA022389. [3] Liew, L. A., et al. (2004), Microfabricated alkali atom vapor cells, *Appl. Phys. Lett.*, *84*, 2694-2696. [4] Schwindt, P. D. D., et al. (2007), Chip-scale atomic magnetometer with improved sensitivity by use of the M-x technique, *Appl. Phys. Lett.*, *90*, 081102, doi: 10.1063/1.2709532.

IDENTIFYING AND QUANTIFYING MINERAL ABUNDANCE THROUGH VSWIR MICROIMAGING SPECTROSCOPY: A COMPARISON TO XRD AND SEM. E. K. Leask[1] and B. L. Ehlmann[1,2], [1]California Institute of Technology, 1200 E. California Blvd., Pasadena, California, 91125 (eleask@caltech.edu), [2]Jet Propulsion Laboratory, 4800 Oak Grove Drive, Pasadena, California, 91109.

Introduction: Visible-shortwave infrared microimaging reflectance spectroscopy is a new technique to identify minerals, quantify abundances, and assess textural relationships at sub-mm scale without destructive sample preparation. Here we used a prototype instrument (Ultra-Compact Imaging Spectrometer, [1]) to image serpentinized igneous rocks and carbonate-rich travertine deposits to evaluate performance relative to traditional techniques: XRD (x-ray diffraction; mineralogical analysis of bulk powders with no texture preservation) and SEM/EDS (scanning electron microscopy/energy dispersive x-ray spectroscopy; analysis of phases and textures using chemical data from polished thin sections). We summarize results discussed further in Leask & Ehlmann (2016) [2].

Methods: **S**amples from the Samail Ophiolite (Oman) are used as an analog for Martian carbonate and serpentine deposits [e.g., 3] to evaluate the ability of VSWIR microimaging spectroscopy to identify minerals present, distinguish carbonates of different chemistries from minerals with absorptions at similar wavelength positions, and to quantify mineral abundances. Rock samples were measured with UCIS over the wavelength range 0.5-2.5 µm, with 10 nm spectral resolution, and a pixel footprint of 81x81 µm (e.g., Fig. 1). Each sample takes ~3 minutes to image. Subsamples of each rock were sent to external laboratories (ActLabs, K-T Geoservices) for x-ray diffraction (XRD) analyses of powdered samples for mineral identification and quantitative abundance estimates. Two samples were polished, imaged with UCIS, then carbon coated, and imaged on a scanning electron microscope (SEM). Energy-dispersive spectroscopy (EDS) maps were obtained over the area of the sample, providing elemental abundance data for direct comparison with UCIS data.

Linear Unmixing. At this spatial scale, many pixels consist of a single mineral grain. As a first-order approximation, we use linear spectral unmixing [4] to estimate the abundance of phases, assuming most mixed spectra result from areal 'checkerboard' mixtures, where endmember spectra combine linearly, proportional to their areal abundance within a pixel. Endmember selection was refined until average RMS errors were under 0.05.

Mineral Identification: In 13 of 15 samples, UCIS identifies all the same major (>5% abundance) mineral phases as XRD analysis (Fig. 2). Exceptions are a very dark sample (002), where UCIS did not detect 10-19% olivine, and brighter sample (011), where UCIS did not identify ~6% quartz found by XRD. Notably, UCIS data reliably differentiated between carbonate minerals (calcite, dolomite, and magnesite) and serpentine with very similar overall spectra, based on the exact position of the 2.3µm absorption [5,6] (Fig. 2C). Specific carbonate minerals can be clearly distinguished when each phase extends over several pixels. UCIS also identified spatially coherent rare phases, below the detection limit of powder XRD. Several clasts in conglomerate sample 001 were identified as Al-bearing serpentine or chlorite due to a small 2.25-µm absorption (caused by Al/Mg-OH vibrational overtones [7]). EDS elemental mapping confirms that these clasts contain much more Al than other clasts. Distinctive 0.9-µm pyroxene absorptions [8; Fig 1C, 2B] are seen in samples 001, 007, and 009, though pyroxene is not detected by XRD. Most 'pyroxene' spectra show different degrees of partial alteration to serpentine (sharp 1.4- and 2.3-µm hydroxyl absorp-

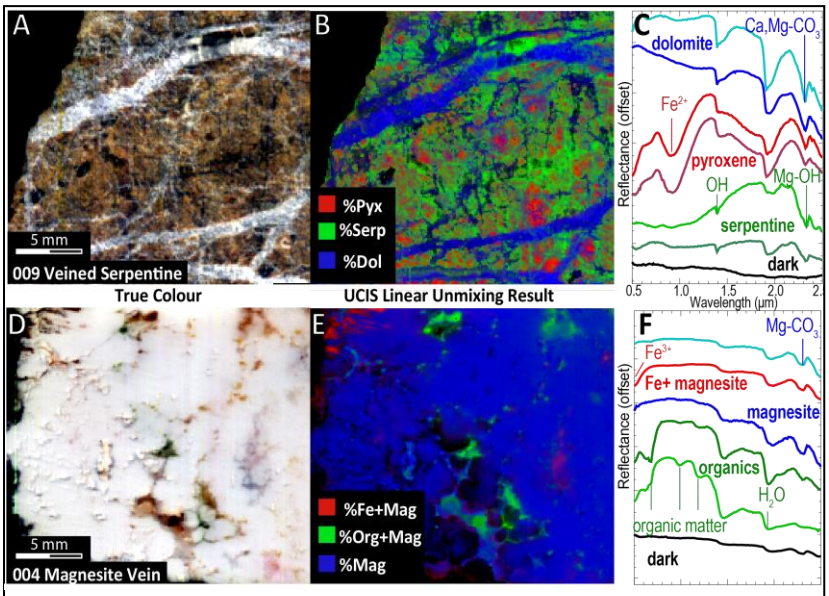

Fig.1. Linear unmixing examples. A-C: Veined serpentinite sample. Unmixing results (B) highlight veins and remnant pyroxene (endmember spectra shown in C). D-F: Magnesite vein sample, with organic matter (green) in porous areas.

tions; Fig. 1C, 1F). These are included in the 'amorphous' fraction of XRD results. In magnesite vein samples 004 and 008, absorption features consistent with organic matter are also noted—a sharp 'red edge' at ~0.8 µm from photosynthetic pigments and minor absorptions in the 1-2µm range associated with C-H (O), and N-H bonds [9] (Fig. 1F).

Mineral Quantification: Abundance estimates between UCIS and XRD are usually the same within 10-15% (median total difference per sample; see Fig. 2A). Scatter between multiple XRD analyses of different subsamples of the same rock is 5-10%. Given the heterogeneous nature of many of the samples (e.g., 001, 018, 021), natural variance in abundance is expected. For sample 001, areal abundances from EDS and UCIS can be directly compared. Here, determinations are very similar (EDS (UCIS)): 41 (42)% serpentine, 31 (25)% calcite, 21 (18)% mixed carbonate and serpentine, and 7 (14) % pyroxene.

Advantages of this technique: A key advantage of VSWIR microimaging spectroscopy vs. XRD is its ability to obtain mineralogical information with petrographic context, allowing process interpretation. Hence with UCIS, we can get a clearer picture of the bulk mineral composition in altered samples and the processes driving alteration by the ability to simultaneously detect the primary mineral and secondary product. EDS also retains spatial relationships, but requires a high degree of sample preparation, which is expensive and time consuming.

Conclusions: In this study, VSWIR microimaging spectroscopy combined with linear spectral unmixing provides estimates of quantitative mineral abundance consistent with abundance estimates from XRD and EDS. The UCIS prototype instrument demonstrated the ability to identify all VSWIR-active phases and differentiate between carbonate minerals and other minerals like serpentines with major absorptions in the same wavelength region. UCIS is especially well-suited to identify spatially coherent rare phases that would be missed by traditional techniques such as XRD, and tie products to reactants. It is an effective, rapid method to survey a set of samples with minimal preparation.

References:

[1] Van Gorp, B., et al. (2014) *J.App. Rem. Sensing 8(1)*, 084988. [2] Leask, E.K.and B.L. Ehlmann (2016) *8th IEEE WHISPERS.* [3] Ehlmann, B. L. and J. F. Mustard (2012) *GRL, 39(11).* [4] Heylen, R., et al. (2011) *IEEE Trans. on Geosci. Rem. Sensing, 49(11),* 4112-4122. [5] Gaffey, S. J. (1987). *JGR: Solid Earth, 92(B2),* 1429-1440. [6] Clark, R. N. (1999). *Man. rem. sensing 3*, 3-58. [7] Bishop, J., et al. (2008). *Clay Minerals, 43(1),* 35-54. [8] Cloutis, E. A. and M. J. Gaffey (1991). *JGR: Planets, 96(E5),* 22809-22826. [9] ASD Inc. (2013) http://cdn2.hubspot.net/ hub/45853/file-244381196-pdf/docs/near-ir_absorption_bands_chart.pdf?t=1454607097572.

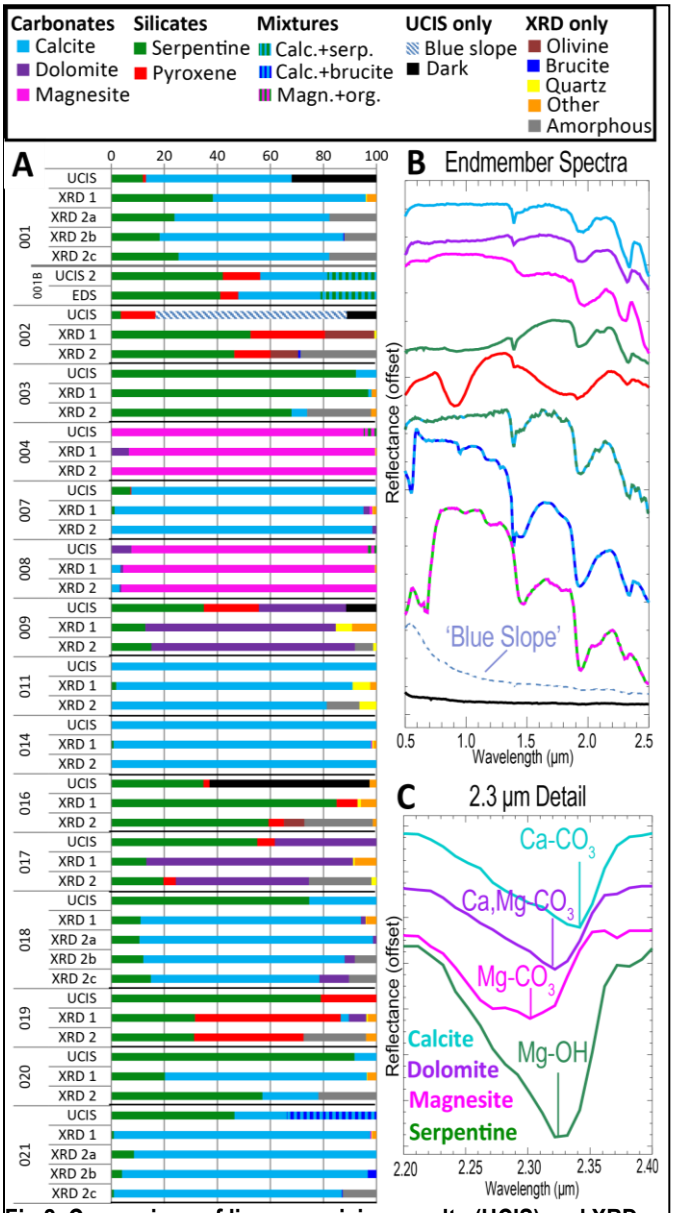

Fig.2. Comparison of linear unmixing results (UCIS) and XRD abundance estimates (A). B: Examples of endmember spectra used in unmixing. C: Zoom showing subtle differences in the 2.3µm absorption between carbonates and serpentine.

The Development of a Highly Integrated Imaging Payload for Space Weather and Maritime Monitoring. H. N. Lerman[1], I. B. Hutchinson[1], N. P. Bannister[1], M. McHugh[1], R. Ingley[1], M. Lester[1], D. Wright[1], S. Milan[1], C. Brunskill[2], D. Garton[2], [1]University of Leicester (Space Research Centre, University of Leicester, Leicester, UK, LE1 7RH, hnl4@le.ac.uk), [2]Satellite Applications Catapult (Satellite Applications Catapult, Harwell, UK, OX11 0QR).

Introduction: CubeSats have very challenging resource limitations (e.g. power, mass, volume and communication) but enable exciting opportunities to develop creative and innovative scientific experiments. Subsystems are required to be compact and efficient whilst being capable of achieving high levels of performance and reliability for various commercial, security and scientific applications.

The CubeSat payload development and optimization presented here is a multi-purpose imaging payload with powerful onboard processing capability that significantly reduces telemetry requirements. The camera is closely integrated with other subsystems to improve autonomy. The primary applications for this payload are space weather monitoring and maritime situational awareness, which both benefit from the acquisition of data at UV wavelengths.

Here, we discuss the results of initial experimental test and describe the optimization and capabilities of the CCD based, UV enhanced camera system, which is highly suitable for use in a compact and efficient CubeSat payload.

Space Weather Monitoring: The interaction of the Solar Wind with the Earth's magnetosphere produces characteristic signatures at UV and optical wavelengths in the auroral ovals of the Northern and Southern hemispheres. Measurements of these emissions provides an opportunity to monitor the magnetosphere activity and morphology, giving an insight into the physical nature of the processes involved. The energy exchange which results from such interactions between the Earth and Sun causes disruption to power transmission systems, causes damage to expensive spacecrafts in LEO, degrades GPS signals, and is a source of danger to astronauts. Hence it is advantageous to observe magnetospheric changes across a variety of timescales and to associate the activity with particular locations in the magnetosphere. For these measurements, the camera system is used in conjunction with a Microchannel Plate (MCP) Optic in a similar configuration to that used for the Mercury Imaging X-Ray Spectrometer onboard ESA's BepiColumbo mission.

Maritime Situational Awareness: The current methods utilized to track and identify vessels at sea are far from perfect. For example, the maritime Automatic Information System, a broadcasting signal which identifies identity and position of a vessel, can be switched off or altered to send incorrect information. Moreover, optical monitoring from space, although useful for spatial resolution and target discrimination, lacks reliability due to the changeability of the weather. However, the imager concept presented here is able to overcome some of these issues, as reported by Bannister and Neyland (2015) [1]. In order to achieve this, the imaging system utilizes data from both optical and near infra-red (NIR) wavelength channels, obtaining using a conventional lens/mirror based system.

Imaging Payload: The multi-purpose imaging payload incorporates a spherical MCP optic and a UV-sensitive CCD focal plane sensor with transmissive filters deposited on a CaF_2 window in front of the CCD. The optic consists of a spherically curved glass plate containing millions of precisely aligned hollow channels whose walls act as grazing-incidence mirrors, and is the key to realizing a low mass, compact instrument [2]. The detector is a full frame imaging device, which is UV enhanced/coated and compromises 2048x512, 13.5μm pixels. A thermal cooling and stabilization system is used to optimize dynamic range and overall performance. The selected detector exhibits a detection efficiency of greater than 50% across the UV wavelength range of interest, ideal for space weather monitoring. It also performs well within the range required for use in maritime domain awareness applications.

Camera Design: In order to facilitate rapid development and optimization of a range of different possible payload configurations, a 3D printer was used to manufacture suitable test environments for the detector/cooling system and optical benches for the lenses, filters and mirrors (see Figure 1, which shows the first re-configurable optical system that was used to verify the UV performance of the camera). The modular system is compact, low mass, light proof and cheap to fabricate. The FPGA based detector system generates all of the necessary biases and clocks required to operate the CCD and incorporates a CDS ASIC for sampling the output from the detector (a space qualified version is available). Low level data processing is performed on an FPGA in order to compress the data stream and generate the various data products that are required to provide appropriate control over the other subsytems. The FPGA is also used to provide closed loop control over the thermal cooling/stabilization sys-

tem and control over the various calibration sources used to characterize detector performance.

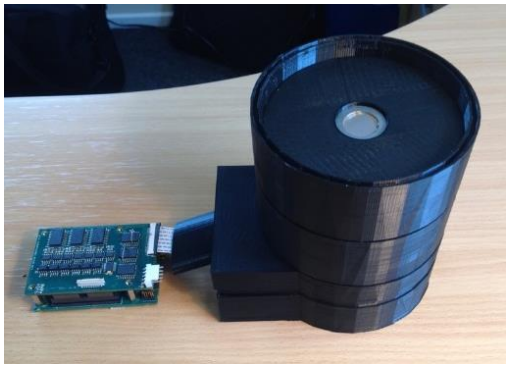

Figure 1: Camera electronics and detector enclosure. The mesh can be seen at the top of the enclosure.

Camera Performance: Initial tests focused on the verification of UV performance. A light-tight enclosure was fabricated and a UV filter and mesh were used along with a Cathodeon v03 deuterium lamp to deliver an appropriate intensity of wavelength constrained light at the focal plane. Dynamic range and detection efficiency measurements were made with the focal plane stabilized at a temperature of 290K. The data obtained were also used to verify the data processing algorithms developed in order to enable autonomous control of the platform. The optical performance of the UV optic was also investigated using the detector/camera system.

A number of different detector operating modes have been investigated during the tests, including on-chip binning, windowing and frame transfer. Early results indicate good UV response and overall instrument dynamic range. We have also investigated the overall performance of particular instrument configurations using instrument radiometric models in conjunction with a detector simulator. The software accounts for specific operating modes and detector noise sources and simulates the expected output given a particular operating scenario and input light field. A typical image obtained with the camera system is shown in Figure 2. The low intensity bands on the left and right of the image are calibration pixels that are not associated with light sensitive parts of the detector. The image incorporates two, 100 row windows on the surface of the detector. Light intensity increases from the bottom to the top of each window and can be used to generate a photon transfer curve for the system (verifying the gain and noise of the system).

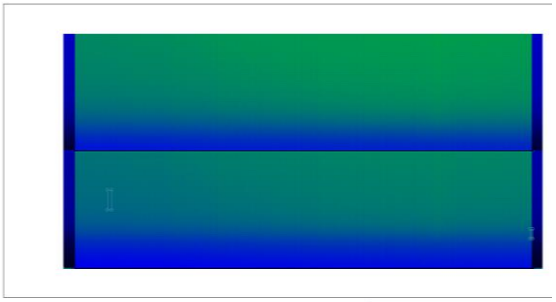

Figure 2: Camera image obtained with the detector/drive electronics, illustrating windowed operation.

References: [1] Bannister N. P. and Neyland D. L. (2015) *IJRS*, *36*, 211-243. [2] Bannister N. P. et al. (2007) *Ann.Geophysicae* 25, 519-532.

Onboard Science Techniques to Optimize Science Data Retrieval from Small Spacecraft. J. Lightholder, D.R. Thompson, W. Huffman, J. Boland, S. Chien, J. Castillo-Rogez, Jet Propulsion Laboratory, California Institute of Technology, (4800 Oak Grove Drive, Pasadena, CA 91109, {jack.a.lightholder, david.r.thompson, justin.s.boland, steve.a.chien, julie.c.castillo}@jpl.nasa.gov).

Introduction: As small spacecraft begin to travel beyond low earth orbit, mission planners are likely to encounter platform constraints that may adversely affect operations and instrument design. These include limits to instrument aperture, low communications bandwidth, and attitude control. Compensatory software based strategies for mitigating these limitations have recently been introduced in order to make efficienct interplanetary small spacecraft a reality. These strategies move the zero-order science data analysis, traditionally completed on the ground, onboard the spacecraft. Moving the science analysis to the spacecraft allows for significant reductions in required bandwith for sending crucial scientific data products. These techniques have additional potential for integration into larger interplanetary missions for increasing overall mission science return.

Goal: Developing software solutions to optimize science return in resource consrained missions is the focus of this work. The Near Earth Asteroid (NEA) Scout mission, launching in 2018 with the Space Launch System Exploration Mission 1, will demonstrate these capabilities as critical mission components.

This 6U CubeSat propelled by a solar sail will perform the reconnaissance of a near earth asteroid via multispectral imaging in the visible. Onboard science techniques at being impemented for detection, navigation towards, and obsrvation of the target. Several unique challenges of the small platform make this objective challenging. First, the encounter will take place at about 1 AU from earth where the downlink rate afforded by the CubeSat is a mere 1 kbps. In addition, the small mass and large solar sail makes stable pointing difficult, so that the Attitude Control System (ACS) will be challenged to achieve the pointing precision needed for long camera integrations to detect the target when in range. Finally, the cubesat platform also requires low instrument mass, compounding the detection challenge. Novel onboard science data analyses will permit image coalignment and coaddition, improving the effective sensitivity without bandwidth requirements of downlinking large image sequences. Automatic coalignment provides resilience to cosmic ray artifacts as well as ACS-induced drift.

Methods: In order to be practically deployed on flight hardware the NEAScout Science toolkit must have a small working memory footprint as well as minimal power requirements. The techniques can broadly be categorized as (1) image radiometric calibration and (2) target detection. Each of these processes is completed onboard the spacecraft, permitting efficient downlink of the finalized scientific data products.

Radiometric Calibration: Flight calibration of optical instrumentation is not a new challenge. However, to optimize volume, cost, and complexity, a shutter has been omitted from the NEAScout Science Imager. While this poses challenges for the collection of dark current and flat fielding frames, the Agile Science toolkit includes an image co-addition software capability which works as a median filter across an image set. Dark current reference frames can be generated without the use of a shutter by taking a collection of zero second exposure images and using co-addition to create a single high fidelity reference frame for dark current subtraction. This process simultaneously eliminates single image events such as cosmic rays. Flat fielding is handlded with pre-launch laboratory calibration in conjunction with non-illuminated pixel querying in flight. By querying these non-illuminated pixels, radiation degredation of the detector can be characterized and adjusted for. These areas will be characterized for stray light preceeding launch and will act as a reference to characterize radiation decay. Detector specific radiometric calibration characterization routines has been written into the science software with coefficients updated automatically in flight based on the results of preceeding flat field and dark current investigations. The generation and processing of calibration data in flight eliminates the need to send these frames to ground for scientific calibration under nominal science operations.

Target Detection: Strategies for early target detection utilize software functionality to support the limited aperture camera equipment available to small spacecraft platforms. Small aperture systems on a spacecraft with minimal pointing accuracy would challenge traditional optical navigation on these platforms; they would reduce single-frame image sensitivity to below the level needed for timely detection of a wide range of small, dark primitive body targets. We address this challenge with software strategies for early target detection that are appropriate for the limited aperture camera equipment available to small spacecraft platforms.

The first step in target detection is to increase the fidelity of the acquired data. This is accomplished with image coaddition on at least ten images taken in rapid sucession. For the NEAScout target at nominal detection distance, these images must carry a signal to noise ratio of 5. The brightest point sources persistent across all images (bright stars) are then identified as image anchor points. The row/column shift between any two images can then be determined by calculating the shift in centroid for any reference star between two images. We search for the optimal cross-correlation over a finite search window based on the expected travel distance of the starfield. Once these shift parameters are known for each image pair, the images are aligned and pixel values are combined. Coaddition is then performed on the aligned stack, increasing the signal to noise ratio to 7 [1]. In addition to increasing the fidelity of the data, the combination strategy uses a triplet-median method that filters single-pixel anomalies such as cosmic rays. This also reduces memory requirements because it is never necessary to store more than a few frames in memory at one time.

A more ambitious objective is to detect the target onboard, so that only the target row and column image coordinates need be downlinked. This involves two coadded image stacks acquired with a time difference permitting a shift in the target across the stationary starfield. Applying a pixel value subtraction between the aligned images will eliminate the background starfield, leaving only the target as an illuminated point source. The coordinate of the point source centroid is then recorded as an onboard data product for later use [2].

Onboard instrument calibration and target detection allow for controlled testing of onboard autonomous systems. The results of these processes, and their intermediary data, are stored onboard to be queued for downlink as needed. Because of the size of resulting data products, they can easily be downlinked for terrestrial validation by the spacecraft team.

Implementation: In order to be practically deployed on CubeSat-class flight hardware the Agile Science toolkit must have a small working memory footprint as well as minimal power requirements. The computer and data handling (C&DH) subsystem onboard NEAScout was in part designed to enable agile science processing. It offers dual core processing with 134 MIPS in full duplex and peak power < 7W.

Testing: The NEAScout software continues to meet mission expectations as the flight ready distribution undergoes testing. Testing involves both synthetically generated data and past mission data available on the Planetary Data System. These include the New Horizons data from the Long Range Reconnaissance Imager (LORRI) upon approach to Pluto [3]; the Rosetta mission encounters of Steins[4] using the wide angle camera and 67P using the navigation camera [5]. Coaddition achieved anticipated improvements in SNR as more images were analyzed. Applying the detection algorithm to raw (uncalibrated) mission data, target detection rates over 95%. Failures are typically due to the unavoidable case of a target obscured by a point source in the star field, resulting in the target being subtracted away with the background star field. This condition can be detected in the resulting data product, which will not conform to mission specific expectations with respect to brightness and general target area. The process for reacquiring the target is to repeat the analysis process with another coadded image stack, taken at a different time. The occurrence rate of this boundary phenomenonpathological case is related to the density of background stars in the reference frame. This can be controlled with exposure time of the images, a mission specific parameter which can be determined before launch or adjusted in flight.

Conclusions: As smaller spacecraft conduct interplenatary travel, communications bandwidth, ACS-inducted drift, power and instrument volume constraints will increasingly hinder the volume of scientific return. Here, novel software addresses the problems of limited ground contact on interplanetary missions as well as the inherent physical limitations imposed by small spacecraft platforms. A unified software solution addresses both problems with minimal software infrastructure overhead.

More generally, moving well-defined data analysis onboard the spacecraft allows for more efficient and effective human interaction while preserving the critical decisions for the human controllers. By reducing the data volume required to downlink for practical scientific decision making, operations teams can access the scientific return of a mission in significantly reduced timescales when compared to the status quo defined by larger missions' science downlink strategies.

References: [1] Huffman W. et al. (2015) The Astronomical Society of the Pacific [2] Thompson D. et al. (2012) *SpaceOps [3]* Cheng A. (2014) NASA Planetary Data System, 2014 *[4]* Hviid S. et al. (2011) ESA Planetary Science Archive [5] Geiger B. (2015) NASA Planetary Data System

AN INFRARED MULTIWAVELENGTH LIDAR FOR COMPOSITIONAL MAPPING. P. G. Lucey[1] ,X. Sun[2], S. X. Li[2], K. Numata[2], E. Mazarico[2], G. A. Neumann[2], J. B. Abshire[2], and D. E. Smith[3], [1]Hawai'i Institute of Geophysics and Planetology, University of Hawai'i at Mānoa, 1680 East-West Road, Honolulu, HI 96822, USA (lucey@higp.hawaii.edu),.[2]NASA Goddard Space Flight Center, Greenbelt MD 20771 USA, [3]Massachusetts Institute of Technology, Cambridge MA, USA

Introduction: Infrared spectral remote sensing has been a mainstay of planetary exploration with its combination of high spatial resolution and rich compositional information content. To date these data have been obtained passively, using spectrometers that exploit solar reflected or thermally emitted photons as the light source. While passive spectral imaging is an exceedingly powerful technique, it is not without its shortcomings. Chief among them are the limitations imposed by the temperature of the source or the intensity of the sun, and the need to photometrically normalize the data which can lead to artifacts or poorly known uncertainties.

A lidar carries its own light source and overcomes these limitations. For example, while limited imaging is available in the permanently shadowed regions of the Moon using light reflected off nearby illuminated surfaces [1,2] quantitative single wavelength reflectance data in regions of permanent shadow are available from the LOLA and MLA laser altimeters [3,4]. These single band laser reflectance measurements can be compared across the entire data

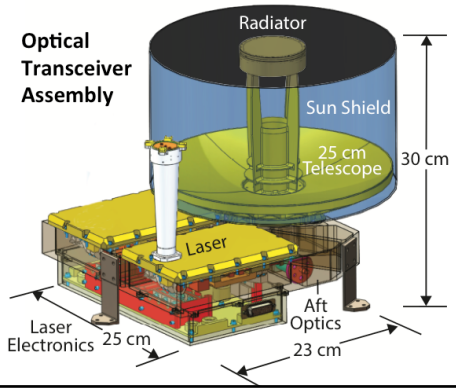

Figure 1. Schematic of multiband laser

sets without the need for any photometric normalization that might, for example, obscure latitude dependent spectral trends. For example, data from LOLA reveals that permanently shadowed regions are brighter than those that receive some illumination, but scattered light imaging using LROC has been unable to detect these subtle differences.

While LOLA and MLA (and MOLA) measurements are single band, obtaining multiple wavelength measurements is now possible (e.g. [5]). Recently we have been developing laser and detector technology to emphasize the 3 micron region of the spectrum most sensitive to water and other volatile species, including methane and simple organics, and to collect data not just in a single band, but at up to 7 wavelengths.

LIDAR Development. Any laser remote sensing system requires both a laser and a receiver and at Goddard we have been developing both for operation in the 3 micron region.

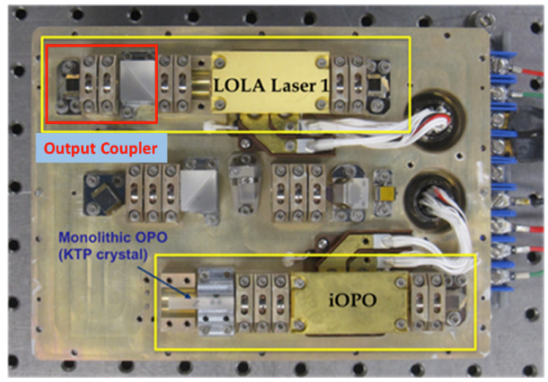

Figure 2. IOPO laser design (*bottom*) in comparison to the LOLA laser (*top*). The IOPO laser is almost identical to the LOLA laser except for the wavelength conversion section.

Lasers. We have been developing two technologies in parallel, each of which converts a 1064 nm laser to infrared output. The two related technologies are Optical Parametric Amplifiers (OPA) [6] and Intracavity Optical Parametric Oscillators (IOPO) [7]. In both cases a LOLA-like pulsed laser provides the principal input energy to a non-linear crystal that accomplishes the down-conversion of the light to infrared wavelengths. The OPA system contains more subsystems, requiring near-IR seed lasers to select the 3 micron region wavelengths, but only requires a single pump, while the IOPO system is simpler and more compact, but imposes more constraints on the choice of the output wavelengths and requires a LOLA-like pump laser for each pair of near-IR and 3 micron region outputs. The TRL of the IOPO approach benefits from the flight heritage of the LOLA laser.

Figure 3. Integrated detector-cooler assembly (IDCA) from the InVEST program for an in-space demonstration on a 3U CubeSat. The IDCA is 8x8x20 cm in size and consumes 7-10 W electrical power.

Detectors. For several years we have been developing infrared lidar detectors based on HgCdTe avalanche photodiodes under the NASA ESTO (Earth Science Technology Office) IIP (Instrument Incubator Program) [8]. This effort has led to small (up to 2x8 and 4x4) arrays of pixels well suited to the spectral detection task. These detectors are sensitive from 0.4 to 4.5 microns and are much more sensitive than the Si APD detectors used in LOLA. These detectors have been successfully used in airborne methane and CO2 lidar measurement campaigns in the laser few years. We are currently qualifying a version of these detectors for the InVEST program for a Cubesat in-space demonstration.

Unique Features. The multiple wavelength lidar system is immune to solar and thermally emitted radiation from the target surface because of the extremely short pulse durations (a few nanoseconds). During the brief laser pulse, the laser is much more intense than the natural sources of radiation. Therefore, day and night measurements can be directly compared.

Proof of Concept: We have conducted experiments demonstrating the technique, and to measuring very small amounts of surface frost condensed from water vapor onto cryogenically cooled lunar simulant. These measurements were supported by the NASA GSFC IRAD program. For these experiments we modified an optical parametric amplifier (OPA) laser that was originally developed for an airborne methane lidar [6]. We added more diode seed lasers to obtain additional wavelengths. This allowed the OPA output to span several wavelengths across the 3 µm water ice absorption band. Some preliminary results are shown in Figure 4.

Applications: For the Moon, reflectance measurements near 3 µm can definitively answer the question of whether water is mobile by comparing

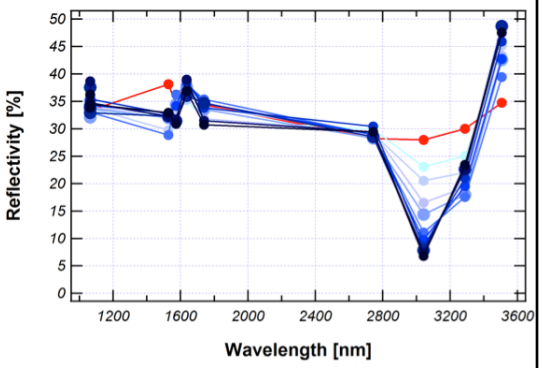

Figure 4. Initial results from laser reflectance measurements made to lunar simulant at ~160 K. The different colors indicate reflectance measured to the cold surface exposed to increasing numbers of water vapor injections, or "loads"

band depths during both day and night. At Io, the instrument can uniquely measure the reflectance of active lava lakes. For icy satellites and Trojans, the instrument can provide high quality characterization of volatile migration by comparing day and night reflectances and bands. For dense comet comae, lidar can measure in three dimensions the particle sizes and the ratio of ice to non-icy species, including organics and salts.

References: [1] Speyerer, E. J., and M. S. Robinson (2011), Analysis of highly illuminated zones near the lunar south pole, *Lunar Planet. Sci.*, **42**, Abstract 2540., [2] Chabot, Nancy L., et al. *Geophysical Research Letters* 39.9 (2012). [3] Lucey, P.G. et al. (2014), , *J. Geophys. Res. Planets* 119, 1665-1679. [4]Zuber, M. T. et al. (2012),., Nature, 486(7403), 378–81. [5] Cohen BA, Hayne PO, Paige DA, Greenhagen BT. Annu. Meet. Lunar Explor. Anal. Group. 2014 Jul 21:3031. [6] Numata, K. et al. (2012), *Journal of Applied Remote Sensing* 6(1), 063561. [7] Oshman, M. K. and S. E. Harris (1968), *IEEE J. Quantum Electron*. QE-4, 491–502. [8] Sun, X., J. B. Abshire, and J. Beck (2014), *Proc. SPIE* 9114.

SPATIAL INTERFEROMETERS FOR REMOTE SENSING AND IN SITU ANALYSIS. P. G. Lucey[1], R. Wright[1], C. Honniball[1], S.T. Crites[2], J. Cahill[3], B.T. Greenhagen[3], T. Glotch[4], [1]Hawai'i Institute of Geophysics and Planetology, University of Hawai'i at Mānoa, 1680 East-West Road, Honolulu, HI 96822, USA (lucey@higp.hawaii.edu), [2]Japan Aerospace Exploration Agency, Institute of Space and Astronautical Science, Kanagawa, Japan, [3]Applied Physical Laboratory, Johns Hopkins University, Laurel MD, [4] Geosciences Department, Stony Brook University, Stony Brook, NY

Introduction: Interferometers have been used as spectrometers in planetary exploration for decades, from Mariner 9 IRIS to MRO TES and MER miniTES, to CIRS on Cassini through IIM on Chang E' 1. Spectral interferometry has characteristics that are distinct from other spectral measurement techniques and broaden the design space for spectrometer applications. Among these characteristics are 1) an intrinsically broad spectral range, typically limited only by the sensitivity of the detector and transmission characteristics of the beamsplitter that is the heart of many such instruments; and when using detectors that are not limited by photon noise but by the inherent noise of the detector, interferometers enjoy a signal to noise advantage over other methods that is approximately equal to the number of bands collected.

While all but one planetary spectral interferometers have been based on the Michelson Interferometer, the IIM on the Change E' 1 lunar orbiter mission used a different approach interferometric approach to collect spectral information [1]. In the Michelson interferometer, the essential interference pattern from which the spectrum is derived is collected as a function of time; the IIM is a variety of so-called spatial interferometers where the interference pattern is collected by a detector array. As a class spatial interferometers have useful features compared to Michelson interferometers, chief among them being a lack of moving parts. The Michelson requires a precise mirror scanning mechanism as well as a fringe counting auxiliary laser system to measure the position of the mirror. With no moving parts, the spatial interferometer requires only a one-time wavelength calibration that can be done on the ground and checked using flight data.

While IIM collected data with a Si CCD, spatial interferometry is well-suited to the collection of data in the infrared portion of the spectrum. Large, low power array detectors are available in the form of microbolometers and thermopile arrays, both of which have rich flight heritage with filter based instruments (MRO THEMIS, LCROSS and LRO Diviner) and Michelson interferometers (Cassini CIRS). The spatial interferometer offers the designer an alternative to filter designs for multispectral or hyperspectral data collection with superior signal to noise ratios when band counts exceed about 10.

Experience with infrared spatial interferometers: Since 1990 the University of Hawaii has been experimenting with infrared imaging spectrometers based on spatial interferometry. Most of these interferometers were, like IIM, of the Sagnac variety but it appears that any interferometer can be used as a spatial interferometer.

We have produced imaging interferometer spectrometers in the 1-2.5 [2], 3-5 [2,3] and 8-14 micron regions [4], with both cooled and uncooled detectors, and used these for airborne hyperspectral imaging, in ground to ground field applications, and as

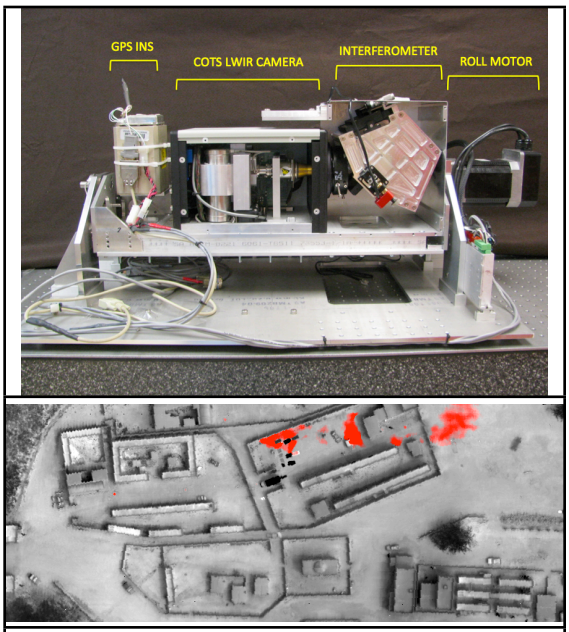

Figure 1. Top: Infrared airborne Sagnac interferometer using a cooled HgCdTe detector array. Bottom, in red, plumes of acetone evaporating from open pans.

spectral microscopes. Development has been supported by NASA PIDDP and IIP (Earth Sciences Instrument Incubator Program) and DARPA.

Airborne Applications: We have flown three types of Sagnac interferometers for airborne applications: one cryogenic instrument operating from 1-5 microns, an uncooled spectrometer using a microbolometer array, and a version with a cooled detector array and uncooled interferometer. The latter instrument was

developed under PIDDP funding and has the advantage of collecting high quality spectral data at high rates,

Figure 2. Backpack Sagnac spectrometer using microbolometer detector. Bottom, color composite of Mojave desert road, 9, 10, and 11 microns.

while not requiring cooling of the interferometer. Figure 1 shows an example of data collected with that instrument detecting acetone vapor.

Ground to ground applications: We have developed several portable instruments for field operations, in this case all Sagnac interferometers using low power microbolometer detectors for imaging data collection from 8-14 microns. Signal to noise ratios of these instrument are very high, with peak response over 1500.

Microsocope Applications: We have implemented an IR hyperspectral microscope using a Sagnac interferometer and have used it to scan lunar soils at 30 micron resolution. Figure 3 shows a variety of minerals detected using this system, including rare quartz and phosphate grains.

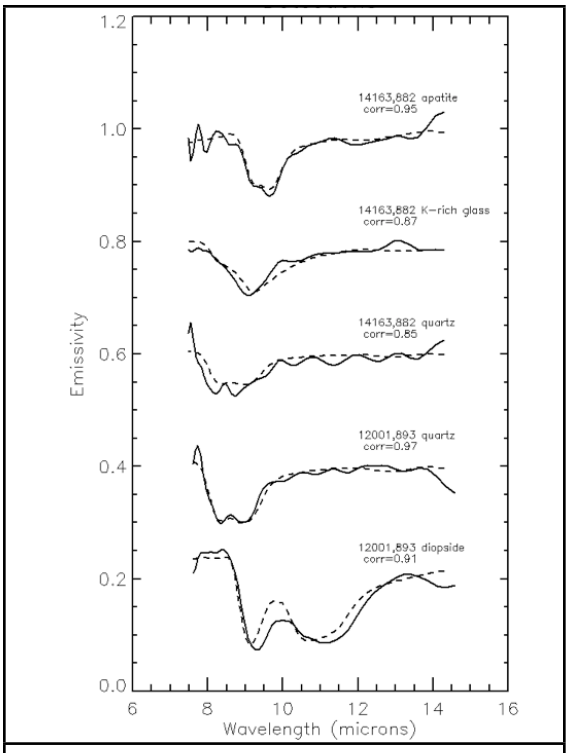

Figure 3. Lunar minerals detected with Sagnac interferometer used as a hyperspectral microscope.

Potential planetary applications: There are three niches we are pursuing with this technology: Spectral imaging from 5-200 microns for outer solar system applications; very high spatial resolution orbital imaging spectroscopy for inner solar system applications; and infrared hyperspectral microscopy for planetary landers.

Conclusions: The spatial interferometer occupies a unique niche for collection of hyperspectral data in the infrared with no moving parts and low power consumption. We have produced more than ten spatial interferometers of various designs and used all of them in field or airborne applications, demonstrating the ability of this technology to collect high quality spectral information. The low power and cooling requirements of this technology makes it ideal for planetary applications.

References: [1] Qiu, Y.H., Wen, D.S., Zhao, B.C., Chen, Z., Qiao, W.D., Acta Photonica Sin 38, 484-488, 2009, [2] Lucey P.G., Williams T., Horton K., Hinck K., Budney C., Rafert J.B., and Rusk T.B., Proc. of the Int. Symposium on Spectral Sensing Research, Gomez R.B. and McKim H., 1992. [3] Honniball CI, Wright R, Lucey PG, Crites ST, SPIE Defense Security 2016 [4]Lucey, P.G., Horton, K.A., Williams, T., Applied Optics, 47(28), F107-F113 (2008).

ENHANCED ENGINEERING CAMERAS (EECAMs) FOR THE MARS 2020 ROVER. J. N. Maki[1], C. M. McKinney[1], R. G. Sellar[1], R. G., Willson[1], D. S. Copley-Woods[1], D. C. Gruel[1], D. L. Nuding[1], M. Valvo[1], T. Goodsall[1], J. McGuire[1], J. Kempenaar[1], T. E. Litwin[1] ([1]Jet Propulsion Laboratory, California Institute of Technology, 4800 Oak Grove Drive, Pasadena, CA 91109, Justin.N.Maki@jpl.nasa.gov).

Introduction: The Mars 2020 Rover will be equipped with a next-generation engineering camera imaging system that represents an upgrade over the previous Mars rover engineering cameras flown on the Mars Exploration Rover (MER) mission [1,2,3] and the Mars Science Laboratory (MSL) rover mission [4]. The previous generation of Navcams and Hazcams, known collectively as the engineering cameras, were designed in the early 2000s as part of the MER development program. A total of 34 individual MER-style cameras have flown to Mars, built in two separate production runs: the original MER run (2003) and a second, build-to-print run for MSL (2008). Newer technologies and electronics parts obsolescence have brought the MER/MSL camera production to a close, with no additional production runs currently scheduled.

The Mars 2020 EECAMs utilize a 20 Megapixel color CMOS sensor, in contrast to the 1 Megapixel grayscale CCD sensor utilized by the MER/MSL cameras. The Mars 2020 Navcams, mounted on a pan/tilt mast, will acquire stereo color panoramas from a height of approximately 2 meters above the Martian surface. The Mars 2020 Hazcams, hard-mounted to the rover body at a height of approximately 0.7 meters above the surface, will acquire color stereo images of the areas immediately in the front and rear of the rover. The Mars 2020 Cachecam, a new camera type, will acquire images of sample materials as they are being processed by the Mars 2020 Sample Caching System. The more capable Mars 2020 EECAMs will help increase the overall efficiency of Mars 2020 rover operations on the surface of Mars. As with the MER/MSL cameras, the Mars 2020 EECAMs are being designed and built by the Instruments Division at the Jet Propulsion Laboratory in Pasadena, CA.

EECAM Instrument Functional Requirements: The Mars 2020 EECAMs inherit the same high-level functional requirements from MER and MSL. The Navcams are required to provide stereo image data for rover traverse planning, targeting of remote sensing instruments, operation of the robotic arm, and the acquisition of panoramas with a 360° field of regard around the rover. The Hazcams are required to provide stereo image data for the onboard detection of navigation hazards during a traverse, terrain context immediately forward and aft of the rover (in particular the areas not viewable by the Navcams) for traverse planning, support for robotic arm operations, support for rover fine positioning, and imaging of the front and rear wheels.

Instrument Description

The EECAMs incorporate proven heritage design principles from MER/MSL: 1) small, ruggedized camera bodies with fixed-focus lenses, 2) a simple camera head with limited processing and storage capabilities; the engineering cameras essentially function as sensor heads only, with image storage and compression functions performed by the spacecraft/rover computer, and 3) cameras mounted together as stereo pairs (the Cachecam, a monoscopic camera, is an exception). The Mars 2020 EECAMs are packaged into a single, compact camera head box (see figure 1).

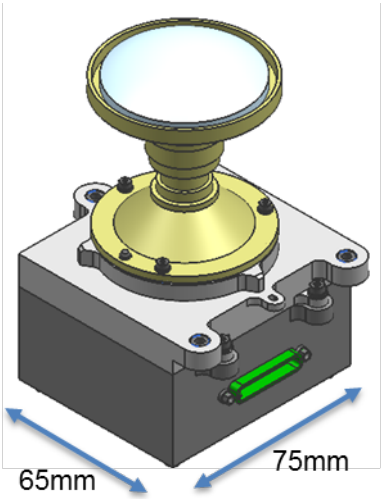

Figure 1. The basic EECAM design consists of a fixed focus lens mounted to a sensor head. Pictured above is the Mars 2020 Navcam camera.

The Mars 2020 EECAMs significantly improve on the MER/MSL designs by adding a CMOSIS CMV-20000, a 20 Megapixel color sensor with a 5120 x 3840 pixel imaging area. The EECAMS lenses have more resolving power than the older MER/MSL designs (as required by the smaller pixel size of the EECAMs), and in the case of the Navcams, also provide a wider field of view. The result of these enhancements is that the Navcam will have more than twice the angular resolution of the MER/MSL Navcam, and the Hazcam will have more than 3 times the angular resolution. Both cameras types will also

produce color images, with better antiblooming capability than the MER/MSL designs. In order to accommodate constraints on downlinked data volume to Earth, the EECAMs have the capability to return images at various reduced resolutions or at full-resolution, depending on the commanded mode.

Table 1. Mars 2020 EECAM Capabilities.
Items in brackets may change, pending final design.

Camera Capabilities	
Sensor Capabilities	
Type	20 MegaPixel CMOS
Optical Format	35 mm
Array Size	5120 x 3840 pixels
Pixel Size and Pitch	6.4 microns
Full well charge	15,000 e^-
Pixel Dark Noise	8 e^- RMS
Pixel Dark Current	125 e^-/s @ 25C
Windowing	Yes, ROI
Shutter	Global
Pixel Quantization	12 bit
Electrical Interface	
Commanding & Data	LVDS
Protocol	MER/MSL/Mars2020 NVMCAM
Power Input	+5 V (+/- 0.5 V)
Power	< [10 W]
Memory	[1 Gbit] SDRAM
Non-Volatile FPGA	MicroSemi Rad-Tolerant [ProASIC3]
Camera System Specifications	
Mass (CBE, no optics)	[< 425 g]
Volume (CBE, no optics)	[75 mm x 85 mm x 55 mm]
Operating Temperature	-55C to +50C
Survival Temperature	-135C to +70C
Mars2020 Optics Configurations	
Navigation Camera (Color)	103° X 77°(H x V), f/12, iFOV ≤ 0.35 mrad
Hazard Camera (Color)	156° X 117°(H x V), f/12, iFOV ≤ 0.54 mrad
Sample Camera (Color)	EFL = [30mm], Focus Distance = 270mm, F/8

The Mars 2020 EECAMs began as a six-month study task in late 2013. After a successful protoype demonstration, the Mars 2020 project approved the new cameras for flight in October 2014. The detailed design is currently underway, with a PDR scheduled for October 2016, a CDR scheduled for April 2017, and delivery to the Mars 2020 project in the fall of 2018. Launch of the Mars 2020 rover mission is scheduled for the summer of 2020.

References:

[1] Maki, J. N., Bell, J., Herkenhoff, K., Squyres, S., Kiely, A., et al (2003) The Mars Exploration Rover Engineering Cameras, J. Geophys. Res., 108(E12), 8071, [2] Bell III, J.F, Squyres, S.W., Herkenhoff, K. E., Maki, J.N., et al. (2003) Mars Exploration Rover Athena Panoramic Camera (Pancam) Investigation, J. Geophys. Res., 108(E12), 8063, [3] Herkenhoff, K., Squyres, S., Bell III, J., Maki, J., et al (2003), Athena Microscopic Imager Investigation, J. Geophys. Res., 108(E12), 8065, [4] Maki, J., D. Thiessen, A. Pourangi, P. Kobzeff, T. Litwin, L. Scherr, S. Elliott, A. Dingizian, and M. Maimone (2012), The Mars Science Laboratory engineering cameras, Space Science Reviews, 170:77-93, [5] Lemmon, et al (2008), The Phoenix Surface Stereo Imager (SSI) Investigation, 39th LPSC XXXIX, No. 1391.

OPTIMISING THE OPERATION AND PERFORMANCE OF A STAND-OFF RAMAN INSTRUMENT DEVELOPED FOR PLANETARY AND LUNAR EXPLORATION. M. McHugh[1*], I.B. Hutchinson[1], R. Ingley[1] and N. Nelms[2]. [1]University of Leicester, Space Research Centre, University Road, Leicester, UK. LE1 7RH [2]European Space Agency, ESTEC, NL-2200 AG Noordwijk, The Netherlands. *mm372@le.ac.uk.

Introduction: Raman spectroscopy is a chemical and structural identification technique based on the vibrational modes of molecles. The technique is fast, non destructive and capable of detecting organics and biogenic materials within unprepared samples [1]. Raman spectroscopy is widely used in many fields (such as biology, chemistry, pharmaceuticals, security/defence and the nuclear waste industry) with instruments spanning a range of configurations from microscopic [2] to telescopic systems [3].

Stand-off Raman spectroscopy is the application of the standard Raman technique over a large distance (more than 120 m in some cases) [4]. The stand-off technique has proven to be a valuable tool in the fields of geology and mineralogy [5] and over the last decade efforts have been concentrated on developing mature, robust, low mass, low volume stand-off systems suitable for planetary exploration [5].

Recently, stand-off Raman spectroscopy was listed as a potential reconnaisance feature of future exploration of planetary surfces such as Mars, the Moon and Europa [6] as it facilitates the acquisitionof detailed mineralogical information from a remote distance, enabling a rover to access regions of interest (that might normally be inaccessible) without the need to re-locate and use limited rover resources. Stand-off Raman spectroscopy has been used to successfully detect carbonates and (hydro-) sulphates (such as calcite, barite, gypsum and other geologically important minerals that provide information geological processes) at a distance of over 10 m [7].

Clegg et al. suggested that an integrated stand-off sytem of complementary techniques such as Raman and Laser Induced Breakdown Spectroscopy (LIBS), operating from the mast of a rover, would be capable of context mineralogy, fine scale imaging, and fine scale elemental composition [8]. Also, in light of the recent Science Definition Report on Europa [9], Sharma et al. reported that a stand-off Raman instrument, similar to existing proto-types, would be capable of measuring and identifying various salts, organic and CO_2 ice on the surface of Europa, potentially to a depth of a few centimetres [10].

It is these advancements [11] that have led to the recent selection of a stand-off Raman instrument (SuperCam) for the NASA 2020 Mars mission payload [7].

A Radiometric Model: One of the many challenges associated with developing a stand-off Raman system is the reduction of various sources of noise that can compromise the relatively small signal collected by the instrument (due to the large distances between the sample and instrument. Background noise in a system can often be reduced by implementing complex operating modes. However complications arise due to the potential impact of radiation damge on the instrument and the limited time, processing power and memory available to efficiently/sucessfully execute the operating modes.

In order to understand the many interrelated parameters, the complicated trade-offs and the impact they have on the overall instrument performance, we have developed a sophisticated radiometric model.The model describes all aspects of the system performance by simulating instrument operation and all of the physical processes involved. For example, the model uses a monte carlo simulation to generate a Raman and fluorescence signal emitted by a sample based on parameters such as the Raman cross section of the sample, laser power, distance to the sample and collection optic configuration. The model then generates levels of ambient light both local to the detector and collected by the instrument. The simulated signal is then convolved and dispersed according to a particular spectrograph deisgn.

The simulation then accounts for specific CCD operations such as pre-scan, integration, post-scan and readout (i.e. as implemented for windowed operationse), and quantum efficiency, read noise and dark current, all of which impact the signal to noise ratio achieved by the instrument.

Radiation induced detector defects can also be accounted for in the model, the effects of which become apparent during the readout stage of operation and in the final simulated image.

The radiometric model offers a method of comparing the performance of various instrument configurations i.e. the performance of an instrument that uses a pulsed lasers and gated detectors (a component with a relatively low TRL currently) compared with a non-gated detector system.

Results: The radiometric model was used to assess three separate stand-off instrument configurations. The first configuration incorporated a continuous laser

and a non-gated detector (similar to an in-situ Raman instrument). The second configuration ultilised a pulsed laser and a non-gated detector and the third incorporated a pulsed laser with a gated detector (the current configuration of instruments such as Super-Cam [5])

Using the model, the SNR values from three different samples were obtained under three different levels of ambient light (low, medium and high). The sample used in the initial stages were sulphur, acetaminophen and β-carotene as they exhibit increasing levels of fluorescence respectively.

Initial results show, as expected, that a high SNR can be obtained with a gated detector (with a pulsed laser) in all cases.

However, the results from a number of the models also indicate that under certain fluorescence and ambient light conditions, a reasonable signal to noise ratios can also be achieved without using a gated detector. Since a gated detector is of relatively low TRL compared to non-gated detectors, identifying scenarios where they may not be required is important in order to reduce system expense and complexity and to increase robustness and reliability..

The radiometric models that are described here have also been used to investigate how the effects of different operating modes (such as frame stacking), detector temperature and energy density at the sample can effect the observed signal to noise ratio, for a given system configuration and operating environment. For example, Figure 1 shows the SNR achieved by the instrument as a function of total integration time. A frame is acquired every 80 seconds (the optimised integration time calculated by the simulation for a given signal). The relationship between SNR and total integration time is shown for three different levels of collected ambient light for two system configurations; a pulsed laser configuration and a continuous laser configuration. It is clear from the results obtained that, while operating in low level ambient light, stacking a frame can significantly decrease the SNR value achieved by the instrument. It is also clear that if the total integration time is limited the SNR may not return to its initial value (the SNR value before the frame was stacked). The plot also shows that the increased excitation energy provided by a pulsed laser consistently generates a higher signal to noise ratio over various ambient light levels. The power of the excitation laser however is often limited due to sample degradation and destruction.

On-going Work: Current work is focused on introducing the impact of radition damage onsystem into the configuration and environmental comparison work

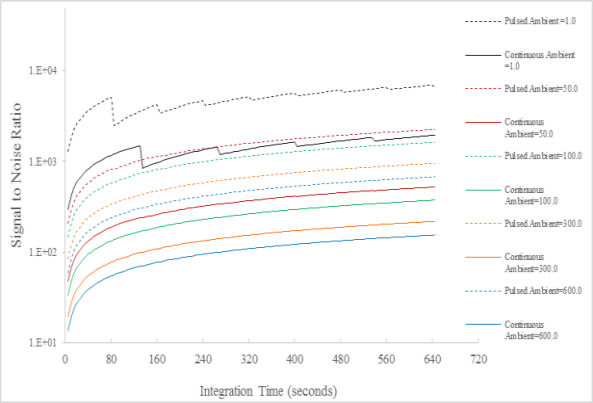

Figure 1: The relationship between the SNR achieved by an instrument and the total ingration time of stacked images.

described above, in order to evaluate the SNR values achived by a particular instrument configuration during a mission lifetime.

The model is currently being validated using spectra obtained by the different configurations for materials such as quartz, calcite, various plagioclases, pyroxenes, feldspars and olivine. These material compose >90% of most lunar rocks [12] and will provide a method to assess the performance of a stand off isntrument during a lunar mission.

References:.[1] Lewis, I.R., and Edwards, H. (2001) CRC Press. [2] Edwards, H.G.M, et al. (2005) Analyst 130.6: 917-923. [3] Misra, A. K. et al. (2005) Spectrochimica Acta A, 61.10: 2281-2287. [4] Rull, Fernando, et al. (2011) Spectrochimica Acta Part A, 80.1: 148-155. [5]Sharma, S. K. (2007), Spectrochimica Acta A, 68.4:1008-1022. [6] Mustard, J. F. et al. (2013), Mars_2020_SDT_Report_Final. Pdf, 154pp. [7] Clegg, S. M., et al. (2015) LPSC Abstract. Vol. 46. [8] Clegg, S.M., et al. (2014), 45th LPSC. [9] Europa Study Team. (2012) National Aeronautics and Space Administration. [10] Sharma, S. K. et al. (2014) LPSC Abstracts. Vol. 45. [11] Sharma, Shiv K., et al. (2003) Spectrochimica Acta Part A, 9.10: 2391-2407. [12] Wang, A., et al. (1995), A. J. Geophys. Res, 100, 21189-21199.

Additional Information: This work was funded by the University of Leicester and ESA (through a Network Partnership Initiative award)

NEW CONCEPT OF SAMPLING THIN ATMOSPHERES OF PLANETARY BODIES FOR RETURN MISSIONS. A. Meshik and O. Pravdvtseva, McDonnell Center for Space Sciences and Physics Department at Washington University, Saint Louis, MO 63130 (ameshik@physics.wustl.edu, olga@physics.wustl.edu).

Introduction: Elemental and isotopic compositions of planetary atmospheres provide valuable information about early evolution of planets, their geological activities, and catastrophic events occurred in the past.

Our laboratory was founded by Charles Hohenberg more than 4 decades ago [1] and half of this time we have been involved in the Genesis NASA mission [2]. Our efforts resulted in precise isotopic compositions of the solar noble gases [3, 4]. These compositions are believed to represent starting material of the Solar System and most likely the composition of protoplanetary disc from which the Sun has been formed.

The "hard" landing of the Genesis return capsule caused significant contamination of solar wind collectors. After years of trials and errors we developed and refined a stepped UV-laser extraction technique which allowed us to extract implanted solar wind "layer-by-layer", effectively separating surface contamination. An example of how this technique has been applied for Ar depth profiling of the polished aluminum solar wind collector is shown in Figure 1.

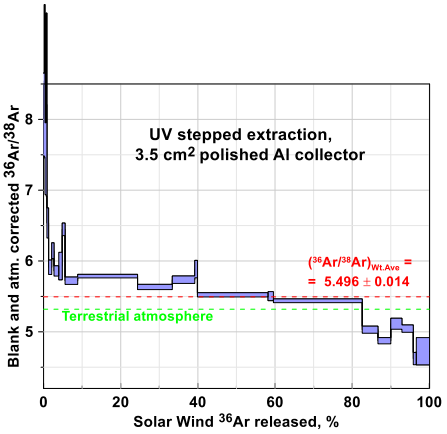

Fig. 1. Depth profile solar wind argon released from Genesis Al-collector shows that the heavier isotope is implanted deeper because the implantation occurred at constant velocity. The weighted average of all extraction steps remains the most precise composition of solar wind Ar to date. Terrestrial atmospheric Ar is depleted in light isotope supporting the partial loss of atmosphere likely during moon forming event.

Here we suggest using this technique, which worked nicely for the Genesis mission, to study volatiles from small planetary bodies. These volatiles can be efficiently captured by portable ion pumps, ion-getter pumps or orbitron pumps which will ionize the ambient gas, implant it into the pump cathode, and bury by sputtering titanium. After return to the Earth the pumps will be disassembled and the cathodes will be processed the same way as our Genesis solar wind collectors. The implantation depths will depend on the operation voltage of the pump, which is typically 7 kV, resulting in energy similar to that of solar wind He (4 keV) and Ne (20 keV).

An ion pump can be miniaturized to meet payload requirements. The orbitron pumps can be scaled down to the size of microchip [5]. This opens the opportunity to bring multiple samples from the planetary atmospheres taken from different altitudes back to the Earth.

This concept can be tried first with high-elevation balloons and/or rockets to study the uppermost terrestrial atmosphere. We may be able to answer the long-standing question about "missing" terrestrial xenon. The search for potential Xe traps (ices, sediments, shales, clathrates...) turned out to be negative. Now only two possibilities remain: (1) the deep Earth interior where pressure and temperature are apparently favorable for Xe to form chemical compounds [6] and (2) because of the lowest (among the noble gases) ionization potential, xenon is photo-ionized in the upper atmosphere and escapes it [7]. The noble gas composition in the thin upper atmosphere can be the key to the "missing xenon paradox".

The Hayabusa mission attempted to capture the asteroidal volatiles, but the capture was not efficient. Our concept could work there since the ion pump would both concentrate and protect the captured volatiles from the later terrestrial exposure.

We realize that many technical problems should be addressed before the concept proposed here becomes feasible. We hope that the successful experience of bringing Solar Wind back to the Earth for precise isotopic analyses can be used for analyses of some planetary volatiles, including the gases in uppermost part of our own terrestrial atmosphere.

References: [1] Meshik A. and Pravdivtseva O. (2016) *47th LPSC*, Houston, TX, Abstract # 1981. [2] The Genesis Mission (2002) *Space Science Reviews* 102, No. 1–2. [3] Meshik A., et al. (2007) *Science* 318, 433-435. [4] Meshik A., Hohenberg C., Pravdivtseva O., and Burnett D. (2014) *Geochim. Cosmochim. Acta* 127, 326–347. [5] Koops H. W. P. (2005) Proceedings of SPIE (Int. Soc. Optical Engineering) Nanotechnology II, 5838, 38. [6] Sanloup C., et al. (2005) Science 310, 1174. [7] Hebrard E. and Marty B. (2014) Earth and Planet Sci. Lett. 385, 40–48.

PLANETARY PROTECTION TECHNOLOGY DEFINITION TEAM: TASKS, STATUS, AND FEEDBACK. M. A. Meyer[1] and J. D. Rummel[2], [1]Planetary Science Division, SMD, NASA HQ, Washington, DC 20546, michael.a.meyer@nasa.gov, [2]SETI Institute, 189 Bernardo Ave, Suite 200, Mountain View, CA 94043, jrummel@seti.org.

Introduction: In accordance with international treaty obligations, NASA maintains a planetary protection policy to avoid the contamination of extraterrestrial bodies during spaceflight missions. Requirements are levied on NASA's Planetary Science program to prevent the contamination of solar system targets of exploration with terrestrial organisms and organic compounds (forward contamination), and to prevent the uncontrolled introduction of extraterrestrial life to the Earth (backward contamination).

In the forward direction, targets of high astrobiological significance due to the potential for native life are of highest concern for planetary protection, because these locations are also more likely to provide habitats for Earth life. Constraints on such missions include the requirement to reduce the biological contamination carried by the spacecraft and ensure prevention of recontamination, constraints on spacecraft operating procedures, and inventories of organic constituents of the spacecraft and organic samples—in addition to the standard requirements to document spacecraft operations, impact potential, and the location of landings or impact points on planetary surfaces or other bodies.

In the backward direction, similar concerns are evinced in the areas of engineering and technologies to ensure encapsulation and containment of the samples while breaking the chain of contact between the sampled planetary environment and the uncontained portion of the spacecraft returning the sample. For future robotic missions to astrobiologically significant destinations, such as ocean worlds, a prime focus has to be on avoiding the release of Earth contamination that may confound future observations and experiments.

Tasks: The Planetary Protection and Technology Definition Team (PPTDT) has been established to provide for optimal planning and the future implementation of missions to astrobiologically significant targets. This Team has been tasked with the following:

- Assess technical and engineering challenges to applying available microbial-reduction methods, including recontamination prevention, to spacecraft hardware and instruments, to meet current NASA requirements on preventing the forward contamination of potentially habitable worlds by future spacecraft missions;
- Provide a list of spacecraft and instrument materials known to be compatible with existing planetary protection protocols;
- Delineate planetary protection protocols/processes available or which appear promising;
- Identify areas ripe for technological development;
- Evaluate technical and engineering challenges to ensuring that spacecraft hardware and instruments can meet organic cleanliness requirements needed to differentiate Earth contamination from extraterrestrial signals;
- Propose approaches for mitigating the identified challenges that would allow instruments to be flown successfully at the required levels of cleanliness and microbial reduction, beginning with identification of commonly used materials and spacecraft hardware that are compatible (or particularly vulnerable) to planetary protection protocols;
- Identify engineering, technology, and scientific research and development that could be funded by NASA to provide future capabilities to field scientific instruments and spacecraft on missions that require microbial reduction and recontamination prevention.

Status and Feedback: The status of the PPTDT's study will be reported along with their initial findings. In addition, feedback is requested from the instrumentation community to ensure that the Team has considered a broad range of instrument challenges, possible planetary protection techniques, and potential approaches.

References: 1) Frick, A., R. Mogul, P. Stabekis, C.A. Conley, and P. Ehrenfreund. Overview of current capabilities and research and technology developments for planetary protection. Advances in Space Research 54: 221–240 (2014). 2) Space Studies Board, National Research Council, Preventing the Forward Contamination of Mars, National Academy Press, Washington, DC (2006).

SETG: NUCLEIC ACID EXTRACTION AND SEQUENCING FOR IN SITU LIFE DETECTION ON MARS.

A. Mojarro[1], J. Hachey[1,3], J. Tani[1], A. Smith[1], S. A. Bhattaru[1], A. Pontefract[1], R. Doebler[2], M. Brown[2], G. Ruvkun[3], M. T. Zuber[1], and C. E. Carr[1,3,*], [1]Department of Earth, Atmospheric and Planetary Science, Massachusetts Institute of Technology, 77 Massachusetts Ave, Cambridge, MA, 02139, [2]Claremont BioSolutions, 1182 Monte Vista Ave #11, Upland, CA, 91786, [3]Department of Molecular Biology, Massachusetts General Hospital, 185 Cambridge Street, Boston, MA, 02114,[*]Corresponding author: chrisc@mit.edu

Introduction: Theoretical and experimental evidence suggest that life on Mars, if it exists, may share a common ancestry with life on Earth due to substantial lithological exchange experienced during the late heavy bombardment period [1]. Moreover, widespread synthesis and delivery of amino acids and nucleobases, *the known building blocks of life,* from the early planetary nebula [2-4] may have biased life on Mars towards a familiar medium of hereditary transference via informational polymers (IPs) (e.g., deoxyribonucleic acid - DNA, and ribonucleic acid - RNA). Thus, biological IPs have the potential to provide *unambiguous* signatures of extraterrestrial life.

We are developing an integrated nucleic acid extraction and sequencing instrument: the Search for Extra-Terrestrial Genomes (SETG) [5,6] for *in situ* life detection on Mars (Fig. 1). SETG implements nucleic acid isolation [7] and leverages the sensitive technologies developed, such as nanopore sequencing, in the present genomics revolution.

Here we provide a brief overview of SETG, having recently achieved technology readiness level 4 (TRL-4) and outline the next steps in the instrument's development (TRL-5-6)

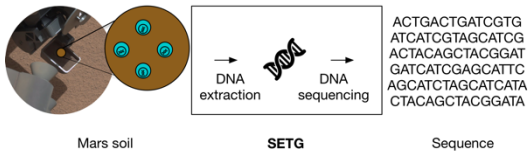

Figure 1: SETG overview, soil sample to genetic sequence.

Science Goals: Searching for IPs, including DNA and RNA, is critical to any comprehensive life detection strategy. Sequence data has revealed that all known life on Earth share ~400 "universal genes" (including the ribosomal RNA) [8,9]. These genes have remained "conserved" for the past 3-4 billion years (e.g., 16s rRNA) [10], thus comparing sequence data from Mars "life" and Earth life could discriminate forward contamination from true life detection and establish a possible common ancestry [11]. Our goals for SETG are to:

- identify related or unrelated nucleic acid-based life
- discern forward contamination among detections
- inform Mars Sample Return (MSR) of potential extant life

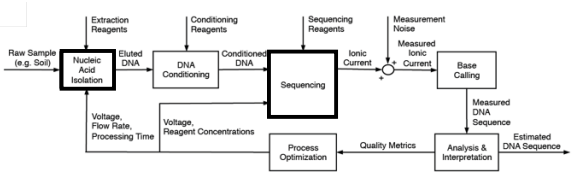

Figure 2: Provisional SETG functional block diagram; nucleic acid isolation and sequencing are discussed in this overview [5].

Instrument Overview: SETG consists of two primary subsystems: *nucleic acid extraction* and *sequencing* (Fig. 2).

Our *nucleic acid extraction* module is based on Claremont BioSolutions, LLC (CBIO) manual PureLyse® rapid (< 3 minutes) genomic DNA/RNA extraction kit [7]. PureLyse® facilitates solid-phase nucleic acid extraction and purification via mechanical bead-beating cell lysis in combination with binding and elution buffers. Furthermore, PureLyse® validations [12] have been conducted on a suite of synthetic Mars analog soils representing Gusev Crater (salt-rich), Meridiani Planum (acidic), Chrysie Planitia (alkaline), Vatistas Borealis (perchlorate-rich), and the global aeolian soil [13].

Sequencing is conducted using Oxford Nanopore Technologies (ONT) MinION Mk 1B sequencer with R9 flowcells (Fig. 3A). ONT performs strand sequencing using protein nanopores anchored in an electrically resistant membrane bilayer. When a voltage is applied to the bilayer, it creates an ionic current through the pores. Extracted IPs are conditioned to contain a motor protein that regulates the movement through the pores, and nucleobases are detected by monitoring the ionic current produced by the translocation of a single strand polymer.

TRL-4: In the context of SETG, TRL-4 implies *automated nucleic acid extraction* accompanied by *automated sequencing* (with intermediate manual handling).

Here we show the results of DNA extracted from 1.56×10^8 spores of *Bacillus subtilis* ATCC 6633 homogenized with 50 mg of synthetic perchlorate-rich Mars analog soil [13]. Spores of *B. subtilis* were selected as a worst case scenario of hardy, tough to lyse cells that can survive in extreme environments [13,14] while perchlorate-rich soil is a foreseeable sample candidate on Mars of astrobiological interest [15].

Automated nucleic acid extraction: Our automated extraction module is a custom Claremont BioSolutions SimplePrep X1 Automated Lysis and Nucleic Acid Extraction Platform (Fig. 3B). The X1 utilizes integrated PureLyse® cartridges to isolate DNA/RNA from tough to lyse microorganisms in soil samples. In addition, we implement sample conditioning protocols to mitigate soil-DNA interactions (e.g. DNA destruction and/or adsorption by soil) (Fig. 4) [12].

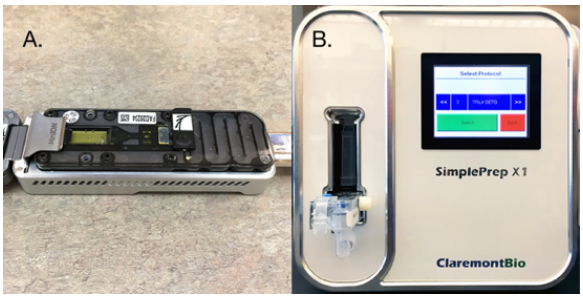

Figure 3: A). MinION Mk 1B with R9 flowcell B). SimplePrep X1 automated lysis and nucleic acid extraction platform.

Figure 4: TRL4 nucleic acid extraction workflow and sample conditioning protocol for synthetic Mars analog soils.

Automated sequencing: Two extractions (*B. subtilis* in perchlorate soil) with the X1 system were prepared using ONT's rapid sequencing kit (SQK-RAD001). This transposon-based method attaches platform specific adapters and motor proteins to DNA (IPs) in two five-minute steps. The conditioned DNA was then sequenced on a 48-hour cycle which yielded ~4 x 10^7 sequences (Fig. 5) of positive *B. subtilis* ATCC 6633 detections (verified with Basic Local Aligment Search Tool, blast.ncbi.nlm.nih.gov/Blast.cgi).

TRL-5-6: The advancement of SETG from TRL4 towards TRL5 is focused on achieving fully-automated end-to-end sample loading to sequencing. We expect to achieve a less than 10 parts per billion (ppb) detection sensitivity from samples containing lower ranges of cell densities analogous to those present in the McMurdo Dry Valleys and the Atacama Desert (1x10^5 spores/g soil). TRL6 is focused on producing a fully-integrated SETG prototype compatible with Mars temperature and pressure, TRL6 will also target an ultimate detection sensitivity of less than 1 ppb [16,17]. Current work using CBIO manual PureLyse® kits and Droplet Digital Polymerase Chain Reaction (ddPCR) DNA detection techniques suggest 1 ppb sensitivity is attainable.

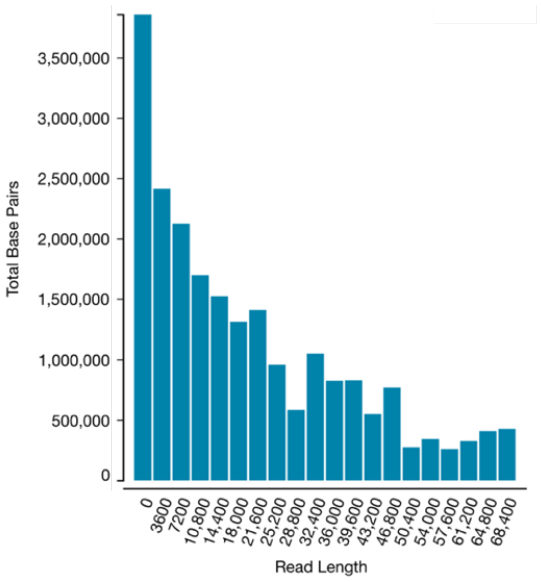

Figure 5: Total base pairs as a function of read lengths. Longer read lengths are a measure of quality sequencing as they aid in genome assembly, leading to more distinct discrimination between sequenced species.

Summary: Life on Mars, if it exists, may potentially be detected by SETG via *in situ* sequencing aboard a future rover or lander mission. Martian metagenomics could also provide unambiguous evidence of life on Mars and discern conserved genetic sequences, unveiling a Mars-Earth shared ancestry. SETG would also provide the first *in situ* characterization of forward contamination.

References: [1] Gladman B.J. et al. (1996) *Science*, *271*, 1387. [2] Ciesla F.J. and Sandford S.A. (2012) *Science*, *336*, 452–454. [3] Nuevo M. et al. (2012) *Astrobiology*, *12*, 295–314. [4] Meinert C. et al. (2016) *Science*, *352*, 208–212. [5]Carr C.E. et al. (2016) *2016 IEEE Aerospace Conference*, 1–15. [6] Lui C. et al. (2011) *2011 IEEE Aerospace Conference*, 1–12. [7] ClaremonBio Solutions (2011) 1–4. [8] Harris J.K. et al. (2003) *Genome Res 13, 407-412*. [9] Makarova K.S. et al. (1999) *Genome Res*, *9*, 608–628. [10] Woese C.R. et al. (1975), *Nature, 254*, 83–86. [11] David L.A. and Alm E.J. (2010) *Nature*, *469*, 93–96. [12] Mojarro A. et al. (2016) *Under Review*. [13] Schuerger A.C. et al. (2012) *Planetary and Space Science*, *72*, 91–101. [14] Horneck G. and Zell M. (2012) *Astrobiology*, *12*, 373–373. [15] Stoker C.R. et al. (2010) *J. Geophys. Res*, *115*, 20–24. [16] Azua-Bustos A. et al. (2015) *Environmental Microbiology Reports*, *7*, 388–394. [17] Goordial J. et al. (2016) *Isme J*, 1–12.

Acknowledgments: This work was supported by NASA MatISSE award NNX15AF85G.

High Sensitivity Planetary Composition Measurements Using Integrating Cavity Enhanced Spectroscopy.

T. Z. Moore[1], K. D. Retherford[1], M. W. Davis[1], U. Raut[1], K.E. Mandt[1], J. D. Mason[2], and V. V. Yakovlev[2], [1]Southwest Research Institute, 6220 Culebra Road, San Antonio, TX 78238, [2]Texas A&M University, College Station, Texas

Introduction: The desire to understand planetary atmospheres, terrestrial chemistry, or search for potential biological markers on Ocean Worlds often involves some form of optical spectroscopy. Common spectroscopic methods include absorption, fluorescence, or Raman based measurements. We present a new approach to planetary spectrographic instruments based on a novel high reflectivity integrating cavity.

The exploration of planetary surfaces using Raman based spectroscopy techniques is relatively new, and promises to play an important role in NASA's future exploration of the Solar System. Similar to the spectral fingerprints available through infrared imaging spectroscopy the Raman excited emissions provide distinct signatures, including those of more complex molecules typically found in trace abundances.

In many ways the initial survey of the Solar System with Raman spectrographs is just beginning at Mars. Future missions including UV fluorescence measurements will have increasingly focused objectives related to biologically interesting species and related design requirements for highly sensitive (low abundance level) measurements in increasingly extreme environments. The need to better adapt UV Raman and fluorescence measurement techniques combined with IR Raman for the high sensitivity needed for life detections motivates us to develop a new instrument optimized for high sensitivity and with multiple excitation source wavelengths.

While many optical spectroscopy techniques have the capability to provide very sensitive measurements, many suffer from significant practical challenges such as scattering within the sample region, small sample volume interaction, weak excitation sources, or weak optical signals. For example, most optical absorption instruments do not measure absorption directly but measure attenuation where the presence of scattering will significantly degrade the measurement. Weak optical signals from Raman or fluorescence based instruments in a laboratory setting require sensitive low noise detectors and often long integration times.

Several techniques have been developed to address many of the issues commonly encountered with optical spectroscopy instruments. However, these techniques often come with an additional cost such as increased complexity.

Integrating Cavity Enhanced Spectroscopy (iCES): Integrating cavities are utilized extensively in optics from irradiance measurements, to detection systems, to the generation of uniform light sources.[1] However, until recently, commonly available integrating cavity materials generally did not have the optical characteristics to be used effectively for sensitive spectroscopy measurements and/or for space flight instrumentation.

Recently, our colleagues at Texas A&M University have developed a new process for fabricating a highly reflective Lambertian reflector from commercially available fumed silica powders. This disruptive advancement in the state-of-the-art integrating cavity material has resulted in significantly higher reflectance with very low absorption. In addition, the cavity has been shown to have excellent performance in the deep UV region of the spectrum.[2]

After fumed silica powder is pressed and sintered, it can be formed into any shape as shown in Figure 1. Cavity ring-down measurements have demonstrated reflectivity of 99.98% throughout the visible spectrum and into the near infrared, from 400 nm to 1.2 μm, and 99.96% into the deep UV, the highest reflectivity of any known Lambertian reflector.[3]

Figure 1. Integrating cavity formed from high purity fumed silica. This integrating cavity has the highest reflectivity of any known Lambertian reflector at 99.98% at 532 nm and 99.96% at 260 nm.

There are several benefits of such a highly reflective integrating cavity. The integrating cavity can be substituted into many instruments where a Fabry-Perot type cavity or Herriott cell is used with the

advantage of not having to mode-match the coherent source to the cavity. Because light reflects incoherently within the cavity, it is possible to use incoherent light as a source as well. In addition, the new integrating cavity has been shown to be insensitive to scattering within the sample, which is a significant limitation to traditional cavity enhanced instruments.[4] The integrating cavity also results in increased sample volume interaction along with build up of the excitation source light within the cavity, providing demonstrated gains of 60 to 100 times. Finally, the cavity collects all of the light within the cavity where it eventually exits through the output port. The collection of light from all directions substantially enhances the optical output signal.

While the integrating cavity method does have many significant benefits there are two basic limitations. 1) The sample must me placed inside of the cavity, requiring one or more moving parts for its use in flight. 2) The cavity may is less appropriate for techniques relying on optical coherence, which is lost when reflected from the walls of the cavity.

Demonstration of ICES: Our collaborators at Texas A&M University have demonstrated the effectiveness of ICES using several different spectroscopy techniques. These techniques include integrating cavity ring-down absorption spectroscopy, fluorescence spectroscopy, Raman spectroscopy, and direct scattering measurements.

Integrating cavity enhanced fluorescence spectroscopy. Sensitive trace measurements of liquid contaminants using integrating cavity enhanced fluorescence spectroscopy to detect urobilin in water was demonstrated. The researchers were able to detect 100×10^{-15} mole (femto-moles) of urobilin with significant signal remaining.[5] The device consisted of a commercially available blue LED, the integrating cavity, and a commercial spectrometer.

Integrating cavity enhanced Raman spectroscopy (ICERS). Initial Raman spectroscopy sensitivity studies are extremely promising where Raman enhancement at 532 nm on the order of 10^5 has been observed (Figure 3). Background measurements show the Raman shift of nitrogen at 2331 cm^{-1} and oxygen at 1556 cm^{-1}. In addition, studies of liquids and bulk materials such as pyrene have shown the ability to measure down to $37x10^{-9}$ moles where the integrating cavity is providing substantial signal enhancement over typical Raman measurement techniques. These measurements can be substantially improved by utilizing UV resonance enhancement of the Raman signal which is now possible.

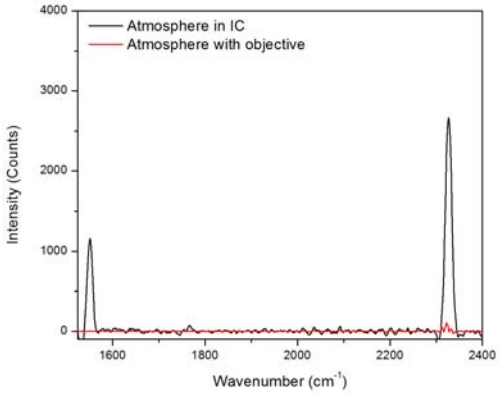

Figure 3. Raman spectrum of atmosphere collected with an integrating cavity (black trace) and with a 20x, 0.5 NA microscope objective. The spectrum collected with the microscope objective was taken over 1 hour while the spectrum taken inside the cavity was taken over 1.2 seconds. Raman spectroscopy of bulk pyrene demonstrated the ability to detect down to 37 nM with a 532 nm excitation source.[7]

Summary: iCES has been demonstrated to provide significant signal enhancement for fluorescence and Raman measurements. In addition, ICES instruments are insensitive to scattering within the sample making it possible to make sensitive absorption measurements. An iCERS instrument is currently under development at SwRI for trace gas analysis and UV resonance enhanced Raman spectroscopy of bulk samples.

References: [1] Beaulieu J. (1999) Tech. Rep. Labsphere, Inc. [2] Mason J. D. et al. (2015) *Appl. Opt.*, 54, 25, 7542-7545. [3] Biler J. N. (2015) *Dissertation Texas A&M Univeristy*, 1151–1154. Cone M. T. (2014) *Dissertation Texas A&M Univeristy*, 33. [4] Cone M. T. et. al. (2014) *Biomedical Optics*, Miami Florida. [5] Bixler J. N. et al. (2014) *PNAS., 111,* 7208-7211. [6] Bixler J. N. (2015) *Dissertation Texas A&M Univeristy*, 54-79. [7] Bixler J. N. (2015) *Dissertation Texas A&M Univeristy*, 62

Microchip Electrophoresis Instrumentation for Determination of Chemical Distributions on Future Spaceflight Missions

M. F. Mora[1] and P. A Willis[1]
[1]Maria.Mora@jpl.nasa.gov, Jet Propulsion Laboratory, California Institute of Technology.

Introduction:

The search for evidence of life beyond Earth is among the highest level goals in planetary exploration and is potentially one of the greatest research opportunities for the future of chemistry. However, despite multiple orbiter and landed missions to extraterrestrial bodies in the solar system, we still haven't found evidence of life. A powerful and highly unambiguous approach in the search for life involves seeking biochemical signatures of life at the molecular level, as expressed in distributions of geometric and stereochemical properties of organic molecules. Microchip electrophoresis (ME) has tremendous promise for aiding in this search. [1-4] Depending on the detection method used, ME allows for the detection of organics as well as inorganic ions. ME also has minimal mass/power/volume requirements, which is essential for instrument payloads on spaceflight missions. However, in terms of spaceflight implementation, this technique is relatively new, and there are still many challenges to be addressed for future implementation on spaceflight missions. Here we will describe the status of ME instruments at JPL and the steps we are taking to someday enable the implementation of this technology on other worlds.[5]

Approach:

We focus here on two detection methods: laser-induced fluorescence (LIF) and capacitively coupled contactless conductivity detection (C^4D). We describe a ME-LIF system we dub The Chemical Laptop [6] (Figure 1), which would provide the sample processing capabilities required for *in situ* analysis on extraterrestrial destinations with parts-per-billion sensitivity in a compact, low-mass, and low-power package. This instrument concept could be adapted to the environmental requirements of a variety of astrobiologically interesting targets lie Europa, Enceladus, or Titan.

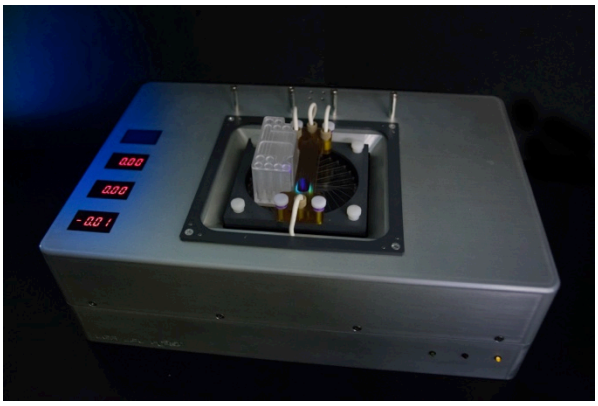

Figure 1. The Chemical Laptop *is a battery-powered, portable, automated, and reprogrammable microchip electrophoresis instrument capable of detection of organic molecules at the ppb and ppt levels*.

This instrument is the first battery-powered and truly portable "end-to-end" ME-LIF astrobiology instrument capable of receiving an unlabeled liquid sample and performing all operations required for analysis. We recently validated The Chemical Laptop by analyzing amino acids in the field.

The search for signatures of life on alien worlds like Mars or Europa imposes a low sensitivity requirement on in situ instrumentation seeking signs of life. Toward this end, we have optimized the optical system on the Chemical Laptop to achieve extremely low instrument detection limits. We demonstrated detection of a 200 pM mixture of amino acid (Figure 2).

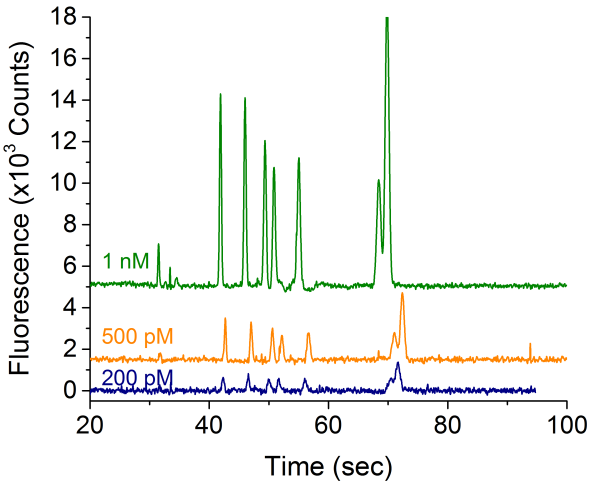

Figure 2. *Analysis of amino acid mixtures at low concentrations obtained with The Chemical Laptop. The lowest concentration analyzed was 200 pM.*

When analyzing "known terrestrial samples" we can select the appropriate methods for analysis and sample processing in such a way that the rest of the sample doesn't interfere with the detection of the compound of interest. On the other hand, analyzing unknown samples like the ones expected on alien worlds is a little more challenging. *Ideally, we need a method of analysis that can detect all of the compounds of interest with a single experiment.* Of course, in most cases this is not possible. **However, we can narrow the search to a certain group of analytes and then develop a method that allows the detection of as many of those compounds as possible.** Towards this end, we are developing ME-C^{4}D methods to simultaneously analyze inorganic and organic ions (i.e. calcium, sodium, perchlorate, amino acids, carboxylic acids etc.), as they are likely to be present at the same time on samples collected from the most relevant astrobiology targets like Mars, Enceladus, or Europa. Figure 3 shows a simulated separation demonstrating simultaneous detection of inorganic cations and amino acids.

This type of instrument also offers key capabilities for human flight applications. For example, we are currently working in collaboration with SBIR partners on the development of a miniaturized ME-C^{4}D instrument to monitor water quality in the ISS.

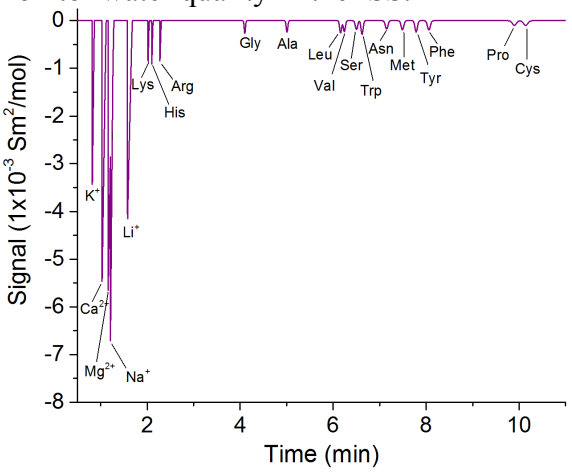

Figure 3. Simulated separation of cations and amino acids *on a 24 cm channel performed with PeakMaster 5.3. Separation buffer consisted of acetic acid 0.5 M. Concentrations of amino acids were set to small and inorganic ions to large. This example demonstrates that is possible to do simultaneous analysis but more importantly that even if inorganic ions are present at much higher concentrations than amino acids they don't hinder their detection*

References:

[1] Mora MF, Greer F, Stockton AM, Bryant S, Willis PA (2011). Anal Chem 83 (22):8636-8641.
[2] Mora MF, Stockton AM, Willis PA (2012). Electrophoresis 33: 2624–2638.
[3] Cable ML, Stockton AM, Mora MF, Willis PA (2013). Anal Chem 85:1124−1131.
[4] Mora MF, Stockton AM, Willis PA (2013). Electrophoresis 34:309–316.
[5] Willis P, Creamer J, Mora M (2015). Analytical and Bioanalytical Chemistry 407 (23):6939-6963.
[6] Willis PA, Mora MF et al. (2015) The Chemical Laptop. U.S. Patent CIT-5905-P5

RAMAN LASER SPECTROMETER FOR 2020 EXOMARS MISSION

A. G. Moral[a,1], F. Rull[b], S.Maurice[c], I. Hutchinson[d], C.P. Canora[a], G. López[b], R. Canchal[a], P. Gallego[a], L. Seoane[e], J.A.R. Prieto[e], A. Santiago[e], P. Santamaría[a], M. Colombo[a], T. Belenguer[a], Y. Parot[c], R. Ingley[d], S. Woodward[f], W.Shulte[g]

[a]Instituto Nacional de Técnica Aerospacial (INTA), *Ctra. Ajalvir, Km 4, 28850 Torrejón de Ardoz,* Spain. [b]University of Valladolid (UVa) - Centro de Astrobiología (CAB). *Av. Francisco valles, 8, Parque Tecnológico de Boecillo, Parcela 203, E-47151 Boecillo, Valladolid, Spain* www.cab.inta.es. www.inta.es. [c]Institut de Recherche en Astrophysique et Planétologie (IRAP), France. www.irap.omp.eu. [d]University of Leicester, UK. www.le.ac.uk. [e]Ingeniería y Sistemas (INSA), Spain. www.insa.es. [f]Rutherford Appleton Laboratory (RAL), UK. www.stfc.ac.uk. [g] OHB System ENG, Germany. www.ohb-system.de

Introduction: The Raman Laser Spectrometer (RLS) is one of the Pasteur Payload instruments, within the ESA's Aurora Exploration Programme, ExoMars mission.

Two missions are part of ExoMars: one consisting of an Orbiter plus an Entry, Descent and Landing Demonstrator (launched in March 14th 2016) and the other including a Rover as part of ESA-Roscosmos collaboration (to be launched in 2020). ExoMars Rover would carry a drill and a suite of instruments dedicated to exobiology and geochemistry research and its main Scientic objective is "Searching for evidence of past and present life on Mars".

Raman Spectroscopy is used to analyze the vibrational modes of a substance either in the solid, liquid or gas state. It relies on the inelastic scattering (Raman Scattering) of monochromatic light produced by atoms and molecules. The radiation-matter interaction results in the energy of the exciting photons to be shifted up or down. The shift in energy appears as a spectral distribution and therefore provides an unique fingerprint by which the substances can be identified and structurally analyzed.

The RLS is being developed by an European Consortium composed by Spanish, UK, French and German partners. It will perform Raman spectroscopy on crushed powdered samples, obtained from 2 meters depth under Mars surface, inside the Rover's Analytical Laboratory Drawer.

The Raman Laser Spectrometer Instrument: The RLS Instrument is composed by the following units:

- SPU (Spectrometer Unit)
- iOH: (Internal Optical Head)
- ICEU (Instrument Control and Excitation Unit)

Other instrument units are EH (Electrical Harness), OH (Optical Harness) and RLS Application SW On-Board.

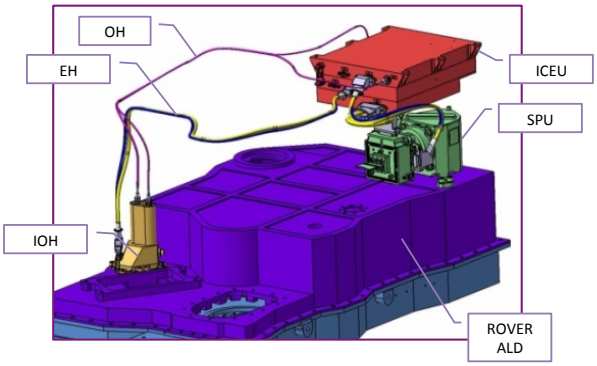

Figure 1: RLS layout over Rover ALD (Analytical Laboratory Drawer)

Results: RLS expected main characteristics are as follows:

- Laser excitation wavelength: 532 nm
- Irradiance on sample: 0.6 - 1.2 kW/cm2
- Spectral range: 150-3800cm-1
- Spectral resolution: between 6 cm-1 and 8 cm-1
- Spectral accuracy: < 1 cm-1
- Spot size: 50 microns

TRL8: After a wide campaign for evaluating Instrument performances by means of simulation tools and development of an instrument prototype, Instrument Structural and Thermal Model was successfully delivered on February 2015.

Since then, the RLS Engineering and Qualification Model has been manufactured and is expected to be delivered by November 2016, after a full qualification testing campaign developed during Q3 & Q4 of 2016.

A summary of main Instrument functionalities obtained during the last months, achieving high levels of scientific performances will be described.

1 Corresponding Author: A. G. Moral moralia@inta.es

LADEEVIEW: ELEMENTAL COMPOSITION ANALYSIS OF LUNAR SURFACE D. Nikolić[1] and M. Darrach[1], [1]Jet Propulsion Laboratory, California Institute of Technology, 4800 Oak Grove Dr., Pasadena, CA 91109, USA

Introduction: In its 2007 final report, the NRC's Committee on the Scientific Context for Exploration of the Moon states that "*over 90% of the molecules in the Moon's atmosphere are currently compositionally unidentified*". The key scientific question to be addressed is the composition and the variability of the lunar atmosphere with solar activity, diurnal cycles, and meteoritic impacts.

The recent global characterization of neutral He and Ar in the lunar exosphere [1,2], along with the discovery of neutral Ne over the night side at levels comparable to He, was performed by the Ion and Neutral Mass Spectrometer (INMS) [3] onboard the Lunar Atmosphere and Dust Environment Explorer (LADEE) [4]. The equatorial distribution of surface densities of these neutral noble gases, as well as detections of exospheric ions [5], revealed novel temporal variations made possible by combined analysis of data from Lunar Reconnaissance Orbiter (LRO) Lyman Alpha Mapping Project (LAMP) [6] and the ARTEMIS mission that monitored the solar wind alpha particle flux to the Moon [7].

Apart from the solar wind alpha particles as the dominant supply of helium to the exosphere, Benna *et al* [2] argue the presence of an internal source of helium at rate of 1.9E23 atoms/s; they also identify neon with the spatial distribution of a surface bound non-condensable gas having the source rate comparable to that of helium, whereas the global transient variability of argon has been coupled to the local enhancement such as those found in the west maria region (see Fig.1).

We present the modular computer program LADEEView designed to aid multi-parameter analysis of mass spectrometry data obtained by the INMS onboard the LADEE spacecraft. LADEEView is an in-house C++ program that utilizes hardware-accelerated rendering of realistic 3D graphics via OpenGL API. As currently envisioned, its primary purpose is to aid researchers in characterization of the global density, composition, and time variability of the lunar surface boundary exosphere.

LADEEView Program Structure: LADEEView aims to be a comprehensive Lunar Data Analyzer with modular architecture for inclusion of data from other instruments. At present stage LADEEView performs detailed cross-analysis of data measured by the INMS onboard LADEE. It uses LADEE SPICE data archived in the Planetary Data System to accurately determine the spacecraft position and orientation with respect to the lunar surface, solar wind and Earth's magnetosphere. From these, the INMS operational field of view is precisely known. Currently LADEEView deploys the completed mass spectrometry module in mapping the elemental abundances along the LADEE trajectories (see Fig.1). These maps are expected to be extremely useful as constraints and input for future models of lunar exosphere especially those that address volatile transport.

The detailed knowledge of lunar surface temperature is crucial for exospheric simulations of volatile transport via ion sputtering processes and for modeling the gas-surface thermal and chemical equilibration. The surface temperature governs the thermal desorption/diffusion of particles from the regolith and affects the initial velocity distribution of exospheric particles. Presently LADEEView uses the topographically smoothed approximation to the temperature of the surface of the Moon as measured by the Diviner Lunar Radiometer Experiment onboard the LRO. However, the actual temperature near the terminator strongly depends on the local topographic features. Therefore, future development of LADEEView will include the digital elevation model (DEM) data from the Lunar Orbiter Laser Altimeter (LOLA) onboard LRO spacecraft. In addition, we plan to enhance the LADEEView with magnetometer spectrograms onboard the Advanced Composition Explorer (ACE) to provide an easy access to local magnetic field strengths influencing the ion trajectories and the efficiency of their detection by the INMS instrument.

The current version of the LADEEView program contains three main components: mass spectra module, SPICE engine, and flyby simulator. Mass Spectra module offers a visualization of the count rate as a function of the mass-to-charge ratio as well as the total number of events detected per each second of measurement. SPICE engine serves to determine the variability of LADEE spacecraft orientation and position with respect to the Moon, Earth, and the Sun. For each recorded event the position and the orientation of the INMS instrument is known in terms of the instrument's field of view at given altitude and velocity; the local solar time as well as the selenographic latitude and longitude are also given for the spacecraft's, Earth's, and Sun's subpoints on the lunar surface. Flyby simulator exhibits the detailed visual information as spacecraft approaches and orbits around the Moon.

LADEEView is scriptable application for a fully automated event search data analysis.

Acknowledgements: This study has been carried out at the Jet Propulsion Laboratory, California Institute of Technology, under a contract with the National Aeronautics and Space Administration. It was supported by the JPL's Research and Technology Development Program. The authors would also like to acknowledge valuable help of Boris Semenov (JPL) during SPICE module validation. Copyright 2016 California Institute of Technology; U.S. Government sponsorship is acknowledged.

References: [1] D. M. Hurley et al. (2016) *Icarus 273*, 45-52; [2] M. Benna et al. (2015) *Geophys Res Lett 42*, 3723-3729; [3] P. R. Mahaffy et al. (2014) *Space Sci Rev 185(1)*, 27-61; [4] R. C. Elphic et al. (2014) *Space Sci Rev 185(1)*, 3-25; [5] J. S. Halekas et al. (2015) *Geophys Res Lett 42(13)*, 5162-5169; [6] S. A. Stern et al. (2012) *Geophys Res Lett 39(12)*, L12202; [7] J. S. Halekas et al (2011) *Space Sci Rev 165*, 93-107; [8] D. J. Lawrence et al. (1998) *Science 281(5382)*, 1484-1489;

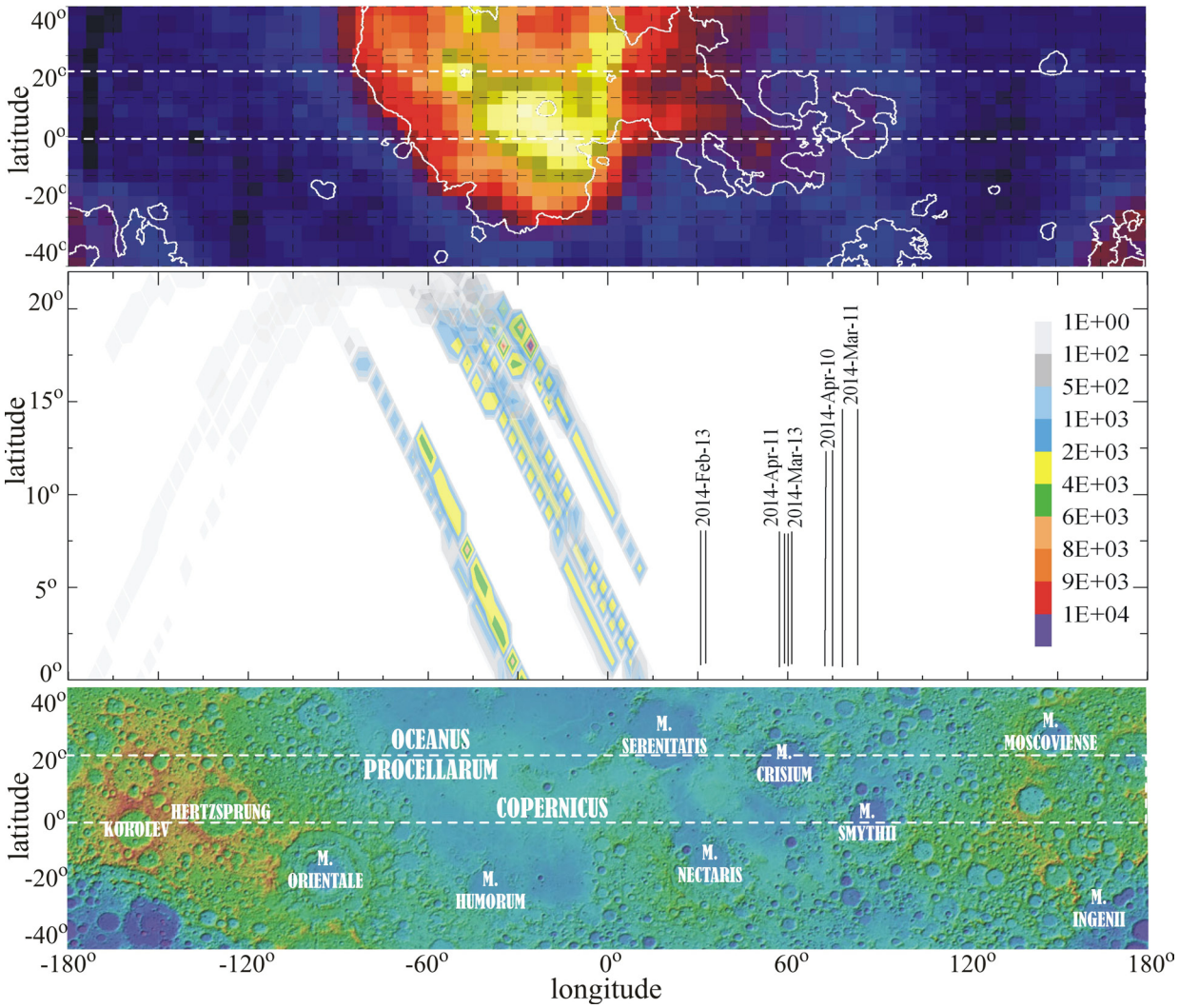

Figure 1: Variability of KREEP-rich materials (potassium K, rare earth elements REE, and phosphorus P) in the lunar highlands around the nearside western maria: (top) delineation of large compositional variation map of ^{40}K [8] with color blue (355 cnts) and yellow (490 cnts); (middle) LADEEView surface number density derived from LADEE INMS closed source neutral count rate within 39.46-40.46Th mass-to-charge channels; vertical lines denote subsolar meridian; (bottom) mid-latitude portion of elevation map (Lunar LOLA Color Hillshade 128ppd v04) with color blue (-6km) and red (+11km).

Astrobionibbler: In Situ Microfluidic Subcritical Water Extraction of Amino Acids

A. C. Noell, A.M. Fisher, N. Takano, K. Fors-Francis, S. Sherrit, and F. Grunthaner
Jet Propulsion Laboratory, California Institute of Technology, 4800 Oak Grove Dr. Pasadena CA 91106, anoell@jpl.nasa.gov

Introduction: Searching for trace levels of organic molecules on Mars or other rocky bodies presents a formidable challenge for robotic instrumentation. One particularly high value target, amino acids, are ideally suited to wet chemical analysis methods such as liquid chromatography (LC) and capillary electrophoresis (CE); because of this, automated microfluidic versions of LC and CE capable of separation and sensitive detection of amino acids and other organic molecules are already demonstrated or under development [1, 2].

However, less work has been done to develop suitable instrumentation for analyte extraction and liquid extract delivery to downstream microfluidic instruments. The Astrobionibbler instrument (ABN) [3, 4], focuses on this problem, with the primary aim of developing a chip based fluidic device for subcritical water extraction (SCWE) of amino acids from powder samples.

Background: The simplest analogy for SCWE and the ABN instrument is that of a French press coffee maker. In a French press a slurry of near boiling water and coffee grinds are allowed to mix for a period of time before a filter helps separate the desired coffee extract from the undesired residual particulates. The main difference in the ABN instrument (and SCWE in general) is the need to allow the system to pressurize so that temperatures greater than the boiling point of water can be reached (but less than the critical point).

The SCWE technique has three features that make it desirable for a planetary *in situ* extraction technique. The first is that it only requires water to perform the extractions, and not any other more reactive or difficult to contain solvents. Second, SCWE allows water to behave like other less polar solvents when desirable because the dielectric constant of water changes dramatically with temperature, especially above 100°C [5]. Third, the high temperatures reached in SCWE can be used to hydrolyze biopolymers such as proteins into their constituent amino acids, increasing our ability to separate and conclusively detect potentially very small amounts of material.

A number of proof-of-principle studies have shown that it is possible to extract both amino acids and polycyclic aromatic hydrocarbons from low organic content Atacama soils using SCWE [5, 6]. Commercially SCWE is a potentially environmentally friendly manner of converting food wastes into useful chemical precursors such as amino acids [7].

Instrument Design and Preliminary Results: The ABN instrument can be broken down into three components:

1. Sample acceptance and slurry preparation: Sample cups of 5 mL volume have been designed to accept solid powder samples and water to create homogenously mixed slurries via sonication with piezoelectric actuators. Using a peristaltic pump it was possible to reproducibly move slurries up to 20% weight from the sample cups to another device. This cup also functions as a "gentle" extractor if desired, allowing comparison of the free soluble species, to those bound in larger polymers. Furthermore, this sort of sonic extractor may be all that is required for icy samples that simply need melting and handling.

2. Microfluidic SCWE extraction chip: A significant challenge in creating a SCWE instrument is withstanding the pressures and temperatures required during extraction. A bonded glass chip has the inherent strength, but proper fabrication/bonding and creating pressurized seals at the interfaces that are easily automatable is non-trivial. Work is ongoing to determine the most robust and reproducible extraction chip fabrication procedure. The problem of fluidic seals has been overcome by using ice plugs in the microfluidic channels as a sealing mechanism. Thermoelectric coolers have been demonstrated to hold ice plug seals against extraction area temperatures >200°C, with the heating generated by both ultrasonication and resistive methods [4].

A series of samples including pure solutions of a test protein (bovine serum albumin), as well as JSC Mars 1A, Atacama, and Antarctic soils have been extracted under a variety of temperatures and durations using a benchtop SCWE. Comparisons between the benchtop SCWE and the ABN system are underway.

3. Particle removal and instrument reuse: After extraction it is necessary to remove the residual solids and deliver only the extract to downstream instruments. ABN achieves this through a combination of a settling cup and an inline filter. By allowing the particles to gravitationally settle out, only those < ~25 μm remain dispersed in the extract after a time period of ~1 hr. A 2 micron inline filter can then provide the purity of extract typically required for a microfluidic device without rapidly clogging due to the gravitational removal of the largest (and largest fraction) of particles.

After the extract has been delivered, piezo agitation can be applied to remix the slurry and then transfer the whole aliquot to waste for reuse of the system.

References:

[1] Mora, M.F., et al. (2011) *Anal. Chem., 83*, 8636-8641.
[2] Skelley, A.M., et al. (2005) *Proceedings of the National Academy of Sciences of the United States of America*, *102*, 1041-1046.
[3] Grunthaner, F.J., et al. (2012) *Concepts and Approaches for Mars Exploration*. Houston, TX: Lunar and Planetary Institute
[4] Sherrit, S., et al. (2016) *SPIE Sensors and Smart Structures Technologies for Civil, Mechanical, and Aerospace Systems*. 9803
[5] Amashukeli, X., et al. (2007) *JGR: Biogeo*, *112*, G04S16.
[6] Stockton, A.M., et al. (2008) *Anal. Chem.*, *81*, 790-796.
[7] Marcet, I., et al. (2016) *Waste Manage. (Oxford)*, *49*, 364-371.

Novel Solid-State Devices as Timing Detectors for Ion Time-Of-Flight Measurements. K. Ogasawara[1], F. Allegrini[1], M. I. Desai[1], S. A. Livi[1], [1]Southwest Research Institute, 6220 Culebra Road, San Antonio, TX 78238, kogasawara@swri.org.

Abstract: This study reports on the performance of Avalanche Photodiode (APD) and Multi-Pixel Photon Counter (MPPC) as a timing detector for ion Time-of-Flight (TOF) mass spectroscopy. We found that the fast signal carrier speed in a reach-through type APD enables an extremely short timescale response with a mass or energy independent <2 ns rise time for <200 keV ions (1-40 AMU) under proper bias voltage operations. When combined with a Microchannel Plate (MCP) to detect start electron signals from an ultra-thin carbon foil, the APD comprises a novel TOF system that successfully operates with a <0.8 ns intrinsic timing resolution even using commercial off-the-shelf constant-fraction discriminators. Thin dead-layer MPPCs are also tested for the capability to directly count secondary electrons to replace the MCPs, and ~keV electrons were detectable. By replacing conventional total-energy detectors and secondary electron detectors in the TOF-E system, APDs and/or MPPCs offer a significant power and mass savings or an anti-coincidence background rejection capability in future space instrumentation.

Introduction: In the space plasma instrumentation, the speed, energy per charge (E/Q), and total E of the incident ions are separately measured and thus their mass (M), E, and charge state (Q) can be uniquely determined [1-3]. Commonly, the TOF section typically employs two Microchannel Plates (MCPs) that measure the signals generated by secondary electrons produced as ions incident on the sensor interact with a thin carbon foil (start signal) and a detector (stop signal). The timing difference between the start and stop signals measured by these MCPs is used to determine the speed of these ions. The total E of the ions is measured by a solid-state detector (SSD) located at the end of the flight path, utilizing a proportional response to the ionization energy loss in the detector. If one could use SSD signals for simultaneous energy and timing analysis, the electrodes and the MCP for stop electron timing signals can be eliminated and a simplified instrument with significant power and mass savings could be possible. In reality, the signal rise time from conventional SSDs is too slow to use in start/stop timing due to the un-saturated slow drift mobility of electrons and holes in silicon (<~10^6 cm/s for full-depletion configurations [4]). The typical response time of traditional SSDs is 10-100 ns [5-7], which is far too long for timing analyses in a TOF-based ion spectrometer (e.g. for space plasmas, this ideally requires <1 ns timing resolution). This study presents a new approach to TOF-based mass spectroscopy that utilizes solid-state APDs and MPPCs as the timing detector for primary ions and secondary electron, respectively. APDs and MPPCs operate with a stronger electric field than non-avalanching silicon SSDs: At a nearly saturating level (~10^7 V/cm) for silicon devices, the mobility of carriers in these detectors is expected to be ~100 times faster than those in the full-depleted active layer of SSDs. However, (1) the timing profile of APD signals and directly initiated by ions, and (2) the capability of MPPCs as a electron counter are not well understood.

Methodology (APD): We study the response of a reach-through type APD with a 145 um depletion layer and a 15 mm^2 active area [8] applied in a TOF system. Ions pass through the inlet slit to the APD, and create secondary electrons in an ultra-thin carbon foil. These secondary electrons, created at both the front and back surfaces, are deflected onto a circular Chevron MCP detector placed below the foil. A ring electrode is kept at an optimized voltage (~-100 V) to minimize the radial dispersion of secondary electrons. The arrival time of these secondary electrons were used as the start signal of the TOF coincidence window in the system. The stop signals from the APD are directly induced by incident ions and fed into the fast pre-amplifier of our TOF measurement system. The APD is biased at +450 V unless otherwise indicated in the text, and operated at room temperature (20 °C).

Key Results (APD): Figure 1 shows a summary of TOF spectra for several ion species having 100 keV total energy collected using the MCP-APD TOF system. From this figure, it is clear that the proposed TOF method provides an excellent TOF mass resolution which is capable of separating the H_2O and Ne (AMU 18 and 20) peaks at the ~3% level. Figure 2 summarizes the TOF results for all investigated ion species with several incident energies (30, 50, 100, 150, and 200 keV) as a function of ion M/Q. Solid curves indicate theoretical values of the ion flight time. These reasonable results thereby validates the functionality of this TOF mass spectrometry concept. Further detailed analysis for the APD timing resolution will be given in the presentation. By averaging all data points for fast ions >2x10^6 m/s, where the carbon foil time straggling is negligible, we estimate that the intrinsic TOF resolution of the MCP-APD TOF system is 780 ps.

Methodology (MPPC): As a secondary electron source, we used one-stage MCP for the simplicity of

the set up and the capability to produce a large number of secondary electrons within a short time window. The particles injecting into the single stage MCP is converted to 100 to 1000 secondary electrons. These electrons are focused into a tiny MPPC active area through three electrodes. The MCP mount can be floated to accelerate the electrons up to 5 keV. The simulated electron travel time is 16 ns with a 0.5 ns dispersion. Assuming that one avalanche of the electron charge cloud is produced in one MCP pore ~1 um in diameter), most of the electrons will be detected within a response time of SiPM to produce significantly stronger signals than 1 p.e. signal. During this experiment, we used UV lamp to stimulate the MCP secondary electrons. The applied MPPC is a UV sensitive type with a 3x3 mm active surface comprised with 50x50 um pixels.The SiPM signals are amplified by a gain of 30, and directly counted by a universal counter.

Key Results (MPPC): Figure 3 shows the MPPC count rate as a function of the threshold level on the counter under various conditions. If we bias the MCP with 1300V, even if the UV lamp is turned off, the MPPC starts counting the electrons corresponding to MCP background counts. These MCP background count profile is totally different in their pulse height compared to the intrinsic MPPC background counts, because the number of MCP secondary electrons contributes to trigger avalanches in many pixels of MPPC. After the UV lamp is turned on, the count rate went high only for the large pulse height component in the count rate profile. This result clearly shows that these counts were produced by the secondary electrons originated in the MCPs, and thus the SiPM can count ~keV electrons. The MPPC intrinsic dark counts could be discriminated from ~3 p.e. threshold level.

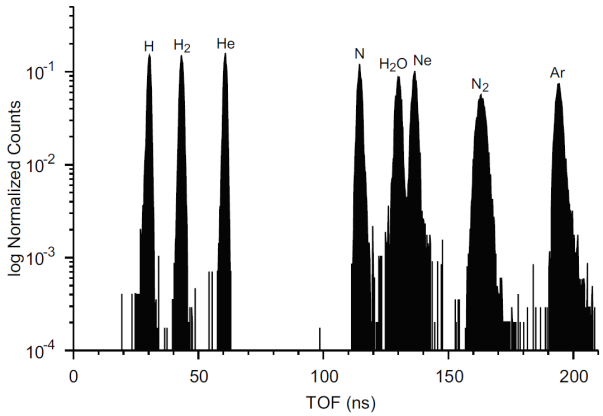

Figure 1: TOF spectra on a logarithmic scale for different ion species at 100 keV total energy obtained by the combination of MCP (Start signal) and APD (Stop signal) measurements. The accumulated counts in each ADC bin are normalized by the total count per each measurement, summed for all species. The foot of the peak prominent around the H_2O spectrum comprises contamination counts from the beam line structure by sputtering (Reproduced from Ref [8]).

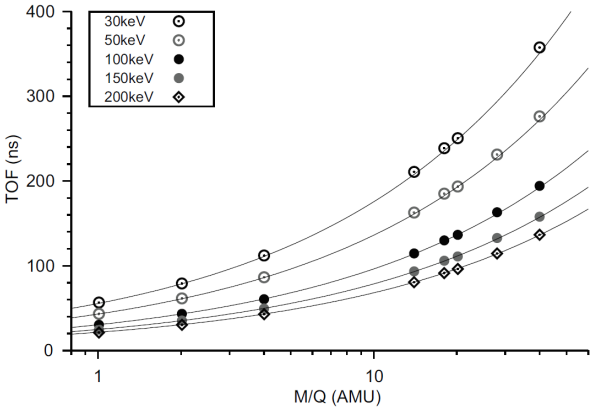

Figure 2: TOF curves as a function of ion mass per charge obtained by the combination of MCP (Start signal) and APD (Stop signal) measurements for 30, 50, 100, 150, and 200 keV ions of various species. Theoretical TOF curves based on a 13.3 cm flight path are shown for each energy (Reproduced from Ref [8]).

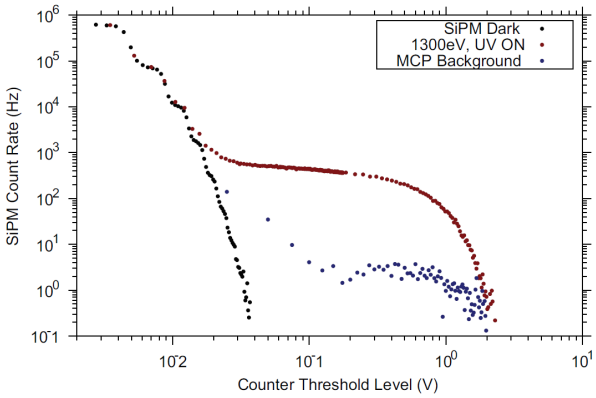

Figure 3: MPPC count rate profile as a function of different threshold levels on the counter. MPPC is biased at 66 V under a temperature of 19 °C in the vacuum chamber. Secondary electron signals are clearly distinguishable from MPPC dark counts.

References:[1] Gloeckler et al. (1985) *IEEE trans. on Geosci. And Remote Sens., 23,* 234-240. [2] Moebius et al. (1985) *IEEE trans. on Geosci. And Remote Sens., 23,* 274-279. [3] Krimigis et al. (2004) *Space. Sci. Rev., 114,* 233-329. [4] Sze (1981) Physics of Semiconductor, Wiley. [5] Pausch et al. (1994) *NIM-A, 349,* 281-284. [6] Mutterer et al. (2000) *IEEE trans. on NS, 47,* 756-759. [7] Lu et al. (2001) *NIM-A, 471,* 374-379. [8] Ogasawara et al. (2015) *Rev. Sci. Instrum., 86,* 083302.

Reducing Impact Fragmentation with a Novel Inlet on a Closed Source Neutral Mass Spectrometer.

Sandra Osburn[1], Brandon Turner[1], Eric T. Sevy[1], and Daniel E. Austin1[1]
[1]Department of Chemistry and Biochemistry, C100 BNSN, Brigham Young University, Provo, UT 84602.

Introduction: Closed-source neutral mass spectrometers are often used on flyby missions to characterize the molecular components of planetary exospheres. For example, the upper atmosphere of Enceladus and Titan were analyzed using an Ion and Neutral Mass Spectrometer (INMS) on the Cassini space probe [1]. In a typical closed source, neutrals are thermalized through multiple bounces within a spherical antechamber prior to ionization and mass anlaysis. The closed source improves sensitivity via a ram pressure enhancement.

A limitation of existing closed-source inlets is that the neutrals are traveling at high speeds (5-20 km/s) when they enter the thermalization chamber, and the high kinetic energy of impact leads to fragmentation before molecules enter the ionization region of the mass spectrometer. Due to this fragmentation the original composition of the molecule may have been altered, giving incorrect composition of the exosphere and possibly missing important compounds that were present. Jaramillo-Botero *et al*. used quantum mechanical based simulatons to determine the velocities at which molecular fragmentation occurs [2]. They showed that dissociative adsorption and scattering occurs at about 6 km/s with the inelastic scattering being the dominate pathway up to 8 km/s. Adiabatic sputtering, implantation, and nonadiabatic fragmentation occur at 15 km/s [2].

Knowing that fragmentation occurs, and even knowing some or all of the fragmentation pathways, does not allow deconvolution of flight data to give correct composition. Only stable, volatile fragments will be observed in the subsequent mass spectrometer. Different organic compounds will likely give similar fragmentation products. Simply detecting these products will not lead to unambiguous identication of the precursor molecules. Fragmentation due to ionization acts in addition to impact fragmentation, and together the two make it very challenging to know the native chemical composition of an exosphere. We present a hardware solution to this problem—an inlet that will reduce the fragmentation of molecules that impact at relevant high velocities.

Inlet Design: We are developing a new design for an inlet that will reduce fragmentation of the incoming molecules. The inlet, intended to replace the conventional spherical antechamber, still provides the advantages of ram-enhanced pressure and improved sensitivity. The reduction in fragmentation can be achieved using the shape of the inlet, which will be detailed in the presentation. Considering that fragmentation occurs as a unimolecular dissociation reaction driven by vibrational energy, collisions with walls of the inlet dissipate energy on a timescale that is fast compared with the vibrational dissociation time. Translational energies as low as 5 eV are sufficient to activate chemical transfromations [3] indicating that the dissipation of the translational energy is necessary to keep the molecule intact. Typical kinetic energies of impact range from a few eV for low molecular weight molecules at low encounter velocities to more than 100 eV for larger molecules and higher flyby velocities.

Preliminary calculations indicate that impact-induced fragmentation will be reduced by 2-3 orders of magnitude for all flyby velocities compared with conventional closed sources. This reduction is sufficient to allow essentially all volatile and semi-volatile organic compounds to be analyzed without chemical modification or fragmentation. In addition, experiments are currently underway to characterize the performance of this inlet using beams of high-velocity neutral molecules in the range of several km/s.

References:

[1] Waite J.H., Lewis Jr. W.S., Kasprzak W.T., Anicich V.G., Block B.P., Cravens T.E., Fletcher G.G., Ip W.-H., Luhmann J.G., McNutt R.L., Niemann H.B., Parejko J.K., Richards J.E., Thorpe R.L., Walter E.M., and Yelle R.V. (2004) *Space Sci. Rev.*, *114*, 113-231. [2] Jaramillo-Botero A., An Q., Cheng M.-J., Goddard III W.A., Beegle L.W., and Hodyss R. (2012) *Phys. Rev. Let.*, *109*, 213201. [3] Jacobs D.C. (2002) *Annu. Rev. Chem. Phys.*, *53*, 379-407.

VISTA: a miniaturized THERMOGRAVIMETER to detect planetary dust and volatiles. E. Palomba[1], F. Dirri[1], A. Longobardo[1], A. Galiano[1], D. Biondi[1], A.Boccaccini[1], E. Zampetti[2], B. Saggin[3], D. Scaccabarozzi[3]

[1] IAPS-INAF, Via Fosso del Cavaliere 100, 00133 Rome, Italy (ernesto.palomba@iaps.inaf.it, fabrizio.dirri@iaps.inaf.it), [2] IIA-CNR, via Salaria km 29,300 Monterotondo, Rome; [3] Politecnico di Milano, Polo Territoriale di Lecco, Lecco, Italy

Introduction: VISTA (Volatile In Situ Thermogravimetry Analyser) is a μ-Thermogravimeter device, developed by a consortium of Italian institutes.
The thermogravimetry technique (TGA) has a wide set of applications, from Space mission to chemical and biological fields [1] as well as to investigate condensation/sublimation and absorption/desorption processes of volatile compounds [2]. TGA can be useful in planetary in-situ missions in order to measure water and organics desorption, whose presence is connected to habitability of the planet/satellite, and to monitor outgassing contamination [3].
The instrument core is a Piezoelectric Crystal Microbalance (PCM), whose crystal is equipped with built-in heater and built-in temperature sensor Crystal oscillation frequency linearly depends on the mass deposited on its sensible area, according to the Sauerbrey equation [4]:

$$\Delta f \propto \frac{f_0^2}{A}\Delta m$$

PCM temperature can be increased by means of an appropriate heater in order to allow sublimation/desorption of the most volatile component of the analyzed sample. This measure gives the volatile content while composition can be inferred by desorption temperature.
Because of the similar temperature desorption range of several volatile species, other physical-chemical parameter have to be obtained by TGA during the sublimation/desorption process, e.g. enthalpy of sublimation/evaporation $\Delta H_{sub,evap}$, entropy of sublimation/evaporation $\Delta S_{sub,evap}$, sublimation/desorption temperature T_{sub} and vapour pressures at a given temperature and pressure (P_{vap}), typical for each compounds [5,6].

VISTA space/planetary applications: VISTA instrument has been studied for space applications and proposed for planetary in-situ missions [7], i.e. it has been studied for Phase A of the ESA proposed missions Marco Polo and selected for MarcoPoloR [8], addressed to a primitive Near Earth Asteroid, and for JUICE (JUpiter ICy moon Explorer), in this case coupled to a Penetrator [9]. In a planetary in-situ mission, VISTA can accomplish the following tasks depending to the planetary environment:

- measurement of abundance of volatile (e.g. water, organics) in planetary/asteroidal regolith an cometary-like activity;
- measurement of dust and ice settling rate, water content in dust and humidity;
- discrimination between water ice and clathrate hydrates (basing on their different sublimation temperature) on icy satellite surfaces;
- determination of composition of non-ice materials on icy satellite surfaces;
- characterization of organic species by measuring its enthalpy of sublimation.

VISTA is composed by two different subsystems: the Sensor Head 1 (SH1), devoted to work at low temperaures (down to -200°C) and to perform heating cycles up to 100°C and the Sensor Head 2 (SH2), able to performs TGA measurements (large temperature range, i.e. >200°C) with a low power budget. The VISTA block diagram is shown in Fig.1.

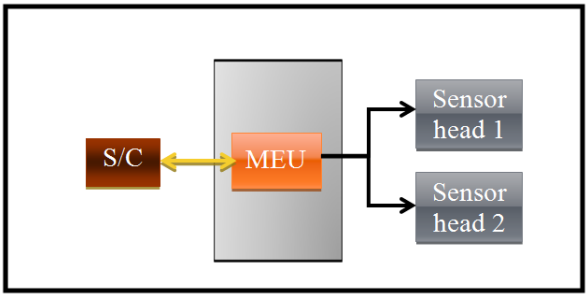

Fig.1. VISTA instrument composed by SH1 and SH2.

SH1 is currently at TRL 6 (Fig.2, *Left*), whereas a laboratory breadboard of SH2 is operative and under test (TRL 4-5) (Fig.2, *Right*). In particular, a dedicated setup has been used to evaluate the SH2 power budget performance: only 0.29 mW are required to obtain a ΔT_v~185°C in vacuum and ΔT_a~100°C in air, whereas to obtain a ΔT=250°C in vacuum only 0.43 mW are needed.

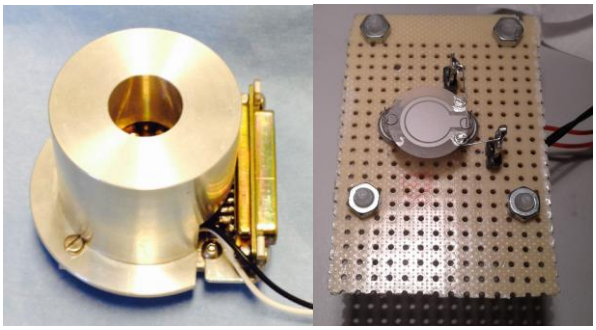

Fig.2. VISTA instrument. Left: SH1 breadboard. Right: SH1 breadboard.

Technical characteristics: VISTA has a very small mass, volume and power requirements and needs a quite small amount of material for the analysis, i.e. less than 1 mg. The main innovation concerns the special design of μ-thermogravimeter, equipped with a built-in heat-er and a built-in thermistor. SH1 and SH2 have its own proximity electronics (including the frequency counter and the temperature control system).
The Main Electronic (ME) board can be shared with other sensors of the scientific package, reducing the instrument load to the sensor heads, only. Technical characteristics of the sensor heads are summarised in Table 1.

Unit	***SH1***	***SH2***
Sensor type	*Quartz Crystal Microbalance*	*$GaPO_4$ Crystal Microbalance*
Resonant Frequency(MHz)	*10*	*5.8*
Mass [g]	*90*	*60*
Volume [mm]	*50x50x38*	*35x35x25*
Power [W]	*1 W (peak); 0.12 (mean)*	*0.62 (peak); 0.37 (mean)*
Data rate	*30 bit/ measurement*	*30 bit/ measurement*
Operating Temperatures [K]	*< 180*	*< 550*
TRL	*6*	*4/5*

Tab.1 VISTA technical characteristics.

Performance Test: a laboratory set-up has been developed in order to use PCM as cold sink (Deposition measurement) for volatiles, to obtain ΔH_{sub} and to perform heating cycles with integrated heaters (TGA measurement).

Deposition Measurement: due to the similar desorption temperatures of different volatile species, ΔH_{sub} has been measured for five Dicarboxylic acids in order to obtain a characterization of each volatile compound.
The sample and the PCM were placed inside a vacuum chamber: the sample, contained in an effusion cell, was heated up to 80°C by means of a resistor whereas the PCM was cooled at -72°C by a cold finger (i.e liquid nitrogen serpentine), in order to allow the molecules deposition coming from the sublimation process.
By measuring two different deposition rates on PCM, R_1 and R_2, at two different sample temperatures T_1 and T_2, it has been possible to infer the ΔH_{sub} of the samples by means of Van't Hoff relation [10]. The obtained results are in good agreement with literature, demonstrating the VISTA ability to measure ΔH_{sub}. Moreover, the presence of some these organic compounds inside meteorites [11] make VISTA useful to know the chemical composition of these samples associated to primitive asteroids [12].
TGA measurement: applying TGA it has been also possible to monitor a sublimation processes and to measure the corresponding ΔH_{sub}, of some Dicarboxylic acids present in Earth's atmospheric aerosol [13]. The exprimental procedure was to perform a deposition of the Adipic acid sample on the crystal's surface, heating the effusion cell up to 100°C, for a total of 29.4 μgcm^{-2}. Therefore, the cell has been switched off while the crystal was heated by using the integrated heater up to 80°C. Then, the difference in mass came back to "zero", i.e. all the deposited sample was desorbed from crystal's surface. The ΔH_{sub} calculated with Langmuir relation [14] is in agreement within 6% with the result calculated with Van't Hoff relation [13].

References:

[1] Freedman A. et al., (2008), Meas. Sci. Technol. 19, 125102, doi:10.1088/0957; [2] Zinzi, A. et al. (2011), *Sen-sors and Actuators A*, 172, 504-510; [3] Wood B.E. et al., (1997), AIAA 97-0841; [4] Sauerbrey, G. (1959), *Z. Phys.*, 155, 206-222; [5] Bilde M. et al., (2015), Chem. Rev. 2015, 115, 4115−4156; [6] Booth A.M. et al., (2009), Atmos. Meas. Tech., 2, 355–361; [7] Palomba E. et al., (2016), *OLEB Journ.*, 46, 2, 273-281; [8] Barucci, M. A. et al. (2011), *Exp. Astronomy*, DOI 10.1007/s10686-011-9231-8; [9] Palomba, E. et al. (2010), *EPSC*, #445; [10] Benson, S.W. (1968), *Thermochemical Kinetics*, 1017; [11] Andersen C.A. et al., (2005), *Int. Jour. of Astrob.*, 4, 1, 13-17; [12] Dirri F. et al. (2016), *OLEB Journ.*, under publication; [13] Dirri, F. et al. (2016), AMT 9, 655-668; [14] Torres L.A. et al., (1994), *Meas. Sci. T*

SOFT X-RAY IMAGER USING MULTILAYER MIRROR OPTICS FOR MARTIAN EXOSPHERIC STUDIES. S. Panini[1], S. Narendranath[2], P. Sreekumar[1], P. S. Athiray[3], M. Nayak [4]. [1]Indian Institute of Astrophysics (panini@iiap.res.in), ISRO Satellite Centre (kcshyama@isac.gov.in) , [3]Manipal Centre for Natural Sciences, [4]Raja Ramanna Centre for Advanced Technology.

Introduction: Planetary X ray measurements in the past have yielded valuable science in several areas such as the surface chemistry, polar auroras, magnetospheres and solar wind interaction with the exosphere. X-ray spectrometers have been flown in several missions primarily to map the surface elemental abundances. We are developing a soft X-ray imager where multilayer mirrors are used to selectively image the energies of interest onto the focal plane detector. This would be thus capable of doing imaging spectroscopy of the Martian exosphere.

Motivation: Planetary exospheric studies on its density structure, temperature profile and composition, enable calculation of escape flux from the planet's atmosphere. This provides important constraints to models on long term atmospheric evolution and volatile inventory. The characteristics of this region of the planetary atmosphere are heavily driven by its interaction with the solar wind. The exosphere also exhibits short term variations that are driven by seasonal changes, dust storms and are strongly coupled to the physical and chemical processes in the thermosphere and ionosphere.

The extended exosphere consists of several species such as H, C, N and O. The exobase altitude and extent is different for the different species. In addition to the thermal population, there is an important non-thermal population of hot atomic species in the Martian exosphere. The current understanding of the density distribution of these atoms is largely based on 3D models rather than direct measurements especially in the extended exosphere.

XMM Newton observations of Mars [1] from Earth's orbit show solar wind charge exchange X-ray emission in the exosphere up to ~ 8 Martian radii. Mapping SWCX emission from an orbit around Mars can provide through forward modeling, a global picture of the neutral atom density profiles and quantify the contribution of this non-thermal escape mechanism.

X-ray imaging spectroscopy is one of the best ways to remotely sample the exospheric species and its dynamic interactions with the solar wind. A compact light weight design is crucial on a planetary mission where resources are limited. This work therefore is targeted towards a design where single reflection optics using multilayer coated mirrors, acts as a telescope with a short focal length for a mission to Mars.

Design: The optics design consists of 24 shells of single reflection grazing incidence mirrors that are Ni coated which will concentrate the X- rays onto a set of multilayer mirrors placed at an angle of 35° from the optical axis (Figure 1). The multilayer mirrors act as monochromators to image specific lines of interest to a detector at the Nasmyth focus. Design parameters of the soft X-ray concentrator and multilayer mirrors are optimized to primarily observe six lines from the Martian exosphere. Sequential operation of each of five multilayer mirrors gives excellent spectral response. Monochromatic multilayers also suppress the background counts. Figure 2 shows the effective area of the optics. Conventional semiconductors (Si) or wide band-bap semiconductors will be considered as focal plane detectors.

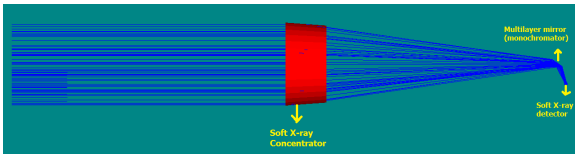

Figure 1: Optical layout of the telescope design

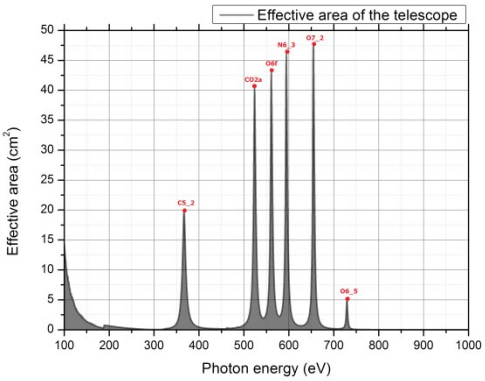

Figure 2: Effective area of the optics

Developments: We have coated silicon substrates with multilayers of W/B_4C (of a range in the number of bilayers from a few to 170 layers) with magnetron sputtering system at the Raja Ramanna Centre for

Advanced Technology (RRCAT), India (Figure 3). These mirrors have been tested for X-ray reflectivity and have gone through thermal cycling for stability checks.

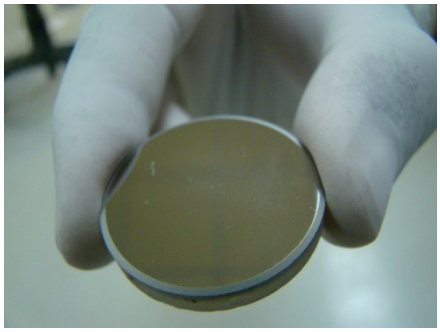

Figure 3: W/B_4C mirror developed using a magnetron sputtering system at RRCAT

Summary: We are developing a soft X-ray imager for Mars that would be capable of coarse imaging of the Martian exosphere at specific lines of interest in the 0.3 to 2 keV energy range. Multilayer mirror coatings have been developed and tested for X-ray reflectivity and thermal stability. The design yields a compact payload with a 100 cm focal length that can fly on a mission to Mars.

Acknowledgements: We thank the staff at RRCAT, Indore, Center for Nanosciences and Engineering, Indian Institute of Science and ISRO environmental facilities for their support in conducting various tests on the multilayer mirrors.

References: [1] Dennerl, K., et al. (2006) A&A, 451, 709-722

ADVANCED POINTING IMAGING CAMERA (APIC) CONCEPT. Ryan S. Park[1], Bruce G. Bills[1], John Jorgensen[2], Insoo Jun[1], Justin N. Maki[1], Alfred S. McEwen[3], Ed Riedel[1], Marc Walch[1], Michael M. Watkins[1], [1]Jet Propulsion Laboratory, California Institute of Technology (Ryan.S.Park@jpl.nasa.gov), [2]Danmarks Tekniske Universitet, [3] The University of Arizona, Lunar and Planetary Laboratory.

Introduction: The Advanced Pointing Imaging Camera (APIC, see Fig. 1) concept is envisioned as an integrated system, with optical bench and flight-proven components, designed for deep-space planetary missions. The APIC concept's unique capabilities include:

- 2 degree-of-freedom (DOF) control capability, allowing rapid and flexible image acquisition, and image motion compensation
- Innovative periscope design capable of simultaneously acquiring images of target and star field for precise image pointing knowledge.

APIC is a part of NASA's New Frontier's Homesteader Program. By the end of CY2016, all of APIC's components will achieve TRL 5-6, making APIC, as a whole, to be TRL 5. More specifically, these tasks would retire:

- Almost all radiation-related issues (including the Jovian system enviroronment). **TRL-5**
- Field-test proven 2-DOF actuation. **TRL-6**.
- Thermally stable optical-bench structure (Carbon-fiber-composite) with arc-second stability in rad-hard environment. **TRL-6**.

Size, mass, and various parameters of interested can be found in Table 1.

Science and Engineering Enabled by APIC: APIC's 2-DOF actuation would allow effective and efficient science/mission operations by providing rapid and flexible imaging capability (e.g., substantial reduction in mission duration and much less constraints on spacecraft operational geometry). APIC's internal image-motion compensation (IMC) using the internal gimbal and attitude knowledge dramatically reduces the operational cost of IMC for any mission, and increase fast flyby mission imaging resolution.

APIC's unique periscope design with high-resolution narrow-angle-camera (NAC), and an optional wide-angle-camera (WAC), would provide important unique science return via the ability to simultaneously take the images of target body and star field, allowing high-resolution surface imaging with extremely precise pointing knowledge. Such imaging data with precise pointing information can accurately measure the tidal deformation and/or libration/precession of the target body, and thereby reveal target body's interior structure. Furthermore, APIC can provide stereo reconstruction of target topography and control network that would provide very accurate determination of the target-relative position of the spacecraft.

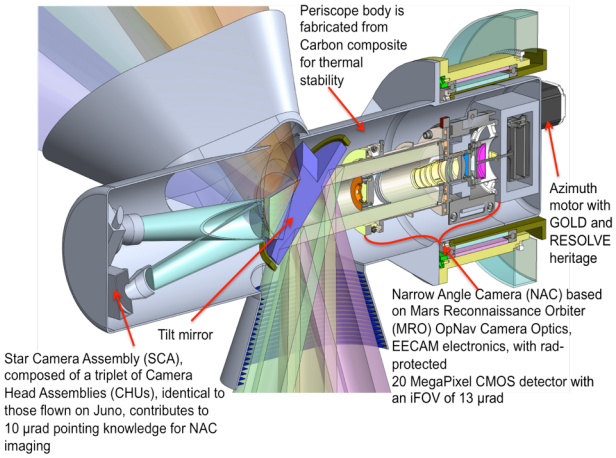

Figure 1: Cut-away view of the Advanced Pointing Imaging Camera (APIC) Instrument concept, which will far advance the planetary imaging state of the art.

Parameters	Values
Dimension	60x19x19cm
Mass	14 kg
Radiation Shielding	4 kg
Power	12 W
Image Resolution	13 µrad (~3 arcsec)
Pointing Knowledge	2 arc-second
Azimuth Range	±80°
Elevation Range	±30°
Azimuth max rate	30°/s
Elevation max rate	30°/s

Table 1: Capabilities and characteristics of the APIC concept.

APIC's combined functionalities would offer a powerful optical navigation capability, that would significantly enhance spacecraft orbit reconstruction and prediction accuracy, and thus, reducing operational cost. Also, APIC can serve as an ideal platform for autonomous navigation. Internal star-finding/tracking can provide backup attitude information for the host spacecraft.

PEP-HI: ENERGETIC ELECTRON, ION, AND NEUTRAL PARTICLE INSTRUMENTATION FOR THE JUICE MISSION. C. W. Parker[1], [1]Johns Hopkins University Applied Physics Laboratory

The Particle Enviornment Package (PEP) is an instrument suite comprising six sensors that is being developed for the European Space Agency's JUptier ICy moon Explorer (JUICE) mission. The Johns Hopkins University Applied Physics Laboratory is developing two sensors for this package, the Jovian Energetic Neutrals and Ions (JENI) sensor and the Jovian Energetic Electron (JoEE) sensor, which are responsible for measurements of the middle to high energy portions of the Jovian particle environment.

The JENI sensor is an ion and neutral particle camera based on the Cassini/INCA and IMAGE/HENA sensors, that will measure energetic (500 eV – 5 MeV) H, He, CNO, and S ions and neutral particles with an energy resolution $\Delta E/E < 14\%$. The 90° x 120° FOV is resolved into 2° x 2° pixels (≥ 10 keV H) and has a geometrical factor that can be adjusted between 0.013 cm^2 sr and 1.8 cm^2 sr by a rotating shutter mechanism. An electrostatic deflection system can be enabled to sweep ions < 300-400 keV/q out of the aperture so that neutral particles can be imaged.

Neutral particle images from JENI are observations of the remote particle environment and compliment the in-situ charged particle measurements of the other PEP instruments. Remote events can be detected and tracked as they evolve prior to reaching the in-situ instruments allowing local measurements to be understood within the context of the Jovian magnetosphere.

The JoEE sensor is an energetic electron (25 keV – 1 MeV) detector with an FOV of 202.5° x 12° divided into nine 22.5° degree sectors. A magnetic spectrometer wheel is employed to bend incoming electron (25 keV – 300 keV) trajectories into a pixelated solid state detector perpendicular to the plane of the aperture. Three sectors (0°, 90°, and 180°) have an SSD detector stack parallel to the aperture plane that will observe electrons energetic enough to traverse the magnetic spectrometer section (≥ 400 keV). A dExE measurement in these detectors will be used to separate electrons from high-energy ions.

JoEE will measure the electron pitch angle distributions to assist in determining magnetic field topology. Distributions on field lines connected to Ganymede, for example, will have much larger loss cones than those on field lines connected to the Jovian magnetosphere.

MEASURING VENUS' BULK ELEMENTAL COMPOSITION WITH BECA

A. M. Parsons[1], J. Grau[2] , D. J. Lawrence[3], J. Miles[4], P.N. Peplowski[3], L. Perkins[4], J. S. Schweitzer[2], R. D. Starr[5]
[1]NASA Goddard Space Flight Center (Greenbelt, MD, Ann.M.Parsons@nasa.gov), [2]Schweitzer Consulting (Ridgefield, CT), [3]Johns Hopkins Applied Physics Laboratory (Laurel, MD), [4]Schlumberger Technology Corporation (Sugar Land, TX), [5]Catholic U. of America (Washington, DC)

Introduction: The Bulk Elemental Composition Analyzer (BECA) instrument uses high energy neutrons and gamma rays to penetrate Venus' surface and measure the bulk elemental composition over a large volume beneath a landed probe (up to 30 cm depth and similar lateral distribution). These data are vital for understanding Venus, as little is currently known about the bulk composition of its surface. While surface x-ray fluorescence measurements were made by the Venera and Vega missions in the 1970s-80s, gamma-ray bulk composition measurements were limited to the naturally radioactive elements [1,2]. With the addition of a pulsed neutron generator, BECA provides a significant improvement over previous Venus bulk composition studies.

Bulk elemental composition measurements of the subsurface of Venus are challenging because of the extreme surface environment (462 ˚C, 93 bars pressure). The instruments included on landed probes of the surface of Venus must therefore be enclosed in a pressure vessel. The high surface temperatures require a thermal control system that can keep the instrumentation and communication electronics within their operating temperature range for as long as possible. Currently, Venus surface probes can operate for only a few hours. It is therefore crucial that the lander instrumentation be able to make statistically significant measurements in a short time.

BECA is well suited for Venus surface measurements since it will be located completely inside the Venus lander. BECA has no moving parts and because neutrons and gamma rays can penetrate the pressure vessel walls, BECA does not require a pressure vessel window or any sample manipulation, a valuable attribute given the difficulties associated with operating external mechanisms and sample handling systems in the harsh Venusian surface environment.

Instrument Description: BECA consists of a Pulsed Neutron Generator (PNG) and a Gamma-Ray Spectrometer (GRS), as shown in Figure 1. The PNG emits isotropic pulses of 14.1 MeV neutrons that penetrate the pressure vessel walls, the dense atmosphere and Venus' surface. Nuclear reactions occur between these incident energetic neutrons and Venus's subsurface material to produce gamma rays with energies specific to the element and nuclear process involved. Thus the energies of the detected gamma rays identify the elements present and their intensities provide the abundance of each element. These gamma rays are energetic enough (0.1–10 MeV) to penetrate the Venus surface, atmosphere and pressure vessel walls to be detected by BECA's cerium bromide ($CeBr_3$) scintillator GRS. The GRS spectra are analyzed to determine the Venus elemental composition from the spectral signature of individual major, minor, and trace radioactive elements in the surface to a depth of tens of cm.

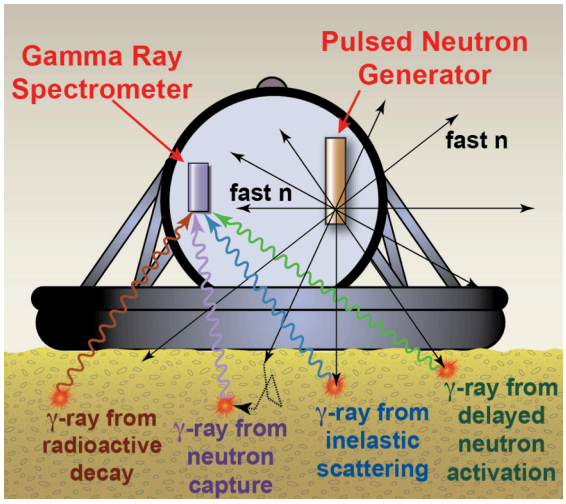

Figure 1. BECA's PNG excites the nuclei in the surface material resulting in the emission of characteristic gamma rays. The detection of these gamma rays by the GRS yields the elemental composition.

BECA's PNG and GRS system is based on Schlumberger Technology Corporation's Litho Scanner* instrument, which is used extensively in the oil industry for determining the elemental composition of material down oil well boreholes [3]. The Litho Scanner is very similar to BECA except that its GRS uses $LaBr_3$ instead of $CeBr_3$. $CeBr_3$ is expected to have the same performance when used with the PNG, but will provide superior measurements of naturally radioactive elements due to its lack of internal background. The Litho Scanner technology is easily adapted to space applications since the oil well environment is similarly harsh. In the oil well configuration, the cylindrical PNG and GRS are co-aligned. Adapting the Litho Scanner to the BECA Venus application requires the

*Trademark of Schlumberger

PNG and GRS to be placed separately within the Venus probe volume as shown schematically in Figure 1. There is significant flexibility in the orientation and placement of the PNG and GRS and instrumental electronics within the lander pressure vessel. Monte Carlo simulations will be employed to optimize the location of the components.

Operational Advantages and Capabilities: A neutron source is required on the surface of Venus because galactic cosmic rays do not penetrate the dense Venusian atmosphere. A deuterium-tritium PNG has multiple advantages over radioactive sources since its higher (14.1 MeV) neutron energy allows the measurement of a wider variety of elements and this neutron source can be turned off during the launch and cruise phase of the mission.

The combination of a PNG with an average isotropic intensity of up to 5×10^8 neutrons per second with the unusually fast light decay time (< 20 ns) of the $CeBr_3$ scintillator GRS allows for count rates of many hundreds of kHz, depending on BECA's distance to the Venus surface. This high gamma ray throughput is necessary to provide the counting statistics needed for the short (~ 1 hour) measurement times currently available for Venus landers.

Test Results: On July 6 and 7, 2016, a Schlumberger Litho Scanner oil well logging tool was used in a series of experiments performed at the Gamma Ray Neutron Test (GNT) facility [4] at NASA's Goddard Space Flight Center. The Litho Scanner tool was mounted above large (1.8 m x 1.8 m x .9 m) granite and basalt monuments and made a series of one-hour elemental composition measurements to demonstrate the successful operation of a BECA prototype in a planar geometry more similar to a planetary lander measurement.

Measurements were made in various configurations to determine how the BECA prototype performance scales with 1) the height of the instrument above the monument, 2) differences in elemental composition between the granite and the basalt as well as additional Ti and S added to the configurations and 3) different thicknesses of polyethylene placed on top of the monuments to represent varying amounts of phase-change material that would be used inside a Venus lander. These tests also provide an experimental benchmark for our Monte Carlo simulations that will be used to determine the elemental measurement precision in an actual Venus probe configuration.

Knowing the independently measured elemental compositions of our basalt and granite monuments from an assay provided by an outside laboratory allows us to quantitatively compare these measurement results with the actual elemental concentrations present in each monument. Some key systematic effects for which this measurement has not been optimized include: the elemental standard spectra have been derived for the fluid-filled oil-well borehole environment, not open-air monuments; and the mineralogical assumptions that inform the conversion of spectral yields to elemental concentrations were designed for sedimentary rocks, not granite or basalt.

Table 1: Preliminary Granite Test Results

Element	Units	Granite Assay	Granite BECA Results
Al	wt%	7.40	7.41
Ca	wt%	0.63	0.74
Fe	wt%	1.14	1.23
Gd	wt-ppm	4.55	4.72
K	wt%	4.32	5.09
Mg	wt%	0.17	0.11
Mn	wt%	0.04	0.04
Na	wt%	2.27	2.09
Si	wt%	34.23	34.65
S	wt%	0.01	0.00
Ti	wt%	0.14	0.18

Table 1 shows preliminary results for one of our measurements of the granite elemental composition. These one-hour measurements were made with an average isotropic PNG neutron output of 3.8×10^8 neutrons/s and with the PNG and $LaBr_3$ GRS of the Schlumberger Litho Scanner tool located 20 cm above a 2.54 cm thick layer of polyethylene placed on top of the bare granite monument. An identical measurement was performed on the basalt monument.

While the absolute statistical uncertainties for the results above were typically less than 0.1 wt%, the overall measurement uncertainties are dominated by a number of systematic effects. We will present the test results for the measured basalt and granite monuments in various configurations and will describe the systematic effects that drive up the measurement uncertainties.

References:

[1] Surkov, Y., et al., (1984), Geophys. Res. Suppl., 88:481-493; [2] Surkov, Y. et al., (1986), Geophys. Res. Suppl., 91:215-218; [3] Radtke, R.J., et al., (2012), SPWLA 53rd Annual Logging Symposium, paper AAA 1–16; [4] Parsons, A.M et al., (2016), 47th Lunar and Planetary Science Conference, 2476.

SIGNAL PROCESSING TECHNIQUES FOR SILICON DRIFT DETECTOR BASED X-RAY SPECTROMETER FOR PLANATARY INSTRUMENTS. A R Patel, M. Shanmugam, T. Ladiya, Physical Research Laboratory (Navarangpura, Ahmedabad-380009, Gujarat,India; arpitp@prl.res.in, shans@prl.res.in, tinkal@prl.res.in).

Introduction: Most radiation detectors require pulse (or signal) processing electronics so that energy or time information involved with radiation interactions can be properly extracted. The objective of this work is to develop and compare various pulse processing techniques for x-ray and Gamma ray spectrometers which can be used for future scientific missions. A preamplifier is the first component in a signal processing chain of a radiation detector which has a main function to extract the signal from the detector without significantly degrading the intrinsic signal-to-noise ratio. CSPA output signal is given to pulse height analyzer for energy spectroscopy.

To study we are developing SDD (silicon drift detector) based x-ray spectrometer using various pulse height analysis techniques. We are working on different techniques of pulse height analysis like Wilkinson ADC technique, Pulse width modulation technique, Digital pulse processing technique and pulse height measurement using peak detector & successive approximation ADC. This study will help to identify the proper processing technique based on planetary instrument specifications like number of detectors, total incoming photon count rate, spectral resolution, size, mass and power. The design details and evaluation results of techniques are presented in this paper.

SDD based Spectrometer with conventional peak detection technique: SDD based spectrometer is mainly divided in two parts. Sensor package and processing package. sensor package consists of SDD module coupled with Charge Sensitive Pre-Amplifier (CSPA), shaping amplifier, HV supply for SDD module, controller for and the Peltier cooler. The analog front end electronics include shaping amplifiers with peaking times of 1µs. The block schematic of spectrometer is shown in figure 1.

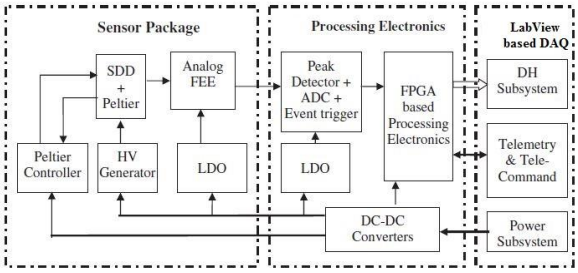

Figure 1. Block schematic of SDD based Spectrometer with conventional Peak detection method.

The hardware setup for SDD based spectrometer is shown in figure 2. With this setup we are getting ~200 ev resolution at 5.9 Kev by putting the Fe55 source in front of the detector.

Figure 2. Set up for SDD based X-ray spectrometer.

Digital Pulse Processing technique for real-time pulse shaping: Shaping amplifier and peak detector use in system limits the count rate and performance at higher count rate, to overcome to this problem digital pulse processing technique is developed which can be used for space instruments. In this system the digitizer replaces both the Shaping Amplifier and the Peak Sensing circuitry by direct digitizing pre-filter output as shown in figure-3.

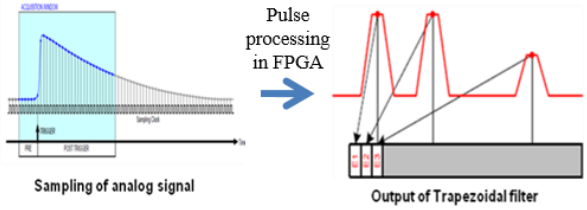

Figure 3. Pulse processing technique (sampling and Trapezoidal filtering)

The pulse shaping is done in digital by means of a trapezoidal filter implemented in FPGA running online on the digitizer data. Efficient recursive algorithm is developed for ACTEL A3P250 FPGA which allow real time implementation of a shaper that can produce either trapezoidal or triangular pulse shape. The setup for large area SDD detector is shown in figure 4 which has an interface with programmable FPGA board. With keeping the X-ray source Fe55 to front of detector we are getting 200 ev resolution at 5.9 Kev. The spectra is shown in figure 5.

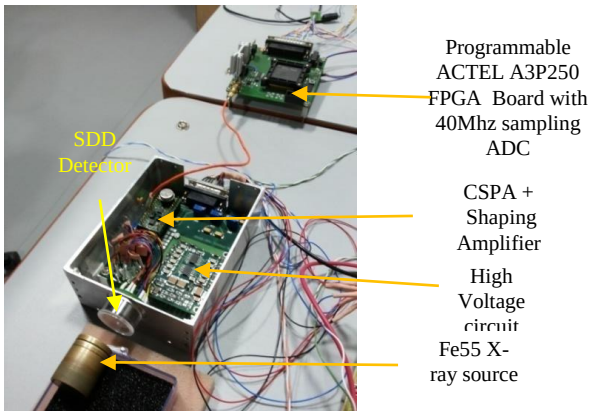

Figure 4. SDD detector setup for digital pulse processing including sampling ADC and on-board programmable FPGA.

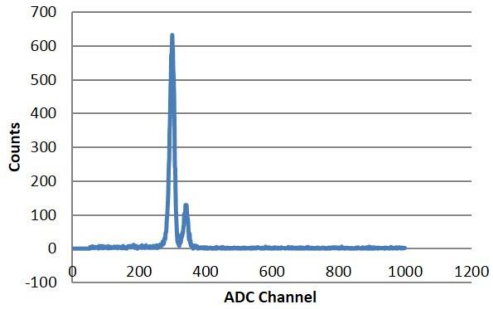

Figure 5. Initial results - Spectra obtained with Fe55 source using digital pulse processing technique.

Designed scheme for Wilkinson ADC technique (linear discharge): This work has been in inspired from the Wilkinson ADC. The detail schematic block diagram is shown figure 6. The comparator compares the shaping amplifier output with discharge output which is delayed by few ns. This delay can help us to identify the peak of shaped pulse. The comparator output pulse is given to a switch to initiate the discharge process. The higher discharge time can help to cover a wide energy.

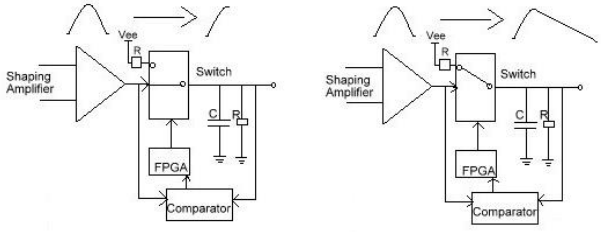

Figure 6. Conceptual method for the linear discharge of the signal.

Figure- 7 shows the shaping amplifier last stage output and the discharge pulse output. The discharge pulse is compared with small reference voltage using fast comparator. The width of the pulse output of comparator has the information about peak height. This pulse is given as an input signal to the FPGA where the logic is implemented to count the number of clocks within the entire width. The Counter clock is at 320 MHz which is generated using FPGA internal PLL block which gives the pulse width resolution of 3.125ns.

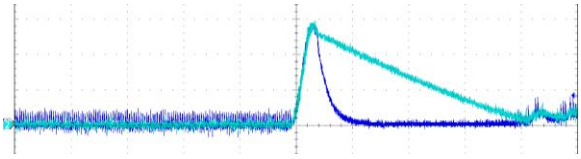

Figure 7. CRO screen showing Shaping amplifier output (Dark Blue) and Linear discharge pulse Output (light Blue).

With this technique we obtain the resolution ~300 ev at 5.9 Kev. We are targeting the 200 ev resolution with this system by making printed boards. Results for this technique will be discussed more at workshop.

PWM technique to measure pulse height: People are mostly use it in the DC signal only, here we are trying to measure the pulse height with use of PWM. We have generated a triangular waveform of frequency ~500Khz with use of integrator circuit. The fast comparator AD8561 is used to compare the triangle wave with Gaussian pulse which is coming from Shaping amplifier output. The output of PWM is shown in figure 8.

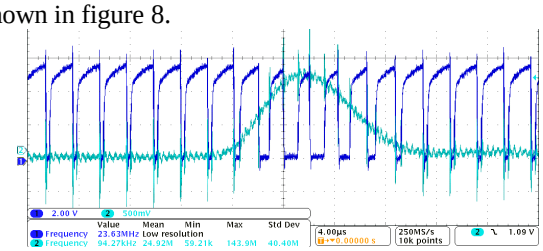

Figure 8. PWM output with Gaussian input pulse.

The PWM output will be given to FPGA to measure the pulse width. The width is proportional to the height of analog pulse. We have made 320Mhz PLL internal to FPGA to measure the pulse width with resolution of 3.125 ns. System with PWM circuit and FPGA is connected with SDD detector and initial results are obtains which shows 300ev resolution at 5.9Kev. Further we like to improve the results by increasing the PLL frequency or by using the Vernier method to measure the pulse width with resolution of <1 ns.We are optimizing all designs for better performance and count rate achievement so the comparative study will be more discussed during workshop.

Venus Heat Flow Instrument Development Michael Pauken[1] Kevin Smith[1], Sutine Sujittosakul[1], Billy C. Li[1], Samad Firdosy[1] Suzanne Smrekar[1], and Paul Morgan[2], [1]Jet Propulsion Laboratory, California Institute of Technology, 4800 Oak Grove Blvd, M/S 125-123, Pasadena, CA 91109, mpauken@jpl.nasa.gov, [2]Colorado School of Mines 1801 19th St., Golden, CO 80401.

Introduction: We are developing an instrument that would help illuminate the evolutionary path that has brought Venus to its unique state today by measuring the heat loss from its interior at the surface. Knowledge of the present day heat flow would allow us to provide an estimate of the lithospheric thickness, the current level of geologic activity, and distinguish between various hypotheses of planetary evolution. Numerous models of Venus' thermal evolution exist. A very low heat flow (<20 mW/m^2) would indicate that either a recent stagnant lid or a very late stage of episodic global overturn is operating [1]. An intermediate value of heat flow (20-40 mW/m^2) would be consistent with a stagnant lid modulated by convective heat flux [2]. High values (> 40 mW/m^2) would indicate a thinner lithosphere and possibly a long period of mantle heating due to the effect of an insulating stagnant lid [3]. The predicted heat flow today is a function of the assumed concentration of radiogenic material, heat of accretion, and most importantly, the style of geologic activity.

Heat flow measurements for Earth, the Moon, and those scheduled for Mars (InSight mission) are based on subsurface temperature measurements below their diurnal and annual variations. On Venus, access to the subsurface is not necessary because there are essentially no diurnal or annual temperature variations due to the thermal stability of its dense lower atmosphere. The surface flux measurement approach described here is possible on Venus because the surface diurnal or annual temperature changes are small ~1 K; [4] and occur at much longer time scales than the time required to measure the surface flux.

Objectives: Our objective is to develop robust a instrument for rapidly measuring heat flow at the Venus surface over the range of 10 to 100+ mW/m^2 with an accuracy of ±5 mW/m^2. This level of accuracy is sufficient to determine whether the interior Venus heat flux is low, intermediate or high.

Configuration: The heat flux sensor would be externally deployed from a lander vehicle as shown in the figure below. The sensor would be located on the end of a boom that places it on the surface. During operation the sensor generates a voltage proportional to the heat flux flowing through it. The electronics located within the lander vehicle measure the generated voltage signal.

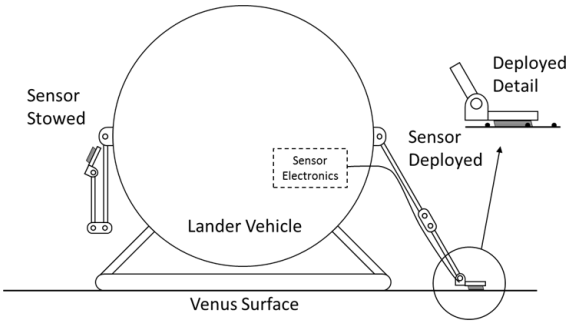

Heat flux sensor instrument shown on a Venus lander vehicle.

Prototype: The heat flux sensor uses the thermoelectric effect of specific semiconductor materials to measure heat flow. Thermoelectric material pairs produce a voltage when they are subjected to temperature gradients. This principle is used by thermocouples to measure temperature.

The sensor, shown in the figure below, has a graphite disk base. Heat flow from the Venus surface would flow into the base, through the thermopiles and then through the top graphite disk. Between the graphite disks are ten thermopiles each with 10-pairs of thermoelectric element (TE) legs. One leg of each thermoelectric pair is an n-type skutterudite semiconductor and the other leg is a p-type. The top of the thermopiles are bonded to a graphite disk that rejects heat by convection and radiation to the ambient environment.

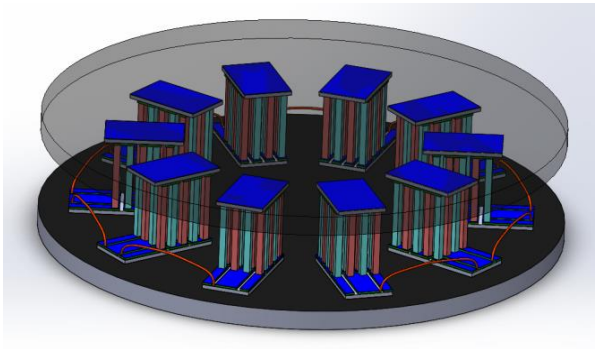

A CAD rendering of the prototype Venus surface heat flux sensor.

Analysis: An analytical model of the heat flux sensor has been developed to understand the performance and capability of the heat flux sensor and to guide the development of a prototype sensor. The analysis was

performed using finite element modeling with COMSOL Multiphysics. Parametric studies of device geometry, effects of conjugate heat transfer, and assumed heat flux from the surface were carried out. The thermoelectric device-based sensor design constitutes a geometry that analytically satisfies the requirements for measuring the surface heat flux in the range of 10 to 100+ mW/m^2 with a resolution of 5mW/m^2.

For the selected n- and p-type semiconductors the Seebeck coefficient is 340 μVolts/K at 750K, Venus' surface temperature. This produces a voltage of 0.12 μVolts per element pair and for an array of 100 elements, the total voltage generated is 12 μVolts for the 5 mW/m^2 heat flux resolution. A plot of the predicted sensor output voltage as a function of input heat flux is shown below at Venus temperature and at ambient temperature.

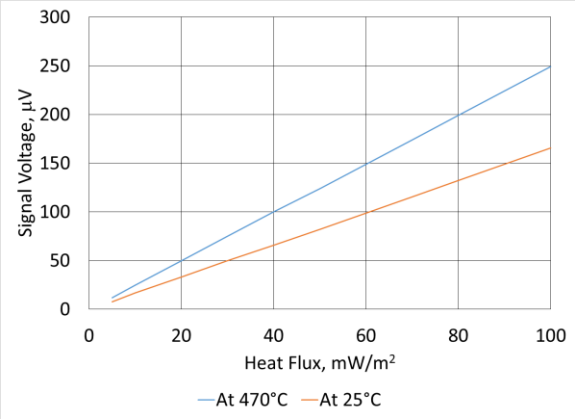

Predicted performance of the Venus heat flux sensor.

References: [1] Parmentier, E. M., and Hess P. C., (1992) *Geophys. Res. Lett., 19*, 2015-2018. [2] Phillips, R.J et al. (1997) in *Venus II*, Univ. Arizona Press. [3] Smrekar, S. E. and Sotin, C. (2012) *Icarus*. [4] Dobrovolskis, A.R. (1993) *Icarus* 103, 276-289.

THE EUROPA SEISMIC PACKAGE (ESP) CONCEPT: 1. SELECTING A BROADBAND MICROSEISMOMETER FOR OCEAN WORLDS. W. T. Pike[1], I. M. Standley[2], S. Calcutt[3], S. Kedar[4], S. D. Vance[4], B. G. Bills[4], [1]Dept. of Electrical and Electronic Engineering, Imperial College, London, UK, [2]Standley Technology Consulting, Claremont, CA, [3]Dept. of Physics, Oxford University, UK, [4]Jet Propulsion Laboratory, Caltech, Pasadena, CA w.t.pike@imperial.ac.uk

Introduction: NASA is currently studying a potential Europa lander mission with instrumentation required to be ready within 3-4 years. The mission would search for life and habitability by probing and analyzing the chemistry of the surface ice in pursuit of evidence for microbiological markers. The Europa Lander concept and subsequent Ocean Worlds landers would also carry seismometers to map the shallow and deep interiors of the moons, which hold the keys to understanding their planetary evolution, their thermal and chemical make-up, and thus their long-term habitability. We summarize the instrument requirements that would enable a seismic system to provide a probe of the habitability of Europa and introduce a candidate microseismometer for a Europa Seismic Package (ESP) concept that meets those requirements, comparing to potential competitor technologies.

Seismology as a Probe of Habitability: Sensitive seismometers are critical for detecting faint motions deep within planetary bodies that can be used to reconstruct composition and temperature structure, while also revealing fundamental processes such as plate and ice tectonics, volcanism, ocean waves, ice flow, geysers and more. Moreover, a seismometer for Europa and other Ocean Worlds will listen for the moons' distinct "vital signs": fluid motion in the shallow subsurface, cryovolcanos, and sub-glacial ocean circulation (Fig. 1).

Prior investigations [1, 2, 3, 4] have considered primary seismic sources, their likely occurrence rates and magnitudes, and how they might be used to measure the thickness of the ice shell and underlying ocean. Europa's internal structure controls its prospects for life by governing the cycling of redox materials, which is key to habitability [5]. A hot metallic core or silicate melts [6] would be strong evidence for an active interior [e.g., 3] and of continued hydrothermal activity producing hydrogen and other electron donors needed to sustain chemical energy for life. The amplitude and frequencies of these expected sources in plotted in Fig. 1.

The SP microseismometer: The measured noise floor of the microseismometer that was successfully delivered to the InSight Mars 2018 mission is also shown in Fig. 1, demonstrating sufficient sensitivity to detect a broad range of Europa's expected seismic activity. While this seismometer is designated as "short period" (in comparison to the CNES-designed very broadband (VBB) seismometer), the SP provides a sensitivity and dynamic range comparable to significantly more massive broadband terrestrial instruments. The sensor is micromachined from single-crystal silicon by through-wafer deep reactive-ion etching to produce a non-magnetic suspension and proof mass with a resonance of 6 Hz [7].

The SP is well suited for accommodation on a potential Europa Lander. It is robust to high shock (> 1000 g) and vibration (> 30 g_{rms}). For qualification SP units have undergone the full thermal cycles of the InSight mission and noise tested down to 208K, with no degradation in the performance in both cases. In addition, the sensor has been tested as functional down to 77K, below the lowest expected temperatures on Europa. All three axes deliver full performance over a tilt range of ±15° on Mars, allowing operation on Europa without leveling. The SP operates in feedback automatically initiated with power on of the electronics, achieving a noise floor

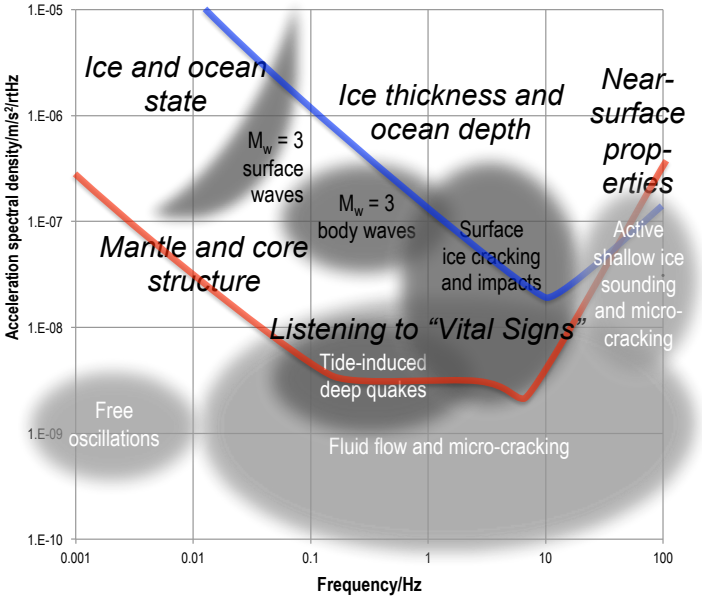

Figure 1: Europa is expected to be seismically active *[2,4] requiring a sensitive, broad-band, high-dynamic-range seismometer such as the SP (red). The expected sources are located in their relevant frequency and amplitude ranges, based on Earth analog (black text) and models (white text), with italicized text indicating the science investigations that are enabled by recording these sources. The sensitivity of a 10 Hz geophone is shown in blue for comparison.*

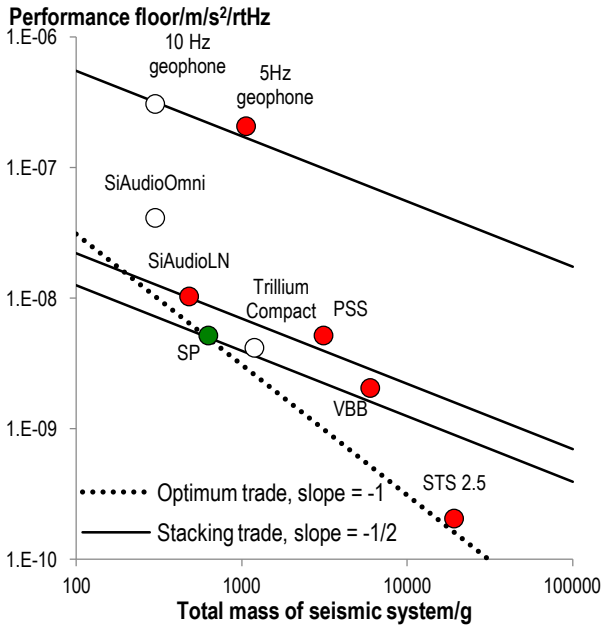

Figure 2: Comparison of sensor performance/mass parameter space. *The SP is the most mature and best suited for Europa: it is the only non-magnetic seismic system delivered for flight (marked in green), with most comparators also requiring leveling (marked in red).*

below 1 ng/√Hz in less than a minute. The total mass for the three-axis SP delivery is 635g while the power requirement is 360 mW.

Comparative Technology Assessment: We have compared the SP with a variety of other possible seismic technologies in terms of performance (noise floor), mass and power:

- Conventional 10 Hz (Fig. 1) and 5 Hz geophones (noise data from [8])
- Two optically sensed miniature seismometers, one requiring tilt [8]
- A geophone developed in Japan for a lunar penetrator, PSS [9]
- A conventional broad-band seismometer, the Trillium Compact [10]
- The Streckeisen STS 2.5, a high sensitivity seismometer with performance designed to match the lowest ambient noise floor of Earth [11]
- The CNES VBB under development for InSight 2018 [12]

The noise floor accounts for the peaked response of the geophones by selecting the lowest noise sensitivity at the extremes of a frequency bandwidth of two orders of magnitude. The mass requirements are estimated for a three-axis seismic system. If the sensor requires tilt under Europa gravity, an additional 75% is added for the mechanism, based on the InSight VBB system. The critical trade for these seismic systems is between performance and mass as their power budgets are comparable. The relationship between these two parameters (fig. 2) gives the general trend of the instrument locations, with a slope of ~ -1. The SP has the highest figure of merit: compared to its nearest neighbors it has twice the performance of the non-flight Silicon Audio Low Noise, 50% the mass of the non-flight Trillium Compact, and 20% the mass of the PSS. Geophones fare poorly in this trade, with lower performance without any mass advantage. One option to improve performance is to use multiple, n, units to push down the noise by $\sqrt{n}$. However, this comes at an increase of n in the mass and hence such "stacked" systems will be distributed along lines of slope -1/2, pushing them away from the optimal trade line.

Two other critical parameters for selection are the deployment and calibration requirements, and the technology maturity. Leveling requires additional mass and more complicated deployment, and introduces additional failure modes, some of which may be hard to predict in the Europa environment. The SP does not need leveling unlike most other competing technologies. It also requires no magnetic calibration from additional sensors, unlike all its comparators. These are important advantages given the strong slopes [13] and variable magnetic environment at Europa [14]. Finally, only the SP has the fully flight-qualified heritage.

Conclusion: The SP stands out as the strongest candidate for development for a Europa payload. We are now adapting its design to meet the environmental challenges of Europa.

Acknowledgments: A portion of this work was funded by the UK Space Agency, and a portion performed at the Jet Propulsion Laboratory, California Institute of Technology, under a contract with NASA. U.S. Government sponsorship is acknowledged.

References: [1] Kovach & Chyba. (2001) *Icarus*, **150**(2):279– 287 [2] Lee et al. (2003), *Icarus* **165**, 144–167 [3] Cammarano et al. (2006) *J. Geophys. Res.,* E12009 [4] Panning et al. (2006) *J. Geophys. Res.*, E12008 [5] Vance et al. (2016) *Geophys. Res. Lett.*, **43**, 4871–4879 [6] Chantel et al. (2016) *Science Advances*, **2**, 5, e1600246 [7] Pike et al. (2013). *Proc. Transducers & Eurosensors XXVII,* 622-625 [8] http://www.siaudio.com/uploads/common/10-15-SA-product-flyer-updates-v2.pdf [9] Yamada et al. (2009) *Planetary Space Science* 57, no. 7: 751-763 [10]http://www.nanometrics.ca/ckfinder/userfiles/files/NMX-TrilliumCompact-%20WEB.pdf [11] http://www.kinemetrics.com/uploads/PDFs/STS-2_5.pdf [12] Robert et al. (2012) *LPSC*, vol. 43 2025 [13] Schenk (2009) *Geophys. Res. Lett.*, 36(15):L15204 [14] Kivelson et al. (2009) *Europa*, ISBN: 9780816528448, 545-570.

PLANETARY GAMMA RAY SPECTROSCOPY WITH STRONTIUM IODIDE

T. H. Prettyman[1], N. Yamashita[1], A. Burger[2], E. Rowe[2], J. Butler[2], M. Groza[2], K. G. Stassun[3], J. L. Lambert[4], J. C. Castillo-Rogez[4], C. A. Raymond,[4] S. M. Feldman,[4] P. R. Beck[5], N. J. Cherepy[5], S. A. Payne[5], [1]Planetary Science Institute (prettyman@psi.edu), Tucson, AZ, [2]Fisk University, Nashville, TN, [3]Vanderbilt University, Nashville, TN, [4]Jet Propulsion Laboratory, California Institute of Technology, Pasadena, CA, [5]Lawrence Livermore National Laboratory, Livermore, CA.

Introduction. The chemical composition of solar system bodies can be determined from gamma ray spectra measured by an instrument deployed on an orbiter, lander, rover, or sonde. Gamma rays are produced by the decay of natural radioelements and, for bodies with thin or no atmosphere, by the interaction of galactic cosmic rays with the regolith. The leakage spectrum of gamma rays can be analyzed to determine the concentration of specific elements, such as H, C, O, Mg, Al, Si, S, Cl, K, Ca, Ti, Fe, Ni, Th, and U. The elemental data is needed to understand chemical and physical processes underlying planetary formation and evolution.

Gamma ray spectroscopy is well established for planetary remote sensing. The elemental composition of surface materials on Mercury, Venus, the Moon, Mars, the near-Earth asteroid 433 Eros, the main belt asteroid 4 Vesta, and the dwarf planet 1 Ceres was determined from passive gamma ray measurements [e.g. 1]. Although some information can be obtained during a close flyby, precise measurements require lengthy accumulation at low altitude (<1 body radius). Future missions may use active interrogation with a pulsed neutron generator or isotopic neutron source for high-throughput, in situ measurements.

Requirements: Sensors with large active volumes made from materials with high density and atomic mass are required to measure gamma rays in the target energy range: a few hundred keV to 10 MeV. High-energy resolution is desired; however, other factors such as payload limitations (mass, volume, power), thermal environment, susceptibility to radiation damage and backgrounds must be considered. For example, sensors optimized for the exploration of main belt asteroids may be poorly suited for a mission to the surface of Venus.

Strontium Iodide: Europium-doped strontium iodide, SrI_2(Eu), is an ultra-bright scintillator with a factor of two to four times better energy resolution at room temperature than scintillators with flight heritage. Improved resolution will enable accurate analyses of elements with gamma rays in the densely populated region below 3 MeV (Fig. 1). Large, single crystals can be manufactured, obviating the need for arrays required for other sensor technologies (e.g. CdZnTe). The scintillation emission spectrum is well matched to the photon detection efficiency of solid-state optical sensors, such as silicon photomultipliers, leading to compact, low-power spectrometers (Fig. 2). These factors combined with the potential for scalability of crystal size and absence of self-activity make SrI_2 an excellent choice among competing scintillators such as $CeBr_3$ and $LaBr_3$ [3].

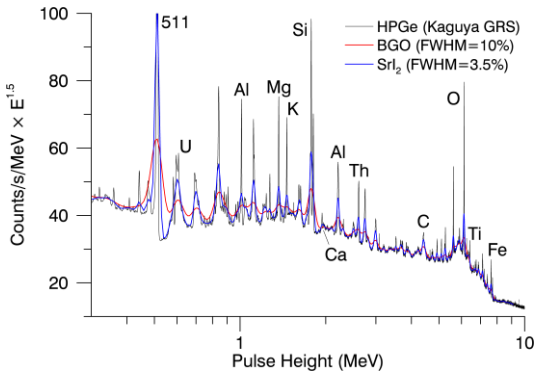

Figure 1. The average lunar spectrum acquired by JAXA/Kaguya (HPGe) was adjusted to illustrate the potential performance of a SrI_2 gamma ray spectrometer.

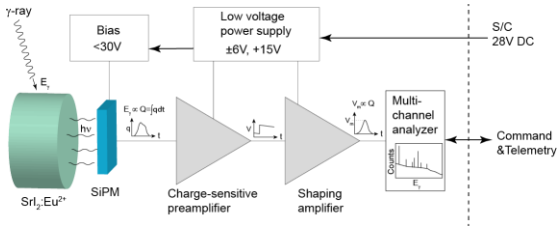

Figure 2. Block diagram for a gamma ray spectrometer with a SrI_2 crystal and silicon photomultiplier (SiPM).

Next steps in the development of SrI_2 for planetary applications include optimizing crystal growth, packaging and readout of large-volume crystals; evaluating radiation damage effects for SrI_2 crystals and optical sensors; determining the response of sensors to energetic particles; and identifying potential sources of background. Successful development will lead to a new generation of high-performance spectrometers that can be deployed on a variety of platforms [e.g. 4] to targets large and small in the inner and outer solar system.

References: [1] Prettyman, T.H. (2014), in Encyclopedia of the Solar System, ISBN:9780124158450. [2] Cherepy, N. J. et al. (2008), *Appl. Phys. Lett., 92*, 083508. [3] Prettyman, T. H. et al. (2015) *SPIE Newsroom*, doi: 10.1117/2.1201510.006162. [4] Egner, J. C. et al., *JATIS*, submitted.

Acknowledgement: This work is funded by the NASA PICASSO program.

Junocam: approach and orbit 1 imaging. M. A. Ravine[1], M. A. Caplinger[1], C. J. Hansen[2], A. P. Ingersoll[3] and S. J. Bolton[4], [1]Malin Space Science Systems, 5880 Pacific Center Blvd, San Diego, CA, ravine@msss.com, [2]Planetary Science Institute, Tucson, AZ, [3]California Institute of Technology, Pasadena, CA, [4]Southwest Research Institute, San Antonio, TX.

Introduction: The Juno mission to Jupiter includes a visible/near infrared camera (Junocam) as part of its science payload. After a five-year cruise, Juno went into orbit around Jupiter on 4 July 2016. Junocam took images of Jupiter and its satellites in the weeks before Jupiter Orbit Insertion (JOI). After having been powered off for a week around JOI, Junocam was turned back on and has been imaging since then. As Juno is in a highly elliptical orbit, the images currently being taken are very low resolution, but show that the instrument is functioning well.

The details of the Junocam development have been documented previously [1]. Our purpose here is to summarize the aspects of the Junocam design relevant to interpreting the images, to present images already acquired and to describe the planned acquisitions for the next periapsis pass on 27 August 2016. During that pass, Juno will pass within 5000 km of Jupiter's cloudtops, with Junocam acquiring the highest resolution images ever taken of Jupiter.

Junocam imaging scheme: The Junocam camera head is fixed-mounted to the Juno spacecraft, with its optic axis pointed perpendicular to the spacecraft spin vector (Figure 1). The 58° wide Junocam field of view is thus swept though 360° by each spacecraft rotation.

Figure 1. The Junocam flight camera head, shortly after it was integrated with the Juno spacecraft.

The instrument can image in four different color bands by means of a fixed color filter array mounted to the Junocam CCD detector. Color images are built up by "pushframe" imaging, as is done with the MRO MARCI [2] and LRO WAC instruments [3]. The four color bands are shown in Figure 2. The three visible bands (blue, green and red) were selected to provide color images similar to what the human eye would see. The fourth band, which overlaps the methane absorption feature centered at 889 nm, was selected to provide images with some vertical discriminability (features that sit higher in the atmosphere have less of their light absorbed by methane in the band, and thus appear brighter).

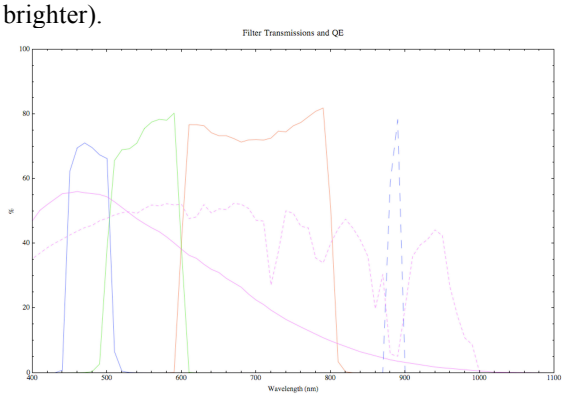

Figure 2. The bandpasses of the four Junocam color filter bands (blue, green, red and 889 nm methane). These are plotted over the quantum efficiency of the Junocam detector and the Jupiter spectrum. This shows the challenge of methane-band imaging, with the reflectivity of Jupiter becoming very low and the detector response likewise.

Because of the low light level at Jupiter—being five times farther from the Sun than Earth, the solar irradiance is twenty-five times lower than at Earth—Junocam incorporates two other features: a relatively fast lens (f/2.7) and the capability to clock the camera's interline transfer CCD detector to track the motion of the target from the rotation of the spacecraft (Time Delay Integration, or TDI). For imaging in the visible bands, only low levels of TDI (1 or 2) are required to get an acceptable signal-to-noise ratio (SNR). For the methane band, the signal levels are low and the instrument response is also low, so large amounts of TDI are required (up to 64 lines, the maximum the instrument can do). With these much longer exposures, the methane band images are more vulnerable to transient radiation hits.

Operations:

Approach. During the three weeks before Juno JOI, Junocam was turned on and acquired three-color visible images of Jupiter and the Galilean Satellites

once every 15 minutes. Over 1300 color images were acquired between 12 and 29 June, which were then assembled into a movie of the approach to Jupiter (see https://www.missionjuno.swri.edu/). An example of one of these frames is shown in Figure 3. This sequence shows the satellites making multiple revolutions about Jupiter and going in and out of eclipse. While Jupiter is small enough to be almost featureless at the beginning, at the spacecraft nears the planet, the classic features become visible (the belts and zones, the Great Red Spot (GRS) and shadows of the satellites crossing the sunlight face of the planet. The raw images are also available for download from the Mission Juno website.

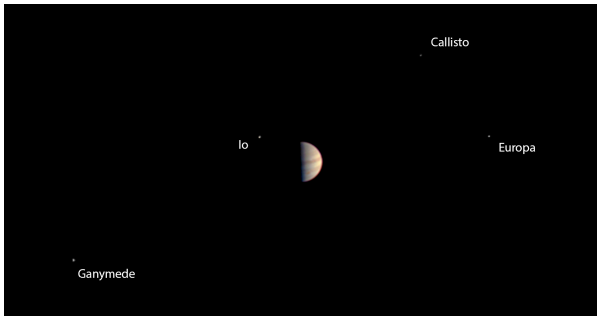

Figure 3. An approach image taken by Junocam of Jupiter and the four Galilean Satellites. The Great Red Spot is visible on the lower (southern) half of the planet (12 to 29 June 2016).

Orbit 1. Five days after JOI, Junocam was powered on and commanded to acquire images of Jupiter. While the spacecraft had passed within 5000 km of the planet during orbit insertion, by 10 July, it was 4.3 million km away. At that distance, although the resolution in the images is low, it was initially still better than the highest resolution of the approach images (see Figure 4).

Figure 4. A Junocam image of Jupiter and the Galilean Satellites (excepting Callisto), taken three days after Jupiter Orbit Insertion. The Great Red Spot is visible south of the equator.

Methane band. Due to data volume constraints, no methane band images were acquired during approach. To determine the actual signal levels from Jupiter in this band, a series of images were taken in the methane filter with 32 lines of TDI. The signal levels were, as expected, somewhat low, but still high enough to discern the features we expected to see in this band: the polar haze, the equatorial band and the GRS. See Figure 5.

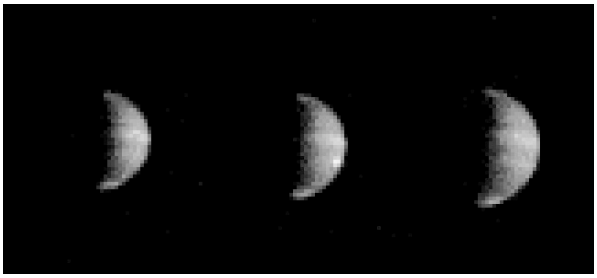

Figure 5. A sequence of three Junocam images in the 889 nm methane absorption band. The polar hazes and equatorial band are visible, as is the GRS in the center image.

First Periapsis (PJ-1). On 27 August 2016, Juno will make its first periapsis pass. Junocam will be on for this entire pass, and will acquire the following images (in priority order):

- Before closest approach, looking "down" on the north pole (RGB color and methane).
- After closest approach, looking "up" at the south pole (RGB color and methane).
- At closest approach, the highest resolution image ever of Jupiter (RGB color).
- An approach time-lapse sequence for the five days preceeding PJ-1.
- Ganymede (resolved but small).

Depending on the constraints of this sequence, we may also attempt long exposures of the poles to determine if Junocam has the capability to detect Jupiter's aurora (the uncertainty is whether the aurora will be brighter than the scattered light from Jupiter in the Junocam wide-field optics in a long exposure).

References: [1] C. J. Hansen, et al. (2014) *Space Science Reviews,* [pp.1-32], doi:110.1007/s11214-014-0079-x. [2] J. F. Bell, et al. (2009) Mars Reconnaissance Orbiter Mars Color Imager (MARCI): Instrument description, calibration, and performance, *Journal of Geophysical Research-Planets* 114, E08S92, doi:10.1029/2008JE003315. [3] M. S. Robinson, et al. (2010) *Space Science Reviews*, [pp.81-124], doi:10.1007/s11214-010-9634-2.

ECAM, a Modular Spaceflight Imaging System—First Flight Deliveries. M. A. Ravine[1], J. A. Schaffner[1] and M. A. Caplinger[1], [1]Malin Space Science Systems, Inc., P.O. Box 910148, San Diego, CA 92191, USA, e-mail: cameras@msss.com.

Introduction: Since 2009, Malin Space Science Systems, Inc. (MSSS) has used our extensive experience in science instruments to develop the modular, space qualified, ECAM imaging platform (Figure 1). While ECAM was originally conceived for engineering camera applications, its flexibile architecture makes it useful for science applications as well. MSSS has delivered four ECAM systems to four different customers and for widely varying missions and is under contract for two additional systems. The variety of real-world applications and interface requirements has proven the flexibility of the architecture, expanded the heritage of the common elements, and provided useful insight for further development. Through a custom, ECAM-derived camera development for NASA Goddard Space Flight Center, MSSS has qualified a new 2592 x 2048 format CMOS sensor with 4.8 µm pixels. In parallel with this custom design, MSSS is developing two new ECAM-compatible cameras based on this sensor (each available in color and monochrome versions); the two cameras provide different balances of volume/mass/power vs. performance/features.

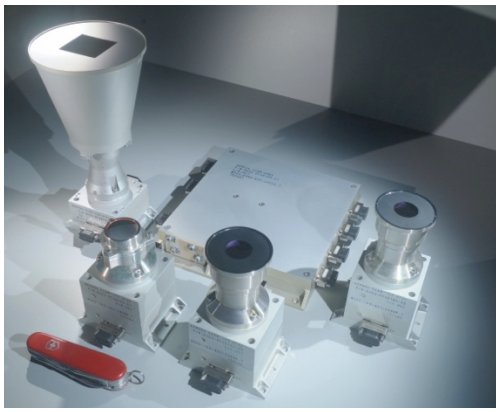

Figure 1. A flight ECAM 4-port Digital Video Recorder and visible CMOS and thermal IR Cameras (DVR4, center; CMOS camera head, left; IR camera heads, front and right; Swiss Army Knife for scale).

ECAM modular spaceflight imaging system platform: Each ECAM system consists of a DVR and one or more camera heads. Camera heads interface to the DVR through a standardized interface that provides power and data on a single cable, with pin counts minimized to reduce cable mass. Examples of delivered flight hardware are shown in Figure 1.

Digital Video Recorders (DVRs). There are three configurations of DVRs, supporting one, four, or eight sensor heads. DVRs include a 128MB volatile buffer and non-volatile buffers of 8, 16, or 32GB. The baseline system performs JPEG (lossy) and Huffman first-difference lossless compression. JPEG2000, LOCO-I, or H.264 compressors may also be implemented. The embedded soft-processor runs the instrument flight software, which implements the higher-level layers of the camera and spacecraft interface protocols and orchestrates all functions performed by the logic peripherals. A flight DVR4 board is shown in Figure 2.

Figure 2. A flight ECAM 4-port DVR PCB.

Visible Wavelength CMOS Camera. The ECAM-C50 acquires 2592 x 1944 format images with 2.2 µm pixel pitch; either Bayer pattern (color) or monochrome versions of this sensor are available. The C50 camera head weighs less than 250 g (without optics or mounting brackets).

Long-Wave Infrared Microbolometer Camera. The ECAM-IR3A uses an uncooled amorphous silicon microbolometer to acquire 640 x 480 format images with 17 µm pixels in the Long Wave Infrared band (8-13µm wavelength). It has a similar (though somewhat larger) mass and form-factor as the C50. An image taken with one of these cameras is shown in Figure 3.

Optics. For the visible camera (C50), there are four standard lens options, ranging from ~90° to 15° fields of view. These optics are fixed focus and are athermalized to provide stable performance over a wide temperature range. There are two standard LWIR lenses, with fields of view of ~20° and ~60°.

Interface. The DVR data interface to the spacecraft is comprised of eight LVDS differential pairs (RS-422 optional) in each direction, split across redundant connectors with independent drivers and receives. The interface is implemented in programmable logic, allowing substantial customization. For the units

already delivered, interfaces have included SpaceWire, low-speed asynchronous, and high-speed synchronous, with both RS-422 and LVDS at the electrical level.

TRL. Flight ECAM systems have been assembled, qualified, and delivered, bringing all components of the baseline ECAM system to TRL 8. With the lauch of OSIRIS-REx in September of 2016, the DVR and visible cameras will be at TRL 9. The IR camera is expected to fly in early CY2017, at which point it will also be at TRL 9.

Figure 3. A thermal IR image of the Moon taken with an ECAM IR3A camera.

ECAM flight deliveries: MSSS delivered three flight ECAM systems in CY2015 and CY2016. They are as follows:

OSIRIS-REx TAGCAMS (Lockheed Martin). The Touch-and-Go Camera System (TAGCAMS) is a multi-purpose imaging system installed on the OSIRIS-REx asteroid sample return mission [2]. TAGCAMS consists of a DVR8 and three C50 camera heads each with ECAM medium field of view (MFOV) lenses. One camera will monitor the delivery of the sample from the asteroid Benuu to the Earth sample return capsule (StowCam, see Figure 4); the other two cameras will image the asteroid and background star field to support optical navigation when the spacecraft is in the vicinity of the asteroid (NavCam). OSIRIS-REx is scheduled for launch in September, 2016, with first operation of these cameras shortly thereafter.

Undisclosed customer #1. The second delivered flight ECAM system is a DVR4 with four camera heads: one C50 color visible camera, and three IR3A thermal infrared cameras (Figure 1). The visible camera has a narrow field lens; the IR cameras have a combination of wide- and narrow-field lenses. The system could operate all the cameras in a streaming mode over three parallel SpaceWire ports to the spacecraft. Launch for this system is expected in early CY2016

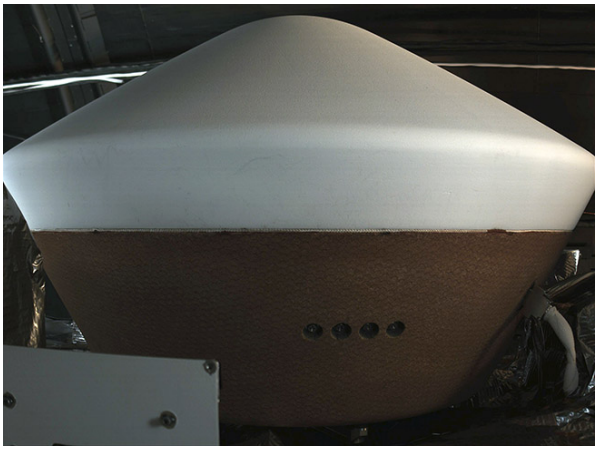

Figure 4. An image of the OSIRIS-REx sample return capsule taken by StowCam after integration with the spacecraft.

Undisclosed customer #2. The third flight ECAM system is a DVR1 system with a single camera head: a C50 color visible camera with a narrow field lens. This system provides after-the-fact knowledge of acquisition time to within 1 ms.

Lessons learned: While each of these programs had their own unique aspects, the recurring theme between them was the need to allocate somewhat more attention to interface and requirements definition early in the program. As expected, each customer had unique interface requirements; Despite this, all could be accommodated with customized FPGA logic, using the single, flexible, data interfaces of the DVR (the only unique hardware configuration being the selection of LVDS or RS-422 drivers and receivers).

References: [1] Schaffner, J. A., M. A. Ravine and M. A. Caplinger (2014), Int'l Workshop on Instrumentation for Planetary Missions, Abstract #1114. [2] Drake, M. J et al., American Geophysical Union, Fall Meeting 2011, abstract #P42A-03.

LOAC-S: a small aerosol optical counter/sizer for planetary measurements of the size distribution and nature of atmospheric particles.

Jean-Baptiste Renard[1] and the LOAC team, Nicolas Verdier[2]
[1] LPC2E-CNRS / Université d'Orléans, 3A avenue de la recherche scientifique, 45071 Orléans, France,
[2] Centre National d'Etudes Spatiales (CNES), DCT/BL/NB, 18 avenue Edouard Belin, 31401 Toulouse cedex 9, France

On Earth, the study of aerosols in the troposphere and in the stratosphere is of major importance both for climate and air quality studies. In the solar system, the atmospheric aerosols size and distribution are key parameters for radiative fluxes assessment not only for solid planets like Mars but also for the gaseous planets like Saturn.

Among the numerous instruments available, aerosol particles counters provide the size distribution in diameter range from few hundreds of nm to few tens of um. Most of them are very sensitive to the nature of aerosols, and this can result in significant biases in the retrieved size distribution. It is not the case for the versatile optical particle/sizer counter (OPC) named LOAC (Light Optical Aerosols Counter), which has been used for years to perform measurements not only at the surface but under all kinds of balloons in the Earth atmosphere (more than 100 flights in the stratosphere since 1993). As a consequence, the instrument reliability is now demonstrated and it is light and compact enough to address planetary missions.

LOAC is an original OPC performing observations at two scattering angles. The first one is around 12°, and is almost insensitive to the nature of the particles; the second one is around 60° and is strongly sensitive to the refractive index of the particles. By combining measurements at the two angles of the light scattered by the particles that cross a laser beam, it is possible to retrieve accurately the size distribution and to estimate the nature of the dominant particles (droplets, carbonaceous, salts and mineral particles) in 19 size classes in the 0.2-19 μm range. This typology is based on calibration charts obtained in the laboratory. Several campaigns of cross-comparison of LOAC with other particle counting instruments and remote sensing photometers have been run to validate both the size distribution derived by LOAC and the retrieved particle number density. The speciation of the aerosols has been validated in well-defined conditions including urban pollution, desert dust episodes, fog, and cloud. Comparison with reference aerosol mass monitoring instruments also shows that the LOAC measurements can be successfully converted to mass concentrations [1].

The weight of LOAC is of about 200g and the consumption is below 3W. Figure 1 presents the LOAC instrument used for measurements under all kinds of balloons, including meteorological balloons.

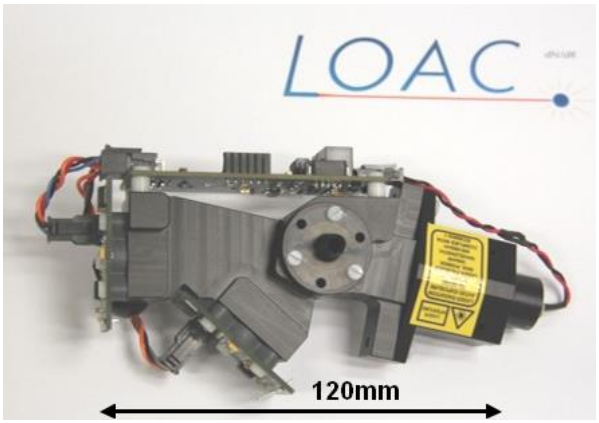

Figure 1: the LOAC instrument

Some hardware and software improvements are in progress for performance enhancements (size detection down to 0.1 μm and concentration above 1000 particles per cm^3), to satisfy the space conditions, and to be able to easily address opportunities for the future planetary missions.

Two main objectives are identified:
- The study of the atmosphere of Saturn, in the frame of the HERA project that will be submitted to the M5 call for proposals of the European Space Agency. This project consist of an entry probe into the cloud forming region of the troposphere, below the region accessible from remote sensing, to better understand the formation and the composition of the Saturn atmosphere. LOAC will provide the size distributions of the aerosols, which are unknown at present.

- The study of the Martian atmosphere, from a lander, a rover or even a balloon, although no mission have been yet identified. LOAC could determine the aerosols size distribution, and could provide a better estimate of the nature of the liquid and solid particles in the atmosphere and at ground, including for the "dust devils".
- Three others objectives can be also considered in the future: the clouds of the Venus atmosphere, the Titian atmosphere, and the comet comae.

References: [1] Renard J.-B. et al. (2016), *Atmos. Meas. Tech., 9*, 1721-1742.

Tests of Microchannel Plate (MCP) Detector Response to MeV Electrons in Support of Juno, JUICE, and Europa Mission UVS Instrument Investigations. K. D. Retherford[1], M.W. Davis[1], T. K. Greathouse[1], R. M. Monreal[1], R. C. Blase[1], U. Raut[1], A. J. Steffl[1], C. M. Cooke[2], O. Siegmund[3], and G. R. Gladstone[1], [1]Southwest Research Institute, 6220 Culebra Road, San Antonio, TX 78238, [2]Research Laboratory of Electronics, Massachusetts Institute of Technology, Cambridge, MA 02139, [3]Sensor Sciences, 3333 Vincent Road, Ste. 103, Pleasant Hill, CA 94523.

Introduction: Beamline tests were conducted at MIT to determine the responsivity of Microchannel Plate (MCP) detectors, typically used in UV instruments, to the energetic MeV electrons expected in the Jupiter and Europa radiation environments during operations by Juno, JUICE, and Europa UVS instruments.

Approach: The response of Microchannel Plate (MCP) detectors to far-UV photons is excellent. MCPs provide a photon-counting capability that is especially useful for high-quality stellar and solar occultation measurements. However, use of MCPs within the Jovian magnetosphere for UV measurements is hampered by their ~30% detection efficiency to energetic electrons and ~1% efficiency to γ-rays. High-Z shielding stops energetic electrons, but creates numerous secondary particles; γ-rays are the most important of these for MCPs. These detected particles are a noise background to the measured far-UV photon signal, and at particularly intense times their combination can approach detector global count rates of ~500 kHz when operating at nominal HV levels. To address the challenges presented by the intense radiation environment experienced during Europa encounters we performed electron beam radiation testing of the Juno-UVS flight spare cross-delay line (XDL) MCP in June 2012 at MIT's High Voltage Research Laboratory (HVRL), and again in Nov. 2013 adding an atomic-layer deposition (ALD) coated test-MCP, to measure the detection efficiency and pulse height distribution characteristics for energetic electrons and γ-rays.

Experiments: A key result from our initial UVS-dedicated SwRI IR&D project in 2012 is a qualitative characterization of our XDL's response to both particles (electrons and γ-rays) and photons as a function of HV level. These results provided confidence that good science data quality is achievable when operating at Europa closest approach and/or in orbit. Comparisons with in-flight data obtained with New Horizons Pluto-Alice MeV electron response measurements at Jupiter [1], LRO-LAMP electron and proton event data, and Juno-UVS Earth proton-belt flyby data, and recent bench tests with radioactive sources at Sensor Sciences increase this confidence. The effects of fluorescence on the detector housing window in the first round of tests prohibited quantitative analyses, which prompted a second round of tests in 2013.

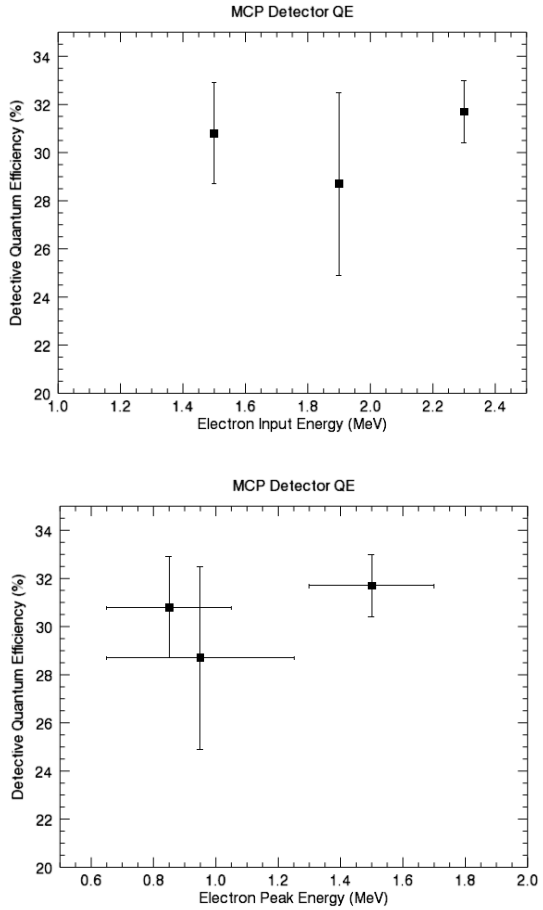

Figure 1. (top) Measured Juno flight spare detector efficiency to electrons as a function of beam input energy. These results agree well with previous measurements of similar MCP detectors. (bottom) MCNP6 modeled response.

Davis et al. [2] report a description of the 2013 test setup and the quantitative results shown in Figure 1-top. The detector response was measured at multiple beam energies ranging from 0.5-2.5 MeV and multiple currents. This response was then checked with MCNP6, a radiation transport simulation tool, to determine the secondary gamma rays produced by the primary electrons striking the detector window (Figure 1-bottom & Figure 2). We report on the measurement approach and the inferred electron and gamma sensitivities.

Results: The measured efficiency of the UVS-style microchannel plate detectors to MeV-level electrons is approximately 31%, consistent with previous measurements with UVS-style detectors, but not consistent with measurements by other microchannel plate detectors with thinner MCP stacks. The measured efficiency of UVS-style detectors to gamma rays is 2.4±0.1% at 0.5 MeV input energy based on the electron-to-gamma conversion of the fused silica window. This measurement is consistent with the 2% QE to gammas reported by Siegmund et al. [3].

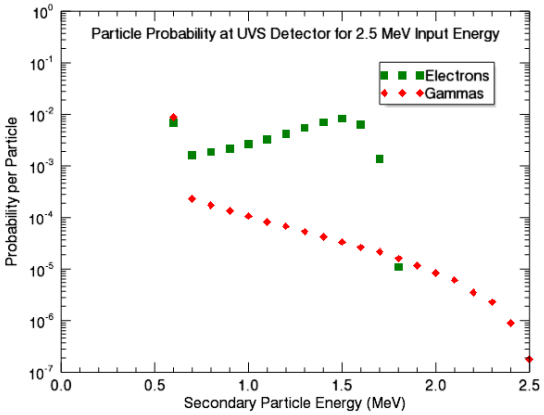

Figure 2. MCNP6 simulation calculation of the probability per particle that a secondary particle reaching the Juno-UVS spare detector within the beamline test setup will have a certain energy for a primary source electron with input energy of 2.5 MeV. Similar calculations were performed for input electron energies of 2.0 MeV, 1.5 MeV, and 0.5 MeV.

Summary: We will discuss several lessons learned to help inform future beamline test experiments dedicated to instrument developments for NASA's next large missions to Europa and ESA's JUICE mission to Ganymede. This information is central to the design of high-Z shielding material for minimizing background count rates for science measurements to be performed by the JUICE-UVS and Europa-UVS instruments.

References:

[1] Steffl, A.J., A.B. Shinn, G.R. Gladstone, J.W. Parker, K.D. Retherford, D.C. Slater, M.H. Versteeg, and S.A. Stern (2012), MeV electrons detected by the Alice UV spectrograph during the *New Horizons* flyby of Jupiter, *J. Geophys. Res., 117*, A10222, doi:10.1029/2012JA017869.

[2] Davis, M.W., T.K. Greathouse, C.M. Cooke, R.C. Blase, G.R. Gladstone, K.D. Retherford (2016) MeV-level electron and gamma ray sensitivities of modern far ultraviolet sensitive microchannel plate detectors, *Proc. of the SPIE*, Proceedings of the SPIE Vol. 9915, doi: 10.1117/12.2232755.

[3] Siegmund, O.H.W., C. Ertley, and J. Vallerga (2015), High Speed Large Format Photon Counting Microchannel Plate Imaging Sensors, *Proceedings of the Advanced Maui Optical and Space Surveillance Technologies Conference*, Maui, Hawaii, id.94.

Laser Limb Sounding Approach for Planetary Atmospheres using Cubesats or SmallSats

Haris Riris[1], James B. Abshire[1], Michael Mumma[1], Geromino Villanueva[1], Thomas Hanisco[1],
[1]Goddard Space Flight Center, 8800 Greenbelt Rd., Greeneblt, MD 20771 (haris.riris@nasa.gov).

Introduction: We describe an approach for an efficient and sensitive way to map trace gas abundances in planetary atmospheres. The approach uses a pair of small satellites flying in formation, in a circular polar orbit. Each satellite carries several tunable single frequency diode lasers and a sensitive optical detector. The laser beam from each satellite is pointed through the limb of the planetary atmosphere to illuminate the other satellite. Tuning the diode laser's wavelengths through trace gas absorption lines allows the gas abundance in the path to be measured at the other satellite's receiver.

Application for Mars Atmosphere: NASA's 2013 Planetary Science Decadal Survey identified mapping gas abundance in planetary atmospheres as an important goal. This new laser limb sounding approach allows the concentration of many key trace gases (such as CH_4, H_2O, HDO and CO_2) to be measured simultaneously and continuously with very high sensitivity.

Recent observations of Mars [1-3] suggest that CH_4 varies in longitude, latitude, and season, but the details are sparsely measured and are poorly understood. The proposed concept will enable mapping the global atmospheric CH_4 concentrations. The technique also allows probing water isotopic ratios (e.g., D/H), a proxy to sub-surface release and water loss. Earth-based observations show strong variations in the D/H ratio in column water vapor, and aspects of their seasonal changes [4]. Measurements from orbit are expected to provide new insights into the processes that control their distribution and ratio. The targeted gases also vary with altitude and one may vary the limb tangent altitude by changing the spacecraft spacing.

Benefits of Approach: There are several important benefits to this novel approach. Unlike solar occultation, which can measure only during sunrise or sunset events, this approach allows continuous measurements, permitting full planetary mapping from polar orbit, even in darkness. The measurement sensitivity is high because the optical path length through the atmosphere is long (1000's of km). The geometry allows the measurement to be made with modest (10-20 mW) laser power using compact diode lasers and sensitive infrared detector [5].

Measurement Scenario: A mission can be accomplished with two smallsats, or 6U cubesats. After deployment the distance between them is adjusted so that they co-orbit with the primary spacecraft and the optical path between the two cubesats passes through the limb of the atmosphere. Each satellite is 3-axis stabilized and carries a payload consisting of a few small tunable single frequency diode lasers, a receiver lens and an optical detector.

The satellites use body-pointing of their payloads. Once two-way pointing is achieved, repetitively sweeping the diode laser's wavelength through its gas absorption line allows the gas absorption line shapes to be measured at the other satellite's receiver. From the line shape the path-integrated gas abundance can be calculated. The limb-tangent altitude can be varied by changing the distance between the satellites. From a circular polar orbit the measurements allow a global map of the trace gases to be made as the planet rotates. Several gases can be measured simultaneously by using different diode lasers, each emitting at a specific wavelength for each gas.

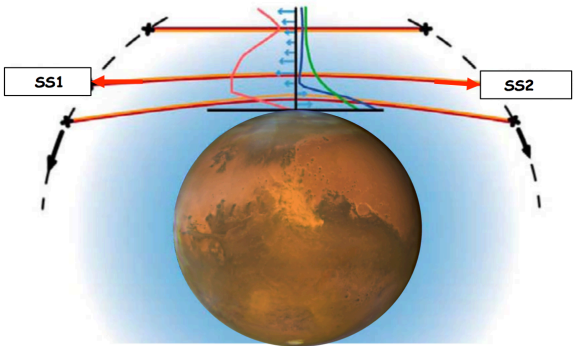

Figure 1. Illustration of the planetary laser limb sounding measurement geometry allowing measurements between two cubesats

Application for Earth's Atmosphere: There are similar benefits from measuring H_2O and HDO globally in the Earth's stratosphere (with the tangent path above the cloud tops) with this approach. Water vapor plays a critical role in the climate system through the direct absorption of infrared radiation and through the formation of cloud and aerosol particles. Reliable long-term climate forecasts require accurate descriptions of the mechanisms that transport water vapor across the tropopause and how this mechanism changes with a changing climate. The isotopic abundance of water vapor is strongly influenced by transport processes, showing large variations depending on the role of deep convection compared to large-scale adiabatic ascent. Measurements of the isotopic abundance of water va-

por (the ratio HDO/H_2O) can be used to quantify the role of convection and constrain the transport processes in global climate models [6].

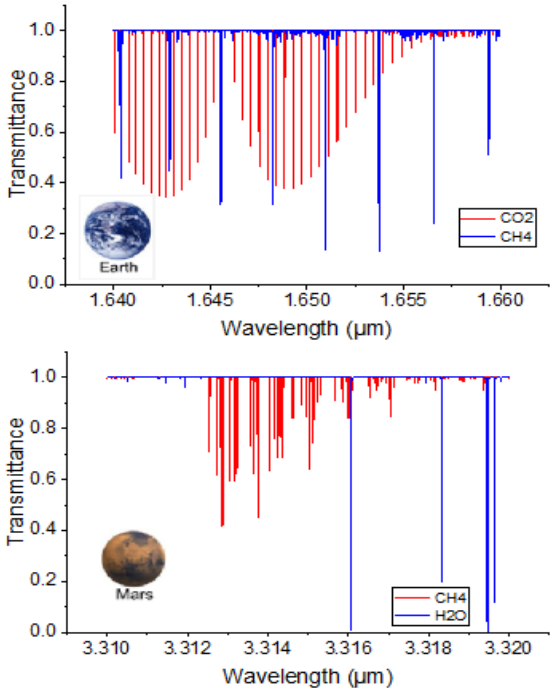

Figure 2. Transmission spectrum through the Earth's (top) and Mars (bottom) atmosphere at 20 km tangent height for candidate gases (CO_2 and CH_4 for Earth and CH_4 and H_2O for Mars).

References:

[1] Mumma, M. J., Villanueva, G. L., Novak, R. E., Hewagama, T., Bonev, B. P., DiSanti, M. A., & Smith, M. D. (2009) Science, 323(5917), 1041-1045.

[2] Webster, C. R., Mahaffy, P. R., Atreya, S. K., Flesch, G. J., Mischna, M. A., Meslin, P. Y., & Martín-Torres, J. (2015). Science, 347(6220), 415-417

[3] Lefevre, F., & Forget, F. (2009). Nature, 460(7256), 720-723.

[4] Villanueva, G. L., Mumma, M. J., Bonev, B. P., Novak, R. E., Barber, R. J., & DiSanti, M. A. (2012). Journal of Quantitative Spectroscopy and Radiative Transfer, 113(3), 202-220.

[5] Beck, J., Welch, T., Mitra, P., Reiff, K., Sun, X., & Abshire, J. (2014). Journal of Electronic Materials, 43(8), 2970-2977.

[6] Worden, J., Kulawik, S., Frankenberg, C., Payne, V., Bowman, K., Cady-Peirara, K., ... & Noone, D. (2012). Atmospheric Measurement Techniques, 5(2), 397-411.

MEDA, THE ENVIRONMENTAL DYNAMICS ANALYZER FOR MARS 2020. J.A. Rodriguez-Manfredi[1], M. de la Torre[2], J.S. Boland[2], N.T. Bridges[3], P. Conrad[4], F. Ferri[5], M. Genzer[6], F. Gómez-Gómez[1], J. Gómez-Elvira[1], A-M. Harri[6], O. Kemppinnen[6], M. Lemmon[7], G. Martínez[8], S. Navarro[1], C. Newman[9], S. Pérez-Hoyos[10], O. Prieto[1], M. Ramos[11], A. Saiz-López[12], A. Sánchez-Lavega[10], J.T. Schofield[2], E. Sebastian[1], M. Smith[4], L.K. Tamppari[2], and the MEDA team. [1]Centro de Astrobiología (INTA-CSIC), Madrid, Spain; [2]Jet Propulsion Laboratory/California Institute of Technology, Pasadena, CA 91109; [3]Applied Physics Laboratory, 11100 Johns Hopkins Road, Laurel, MD 20723; [4]NASA Goddard Space Flight Center, 8800 Greenbelt Rd, Greenbelt, MD 20771; [5]Università degli Studi di Padova, Centro Di Ateneo Di Studi E Attivita' Spaziali "Giuseppe Colombo" (CISAS), Padova Italy; [6]Finnish Meteorological Institute, Erik Palménin aukio 1, 00560 Helsinki, Finland; [7]Texas A&M University, College Station, TX 77843; [8]University of Michigan, 500 S State St, Ann Arbor, MI 48109; [9]Ashima Research, 600 S. Lake Ave, Suite 104, Pasadena, CA 91106; [10]University of Basque Country, Bilbao, Spain; [11]University of Alcalá, Plaza de San Diego, 28801, Alcalá de Henares, Spain; [12]Institute Physical-Chemistry Rocasolano, CSIC, Serrano 119, 28016, Madrid, Spain.

Introduction: The *Mars Environmental Dynamics Analyzer* (MEDA) is a suite of environmental sensors that compose one of seven instruments being developed for science investigations aboard the NASA Mars 2020 rover [1].

MEDA is an international collaboration to combine a mostly contributed set of sensors that can address two M-2020 investigation goals: "characterization of dust size and morphology", and "surface weather measurements". MEDA also responds to Mars Program objectives and Mars Strategic Knowledge Gap investigations for Human Exploration identified by the MEPAG [2].

The MEDA payload carries high heritage from the currently-in-use Remote Environmental Monitoring Station (REMS) [3] and PanCam/HazCam [4] instruments aboard the Mars Science Laboratory (MSL) mission. MEDA can monitor dust and surface meteorology autonomously and will be capable of sampling environmental conditions in parallel to other Mars 2020 investigations [such as e.g. the *Mars Oxygen ISRU Experiment* (MOXIE), designed to produce oxygen from Martian atmospheric carbon dioxide].

MEDA investigations: MEDA's sensors will characterize the climate near the Martian surface. Those sensors are a dust and optical radiation sensor (RDS) that includes a camera (SkyCam), pressure sensor (PS), relative humidity sensor (HS), wind sensor (WS), 5 air temperature sensors (ATS), and a thermal infrared sensor (TIRS) for net flux and ground temperature.

The solar radiation sensor is designed to track direct and diffuse radiation in a geometry that characterizes both the prevailing environmental dust properties [5,6] and the behavior of solar radiation on subdiurnal time scales. This helps constrain and model the impact of solar radiation on local photochemistry, thus supporting assessments of the preservation potential for organics on a cache sample. The other sensors will enable comparisons to the environments found at other locations explored by environmental packages aboard previous landers and rovers on Mars. The MSL REMS heritage additionally permits easy comparisons to the meteorological station currently operating on Gale Crater.

MEDA's investigations are to measure:

a. The physical and optical properties of the local atmospheric aerosols. Particle abundance, size distribution, shape, phase function, and how these optical properties relate to the meteorological cycles (diurnal, seasonal, interannual).

b. The conditions leading to dust lifting and how the aerosol diurnal cycle responds to the local atmospheric wind regimes.

c. How the current environmental pressure, temperature, relative humidity, solar radiation, net infrared radiation, and winds at the landing site differ from those at the Viking, Phoenix, Pathfinder, and Curiosity locations.

d. The relationship between the surface environment and the large-scale dynamics observed from orbiting instruments.

e. The energy and water fluxes between the surface and the lower atmosphere of Mars near the rover.

f. The annual cycles of the solar UV, visible and NIR radiation on the surface of Mars.

g. The environmental context for weathering and preservation potential of a possible cache sample.

h. How pressure, humidity, temperature and winds influence the ISRU engineering efficiency.

i. How the MEDA observations agree with models extrapolations to the Martian surface.

MEDA Operations approach: To ensure these objectives, MEDA will be able to measure with 1Hz frequency for at least 5 minutes each 30 minutes. This occurs autonomously even if the rover is asleep. Over this basic operarions scenario, the M-2020 Science

teams will be able to add as many 5 minute blocks as desired to fill up to 24 hours/sol anytime that rover power and data volume enables for it.

Development status: To ensure the investigation goals, the MEDA sensor locations have been selected searching to minimize the influence of the rover geometry on the sensors. This required for some sensors to be upwind of the rover. As a consequence there are several ATS and WS all distributed such that there is always one upwind of the rover. Two MEDA air temperature sensors will be accommodated on the sides of the rover providing local lapse rate information, the RDS will be on the rover deck, the pressure sensor and the MEDA CPU will be inside the rover and the rest of sensors, HS, TIRS, and 3 ATS will be on the rover Remote Sensing Mast.

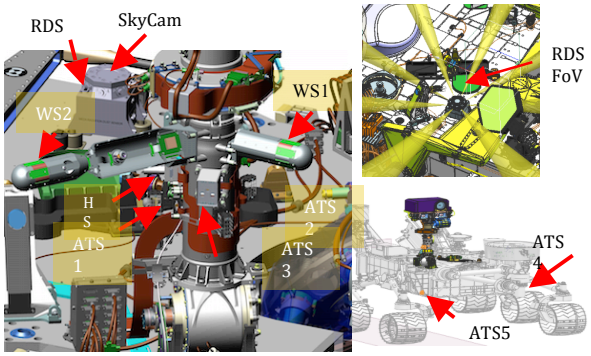

References:

[1] NASA Mars 2020 Press Release and Press Kits, http://www.nasa.gov/press/2014/july/nasa-announces-mars-2020-rover-payload-to-explore-the-red-planet-as-never-before/. [2] P-SAG (2012) Analysis of Strategic Knowledge Gaps Associated with Potential Human Missions to the Martian System: Final report of the Precursor Strategy Analysis Group (P-SAG), D.W. Beaty and M.H. Carr (co-chairs) + 25 co-authors, sponsored by MEPAG/SBAG, 72 pp., posted July 2012, by the Mars Exploration Program Analysis Group (MEPAG) at http://mepag.jpl.nasa.gov/reports/ . [3] Gómez-Elvira, J. et al. (2012), /SSR, 170,/ 583-640. [4] Bell III, J. F., S. W. Squyres, K. E. Herkenhoff, et al., The Mars Exploration Rover Athena Panoramic Camera (Pancam) investigation, J. Geophys. Res. 108(E12), doi:10.1029/2003JE002070, 2003. [5] Dubovik, O., and M. D. King (2000), A flexible inversion algorithm for retrieval of aerosol optical properties from Sun and sky radiance measurements, J. Geophys. Res., 105(D16), 20673–20696, doi:10.1029/2000JD900282 http://dx.doi.org/10.1029/2000JD900282. [6] Lemmon, M. T., M. J. Wolff, M. D. Smith, R. T. Clancy, D. Banfield, G. A. Landis, A. Ghosh, P. H. Smith, N. Spanovich, B. Whitney, P. Whelley, R. Greeley, S. Thompson, J. F. Bell III, and S. W. Squyres. 2004. Atmospheric Imaging Results from the Mars Exploration Rovers: Spirit and Opportunity. /Science/ 306

Acknowledgements: Support for this work is gratefully acknowledged to the Spanish Ministerio for Economia y Competitividad (Spain), FMI (Finnish team), and NASA HEOMD (US team).

THE MINIATURIZED MÖSSBAUER SPECTROMETER MIMOS II FOR THE ASTEROID REDIRECT MISSION (ARM): QUANTATIVE IRON MINERALOGY AND OXIDATION STATES.

C. Schröder[1], G. Klingelhöfer[2], R. V. Morris[3], A. S. Yen[4], F. Renz[5], and T. G. Graff[6], [1]Biological and Environmental Sciences, University of Stirling, Stirling FK9 4LA, Scotland, UK, christian.schroeder@stir.ac.uk, [2]Institute of Inorganic Chemistry and Analytical Chemistry, Johannes Gutenberg-University, Staudinger Weg 9, 55128 Mainz, Germany, [3]XI3/Exploration Integration and Science Directorate, NASA Johnson Space Center, 2101 NASA Parkway, Houston, TX 77058, USA, [4]Jet Propulsion Laboratory, California Institute of Technology, Pasadena, CA 91109, USA, [5]Institut für Anorganische Chemie, Leibniz Universität Hannover, Callinstr. 9, 30167 Hannover, Germany, [6]Jacobs Technology, NASA Johnson Space Center, Houston, TX, USA.

Introduction: The miniaturized Mössbauer spectrometer MIMOS II [1] is an off-the-shelf instrument with proven flight heritage. It has been successfully deployed during NASA's Mars Exploration Rover (MER) mission [2-4] and was on-board the UK-led Beagle 2 Mars lander [5] and the Russian Phobos-Grunt sample return mission [6]. A Mössbauer spectrometer has been suggested for ASTEX, a DLR Near-Earth Asteroid (NEA) mission study [7], and the potential payload to be hosted by the Asteroid Redirect Mission (ARM) [8]. Here we make the case for in situ asteroid characterization with Mössbauer spectroscopy on the ARM employing one of three available fully-qualified flight-spare Mössbauer instruments.

Instrument Description: MIMOS II [1] consists of a sensor head (Fig. 1) and an electronics board. The sensor head can be mounted on e.g. a robotic arm (see Fig. 2 for a MER instrument) and needs to be brought in physical contact with the sample to be analyzed. No sample preparation is necessary. The sensor head carries the radiation source (^{57}Co, halflife 270 d) and detector system, and has a volume of 50×50×90mm³. The electronics board holds data acquisition and instrument control units (CPU + FPGA), voltage converters, and electrical and data interfaces to the spacecraft. It is 100×160×25mm³. The whole system including connecting cables weighs <500 g, power consumption is 4W during data acquisition, and data product size per analysis is 512 kBytes (4 Mbit).

Asteroid Redirect Mission: ARM consists of the Asteroid Redirect Robotic Mission (ARRM) to be followed by the Asteroid Redirect Crewed Mission (ARCM). ARRM will visit a larger than ~100 m diameter NEA and collect a meter-sized boulder and regolith from its surface. The boulder will be used for a gravity tractor asteroid deflection demonstration before it will be transported to a stable orbit around the Moon where astronauts can explore it and return samples to Earth during the ARCM [8]. Asteroid 2008 EV_5 has been used to support mission design studies but the final target asteroid has yet to be selected. Asteroid 2008 EV_5 is probably a CR-type carbonaceous chondrite.

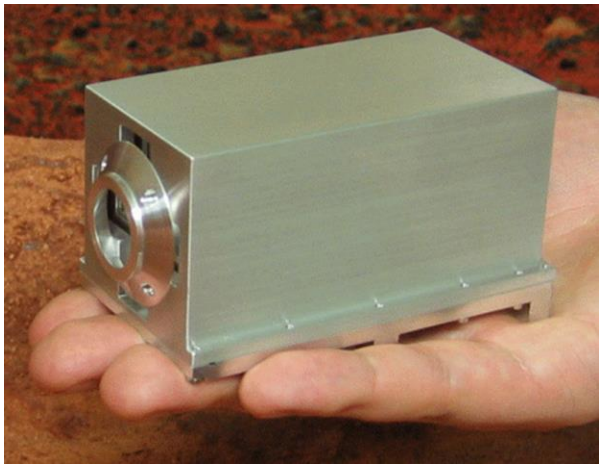

Fig. 1. The MIMOS II sensorhead. Credit: University of Mainz.

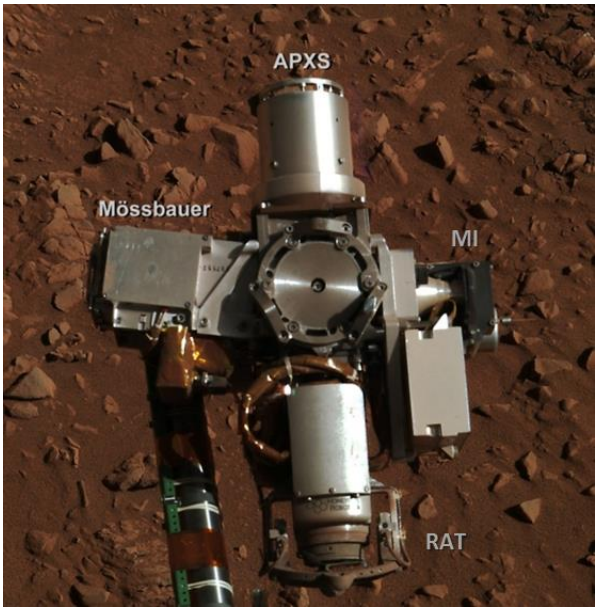

Fig. 2. A MIMOS II sensorhead (Mössbauer) mounted on Mars Exploration Rover Spirit's robotic arm, together with the Alpha Particle X-ray Spectrometer (APXS), the Microscopic Imager (MI), and the Rock Abrasion Tool (RAT). Credit: NASA/JPL/Cornell.

Mössbauer Investigations Related to ARM and NASA Goals: Mössbauer spectroscopy identifies Fe-bearing mineral phases (e.g., silicates, oxides, and sulfides) and Fe oxidation states, and determines the quantitative distribution of Fe between mineral phases and oxidation states. It also yields insights into magnetic properties. This information is vital to support ARM and NASA goals regarding science, planetary defense, asteroidal resources and ISRU, as demonstrated by the examples given below.

Science. Asteroid 2008 EV5 is likely a CR carbonaceous chondrite on the basis of its reflectance spectrum and albedo but could also be a CI, CM, or CK chondrite. Such uncertainty is the case for most asteroids. This uncertainty in composition can be removed by establishing a firm link to a single group of meteorites through knowledge of the geochemical and mineralogical composition. Importantly, the MB instrument can "see through" more than a millimetre of basaltic dust and obtain information on the solid substrate beneath. Modal mineralogy or the distribution of Fe^{2+} in the silicate olivine and Fe^0 in metal phases can be used to differentiate between meteorite groups [9,10], which works particularly well when complemented by chemical composition and/or magnetic susceptibility measurements. For example, using Mars Exploration Rover Opportunity's Alpha Particle X-ray Spectrometer (APXS) and Mössbauer spectrometer on Bounce Rock, a boulder float at Meridiani Planum, we identified the first rock on Mars similar in composition to the shergottite group of meteorites who originated on Mars [11]. We also identified and grouped both iron and stony meteorites on Mars [12,13], and could establish that fragments of the latter encountered by Opportunity were most likely paired [13].

Carbonaceous chondrites and their parent asteroids are particularly interesting targets because they display a history of aqueous alteration. The abundance of the mixed-valent Fe-oxide magnetite can be used as a tracer for the extent of aqueous alteration. Fe-bearing minerals and Fe oxidation states can also be used to trace the thermal and shock history of meteorites or asteroids. Magnetite and metal phases influence the electromagnetic properties of an asteroid.

Space weathering can alter the optical spectrum and albedo of an asteroid and may thus lead to uncertainty when comparing to known groups of meteorites. These effects may not be apparent through geochemical changes but changes in Fe oxidation states only. The Fe^0 content of surface fines, for example, is a measure of exposure time [14], which may be used to constrain the flux of micrometeoroids. At the opposite end, we have used the oxidation of metallic Fe in stony meteorites on Mars to demonstrate extremely slow chemical weathering rates under the current extremely arid conditions [15].

Planetary defense. The knowledge of physical or geotechnical properties such as density, porosity, shear strength, compressive strength or tensile strength is essential for planetary defense purposes. By ascertaining the link between asteroid and correct group of meteorites, many of these properties can be obtained from the meteorites in collections. A good knowledge of mineralogy and Fe oxidation states further enables estimating coefficients of thermal expansion or electromagnetic properties. Asteroids may have been weakened through thermal and shock events.

Asteroidal resources and ISRU. Asteroids may be used in several ways for in situ resource utilization during human exploration. Knowledge of the mineralogical compositions helps to assess the radiation protective properties of asteroidal materials, as well as the potential to yield precious water or oxygen. In experiments with lunar regolith, the yield of oxygen that can be extracted is directly proportional to FeO content [16]. Several oxygen extraction hardware concepts were evaluated during two field tests on Mauna Kea, Hawaii, in 2008 [17,18] and 2010 [19,20]. MIMOS II worked successfully as both a process monitor and a prospecting tool. Feedstock would be selected for high FeO content and mineral content: Ilmenite is reduced at 900°C, olivine at 1000°C and all other FeO-bearing phases at 1100°C.

References: [1] Klingelhöfer G. et al. (2003) *JGR, 108*(E12), 8067. [2] Morris R. V. et al. (2004) *Science, 305*, 833-836. [3] Klingelhöfer G. et al. (2004) *Science, 306*, 1740-1745. [4] Morris R.V. et al. (2010) *Science, 329*, 421-424. [5] Pullan D. et al. (2003) ESA SP-1240. [6] Rodionov D. et al. (2010) *Solar Syst. Res., 44*, 362-370. [7] Nathues A. (2008) Asteroids, Comets, Meteors, abstract #8076. [8] Mazanek D. D. et al. (2016) NASA/TM–2016-219011. [9] Bland P. A. et al. (2004) *Meteorit. Planet. Sci., 39*, 3-16. [10] Righter K. et al. (2013) *Meteorit. Planet. Sci., 48*(s1), 5232. [11] Zipfel J. et al. (2011) *Meteoritics & Planet. Sci., 46*, 1- 20. [12] Schröder C. et al. (2008) *JGR, 113*, E06S22. [13] Schröder C. et al. (2010) *JGR, 115*, E00F09. [14] Morris R. V. et al. (1998) *Hyperfine Interact., 117*, 405-432. [15] Schröder C. et al. (2016) *Nat. Commun.* in press. [16] Allen C. C. et al. (1994) *JGR, 99*(E11), 23173-23185. [17] Morris R. V. et al. (2009) Lunar Base Symposium, Abstract #A5-5. [18] Schröder C. et al. (2011) *Geochem.-Explor. Env. A., 11*, 129-143. [19] Klingelhöfer G. et al. (2011) *LPS XLII*, Abstract #2810. [20] ten Kate I. et al. (2013) *J. Aerospace Eng.*, 26, 183-196.

ON-BOARD ORBIT PROPAGATOR USING KUSTAANHEIMO-STIEFEL ELEMENTS FOR MARS MICRO ORBITERS

Harishkumar Sellamuthu and Ram Krishan Sharma,
Department of Aerospace Engineering, Karunya University, Karunya Nagar, Coimbatore – 641114, Tamil Nadu, India

Introduction: Economization of the small satellite systems becomes essential especially for planetary and small body orbiters. The quality of the payload and the dimensions of the spacecraft subsystems including Attitude and Orbit Control (AOCS), Power, Thermal Control and Communications are mutually dependent. Mars orbiting missions have long phases of non-communication with Earth and use non-GPS orbit navigation. A competent level of autonomy should be achieved in the on-board navigation and guidance software which eventually affects the performance and quality of the AOCS subsytem. The integral part of the navigation and guidance software is the on-board orbit propagation algorithm. Although widely used, numerical integration algorithms for orbit propagators with complex force models are expensive in terms of memory allocation and power consumption, and not suitable for implementation in small and low-cost spacecrafts. In view of the stringent memory and power budget, a simple and robust propagation flight software becomes essential and analytical methods come handy with closed-form solution which can be evaluated to high accuracy comparable to numerical integration algorithms.

KS Element Orbit Propagator: The major perturbing forces affecting the motion of the satellites around Mars are the oblateness, atmospheric drag, and third-body attraction from its satellites and the Sun. The main perturbations outside the low altitude atmosphere of Mars are the solar gravity and the planetary oblateness effects. Due to the non-linear nature of the classical Newtonian equations of motion, during spacecraft close approaches to the central body, they exhibit singularities and are unstable for long-term orbit propagation. Using regularization method due to Kustaanheimo and Stiefel (KS), linear differential equations of a harmonic oscillator with constant frequency is obtained and extended to perturbed motion. KS regular equations of motion can be used to produce singularity-free analytical solutions. The equations are smoothed for eccentric orbits and generalized eccentric anomaly is the independent variable. In the present study, a new analytical solution concurrently with numerical integration algorithm is developed in terms of KS regular elements with solar gravity perturbation and oblateness of the Mars. The algorithm utilizes an analytically computed areocentric solar coordinates and second zonal harmonics (J_2) of Mars.

Conclusion: The analytical solutions will be compared with the numerically integrated values. The elegance of the analytical solution is the existence of symmetry between the equations of motion which allows solving of only two out of nine equations while the rest are solved by altering the initial conditions, instead of six. The symmetric characteristics of the KS element equations will reduce the computational time, and the on-board memory requirement is minimized considerably due to simple transcendental function addition and subtraction operations. The major applications include development of on-board orbit propagation algorithms, and mission analysis for small spacecraft missions about Mars.

Common Region Detection Algorithm for Adjacent Lunar Surface Images using Crater Matching. M. G. Seo[1], M. H. Cho[2] and M. J. Tahk[3], [1]KAIST (Korea Advanced Institute of Science and Technology 291, Daehak-ro, Yuseong-gu, Daejeon, 34141, Korea, mgseo@fdcl.kaist.ac.kr), [2]KAIST (Korea Advanced Institute of Science and Technology 291, Daehak-ro, Yuseong-gu, Daejeon, 34141, Korea, mhcho@fdcl.kaist.ac.kr) , [3]KAIST (Korea Advanced Institute of Science and Technology 291, Daehak-ro, Yuseong-gu, Daejeon, 34141, Korea, mjtahk@fdcl.kaist.ac.kr).

Introduction: The digital elevation model (DEM) of the lunar lunar surface is vital information for lunar exploration missions. The algorithms to construct DEM of the certain region using a camera image has been developed in previous studies. In order to construct the high-resolution DEM of a broad area, a single high-resolution image over that region is required. Since the resolving power of a camera is limited, a high resolution image of a large area is difficult to acquire.

Another method is to construct DEMs from the partial images of the designated area and combine them into a single DEM. This method needs the information of the relative position and attitude angle between images. Especially for images of adjacent areas, the overlapping regions of two images are defined from this information. This indicates that the relative position and attitude angle between those two images should be exactly known to make the overlapping regions to contain only the duplicately taken area.

This paper deals with the algorithm to figure out the common region of the given two neighboring lunar surface images using crater matching. Craters are approximated as circles using the algorithms addressed in the previous studies.[1,2] The proposed algorithm calculates the relative position and attitude angle of two images, which minimize the newly defined cost function. This cost function is defined as the average of the distances between the centers of two circles with the similar radius on the overlapping region of each image.

Crater Detection Algorithm: The algorithms to detect and approximate craters as simple geometric figures has been studied in various articles.[1,3,4] The craters are approximated as circles for simple crater matching algorithm in this paper. The algorithms proposed in [1] are applied for crater edge detection and pairing. The paired edges are approximated as circles with the method introduced in [2]. This method calculates suitable circle on each crater based on least square fitting and uses finite number of points on edges.

Crater Matching Algorithm: The craters on the two images are approximated as circles and their positions and radii are given from the algorithms introduced in the previous section.

The altitude and the relative attitude of the camera against the image normal vector are assumed to be identical for two images. Under this assumption, the difference between radiuses of the circles, derived from same crater on each image, are considered to be small. One of the image is defined as Image A and the other is called Image B in this paper.

An orthogonal coordinate system is defined with its origin at the center of Image A. Its x-axis is defined to be parallel to the horizontal sides of the image. The position of the center of Image B, (x_B, y_B), is defined in this coordinate system. The attitude angle of Image B with respect to Image A, θ_B, is defined as the angle between x-axis and the horizontal side of Image B. Those definitions are addressed in Fig. 1.

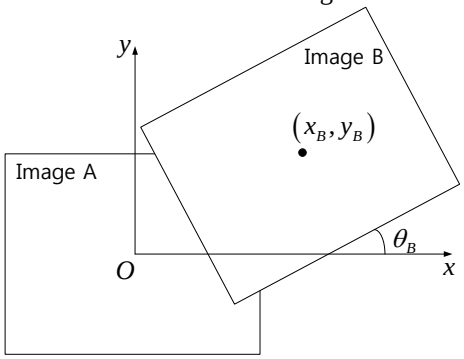

Fig. 1 Coordinate System and Parameters

It is obvious as shown in Fig. 1, the overlapping region of two images are given from (x_B, y_B) and θ_B. The crater matcing algorithm is proposed to find the proper (x_B, y_B) and θ_B which makes the overlapping region to be the actual common area. This is accomplished by figure out (x_B, y_B) and θ_B which minimizes the objective function $J(x_B, y_B, \theta_B)$.

$$\min_{x_B, y_B, \theta_B} J(x_B, y_B, \theta_B) \tag{1}$$

$J(x_B, y_B, \theta_B)$ is defined as the average of the distances between the centers of two circles approximated from the same crater. The process to calculate $J(x_B, y_B, \theta_B)$ is given as follows.

a. Figure out the circles whose centers are on the overlapping region of each image. Let the number of them on Image A as n, and that of Image B as m.

b. Sort the circles on each image in descending order of their radiuses. The i-th circle of Image A is symbolized as $C_{A,i}$, and the j-th circle of Image B is defined as $C_{B,j}$.

c. In $n<m$ cases, from $i=1$ to $i=n$, search the nearest $C_{B,j}$ whose radius and that of $C_{A,i}$ differs by a small threshold value designed by the user, and pair those two circles. $C_{B,j}$ s, those paired with $C_{A,k}$ s of $k=1,\cdots,i-1$, are excluded from the search process for $C_{A,i}$. In $n>m$ cases, the same searching and pairing processes are conducted for $C_{B,j}$ from $j=1$ to $j=m$.

d. When the number of pairs obtained from c. is l ($l\le n$ for $n<m$ case, $l\le m$ for $n>m$ case), $J(x_B,y_B,\theta_B)$ is calculated as below. $d_k(x_B,y_B,\theta_B)$ is defined as the distance between two circles of k-th pair $(k=1,\cdots,l)$.

$$J(x_B,y_B,\theta_B)=\frac{1}{l}\sum_{k=1}^{l}d_k(x_B,y_B,\theta_B) \qquad (2)$$

In the case where the only one crator exists on the overlapping regions, θ_B is not able to be uniquely defined with the proposed detection algorithm. In order to prevent this drawback, $J(x_B,y_B,\theta_B)$ is defined to be a extremely huge number for $n\le 1$ or $m\le 1$ cases.

Image Merging: The image merging test is conducted with two neighboring lunar surface images to show the performance of the proposed algorithm. The following lunar surface image is obtained from [5].

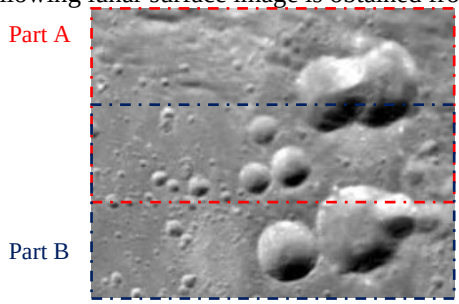

Fig. 2 Lunar Surface Image

Image A is defined as Part A of Fig.2. Image B is obtained by rotating Part B by 180° clockwise. The crater detection results with those two images are presented.

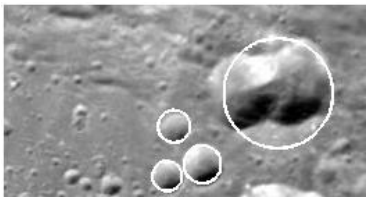

Fig. 3 Crater Detection with Image A

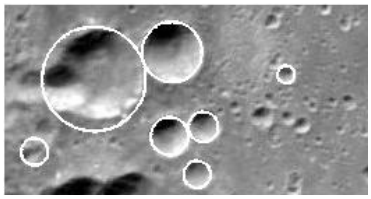

Fig. 4 Crater Detection with Image B

The relative position and attitude of Image B with respect to Image A is given from the crater matching algorithm. The optimal solution is obtained with the optimization tool of MATLAB, called 'fminsearch'.

$$(x_B,y_B)=(2.2154,-72.7507)\quad \theta_B=176.7808^\circ$$
$$J(x_B,y_B,\theta_B)=0.8913 \qquad (3)$$

The image merging is conducted by applying the relative position and attitude angle condition in (3) to Image A and Image B. The merged image is obtained by defining the grayscale values of pixels on the overlapping region as the average values of two images.

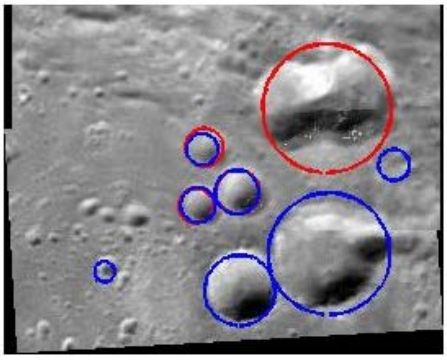

Fig. 5 Merged Image using Crater Matching

Conclusion: The algorithm to figure out the common area of two partially overlapping lunar surface images is proposed in this paper. The performance of this algorithm is demonstrated by the image merging test.

Acknowledgment: This work was supported by the National Research Foundation of Korea(NRF) Grant funded by the Korean Government(MSIP)(No. 2014M1A3A3A03034589).

References: [1] Jeon. B. J. et al. (2013) Asia-Pacific International Symposium on Aerospace Technology [2] Pratt. V. (1987), ACM SIGGRAPH Computer Graphics., Vol. 21, No. 4 [3] Jiang. H. et al. (2010) Intelligent Control and Information Processing, 2010 International Conference on [4] Junhua. F. et al. (2010) Systems and Control in Astronautics, 2010 3rd International Symposium on [5] NASA Planetary Data System (Planetary Image Locator Tool, http://pilot.wr.usgos.gov, (Searching Date : 07.23.16)

LENSLESS DIGITAL HOLOGRAPHIC MICROSCOPY FOR LIFE DETECTION. E. Serabyn[1], K. Liewer[1], J.K. Wallace[1], S. Rider[1], C. Lindensmith[1] and J. Nadeau[2], [1]Jet Propulsion Laboratory, California Institute of Technology, 4800 Oak Grove Drive, Pasadena, CA 91109, [2]California Institute of Technology, Pasadena, CA 91125.

Introduction: Microscopy capable of volume imaging can be used to search for microbial life on ocean worlds. Here we discuss our digital holographic microscope (DHM) systems, which provide high resolution, compactness and stability. Our most recent lensless DHM provides micron-scale resolution in a very compact package.

Background: Microbial motions can deviate noticeably from the average flow, so one way of identifying microbial life in aqueous or icy environments is the use of microscopic techniques that are sensitive to full 3-dimensional volumes, wherein the motions of any particulates or microbes present can be tracked. We have thus been developing a series of deployable digital holographic microscopes.

Digital holographic microscopy [1] has many advantages, including instantaneous 3-d volume imaging, high lateral resolution (micron scale), a large depth of field (mm-range), a large field of view, and compressed data sampling. Our initial submersible DHM for (terrestrial) field science [2] has been deployed to Greenland once, but its lens-based optics left this instrument larger than desirable for space missions. We thus have also been investigating "lensless" approaches [1] to digital holographic microscopy.

Lensless DHM: Our lensless DHM configurations rely on fiber-injection of the object and reference beams, and a small (few cm) free-space path from the sample plane to the detector plane. Our initial lensless system still relied on a lens-based optical relay to provide the desired focal ratio for both beams (in order to fully illuminate the detector array), but the imaging part of the optical system is lensless (i.e., from the final source focal plane just prior to the sample to the detector array). This system demonstrated micron-scale resolution over a large field of view, once aberrations were corrected by viewing a clear glass region.

As miniaturization for space-flight applications is a priority, we eliminated the initial relay by incorporating gradient-index lenses into the source assembly, leaving a free-space propagation distance of only a few cm. Such a compact system has many immediate applications, both terrestrial and space-based, including the search for microbial life on ocean worlds.

References: [1] M.K. Kim (2011) *Digital Holographic Microscopy* (Springer). [2] J.K. Wallace, S. Rider, E. Serabyn, J. Kühn, K. Liewer, J. Deming, G. Showalter, C. Lindensmith and J. Nadeau (2015), Opt. Exp. **23**, 17367.

A MINIATURE GAS CHROMATOGRAPH MAS SPECTROMETER (GCMS) FOR PLANETARY ATMOSPHERES IN SITU STUDIES. J.Simcic, S. Madzunkov, B. Bae, D. Nikolic, E. Neidholdt, M. Darrach, Planetary Surface Instruments Group, Jet Propulsion Laboratory, 4800 Oak Grove Drive, Pasadena, CA, 91109, jurij.simcic@jpl.nasa.gov

Introduction: There is a particular need for the development of miniaturized, high-G load tolerant, low-mass, low-power instruments for in situ studies of trace organic compounds, small inorganic molecules and their isotopes in planetary materials. Presented herein are the latest achievements in developing an instrument with the same analytical performance of commercial GCMS systems but approximately an order of magnitude smaller and optimized for space missions. The Jet Propulsion Laboratory (JPL) Planetary Surface Instruments (PSI) group has developed an instrument consisting of a quadrupole ion trap (QIT) Mass Spectrometer (MS), integrated with a Micro-Electro-Mechanical Systems (MEMS) Gas Chromatograph (GC), developed for human spaceflight applications for NASA Advanced Exploration Systems (AES).

JPL's miniaturized GCMS has been under continuous development at JPL's PSI Group for the last decade. The instrument inherits its basic design from the Vehicle Cabin Atmosphere Monitor (VCAM)[1,2], an autonomous GCMS operated continuously aboard the International Space Station (ISS) for monitoring the cabin atmosphere for major constituents and trace species from 2010 to 2012. VCAM has intrinsic characteristics comparable to commercial Earth-based analytical GCMS systems with total mass of 30 kg and average power consumption of 100W. It has a unique design enabling it to perform two very different tasks: a) trace organic measurements at parts-per-billion (ppb) concentrations; b) major constituent analysis (MCA) where the percent concentration of major gases present in ISS atmosphere, specifically N_2, O_2, CO_2 and Ar, are measured.

Compared to VCAM, our current GCMS instrument embodies several major improvements. The MS is redesigned to be more compact and robust using a unique wireless design in which all electrical connections to the electrodes are achieved through the mounting posts, thus eliminating the need for electrical wires, which represent liability in high-G environment. Also the end-cap electrodes of the QIT are electrically-isolated from the instrument's ground to enable supplemental modes of operation using additional dipole radio frequency (RF) field[3]. The MS uses electron impact ionization for producing ions inside the QIT by means of a redesigned electron gun, consisting of tantalum disc cathode emitter and three focusing electrodes. The electron gun can now be utilized either in traditional axial geometry, where a parallel electron beam traverses the central z-axis of the QIT through the holes in the top and bottom caps, or side geometry, where the ionization is achieved through the hole in the ring electrode. In the effort to minimize the size of the instrument, MS is hosted in a 3D printed Titanium vacuum chamber and sandwiched between two custom made flanges with electric feedthrough pin patterns exactly matching the electrical contacts of the MS. Operational vacuum level of $1.5x10^{-10}$ torr was achieved using a combination of ion-getter pumps which allows us to further reduce mas, power consumption and eliminate the risk of mechanical failure of turbo-molecular pump in high-G environment. As well, the GC system is fundamentally changed by implementing a new MEMS technology. The MEMS GC technology requires less material (grams instead of kilograms), much less power and a low carrier gas flow, and at the same time enables faster injection times.

The new instrument, the Spacecraft Atmosphere Monitor (S.A.M.) with miniaturized vacuum chamber, pumps, and all the electronics presently weighs around 6.8 kg and has a volume of 10.2L. During operation S.A.M. consumes approximately 35W of power. The QIT-MS resonant ejection operation and precise control of the ionization of the neutral gas sample achieves an improvement in the analytical performance of the instrument, a sensitivity of 10^{15} counts/Torr/sec and dynamic range of 10^6 [4]. The low instrument mass, coupled with its high analytical capabilities, makes the instrument ideally suitable for wide range of applications such as trace contaminant and major constituent monitoring in crewed space exploration vehicles or robotic planetary missions.

References: [1] A. Chutjian, M. Darrach, et al., SAE Technical Paper Series 2007- 01-3150, (2007), [2] M. Darrach et al. SAE Technical Paper Series 2008-01-2045, (2008), [3] J. MacAskill, et al. AIP Conf. Proc. 1336, pp. 127-131, [4] M. Darrach et al, IEEE Aerospace Conference Proceedings, Big Sky, MT, 2015, pp. 1-13.

ADVANCED ION MASS SPECTROMETER FOR GIANT PLANET IONOSPHERES, MAGNETOSPHERES AND MOONS. E. C. Sittler[1], J. F. Cooper[2], N. Paschalidis[3], S. L. Jones[4], W. L. Brinckerhoff[5], W. R. Paterson[6], A. Ali[7], M. A. Coplan[8], D. Chornay[9], S. J. Sturner[10], M. Benna[11], F. B. Bateman[12], D. Fontaine[13], C. Verdeil[14], N. Andre[15], M. Blanc[16] and P. Wurz[17], [1]NASA Goddard Space Flight Center, 8800 Greenbelt Road, Greenbelt, MD, 20771, USA, Edward.c.sittler@nasa.gov, [2]NASA Goddard Space Flight Center, 8800 Greenbelt Road, Greenbelt, MD, 20771, USA, john.f.cooper@nasa.gov, [3]NASA Goddard Space Flight Center, 8800 Greenbelt Road, Greenbelt, MD, 20771, USA, Nikolaos.paschalidis@nasa.gov, [4]NASA Goddard Space Flight Center, 8800 Greenbelt Road, Greenbelt, MD, 20771, USA, sarah.l.jones@nasa.gov, [5]NASA Goddard Space Flight Center, 8800 Greenbelt Road, Greenbelt, MD, 20771, USA, william.b.brinckerhoff@nasa.gov, [6]NASA Goddard Space Flight Center, 8800 Greenbelt Road, Greenbelt, MD, 20771, USA, william.r.paterson@nasa.gov, [7]Science Systems Applications, Inc., 6301 Ivy Lane, Suite 510, Greenbelt, MD, 20770, [8]University of Maryland, College Park, MD, coplan@umd.edu, [9]University of Maryland, College Park, MD/NASA Goddard Space Flight Center, 8800 Greenbelt Road, Greenbelt, MD, 20771, dennis.j.chornay@nasa.gov, [10]University of Maryland Baltimore County/NASA Goddard Space Flight Center, 8800 Greenbelt Road, Greenbelt, MD, 20771, steven.j.sturner@nasa.gov, [11]University of Maryland Baltimore County/NASA Goddard Space Flight Center, 8800 Greenbelt Road, Greenbelt, MD, 20771, mehdi.benna-1@nasa.gov, [12]National Institute of Technology and Standards, Gaithersburg, MD, USA, fred.bateman@nist.gov, [13]LPP-CNRS Ecole Polytechnique, Route de Saclay, 91128, Palaiseau, FR, Dominique.fontaine@lpp.polytechnique.fr, [14]LPP-CNRS, 4 Place de Jussieu, tour 24-34, 75252, Paris, Cedex, FR, Christophe.verdeil@lpp.polytechnique.fr, [15]IRAP, Center National de la Recherche Scientifique, Toulouse, FR, Nicolas.andre@irap.omp.eu, [16]IRAP, Center National de la Recherche Scientifique, Toulouse, FR, michel.blanc@irap.omp.eu, [17]University of Bern, Physikalisches Institut, Bern, Switzerland, peter.wurz@space.unibe.ch

Introduction: The Advanced Ion Mass Spectrometer (AIMS) has been under development from various NASA sources (NASA Living with a Star Instrument Development (LWSID), NASA Astrobiology Instrument Development (ASTID), NASA Goddard Internal Research and Development (IRAD)s) to measure elemental, isotopic, and simple molecular composition abundances of 1 V to 25 kV hot ions with wide field-of-view (FOV) in the 1 – 60 amu mass range at mass resolution $M/\Delta M \leq 60$ over a wide dynamic range of particle intensities and penetrating radiation background from the inner magnetospheres of Jupiter and Saturn to the outer magnetospheric boundary regions and the upstream solar wind. This instrument will work for both spinning spacecraft and 3-axis stabilized spacecraft with wide field-of-view capability in both cases. AIMS will measure the ion velocity distribution functions (VDF) for the individual ion species. Ion velocity moments of the ion VDF will give the fluid parameters (density, flow velocity and temperature) of the individual ion species. Outer planet mission applications are Io Observer, (IoO), Jupiter Europa Orbiter (EurO), Europa Multiple Flyby Mission (EMFM), Enceladus Orbiter (EncO), and Uranus Orbiter and Probe (UOAP) as described in the decadal survey, but would also be valuable for inclusion on other missions to outer planet destinations such as Enceladus-Titan Joint Mission (ETJM), and Neptune-Triton and for future missions to terrestrial planets, Venus and Mars, the Moon, asteroids, and comets, and geospace applications to the Earth.

Rational for AIMS: The four giant planets of our solar system all have planetary magnetic fields containing hot plasma ions and electrons originating from solar, interplanetary, and internal magnetospheric sources. Plasma interactions both implant into, and erode materials from, moons of these planets, while also partly (Europa, Io) or wholly (Titan) obscuring subtle magnetic signatures of liquid oceans below the moon surfaces. Remote sensing analysis of surface composition at Europa, Enceladus, and other airless icy moons must account for effects of space weathering by the hot plasma and energetic radiation environments of those moons. The extreme radiation environments of Io and Europa, and the large abundances of foreground water group ions (O^+, OH^+, H_2O^+, H_3O^+) and nitrogen ions respectively at Enceladus and Titan, make precision measurements of plasma ion velocity moment fluid parameters (density, flow velocity, temperature) and abundances very challenging. Nevertheless, these worlds have significant decadal survey priorities for 2013–2022 (Visions and Voyages, 2012), all except Io also being potentially habitable ocean worlds as targets of NASA's new Ocean Worlds Exploration Program [1]. Advanced plasma instrumentation like AIMS is needed to operate in and to understand the complex plasma-field-radiation interactions in these environments.

Europa science objectives of the decadal survey are already covered in part by NASA's Europa Multiple Flyby Mission (EMFM), but later delivery of a Europa

lander could be accompanied by an orbiter platform and more fully achieve all objectives.

For all of these missions, AIMS would measure the full energy/charge, mass/charge, mass, and angular distributions of the local hot plasma environments to support the following science objectives: (1) Ocean: subsurface ocean detection and global characterization at icy moons by induced magnetic fields against background of local ionospheric and magnetospheric ion currents. (2) Chemistry: ionic characterization of moon surface and atmospheric composition indicative of moon origins and evolution, internal geologic activity, volcanism, and potential habitability. (3) Magnetosphere: Evaluation of moon connections to hot plasma sources, transport processes, and sinks in the giant planet system.

AIMS Approach: The AIMS approach has a multi-mission capability because sub-systems can be removed or added to meet the planetary mission requirements. Emphasis is on an Europa class mission due to its most demanding radiation environment If this can be achieved, then the instrument has the necessary capability for missions with less demanding environments. A lower resource version would have greater emphasis on the major ions which could be applicable, for example, to support magnetometer measurements of Europa's ocean. The most capable higher resource option for which ion composition has the greatest emphasis, would measure both the major ion and minor ion species which will require a wider dynamic range in particle intensities so measurements of the more tenuous magnetospheric plasmas and denser plasmas within planetary ionospheres can both be made. The design of AIMS can be optimized for science operations in extreme radiation environments as would be encountered at Io and Europa, while also allowing full measurements in the more quiescent environments of the outer magnetospheric boundary regions and the upstream solar wind.

AIMS Design: Our design approach is to increase the signal to noise (S/N) within the instrument by 1) reduce foreground noise so scattering by major ions cannot hide the peaks of the minor ions by using our Circular Wien Filter (CWF) design with tophat electrostatic analyzer (ESA) for wide field-of-view capability and 2) reduce background noise due to penetrating particles by developing an effective gradient-Z radiation shielding design and by developing a technique that reduces the area of the detectors within the shielded cavity of AIMS without reducing geometric factor (GF) or sensitive area of AIMS. Reducing detector area also allows the shielding mass to be reduced. We have been measuring the response of microchannel plates (MCPs) to penetrating electrons and their secondaries from 100 keV to 1.5 MeV electrons using the NASA Goddard Van de Graaff accelerator and 8 MeV to 27 MeV using the National Institute of Standards and Technology (NIST) linear accelerator with and without shielding. Other mitigating techniques can also be used. By combining the mass-per-charge (M/Q) selection capabilities of the CWF + ESA, and the Linear Electric Field (LEF) time-of-flight (TOF) sub-assembly, we can separate ions of similar M/Q like O^+/S^{++} and O_2^+/S^+; our LEF will use novel tapered design whose concept was originated by the Goddard AIMS group. The tapered LEF reduces the sensor mass and allows one to optimize the performance of the LEF. A solid state detector (SSD) is included for high charge state ion measurements such as solar wind high charge state ions entering into giant planet magnetospheres [2]. The LEF allows one to locate the SSD near ground potential for a low mass and low risk design. We also have the capability to detune the instrument's GF by > 1000. Laboratory measurements of the AIMS prototype instrument performance will be presented along with our measurements of MCP response to energetic electrons and radiation shielding design approach.

References:

[1] McEwen, A., New study team: Roadmaps to Ocean Worlds (ROW), (2016) *Outer Planets Assessment Group*, San Antonio, Texas, Feburary 1-2, 2016. [2] Geiss, J., G. Gloeckler, H. Balsiger, L. A. Fisk, A. B. Galvin, F. Gliem, D. C. Hamilton, F. M. Ipavich, S. Livi, U. Mall, K. W. Ogilvie, R. von Steiger, and B. Wilken, (1992), *Science, 257*, 1535 – 1539.

Acknowledgements: We would like to acknowledge the support we received from the Astrobiology Instrument Development (ASTID) program and support from the Goddard Chief Technologists Internal Research and Development (IRAD) Program.

SUMMARY OF GSA 2016 SESSION T39: 'GO SMALL OR GO HOME: MICROBEAM TECHNIQUES APPLIED TO IGNEOUS, METAMORPHIC, AND SEDIMENTARY PETROLOGY OF EARTH AND PLANETARY MATERIALS'. A.K. Souders[1] and P.J. Sylvester[1], [1]Department of Geosciences, Texas Tech University, Lubbock, TX 79409 (kate.souders@ttu.edu; paul.sylvester@ttu.edu)

Introduction: Recent advances in in-situ analytical methods (e.g EPMA, SEM/TEM, EBSD, SIMS, LA-(MC)-ICPMS) have inspired new method development and applications for Earth and planetary geochemistry. Unlike traditional bulk geochemical approaches, in-situ measurements provide chemical and isotopic compositions of particles and minerals down to the submicron levels while, in some cases, preserving the petrographic relationships between phases. These geochemical measurements enable us to gain a better understanding of the magmatic and metamorphic histories of planetary crusts, sedimentary provenance, diagenesis, impact processes, and nucleosynthesis and stellar evolution.

This presentation will provide a summary of the 2016 Geological Society of America Annual Meeting topical session 'Go Small or Go Home: Microbeam Techniques Applied to Igneous, Metamorphic, and Sedimentary Petrology of Earth and Planetary Materials'. Particular emphasis will be placed on the latest technology developments and applications that provide new observations and/or improved data quality for a wide range of Earth and planetary materials.

Design of an Integrated LC-MS Prototype for an *in situ* Mission to an Icy Body in the Solar System

A. E. Southard[1], S. A. Getty[2], J.P. Ferrance[3], M. A. Balvin[2], J. E. Elsila[2], D. Stewart[2], B. Stamos[4], C. Kotecki[2], D. P. Glavin[2], [1]Universities Space Research Association (Adrian.e.southard@nasa.gov), [2]NASA GSFC, [3]J2F Engineering, [4]Univ. of Texas at Arlington

Introduction: Future high-priority planetary exploration will target destinations that are likely host to a broad diversity of inorganic and organic composition. Primitive bodies, such as comets and carbonaceous asteroids, are thought to have contributed an inventory of prebiotic chemistry to the early Earth, and cataloging their present-day, cryo-trapped organic diversity can offer details about the breadth of organic astrochemistry that is representative of the Solar System's origins and evolution. Major classes of organics likely to be present on these primitive, small bodies include polycyclic aromatics, carboxylic acids, alcohols, aldehydes and ketones, amines, nucleobases, and amino acids. The diversity of organic material on these primitive bodies can be challenging to fully characterize by mass analysis alone; liquid chromatography can offer additional discrimination based on functional group chemistry and/or size effects to alleviate ambiguity.

Liquid chromatography-mass spectrometry (LC-MS) has enabled detailed and sensitive terrestrial investigations of meteoritic materials, interplanetary dust, and returned cometary particles[1]. It has been used to detect extraterrestrial amino acids in meteorites [2]–[4] and to quantify enantiomeric excess [4]. LC-MS is a sensitive, versatile approach to analyzing non-volatile organics with little to no degradation of the analytes.

The development goal of the OASIS instrument (Organics Analyzer for Sampling Icy Surfaces) is to implement LC-MS in a spaceflight-compatible package [5]. We estimate that an eventual flight-ready OASIS Instrument could weigh as little as 5 kg and consume only 3 W of power, even for the case of a cold surface of an icy satellite or comet. While separations of a range of molecular classes relevant to life could be performed, here we discuss results achieved for amino acids and nucleobases uaing the analytical column of the OASIS instrument.

Design: The OASIS instrument utilizes a four stage vacuum interface (Figure 1) designed to transmit ion current from a spray tip at the outlet of an LC analytical column into a prototype time-of-flight mass spectrometer [7], measuring 8x30 x 4 cm^3.

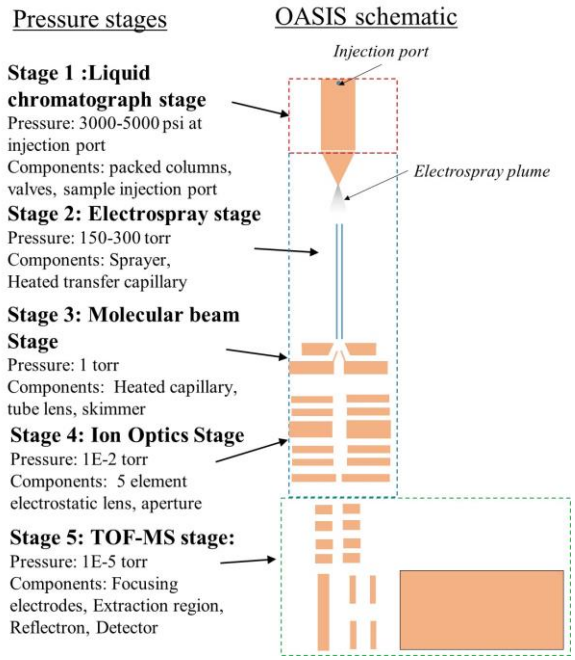

Figure 1 Schematic of the multi-stage interface between the OASIS microchip and a custom time-of-flight mass spectrometer

The LC analytical column and spray tip are integrated into a custom microchip (2 cm x 3 cm x 0.1 cm) with integrated heaters. The microchip was designed to sustain high delivery pressure (>5000 psi), minimize background contamination, and integrate the LC column to a spray tip with minimal dead volume, which can lead to degradation in the chromatography.

Results: Electrospray ionization (ESI) of a mixture of adenine and phenolphthalein standards was demonstrated from the nozzle component of a microchip using a commercial Waters TOF-MS for detection[6]. For this component-level demonstration, no chromatography was performed.

A packed column on a precursor microchip (without nozzle) is shown in Figure 2. For analytical testing, the 8 cm long, 75 micron inner diameter microchip column was packed with a commercial chiral stationary phase and connected to a 20 micron inner diameter commercial ESI tip (Waters). Separations of the chiral forms of four amino acids using the microchip column are shown in Figure 3. Resolution of the microchips with integrated spray tips is expected to surpass that

achieved here due to the reduced dead volume in the integrated microchips.

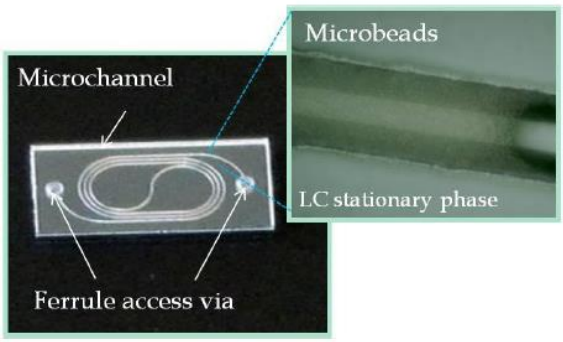

Figure 2 OASIS microchip without integrated spray tip (left) and picture of packed stationary phase (right)

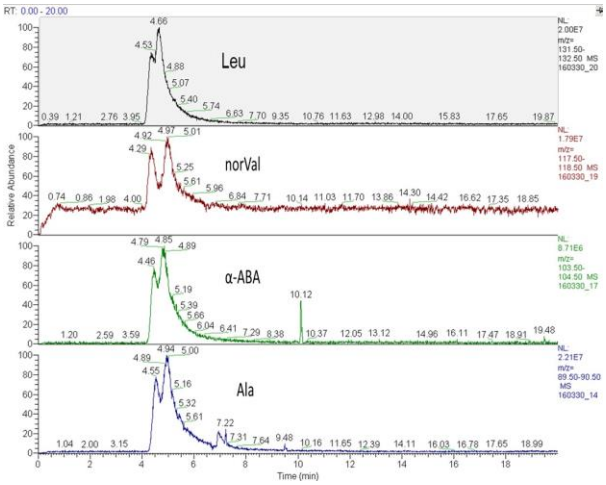

Figure 3 The amino acids leucine(Leu), norvaline(norVal), homoalanine(α-ABA), and alanine(Ala) in a 95:05 methanol:water 1% formic acid solution were separated by an OASIS microchip analytical column and detected using a commercial mass spectrometer (Thermo LTQ orbitrap XL)

A challenging aspect of the microchip to TOF-MS interface (Figure 1) is the efficient transfer of analyte from stage 1 where pressures are greater than the vapor pressure of the sprayed solvent, as required by ESI, to the fourth stage where pressures are in the microtorr regime. This transfer is dominated by gas flow at higher pressures, but the second stage is characterized by sufficiently low pressure for electrostatic forces to steer and focus the charged analytes. The second stage uses a ring electrode to direct ions through a skimmer opposite the capillary. A multi-element electrostatic lens in the third stage (Figure 4) is then used to focus ions through a second skimmer (not shown) into the final (fourth) TOF-MS stage.

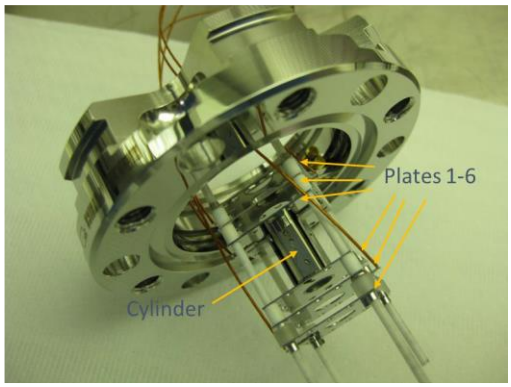

Figure 4 A five element electrostatic lens built from plates, with apertures, and a hollow, cylindrical element (Kimball Physics eV parts)

We monitored transfer efficiency through the various lens elements by examining the currents reaching the transfer capillary, skimmer, and the plates in stages 2 and 3. Currents intercepted by the heated transfer capillary are readily measurable in the tens of nanoamp range at flow rates of 0.5 uL/min (80:20 methanol:water, 10% formic acid, 0.5 mM adenine). Currents transmitted throught the ion optics stage are in the tens of picoamps. Most of the losses appear to be within stage 2; however, characterization of currents at the spray tip is underway to also assess losses in the capillary transfer region. While the transmission of current does not guarantee a proportionate response in isolated, charged analyte[8], it represents practical way to insure good mechanical alignment and allows for optimization of focusing of the electrostatic lens of stage 3.

References: [1] Burton *et al. Chem. Soc. Rev.*, vol. 41, no. 16, pp. 5459–5472, Jul. 2012. [2] M. P. Callahan *et al. Meteorit. Planet. Sci.*, vol. 48, no. 5, pp. 786–795, May 2013. [3] Elsila *et al. Meteorit. Planet. Sci.*, vol. 44, no. 9, pp. 1323–1330, 2009. [4] Glavin *et al. Meteorit. Planet. Sci.*, vol. 41, no. 6, pp. 889–902, 2006. [5] Getty *et al.* (2013) *IEEE Aerospace Conference*, 2013, pp. 1–8. [6] Southard *et al.* (2014) IEEE Aerospace Conference 2014, pp. 1-7. [7] Glavin *et al. Aerospace Conference, 2012 IEEE*, 2012, pp. 1–11. [8]Page *et al.* (2007) J. Amer. Soc. Mass. Spec., vol 18, no. 9, pp. 1582-1590, Sep. 2007

Mars Organic Molecule Analyzer (MOMA) as an example for Contamination Control for Life Detection Instrumentation. H. Steininger[1], F. Goesmann[1], F. Raulin[2], W. B. Brinckerhoff[3], P. R. Mahaffy[3], C. Szopa[4], MOMA Team, [1]Max Planck Institute for Solar System Research (MPS), 37077 Göttingen, Germany (steininger@mps.mpg.de), [2]LISA, Universités Paris Est-Créteil, Paris , Denis Diderot et CNRS, CMC, 94010 Créteil cedex, France, [3]NASA Goddard Space Flight Center, Greenbelt, Maryland 20771, USA Laurel, MD, [4]UMPC Univ. Paris 6 , Universités Versailles St-Quentin, Paris , CNRS/INSU, LATMOS-IPSL, 75055 Créteil cedex, France.

Introduction: The Mars Organic Molecule Analyzer (MOMA) is a combined pyrolysis gas chromatograph mass spectrometer (GC-MS) and laser desorption mass spectrometer (LD-MS). It will be the key instrument of the ESA Roscosmos ExoMars 2020 mission to search for extinct and extant life on Mars. Additionally the instrument should detect the organic background on Mars, e.g. the one caused by meteoritic influx. The drill system on board ExoMars is capable to provide a drill core from down to 2 m depth. The sensitivity of the instrument to organic contamination is high and even a small background of organic contamination would make the identification of martian organics challenging. Contamination of biological origine could lead to a false positive life detection on Mars. This makes the Contamination Control one of the key points for the scientific success of the mission.

Laser desorption-Mass Spectrometry: Laser desorption-mass spectrometry is a method to detect large organic molecules without degrading them during the volatilization step. This method needs a laser source in the UV-range.

In the MOMA instrument a solid-state laser source generates UV light (λ = 266 nm) with a 1-ns pulse width. A miniaturized linear ion trap mass spectrometer similar to a Thermo LTQ ion trap is used to detect the generated ions.

A crushed sample from the drill is moved under the laser and the mass spectrometer. The laser pulses generate plumes of ions which are injected into the mass spectrometer via gas flow and electrostatic voltages through the aperture valve and capillary ion inlet. After closing of the valve the pressure in the MS is reduced to the working conditions of the linear ion trap mass spectrometer and the ions are analyzed..

Gas Chromatography-Mass Spectrometry: The MOMA instrument is capable to submit the sample to a derivatization process, consisting of the reaction of the sample components with specific reactants (MTBSTFA, DMF-DMA or TMAH) which increase the volatility of complex organic species. In the pyrolysis mode the sample material can be heated to above 850°C. In this step most of refractory organic compounds break down and can be analyzed by the GC-MS.

Contamination Control: Several issues defined the requirements and the implemention of the contamination control approach within the instrument and in the entire rover. The science requirements of several instruments had to be combined and molded into top level CC requirement of the mission. The changes in the instrument payload led to a challenging task to combine the requirements. The original set of instruments was chosen to cover most of the possible biomarkers and organic compounds in several sensitivity ranges. There were highly specific instruments with a narrow field of view and other instruments with a broad spectrum but much higher detection threshold, like MOMA. The first more complex requirement for the mission would have been hard to verify and hard to implement for the instruments because it would have needed test methods of the same complexity. With the decreasing number of life detection instruments on the mission the requirement became less complex and was by a large part influenced by the needs of the MOMA instrument. The situation for the rover was simplified by the approach of an ultra-clean part of the rover interior. All the sample processing and science observations are happening in this ultra-clean zone. Although now the number of instrument groups affected by the stringent CC requirements was small the test procedures and the effective implementation of the CC requirement into the assembly and integration of the instruments and rover was challenging. The amount of contamination at the beginning of the science mission on Mars was fixed, but the distribution to the individual teams and the approach of every team to meet the requirements had to be implemented.

The allowed amounts of organic contamination were in the ng range and for every instrument parts cleaning procedures and verification methods had to be tested and approved. But the final prove of concept that every part of the ultra clean zone was clean enough would first be tested with the qualification model of the rover enterior.

For sample return missions the requirements have to be even more stringent because laboratories here on earth have a larger pool of methods compared to space instruments for life detection. This would make the Contamination Control the driver of a lot of technical inovations to meet the requirements.

.

BROADBAND GROUND PENETRATING RADAR WITH CONFORMAL ANTENNAS FOR SUBSURFACE IMAGE FROM A ROVER. D. E. Stillman[1], C. Oden[2], R. E. Grimm[1], and B. Pyke[2], [1]Dept. of Space Studies, Southwest Research Institute, 1050 Walnut St. #300, Boulder, CO 80302 (dstillman@boulder.swri.edu), [2]Earth Science Systems, Wheat Ridge, CO.

Introduction: Ground-Penetrating Radar (GPR) provides geologic context via subsurface imaging and will be flown on the next two Mars rovers (WISDOM [1] on ExoMars and RIMFAX [2] on Mars 2020). The ExoMars antennas cannot be easily attached to an MSL class rover because the front of the rover is used for the arm and the rear is used for the RTG. RIMFAX had to change the location of its antenna post selection because their proposed location was not approved by the rover engineers. In fact, these engineers suggested moving the antenna to the belly of the rover, but RIMFAX decided against this. The motivation of this research is to design a broadband radar antenna that conforms to the rover belly, while maximizing the scientific capabilities of the GPR. Therefore, we have designed our antennas to be as thin as possible so that rover mobility is not compromised. Furthermore, we aim to design a GPR with: (1) high bandwidth – which controls the resolution and allows certain mineralogies and rock units to be discriminated based on their frequency-dependent EM or scattering properties, (2) high antenna efficiency at low frequency – which controls the depth of penetration, and (3) high dynamic range – which also controls the depth of penetration and allows the detection of interfaces with small changes.

Antenna Design / Polarization: We have designed and field-tested a prototype GPR that utilizes bistatic circularly polarized spiral antennas (**Fig. 1**). This antenna type was chosen because they have an inherent broadband response and provide a better low frequency response compared with similarly sized linearly polarized antennas. The resulting spiral antennas provide high gain (0 to 8 dBi) from 200 to 1000 MHz (**Fig. 2**).

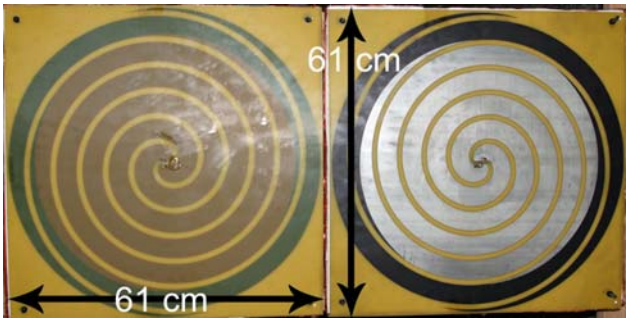

Figure 1. Spiral antennas sized to be mounted to the underbelly of a MSL-class rover and efficiently radiate energy down to 200 MHz.

Thickness: Antennas output energy both upward and downward. Upward energy reflects via the rover belly back downwards, thus interferes with subsurface reflected energy. To minimize this we use 1) an antenna with a high metallization ratio so less energy can transmit through the antenna and into the subsurface, and 2) space qualified attenuative foam to attenuate energy above the antenna.

Our antenna testing shows that a backplane decreases antenna gain at low frequency and slightly raises gain at high frequency. As the thickness of attenuative foam increases low frequency gain was recovered. Overall, we found a 4.6 cm total antenna and foam thickness produced reasonable results of antenna gain.

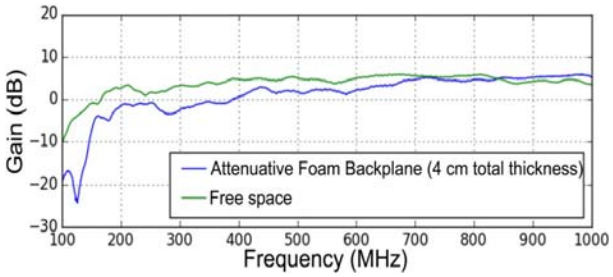

Figure 2. 4 cm of attenuative foam produces good bandwidth from 200 – 1000 MHz.

Field Test: The antennas are mounted on the platform shown below to simulate emplacement on an MSL-class rover (**Fig. 3**). The field test was performed to test the antennas, thus we used commercial impulse GPR electronics with a center frequency of 500 MHz and a dynamic range of ~150 dB. Field location is at Earth Science Systems GPR test pit near Bennett, CO where multiple pipes are buried in sand. Radargram from the field test shows the capability of detecting three metal pipes and the sand-clay interface at 3 to 3.7 m deep (**Fig. 4**).

Figure 3. Field test of antennas.

Dynamic Range: There are three different techniques to operate a GPR: (1) Impulse – where a broadband pulse is quickly transmitted and then the reflected energy is measured as a function of time, (2) Continuous Wave (CW) – where the transmitter sweeps through a number of frequencies and both the transmitter and receiver are always on, and (3) Gated CW – where the transmitter emits a single frequency or chirp and then turns off, and the receiver is always turned on. For the single frequency mode, the process is repeated with a different frequency until the entire bandwidth has been swept through.

We evaluated which GPR operational mode was able to obtain the highest dynamic range (DR: the ratio between the largest and smallest values of energy the GPR can measure). We also assumed that range gain (where received energy is amplified with time before being digitized) was used when the transmitter was off. DR is important because it allows us to image smaller reflection caused by changes in electrical or magnetic properties and it allows deeper penetration as signals are attenuated as they propagate.

We chose to use a Gated CW operational mode because it produces the largest DR (**Table 1**). This occurs because Gated CW is able to emit for energy into the ground longer than the impulse operation and receives energy at depth when the transmitter being off, thus allowing range gain. A broadband gated CW radar has many of operational benefits. As the high frequencies will get absorbed faster than low frequencies, therefore the radar could be programmed to measure at high frequencies for a longer period to increase resolution. Similarly, the radar can measure at lower frequencies for a longer period to increase depth of penetration. Thus, we are building in flexibility to perform high resolution shallow imaging and deep imaging.

Summary: We are building a GPR that maximizes depth of penetration and resolution with conformal antennas that efficiently radiate energy from 200 – 1000 MHz with a system high dynamic range (~180 dB). We have built and field-tested our bistatic circularly polarized spiral antennas that could be mounted to the underbelly of a MSL-class rover. We are currently testing the electronics so that we can operate the radar in a gated CW mode to maximized dynamic range.

This broadband radar system will allow for maximum versatility; thus allowing high resolution shallow mapping and deep mapping. Furthermore, the frequency range can be changed to increase the dynamic range at low frequency (i.e. to see deeper) or at high frequency (i.e. to increase resolution). Broadband surveys allow certain mineralogies and rock units to be discriminated based on their frequency-dependent EM or scattering properties. Overall, we estimate that this radar should provide penetration to tens of meters in martian regolith or hundreds of meters in ice-rich regolith.

Table 1. Comparison of the dynamic range (DR) of three operational modes. Note an increase in the T_{trace} by a factor of 10 also increases the DR by 10.

Radar type	Power	Duty Cycle	DR (T_{trace} = 0.1 s)
Impulse + range gain	1 W*	0.1%	158 dB
CW	4 mW**	100%	164 dB
Gated CW + range gain	1 W	10%	178 dB

* Higher power can be obtained but requires bigger pulse repetition rate, which lowers T_{trace} and causes a decrease in transmitted energy and DR.

** No value in increasing power because transmitter and receiver are always on.

References: [1] Ciarletti et al. (2011) *Proc. IEEE, 99*, 824-836. [2] Hamran et al., (2014) *2nd Intern. Workshop on Instrum. for Planet. Missions*, 1034.

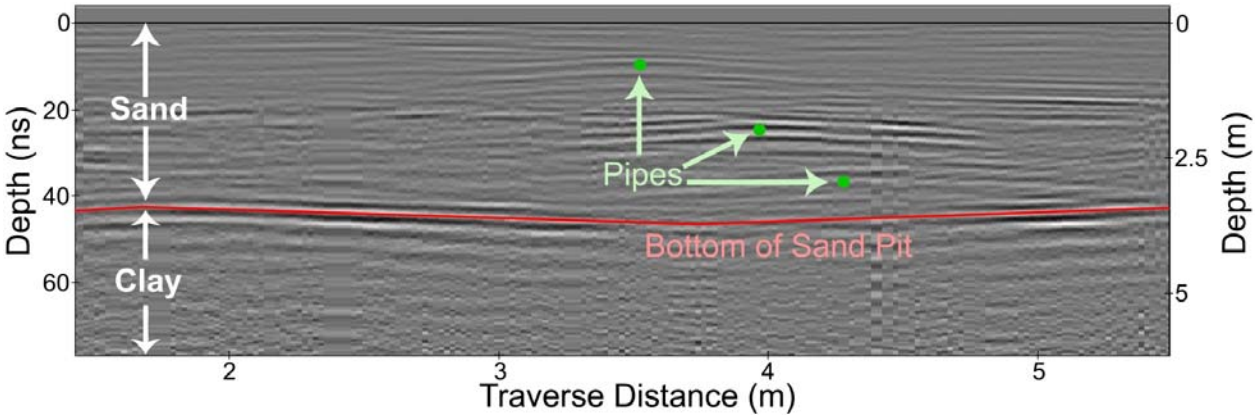

Figure 4. Radargram showing detectability of three pipes and the bottom of the sand pit.

AN ORGANIC ANALYZER INSTRUMENT FOR HIGHLY SENSITIVE IN SITU ORGANIC DETECTION ON AN ICE SHELL IMPACT PENETRATOR DESCENT PROBE. A. M. Stockton[1*], Z. Duca[1], M. Cato[1], T. Cantrell[1], S. Foreman[2], J. Kim[2], P. Putman[3], and B. Schmidt[1], [1]Georgia Institute of Technology, GA, USA, [2]Texas Tech University, TX, USA, [3]Sierra Lobo, OH, USA.

Introduction: Kinetic penetrators have the potential to enable low cost in situ measurements of the ice shells of astrobiologically exciting worlds including Europa and Enceladus [1]. Their small size and mass, critical to limiting their kinetic energy to an acceptable range, makes them ideal small landers riding on primarily orbiter missions, while still enabling sampling at several m depth due simply to burial and excavation. In situ microfluidic-based organic analysis systems are a powerful, miniaturized approach for detecting markers of habitability and recent biological activity.

Quantitative, compositional, and chiral analysis of small organic molecules *in situ* provides important information for studying planetary formation and evolution, and, more excitingly, also can provide signatures of past or present life. The Extraterrestrial Organic Analyzer (EOA), with microchip capillary electrophoresis (μCE) and laser-induced fluorescence (LIF) detection, is the only technique currently ready for space flight that has the resolution, selectivity, and sensitivity to provide these analyses. Through both in-lab [2,3] and field [4] testing, μCE-LIF has demonstrated the capability to provide highly sensitive (sub parts-per-trillion, or pptr) automated quantitative compositional chiral analysis of multiple organic compound classes [5,6], including polycyclic aromatic hydrocarbons (PAHs) [7], amino acids [8], aldehydes and ketones [9], carboxylic acids [10], thiols [11], and amines [12]. Lander or fly-by missions have largely been the focus for the development of μCE-LIF, as proposed in the Mars Organic Analyzer (MOA) and the Enceladus Organic Analyzer.

Concept: Development of microfluidic technology, like that of the Mars Organic Analyzer (MOA) [2-12] and Enceladus Organic Analyzer (EOA), has led to an instrument capable of in situ organic chemical analysis compatible with a kinetic penetrator platform. This technology uses an integrated microfluidic processor to prepare samples for analysis via fluorescent derivatization prior to highly sensitive laser-induced fluorescence (LIF) detection. Selective derivatization in the presence of a chiral selector enables distinction between amino acid enantiomers.

Programmable microfluidic architechtures enable automated, complex microfluidic manipulation on-chip, including mixing, dilutions, fluorescent derivatization, and transfer [6]. Recently, we have shown that microdevices retain functionality of their pneumatically-actuated monolithic membrane microvalves after 10+ years in storage [13]. Here, we show the continued development of the microfluidic and LIF subsystems for a kinetic impactor mission. Preliminary results have shown promising suitability of microdevices during a 50000g impact, indicating that PMA and LIF are valid in situ techniques for this extreme planetary mission format.

Instrument Development: Finite element analysis of the core microfluidic processing and analytical device indicated that the device itself is more than capable of surviving the stresses associated with an impact acceleration of >50,000g. However, a number of developments were still required to enable a flight-ready system.

Preliminary experiments indicated that moving from a pneumatically-actuated to a hydraulically-actuated microvalve system may provide better impact resistance. A hydraulically-actuated microvalve system was developed and tested. A modification of an established microfabricated LIF detection system would use indium bump bonding to permanently weld optical components using standard microfabrication techniques with perfect alignment. Recent work has also focused on developing and characterizing impact-resistant electronics.

Summary: This work shows the low-TRL development of EOA's LIF and microfluidic subsystems for future planetary impact penetrator missions. With correct structural decisions and optimizations, EOA can survive a 50,000g impact, making it the only current optical instrument with this capability.

References: [1] Gowen et al., Adv. Space Res., 2011, 725. [2] Skelley et al, PNAS USA, 2005, 102, 1041. [3] Benhabib, M. et al. (2010) Anal. Chem., 82, 2372-2379. [4] Skelley, A. et al. (2007) JGR., 111, G04S11. [5] Kim J., et al, Anal. Chem., 2013, 85, 7682. [6] Kim, J. et al. (2016) Lab Chip. 16, 812-819. [7] Stockton, A. et al. (2009) Anal. Chem., 81, 790-7906. [8] Chiesl, T. et al. (2009) Anal. Chem., 81, 2537-2544. [9] Stockton, A. et al. (2010) Electrophoresis, 31, 3642-3649. [10] Stockton, A. et al. (2011) Astrobiology, 11, 519-528 [11] Mora, M. et al. (2013) Electrophoresis, 34, 309-216. [12] Cable, M. et al. (2013) Anal. Chem., 85, 1124-1131. [13] Duca, Z. et al. (2015) EPSC, Abstract #416.

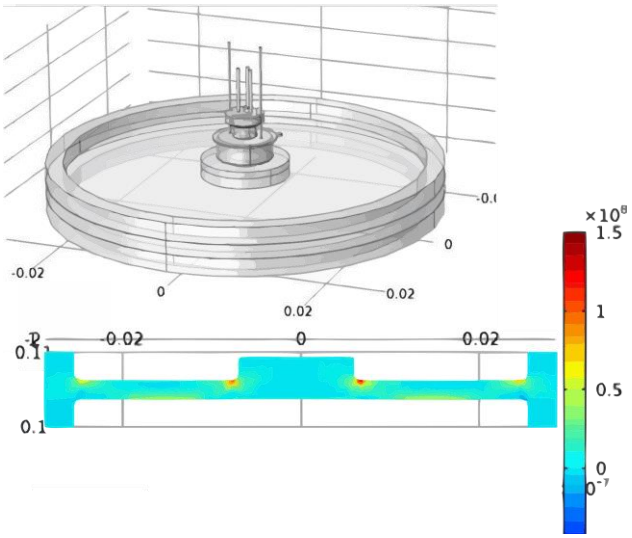

Figure 1: Structural (top) and stress (bottom) model of a centered optical stack without support structures

A SUBMILLIMETER SOUNDER FOR MEASURING MARTIAN WINDS AND WATER. L. K. Tamppari[1], N. J. Livesey[1], and W. G. Read[1], [1]Jet Propulsion Laboratory/Caltech, 4800 Oak Grove Dr., Pasadena, CA 91109.

Introduction: The winds on Mars are almost completely unknown, yet are critical for understanding fundamental Martian processes, such as the dust and water cycles, and for ensuring safe landing of robotic and human spacecraft. Previous Martian surface wind measurements are limited to the Viking, Pathfinder, Phoenix and Curiosity landed missions; all single locations with only the Vikings operating contemporaneously. A few other indirect wind measurements have been made through application of techniques such as thermal wind balance, and through examinination of wind generated features on the surface, and cloud motions. A few Earth-based observations of winds have been made, but they are severely limited in time and represent averages over very large regions of the atmosphere. Given this dearth of measurements, most studies of Martian winds are model-based in nature and only limited validation has been possible for the conclusions drawn.

The need for a global, long-term wind measurement set is great, as discussed by NASA's Next Orbiter Science Analysis Group [NEX-SAG; 1]. This group was chartered by the Mars Exploration Program Analysis Group in 2015 to evaluate the science priorities for a potential Mars orbiter envisioned to launch as early as 2022. One of the five compelling science objectives noted was to *"Measure winds and characterize transport and other dynamic processes to understand current climate, water, and dust cycles, with extrapolation to past climates"* and a Finding was *"Observation of wind velocity is the single most valuable new measurement that can be made to advance knowledge of atmospheric dynamic processes. Near-simultaneous observations of atmospheric wind velocities, temperatures, aerosols, and water vapor with global coverage are required to properly understand the complex interactions that define the current climate."* The NEX-SAG further identified that a long-wavelength atmospheric sounder could meet this objective.

Science Motivation: The various Mars orbiting spacecraft that have been flown to date have characterized the Martian atmosphere fairly well in terms of temperature, pressure, dust and ice aerosols, and column water vapor amount. The ExoMars Trace Gas Orbiter will measure profiles of the abundance of many key trace gases, and MAVEN is studying the upper atmosphere and its interaction with the space environment.

However, fundamental questions regarding the nature of the current and past Martian climate remain. Addressing these questions requires an understanding of the atmospheric general circulation and its variability, for which global wind measurements are necessary, and have remained and missing piece in basic atmospheric characterization. Further, measurements of temperature, aerosol and water vapor are needed simultaneously with any wind measurements, to fully understand the impact of thermal forcing on wind, and the consequences for aerosol/vapor transport. Specific science examples, relating to key questions involving two major cycles operating in the Martian atmosphere, are discussed below.

Winds, Temperature and the dust cycle. Dust storms (Fig. 1) are a major part of the Martian climatology, and affect the atmospheric state on local to global scales. However, their genesis and evolution are not well understood, particularly with regard to the generation of global dust storms. At the most basic level, it is still not understood why some storms become global while others remain regional or local. Intriguingly, a "flushing" storm originating in the northern hemisphere and migrating southwards was seen just prior to the 2007 global dust storm [2], providing a possible mechanism for the incitement of the global dust storm. However, a similar flushing storm in a later Mars year did not lead to a global dust storm. Key related questions are: what are the wind velocity and associated temperature profiles within and surrounding large dust storm, and how do these vary with season and location or for similar storms expressed in different years? **Measurement of the winds and associated atmospheric temperatures are essential for enhancing understanding of dust storm initiation, progression, and variabitlity.**

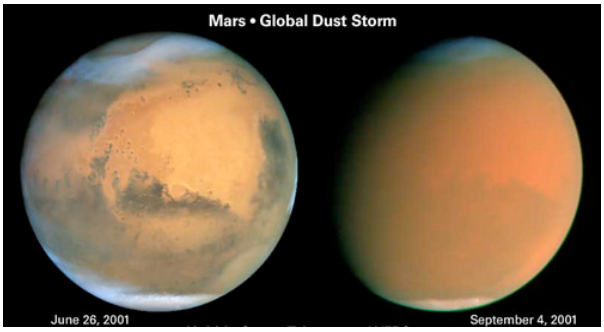

Figure 1: An example of a global dust storm on Mars (this one in 2001). Image credit: HST.

Winds and the water cycle. One of the biggest mysteries on Mars is when, and under what conditions, was there sustained surface water. Given that such flow is not sustained today, although geomorphic and geologic evidence shows clearly that it was in the past, the question then becomes, how and when did the Mar-

tain climate change? Simultaneous measurements of the vertical profile of wind and water vapor abundance are essential for understanding how much vapor mass is transported by the atmospheric circulation. Key questions include: is there net cross-hemisphere transport today and is transport influenced by seasonally or orbitally forced behavior of possible sources and sinks (e.g., polar cap and high-mid latitude regolith)? Further, understanding behavior in today's climate is critical for understanding climate change and the rate thereof. Tyler and Barnes [5] show transient eddies that generate winds within the boundary layer (~10 km) that blow directly over the north polar cap, particularly at L_s=120°. This could increase sublimation rates due to the effect of strong near surface winds and, by bringing in warm air over the polar cap, both enable greater sublimation and carry moist air away. Measurements of winds and water vapor vertical profiles will enable testing of such hypotheses. **Understanding of the current wind velocities and water vapor vertical profiles as a function of season is essential for quantifying transport and validating models. This in turn can be used to gain insight into the current climate and climate history of Mars**.

Engineering motivation: Wind profiles are critical for entry, descent, and landing to, and in the future ascent from, the surface of Mars. Currently, unvalidated model output (from usually ≥2 models to guard against potential errors) is used to provide guidance for spacecraft design and landing parameters. This may result in over-design of spacecraft or, at worst, mis-prediction of the wind field leading to failure. **Global wind measurements are needed for guiding appropriate spacecraft design.**

Sub-millimeter instrument design concept: A passive submillimeter limb sounding instrument is ideally suited to provide the needed wind, water vapor, and temperature profile measurements. The technique has high hertitage in Earth-science, and dramatic advances in associated technology in the past decade (driven in part by the communications industry) enable significant reductions in needed power, mass and complexity. Such an instrument can make meaurements both day and night, and in the presence of atmospheric dust loading. Per the NEX-SAG report, our instrument design will be optimized to deliver measurements of winds, temperature, and water vapor between 0–80 km, at ~ 5 km vertical resolution.

Our concept for such an instrument builds on prior JPL-led instruments such as the Microwave Limb Sounder currently flying on EOS *Aura* [6], and the MIRO instrument aboard *Rosetta* [7]. The instrument would employ a single, steerable antenna (~30 cm diameter), and observe a diverse set of spectral lines, both weak and strong, from multiple species to cover the full range of altitude desired. The antenna would be 2-axis gimbaled for steerable limb and near-nadir views, enabling continuous instrument operation during spacecraft maneauvers for special campaign observations, or as the spacecraft orbit changes. Fig. 2 shows a block diagram of the instrument.

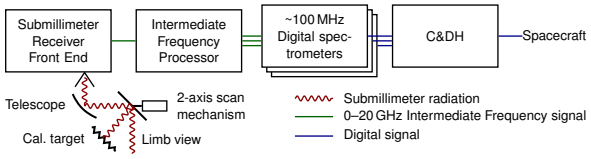

Figure 2: Block diagram of instrument

Performance Analysis. Initial simulations have been undertaken to show performance of our notional sub-mm sounder (Fig. 3). These simulations employed algorithms and software developed for Aura MLS (suitably adapted to the Martian atmosphere) to model performance of the the instrument under conditions taken from the Mars Climate Database.

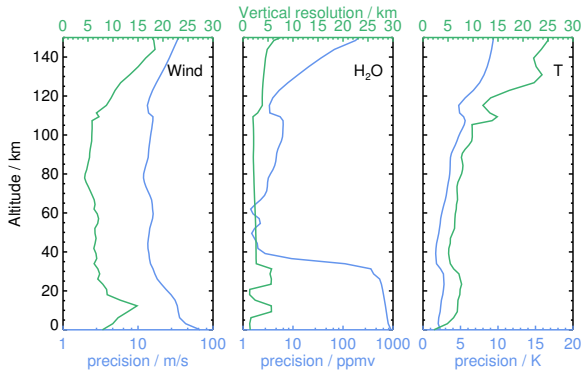

Figure 3: Example preliminary results from simulated retrievals, showing estimated precision and vertical resolution for line of sight wind, water vapor and Temperature from a 550 GHz submm limb sounder.

References:

[1] MEPAG NEX-SAG Report (2015), Report from the Next Orbiter Science Analysis Group (NEX-SAG), *Chaired by* B. Campbell and R. Zurek, 77 pages posted December, 2015 by the Mars Exploration Program Analysis Group (MEPAG) at http://mepag.nasa.gov/reports.cfm.

[2] Wang, H. and Richardson, M.I. (2013) *Icarus*.

[3] Piqueux, S. A. *et al.* (2014) *Icarus*.

[4] Cantor, B. A., et al. (2010) *Icarus* 208, 61–81.

[5] Tyler, D., Jr., Barnes, J. R. (2005) *J. Geophys. Res.*, 110, E06007.

[6] Waters, J.W. *et al.* (2006) *IEEE Trans. Geosci. Remote Sensing 44*, 1075–1092.

[7] Gulkis, S. et al. (2007), *Space Sci Rev*, *128*(1-4), 561–597.

THE EUROPA IMAGING SYSTEM (EIS), A CAMERA SUITE TO INVESTIGATE EUROPA'S GEOLOGY, ICE SHELL, AND POTENTIAL FOR CURRENT ACTIVITY. E. P. Turtle[1], A. S. McEwen[2], S. N. Osterman[1], J. D. Boldt[1], K. Strohbehn[1], and the EIS Science Team, [1]Johns Hopkins Univ. Applied Physics Lab., Laurel, MD; Elizabeth.Turtle@jhuapl.edu, [2]Univ. Arizona, Tucson, AZ.

Introduction: Based on the Europa Clipper mission concept [1], NASA's Europa Multiple Flyby Mission, planned for launch in 2022, will perform more than 40 flybys of Europa with altitudes at closest approach as low as 25 km. The science payload [2] includes the Europa Imaging System (EIS), a camera suite designed to provide global decameter-scale coverage, topographic and color mapping, and unprecedented sub-meter-scale imaging. EIS combines narrow-angle and wide-angle cameras (Fig. 1) to address Europa Mission science goals of investigating Europa's geology, composition, ice shell and ocean.

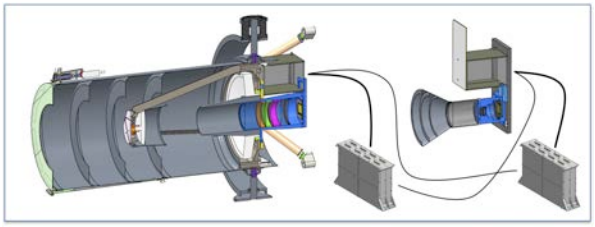

Figure 1: (Left) EIS NAC, (right) EIS WAC, and identical, cross-strapped DPUs (in spacecraft vault).

EIS science objectives include:

• constraining the formation processes of surface features by characterizing endogenic geologic structures, surface units, global cross-cutting relationships, and relationships to Europa's subsurface structure and potential near-surface water [*e.g.*, 3];

• searching for evidence of recent or current activity, including potential plumes [4];

• characterizing the ice shell by constraining its thickness and correlating surface features with subsurface structures detected by ice penetrating radar [5];

• characterizing scientifically compelling landing sites and hazards by determining the nature of the surface at scales relevant to a potential lander [6].

EIS Narrow-angle Camera (NAC): The NAC is derived from *New Horizons* LORRI [7] heritage and has a 2.3° cross-track x 1.2° along-track field of view (FOV) and a 10-µrad instantaneous FOV (IFOV) to achieve 0.5-m pixel scale over a 2-km-wide swath from 50-km altitude. It is mounted on a 2-axis ±30° gimbal to enable NAC targeting independent of S/C pointing. Use of a gimbal makes near-global (>95%; Fig. 2) mapping of Europa possible at ≤50-m pixel scale (to date, only ~14% of Europa has been imaged at ≤500 m/pixel), as well as regional stereo imaging. The gimbal slew rate is specifically designed to be able to perform very high-resolution stereo imaging from as close as 50-km altitude during high-speed (~4.5 m/s) flybys. These observations will generate digital topographic models (DTMs) with 2-m spatial scale and 0.25-m vertical precision over the 2-km swath.

The NAC will also perform high-phase-angle observations to search for potential plumes; a pixel scale of 10 km from 1E6 km range means that the NAC can take advantage of good illumination geometry for forward scattering by potential plumes even when the spacecraft is distant from Europa.

EIS Wide-angle Camera (WAC): The WAC, derived from *MESSENGER* MDIS [8] heritage, has a 48° cross-track x 24° along-track FOV, with a 218-µrad IFOV. The along-track FOV is designed provide sufficient convergence angle to acquire pushbroom stereo swaths along flyby ground-tracks (Fig. 3). From 50-km altitude, the WAC achieves 11-m pixel scale over a 44-km-wide swath, generating DTMs with 32-m spatial scale and 4-m vertical precision. These data also support characterization of surface clutter for interpretation of radar deep and shallow sounding modes.

Detectors and electronics: The cameras have identical radiation-hard 4k x 2k CMOS detectors [9] which function in both pushbroom and framing modes and have rapid readout for imaging during fast flybys and to minimize radiation-induced noise. Color observations are acquired by pushbroom imaging with six broadband filters on a substrate in front of the detector.

APL's radiation-hardened data processing unit (DPU) uses innovative real-time processing for pushbroom imaging [10], including WAC 3-line stereo, digital time delay integration (TDI) to enhance signal-to-noise ratio (SNR), and collecting data to measure and correct pointing jitter [11], taking full advantage of the rapid, random-access readout of the CMOS arrays. The cameras have identical DPUs, which are cross-strapped for redundancy.

Summary: EIS will provide comprehensive data sets essential to fulfilling the goal of exploring Europa to investigate its habitability and will perform collaborative science with other investigations, including cartographic and geologic mapping, regional and high-resolution digital topography, GIS products, color and photometric data products, a database of plume-search observations, and a geodetic control network tied to radar altimetry [5].

References: [1] Pappalardo R. T. *et al.* (2015) *AGU Fall Meeting*, Abstract #P13E-01. [2] Pappalardo R. T. *et al.* (2015) *LPSC* **46**, Abstract #2673. [3] Schmidt B. E. *et al.* (2015) *Nature* **479**, 502-505. [4] Roth L. *et al.* (2014) *Science* **343**, 171-174. [5] Moussessian A. *et al.* (2015) *AGU Fall Meeting*, Abstract #P13E-05. [6] Pappalardo R. T. *et al.* (2013) *Astrobiology* **13**, 740-773. [7] Cheng A.F. et al. (2008) Space Sci. Rev. 140, 189-215. [8] Hawkins S.E. et al. (2007) Space Sci. Rev. 131, 247-338. [9] Janesick J. *et al.* (2014) *Proc. SPIE* **9211**, 921106. [10] McEwen A.S. et al. (2012) Intl. Wkshp. Instr. Planet. 1, 1041. [11] Mattson S.M. et al. (2009) EPSC 4, 604-1.

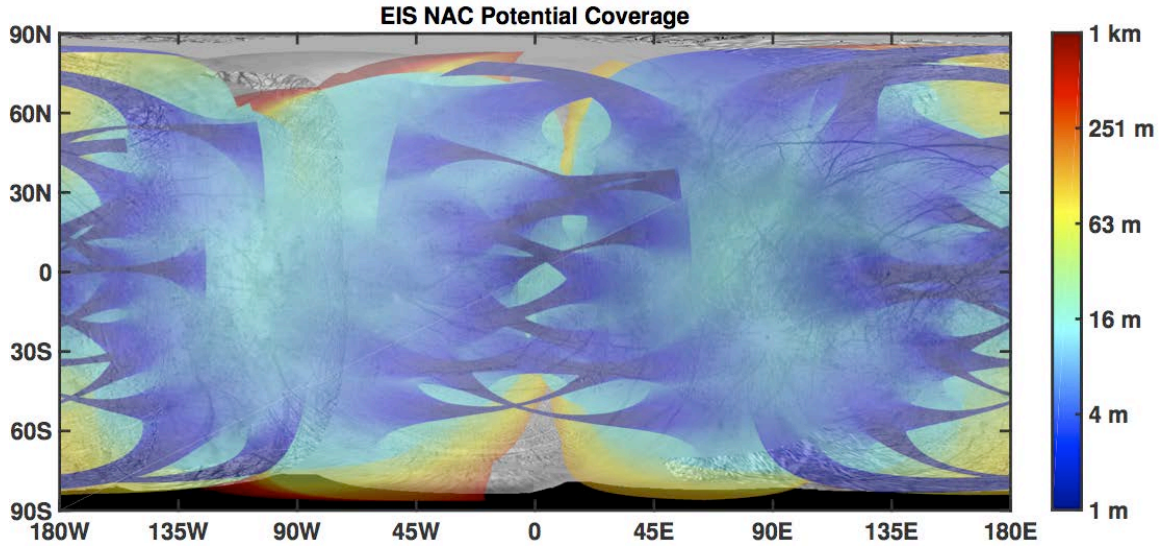

Figure 2. Areas of Europa's surface accessible for imaging by EIS NAC using the 2-axis ±30° gimbal. The NAC can image a swath 2.3° wide (2-km wide, with 0.5-m pixel scale from 50-km altitude), up to 30° from the nadir ground-track. In this way, mapping of >95% of Europa at ≤50 m/pixel is possible (with data volume being the limiting factor). Imaging coverage is color-coded by pixel scale and shown for a potential mission trajectory (15F10) when the spacecraft altitude is below 1000 km.

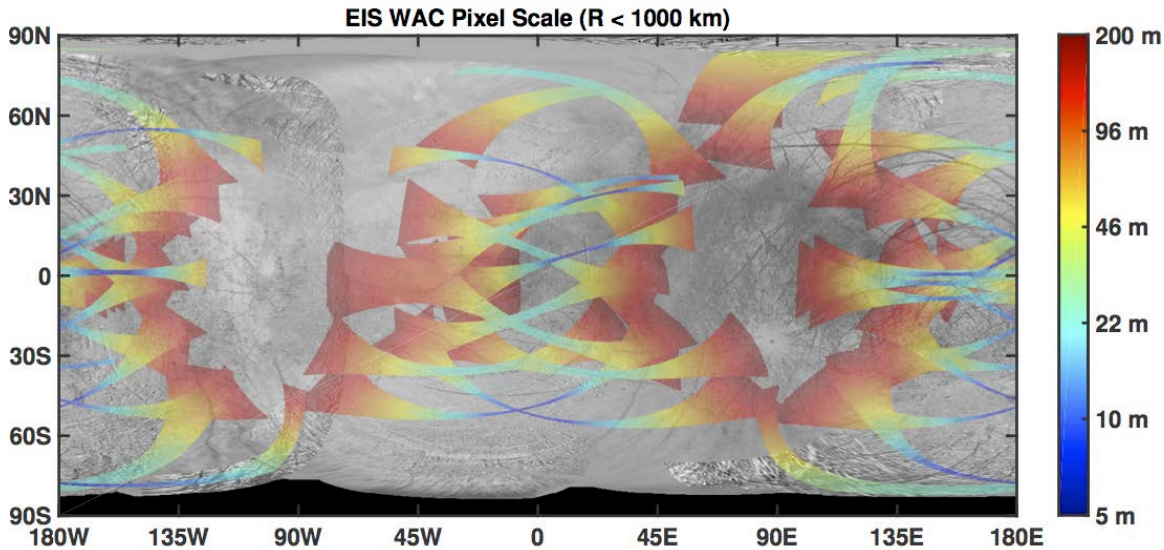

Figure 3. EIS WAC imaging coverage includes 3-line stereo and 6-color imaging, color-coded by pixel scale. The WAC images a swath 48° wide (45-km wide, with 11-m pixel scale from 50-km altitude). Imaging coverage is color-coded by pixel scale and shown for a potential mission trajectory (15F10) when the spacecraft altitude is below 1000 km.

ORGANIC DETECTION IN OCEAN WORLD ANALOGS WITH A TWO-STEP LASER DESORPTION/IONIZATION TIME-OF-FLIGHT MASS SPECTROMETER. K. Uckert[1], S. Getty[2], A. Grubisic[3], X. Li[4], A. W. Yu[2], M. E. Fahey[2], W. B. Brinckerhoff[2], S. X. Li[2], T. Cornish[5], B. Farcy[4], J. E. Elsila[2], [1]New Mexico State University (Department of Astronomy, Las Cruces, New Mexico 88003; kuckert@astronomy.nmsu.edu), [2]NASA Goddard Space Flight Center (8800 Greenbelt Road, Mailstop 699, Greenbelt, MD 20771), [3]University of Maryland (Department of Astronomy, College Park, MD 20742), [4]University of Maryland, Baltimore County (Baltimore, MD 21250), [5]C & E Research, Inc. (Columbia, MD 21045).

Introduction: The detection of organics on other planetary surfaces provides insight into the chemical and geological evolution of a Solar System body of interest and can inform our understanding of its potential habitability. In this study, we explore the analytical advantages offered by a prototype two-step laser desorption/ionization time-of-flight mass spectrometer (L2MS) by exploiting the resonance-enhanced desorption of analyte. We demonstrate the ability of the L2MS to detect hydrocarbons in organically-doped analog minerals, including cryogenic Ocean World-relevant ices and mixtures.

Methods & Instrumentation: L2MS is compatible with a future *in situ* science payload, and operates by generating a neutral plume of desorbed analyte with an IR desorption laser pulse, followed at a delay by an UV laser pulse, ionizing the plume. Desorption of analyte, including trace organic species, may be enhanced by selecting the wavelength of the IR desorption laser to coincide with IR absorption features associated with vibration transitions of minerals or organic functional groups. For the results presented here, we employ a breadboard mid-infrared (MIR) desorption laser (3.457 μm) with a discrete wavelength, selected to overlap the C-H stretch vibrational transition of certain aromatic hydrocarbons. Additional selectivity to aromatic species is provided by the 266 nm UV ionization laser pulse via the UV resonance-enhanced multiphoton ionization effects [1]. The use of distinct laser wavelengths allows efficient coupling to the vibrational and electronic spectra of the analyte in independent desorption and ionization steps, mitigating excess energy that can lead to fragmentation during the ionization process and leading to selectivity that can aid in data interpretation.

In single-laser positive-ion laser desorption/ionization mass spectrometry (LDMS), salts frequently overwhelm the mass spectrum; in contrast, L2MS is insensitive to salt and other dominant inorganic cations and targets certain high-priority classes of organic molecules, such as polycyclic aromatic hydrocarbons, organic acids, amino acids, and nucleobases [2,3] in complex mixtures. A detailed description of the development, specifications, and sensitivity of this instrument has been reported previously [2,3,4].

To measure samples at cryogenic temperatures relevant to Ocean Worlds, such as Europa and Enceladus, we recently integrated a cooled sample stage into our L2MS testbed (Figure 2). A liquid nitrogen cooling loop is in thermal contact with the sample probe to provide

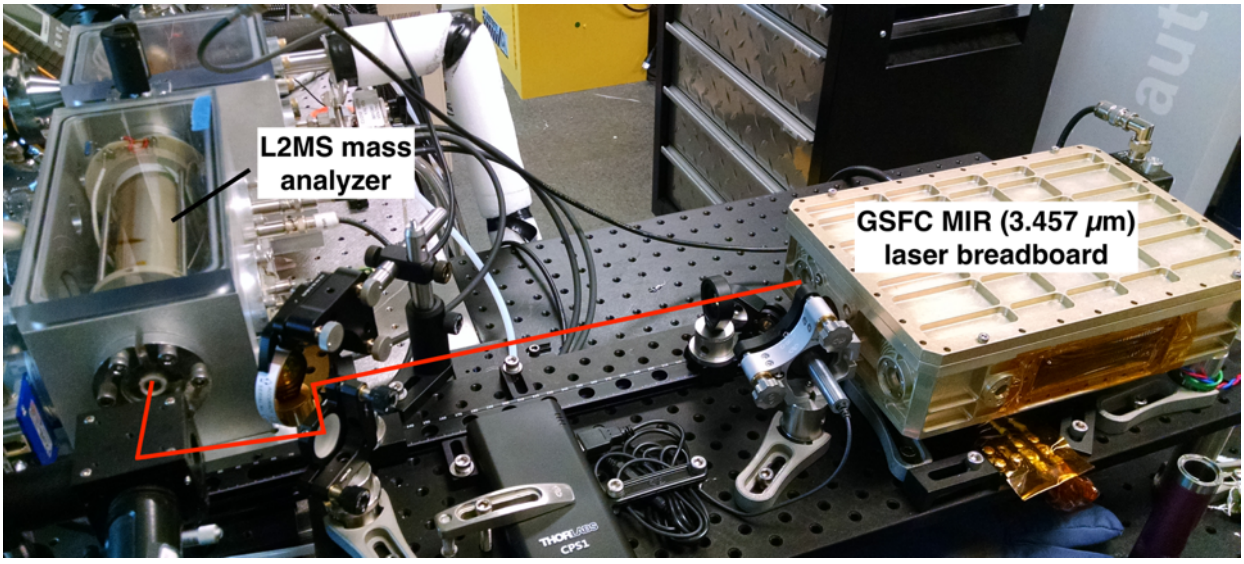

Figure 1: A photograph of the breadboard MIR laser (laser path in red) and the L2MS mass analyzer.

temperatures sufficiently low as to mitigate sublimation of water ice mixtures under high vacuum conditions.

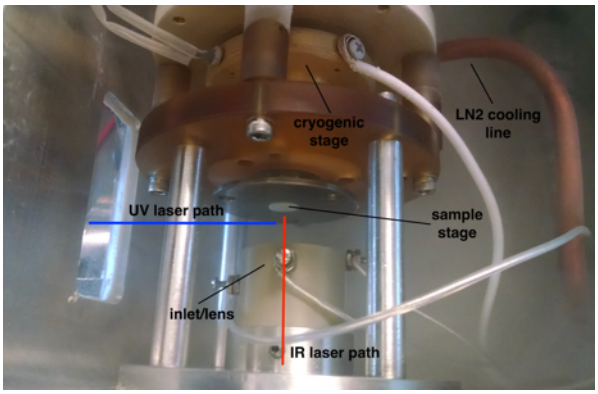

Figure 2: A photograph of the cold sample stage, including the orientation of the orthogonal IR (red) and UV (blue) laser paths relative to the sample.

Results: A mass spectrum of caffeic acid encapsulated by a thin layer of water ice is presented in Figure 3, and clearly shows the caffeic acid parent peak (*m/z* 180 Da). With excess ionization laser energy, minor diagnostic fragments are revealed to corroborate structural assignment of the base peak (*m/z* 163 Da: M-OH; *m/z* 136 Da: M-2•OH).

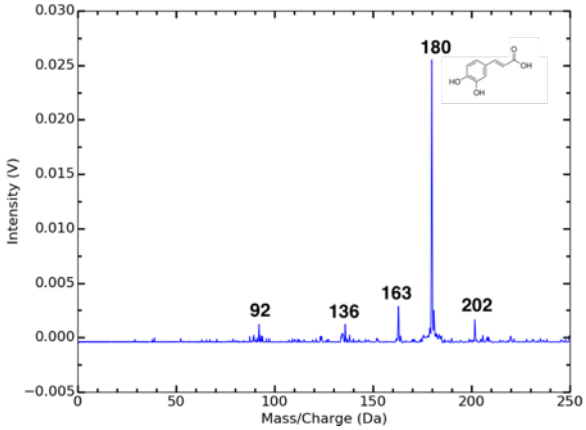

Figure 3: A mass spectrum of caffeic acid coated with water ice, measured at cryogenic temperatures.

We investigated the limit of detection of the L2MS by measuring caffeic acid ($C_9H_8O_4$) (Sigma Aldrich Co.) mixed with epsomite ($MgSO_4•7H_2O$) (Sigma Aldrich Co.) at several concentrations. Epsomite has been identified spectrally on Europa's surface [4], and may be sourced from the subsurface ocean [5], making it a relevant Europa analog salt for our laboratory studies.

Samples were prepared by adding a solution of caffeic acid dissolved in ethanol to epsomite powdered to a <150 µm grain size. We measured a quantity of the organic solution to achieve a 10,000 ppm (1 wt%), 1,000 ppm (0.1 wt%), and 100 ppm (0.01%) concentration series of caffeic acid in mineral concentration. The powdered mixture was dried, pressed onto a stainless steel stub, and mounted onto the sample probe.

The mass spectra of the caffeic acid epsomite mixtures are presented in Figure 4, showing the caffeic acid parent peak (*m/z* 180 Da) and common ionization fragments. An internal calibration standard, pyrene (*m/z* 202 Da) is also present in the spectrum. The limit of detection of caffeic acid embedded in a mineral matrix of the L2MS is approximately 20 ppm (assuming threshold signal-to-noise ratio > 10 is necessary for a detection) or better. Similar quantification of limits of detection will be pursued for a suite of organic analog compound classes in future work.

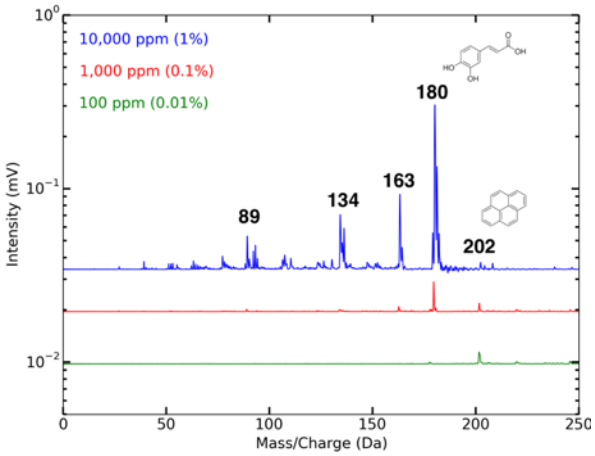

Figure 4: Mass spectra of caffeic acid in epsomite at various concentrations (1%, 0.1%, 0.01%).

Conclusions: We explore the resonance-enhanced detection of analyte on Ocean World analog samples with a two-step laser mass spectrometer to demonstrate the value of this technique in the *in situ* detection and characterization of the organic and molecular biosignature inventory on other planetary surfaces. L2MS has the potential to preserve high-molecular weight biosignatures against excessive fragmentation, and offers an analytical mode with selectivity to certain high-priority classes of organics that may be otherwise obscured in a complex mass spectrum.

References: [1] Han J. H., et al. (1988) *Science* 239(4847):1523 – 1525 [2] Getty S. A. et al. (2014) *Aerosp. Conf. Proc.*, 1 – 6. [3] Getty S. A. et al. (2013) *LPS XLIV*, Abstract #1719. [4] Getty S. A. et al. (2014) *International Workshop on Instrumentation for Planetary Missions*. [4] McCord T. B. et al. (2001) *JGR*, 106, 3311–3319. [5] Dalton III J. B. et al. (2012) *JGR: Planets,* 117:E3.

Acknowledgements: This work was supported by a NASA Space Technology Research Fellowship (NNX13AL49H) and grants from NASA's PIDD and EPSCOR (NNX08AV85) programs.

SEIS EXPERIMENT FOR THE INSIGHT MISSION: TOWARDS 2018 LAUNCH

N. Verdier[1], P. Lognonné[2], W. B. Banerdt[3], S. DeRaucourt[2], F. Ijpelaan[1], L. Kerjean[1], G. Pont[1], A. Sylvestre-Baron[1], P. Laudet[1], P. Bousquet[1], T. Hoffman[3], J. Umland, B[3]. Bone[3], K. Hurst[3], D. Giardini[5], P. Zweifel[5], C. Bramanti[9], W. T. Pike[6], S. Calcutt[7], D. Mimoun[4], M. Bierwirth[8], U. Christensen[8] and the SEIS team

[1]CNES, Toulouse, France, (philippe.laudet@cnes.fr), [2]Département de Géophysique Spatiale et planétaire, IPGP, Paris, France (lognonne@ipgp.fr), [3]Jet Propulsion Laboratory, Pasadena, California, USA, (william.b.banerdt@jpl.nasa.gov), [4]Institut Supérieur de l'Aéronautique et de l'Espace Name, Toulouse, France, [5]ETH, Zürich, Switzerland, [6]Imperial College, London, UK, [7]Oxford University, Oxford, UK, [8]MPS, Gottingen, Germany, [9]ESA/Prodex Noordwijk, NL

Introduction: The InSight NASA Discovery mission will provide unprecedented data on Mars' deep interior structure and more generally on the mechanisms that shaped telluric planets in our solar system. The French contribution to InSight, the SEIS seismometer, will perform essential measurements of Mars' tectonic activity that will enable us to characterize the nature and size of its core and the thickness of its crust.

After giving an outline of the InSight mission, with a focus on SEIS activities on Mars, we will describe the SEIS instrument and its performances, and provide a status of its development at the time of the workshop.

Insight mission [1]: Insight is led by the Jet Propulsion Laboratory. It will deploy at the surface of Mars on November 26th, 2018 a set of seismometers called SEIS (Seismic Experiment for Interior Structure), and a suite of complementary instruments, such as a precision temperature sensor, a micro-barometer, a magnetometer and a wind sensor, making it the first broadband seismic broadband station on another planet. A heat flow sensor and geodetic measurements, HP^3, will provide additional science measurements, in order to constrain the internal structure of Mars.

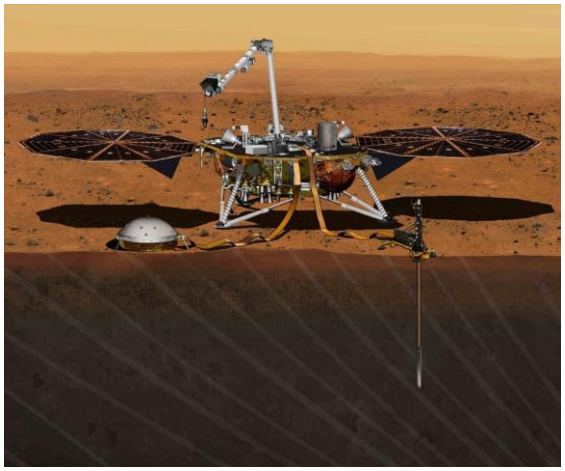

Figure 1 : Insight's lander on the surface of Mars, with SEIS on the left and HP^3 on the right

The INSIGHT lander reuses extensively the cruise bus and the Entry-Descent and Landing System of PHOENIX, which performed a successful mission on Mars Northern terrains in 2008.

SEIS instrument [2]: SEIS is provided by CNES, the French Space Agency, which manages a wide consortium including IPGP of Paris, Imperial College of London, Oxford University, MPS of Gottingen, ETH of Zürich, ISAE from Toulouse and the Jet Propulsion Laboratory of Pasadena.

SEIS accommodates two independent, 3 axis seismometers: an ultra-sensitive Very Broad Band (VBB) oblique seismometer and a miniature, Short Period (SP) seismometer. Both seismometers, and their respective signal preamplifier stages, are mounted on a common structure which can be precisely leveled through 3 legs with adjustable legs. They are thermally insulated, and protected from the Martian wind, by an aerogel thermal blanket and WTS (wind shield) and connected by a flexible cable tether to the E-box, a set of electronic cards located inside the Lander thermal enclosure.

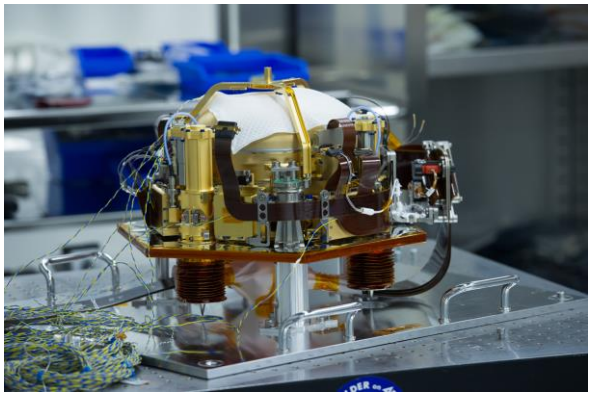

Figure 2 : SEIS flight model in 2015 during environmental test

Several challenges have been overcome to design and realize the planetary seismometer, which exhibits a self-noise of about 10-9 m/s2/sqrt(Hz) in the seismic

bandwidth for its very broadband component. These challenges implied a very complex hardware, both from a mechanical point of view and from an electronic point of view. In particular, keeping the VBBs in vacuum is essential in order to achieve the noise target.

Insight was originally planned for a launch in March 2016. Accordingly, in August 2015, the SEIS Flight Model was fully functional. Unfortunately, it was affected during thermal qualification testing by a leak in the evacuated container that keeps its three seismometers in a vacuum. This led to a loss of performance that was soon judged unacceptable by both the InSight and SEIS Principal Investigators. A joint JPL-CNES Tiger Team worked very hard during the fall of 2015 to locate and fix that leak, but the schedule pressure the team to opt for a repair of the existing Flight Model, which limited the range of solutions. This could however not be achieved in time, and the launch had to be postponed to the next Mars window, in May 2018. In that new time frame, some redesign of the evacuated container has taken place after the root cause of the leak has been identified in one of the feed through electrical connectors. The 2nd phase of SEIS development plan with this new evacuated container will be presented at the workshop.

References :

[1] W. B. Banerdt et al, "INSIGHT: a Discovery mission to explore the interior of Mars", 44th Lunar and Planetary Science Conference (2013)

[2] Ph. Laudet et al, "The SEIS Experiment for the Insight Mission: Development and management plan", EPSC2015-726, 201

INSTRUMENT SCIENCE AUTONOMY FOR ORBITAL AND FLYBY PLANETARY MISSIONS. K.L. Wagstaff, A. Altinok, B. Bue, S.A. Chien, and L. Mandrake, Jet Propulsion Laboratory, California Institute of Technology, (4800 Oak Grove Drive, Pasadena, CA 91109, kiri.wagstaff@jpl.nasa.gov).

Introduction: Spacecraft instruments today can do more than passively collect and transmit data. Onboard data analysis and autonomous response enable the capture of dynamic or short-lived events as well as increasing overall mission science return. These capabilities have been developed and demonstrated for a variety of spacecraft. This abstract describes capabilities for orbital and flyby missions; autonomous science for surface missions is described in [1].

Orbital or flyby planetary missions may operate at great distances from the Earth. Communications are limited by the speed of light as well as the fact that the Deep Space Network is a resource that is shared by all active planetary missions. Onboard data analysis can enable instruments to exploit gaps between communication opportunities and make better use of available downlink volume by identifying features of interest to inform data prioritization, generating compressed data summaries, or filtering out poor quality data. Instruments can also automatically collect additional observations or alert other instruments to an event of interest (cross-instrument coordination). Next we describe examples of current instrument science autonomy capabilities and how they could apply to future instruments.

Surface feature detection: To detect known features of interest, we can train a machine learning classifier with labeled examples and then deploy it to analyze new data as it is collected. For example, we trained a classifier to detect tiny sulfur deposits on top of arctic glaciers as a proxy for the kind of microbial biosignatures that could potentially manifest on Europa [2]. The classifier operates on data collected by Hyperion, a pushbroom hyperspectral imager on the EO-1 Earth orbiter. The study region (Borup Fiord) is considered one of the best Europa analog sites on Earth. We used the trained classifier on EO-1 to monitor the seasonal appearance and disappearance of sulfur deposits from orbit [3] (see Fig. 1).

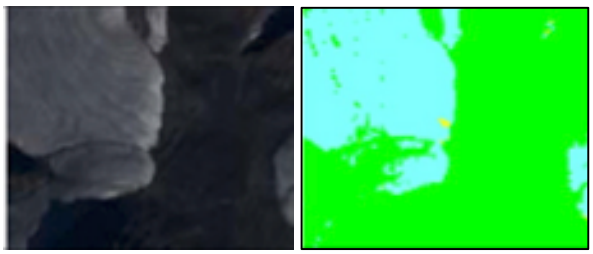

Fig. 1. Supraglacial sulfur deposits (marked in yellow) detected by a classifier onboard the EO-1 Earth orbiter [3].

We also devised a statistical method that can detect and track the seasonal CO_2 and water ice caps on Mars using THEMIS infra-red images collected by the Mars Odyssey orbiter [4]. This method separates image regions into CO_2 ice, water ice, and defrosted terrain. It could potentially be used by thermal imagers studying icy bodies such as Europa, Ganymede, and Enceladus to characterize ice composition and potentially identify slightly warmer regions where the ice crust has thinned. These areas are of great astrobiological interest.

Detection of dynamic or short-lived events: Onboard analysis of instrument data is perhaps best motivated when the goal is to detect dynamic or short-lived events, such as plumes from Enceladus or Europa. We developed an algorithm to detect and track emissions from moons or irregularly shaped bodies (asteroids, comets) in real-time to enable fast follow-up and characterization [5]. The algorithm uses a convex hull model to distinguish the body under observation from any emitted material. We tested this approach on 756 Cassini ISS-NAC images of Enceladus, in which it detected 49 real plumes and 22 false positives. Most of the false positives (77%) came from poor quality or non-limb images which should be filtered out prior to this analysis. We also applied plume detection to 45 EPOXI MRI images of comet Hartley 2, which has an irregular shape and multiple active jets. The largest jet was correctly identified and localized in every image. Example results are shown in Fig. 2.

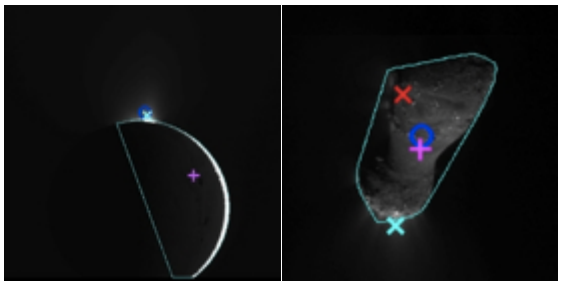

Fig. 2. Automated plume detection (cyan x) for Enceladus (left) and comet Hartley 2 (right) [5]. Other markers are for competing methods that did not perform as well.

Data quality filtering: Assessing data content prior to its transmission to Earth can also yield operational benefits by filtering out low-quality data and thereby reducing the volume of data to be transmitted. The IPEX Earth orbiting CubeSat used a trained classifier to determine cloud cover so that images in which the surface is

visible receive higher priority [6]. An example result from its onboard deployment is shown in Fig. 3.

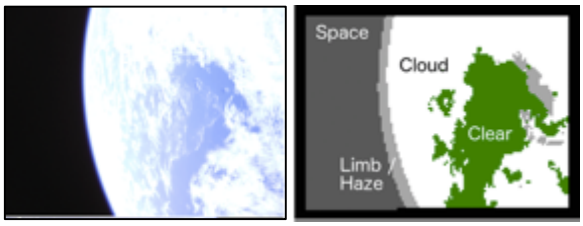

Fig. 3. Onboard classification of IPEX CubeSat Earth image regions into space, limb, cloud, and clear to prioritize cloud-free images. [6]

IPEX had only low-resolution commercial cameras onboard. We have re-trained the cloud classifier to operate on high-resolution (30 m/pixel) Hyperion data, and we are currently in the process of uploading this algorithm to the EO-1 Earth orbiter. Imaging instruments on a Titan balloon could employ the same technology to prioritize images that capture surface features over those that are obscured by haze.

Novelty detection: Training a machine learning algorithm to detect relevant surface or atmospheric features requires advance knowledge and several examples of the feature of interest. However, planetary missions aim to explore and characterize bodies for which our knowledge in incomplete. They may discover new phenomena or processes that manifest in ways we cannot predict in advance. The ability to detect novel or unexpected features is especially relevant to the search for life. We previously developed a novelty detector for imaging instruments that calculates the visual *salience* of each region within an image. Onboard IPEX, it identified three small lakes in Tibet despite no prior training or guidance about bodies of water [7]. Hydrocarbon lakes on Titan could be detected in a similar fashion. We are uploading this algorithm to EO-1 as well.

Monitoring: Some science objectives focus not on particular features but instead on continuous monitoring of an atmospheric or environmental property. One example is the aerosol opacity of the Mars atmosphere. We devised a regression algorithm to estimate the dust and water ice content of the atmosphere from THEMIS data [8]. Like most imaging instruments, THEMIS is able to collect more data than it can downlink. By running this algorithm onboard Mars Odyssey, we would obtain much greater temporal and spatial coverage of the Mars atmosphere instead of being restricted to only those frames transmitted to Earth. We also envisioned operational scenarios in which a high opacity detection (potentially indicating the formation of a dust storm or the presence of a water ice cloud) would trigger the transmission of a subset of the full THEMIS data centered on that location. The opacity estimation algorithm predicted ice opacity with an RMSE of 0.016, well within the uncertainty in the reference model (0.040). Dust opacity (see Fig. 4) was more challenging (RMSE 0.087) because atmospheric dust can be easily confused with surface dust, but it was sufficiently reliable to detect potential dust storms. Similar atmospheric monitoring would be valuable for a Titan orbiter.

Lessons learned and recommendations for future instruments: Future instrument development will benefit most from autonomous science by integrating it into the initial instrument design and test plans to ensure that relevant science objectives are addressed and resource constraints (memory, computation, response time) are met. It is also vital to characterize the impact of operating on uncalibrated data and identify any necessary adjustments (e.g., we employed an empirical calibration for THEMIS data to compensate for temperature drift of the focal plane array that corrected ice temperature measurements by about 15 K [4]).

References: [1] Francis R. et al. (2016) *3rd Workshop on Inst. for Planet. Miss.* (this meeting). [2] Mandrake, L. et al. (2012) *ACM TIST 3*, A77. [3] Gleeson, D.F. et al. (2010) *Remote Sens. Env. 114*, 1297-1311. [4] Wagstaff, K.L. et al. (2008) *Planet. & Space Sci. 56*, 256-265. [5] Wagstaff, K.L. et al. (2014) *ApJ 794*. [6] Altinok, A. et al. (2016) *J. of Field Robotics, 33*, 187-204. [7] Chien, S. et al. (2016) *J. of Aero. Inf. Sys.* [8] Castaño, R. et al. (2007) *13th KDD*.

This work was carried out at the Jet Propulsion Laboratory, California Institute of Technology, under a contract with NASA.

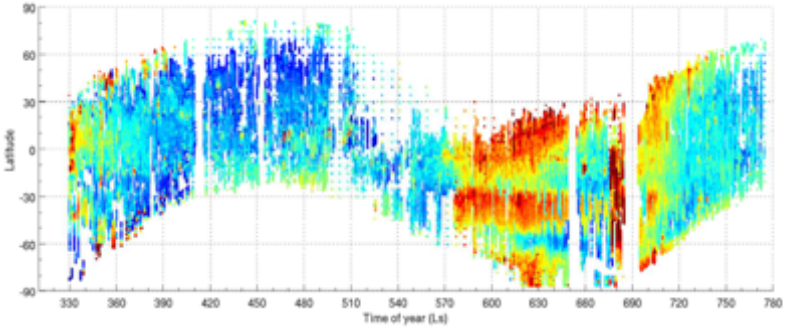

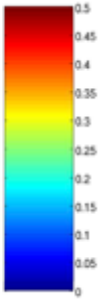

Fig. 4. Estimation of atmospheric dust opacity from Mars Odyssey THEMIS data as a function of time of year (Ls) and latitude [8]. Regional dust storms appear from Ls 580-650.

TWO HIGH PERFORMANCE *In Situ* RAMAN SPECTROMETERS FOR LANDED PLANETARY MISSIONS. Alian Wang[1], James Lambert[2], Ian Hutchinson[3], Steve Monacos[2], Melissa McHugh[3], J. Wei[1], Y.C. Yan[1]. [1]Dept. Earth and Planetary Sciences and McDonnell Center for Space Sciences, Washington University in St. Louis, [2]Jet Propulsion Laboratory, [3]University of Leicester, UK (alianw@levee.wustl.edu).

Fig.1 MMRS on Zoe rover in Atacama (TRL5)

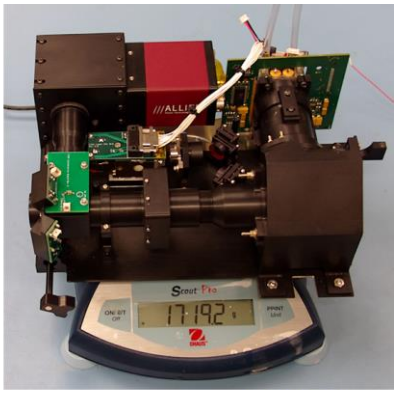

Fig. 2. CIRS prototype (to TRL6)

Supported by PIDDP. MIDP, ASTEP, and recently by MatISSE program, we have accomplished the design, building, and testing two high performance i*n situ* Raman spectrometers: the Mars Microbeam Raman Spectrometer (MMRS) and the Compact Integrated Raman Spectrometer (CIRS).

MMRS (**Fig. 1**) has a separate Raman probe connected through optical fiber to Raman spectrometer [1-3]. MMRS was tested during three field seasons (2012-2015) in Atacama Desert, twice on Zoe rover (> 50 km traverse each time) and once stand-alone. These field studies demonstrated a solid science performance and robust engineering of MMRS (TRL 5). A new paper was published in 2015[4].

CIRS (Fig. 2) was developed on the basis of mature MMRS technology but having an all-optics-in-one architecture (i.e., without optical fiber). The development of CIRS was supported by MatISSE program, with a goal to reach TRL 6 [5, 6]. Currently, a prototype of CIRS was built and tested. We will report here the results from a set of performance tests accomplished in August 2016.

MISSIONS: Both MMRS & CIRS are suitable for *definitive molecular identification* during landed planetary missions. The detailed requirements of a specific mission will determine the selection among the two.

A few common features of MMRS & CIRS are:

(1) both have wide spectral range and necessary spectral resolution to achieve the goal of comprehensive molecular ID;

(2) both are highly sensitive, capable of obtaining a spectrum from a solid sample within <1s to 1min;

(3). both allow the laser excitation and Raman photon collection through an optically transparent window (fused silica or sapphire), thus supporting simple deployments on a Venus lander or on an ISRU platform of a lunar mission, in addition to the direct arm-deployment by a rover on Mars.

CIRS performance

The Raman spectral range of CIRS is 4432 - 183 cm^{-1}, with a spectral resolution ~ 9 cm^{-1}.

CIRS has a context imager, illuminated by a set of UV LED (275 nm) and blue LED (467 nm). It has a Field of View (FOV) ~ 37x26 mm and a chip format of 1600x1200 pixels. The laser spot and the context image of the sample are seen in the same image.

A recent test revealed that CIRS laser beam diameter at focus is 35.7 µm. It has a slow-growing beam profile, that only double its diameter at ± 4.5 mm from the focus, **Fig. 3.** With this beam profile, the measured *Raman sampling depth* (i.e., the off-focus Raman measurement with recognizable peaks) is > 9.375 mm from a quartz at 8s integration, and ~ 3.125 mm from a dark pyroxene at 64s integration (**Fig. 4**).

Figure 3. CIRS laser beam profile near focus

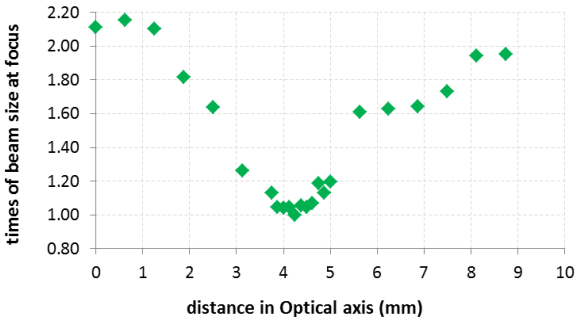

The small diameter of laser beam is designed to detect minor and trace species in a geological sample (rock or soil). The slow-growing beam profile is designed to tolerant the surface roughness of an unprepared geological sample during a robotic exploration.

The optical throughput of CIRS is about 90% in excitation path and about 20% in collection path. It enables the mineral spectrum with good S/N to be obtained in less than 1s for strong Raman scatterers, or

maximum near 1 min for weak Raman scatterers, **Figure 5.** Reduced carbon in chert with TOC@8x10^{-4} was detected by CIRS from a 4s integration.

Through a study of nearly 30 extraterrestrial samples (lunar, martian, and other meteorites) using fluorescence microscopy and Raman spectroscopy [7, 8] we have demonstrated that fluorescence emission from these materials are low-to-non-existence. Thus, fluorescence is not a threat to planetary Raman spectroscopy using CW 532 nm excitation. For its occasional occurrence, our solution is to conduct SERDS (Shifted Excitation Raman Differentiate Spectroscopy) without changing any hardware in CIRS [8].

The realization of SERDS in CIRS is by adjusting the excitation wavelength of its CW laser source. We have found a 15 cm^{-1} shift can be produced by 12°C temperature adjustment of the frequency-doubling crystal of the CIRS laser unit, as shown in **Fig 6.** This shift is enough to distinguish Raman peak from fluorescence signals, **Fig. 7.**

Comparison with other Raman architectures: Comparing with *a remote-Raman architecture*, an *in situ* Raman has:

(1) A capability of detect minor and trace species, due to the small sampling spot (20-30 μm vs. 500-1000 μm);

(2) A much higher (10^2 to 10^4 times) Raman signal collectivity, using a f/2 optics vs. f/20 to f/100 optics;

(3) A lower risk of sample damage (cw laser vs. pulse laser).

Comparing with *a pulse UV- Raman architecture*, the CW green Raman has:

(1) > two orders of magnitude stronger Raman signal on minerals [5], and on reduced carbon and biomarkers [9, 10];

(2). A lower risk for sample damage.

In the aspect of engineering, MMRS & CIRS use ordinary CCD, optics and filters for visible light, and a mature compact CW 532nm laser. They have higher TRL (in both component levels and in system level) than other Raman architectures.

Acknowledgement: USA NASA MatISSE NNX13AM22G; UK Space Agency CREST 2 grant: ST/L005581/1.

References: [1] Wang et al., 1995, JGR, 100, 21189-21199; [2] Wang et al., 1998, Appl. Spec, 52, 477-487; [3] Wang et al., 2003, JGR, doi:10.1029/2002JE001902; [4] Wei et al., 2015, J. Raman Spec., v10,, DOI: 10.1002/jrs.4656; [5] Wang et al., 2014, abs. 1090, 2nd IPM; [6] Lambert et al., 2014, abs 1136, 2nd IPM; [7] Wei et al., 2014, abs 1112, 2nd IPM; [8] Yan et al., 2016, abs2210, 47th LPSc; [9] Wei et al., 2014 LPSC, abs # 2847. [10] Beegle et al., 2014, LPSC, abs# 2835.

Figure 4. Test of *Raman Sampling depth* (raw spectra)

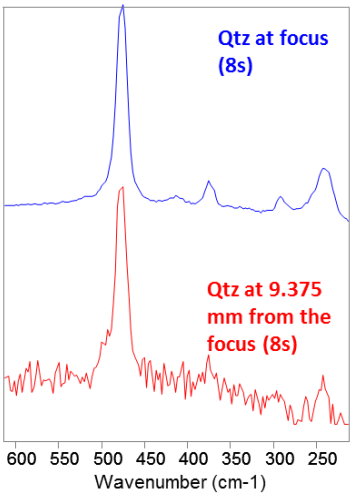

Figure 5. Raw CIRS spectra of strong and weak Raman scatterers

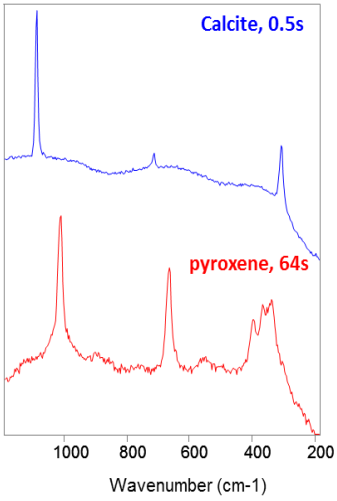

Figure 6. Laser wavelength shift as *f(T)*

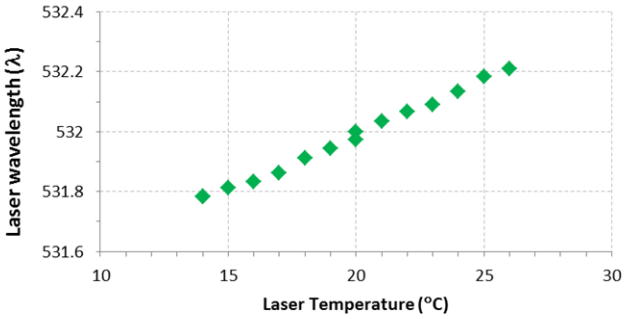

Figure7. To distinguish Raman peak of apatite from REE fluorescence using SERDS

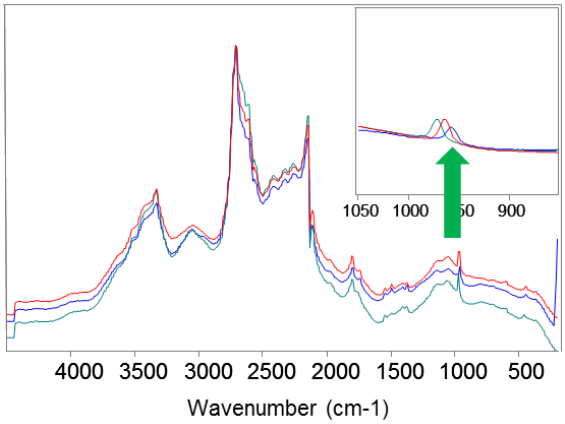

TUNABLE LASER SPECTROMETERS FOR PLANETARY SCIENCE. C. R. Webster[1], G. J. Flesch[1], S. Forouhar[1], L. E. Christensen[1], R. Briggs[1], D. Keymeulen[1], J. Blacksberg[1], E. Alerstam[1], and P. R. Mahaffy[2], [1]Jet Propulsion Laboratory, California Institute of Technology, 4800 Oak Grove Drive, Pasadena, CA 91109; Chris.R.Webster@jpl.nasa.gov [2]NASA Goddard Space Flight Center (GSFC), 8800 Greenbelt Rd., Greenbelt, Md., 20771. Paul.R.Mahaffy@nasa.gov

Introduction: Accompanying the development of lasers operating at room temperature, tunable laser spectrometer instruments have enjoyed a huge growth in capability for a wide range of applications in scientific research, medicine, industry, Earth and planetary space missions. Miniaturization has enabled the development of powerful new instruments for planetary missions to planets, satellites and primitive bodies and for the International Space Station (ISS) cabin monitoring.

The first atmospheric measurements were made in the 1980's [1] using the newly invented lead-salt tunable diode lasers that required liquid helium cooling and produced only a few microwatts of output power. The BLISS high-altitude balloon instrument weighed 1,500 kg and a single laser package (cryostat) weighed 70 kg. By the 1990's when liquid-nitrogen cooled lasers were available, several groups [2] from all over the world were flying tunable laser spectrometers on a wide variety of aircraft to understand Earth's ozone hole chemistry and dynamics. In the early 2000's with Quantum Cascade (QC) lasers available, the transition to room temperature operation began in earnest [3], so that by 2005 miniature laser spectrometers were being considered for planetary missions.

Today, room temperature QC, Interband Cascade (IC) and tunable diode lasers are available [4] over a large wavelength region, accessing molecules of interest to planetary science not just at the shorter near-IR wavelengths but also mid-IR wavelengths (Fig. 1) from HF (2.3 µm) to NH_3 (10 µm).

IR Tunable Laser Spectroscopy: Tunable laser spectrometers are uniquely suited to making high-precision gas abundance and stable isotope ratios because of their ability to scan at ultra-high resolution (0.0001 cm^{-1}) over targeted individual rovibrational spectral lines of the gas of interest without interferences that can be of concern with mass spectrometers.

For light molecules at pressures below ~100 mbar, IR tunable laser spectroscopy offers a direct, non-invasive, unambiguous method for measuring stable isotope ratios to sensitivities of ~1‰ for planetary low-mass (<3 kg), all-solid-state instruments. Tunable laser spectrometers are well suited to H_2O, NO, NO_2, HNO_3, O_3, CO, CO_2, NH_3, SO_2, HCl, N_2O and CH_4.

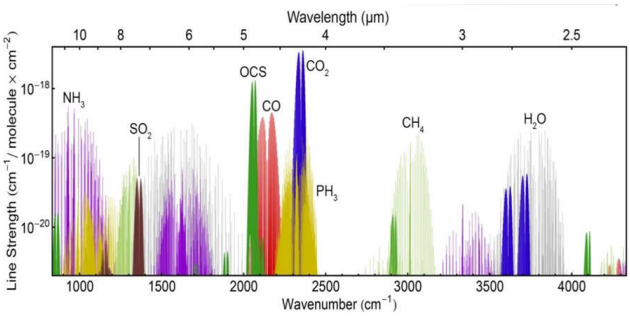

Fig. 1. IR bands of species of interest to planetary science, in particular for Venus, Saturn and Uranus.

Stable isotope ratios in C, H, N, O and S are powerful indicators of a wide variety of planetary geophysical processes that can identify origin, transport, temperature history, radiation exposure, atmospheric escape, environmental habitability and biology [5].

TLS in SAM on MSL's Curiosity Rover: The Tunable Laser Spectrometer (TLS) is one of three instruments that make up the Sample Analysis at Mars (SAM) suite [6] on the Curiosity rover.

During its' first three years in operation, TLS has determined the abundance of methane on Mars [7] and its variability at the Gale crater region, as will be updated during the workshop. In addition, both TLS and SAM's Quadrupole Mass Spectrometer (QMS) have measured atmospheric isotope ratios (see table with references [8, 9, 10, 11]) at unprecedented precision that in comparison with meteoritic data, tell a story of prolonged atmospheric escape that has been ongoing for nearly 4 billion years.

In addition to atmospheric measurements, TLS complements the SAM QMS in analyzing gases evolved from pyrolyzing rock samples acquired by Curiosity, at Rocknest [12], John Klein, and Cumberland sites. One important result [13] is measurement of the D/H in clays from Yellowknife bay. The low value of the measured D/H (~3 times SMOW) indicates that the mudstone was created significantly before much of the atmospheric escape occurred, and when Mars had a global equivalent layer of water of around 150 m.

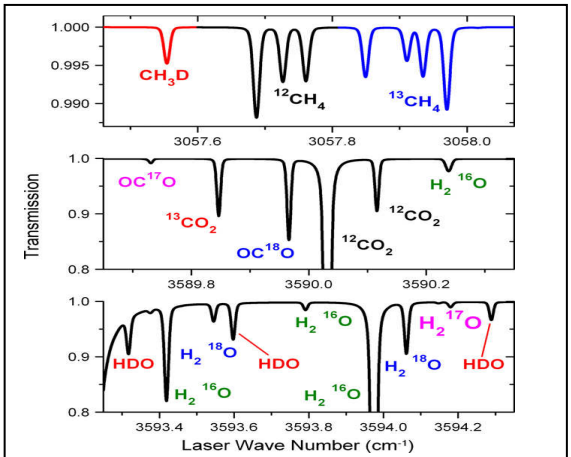

Fig. 2. Spectral scan regions used by MSL-SAM's TLS instrument for measuring isotope ratios in H, C, O. For the methane scan, the vertical axis for $^{13}CH_4$ and CH_3D is multiplied by 100, 500.

TLS for Venus, Saturn, Titan and Uranus Probes: In combination with the QMS, TLS is currently on strawman payloads for Discovery and New Frontiers missions that include atmospheric probes, for example for Venus, Saturn [14], Titan [15] and Uranus. In these applications in which a probe is descending very fast through the upper atmosphere, TLS will be upgraded with fast, agile digital electronics that drive several lasers simultaneously to maximize the data quality and return during these short but very important missions. Target gases include CO, OCS, H_2O, CO_2, SO_2, NH_3 and PH_3 (Fig. 1) and a variety of important isotope ratios. Requirements are typically 1-2% for D/H, and 2‰ for the triple isotopes in S.

TLS as a Combustion Monitor for ISS: In addition to developing TLS for future planetary missions, JPL is building a 5-channel TLS for the International Space Station (ISS) that will serve as a cabin monitor, providing detection of CO, HCN, HF, HCl, and CO_2 as an early warning system of possible fire hazards. For this application, NASA requires improved accuracy, response time and especially maintainability over existing electrochemical sensors.

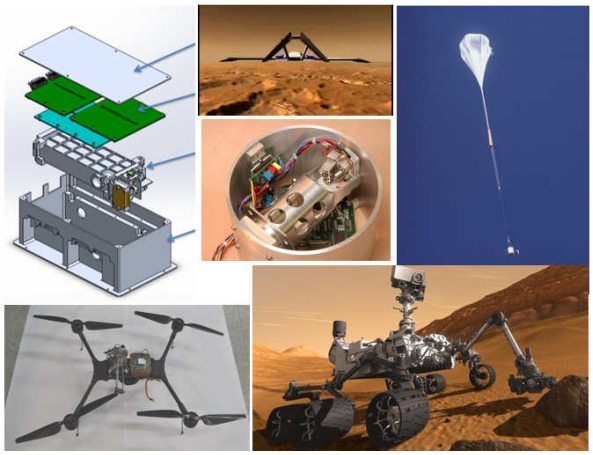

Fig. 3. Planetary tunable laser spectrometers in a variety of platforms: for CubeSats, Mars airplane, planetary probes, balloons, quadcopters and rovers.

We will review science results to date from TLS-SAM-MSL and also discuss laser spectrometers planned for future missions including the ExoMars lander.

References: [1] Webster C.R. and R.D. May, *J. Geophys. Res.* 92, 11931-11950 (1987). [2] Webster C.R. et al., *Science* 261, 1130-1134 (1993). [3] Webster C.R. et al., *Applied Optics*, 40, 321-326, 2001. [4] Forouhar S. et al., Appl. Phys. Lett. 105 051110 (2014) doi: 10.1063/1.4892655 [5] Criss R.E. (1999) *Principles of Stable Isotope Composition*, Oxford University Press, ISBN 0195117751; [6] P. R. Mahaffy, et al., *Space Science Rev.*170, 401 (2012). [7] C. R. Webster et al., *Science* 342, 355 (2013). [8] S. Atreya et al. [9] Mahaffy P.R. et al., doi: 10.1126/science.1237966, *Science* 341, 263 (2013) [10] Wong et al., Geophys. Res. Lett.; [11] C. R. Webster, et al., *Science* 341, 260 (2013). [12] L. Leshin et al., *Science* 341, (2013) DOI: 10.1126/Science 1238937. [13] P.R. Mahaffy et al., "The Deuterium to Hydrogen ratio in the Water that Formed the Yellowknife Bay Mudstones in Gale Crater", LPSC abstract 2014. [14] Mousis O. et al. IPPW 2013 Saturn poster [15] Webster C.R. et al., *Appl. Opt.* 29, 907-917, (1990).

Acknowledgments: Part of the research described here was carried out at the Jet Propulsion Laboratory, California Institute of Technology, under a contract with the National Aeronautics and Space Administration (NASA).

The Plasma Instrument for Magnetic Sounding (PIMS) for the Europa Mission. J. H. Westlake[1], R. L. McNutt[1], J. C. Kasper[2], A. W. Case[3], A. M. Rymer[1], M. L. Stevens[3], X. Jia[2], C. Paty[4], K. K. Khurana[5], M. G. Kivelson[5], J. A. Slavin[2], H. T. Smith[1], H. Korth[1], N. Krupp[6], E. Roussous[6], J. Saur[7] [1]Johns Hopkins University Applied Physics Laboratory, [2]University of Michigan, [3]Smithsonian Astrophysical Observatory, [4]Georgia Institute of Technology, [5]University of California, Los Angeles, [6]Max Planck Institute for Solar System Research, [7]University of Cologne.

Europa exists in a complicated plasma environment where the tilt of Jupiter's magnetic field and rapid rotation rate leads to a dynamic interaction with Europa's ionospheric plasma. While understanding this plasma interaction is interesting in its own right, it is crucial for successfully magnetically sounding Europa's subsurface ocean. In magnetic sounding, currents induced in Europa by the changing Jovian plasma produce a detectable secondary magnetic field that reflects properties of Europa's subsurface ocean such as depth and conductivity. This technique was successfully employed with Galileo observations of Europa to demonstrate that Europa indeed has a subsurface ocean containing more liquid water than Earth's oceans. While these Galileo observations contributed to the renewed interest in Europa, the results raised major questions that remain unanswered, in part due to the large uncertainties in the ice shell thickness, ocean depth, and ocean salinity due to limitations in the observations. Here we present the scientific goals of the Plasma Instrument for Magnetic Sounding (PIMS), one of the 9 instruments selected for the Europa Multiple Flyby Mission. We specifically address how PIMS plasma measurements will transform the accuracy of magnetic sounding of Europa's subsurface oceans. We also present synergistic science with other Europa instrumentation such as the ultraviolet spectrometer, mass spectrometer, and the radar.

SUPERCAM REMOTE SENSING ON THE MARS 2020 ROVER: SCIENCE GOALS AND OVERVIEW

R.C. Wiens[1], S. Maurice[2], F. Rull[3] and the SuperCam Team; [1]Los Alamos National Laboratory, Los Alamos, NM, USA, rwiens@lanl.gov; [2]IRAP, Observatoire Midi-Pyrénées, Toulouse, France; [3]U. Valladolid-CSIC, Valladolid, Spain

Introduction: The Mars 2020 Science Definition Team (SDT) Report [1] emphasized the importance of fine-scale measurements, suggesting that the numerous pin-point observations made at remote distances by ChemCam was a very desirable capability. However, the 2020 SDT made it clear that the new rover's remote sensing needed to have strong capabilities in mineralogy [1], which is covered only minimally on MSL via ChemCam's passive 0.4-0.85 µm [2] and Mastcam multispectral observations [3]. The SuperCam instrument suite that was selected for Mars 2020 provides five remote techniques: two for mineralogy, one for chemistry, one for morphology, and one acoustic. These techniques are, respectively, remote Raman spectroscopy, passive visible and infrared (VISIR) reflectance spectroscopy, laser-induced breakdown spectroscopy (LIBS), color remote micro-imaging (RMI), and a microphone. All of the optical spectroscopy techniques plus the imaging are co-bore sighted, fulfilling a desire stated by the SDT for multiple co-registered observations [1]. In this presentation we give an overview of the science objectives and the implementation. A separate presentation provides technical details of SuperCam's mast unit [4].

Science objectives:

1) *Rock Compositions*: Detailed mineral, chemical, textural, and acoustic characterization of rocks will help to determine the geological diversity of the site, to identify key processes relevant to its aqueous history, and to document the context of the sample cache.

2) *Sedimentary Stratigraphy*: Characterization of the texture, hardness, and composition of the sedimentary structures will provide strong constraints for the aqueous processes as well as its potential habitability.

3) *Organics and Biosignatures*: SuperCam will analyze astrobiologically relevant materials without requiring contact, determining the best area for contact science and caching, and will allow exclusive interrogation of areas inaccessible to the rover arm.

4) *Volatiles*: SuperCam will constrain the aqueous processes involving volatiles and provide data on volatile content for the documentation of cached material.

5) *Context Morphology and Texture*: High resolution color images will provide detailed information on dust covering and a visual approach to oxidation states of layers relevant for aqueous processes.

6) *Coatings and Varnishes*: Analyses of coatings will allow the identification of late-stage weathering and its relationships to exobiological material.

7) *Regolith Characterization*: SuperCam will address soil diversity at the landing site and will characterize the soil potential for biosignature preservation. Additionally, LIBS detection of hazardous elements in dust will provide important data for future human exploration.

8) *Atmospheric Characterization*: Column density measurements of atmospheric molecules, water ice, and dust characteristics will address the radiative balance of the Mars atmosphere. Acoustic sampling will help understand local instabilities (wind gusts).

Remote Sensing and Sampling Scales; Dust Removal: All of the techniques operate within the arm work zone, with a closest distance from the instrument of 2.0 meters, looking straight down. Fig. 1 shows the distance extent of each of the different techniques, giving a range of capabilities depending on the sample distance. Observational footprints are ~0.8 mrad for Raman, ~1.0 mrad for VISIR, 0.3-0.5 µm for LIBS, and an RMI field of view of 20 mrad and pixel FOV of 19 µrad. As such, the RMI provides the highest resolution remote imaging of all of the rover cameras. The LIBS laser shock wave brushes dust from the rock surface over an area large enough for the analytical footprints of all of the spectral techniques, providing unique and important access to the surface of the rock (Fig. 2).

Implementation of Techniques: *LIBS* is performed much the same as on ChemCam [5, 6] with similar laser wavelength and energy, a similar telescope, and a similar spectral range. Two of the three

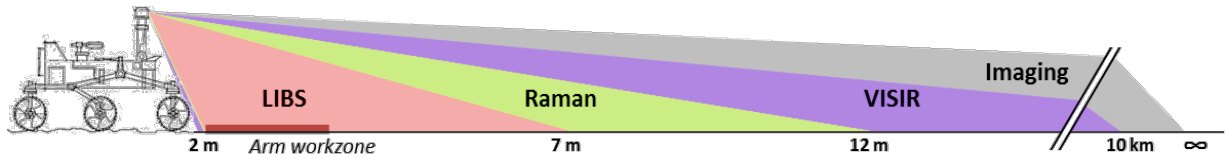

Fig. 1. Extent of SuperCam analytical capabilities. All techniques work within the arm work zone. The microphone (not shown) senses the laser shock waves to 4 m.

spectrometers are exact copies of ChemCam, while the third uses a higher-resolution spectrometer (Fig. 3) with an intensified, gated CCD which will allow time-resolved LIBS. *Remote Raman spectroscopy* is performed with a frequency-doubled YAG laser at 532 nm (green) in time-resolved mode, which eliminates much of the interfering fluorescence. The exposure can also be delayed, facilitating time-resolved fluorescence studies. The spectral resolution is ≤ 10 cm^{-1}, provided by the transmission spectrometer shown in Fig. 3. The *VISIR reflectance spectroscopy* is provided by the visible-range spectrometers used for LIBS and Raman spectroscopy (0.40-0.46, 0.53-0.85 µm) along with a wavelength-scanning AOTF infrared spectrometer that covers 1.3-2.6 µm, providing many important mineral signatures. The *RMI* imager employs a CMOS device with a Bayer color filter and high-dynamic-range (HDR) software. The *Microphone*, a Knowles electret identical to the ones installed (but never used) on Mars 98 and Phoenix, is mounted on the mast. Its primary purpose is to record the laser shock waves, which provide information on the hardness of the rock. It can also record wind and rover sounds.

Architecture: The SuperCam architecture is shown in the block diagram in Fig. 4. Overall, it is similar to ChemCam, consisting of separate Mast and Body Units built in France and at Los Alamos, respectively. The Mast Unit (MU) consists of a 110 mm diameter telescope, RMI camera, laser, and IR spectrometer. Light is provided to the Body Unit (BU) spectrometers via a fiber optic cable. The BU provides overall control and data handling for the instrument, with a number of functions handled in the MU. In addition, a significant effort is underway on the on-board calibration targets, ~28 geological and color standards designed for calibration of all three spectral modes and imaging.

Status: Prototypes of all subsystems have been built. A first end-to-end test was carried out with development unit parts in May, 2016, demonstrating Raman spectroscopy to 12 m along with LIBS. A more comprehensive test is scheduled for October, with a qualification unit being built in early 2017 and the flight unit in 2018.

References: [1] Mustard et al. (2013): Report of the Mars 2020 Science Definition Team. [2] Johnson J.R., et al. (2015) Icarus 249, 74-92 http://dx.doi.org/10.1016/j.icarus.2014.02.028. [3] Bell J.F. III, et al. (2012) Mastcam multispectral imaging on the Mars Science Laboratory rover: Wavelength coverage and imaging strategies at the Gale crater field site. Lunar Planet. Sci. XLIII, 2541. [4] Deleuze M., et al. (2016) The SuperCam Mast Unit on the NASA Mars2020 Mission, this meeting. [5] Wiens R.C., et al. (2012) Spa. Sci. Rev. 170, 167-227, doi 10.1007/S11214-012-9902-4. [6] Maurice S., et al. (2012) Spa. Sci. Rev. 170, 95-166, DOI 10.1007/s11214-012-9912-2.

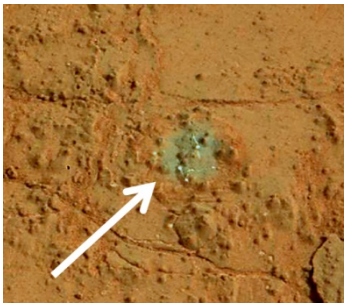

Fig. 2. ChemCam dust removal (2x2 raster) reveals gray mudstones in Gale. All SuperCam techniques will benefit from dust removal.

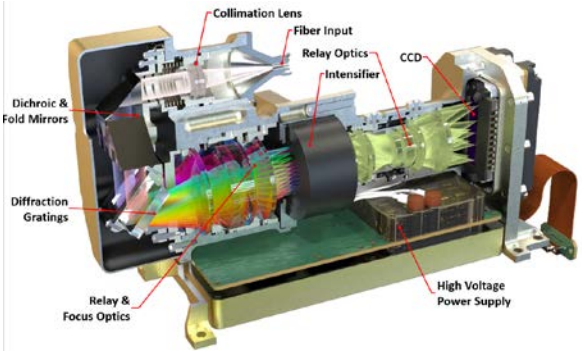

Fig. 3. SuperCam transmission spectrometer covers 535-850 nm (150-4000+ cm^{-1}) range with 10 cm^{-1} resolution.

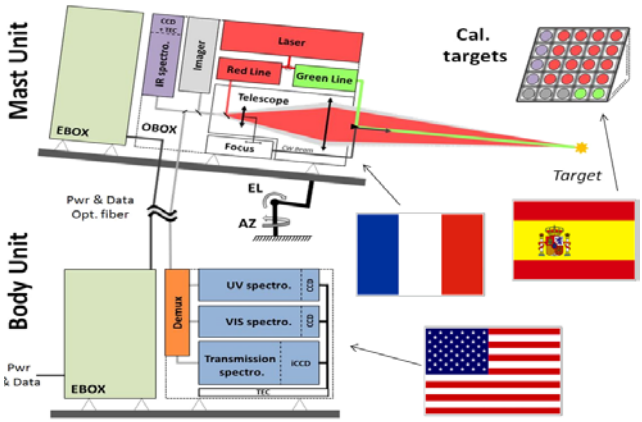

Fig. 4. SuperCam schematic diagram.

MAXIMIZING SCIENCE RETURN ON ASTROBIOLOGY AND PLANETARY MISSIONS USING INTEGRATED LIQUID-HANDLING CHEMICAL ANALYSIS SYSTEMS – A STATUS REPORT

P.A. Willis[1], M.F. Mora[1], J.S. Creamer[1], F. Kehl[1], [1]Peter.A.Willis@jpl.nasa.gov, Jet Propulsion Laboratory, California Institute of Technology, Pasadena CA 91109.

Introduction:

The use of liquids for in situ chemical analysis on planetary missions enables measurements of key organic molecules at parts-per-billion levels in samples that are challenging to analyze using current high-TRL gas phase techniques. This capability becomes particularly valuable when the scientific objective of an in situ chemical analysis involves the search for polar molecules indicative of water-based extant life. These molecules, for example amino acids (building blocks of proteins) and carboxylic acids (constituents of cell membranes), have a very low vapor pressure, and in order to perform a gas phase analysis, one must first perform a sample preparation step in which the molecule is first derivatized to increase its volatility. This process is has been shown to be problematic if the samples contain minerals[1]. Additionally if one wanted to use this type of analysis for a water-based sample, the derivatization agent would preferentially react with the water as well, severely constraining the efficiency of analysis. **An obvious approach to avoid these difficulties in the analysis of liquids is to simply leave them in the liquid state, and use a liquid separation method prior to analysis.** This would be the natural approach to take on an ocean world mission, for example, where ice samples could be acquired by a spacecraft, melted and transferred to an instrument system for direct analysis in that state. The obvious challenge with liquid-based analyses of this kind, of course, is that these systems are low TRL, with little NASA heritage. To that end, our team at JPL has been developing all the necessary "building block" components required for this sort of chemical analysis system (Figure 1) and we are currently in the process of validating a number of different portable automated analyzers that utilize these subsystems, that we have optimized for a range of applications on future missions of exploration (Figures 2 and 3). This contribution will summarize our scientific and technical progress in this area, and highlight the kinds of enhancements to science return on NASA missions that these technologies could provide.

Approach:

The possible pathways for sample flow and analysis we are developing are shown in Figure 1. In all cases, samples (either solid, liquid, or mixtures) are first ingested by the system. For this purpose we have developed a portable subcritical water extraction system (Figure 2) that incorporates elements from a host of previous extraction systems developed at JPL and elsewhere. The liquid output from this extractor is then transferred into a microfluidic based flow injection analysis system (MicroFIA) capable of electrical measurements of pH, conductivity, ORP, and selected ions, as well as performing colorimetric absorbance measurements of ions. To support these measurement capabilities, this system also contains all necessary valving, pumping, and reagent storage capabilities and is battery powered. This system can also act as a "standalone" oceanography sensor for the processing of filtered seawater or lakewater onboard a buoy or underwater explorer.

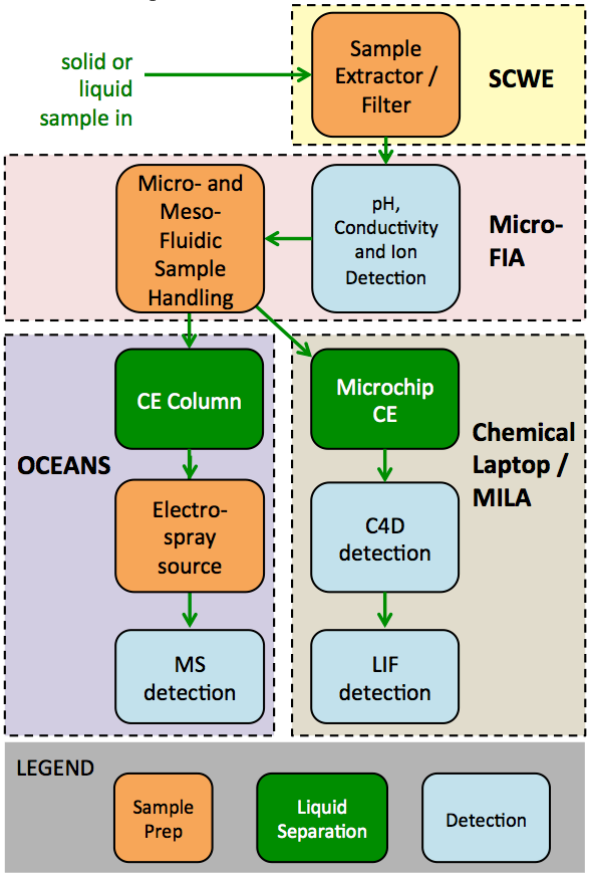

Figure 1. Block diagram displaying sample flow through sample preparation, separation, and detection modules (rounded boxes) under development by our team. We are integrating these modules into complete portable analyzers for use in the field (see Fig 2 and 3).

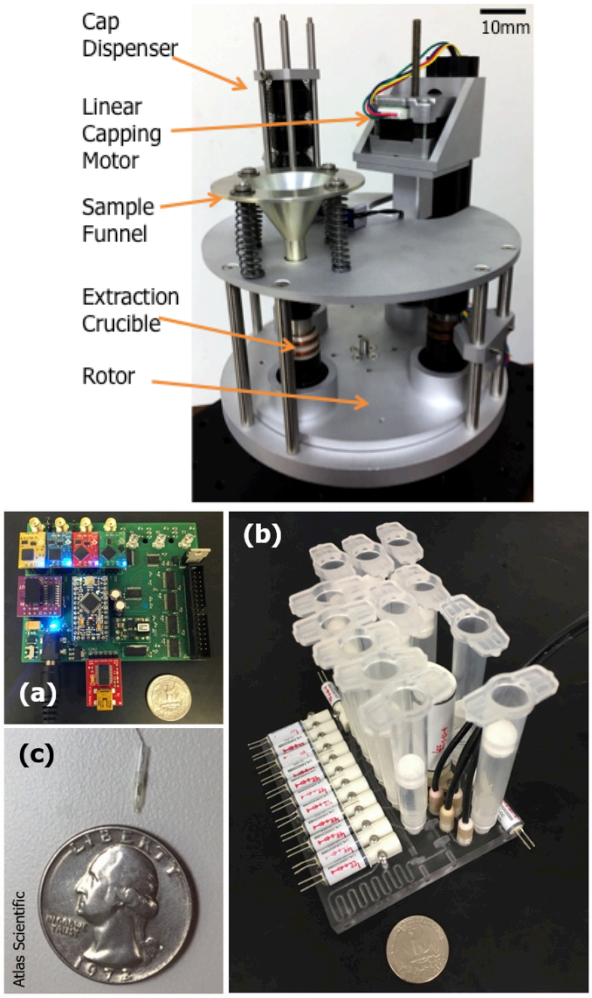

Figure 2. SCWE (*top*) and **MicroFIA** (*bottom* - (a) electronics, (b) assembly, and (c) miniature pH half cell.)

Following initial characterization by the MicroFIA subsystem, liquid samples are separated into their components using electrophoresis, and then detected. Depending upon the form of analysis performed, liquid preparation of these samples must be performed before separation. The bulk of our past efforts have been in the area of microchip electrophoresis coupled to laser-induced fluorescence detection [2]. This requires labeling of samples with a fluorescent dye prior to analysis. We have developed new capillary electrophoresis methods for chiral amino acid analysis that capable of chirally resolving 17 amino acids simultaneously, while still maintaining parts-per-billion detection. The portable system we have validated in the field for performing these analyses is the Chemical Laptop (Figure 3), which we have demonstrated to have an instrumental limit of detection of amino acids of 200pM. We are also currently enhancing this system via the addition of contactless capacitatively coupled conductivity detection (C4D), which, although less sensitive that LIF detection, requires no labeling step and can be used to analyze ions and other inorganic species. Additionally, in partnership with SCIEX we have also recently completed a complete design for a system we dub the Organic Capillary Electrophoresis Analysis System (OCEANS) which couples liquid separations with mass spectrometry detection as well. The design of this system (not yet built) is given in the bottom of Figure 3.

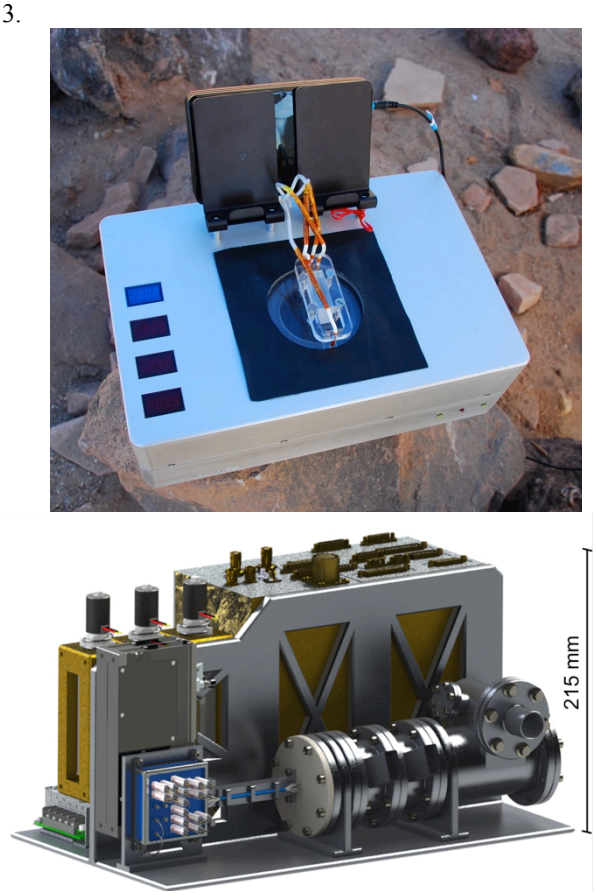

Figure 3. Chemical Laptop (*top* - validated in the field) and the Organic Capillary Electrophoresis Analysis System (**OCEANS**, *bottom* – CAD design of system; key components currently being fabricated, preliminary data acquired).

References:

[1] Stalport F, Glavin DP, Eigenbrode JL, Bish D, Blake D, Coll P, Szopa C, Buch A, McAdam A, Dworkin JP, Mahaffy PR (2012). Planetary and Space Science 67 (1):1-13.

[2] Willis PA, Creamer JS, Mora MF (2015). Analytical and Bioanalytical Chemistry 407 (23):6939-6963.

FROM MARS TO JUPITER AND BEYOND: IN SITU ATMOSPHERIC STUDIES WITH SYNERGISTIC INSTRUMENT PAYLOADS. Michael H. Wong, UC Berkeley (Astronomy) and University of Michigan (Climate and Space). mikewong@astro.berkeley.edu

Introduction: Atmospheres are exciting but challenging targets for in situ studies. As with past missions, future in situ atmospheric measurements (from e.g., Saturn or ice giant probes) may be difficult to interpret due to variability over temporal, horizontal, and vertical dimensions. One approach to these challenges is to conduct studies using a distributed array of sensors, such as a multiprobes [1]. But at a single location, it is essential to employ a synergistic instrument payload capable of inferring the effects of variability on the measurements obtained. Simultaneous global/regional context data are also very important.

The in situ investigations of the martian and jovian atmospheres by the flagship-class Curiosity Rover and Galileo Probe provide important case studies for instrument complementarity. Very rarely are science questions addressed with a single instrument. I will discuss how data from multiple instruments in each payload combine to deliver the clearest picture of atmospheric dynamics, composition, evolution, chemistry, and physics.

Instrumentation: The Galileo Probe's payload was specifically designed to study the gas composition, atmospheric structure, aerosols, and radiative fluxes in Jupiter's atmosphere, with the mission and instrumentation described in [2]. Curiosity carries a meteorology package [3], as well as multiple instruments for sample analysis and remote sensing that also collect data constraining aerosols and atmospheric composition [4].

Cloud physics and chemistry on Jupiter: The nephelometer measured aerosol opacity and scattering properties [5], but determining the cloud composition required complementary information from the atmospheric structure instrument (ASI) [6], which gave the temperature/pressure conditions within aerosol layers needed to compare with compositional cloud models [7]. The Galileo Probe descended into a meteorologically anomalous "hot spot," as shown by highly important ground-based context observations [8]. Within these features, large-scale downwelling produces generally cloud-free conditions and depleted condensable gases [9], but the ASI detected stable regions [10] corresponding to downwardly-displaced cloud layers, an interpretation supported by mass spectral composition measurements [11].

The large-scale downwelling could be reconciled with the continued presence of clouds if small-scale turbulence was responsible for condensation [12], a scenario that could have been confirmed if the probe had carried an imaging experiment (and had the bandwidth to transmit the data). A Net-Flux Radiometer on board the probe at least provided enough photometric information to determine sky color (Fig. 1). Future probes with imagers would provide additional constraints on cloud types in the descent area. Probe imaging data from future missions would help interpret ground-based or orbital/flyby observations with coarser spatial resolution.

Composition and origin of Jupiter's atmosphere: Spatial variation at Jupiter prevented the Galileo Probe from measuring Jupiter's O/H ratio, leaving a strong science driver for the Microwave Radiometer on Juno [13]. The N/H ratio however was measured by the mass spectrometer [14], with confirmation by the probe radio signal attenuation [15,16] and now finally by ground-based thermal radio spectroscopy [17]. Other heavier elemental ratios like He/H and C/H were easily measured by the probe [18] because helium and methane are invariable in Jupiter's troposphere, but CH_4 may also be horizontally and vertically variable on the ice giants. An accurate measurement there will rely on knowledge of local meteorological conditions,

Fig. 1. Visualization of the Galileo Probe descent, just before ejection of the heat shield [19]. For this science-education planetarium movie, we determined the approximate sky color as a function of descent time using NFR data (pers. comm., L.A. Sromovsky).

as was the case for the Jupiter probe. Heavy element relative abundances are related to the composition of planetesimals that formed the planet, so measuring abundances of volatiles and noble gases on the ice giants will provide additional constraints on conditions in the proto-planetary disk.

Martian chemical variability: Instrumentation on the Curiosity rover has been used to study unexpected chemical variability in the martian atmosphere. Methane, a potential biomarker, had previously shown spatial and temporal variability [20]. Specialized instrumentation on Curiosity, the SAM/TLS [21], additionally found that even the low-level background of CH_4 was inexplicably variable [22]. This variability is now being correlated with variable environmental conditions, which are determined by data from the weather sensors (REMS) [4,23] as well as models of UV flux constrained by the MASTCAM imager [24]. Other molecules—O_2 and CO—have been observed to vary using both the SAM mass spectrometer and the ChemCam passive spectrometer [25,26]; CO variability is somewhat inconsistent between ground-based telescopes and orbiters [27,28]. Photochemical lifetimes of all these molecules are long compared to the length of the martian year, so the observed variability may be suggestive of new chemical processes. Explaining these processes will require synthesis of observations of dust, solar radiation, temperature, and humidity from the rover instrument suite.

Conclusion: Whether we have "been there" or not, important questions remain about the workings of planetary atmospheres, as well as their origins. Most of these questions cannot be answered by a single instrument; instead, synergistic payloads are needed to disentangle the effects of temporal and spatial variability.

References: [1] Atreya S.K. and Wong A. (2005) *Sp. Sci. Rev.* 116, 121–136. [2] Young R.E. (1998) *JGR* 103, 22775–22790. [3] Gómez-Elvira et al. (2012) *Sp. Sci. Rev.* 170, 583–640. [4] Grotzinger et al. (2012) *Sp. Sci. Rev.* 170, 5–56. [5] Ragent B. et al. (1998) *JGR* 103, 22891–22910. [6] Seiff et al. (1998) *JGR* 103, 22857–22890. [7] Atreya S.K. et al. (1999) *Planet. Sp. Sci.* 47, 1243–1262. [8] Orton et al. (1998) *JGR* 103, 222791–22814. [9] Friedson A.J. (2005) *Icarus* 177, 1–17. [10] Magalhães et al. (2002) *Icarus* 158, 410–433. [11] Wong M.H. (2009) *Icarus* 199, 231–235. [12] Wong M.H. et al. (2015) *Icarus* 245, 273–281. [13] Janssen M.A. et al. (2005) *Icaurs* 173, 447–453. [14] Wong M.H. et al. (2004) *Icarus* 171, 153–170. [15] Folkner W.M. et al. (1998) *JGR* 103, 22847–22856. [16] Hanley T.R. et al. (2009) *Icarus* 202, 316–335. [17] de Pater I. et al. (2016) *Science* 352, 1198–1201. [18] Niemann H.B. et al. (1998) *JGR* 103, 22831–22846. [19] Emmart, C. et al. (2013) *Dark Universe*, AMNH (http://imdb.com/title/tt4430482). [20] Krasnopolsky V.A. et al. (2004) *Icarus* 172, 537–547. [21] Mahaffy P.R. et al. (2012) *Sp. Sci. Rev.* 170, 401–478. [22] Webster C.R. et al. (2015) *Science* 347, 415–417; Webster C.R. et al. (2016) *AGU Fall Meeting* Abstract, submitted. [23] Smith M.D. et al. (2016) *Icarus*, in press (doi:10.1016/j.icarus.2016.07.012). [24] Martínez G.M. et al. (2016) *Fisica de la Tierra*, submitted. [25] Trainer M.G. et al. (2016) *LPSC XLVII*, Abstract 1739. [26] McConnochie T.H. et al. (2015) *AGU Fall Meeting* Abstract P22A-08. [27] Krasnopolsky V.A. (2015) *Icarus* 253, 149–155. [28] Toigo A.D. et al. (2013) *JGR* 118, 89–104.

PERFORMANCE OF IMAGE REGISTRATION-BASED INSTRUMENT PLACEMENT FOR PIXL. K. Wu[1,2], G. B. Doran[2], D. R. Thompson[2], A. C. Allwood[2], D. T. Flannery[2], R. F. Sharrow[2], D. A. K. Pedersen[3], C. C. Liebe[2], [1]Massachusetts Institute of Technology, [2]Jet Propulsion Laboratory, California Institute of Technology, [3]Technical University of Denmark.

Introduction: A key part of the Mars 2020 Rover's mission involves determining Mars's past ability to support life by characterizing spatially-resolved microscale elemental chemistry of geological targets. The mission will accomplish this using PIXL (Planetary Instrument for X-Ray Lithochemistry), an X-ray fluorescence spectrometer mounted on the rover's Instrument Deployment Device [1]. PIXL requires precise placement relative to the target surface, which would traditionally require multiple rounds of communication between the rover and Earth due to arm thermal expansion and kinematic errors, causing delays and lost opportunities for acquiring data [2]. Because Mars 2020 will have limited time to acquire data at each site, automation of instrument placement has the potential to greatly increase the science yield from the mission [3]. Moreover, closed-loop servoing onboard the spacecraft will permit precision placement to tolerances that would not otherwise be achievable due to the natural thermal expansion and contraction of the rover arm between communication cycles. This high precision will be critical for taking full advantage of the PIXL spatial resolution of ~100μm. A new algorithm for closed-loop instrument placement using image registration on context images, photos of the location and orientation of the instrument, has been developed and tested on images from previous Mars missions [2]. This paper presents a performance analysis evaluating the application of this algorithm to PIXL images under Mars-representative imaging conditions in order to inform mission design and predict system-level performance.

Method: To collect a representative image data set for testing the algorithm, we imaged Mars-representative rocks using a realistic testbed designed to accurately simulate the essential features of flight hardware, including a PIXL context camera, illumination, optics, and imaging geometry. The test data set assumed no dust deposition on the camera lens. We simulated rover slippage by translating the rock and camera relative to each other with precision linear stages. Images were acquired in 0.5 cm steps over a 2.5 cm range in three axes. We also acquired images at standoffs greater than optimum (2.5 cm), which may occur during instrument placement or when imaging targets with high surface relief.

The algorithm must also perform under changes in solar illumination. For simulating Martian nighttime, we placed the instrument in a dark room with the camera's flash as the only source of illumination. For worst-case daytime lighting, the field of view was exposed to simulated Mars solar illumination parallel to the surface of the target. Registrations across these two conditions test the robustness of the algorithm to illumination angle and intensity changes.

Image targets included natural and abraded surfaces of representative rock samples. Both natural and abraded surfaces will be potential targets of interest on Mars.

Figure 1. Examples of rocks imaged.

Analysis: We established a ground truth homography by manually matching points in each pair of images to derive a homography matrix. This was done for each pair of images with 0.5cm translation between them. For pairs with greater translations, the ground truth was obtained by chaining the homographic transformation for image pairs to calculate a cumulative translation. To ensure that small errors did not accumulate, we spot checked some of these cases visually.

We then applied the flight code algorithm to pairs of the collected images to automatically determine homography matrices in a manner similar to what would occur during closed-loop operation onboard the rover. After using the algorithm-generated homography to transform randomly selected points in the source images, we compared the automatic solutions to the manual solutions for quantitative performance statistics.

Using the differences between the selected point coordinates, we estimated the 3σ error bound of the algorithm over the different conditions. Our performance model will help inform operations planning and make recommendations for use of the algorithm. The

PIXL instrument placement approach represents an evolutionary technology advancement and has outsized significance, both for improving data collection efficiency and for enabling placement precision superior to that achieved in any prior mission.

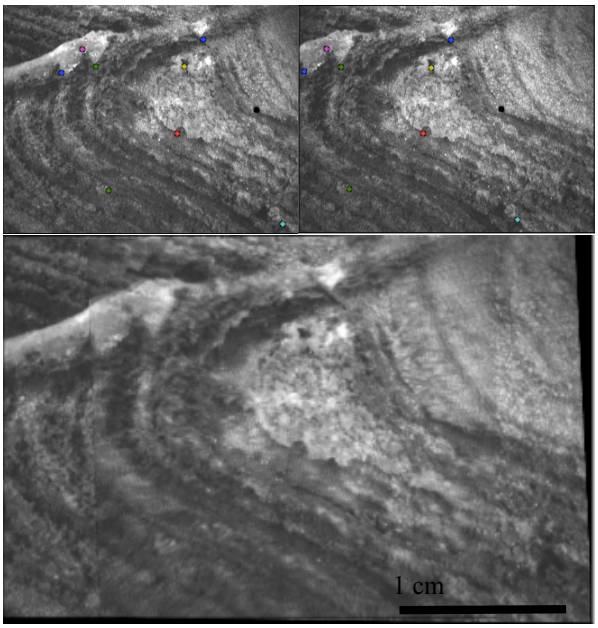

Figure 2. Two test images (top) of a grooved rock, merged (bottom) using manual point matching for establishing ground truth.

References: [1] Allwood A. C. et al., (2015) *IEEE Aerospace Conference*., 1-13. [2] Doran G. et al., (2016) *International Joint Conference on Artificial Intelligence*. [3] Thompson D. R. et al., (2015), *Astrobiology,* 15(11), 961–976.

1 M CLASS DRILL FOR ACQUISITION AND TRANSFER OF VOLATILE RICH SAMPLES ON THE MOON, MARS, AND OCEAN WORLDS. K. Zacny[1], G. Paulsen[1], [1]Honeybee Robotics, Pasadena, CA, zacny@honeybeerobotics.com,

Introduction: For over a decade, Honeybee Robotics has been developing 1 m class sample acquisition drills for accessing volatile rich planetary regolith on Mars and the Moon. The latest drill system is at TRL6 and ready to be infused into missions requiring acquisition of samples from approx. 20 cm to 2 m depth (the drill is scalable with respect to the depth), on any planetary surfaces (Mars, Moon, Comets, Ocean Worlds)

TRL4 Icebreaker Drill: The technology for 1 m class drill started with the development of the TRL4 Icebreaker drill for the Mars Icebreaker mission (**Figure 1**). The drill has been extensively tested in the Arctic, Antarctica, and Mars chamber as shown in **Figure 2**. The system demonstrated drilling in rocks, ice cemented ground, and ice with low power (100-200 Watt), low Weight on Bit (<100 N) and high penetration rate (1 m/hr). During drilling in Dry Valleys, the bit temperature never exceeded -5 °C (in the ground temperature of -19 °C). These tests have shown that drilling on Mars, in ice cemented ground with limited power, energy and Weight on Bit, and collecting samples in discrete depth intervals is possible within the mass, power, and energy levels of a Phoenix-size lander.

The drill uses a bite sampling approach whereby samples (nominally 10 cc in volume) are captured at the lowest section of the auger. The auger is then pulled out of the hole and sample is transferred to a cup or a funnel. The auger is lowered back into the same hole to drill another 10 cm and capture another ~10 cc sample. This process continues all the way to 100 cm depth. The process can be sped up if needed, i.e. the drill can drill all the way to say 70 cm and capture sample between 60 cm and 70 cm depth. This approach preserves stratigraphy (in bites), allows subsurface to cool, and reduces auger torque and power because sample does not need to be augered to the surface.

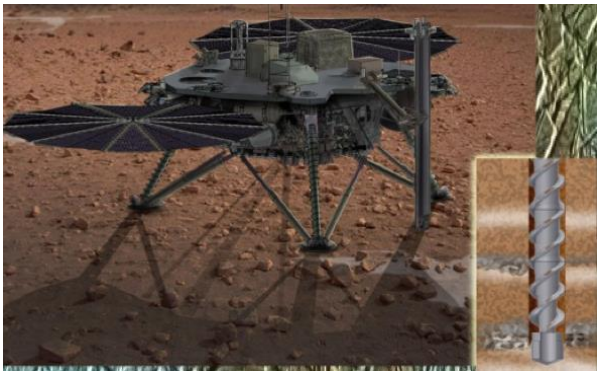

Figure 1. Mars Icebreaker mission concept. [1]

Figure 2. IceBreaker drill in the University Valley, Antarctica. [2, 3]

TRL4/5 LITA Drill: The next generation drill called the LITA drill (Life In The Atacama) achieved TRL 4/5 through significant reduction of mass (the Icebreaker drill weighed 40 kg while the LITA drill weighed 10 kg). The LITA drill has been deployed from a CMU rover in Atacama and in Greenland [4].

The goals of the field campaign were to demonstrate full autonomy the rate end-to-end sample acquisition and delivery from a variety of soils and rocks. During the course of the field deployment 6 holes have been drilled. The autonomy has been successfully demonstrated every time. In all cases, the average drilling power was less than 15 Watts because percussive system did not have to be engaged for most of the time. The Weight on Bit was also low, at 50 N or less. It took approximately 1.5 hours for the end-to-end sample acquisition and delivery.

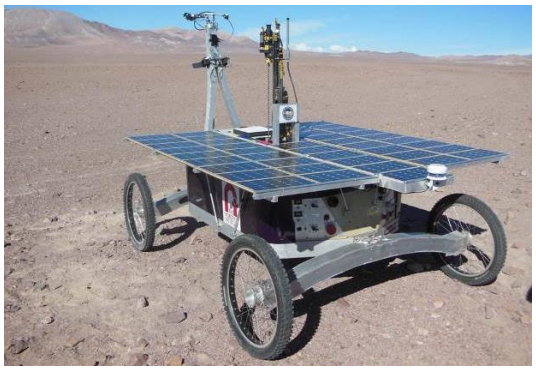

Figure 3. The LITA drill in Atacama deployed off CMU rover. [4]

TRL 5 Resource Prospector Drill: A LITA drill has been modified to reach TRL5 via changes to the drill actuators, lubrication, drill bit designs and so on.

It has subsequently been deployed from a Resource Prospector rover at NASA JSC (Figure 4) and has undergone thermal vacuum tests at NASA GRC [6]. During these vacuum tests, the drill captured volatile rich samples (NU-LHT-3M with 5wt% water) at -100 °C and deposited them into cups. The drill has also successfully withstood vibration tests (Figure 5).

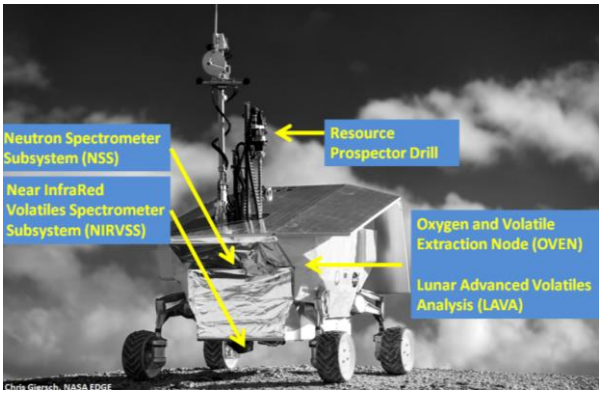

Figure 4. The Resource Prospector (RP) rover with Honeybee 1 m class drill. [5]

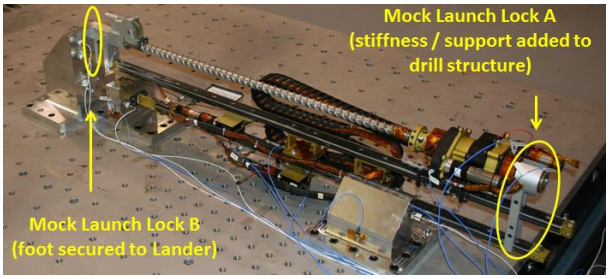

Figure 5. LITA drill setup for Vibration Tests at NASA KSC. [7]

TRL6 Resource Prospector drill: The latest 1 m class drill is being fabricated and will be available in October 2016. The drill has four actuators - two to drive rotary-percussive drill head and two to lower the deployment stage and the auger into the ground. The total rated power is approx. 500 Watt. The drill weighs approx. 15 kg. we plan to fabricate three such drills. First copy will be delivered to NASA KSC for testing for the Resource Prospector mission, second copy will be delivered to NASA Ames for integration with the K-Rex2 rover and deployment in the Atacama and the third copy will remain at Honeybee Robotics for further testing. All three drills in the course of their life will undergo further field deployment (Arctic, Atacama), chamber tests (Mars chamber at Honeybee Robotics and Lunar chamber at NASA Glenn Research Center). The drills will be deployed on two rovers (NASA JSC and NASA Ames). They will also undergo vibration tests at a subsystem level and as part of the entire system (while mounted on the rover). Finally, the drill will undergo thermal vacuum tests.

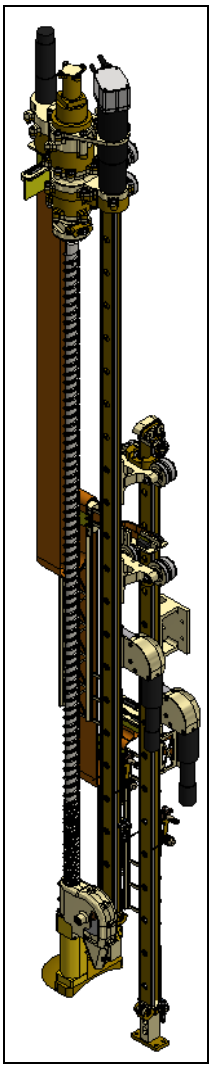

Parameter	Value
Bit Diam. (mm)	25.4
Auger Max (RPM)	120
Auger Torque Cont. (Nm)	14.9
Auger Max Cont. Power Out (W)	187
Percuss Energy (JPB)	4.0
Percuss Rate Max (BPM)	1160
Drill Stroke (mm)	~1186
Drill Depth (mm)	~1000
Deployment Stroke (mm)	~800
Z Stage Force Cont. (N)	~508
Total Mass (kg)	~15

Figure 6. TRL6 - 1 m drill.

References: [1] McKay et al., (2013), The Icebreaker Life Mission to Mars: A search for biomolecular evidence for life, Astrob. [2] Zacny, et al., (2013), Reaching 1 m Deep on Mars: The Icebreaker Drill, Astrob. [3] Paulsen et al., (2011), Testing of a 1 meter Mars IceBreaker Drill in a 3.5 meter Vacuum Chamber and in an Antarctic Mars Analog Site, AIAA Space. [4] Cabrol et al., (2015) Life in the Atacama: Science and Technology Pathways to the Robotic Search for Life on Mars, LPSC. [5] Andrews et al., (2014), Resource Prospecting Mission, AIAA Space. [6] Kleinhenz et al., (2015), Impact of Drilling Operations on Lunar Volatiles Capture: Thermal Vac Tests, AIAA SciTech.

Acknowledgements: The drill system was funded by NASA.